МІНІСТЕРСТВО ОСВІТИ І НАУКИ УКРАЇНИ
ДВНЗ «Прикарпатський національний університет імені Василя Стефаника»
Фізико-хімічний інститут
НОЦ «Наноматеріали в пристроях генерування та накопичення енергії»
АКАДЕМІЯ НАУК ВИЩОЇ ШКОЛИ УКРАЇНИ
ДЕРЖАВНЕ АГЕНТСТВО З ПИТАНЬ НАУКИ, ІННОВАЦІЇ ТА ІНФОРМАЦІЇ УКРАЇНИ
Державний фонд фундаментальних досліджень
НАЦІОНАЛЬНА АКАДЕМІЯ НАУК УКРАЇНИ
Інститут фізики напівпровідників ім. В.Є. Лашкарьова
Інститут хімії поверхні ім. О.О. Чуйка
Інститут металофізики ім. Г.В. Курдюмова
Інститут загальної і неорганічної хімії ім. В.І. Вернадського
Українське фізичне товариство
Івано-Франківський ЦНТІ
Інститут інноваційних досліджень
Інститут загальної фізики РАН (Російська Федерація)
Інститут фізики ім. Б.І. Степанова НАН Білорусі (Республіка Білорусь)
Університет Газі (Туреччина)

ФІЗИКА І ТЕХНОЛОГІЯ ТОНКИХ ПЛІВОК ТА НАНОСИСТЕМ

Матеріали XIV Міжнародної конференції
МКФТТПН-XIV

20-25 травня 2013 р.

Івано-Франківськ
Україна

УДК 539.2
ББК 22.373.1

Ф 83

Фізика і технологія тонких плівок та наносистем. ***Матеріали XIV Міжнародної конференції*** / За заг. ред. заслуженого діяча науки і техніки України, д.х.н., проф. **Фреїка Д.М**. – Івано-Франківськ: Видавництво Прикарпатського національного університету імені Василя Стефаника, 2013. – 624 с.

Представлено результати теоретичних і експериментальних досліджень з наступних питань: технологія тонких плівок (метали, напівпровідники, діелектрики, провідні полімери) і методи їх дослідження; фізико-хімічні властивості плівок; нанотехнології і наноматеріали, квантово-розмірні структури; тонкоплівкові елементи електронних пристроїв, наноелектроніка, функціональні кристалічні матеріали: ріст, фізичні властивості, використання.

Матеріали підготовлено до друку Організаційним комітетом та Редакційною колегією конференції і подано в авторській редакції.

Для наукових та інженерних працівників, що займаються проблемами тонкоплівкового матеріалознавства та мікроелектроніки.

Рекомендовано до друку науково-технічною радою Фізико-хімічного інституту ДВНЗ «Прикарпатський національний університет імені Василя Стефаника»

Р е ц е н з е н т и:
Литовченко В.Г.
чл.-кор. НАН України, завідувач відділенням Інституту фізики напівпровідників ім. В.Є. Лашкарьова НАН України
Готра З.Ю.
доктор технічних наук, професор, завідувач кафедри електронних приладів Національного університету «Львівська політехніка»
Рубіш В.М.
доктор фізико-математичних наук, професор, директор Ужгородсьеого науково технологічного центру оптичних носіїв інформації

УДК 539.2
ББК 22.373.1

вул. Шевченка, 57, м. Івано-Франківськ, 76018, Україна
Тел., факс (0342)596082
E-mail: freik@pu.if.ua

MINISTRY OF EDUCATION AND SCIENCE OF UKRAINE
'Vasyl Stefanyk' Precarpathian National University
Physico-Chemical Institute
SEC "Nanomaterials in Accumulation and Generation of Energy Devices"
ACADEMY OF SCIENCE OF HIGH SCHOOL OF UKRAINE
STATE AGENCY OF SCIENCE, INNOVATION AND INFORMATION OF UKRAINE
State Fund Of Fundamental Research
NATIONAL ACADEMY OF SCIENCE OF UKRAINE
'V.E. Lashkarev' Institute of Semiconductor Physics
'G.V. Kurdyumov' Institute of the Physics of Metals
'V.I. Vernadsky' Institute of General and Inorganic Chemistry
Chuiko Institute of Surface Chemistry
Ukraine Physics Society
Ivano-Frankivsk CSII
Institute of innovation research
Institute of General Physics RAS (Russia)
B.I. Stepanov Institute of Physics NAS of Belarus (Belarus)
Gazy University (Turkey)

PHYSICS AND TECHNOLOGY OF THIN FILMSAND NANOSYSTEMS

XIV INTERNATIONAL CONFERENCE

Materials

20-25, May, 2013

Ivano-Frankivsk, Ukraine

МИНИСТЕРСТВО ПРОСВЕЩЕНИЯ И НАУКИ УКРАИНЫ
ГВУЗ «Прикарпатский национальный университет имени Василия Стефаника»
Физико-химический институт
НОЦ «Наноматериалы в приборах генерирования и накопления энергии»
АКАДЕМІЯ НАУК ВИЩОЇ ШКОЛЫ УКРАИНИ
ГОСУДАРСТВЕННОЕ АГЕНТСТВО ПО ВОПРОСАМ НАУКИ, ИННОВАЦИИ И ИНФОРМАЦИИ УКРАИНЫ
Государственный фонд фундаментальных исследований
НАЦИОНАЛЬНАЯ АКАДЕМИЯ НАУК УКРАИНЫ
Институт физики полупроводников имени В.Е. Лашкарева
Институт металлофизики имени Г.В. Курдюмова
Институт общей и неорганической химии имени В.И. Вернадского
Институт химии поверхности им. О.О.Чуйка
Украинское физическое общество
Ивано-Франковский ЦНТИ
Институт инновационных исследований
Институт общей физики РАН (Росийская Федерация)
Институт физики им. Б.И. Степанова НАН Белоруси (Республика Белорусь)
Университет Гази (Турция)

ФИЗИКА И ТЕХНОЛОГИЯ ТОНКИХ ПЛЁНОК И НАНОСИСТЕМ

XIV МЕЖДУНАРОДНАЯ КОНФЕРЕНЦИЯ

Материалы

20-25 мая 2013 года

Ивано-Франковск, Украина

Physics and Technology of Thin Films and Nanosystems. ***Materials of XIVI International Conference*** / Ed by Honored engineer and techniques of Ukraine, Dr. Chem.Sci., Prof. **Freik D.M**. – Ivano-Frankivsk: A publisn-designing department of 'Vasyl Stefanyk' Precarpathian National University, 2013. – 624 c.

The results of theoretical and experimental researches in directions are submitted: technology of thin films (metals, semiconductors, dielectrics, and carrying out polymers) and methods of their investigation; physic-chemical properties of thin films; nanotechnology and nanomaterials, quantum-size structures; thin-film devices of electronics, crystal's growth and their physical properties.

The materials preformed for printing by Organizational Committee and Editorial Board of Conference, are conveyed in authoring edition.

For the scientific and engineering workers on thin-film material sciences and microelectronics.

It is recommended for printing by Scientific and Technical Advice of Physico-Chemical Institute at the 'Vasyl Stefanyk' Precarpathian National University.

Физика и технология тонких пленок и наносистем. ***Материалы XIV Международной конференции*** / Под общ. ред. заслуженного деятеля науки и техники Украины, д.х.н., проф. **Фреика Д.М.** – Ивано-Франковск: Издательство Прикарпатского национального университета имени Василия Стефаника, 2013. – 624 с.

Предоставлены результаты теоретических и экспериментальных исследований в следующих направлениях: технология тонких пленок (металлы, полупроводники, диэлектрики, проводящие полимеры) и методы их исследования; физико-химические свойства пленок; нанотехнологии и наноматериалы, квантово-размерные структуры; тонкопленочные элементы электронных приборов, наноэлектроника, функциональные кристаллические материалы: рост, физические свойства, использование.

Материалы подготовлены к печати Организационным комитетом и редакционной коллегией конференции, поданы в авторской редакции.

Для научных и инженерных работников занимающимися вопросами тонкопленочного материаловедения и микроэлектроники.

Рекомендовано к печати научно-техническим советом Физико-химического института ГВУЗ «Прикарпатский национальный университет имени Василия Стефаника».

ОРГАНІЗАЦІЙНИЙ КОМІТЕТ

Бюро

Загороднюк А., Литовченко В., Фреїк Д.

Міжнародний

Анатичук Л. (Україна), **Ахиска Р.** (Туреччина), **Бабанли М.** (Азербайджан), **Бєляєв О.** (Україна), **Блонський І.** (Україна), **Бродин М.** (Україна), **Булавін Л.** (Україна), **Власенко О.** (Україна), **Волков С.** (Україна), **Вуйцік В.** (Польща), **Галущак М.** (Україна), **Горбик П.** (Україна), **Готра З.** (Україна), **Грігоніс А.** (Литва), **Гриньов Б.** (Україна), **Гуревич Ю.** (Мексика), **Жуковскі П.** (Польща), **Зломанов В.** (Росія), **Івасишин О.** (Україна), **Калінкін І.** (Росія), **Картель М.** (Україна), **Кияк Б.** (Україна), **Кікінеші О.** (Угорщина), **Комаров Ф.** (Білорусь), **Кучмій С.** (Україна), **Мазуренко Є.** (Україна), **Малашкевич Г.** (Білорусь), **Мачулін В.** (Україна), **Міттова І.** (Росія), **Младенов Г.** (Болгарія), **Мовчан Б.** (Україна), **Наумовець А.** (Україна), **Находкін М.** (Україна), **Нікіфоров К.** (Росія), **Новиков М.** (Україна), **Остафійчук Б.** (Україна), **Панасюк В.** (Україна), **Птушинський Ю.** (Україна), **Раренко І.** (Україна), **Свєчніков С.** (Україна), **Сидоренко С.** (Україна), **Сизов Ф.** (Україна), **Скатков Л.** (Ізраїль), **Солонін Ю.** (Україна), **Стасюк І.** (Україна), **Стріха М.** (Україна), **Харченко М.** (Україна), **Челідзе Т.** (Грузія), **Чобанюк В.** (Україна), **Тигиняну І.** (Молдова), **Томчук П.** (Україна), **Уваров В.** (Україна), **Фірстов С.** (Україна), **Фістуль В.** (Росія), **Шпілевський Е.** (Білорусь), **Шпотюк О.** (Україна)

Національний

Бойчук В. (Дрогобич), **Буджак Я.** (Львів), **Гасюк І.** (Івано-Франківськ), **Дзумедзей Р.** (Івано-Франківськ), **Дзундза Б.** (Івано-Франківськ), **Дмитрук М.** (Київ), **Дружинін А.** (Львів), **Запухляк Р.** (Івано-Франківськ), **Зауличний Я.** (Київ), **Зінченко В.** (Одеса), **Зиман З.** (Харків), **Ігнатенко П.** (Донецьк), **Кідалов В.** (Бердянськ), **Кланічка В.** (Івано-Франківськ), **Коваленко О.** (Дніпропетровськ), **Корбутяк Д.** (Київ), **Куницький Ю.** (Київ), **Лашкарьов Г.** (Київ), **Лєпіх Я.** (Одеса), **Ліщинський І.** (Івано-Франківськ), **Лоп'янко М.** (Івано-Франківськ), **Матвеєва Л.** (Київ), **Мельничук О.** (Ніжин), **Миколайчук О.** (Львів), **Миронюк І.** (Івано-Франківськ), **Никируй Л.** (Івано-Франківськ), **Похмурський В.** (Львів), **Прокопів В.** (Івано-Франківськ), **Проценко І.** (Суми), **Прокопенко І.** (Київ), **Пташенко О.** (Одеса), **Рогачова О.** (Харків), **Рубіш В.** (Ужгород), **Рувінський М.** (Івано-Франківськ), **Середа Б.** (Запоріжжя), **Смертенко П.** (Київ), **Стасюк З.** (Львів), **Стронський О.** (Київ), **Студеняк І.** (Ужгород), **Ткач М.** (Чернівці), **Томашик В.** (Київ), **Чуйко Г.** (Херсон)

Секретаріат

Межиловська Л. – вчений секретар конференції
Борик В., Гургула Г., Паращук Т., Потяк В., Соколов О. – секретарі

ORGANIZING COMMITTEE

Bureau

D. Freik, V. Lytovchenko, A. Zagorodnyuk

International

R. Ahiska (Turkey), **L. Anatychyk** (Ukraine), **M. Babanly** (Azerbaijan), **O. Belyaev** (Ukraine), **I. Blonskiy** (Ukraine), **M. Brodyn** (Ukraine), **L. Bulavin** (Ukraine), **V. Chobanyuk** (Ukraine), **S. Firstov** (Ukraine), **V. Fistulj** (Russia), **M. Galushchak** (Ukraine), **P. Gorbyk** (Ukraine), **Z. Gotra** (Ukraine), **A. Grigonis** (Lithuania), **B. Grynyov** (Ukraine), **Yu. Gurevich** (Mexico), **O. Ivasyshyn** (Ukraine), **I. Kalinkin** (Russia), **M. Kartel** (Ukraine), **M. Kharchenko** (Ukraine), **O. Kikineshi** (Hungary), **F. Komarov** (Belarus), **S. Kuchmij** (Ukraine), **B. Kyyak** (Ukraine), **V. Machulin** (Ukraine), **G. Malashkevich** (Belarus), **Ye. Mazurenko** (Ukraine), **I. Mittova** (Russia), **G. Mladenov** (Bulgaria), **B. Movchan** (Ukraine), **A. Naumovetsj** (Ukraine), **M. Nahodkin** (Ukraine), **K. Nikiforov** (Russia), **M. Novykov** (Ukraine), **B. Ostafiychuk** (Ukraine), **V. Panasjuk** (Ukraine), **Yu. Ptushynskiy** (Ukraine), **I. Rarenko** (Ukraine), **E. Shpilevsky** (Belarus), **O. Shpotyuk** (Ukraine), **F. Sizov** (Ukraine), **L. Skatkov** (Israel), **Yu. Solonin** (Ukraine), **I. Stasjuk** (Ukraine), **M. Striha** (Ukraine), **S. Svechnikov** (Ukraine), **S. Sydorenko** (Ukraine), **T. Tchelidze** (Georgia), **P. Tomchuk** (Ukraine), **I. Tiginyanu** (Moldova), **V. Uvarov** (Ukraine), **O. Vlasenko** (Ukraine), **S. Volkov** (Ukraine), **V. Wojcik** (Poland), **V. Zlomanov** (Russia), **P. Zukowski** (Poland)

National

V. Boychuk (Drogobych), **Ya. Budzhak** (Lviv), **G. Chuyko** (Kherson), **M. Dmytruk** (Kyiv), **A. Druzhynin** (Lviv), **R. Dzumedzey** (Ivano-Frankivsk), **B. Dzundza** (Ivano-Frankivsk), **I. Gasyuk** (Ivano-Frankivsk), **P. Ignatenko** (Donetsk), **V. Kidalov** (Berdyansk), **V. Klanichka** (Ivano-Frankivsk), **D. Korbutyak** (Kyiv), **O. Kovalenko** (Dnipropetrovsk), **Yu. Kunitskiy** (Kyiv), **G. Lashkaryov** (Kyiv), **I. Lepikh** (Odesa), **I. Lishchynskyy** (Ivano-Frankivsk), **M. Lopyanko** (Ivano-Frankivsk), **L. Matveeva** (Kyiv), **Yu. Melnychuk** (Nizhyn), **O. Mykolaychuk** (Lviv), **I. Myronyuk** (Ukraine), **L. Nykyruy** (Ivano-Frankivsk), **V. Pohmursjkyy** (Lviv), **V. Prokopiv** (Ivano-Frankivsk), **I. Protsenko** (Sumy), **I. Prokopenko** (Kyiv), **O. Ptashchenko** (Odesa), **O. Rogachova** (Kharkiv), **V. Rubish** (Uzhgorod), **M. Ruvinskyy** (Ivano-Frankivsk), **B. Sereda** (Zaporizzhya), **P. Smertenko** (Kyiv), **Z. Stasyuk** (Lviv), **O. Stronsjkyy** (Kyiv), **I. Studenyak** (Uzhgorod), **M. Tkach** (Chernivtsi), **V. Tomashyk** (Kyiv), **R. Zapykhlyak** (Ivano-Frankivsk), **I. Zaulychnyy** (Kyiv), **Z. Zyman** (Kharkiv), **V. Zinchenko** (Odesa)

Secretariate

Scientific Secretary – **L. Mezhylovska**
Secretaries – **V. Boryk, G. Gurgula, T. Parashchuk, V. Potyak, O. Sokolov**

Вельмишановні пані та панове! Колеги! Друзі! Учасники XIV МКФТТПН – 2013!

Прикарпатський край і прикарпатці у черговий раз раді зустрічі з Вами! Новий час лине невпинно, постають нові реалії і нові вимоги до науки і нас, науковців. Окрім глибоких теоретичних ідей, необхідні й конкретні практичні рекомендації, а ще краще розробки, які би втілювали у життя новітні досягнення, технології, що визначають подальший цивілізаційний поступ.

Переконаний, що наша конференція буде належним внеском наукової спільноти у розв'язанні відзначних проблем.

Нових звершень та успішної роботи!

З великою повагою,
голова Оргкомітету
МКФТТПН-XIV

Дмитро Фреїк

м.Івано-Франківська, Україна
20 травня 2013 р.

Ladies and Gentlemen! Dear Colleagues Participants XIV ICPTTFN – 2013!

Precarpathian region and precarpathians once again are pleased to meet you! The new time is flying relentlessly; new realities and new challenges are facing to science and to scientists. Besides the deep theoretical ideas, specific practical recommendations are necessary and even better developments that would embody the latest achievements in life, technology, determining the further progress of civilization.

I am convinced that our conference will properly contribute scientific community in solving of significant problems.

New achievements and success!

With great respect,

Chairman of the Organizing Committee
ICPTTFN-XIV

Dmytro Freik

Ivano-Frankivsk, Ukraine
May, 20, 2013.

ПЛЕНАРНІ ДОПОВІДІ
21-24 травня 2013 р.

PLENARY REPORT
May, 21-24, 2013

Thermoelectric Module Structures

Ahiska R.[1], Mamur H.[2]

[1]*Gazi University, Ankara, Turkey*
[2]*Cankiri Karatekin University, Cankiri, Turkey*

Thermoelectric (TE) power generation technology aims to convert thermal energy into electrical energy. In the production of electrical energy, thermoelectric generators (TEG) consisted of large–bulk thermoelectric module (TEM) are preferred for high–power applications and TEGs (micro TEG - μTEG) consisted of thin film TEM are preferred for low-power applications. μTEGs require less thickness than the 50 μm thickness TE elements. Thickness of commercially available and widely used the bulks TEGs usually are over 500 μm. When it is below of this value, production efficiency decreases considerably.

μTEG is smaller and thinner than the bulk TEG. Therefore they take up less space and it is seen that μTEGs can directly integration industry-standard production methods as promising. Thin films in the μTEG are the segment layer materials thickness from one nm to a few nm. Thin film TE materials can be enlarged with different ways. μTEGs mainly consists of several kinds of structure such as Swiss roll, film and thermopile, and thermopile has relatively higher power density and therefore is more valuable for researching. The bulk integrated TEG produces the highest output power and voltage. It easily produces sufficient power at a high enough voltage to power a variety of low power sensors even when harvesting energy from temperature differences as low as 5 °C. μTEGs are more efficient for applications used acquisition of electrical energy in the high temperature difference [1].

For μTEG and bulk TEG performance, three factors turn out to be crucial: increasing the thermal resistance of the generator, decreasing thermal resistance of heat source–sink of heat–sink system consisting of TEG block and the contact to heat source and sink, respectively, and finally minimizing the electrical resistance. TE materials used in the TEMs shows a large variety. These are TEM materials including different material systems from semiconductors to ceramic, different crystal shapes from mono crystal, polycrystalline to nano-composites, and different sizes from bulk, film and wire to cluster. Improving of the figure of merit ***ZT*** of the TE materials is quite difficult due to the basic properties of the materials. In recent years, studies on improving of the figure of merit ***ZT*** of the TEM materials is moving towards the use of nanostructured materials [2]. The nanostructured materials such as quantum wells (QW), superlattices, nanowires, and nano grains are generally used as nano structured materials in the production of new TEGs. The TE conductivity can be quite reduced owing to the nanostructured materials.

The new nano materials called as QW are made up of 10 nm thick silicon and SiGe films. These have contributed to improving of the TE figure of merit *ZT*. Thermoelements having the figure of merit *ZT* greater than 3 have been obtained with the materials at room temperature. This value is a significant improvement compared to the bulk TEGs having the figure of merit *ZT* less than 1. Conversion efficiency of TEGs made of the QW materials is approaching up to 20 % [3].

In recent years, development efforts on the nano structured TE materials from nanocrystals to nanowires show great advantages, compared to the performance of the bulk crystal with the same chemical composition on account of dramatically reduced thermal conductivity [4]. But critical gaps still remain. Therefore, this restricts pratical manufacture, scalable, and wide deployment of nano TE devices.

Energy conversion technologys requires several conditions such as (1) the simplicity of the process and scalability of materials, (2) economical sustainment in the manufacture and recycling, (3) compatibility and integrability with existing manufacture infrastructure, and (4) performance improvability. These requirements determine the direction of future research for the nanostructured TE [5].

Acknowledgements

This study is supported by the Ankara Chamber Of Industry 1. Industrial District Office as Thermoelectric technology development project in Turkey.

1. Bierschenk, J. Optimized thermoelectric for energy harvesting applications // 17th International Symposium on the Applications of Ferroelectrics. –2008. – Santa Re, –P. 1–4.
2. Liu, W., Yan, X., Chen, G. and Ren, Z. Recent advances in thermoelectric nanocomposites. // Nano Energy. –2012. –V. 1. –P. 42–56.
3. Kim, D. H., Kim, C., Ha, D. W. and Kim, H. Fabrication and thermoelectric properties of crystal–aligned nano–structured Bi_2Te_3. // Journal Alloy Compounds. –2011. –V. 509. –P. 5211–5215.
4. Chen, T. G., Yu, P., Chou, R. H. and Pan, C. L. Phonon thermal conductivity suppression of bulk silicon nanowire composites for efficient thermoelectric conversion. // Optics Express. –2010. –V. 18. –P. 467–479.
5. Wu, Y., Finefrock, S. W. and Yang, H. Nanostructured thermoelectric: Opportunities and challenges. // Nano Energy. –2012. –V. 1. –P. 651–653.

Thin Films as Suitable Subjects for Nanomaterials Science Development

Andrievski R.A.

Institute of Problems of Chemical Physics, Russian Academy of Sciences
Chernogolovka, Moscow Region, Russia

Many phenomena in the nanomaterials science such as the features of brittle/plastic deformation, superhardness and superplasticity, conversation of phase diagrams in nanointerval, nature of size effects in nanomaterials, change of physical, mechanical and chemical properties in the nanostate, etc., can be studied with using thin films [1]. As compared with bulk nanomaterials thin films have many advantages such as high purity, minimum porosity and possibility to study subjects with very small grain size (up to 2-3 nm). The investigation results of structure and properties of films-based high-melting point borides, carbides and nitrides (TiB_2, TiC, TiN, B_4C, SiC, Si_3N_4, AlN and their systems) are generalized and discussed in details. The special attention is devoted to the characteristics of their thermal, irradiation and corrosion stability, i.e. to the behavior at extreme conditions [2].

1. Andrievski R.A. Nanostructured superhard films as typical nanomaterials // Surface & Coatings Technology. – 2007. – V.201. – P. 6112-6116.
2. Andrievski R.A. The Fundamentals of Nanostructured Materials Science. The Possibilities and Challenges. Publishing house “BINOM. Laboratory of Knowledge”, Moscow, 2012. – 252 p. (in Russian).

Spatiotemporal Autolocalization of Femtosecond Laser Pulses in Transparent Kerr Media

Blonskyi I.V., Kadan V.M.

Institute of Physics NAS of Ukraine, Kyiv, Ukraine

Non-linear dynamics of powerful femtosecond laser pulses in Kerr media results in their spatiotemporal localization, which manifests itself in space as an appearance of long and narrow filaments featuring high fluence and associated plasma channel. In time domain temporal self-compression of the femtosecond laser pulses and their subsequent splitting occure in the filament mode. Complex physics of interrelated nonlinear processes and a number of important possible applications attracts the attention of researchers to the filamentation phenomenon.

We report the results of our study of the femtosecond filamentation in transparent Kerr media, made at the Department of Photonic Processes of the Institute of Physics NASU. These researches became possible since the opening in the year 2006 of the Laser Femtosecond Center for Collective Use.

The report outlines the following topics:

– basic physical principles of the filamentation phenomenon;

– development of several new experimental time-resolved techniques for the study of the interaction of ultrafast laser pulses with different media;

– our results on the non-linear dynamics of femtosecond filamentation in fused silica and optical glass; particularly, superluminal propagation of the axial maximum of the filament; defocusing and expulsion of light from the plasma-occupied channel at the trail of the femtosecond filament; relaxation dynamics of the laser-induced plasma channel.

– our latest results on the temporal self-compression of the femtosecond pulse from the initial 150 fs down to the 65 fs duration, and extraction of the compressed component of the pulse from more temporally wide background;

– improvement of the temporal resolution of the time-resolved experimental techniques using the compressed pulse;

– direct observation of the self-compression and temporal splitting of the filamented laser pulse using the improved femtosecond time-resolved optical polarigraphy;

– influence of the interaction of the filaments on the spatial localization of the femtosecond pulses;

– mechanisms of Cherenkov phase-matching in Raman-seeded four-wave mixing by a femtosecond Bessel beam;

– femtosecond filamentation in chalcogenide semiconductor glasses and permanent filament-induced waveguides in these materials;

– generation of powerful femtosecond optical vortices and specific features of their filamentation.

Structure Similarity of the Amorphous and Crystalline Materials of Certain Chemical Composition

Bobyk M.Yu., Ivanitsky V.P., Ryaboschuk M.M.

Uzhgorod national university, Uzhgorod, Ukraine

At this report we discuss important methodic question: to what extent the amorphous and crystalline samples of certain chemical composition are structurally similar? For example, the same atoms may manifest themselves differently in the amorphous and crystalline structure. The amorphous Si:H films are a bright example. The hydrogen atoms could be implanted into the silicon crystals as well. However, in the crystalline lattice they are the defects, whereas in the amorphous films the hydrogen atoms generate new structural configurations, which differ considerably from pure silicon ones. These configurations are fixed as steric obstacles due to a large strength of the Si-H bonds and the geometric shape, which they acquire in the atomic network. Being distributed in the amorphous structure, they serve the effective barriers for the crystallization processes. At the same time the hydrogen atoms passivate the 'broken' silicon bonds and, thus, efficiently change the electro-physical properties of the amorphous Si-H films. Thus, besides the mentioned above, here, in our opinion, one has to consider some crucial moments.

1. Only for a very limited circle of the amorphous substances there exist their crystalline analogs (basically, they are the elementary substances and compounds of the stoichiometric compositions of the complex systems). The overwhelming majority of the amorphous substances have no crystalline analogs and the question of the structural similarity has no sense for them. For example, what should we consider the crystalline analog of the $Ge_5As_{15}S_{80}$ glass?

2. If the substance exists both in the crystalline and in the amorphous state, one may surely find separate small structural fragments in the amorphous state, which have the structure almost identical to the crystalline one. In this case the degree of distinction of these structures will be determined by the quantitative deviations of the functional and probabilistic short range order (SRO).

3. In any amorphous substance, which has the crystalline analog, separate structural fragments must necessarily occur with SRO, which both quantitatively and qualitatively differ from the typically crystalline fragments (e.g., in the region of the existence of the amorphous germanium and silicon with 5 and 7 atomic circles in the amorphous matrix).

4. The structural elements untypical for their crystalline analogs may occur in the amorphous substances (for example, the As_4S_4 molecules in the amorphous As_2S_3 films).

5. With increasing size of the structural fragments the degree of their similarity will decrease for the amorphous and crystalline substances. The spatial limits remain here unclear question related to such structural similarity.

A spherical Quantum Dot with Two Donor Impurities

Boichuk V.I., Bilynskyi I.V., Leshko R.Ya., Turyanska L.M.

Department of Theoretical Physics, Ivan Franko Drohobych State Pedagogical University, Drohobych, Lviv region, Ukraine

The most actual task of modern nanotechnologies is the development of new high-performance devices with improved parameters. All devices, which are constructed on the basis of both the bulk and nanoscaled semiconductors, depend strongly on the presence of impurities.

The physical properties of the spherical quantum dot (QD) such as the dipole transition, oscillator strength, and optical absorption coefficient can significantly depend on a presence of impurities in QD's. There are many theoretical works, such as [1–3], which are aimed to study of both central and off-central impurity in the QD. But the QD can contain more then one impurity. The number of impurities depends on different factors, such as concentration of impurities during the doping, purity materials, and etc.

There are not many theoretical works in which the energy spectrum of the QD with two or more impurities was studied. That is why in our opinion, it is expedient to extend the calculation for the case of two of impurities located beyond the center, and consider these impurities on the surface of the QD too.

In this work we present the calculation results of the singlet and triplet states of two impurities in the QD. The wave function of two-electrons system was constructed by the use of the Heitler-London method. One-electron functions were choose on the basis of the variational function [2]. The results show nonmonotonic dependence of the energy of the system on the impurity position in the QD. This fact is caused by the Coulomb and exchange interaction and by the confinement potential.

The absorption coefficients (ACs) associated with intersublevel transitions between singlet-singlet and triplet-triplet states were calculated too. It is shown that the AC depends on both the quantum confinement and the position of impurities in the QD.

1. M. Tkach, V. Holovatsky, Ya. Berezovsky, *Physics and Chemistry Solid State*, 4 (2003), 213.
2. V.I. Boichuk, I.V. Bilynskyi, R.Ya. Leshko, L.M. Turyanska, *Physica E: Low-dimensional Systems and Nanostructures*, **44,** (2011), 476.
3. V.I. Boichuk, R.Ya. Leshko, I.V. Bilynskyi, L.M. Turyanska, *Condensed Matter Physics*, **15**, (2012), 33702.

Crystalline Thin Film PbSe as Quantum Dimensional Structure

Budzhak J.S.

Lviv Polytechnic National University, Lviv, Ukraine

It is known that there is a spatial quantization of energy spectrum of current carriers in thin crystalline conductive films. Due to this a number of thin films' kinetic properties have correlation dependence on their thickness d.

Intensive chemical potential m of current carriers in the conditions of spectrum spatial quantization for impuritive thin film crystals, which are doped with donors and acceptors of the same type, was determined in this work. Chemical potential was determined from the neutrality equation with the condition that there are no transitions in the crystal or we can ignore them.

In the calculations of this work there is the formula of concentration of current carriers in thin films in the conditions of spatial quantization [1]:

$$n(d,T,m) = \frac{1}{2d^3} \cdot x(d,T) \sum_{l=1}^{\infty} \ln\left[1 + \exp\left(m - \frac{p}{x(d,T)} l^2\right)\right] \qquad (1)$$

where $x(d,T) = \frac{8pm^* d^2 kT}{h}$, m^* - effective mass of the charge carrier, d – film thickness, k - Boltzmann constant, T – crystal temperature, h - Planck's constant, m - intensive chemical potential.

This formula made the possibility to calculate mp and ap for the typical germanium crystal of p-type conductivity, results are shown on 1 and 2 figures.

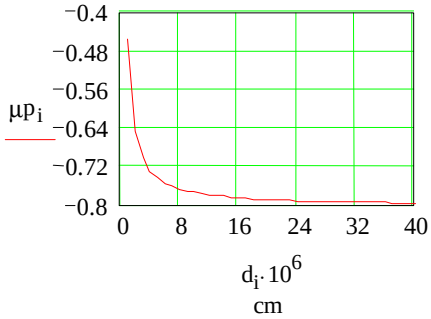

Fig.1.
Intensive chemical potential dependence on d with T=300 K.

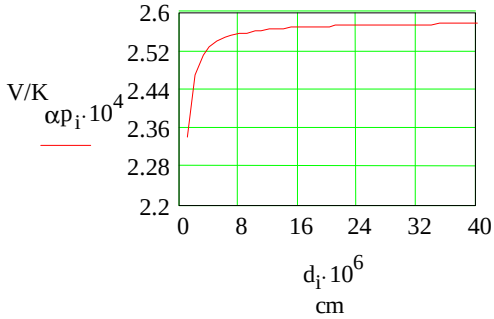

Fig.2.
Seeback coefficient dependence on d with T=300

1. J. S. Budzhak, O. V. Zub Thin crystal film as quantum dimensional structure // Eastern European journal of enterprise technologies //scientific magazine. - Kharkov: Technological center, 2010. - Vol. 2/5 (44). - 73 p.

Surface Modification and Performance of Nanoporous Carbon Electrode Material

Budzulyak I.M., Kuzyshyn M.M., Rachiy B.I., Mykyteichuk P.M.

Precarpathian National University named after Vasyl Stefanyk, Ivano-Frankivsk, Ukraine

Nanoporous carbon materials (NCM) are the main materials used as the electrodes of electrochemical capacitors (EC). It has been accepted that the electrochemical capacitance of carbon materials depends to a great extent on their pore structure and surface functional groups. These properties of carbon materials can be changed by heat or chemical treatment.

Nitric acid was used in the oxidation treatment of NCM, which prepared from raw materials [1]. The oxidation was conducted by wetting 12 g of the carbon materials in 160 ml 70% nitric acid solution in a magnetic stirrer for 3 h at room temperature. It was filtered and washed with deionized water to neutral pH. Then the product was dried at 60 °C for 24 h in air. The obtained sample was subjected to carbonization at different temperatures under Ar flow for 1 h.

The physical characteristics of the NCM determined from N_2 adsorption are given in Table 1. Both the surface area and pore volume decrease due to the treatment with nitric acid, indicating that the introduction of the surface oxides has hindered the access of N_2 into the carbon micropores. Upon carbonization in Ar flow to remove the hindering oxides, a slight porosity increase of the oxidized samples can be observed.

The data of the specific capacitances obtained from discharge plot at the current of 50 mA of the samples carbonated at different temperatures are listed in Table 1. As to the effect of oxidation, the results reflect that the specific capacitance of NCM increases upon nitric acid treatment by 30%. The extent of carbonization in Ar following the oxidation shows a great influence on the performance of EC. The capacitance increases with the carbonization temperature and reaches a maximum value at a temperature of 450 °C.

Table 1

The physical characteristics of the nanoporous carbon materials

Sample	C	CN0	CN1	CN2	CN3	CN4	CN5	CN6
Temperature, °C	-	-	150	250	350	450	550	650
Surface area, m^2/g	1257	1158	1197	1251	1308	1339	1329	1292
Total pore volume, cm^3/g	0,539	0,493	0,506	0,539	0,554	0,578	0,558	0,547
Specific capacitance, F/g	114	161	167	171	175	178	172	169

1. B.I. Rachiy. Morphology and electrochemical properties of thermally modified nanoporous carbon // Bulletin of the Precarpathian National University named after V.Stefanyk. Series of Chemistry. – 2011. – № 12. – P.61-72.

Examination of Nanosized Structures of Gold Thin Films by Scanning Fluorescent Probe Microscopy

Chornii V.[1], Nedilko S.[1], Hizhnyi Yu.[1], Chukova O.[1], Terebilenko K.[1], Slobodyanik M.[1], Aigouy L[2]

[1]*Taras Shevchenko National University of Kyiv, Kyiv, Ukraine*
[2]*UMR 8213 Institut de Physique, Laboratoire de Physique et d'Etude des Matériaux, France*

Modern technological applications require measurements of nanosized structures of thin films with a spatial resolution much smaller than the micrometer. This work presents results on examination of nanosized structures of gold thin films by scanning fluorescent probe microscope. Two types of materials are used as fluorescent probes: Eu-doped vanadates $LaVO_4$ and cromium-doped composites $NaAl(MoO_4)_2$:Cr/Al_2O_3:Cr. The main aim of presented studies is to show a principal possibility of using the submicron particles of the mentioned materials for effective measurements of the nonosized structure of thin metallic films.

Luminescent particles were stuck on a cantilever of the probe microscope. A 80 nm-thick gold layer with holes of 500 nm diameter deposited on SiO_2 substrate, was used as sample on which surface the optical near-field distribution is studied. The sample was irradiated from the bottom side by diode-pumped laser with λ_{ex} = 532 nm. The surface image (topography and surface distribution of the luminescence intensity) of the sample was formed by computer-driven optical system. The PL spectra of the $LaEuVO_4$ particle and results of the scanning of the sample are shown in Fig. 1. The spectra consist of sharp peaks of Eu^{3+}-related emission. Luminescence image of the sample surface was obtained by numerical integration of the luminescence signal in 610-620 nm region.

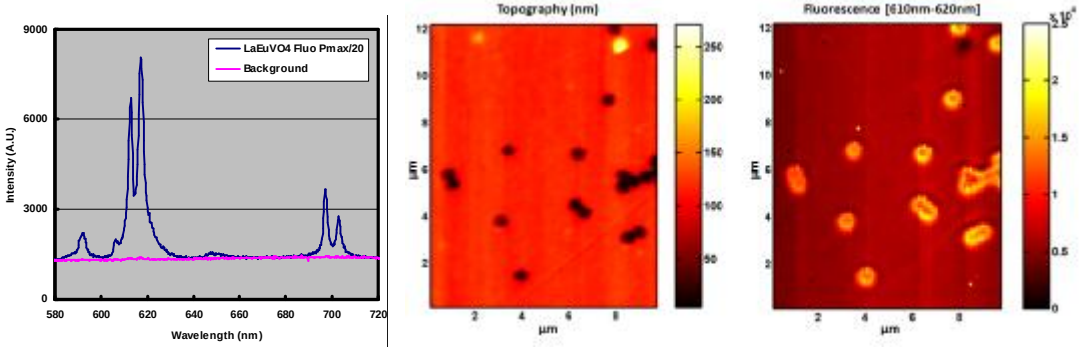

Fig.1 PL spectra of $LaEuVO_4$ microparticle, λ_{ex} = 532 nm (left), Topography (middle) and luminescence image of the gold sample (right).

Perspectives of application of studied luminescence particles in various applications of scanning probe microscopy are discussed.

This work is supported by NASU-CNRS project "Development of luminescent nanothermometers (LNTs) and use for high resolution thermal imaging".

Surface-Enhanced Photophysical Phenomena and Plasmonic Photovoltaics

Dmitruk N.L.

Institute for Physics of Semiconductors, NAS of Ukraine, Kyiv, Ukraine,

When electromagnetic wave or light in optical (visible) range illuminates a so-called surface-active medium, which has negative dielectric function $\varepsilon(\omega)$ in some spectral diapason, the surface electromagnetic waves (surface polaritons) or surface quasiparticles (oscillations) are excited. As surface-active medium it is convenient to use a metal in the spectral region below the plasma frequency, ω_p, or polar dielectric/semiconductor in the region of the phonon transversal-longitudinal splitting, ω_{TO}-ω_{LO}, or exciton semiconductor etc. Then one say about surface plasmon (phonon, exciton or mixed plasmon-phonon) polaritons (oscillations). Since surface polaritons are eigen-oscillations of the limited medium, their excitation leads to strong resonant increase in the electromagnetic fields intensity at the interface. This increase is proportional to the $g^2 = (\mathrm{Re}e(w)/\mathrm{Im}e(w))^2$ ratio. Thus, the field intensity or the energy stored near surface (rough surface, nanoparticle, periodic array of nano(micro)objects) is increased by the factor of $g^2 \approx 10^3 - 10^4$, while the Raman scattering cross section is increased by the factor of $G \approx g^4 \approx 10^6 \div 10^8$. Surface plasmon polaritons (SPP) and surface (localized) plasmons (SP) are especially attractive for practical applications in view of their localization in the visible spectral range, where various electron-hole transitions in many semiconductors and maximum of solar energy spectrum are located.

So, SP or SPP excitation leads to localization, concentration and enhancement of electromagnetic (E/M) fields in solids. This enhancement leads to increase of various photophysical phenomena called the surface enhancement effect, which has a broad range of practical applications, such as:

- infrared absorption by various adsorbed substances (SEIRA);
- surface enhanced Raman scattering (SERS) up to 10^{10} times;
- photo-, electroluminescence enhancement up to 10^2-10^3;
- photocurrent of various barrier semiconductor structures (photodetectors, solar cells (SC); using nanoplasmonics principles and recent advances in the control of light at the nanometre/micometre length scales will allow the development of SC with efficiencies in the 50-70% range;
- sensoric applications, when a single nanodevice that detects the presence of a single molecule would perhaps be the ultimate sensor;
- optical antennas, as some nanoscale resonators with high Q-factor (wavelength selectivity) and possible enhancement of detectivity at resonant conditions.

Besides, resent progress in nanotechnology has enabled to fabricate subwavelength devices for improving the exchange of optical energy with nanoscale matter (antenna, photon collection, photon-emitter interaction, non-linear

optical phenomena, including near-field scanning optical microscopy with subwavelength resolution etc.).

In this report several ways to enhance the SC efficiency by using the plasmonics principles will be considered in detail (plasmonic photovoltaics):

1) Enhancement up to twice of light transmittance into the absorptive layer of SC with anticorrelated reliefs of emitter and the short-circuit current increase predicted theoretically, which is caused by excitation of SPP;

2) The photocurrent enhancement by metal nanoparticles, incorporated into SC interface, due to light scattering with SP excitation, have been calculated in dependence on spherical particle size and their interdistances;

3) Using the differential formalism method for solving the Maxwell's equations in curvilinear coordinate system, the averaged photocurrent of SC with periodical metal nanowire array has been calculated in dependence on the distance of nanowires from the SC interface; existence of some optimal distance $d \approx 100$ nm for the Au-GaAs system is predicted, which is conditioned by near-field localization;

4) In dependence on the metal plasmon-carrying nanoparticles size D, the enhancement effect caused by light scattering ($D \geq 100$ nm for Au, Ag) or by near-field increase ($D \leq 50$ nm) around metal nanoparticles/nanowires;

5) Experimentally the double effect of the SC efficiency increase for the gold nanowires array on ridges of the quasiperiodical microrelief fabricated with self-organized anisotropic etching of GaAs (100) has been studied.

1. N.L.Dmitruk, A.V.Korovin, I.B.Mamontova. Efficiency enhancement of surface barrier solar cells due to excitation of surface plasmon polaritons. Semicond. Sci. Technol. 2009. v.24. p.125011.

2. N.L.Dmitruk, A.V.Korovin. Plasmonic photovoltaics: photocurrent enhancement by metal nanoparticles on solar cells interface. Proc. of the 24th European Photovoltaic Solar Energy Conference and Exhibition. 21-25 September 2009. Hamburg, Germany. pp.566-569.

3. N.L.Dmitruk, A.V.Korovin. Plasmonic photovoltaics: metal nanowires on solar cell interface. Proc. of 25th European Photovoltaic Solar Energy Conference and Exhibition and 5th World Conference on Photovoltaic Energy Conversion, 6–10 September 2010, Valencia, Spain, pp.385-388.

4. S.Mamykin, N.Dmitruk, A.Korovin, D.Naumenko, A.Dmytruk, Yeon-Su Park. Local plasmons contribution into photocurrent of Au/GaAs surface barrier structure with Au nanoparticles on interface. *S*emiconductor Physics, Quantum Electronics & Optoelectronics. 2009. v.12, N4. p.315-320.

5. N.L.Dmitruk, A.V.Korovin. Plasmonic photovoltaics: near-field of metal nanowire assemblies for solar cell efficiency enhancement. Proc. of 26th European Photovoltaic Solar Energy Conference and Exhibition, September 5-9, 2011. Hamburg, Germany, pp. 237-240.

6. N.L.Dmitruk, A.V.Korovin, O.Yu.Borkovskaya, A.M.Dmytruk, I.B.Mamontova, S.V.Mamykin. Plasmonic photovoltaics: self-organized metal nanowires on the solar cell surface/interface. Proc. of 27th European Photovoltaic Solar Energy Conference and Exhibition. September 24–28, 2012. Frankfurt, Germany. pp. 408-411.

Charge Carrier Transport of Polysilicon in Soi Structures at Low Temperatures

Druzhinin A.A.[1,3], Kogut I.T.[1,2], Khoverko Yu.N.[1,3], Vuitsyk A.N.[1]

[1]*Lviv Polytechnic National University, Lviv, Ukraine,*
[2]*Vasyl Stefanyk Precarpathian National University, Ivano-Frankivsk, Ukraine*
[3]*International Laboratory of High Magnetic Fields and Low Temperatures, Wroclaw, Poland*

The paper deals with investigation of electrophysical properties of polysilicon layers in SOI structures with charge carrier concentration of about 2,4 10^{18}cm^{-3} that is near to metal-insulator transition. Samples were prepared by LPCVD method. The doping process of polysilicon was carried out by ion implantation of boron impurity. Low-temparature studies of SOI structures were carried out at temperature range 4,2–300 К and magnetic fields up to 14 Т. Investigation results of magnetic properties have shown the presence of negative magnetoresistance at low magnetic fields and it becomes positive at 4,2 К. The conductivity of such samples at low-temperature region varies according to Mott law ($\ln\rho \sim T^{-1/4}$) [1].

The exponentially high values of positive magnetoresistance indicates a hopping conduction the posistive component of which is related to the compression of localized state wave function at magnetic field. The model that predicts the hopping probability determined by the degree of spin polarization at magnetic field has been proposed. Based on experimental results for magnetoresistance it was found the localization length, density of states and jump distance of charge carriers for low-temperature conduction which are equal: α_1=6 Å, g_1=1,3 10^{21} eV cm^{-3}, 31<R<36, α_2=23 Å, g_2=2 10^{19} eV·cm^{-3}, 121<R<140. It was established that with temperature decreasing the probability of hopps spatially ranged but energeticaly closely to centers of localization increases what results in decreasing of activation energy of hopping conduction.

Taking into account a significant resistance temperature dependence of polysilicon layers at low temperatures it was estimated that the temperature coefficient of resistance is equal to 9%×К$^{-1}$ in temperature range 4,2–50 К. Such polysilicon layers can be recommended for making highly sensitive sensors of cryogenic temperatures. The calibration of polysilion resistor as sensitive element of temperature sensor with free-carrier concentration $p_{300K}\approx 2{,}4\times10^{18}$ in temperature range 4,2–150 К cm^{-3} was made.

1. Druzhinin A., Maryamova I., Kogut I., Pankov Yu., Khoverko Yu., Palewski T. Polysilicon-on-insulator layers at cryogenic temperatures and high magnetic fields // D. Flandre et al. (eds.), Science and Technology of Semiconductor-On-Insulator Structures and Devices Operating in a Harsh Environment. – Kluwer Academic Publishers. – 2005. – P. 297–302.

Nanoporous Silicon Layers for Hydrogen Fuel Cells

Dzhafarov T.D.[1], Aydin Yuksel S.[2], Aydin M.[2]

[1]*Institute of Physics, Azerbaijan National Academy of Sciences,Baku, Azerbaijan*
[2]*Department of Physics, Yildiz Technical University, Istanbul, Turkey*

Hydrogen fuel cells have been investigated as efficient and sustained sources of clean energy. However the use of hydrogen in hydrogen fuel cells poses a lot of problems related with production, storage and transportation of liquefied hydrogen. Nowadays, miniature fuel cells are under active attention for the supply of portable applications (mobile electronic devices, telecommunication, military equipment, etc.). The direct methanol fuel cell (DMFC) based on proton exchange membrane (PEM) with organic polymer membrane (Nafion®) as proton conductor have been developed for small power-supply units. But DMFC has disadvantages related with formation of the CO pollutant gas and high temperature operation (80-100^{o}C). Carbon free and not explosive ammonia (NH_3) and hydrochloric acid known as a good hydrogen carrier have received little consideration for use a direct fuel for PEM type of fuel cells. The fabrication of most portable electronic devices was based on standard micro-fabrication technique, but DMFC type fuel cell with polymer membrane is not readily integrated with this technique. For overcome above disadvantages we used the nanoporous silicon layer as proton-conducting membrane. Fabrication and characterization of Au/Porous silicon/Silicon (Au/PS/Si) and Au/TiO_x/Porous silicon/Silicon (Au/TiO_x/PS/Si)-type direct ammonia and hydrochloric acid fuel cells have been presented in this work.

Porous silicon presents a network of silicon in nano (micro)-sized regions of huge surface (up to 800 m^2/cm^3). The structure of porous silicon is like a sponge or columnar where quantum confinement effects play fundamental role. Existence of pores determining large ion (proton) conductivity along the pores opens new perspectives for using porous silicon-based structures as hydrogen fuel cells. The Au/PS/Si and were fabricated by first creating the nanoporous silicon layer in single-crystalline Si using the anodic etching and then deposition Au catalyst layer onto the porous silicon. In addition, the Au/TiO_x/PS/Si cells with thin titanium dioxide film have been also investigated. The TiO_x films were deposited on porous silicon layer using spin coating technique. The study of fuel cell characteristics was carried out using ammonia solution or hydrochloric acid solution as fuel. The open circuit voltage up to 1.20 V and maximum power density about of 1-3 mW/cm^2 at room temperature was achieved using H_2SO_4:H_2O and NH_3:H_2O solution as fuel. These results demonstrated that the PS/Si-type fuel cells with nanoporous silicon layer operating at room temperature can be considered as the most promising type of low cost direct ammonia or direct hydrochloric acid fuel cell for small power-supply units.

Formation and Properties of Gd Nanofilms on Si (113)

Fedorchenko M.I., Nakhodkin M.G.

Taras Shevchenko National University of Kyiv, Ukraine

The investigation of rare-earth metals/Si interfaces is important because the forming on silicon surfaces thin films of REM silicide are perspective for using in micro- and nanoelectronics. It is known that submonolayer coverages of Gd form nanowires on the high-index Si(113) surface. One-dimensional nanowires have attracted significant attention due to their unusual physical properties and potential applications in nanoelectronic, nanophotonic, molecular-electronic and magnetoelectronic devices. It is also known that GdB_6 nanowire emitters of rectangular cross-section with about 50 nm in lateral dimension and several microns in length have the lowest work function in the rare-earth hexaboride family about 1.5 eV.

High-index Si(113) is of increasing attention as substrate for electronic device applications. It inherent structural anisotropy reduces antiphase domain formation, threading dislocation pileup, and surface roughness during heteroepitaxy, resulting to improved epitaxial layers and novel electronic properties.

The aim of the present work was to study experimentally the adsorption of Gd on high-index Si(113) surfaces and to determine the correlation between structure, electronic and adsorption properties of such interfaces.

The experiments were done in the homemade ultra-high vacuum chamber with a base pressure $\approx 2\times10^{-10}$ Torr. Gd was evaporated by resistive heating of a tantalum filament. The evaporation rate of 0.02 monolayer (ML) per min was monitored by a quartz microbalance. Auger electron spectroscopy, low-energy electron diffraction, ultra-violet photoelectron spectroscopy (UPS) were used for analyzing the adsorption system.

The Si(LVV), Gd(NON) and Gd(NVV) Auger lineshapes were investigated with increasing of Θ_{Gd}. They indicate on forming a well-defined silicide-type interfacial reaction product.

UPS measurements have shown that the work function of Si(113) surface monotonously decreases with increasing of Θ_{Gd}. At $\Theta_{Gd} \approx$ 6ML the work function decreases to $\approx$ 1.2eV and becomes stabilized.

The exposure of Gd nanofilms in CO atmosphere was accompanied by the reduction of electronic state density near the Fermy level, oxidation of Gd atoms and decreasing work function to 0.7–0.3 eV.

The annealing of Si(113):Gd:CO system has shown that the work function has remained $\leq$ 1.0 eV at temperatures $\leq$ 600°C.

The preliminary model that provides the explanation of correlation between structure and the work function of Si(113):Gd:CO system is discussed.

Numerical Modeling of Two-Level System Fluorescence Nearby Metallic Nano Particle with Accounting the Contribution of Tunneling of Electron from the System to the Particle

Fedorovich S.V., Protsenko I.E.

P.N. Lebedev Physical Institute of the Russian Academy of Sciences, Moscow
Plasmonics ltd, Skolkovo, Moscow Region.

At experimental researches of solar cells (SC) established that metal nano-particles placed on the dielectric spacer on SC surface increase SC fluorescence and generation of photo-electrons. Maximal increase of the fluorescence rate have been observed at thickness of spacer d= 20-30 nm. Then fluorescence rate was decreased at d=10-15 nm. At thickness of spacer d<10 nm fluorescence rate falls to zero; our model suggests the reason for that.

We present results of numerical modeling of radiation of two-level system (TLS) near metallic nano-particle at resonant interaction of TLS radiation with plasmon modes of the particle. Computations were made for different polarizations of radiation by dipole approximation method and by multipole expansion method. Contribution of non-radiative process of electron tunneling from two-level system to the nano-particle was taken into account using quasi-classical approximation. Tunneling rate and spontaneous decay rate of TLS excited electron were estimated. They are compared at distances between particle and TLS about 10-15 nm (see Fig.), that explains results of experiments with SC with metal nanoparticles. Our results will also be used in the modeling of plasmonic nano-lasers.

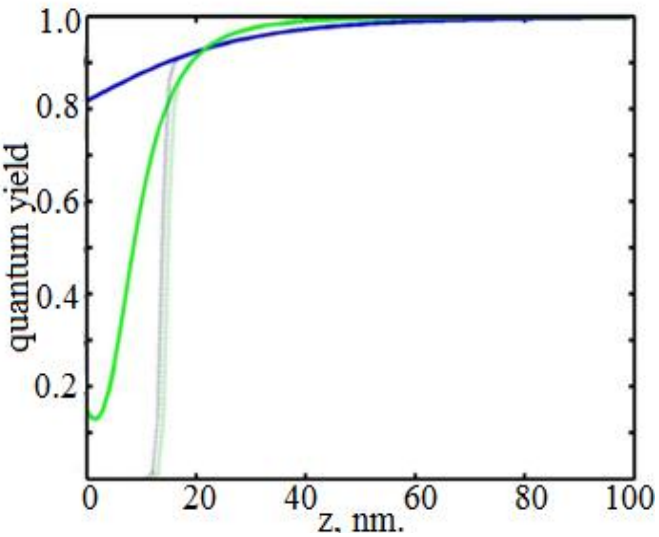

Quantum yeild as function of nanoparticle-TLS separation. Radiation wavelength is λ= 650 nm. and ε= -12.99+i1.09 (gold particle of radius40 nm.). The blue curve is polarization along Z axes; the green bold curve is polarization along X axes; the blue dashed curve is polarization along Z axes witn tunneling; the green dashed curve is polarization along X axes with

1. O.V. Dementeva, S.A. Kazaryan, I.E. Protsenko, et al. II Nanotechnology International Forum, Moscow, October 6-9 2009.

Quantum-size and Nanocomposite Thermoelectric Materials: Technology, Properties, Use

Freik D.M.

Vasyl Stefanyk Precarpathian National University, Ivano-Frankivsk, Ukraine

The environment is filled with a large number of so-called gratuitous energy that is still not effectively used by humanity. The fact that a very urgent need is to improve the efficiency of its conversion into electricity using primarily solid-state thermoelectric modules based on semiconductor materials.. The main thermoelectric parameter is the dimensionless thermoelectric figure of merit ZT ($ZT = S^2\sigma/\chi$, T -absolute temperature). Practical sense are the materials characterized by $ZT \approx 1$ (efficiency = 3-6%). If $ZT = 2 \div 3$ (efficiency: 20%), it would have led to a sharp increase in their use, while at $ZT = 3 \div 4$ thermoelectric converters could compete with conventional electric generators. In this connection it is important to continue to search for efficient thermoelectric materials.

Note, that the Seebeck coefficient (thermoelectric power) (S) and electrical conductivity (σ) are defined only by electronic subsystem of the crystal, and thermal conductivity (χ) in the first approximation – by phonon and electron subsystems ($\chi = \chi_l + \chi_e$). So, to maximize thermoefficiency Z of material it is needed the thermal conductivity to be minimal at maximum electrical conductivity. It takes material such as "phonon glass" and "electronic metal"?!

Recent advances in nanotechnology give some perspective to solve assigned problems [1,2]. It is believed now that the main direction of improvement of thermoelectric properties of materials is the use of spatially inhomogeneous structures with dimensions comparable to the characteristics wavelength of electrons and phonons, that are in nanoscale area. These systems should include quantum dots, wire and wells and created on the basis superlattice of quantum dots, wires and nanocomposites.

Potential impact on electronic and phonon subsystems of new structures by one more parameter – size – significantly expands ways to improve the thermoelectric figure of merit. In such structures there have been two main strategies (using quantum-size effects to enhance the Seebeck coefficient S and to control S and the conductivity σ somewhat independently; the introduction of numerous boundaries that scatter phonons more effectively than electrons and also scatter mainly those phonons which have the greatest contribution to the thermal conductivity) and three conceptions of their future development ("carrier-pocket" engineering, filtering energy, transition semimetal-semiconductor (SMSC-transition)).

The spatial place among nanothermoelectric materials is occupied by composites. This is because the introduction of many surfaces in the host material can significantly reduce the thermal conductivity, and the filtering of

carriers and quantum size effects (QSE) increase S, which leads to increase ZT. In particular, nanoparticles of ~ 10 nm greatly reduce the amount of thermal conductivity. It is crucial that the shortwave phonons in nanocomposites are dispersed by point defects, while medium and long-wave – on the nanoparticles. It was revealed a marked dispersion (scattering coefficient ~ 3) which is the characteristic of PbTe with metal particles ErAs (increase of ZT by 2 times) χ = (5-6) W $m^{-1}K^0$.

It was defined the strategy for further development of new nanocomposite materials among which are the following: modulation of doping compared with uniform doping, coherent nano-inclusion compared to incoherent; ordered limits compared with random; modified grain compared with unmodified grains, spherical cavities in comparison with column. The idea of ordered nanocomposites is a new concept with a variety of well-organized nanostructures to repair electronic transport channel, unlike the most conventional nanocomposites with individual nanostructures.

In connection with said above the thermoelectricity is facing to following problems: the creation of new materials with low thermal conductivity and high thermoelectric figure of merit ZT; development of theory and technology of spatially inhomogeneous materials: composites and quantum-dimensional structures based on superlattices, quantum wells, quantum wires, quantum dots, promoting of thermoelectricity as a promising form of alternative energy.

1. Freik D.M. Nanostructured thermoelectric materials: challenges, technologies, properties // *Physics and Chemistry of Solids* **14**(2) P.280-299 (2013).
2. [2]. Dresselhaus M.S., Chen G., Tang M.I.,Yang R., Lee H., Wang D., Ren Z., Fleurial J-P., Gagna P. New Directions tar Low-Dimensional Thermoelectric Materials // *Adv. Mater* **19** pp. 1043-1053 (2007).

The work supported by an integrated project of MES of Ukraine (N 0113U000185) and by projects of FRSF State Agency for Innovation and Informatization of Ukraine. (Contracts: R54, F53, 3), NAS of Ukraine (N 0110U006281)

Influence of Technological Factors of Growing on the Defects Formation Process and Properties of Lead Chalcogenides Thin Films

Galushchak M.O.

Ivano-Frankivsk National Technical University of Oil and Gas, Ivano-Frankivsk, Ukraine

Was investigate films grown from the vapor phase by 'hot wall' method. Pre-synthesized compounds used as main sample with the initial carrier concentration ~ $2\cdot10^{17}$cm^{-3}. The pure chalcogen powder served as additional source. Substrate chips were fresh single crystals (111) BaF_2 and (100) NaCl. The temperature of the main sources (temperature evaporation) was T_e = 820 K, the temperature of the chamber walls was T_w = 850 K. The temperature substrates T_S varied in the range from 400 K to 720 K. Partial pressure changed of chalcogen vapor in the zone of deposition of films by temperatures of additional evaporator. The growth rate of films was ~ $3\cdot10^{-9}$ m$\cdot$s^{-1}, and their thickness - $(0{,}05\text{-}10)\cdot10^{-6}$m.

The results of the experiments revealed that films deposited in the form of mosaic crystals with average linear dimensions $(2 – 5)\cdot10^{-6}$ m, oriented plane (111) parallel to the substrate surface for BaF_2 and (100) to NaCl. The type of the films conductivity and carrier concentration was determined by technological factors of growth. Thus, for PbTe films at low vapor pressure of tellurium P_{Te} = ($10^{-7} – 10^{-2}$) Pa formed n-type of condensate. Further increase in the vapor pressure of the chalcogen in the deposition area leads to decrease in the electron concentration and conductivity type inversion followed by increasing concentration of holes.

Quasi-chemical model proposed for an explanation of the defect subsystem that takes into account the possibility of different charge states of intrinsic point defects formation in the cation sublattice of films PbX (X = S, Se, Te) of interstitial atoms and vacancies of lead ($Pb_i^+, Pb_i^{2+}, Pb_i^0, V_{Pb}^-, V_{Pb}^{2-}, V_{Pb}^0$).

In particular, for PbTe films with increasing nominal pressure, defined and controlled independent of the sample at a fixed temperature PbTe source of pure tellurium, increasing the concentration of singly charged lead vacancies and decreases the concentration of singly charged interstitial atoms of lead. Doubly charged defects are highly compensated. The concentration is ~ $(1 – 6)\cdot10^{20}$ cm^{-3} according to the calculations, which is one or two orders of magnitude higher than the concentration of singly charged defects, which in turn is dominated by the concentration of neutral defects. Vital role in changing the concentration of charge carriers has single-charged defects, due to the strong, but not full compensation of doubly charged defects.

High concentration of singly charged and doubly charged vacancies interstitial atoms lead observed for PbSe films to several orders of magnitude higher than the concentration of defects other charge states ($Pb_i^0, Pb_i^+, V_{Pb}^0, V_{Pb}^{2-}$).

The concentration of neutral atoms interstitial of lead (Pb_i^0) is lowest, and the concentration of neutral vacancies (V_{Pb}^0) is comparable with the concentration of doubly charged vacancies (V_{Pb}^{2-}).

The doubly charged vacancies and interstitial atoms of lead are the predominant defects in the cation sublattice PbS films, that is similar to the case of PbTe. Point inversion of conductivity for PbS biased towards higher values of vapor pressure and sulfur deposition temperatures compared to PbSe and PbTe, due to the values of enthalpies of defects formation.

The experimental data and theoretical calculations of the concentration of charge carriers correspond to model of disordered cationic sublattice of the lead chalcogenides on the mechanism by Frenkel.

Kinetics of InSe Single Crystals Intercalated by Nickel

Grygorchak I.[1], Tovstyuk N.[1,2], Fomenko V.[2], Seredyuk B.[3]

[1]*National University "Lvivska Politechnika", Lviv, Ukraine*
[2]*Ivan Franko Lviv National University, Lviv, Ukraine*
[3]*Academy of Land Forces named after Hetman Petro Sahaydachniy, Lviv, Ukraine.*

In this paper we study kinetic properties of the semiconductors of complicated molecular structure (Se-In-In-Se monoatomic layers in sandwiches) intercalated by nickel. Such structures are very important in spintronics because one can manage their magnetic properties in electric or optic way.

Frequency dependence of real component of complex impedance of intercalate Ni_xInSe (x<2 at.%) $\rho(\omega)$ showed that for all value of Ni concentration x beside x=1,25at.% $\rho(x)$ is inverse function to the change of lattice parameter c. Taking into account significant decrease of lattice parameter, such effect can be explained by the formation of quasimolecules by forming bonds between Se-In-In-Se sandwiches via inserted nickel ions. To itemize the mechanism of current transit in the synthesized intercalates Nyquist diagrams of the dependence of implicit component of complex impedance on its real component were built. It was found that Nyquist diagram had the expected character for the pure InSe layer crystal. It had one-head arc that reflected capacitive response of localized states and frequency dependent impedance, demonstrating that hopping mechanism of charge carriers over localized states or their exciting in the tails of density of states or delocalized bands mainly contribute to general conductivity. After intercalation frequency dependent impedance was transformed into either one-head arc but with the synthetic structure or a pronounced two-or three head arc structure depending on state of distribution and ratio of relaxation times. It confirms the modification of energy shape of the initial InSe lattice by barriers formed by nickel. The most nonordinary factor is deformation of low frequency branch $\rho(\omega)$ at x=0,25 and x=0,75, at which $\rho(x)$ had absolute maxima. It can be shown by complex amplitude method that these two maxima can be caused by the inductive response of the crystal. The most interesting is that at strong deformation $\rho(\omega)$ for x=0,75 a low frequency branch of Nyquist diagram moved to the IV – inductive quandrant of the complex impedance plain. This phenomena of "negative" capacitance is widely known in the literature. However, its mechanism is not properly explained, and its nature is not known. According to the most general mechanism the appearance of inductive capacitance occurs even when charge is inserted into the layers of small or subsmall sizes, i.e. the several nanometers range.

Effect of Layer by Layer Growth Method in Magnetron Sputtering on Deposition Transparent Conductive Aluminum Doped ZnO Thin Films

Ievtushenko A.I.[1], Lashkarev G.V.[1], Lazorenko V.I.[1], Klochkov L.O.[1], Bykov O.I.[1], Tkach V.M.[2], Kutsay O.M.[2], Starik S.P.[2], Lytvyn O.S.[3], Dusheyko M.G.[4], Baturin V.A.[5], Karpenko A.Y.[5]

[1]*I. Frantsevich Institute for Problems of Materials Science, NASU, Kyiv, Ukraine*
[2]*Bakul Institute for Superhard Materials, Kyiv, Ukraine*
[3]*V. Lashkarev Institute of Semiconductor Physic, NASU, Kyiv, Ukraine*
[4]*National Technical University of Ukraine "KPI", Kyiv, Ukraine*
[5]*Institute of Applied Physics, Sumy, Ukraine*

Novel oxide materials are very interesting for substitution of existing traditional ones in various fields of electronics and optoelectronics. Especially the technological receptions and parameters of growth of transparent conductive films based on them attracting more attention of researchers.

The top difficulty of popular indium tin oxide (ITO) is a limited world reserve of indium. Diametric to ITO, zinc oxide has ecological and economical advantages because its components zinc and oxygen are widely apportioned in Earth. Consequently, ZnO films doped by aluminum (AZO), gallium (GZO) or indium (IZO) are the best suited candidates for replacement ITO ones. The creating of technology for growth of transparent conductive films based on aluminum doped ZnO films will have the commercial future.

Hence the high quality aluminum doped ZnO films were condensed on glass substrates by layer by layer deposition method [1, 2] at a magnetron sputtering of Zn:1.4%Al target. The content of aluminum in the doped ZnO films was about 2,4 atomic %. The report presents the results of oxygen pressure influence on structural, morphological, electrical and optical properties of aluminum doped ZnO films. The comparative studies of transparent conductive films deposited by traditional magnetron sputtering method and layer by layer growth method in magnetron sputtering will be represented.

It is determined that optimal oxygen pressure of 0.03 Pa in the deposition chamber leads to the following aluminum doped ZnO films characteristics: the resistivity is $6 \cdot 10^{-4}$ Ohm·cm, transparency - 95% and roughness - 6 nm. Our investigations of proposed magnetron technology and the prospects of its applications will be discussed.

1. A.I. Ievtushenko, V.A. Karpyna, V.I. Lazorenko, G.V. Lashkarev, et al. *Thin Solid Films*, **518**, 16, pp. 4529–4532 (2010).
2. A.I. Ievtushenko, G.V. Lashkarev, V.I. Lazorenko, V.A.Karpyna, et al. *Physica Statatus Solidi (a)*, **207**, 7, pp. 1746–1750 (2010).

Possibilities of Pulse Plating for Creation of Zinc Oxide Hierarchical Nanostructures

Klochko N.P.[1], Khrypunov G.S.[1], Myagchenko Y.O.[2], Melnychuk E.E.[2], Kopach V.R.[1], Klepikova K.S.[1], Lyubov V.M.[1], Kopach A.V.[1]

[1]National Technical University "Kharkiv Polytechnic Institute", Kharkiv, Ukraine
[2] Taras Shevchenko National University of Kyiv, Kyiv, Ukraine

Zinc oxide nanostructures are objects of study in the field of optoelectronics, solar power engineering, nanosensorics, and catalysis. A dye-sensitized solar cell (DSSC) with zinc oxide (ZnO) anode is a promising route toward solar energy conversion. The central idea is to simulate natural light harvesting procedures in photosynthesis by combining dye sensitizers with semiconductors. The DSSC in the near future should be advantageous in both low-cost and high-efficiency, relative to the more established photovoltaic technologies based on monocrystalline silicon and polycrystalline thin film semiconductors in the case of overcoming of some technological challenges. ZnO one dimensional (1D) nanostructures are highly relevant for efficient charge collection in DSSCs. However, even for dense arrays of very long wires, the global surface area developed by these structures is insufficient to permit a very high solar light collection by the sensitizer. Therefore, the growth of multiscale hierarchical structures is an interesting mean to increase significantly the quantity of dye immobilized in the photoanode and to insure a fast charge collection. The objective of this study is to determine the effect of the pulse electrolysis parameters on the morphology, structural parameters, and optical properties of ZnO layers to implement the controlled growth of nanocrystalline zinc oxide geometrically diverse structures in the pulsed electrodeposition mode. The systematic features of the growth of zinc oxide nanostructures during pulse plating on a cathode substrate were determined by analyzing the electrochemical processes in an aqueous nitrate electrolyte and by the results of a study using X-ray diffraction, optical spectrophotometry, and atomic-force microscopy. Studies of effects of the pulse electrodeposition regimes on structural and substructure parameters, morphology and optical properties of zinc oxide arrays made it possible to identify modes that are optimal for the formation nanorods of this material oriented perpendicular to the substrate surface: the bath temperature 70-85 °C, duty cycle (i. e. relation of the cathode potential pulse duration to the pulse period) 0.4, the pulse frequency 2 Hz. The nanorods sizes can be varied by heating or cooling the electrolyte in the above-mentioned range, making small nanorods electrodeposited on the surface of larger ones and thus forming hierarchical nanostructures. By changing the duty cycle, the surface morphology of arrays is modified up to the formation of zinc oxide mesoporous networks, which together with ZnO nanorods can form hierarchical nanostructures with large specific surface areas.

Magnetooptical and Magnetoresistive Properties of Thin Film Granular Solid Solution

Kondrakhova D. M., Cheshko I.V., Protsenko I.Yu., Shabel'nyk Yu.M.

Sumy State University, Sumy, Ukraine

Research magnetooptical properties by equatorial magnetooptical Kerr effect (MOKE) and magnetoresistive properties (MR) provide insight into the regularities stabilize different magnetic states in thin film systems based on materials with possible spin-depended electron scattering. In some film systems can be realized formation conditions of granular magnetic components. Greater propensity to it was shown by systems on base Co and Cu and in lesser degree on base Co and Au or Ag. Stage of granular state formation can also be traced to changing forms of MOKE hysteresis loops and MR curves. Granular alloys do not have continuous stratified magnetic formations with domain structure which have rectangular MOKE loops form unlike monolayers ferromagnetic film and multi-layered with non-diffuse interfaces. After heat treatment as a result of diffusive processes appear the areas of the heterogeneous magnetic states, which results in blurring of form MOKE curves. It can be traced for the film systems on base Co and Au, Co and Ag or Fe and Cu. For the systems on base Fe and Cr or Co and Cu the MOKE loops and MR curves general form substantially does not change after heat treatment. In these systems processes of formation of solid solution (s.s.) take place already during condensation stage. In the systems on base Co and Ag after heat treatment to T=900 K is stabilized magnetic Co granules in the non-magnetic matrix of the s.s. (Ag, Co) [1]. Magnetic granules in these s.s. especially when a large difference in size have wide range of the magnetic field remagnetization. It is shown that for film granular alloys on base Ag and Co characteristic MR=(0,40-0,50)% at the c_{Co}=38 at.%. At the increase of Co atoms concentration at first the size of MR grows almost in three times and MR =(1,5-1,8)% at the c_{Co}=60 at.%, and then decrease to MR= (0,4-0,5)% at the c_{Co}=70 at.%. And we can see insignificant growing MR at T= 800 K and his diminishing is at T= 900 K. In other system to feel like granulation magnetic components on base Co and Cu it is possible to look after passing to «wide» MOKE loop after heat treatment and, as a result, partial disintegration of s.s. (Cu, Co) with Co granules formation.

This work was performed by the project №0112U001381 (2012-2014 years).

1. Pazukha I.M., Protsenko I.Yu., Shabel’nyk Yu.M. Magnetoresistive properties of granular film alloys based on Ag and Co // Physics and Chemistry of Solid State. - 2012. - V.13, №4. – P. 907 - 915.

Radiation spectrum of sequence of electrons moving in spiral in transparent medium

Konstantinovich A. V.[1], Konstantinovich I. A.[1,2]

[1]*Chernivtsi National University, Chernivtsi, Ukraine*
[2]*Institute of Thermoelectrics, National Academy of Sciences and Ministry of Education and Science of Ukraine, Chernivtsi, Ukraine*

The time-averaged radiation power $\overline{P}^{rad}$ of sequence of electrons moving one by one along a spiral in transparent medium can be calculated by the instrumentality of spectral distribution $W(\omega)$ [1]

$$\overline{P}^{rad} = \int_0^\infty W(\omega) d\omega,$$

$$W(\omega) = \frac{2e^2}{\pi c^2} \int_0^\infty dx \mu(\omega) S_N(\omega)\, \omega \frac{\sin\left\{\frac{n(\omega)}{c}\omega\eta(x)\right\}}{\eta(x)} \cos\omega x \left[V_\perp^2 \cos(\omega_0 x) + V_\parallel^2 - \frac{c^2}{n^2(\omega)}\right],$$

where $\eta(x) = \sqrt{V_\parallel^2 x^2 + 4\frac{V_\perp^2}{\omega_0^2}\sin^2\left(\frac{\omega_0}{2}x\right)}$, ω is the cyclic frequency, $r_0 = V_\perp \omega_0^{-1}$, $\omega_0 = ec^2 B^{ext} \widetilde{E}^{-1}$, $\widetilde{E} = c\sqrt{p^2 + m_0^2 c^2}$, the magnetic induction vector $\vec{B}^{ext} \| 0Z$, $V_\perp$ and $V_\parallel$ are the components of the velocity, $\vec{p}$ and $\widetilde{E}$ are the momentum and energy of the electron, e and m_0 are its charge and rest mass, respectively, Δt_l is the time shift of the l^{th} electron, c is the velocity of light in vacuum.

In the case of sequence of electrons moving one by one along a spiral the coherence factor $S_N(\omega)$ takes the form:

$$S_N(\omega) = \sum_{l,j=1}^{N} \cos\left\{\omega\left(\Delta t_l - \Delta t_j\right)\right\}.$$

The fine structure of synchrotron and synchrotron-Cherenkov radiation spectrum of the one, two, three, and four electrons moving in the spiral in transparent medium near the Cherenkov threshold are investigated combining analytical and numerical methods.

For the case when the longitudinal component of velocity (parallel to the magnetic induction vector $\vec{B}^{ext}$) is bigger than the light phase velocity ($V_\parallel > c/n(\omega)$) in transparent medium the hopping at the lower boundary of harmonic $m = -1$ for one, two, three and four electrons moving one by one happens at the same frequency.

1. A.V. Konstantinovich, I.A. Konstantinovich. Influence of Normal and Anomalous Doppler Effects on Synchrotron-Cherenkov Radiation//Romanian J. of Physics. – 2012.– V. 57, Nos 9–10.– P.1356–1366.

Luminescent Properties of A_2B_6 Semiconductor Quantum Dots

D.V. Korbutyak, S.I. Budzulyak, S.M. Kalytchuk, Yu.V. Kryuchenko

V Lashkarev Institute of Semiconductor Physics, National Academy of Sciences of Ukraine, Kyiv, Ukraine

Quantum dots (QDs) manufactured from semiconductor materials have many unique properties including high mechanical strength, high quantum yield of radiation, controlled radiation range etc. For this reason they are increasingly being used in various fields of opto- and nanoelectronics. In particular they are used as fluorescent labels in medical diagnostics, in high resolution nightly vision devices, in solar cells, field transistors, etc. Among the large number of QD practical applications important places are occupied by light-emitting devices (light-emitting diodes, white light sources, low-threshold lasers) [1]. Due to very narrow emission range of monodisperse QDs (line width at radiation intensity half-maximum is 18-30 nm) the QD LEDs emit rich colors with much better spectral purity than that of liquid crystals or organic LEDs. Significant advantages of QD LEDs are also their high efficiency, low power consumption, long service term, high-speed performance, resistance to vibrations and impacts, controlled profile of light beam, possibility to obtain practically arbitrary color of radiation by selecting the material and QD size. Sources of white light can be obtained by additive mixing of red, green and blue colors emitted by QDs of the same material but having different sizes or by QDs made from different semiconductor compounds.

Widespread practical application of A_2B_6 QDs as light-emitting devices requires finding optimal ways of QD synthesis and surface passivation to reduce nonradiative losses, detailed study of the radiative recombination mechanisms, a theoretical analysis of the characteristics of size quantization in QDs, the influence of barrier matrix parameters on the spectrum and luminescence intensity and so on. The report presents the results of our works and works of other authors devoted to the synthesis technology of colloidal A_2B_6 QDs (CdTe, CdSe, CdS) and their transfer from colloidal solutions into the polymer matrix, as well as to the study of characteristics of the photoluminescence (PL) spectra as functions of QD size, parameters of matrix material, temperature and so on.

Recent scientific progress has resulted in the development of hybrid nanostructures composed of semiconductor QDs and metal nanoparticles (NPs). These hybrid structures promise to produce a new generation of nanoscale optoelectronic devices that combine the best attributes of each component material. In such nanostructures the excitations in semiconductor QDs are coupled with plasma oscillations in metal NPs by the near-field interaction. The resonant exciton-plasmon interparticle coupling leads to variety of new phenomena. In particular localization of QDs in the vicinity of metal NPs is known as one of the most efficient ways to increase their PL. However, up to

now rigorous theoretical studies have been made only for the case of point emitters (dipoles) placed near metal NPs. Considering the emitter as a point dipole is completely justified in the case of isolated atom or molecule luminophore. However, by studying radiation of semiconductor QD in a vicinity of metal NP the QD *a priori* can not be considered as a point dipole (especially at comparable QD and NP sizes). Therefore, all previous theoretical approaches in fact can not be directly applied to this system.

In the present work a model is proposed allowing considering radiation of semiconductor quantum dot (QD) in a vicinity of metal nanoparticle (NP) as radiation of an ensemble of unit cells, from which the QD consists. It is shown that each unit cell of QD can be considered as a separate radiating point dipole. Relations are obtained between the coefficients of multipole expansions of electromagnetic fields in two spherical coordinate systems centered in the semiconductor QD and the metal NP. The relations allow using separately spherical symmetry of the QD and the NP despite the "QD + NP" structure as a whole is not spherically symmetric. It is shown, that contribution of a particular QD unit cell into the total QD radiation is proportional to the value of the envelope exciton wave function in corresponding QD node. Summing contributions from all QD unit cells makes possible to find characteristic radiative and nonradiative times in "QD + NP" structure and evaluate their decrease relatively to that of isolated QD due to resonant excitation of dipole and higher order multipole plasma oscillations in metal NP. In the metal NP not only contribution of free carriers to NP dielectric function is taken into account (Drude term) but that of bound carriers too due to possible interband transitions in real metals in the actual frequency range. Besides, to cover the cases of extremely small metal NPs (less then 10 nm in size) a spatial dispersion in NP dielectric function is also accounted. All electromagnetic fields in the nonspherical "semiconductor QD + metal NP" structure are calculated consistently in the single scattering approximation for the case of radiation of a point dipole located inside QD. It enables finding the power and the rate of radiation as well as the intensity of electromagnetic energy absorption and the rate of nonradiative losses in the system under consideration. Hence the efficiency of radiation depending on the distance D between QD and NP, NP and QD radii and other parameters as well as its change relatively to the case of isolated QD could be calculated. Multiple scatterings of electromagnetic field in the structure could be accounted too using the obtained relations between the coefficients of the electromagnetic field multipole expansions in two different spherical coordinate systems with the centers in QD and NP.

1. Корбутяк Д.В., Коваленко О.В., Будзуляк С.І., Калитчук С.М., Купчак І.М. Світловипромінюючі властивості квантових точок напівпровідникових сполук A_2B_6 // Український фізичний журнал. Огляди. – 2012.- **Т.7,** № 1. – С. 48-95.

Establishment of the Ukrainian Academy of Sciences

Kozyrski W.H.[1], Shenderovskyj V.A.[2]

[1] *The Bogolubov Institute for Theoretical Physics, Kiev, Ukraine*
[2] *Istitute of Physics, Kiev, Ukraine*

Here we expose the short sketch of some crucial points in the history of establishment of the Ukrainian Academy of Sciences.

The idea to have representative national scientific institution was grown in the mind of Ukrainian intelectuals during the second half of XIX century.

However, Ukrainians at that time had not own state. Therefore, the idea remained to be the idea itself. However, patriotic intelectuals gone step by step to this goal. And Shevchenko Scientific Society at Lviv and Ukrainian Scientific Society at Kiev were the first corner stones for the idea realization.

In March 1917 in Kiev the Commission to create Academy of Sciences was completed from Ukrainian Scientific Society Fellows. On March 29 at the General USS meeting M. Hrushevsky suggested to establish Ukrainian Academy of Sciences. Known Ukrainian historian and publicman M. Vasilenko support this idea and made very much torealize it. From the beginning of his work as the minister of education and art in a hetman government he actively realizes this idea. In his turn, M. Hrushevsky had the opinion that the Academy of Sciences must be Scientific Society of Shevchenko Scientific Society type.

At the beginning of May 1918 M. Vasylenko invites to Kiev V.Vernadsky to participate in Ukrainian Academy of Sciences establishing. He, as well as V. Vernadsky, consider Academy of Sciences as public institution carrying out research not only in the area of social sciences but also natural and technical. He considered that the formation of Ukrainian Academy of Sciences “has a large national value”. As a Fellow of the USS, he knew that majority of society divided conception of M. Hrushevsky.

The first meeting of Commission took place on July, 9 in M.Vasilenko office at the Folk Education Ministry. There were V. Vernadsky, D. Bahalij, M. Kaschenko, J. Kosonogov, H. Pavlucky, O. Speransky, E.Tymchenko, P. Tutkovsky, V. Modzalevsky. M.Vasilenko considered the major condition to restore neglected economy “that scientific creativity rises and the state organizes scientific research activity in scientific way. Never this task stood in front of the State authorities in such amounts and such urgency as it is now”.

Although on October 19 M. Vasylenko resigned from the post of Minister, his successor in Fedor Lyzohub Government Peter Stebnyckyj (24.10 –14.11 1918) in 3 weeks had taken all the prepairing and coordinating actions and led the establishment of the Ukrainian Academy of Sciences in Kiev to a successful completion. At November 14, 1918 Hetman P. Skoropadsky signed the Llaw on the establishment of the Academy of Sciences in Kiev approved by the Council of Ministers, as well as the Statute and Staffs of the UAS and its institutions.

On November 14, 1918, also an order by Hetman was issued for the Ministry of education and art listing the first UAS full members (academicians): D. Bahalij, A. Krymsky, M. Petrov, S. Smal-Stocky (historical and philological sciences), V. Vernadsky, S. Tymoshenko, M. Kaschenko, P. Tutkovsky (physical and mathematical sciences), M. Tuhan-Baranovsky, F. Taranovsky, V. Kosynsky, O.Levicky (social sciences).

P. Skoropadsky have seen M. Hrushevsky as President considering him to be the most honourable figure: “Before to open the Ukrainian Academy of Sciences, we were thinking for a long time who was to be its Chairman. I had the opinion – and all agreed with me, that's high and honorable place belongs to Hrushevsky in Ukraine. So I asked to clear how would he offer to such an attitude. The response was strongly negative.”

The inaugural General Assembly at 27.11.1918 have elected Vernadsky as the Head - the President of the Ukrainian Academy of Sciences A.Krymsky as Permanent Secretary. Hetman Government allocated funds for the first scientific research chairs, institutes, and so on.

1921, to emphasize the all-Ukrainian nature of Academy, it was named the All-Ukrainian Academy of Sciences (A-UAS).

After Volodymyr Vernadsky, Professor Mykola Vasylenko (July 1921-February 1922), historian Orest Levytsky (March-May 1922), botanist Vladimir Lipsky (1922-1928), microbiologist and epidemiologist Danylo Zabolotny (1928-1929) were Presidents of the Academy.

Almost to the end of the 1920s the A-UAS retains some autonomy. However, in 1928 due to the changes in the procedure of elections and strengthening of repressions the authorities totally took control of the activities of the Academy of Sciences.

At 1929 the elections passed at extended meeting of the new structure – the Council of the Academy of Sciences consisted of representatives of the Commissariat of education. The number of vacancies was significantly extended (to 34) to push through along with scientists to be elected the bolshevik’s nominations. Vote on nominations was opened.

The elections of the Academy Presidium confirmed the powers of the President D. Zabolotny elected in May 1928.

1928 A. Krymsky was discharged from his duties of Permanent Secretary of the All-Ukrainian Academy of Sciences.

In the summer of 1929, two members of the Academy S. Efremov and M. Slabcenko were arrested and 24 employees of the Academy of Sciences being accused to belong to the mythic counter-revolutionary organization "Union of of the liberation of Ukraine" and sentenced to long terms of imprisonment. 1930-31 "cleaning" of A-UAS continued.

Historical institutions created by M. Hrushevsky have experienced the complete defeat, Hrushevsky himself was arrested and forced to live in Moscow.

Formation of Gradient Materials ZnS by Self-Propagating High-Temperature (SHS) Synthesis

Kozytskyi S.V.

National Maritime Academy, Odesa, Ukraine

It is known that SHS method is successfully applied in aim to obtain a poly-crystalline ***ZnS***. In this report we show that during the crystallization of the systems, those looks as cylinders of 70 mm in diameter and 20-30 mm in a height, the gradient material may be obtained due to high speed of the process.

Really, during the formation of ***ZnS*** the initial solution of $Zn_{1-x}S_x$ is consequently saturated by sulfur (***x*** increases up to 0,5). In this situation the density of the solution decreases until it formed a stoichiometric ***ZnS***. The probability of this is the highest in the center of cylinder. The short period of crystallization (about 100 s) leads to formation of gradients of concentration and temperature, when at the top and bottom parts of the cylinder there are the excess of zinc and lower temperature.

In case when in the upper part of the sample the elementary volume of $Zn_{1-x}S_x$ solution will move up due to fluctuation, its temperature will fall down because the rate of thermal diffusion is significantly greater than the rate of diffusion of concentration. In this situation its chemical state will not change. Due to buoyant force it will continue motion to the top of the sample. In case when this elementary volume will move down (due to fluctuation), its temperature will quickly arise and it will continue its motion to the center of the sample. So, the gradients of temperature and concentration lead to non-stable plane boarder, and in the upper part of cylinder the process of equalization of sulfur concentration in $Zn_{1-x}S_x$ solution will take place.

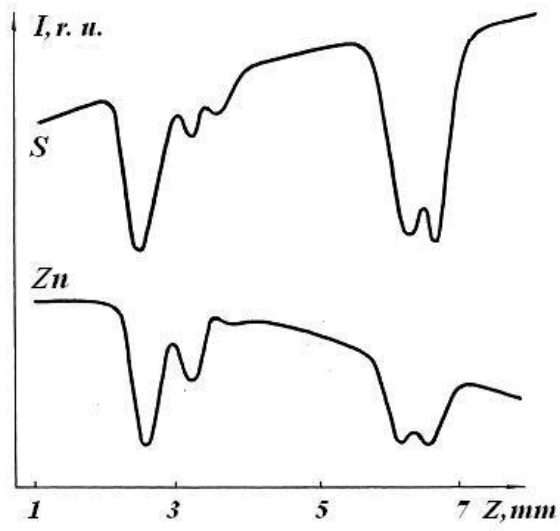

Another situation occurs in the bottom part of the sample. In case when the elementary volume of $Zn_{1-x}S_x$ solution will move up (or down) due to fluctuation, its temperature quickly reaches the ambient temperature of the solution, with no changes in concentration. So due to buoyant and gravity forces returns to the same position and the chemical reaction continued. The distributions of elements in the sample were determined with X-ray microanalysis "Kamebaks" (fig.1).

Thus, the formation of non-stoichiometric material with different concen-tration of sulfur in SHS process is determined by essentially non-equilibrium state of the system, because only in such systems this may take place.

Change of Magnetic Characteristics of Magnetic Nanofilms and Control Spin Current under Laser Radiation

Krupa M.M., Sharai I.V.

Institute of Magnetism NASU, Kyiv, Ukraine

For the high-frequency components of spintronics requires high-speed control system magnetized materials in the local microregions. Solve this problem using conventional magnetic systems is extremely difficult. Promising is the use of short laser pulses to control the spin current in multilayer magnetic films. The laser light can excite the current along the laser beam and obtain a strong magnetic field due to the inverse Faraday effect.

For the high-frequency components of spintronics requires high-speed control system magnetized materials in the local microregions. Solve this problem using conventional magnetic systems is extremely difficult. Promising is the use of short laser pulses to control the spin current in multilayer magnetic films. The laser light can excite the current along the laser beam and obtain a strong magnetic field due to the inverse Faraday effect.

This article describes some of the features of the foton drag effect of the electrons, the mechanisms of magnetization reversal in magnetic nanofilms under laser irradiation and the results of studies of the effect of nanosecond and picosecond laser pulses on the magnetic properties of NiFe films, and the conductivity of tunnel junctions and the mechanisms of magnetization reversal of magnetic nanofilms under laser irradiation, and the results of studies of the effect of nano-and picosecond laser pulses on the magnetic properties of NiFe films, and the conductivity of tunnel junctions $Tb_{19}Co_5Fe_{76}/Pr_6O_{11}/Tb_{22}Co_5Fe_{73}$ and $Co_{80}Fe_{20}/Pr_6O_{11}/Co_{30}Fe_{70}$. It is shown that by using ultra-short laser pulses can change the structure and magnetic properties of thin films, and to study the dynamics of the magnetization reversal and spin current control in high-speed devices of spintronics.

Hysteretic Phenomena in Graphene's Conductivity

Kurchak A.I.[1], Morozovska A.N.[2], Strikha M.V.[1]

[1]V.Lashkariov Institute of Semiconductor Physics, NAS,Kyiv, Ukraine;
[2]Institute of Physics, NAS, Kyiv, Ukraine,

Despite a remarkable symmetry of the graphene's band structure, a hysteretic behavior of the graphene's resistivity with gate voltage V_g onward and backward sweeps is often observed in ambient conditions. The mechanism of this hysteresis can be different, depending on the charge transfer between graphene and its environment. Two types of hysteresis directions are observed experimentally [1]: a direct one and an inverse one (the last is also defined as an 'antihysteresis' for the systems on ferroelectric substrate). This hysteresis in the graphene-on-ferroelectric systems had already enabled the construction of the robust elements of non-volatile memory of new generation [2, 3]. These elements work for more than 10^5 switches and preserve information for more than 1000 s. Such systems can be characterized theoretically by the ultrafast rate of switching (~ 10-100 fs) (for details see rev. [4]).

The direct and opposite hysteresis can be attributed to two rival mechanisms: capacitive coupling and charge carriers trapping from graphene, respectively. A quantitative model for these competing hysteretic mechanisms in graphene channel resistivity on a substrate of different nature – a direct one (caused by adsorbates with dipole moment on surface, e.g. water, as it is presented in fig.1a and an inverse one (caused by capture of free carriers onto localized states on graphene-substrate interface) was proposed in [5, 6].

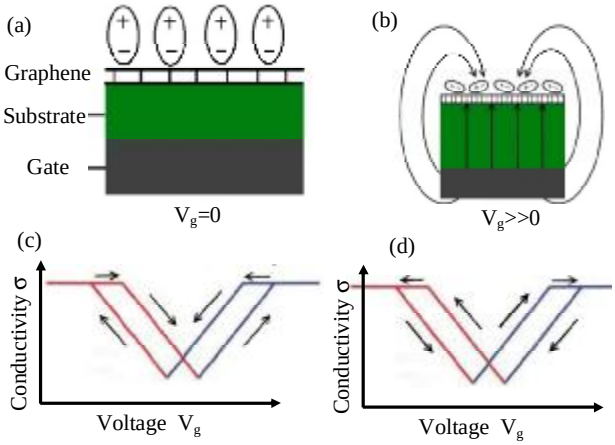

Fig.1. (a) Graphene with adsorbed dipoles at the surface. (b) Dipoles reorientation under high gate voltages. Direct (c) and inverse (d) conductivity hysteresis $\sigma(V_g)$.

This model leads in the first case to non-zero concentration of holes in graphene, at zero V_g, equal to

$$n_{p0} = P_0 / e \qquad (1)$$

where P_0 is the absorbed molecules layer polarization, i.e. the electro-neutrality point on V_g scale is shifted to positive voltages. Therefore the linear

dependence $n(V_g)$ is shifted initially to smaller values of electron concentrations (and greater values of holes concentrations). Further increase of V_g ruins finally the polarization, as it is presented in fig.1b, and for the backward sweep of V_g the dependence $n(V_g)$ is governed by the fleet capacitor correlation, with electro-neutrality point at zero V_g. Therefore the hysteresis in the dependence of conductivity $\sigma(V_g)$ occurs (fig.1c). However, it V_g sweeps rate is slow enough, the spontaneous polarization on graphene's surface restores with time as:

$$P(t) = P_0(1 - \exp(-t/t)) \quad (2)$$

If the time, when V_g reaches electro-neutrality, is of τ constant order or greater, the two electro-neutrality points in fig.1c trends to one and the hysteresis vanishes.

The second channel was examined in [5]. If there are localized interface states with E_T energy and n_T concentration, electrons from graphene are captured onto them when Fermi energy reaches E_T on V_g onward sweep, and $n(V_g)$ shifts in n_T value lower. The characteristic lifetime of electrons on interface states τ_c is rather long [5], therefore this shift remains in $n(V_g)$ dependence on V_g backward sweep as well, and this causes the inverse hysteretic loop, presented in fig.1d.

Mention, that due to hierarchy of times $\tau_c >> \tau$ the realistic sweep rate variation vanishes the direct hysteresis primarily. This was observed experimentally in [1], and τ = 3,4 s can be obtained from it's data [6]. This time is many orders of value longer than the relaxation time of free dipoles due to strong chemical bonds of adsorbates to graphene's surface. Another experimental result of [1] that can be explained within our model is that hysteresis could be swept with the decrease of V_g sweep rate from direct to inverse one for low temperatures, but for room temperatures it was inverse one only. Although chemical nature of adsorbate (water) was the same, τ for ice is many orders greater, than for liquid, therefore no direct hysteresis could be observed for room temperature due to rapid polarization renewal. Thus, possible discrimination of these two channels by variation of the gate voltage sweep rate was proposed: the slow sweep suppresses the direct channel and does not influence greatly for the realistic sweep rate the opposite one. The theory's predictions are in a qualitative agreement with experimental data and can be useful for understanding of the graphene's structures operation in ambient conditions.

This work was supported by Fundamental Research Fund of Ukraine, NAS of Ukraine and STCU.

1. H.Wang, Y.Wu, C.Cong, et all. ACS Nano **4(12),** 7221 (2010).
2. Yi Zheng, G.-X. Ni, 3.-T. Toh et al, Appl. Phys. Lett. **94**, 163505 (2009).
3. X. Hong, J. Hoffman, A. Posadas, et all. Appl. Phys. Lett. **97**, 033114 (2010).
4. M.Strikha. Ukr. J. Phys. Reviews. **7**, 31 (2012).
5. M.Strikha. JETP Lett., **95,** 198 (2012).
6. A.I.Kurchak, A.N.Morozovska, M.V.Strikha. Ukr. J. Phys. *In press.*

Virtual Reality and Practical Aspects of Diamond Polycrystalline Films Spectral Mapping

Kutsay O.M., Garaschenko V.V., Starik S.P., Gorohov V.Yu., Belyaeva T.M., Lutsenko O.V., Tkach V.M., Gontar A.G., Novikov N.V.

V. Bakul Institute for Superhard Materials of the National Academy of Science of Ukraine, Kyiv, Ukraine

The “virtual reality” terminology is often used to describe a wide variety of data commonly associated with highly visual and 3D environments. The topography results of the spatial distribution of the vibration band intensities by the FTIR microspectroscopy data have been presented as 3D or 2D images for different types of the diamond polycrystalline films grown by chemical vapor deposition (CVD). The practical issues of using such techniques for the spatial analysis of the structural perfection and the impurity composition of the investigated diamond materials have been considered.

By the own experience in the CVD coating technology [1-5] the nowadays and possible future of practical applications of diamond polycrystalline films will be critically analyzed.

1. Novikov N.V., Gontar A.G., Khandozhko S.I., et al. // Diamond Rel. Mater. **9** (2000) 792.
2. Romanko L.A., Gontar A.G., Kutsay A.M., et al. // Diamond Rel. Mater. **9** (2000) 801.
3. Kutsay O.M., Gontar A.G., Novikov N.V., et al. // Diamond Rel. Mater. **10** (2001) 1846.
4. Kutsay O., Loginova O., Gontar A., et al. // Diamond Rel. Mater. **17** (2008) 1689.
5. Fodchuk I.M., Tkach V.M., Ralchenko V.G. et al. // Diamond Rel. Mater. **19** (2010) 409.

State of Art and Prospectives for Researches and Applications of ZnO in Electronics

Lashkarev G.V., Ievtushenko A.I., Karpyna V.A., Myronyuk D.V., Shtepliuk I.I., Khranovskyy V.D., Lazorenko V.I., Poznyak I.I., Petrosyan L.I.

I.N. Frantsevich Institute for Problems of Materials Science, NASU, Kyiv, Ukraine

Nowadays ZnO is the mostly investigating wide-gap semiconductor. This is demonstrated by numerical publications (7015 in 2012 year) and by a lot of conferences and symposiums devoted to it. In this report the main applications of ZnO in electronics are considered and the ways for further scientific researches are discussed.

One of prospective areas of possible applications of ZnO and its alloys with MgO is a development on its basis photodetectors for ultraviolet radiation. However ZnO has such problems as bad speed of response and small photosensitivity in different types of detectors on its basis. The application of layer by layer technology of magnetron sputtering allowed to deposit textured ZnO films of high perfection. Nitrogen doping of ZnO leads to an increase of the photosensitivity and speed of response. The phototransistors on the basis of nitrogen doped ZnO films display a significant photosensitivity ~210 A/W at λ = 390 nm with time constant of ~ 100 ns that is one of the best results in the world.

Many researchers pay attention to investigation of ZnO nanostructures as well as ZnO films covered by metal nanoparticles. The inclusion of nanoparticles into ZnO may offer unique properties or enhance their electrical and optical properties. It is possible to realize electronic states with higher oscillator strength due to the quantum phenomena effect or create surface plasmon waves leading to significant enhancing of photoluminescence. For example, optical sensors based on surface plasmon resonance can be created on composite structures such as ZnO-Ag nanoparticles.

An important step in a design of ZnO based devices is optoelectronic band gap engineering for creation quantum wells. Cd substitution of Zn in ZnO serves the purpose of band gap narrowing, keeping the crystalline structure and lattice period close to ZnO. Quantum wells are the key elements in ZnO based light emitters and detectors. The electrical and optical properties of n-ZnCdO/p-SiC heterostructures are reported.

For space applications and nuclear researches semiconductor devices have to operate in harsh radiation conditions involving high energy particles. An important point for such applications is the high radiation resistivity of the semiconducting materials. The impact of radiation on properties of ZnO and other semiconductors (Si, GaAs, GaN, SiC) are considered and compared.

Measuring of Radiation in the Far Infrared Spectrum Region by Indirect Method

Lepikh Ya.I., Ivanchenko I.A., Budiyanskaya L.M.

I.I.Mechnikov National University, Odessa, Ukraine

Abstract: The investigation of indirect method of irradiation in far (~10 microns) IR-area of spectrum measuremet with the use of uncooled photodetector based on anisotype heterojunction, distinguished by layers conductivity various multiplicity at radiation absorption results are represented.

There are methods known for radiation registration in the far (~ 10 microns) infrared spectrum region, based on own photoconductivity direct measurements in narrow-gap semiconductor [1]. However, most of them can work efficiently at much lower temperatures, what has a number of known deficiencies. Therefore, the problem uncooled photodetectors creating in this spectrum region is relevant.

One solution of this problem is transition to indirect information signal measurement. This feature is associated with using anise-type heterojunction as a photodetector formed by semiconductors with significant differences in the crystal structure and the energy that was studied in this paper.

If heterojunction is made by the scheme of optical window-absorber [2], the long-wave infrared radiation passes through the top layer of wide semiconductor and is absorbed in the lower layer of the narrow-gap semiconductor. As a result, in the volume of narrow-gap semiconductor generates electron-hole pairs which n-p-type heterojunction are separated by the junction field for minority carriers - holes in wideband -and electrons in narrow-band semiconductors. Both heterojunction layers specific conductivity increases by the value of photoconductivity.

The absorption of radiation in the semiconductor accompanied by an increase of its conductivity σ_o on the value of photoconductivity $\Delta\sigma$. Conductivity multiplicity during irradiation is determined by the values of both equilibrium and non-equilibrium parameters of semiconductors. [3]

$$\frac{\Delta s}{s_o} = \frac{\Delta p + b\Delta n}{p_o + bn_o}, \qquad (1)$$

where n_o and p_o - free carrier equilibrium concentration in the absence of irradiation,

Δn and Δp - free carrier concentration increase as a result of irradiation

$b = \frac{m_n}{m_p}$, $\mu_п$ and μ_p - electrons and holes mobility, respectively.

From equation (1) follows that with an equal growth of non-equilibrium carriers what is typical for own absorption, semiconductors with high concentrations of the major carriers (low resistance) have less multiplicity of

conductivity changing than semiconductors with low major carriers concentrations (high resistance).

Thus, if the n-layer heterojunction is high resistant while the p-layer one is low resistant, which is logical in terms of band gap, the change in conductivity in the upper layer is more significant than in the lower one, i.e., the modulation of its conductivity occurs. Accordingly, the magnitude of photoconductivity photocurrent, which flows through the heterojunction and its layers, is divided. This relationship is the basis of the indirect method long-wave infrared radiation measuring.

Experimental confirmation of heterojunction and its layers photoactivity is spectral characteristics of n (CdSe)-p (Pb_{1-x} Sn_xSe) heterostructure (fig. 1) at room temperature.

Maximum in 10 microns range corresponds intrinsic absorption in the lower layer, as a result generated electrons are passed into the upper layer and make photocurrent I.

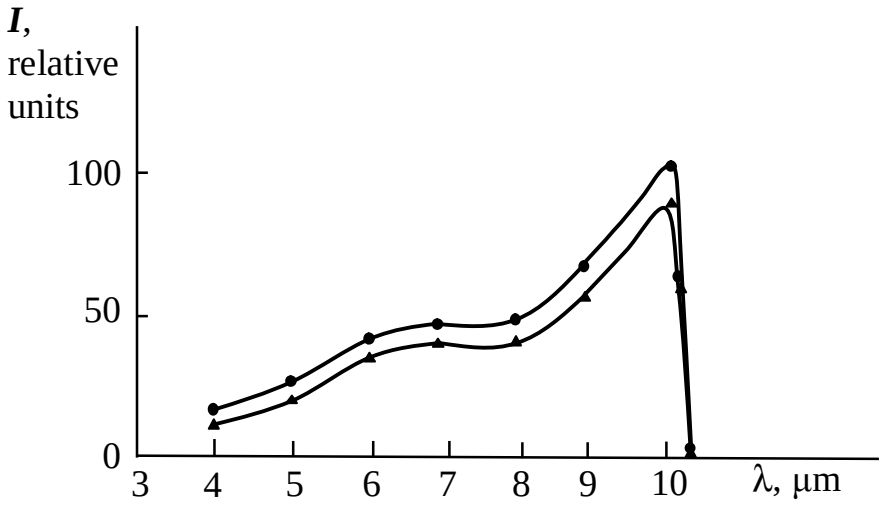

Fig. 1 Spectral characteristics of n (CdSe)-p (Pb_{1-x} Sn_xSe) heterostructure • – across the structure, ▲ – along CdSe upper layer.

I occurrence in the upper layer of a heterojunction explain its equivalent circuit, which is photodetector as a dynamo with a connected parallel to the diode [2], series resistor that takes into account the presence of distributed resistance layer heterojunction and contact transitions, and parallel-connected resistor equal to the resistance of the internal circuits of non-load circuit.

1. Sizov F.F. Photoelectronics for vision systems in "invisible" spectrum range. – Kyiv: Akademperyodyka, 2008. - 460 p.
2. Serdyuk V. Physics of solar elements. - Odessa: Logos, 1994. - 333 p.
3. Physical basis of the semiconductor infrared photo electronics. Current trends, new materials / A.V. Lubchenco, E. Salkov, F.F. Sizov. - Kiev: Naukova Dumka, 1984, 256 p.

Electric Field Confinement Effect on Charge Transport in Polycrystalline Organic Thin Film Transistors

Li X.[1], Kadashchuk A.[2,3], Fishchuk I. I.[3], Gelinck G.[1], Genoe J.[2], Heremans P.[2], and Bässler H.[4]

[1]*Holst Centre/TNO, High Tech Campus 31, Eindhoven, The Netherlands*
[2]*IMEC v.z.w., Kapeldreef 75, Leuven, Belgium*
[3]*Institute of Physics, NAS of Ukraine, Kyiv, Ukraine*
[4]*Experimental Physics II, University of Bayreuth, Bayreuth, Germany*

It is known that that the charge-carrier mobility in organic semiconductors is only weakly dependent on the lateral (source-drain) electric field at low fields. However, in our study, the experimental charge-carrier mobility in organic field-effect transistors using 6,13-bis(triisopropyl-silylethynyl) pentacene (TIPS-PEN) is found to be surprisingly field-dependent at low source-drain fields [1]. Corroborated by scanning Kelvin probe measurements, we explain this experimental observation by the severe difference between local conductivities within grains and at grain boundaries. The lower charge-carrier mobility in the disordered grain boundaries causes the major part of the source-drain voltage to drop over the boundaries, ***i.e.*** the local electric field in these boundaries is high. By rigorously accounting for the field-dependence of the mobility at the grain boundaries and inside the grains separately, we have shown that the overall field-dependence is strong because it is dominated by the disordered grain boundaries where the lateral field is high. We further confirm this picture by verifying that the charge-carrier mobility in channels without grain boundaries, made from the same organic semiconductor, is not significantly field-dependent. Finally, we show that our model allows to quantitatively describe the source-drain field dependence of the mobility in polycrystalline organic transistors.

1. X. Li, A. Kadashchuk, I.I. Fishchuk, W.T.T. Smaal, G. Gelinck, D.J. Broer, J. Genoe, P. Heremans, H. Bässler, *Phys. Rev. Lett.* **108**, 066601 (2012).

Quantum Chemistry and Molecular Dynamics Methods for Calculations of the Structure and Properties of Nanosystems

Lobanov V.V.

Chuiko Institute of Surface Chemistry of National Academy of Sciences of Ukraine
17 General Naumov Str., Kyiv, 03164, Ukraine

The complex scientific fields, united by the prefix "nano" to the names of the classical disciplines dominates modern science. It aims to study on the physical and chemical properties of nanosystems and their temporal evolution. Usually, the nanosystem believed nanobodies (nanoparticles) and their environment. The medium is inhomogeneous, bodies included in a nanosystem are not identical. The goal of quantum chemistry and molecular dynamics simulation of nanosystems is to identify the state of nanobodies as connected with the properties of the atoms of the nanosystem, and to develop a theory of its change over time. The most complete and comprehensive analysis of the nanosystem status can be obtained only on the basis of the molecular-kinetic theory involving quantum mechanics as the principal method of calculation of the interaction energy between the atoms and molecules of nanosystem, specifically computing schemes of the quantum mechanics (see diagram). Theoretical methods are extremely fruitful in the study of nanosystems, the experimental details on them being extremely difficult, by obtained hardly reproduceable or there is some doubt as to what is actually measured.

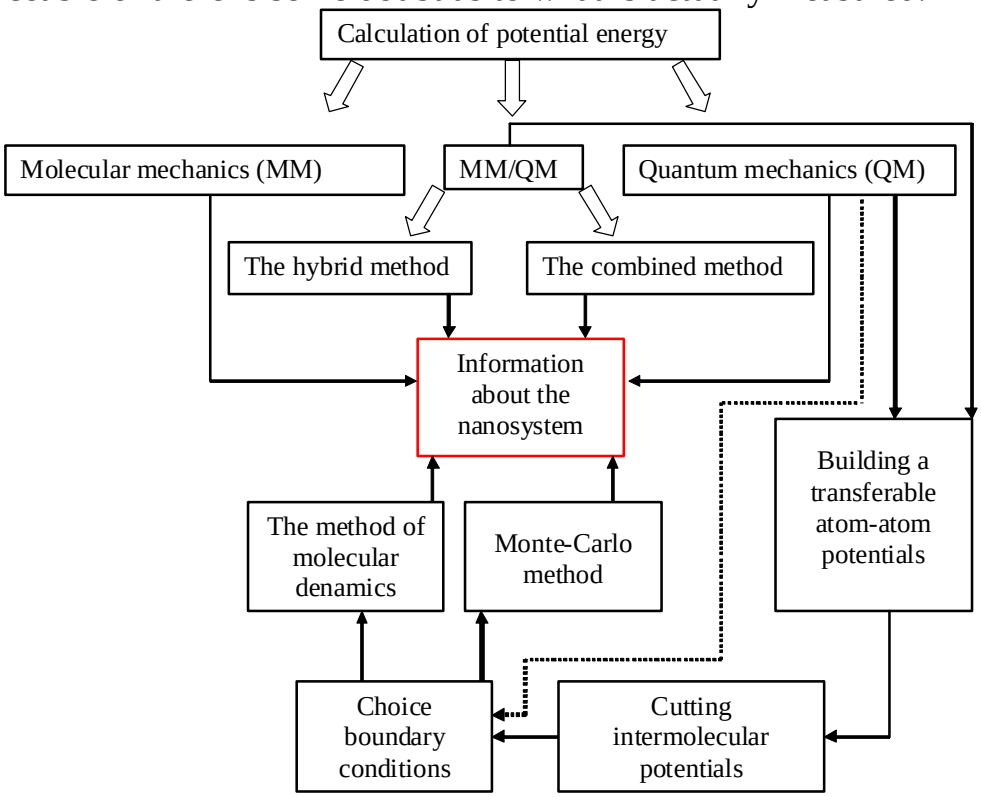

Interesting for experimenters information about the properties, structure, and, importantly, the evolution of nanoparticles and nanosystems, can only be obtained within a reasonable symbiosis of quantum-chemical and statistical methods. All this stimulated the rapid development of calculation methods: the the method of molecular dynamics (MMD) and Monte Carlo (MMC). In these techniques, environmental conditions can be varied such as pressure, volume, temperature, one may produce different types of interaction between the components of nanosystems and study on the macroscopic properties as dependent on molecular configurations.

When calculating the potential energy of nanosystems, containing one or more large biomolecules, one can use three different approximations: only the quantum mechanical (QM), a classic one in the molecular mechanics (MM), mixed way (QM/MM). Purely quantum mechanical approach is the most rigorous, but in practice, it is not useful for the consideration of nanosystems because of the enormous cost of such a model, even when using the approximate (semi-empirical) computational schemes.

To calculate the potential energy surface, molecular mechanics uses empirically derived set of equations, mathematical form of which is borrowed from classical mechanics. This system of potential function, called the force field, contains some variable parameters, their numerical value being chosen optimally so as to obtain the best agreement between the calculated and experimental characteristics of the molecule, such as spatial structure, energy conformational transitions, the heat of formation, etc. The method uses one common assumption about the possibility of transferring the relevant parameters and force constants from one molecule to another. In other words, the numerical values being determined on an example of some simple molecules are then used as fixed values for other related compounds. It is impossible to rigorously prove how true this assumption.

In the mixed approach, the entire biomolecule or some portion (e.g. enzyme active site) is considered in the QM, while the remainder of the system, including water molecules is under study by MM. Methods QM/MM can be used to study the reactivity of macromolecules or for analyzing the fine details of small molecules of solvation. Despite the fact that reliable information about the potential energy nanosystems, as already noted, can only be obtained in terms of quantum mechanics, classic approaches based on molecular mechanics for its preliminary examination still in the course.

Properties of Catalitic-Active Compozitions, Formed on the Nanoporous Layers Base

Lytovchenko V.H.

Institute of Semiconductor Physics. VE Sci Academy of Sciences of Ukraine
e-mail: lvg@isp.kiev.ua

Recently catalytically active composites are widely used in the field of sensory environmentally harmful and explosive gases and liquids, in particular, such as hydrogen sulfide, CO, H_2, methane, etc. According to several studies, the sensitivity of composites can dramatically increase a number of ways: they form a nanocrystalline structure, small size clusters built using some transition metals, using a porous semiconductor surface (in many cases it is - silicon) with built-in time clusters of transition metals and their oxides.

Recently proposed a new approach to obtain catalytically active systems using low-cost transition metals and their oxides, inactive in conventional "bulk" configurations, namely, the nanoscale phases (Cu, W, WO_3, CuOx et al.).

The theoretical basis of such developments is the idea of changing the structural configuration of electronic levels and nature of hybridization in forming micro-clusters transient carriers and their oxides (or, more generally, in compounds with strong acceptor active elements as F, Cl, S), due to the emergence nanoclusters in free (previously completely filled) d-orbitals, which are most active in the dissociation of molecules, and thus in the catalytic cleavage of molecules.

In this regard, some studies have been carried out calculations of electron configurations electron states and spectra of polyatomic molecules and nano sized clusters from first principles based on the state density functions and estimates the parameters of adsorption of certain molecules based on heterogeneous adsorption isotherms, accompanied by charging the surface the catalytic decomposition of molecules.

The model takes into account the potential energy as part of short orbital s, hybrid and Sp and lond d-orbitals and indicates the presence prekorsov states with the participation of d-orbitals, which dramatically increases the probability of dissociation due to the effect of capture molecules near the surface in such semiseized surface condition.

The phenomenological method of crystal field enables qualitatively trace the change in electronic configuration of the transition from atomic to cluster state of matter due to d electron capture to a series of energy (in the cluster) s orbital, thus are created the situation with partially filled d-orbitals (as is the case

in case of Pd and Cu). Calculations of binding energies for clusters of small size silicon adsorption on copper atoms which indicate the presence of structural surface Si cluster configurations where a large density of electronic links with Cu atoms transferred to Si, therefore, in principle, in this case, the possible release of a 10-d-orbitals of the atom Cu, and thereby converting the latter into a catalytically active substance. This is confirmed by calculations of the spectrum of electronic states for 62Cu cluster and its strong shift in the energy region higher states of oxygen atoms in addition to its deposition in various positions of the surface of the cluster.

The method create a layer of porous matrix of different diameter pores on the surface of silicon and deposition of active composites CuPd, WO_3Pd, CuO_x with particle size of 10-50 nm.

Refined the technological route a catalytically active nanostructured layers and made laboratory sample gas sensors based on MOS structures with transition layer porous composite.

It is shown that due to the high sensitivity of the proposed structure can operate without additional heating, as is required for traditional sensors H_2S even using Pt catalysts.

Solidification Paths Confirmation by the Mass Balances

Lutsyk V.

Institute of Physical Materials Science SB RAS, Ulan-Ude, Russian Federation

Computer model of phase diagram is a vigorous tool to design the miscrostructure of heterogeneous material and to decipher its genotype [1-2]. Investigation of 52 concentration fields of CaO-Al_2O_3-SiO_2 system (Fig.), that belong to the primary crystallization of component C(CaO) and neighbor compounds C_3S=R1 and C_3A=R6 (19 two-, 21 one- and 12 zero-dimensional fields) reveals that there are 18 fields (12 one-dimensional and 6 zero-dimensional) without the unique set of microconstituents.

As an example a two-dimensional field Q_2-8-9 within a subsystem $R_2R_6R_7$ (R7=$C_{12}A_7$, R2=C_2S) is analyzed (Fig., a). Vertical line in the mass centre G intersects the phase regions $L+R_1$, $L+R_1+R_2$, $L+R_2+R_6$, $R_2+R_6+R_7$, two planes of four-phase regrouping of phases (at the temperature of invariant points Q_2 and Q_3). The composition of melt changes along the extension of segment R_1-G_1 to liquidus line e_1Q_2 when the point G passes through the region L+CaO. Then mass center G falls into phase regions $L+R_1+R_2$ and $L+R_2+R_6$ (with the reaction Q2: $L^{Q2}+R_1 \rightarrow R_2^{Q2}+R_6^{Q2}$ between them) and the melt moves along the liquidus curves e_1Q_2 and Q_2Q_3. Solidification finishes on the subsolidus simplex $R_2R_6R_7$ at the temperature of point Q_3. The diagram of vertical mass balance (Fig., b) confirms the phase reactions $L^1 \rightarrow R_1^1$, $L^{e1} \rightarrow R_1^{R2}+R_2^{R1}$, $L^{Q2}+R_1 \rightarrow R_2^{Q2}+R_6^{Q2}$, $L^{e\text{п}} \rightarrow R_2^{R6,e\text{п}}+R_6^{R2,e\text{п}}$, $L^{Q3}+R_6 \rightarrow R_2^{Q3}+R_7^{Q3}$ with the forming of microconstituents R_2^{R1}, R_2^{Q2}, R_6^{Q2}, $R_2^{R6,e\text{п}}$, $R_6^{R2,e\text{п}}$, R_2^{Q3}, R_7^{Q3}. Since the solidification finishes on the simplex $R_2R_6R_7$, then the crystals R_1^1 and R_1^{R2} are absent as the microconstituents (they are expended during quasiperitectic reaction Q_2).

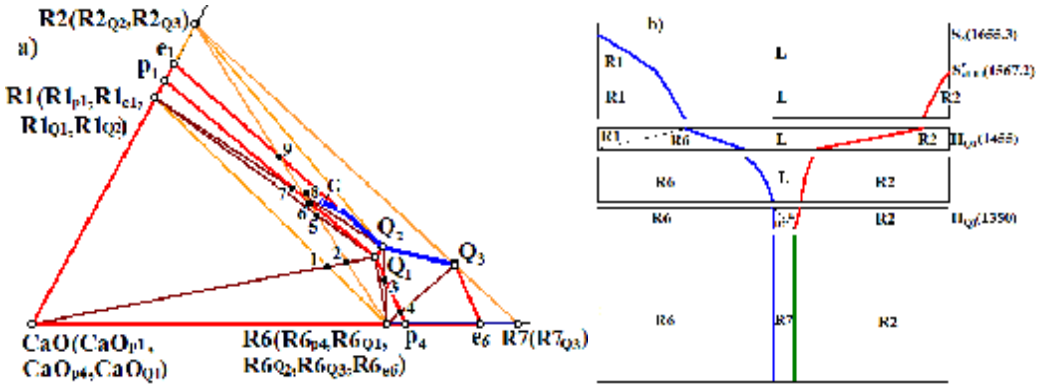

1. V.I. Lutsyk, A.E. Zelenaya. Crystallization Paths and Microstructure Formation in Ternary Oxide Systems with Stoichiometric Compounds // Solid State Phenomena, (2013) (to be published).
2. V.I. Lutsyk. Crystallization path as a genotype of multicomponent material // Bull. Buryat Scientific Centre of RAS, #5, pp. 78-97 (2012). (In Russian).

Luminophors on the Basis of Activated Ultradisperse Diamond

Malashkevich G.E.[1], Lapina V.A.[1], Opitz J.[2] Pershukevich P.P.[1]

[1]*B.I.Stepanov Institute of Physics of the NAS of Belarus, Minsk, Belarus*
[2]*Fraunhofer Institute of nondestructive testing, Dresden, Germany*

Ultradisperse diamond (UDD) powders obtained using detonation synthesis consist of nanoparticles that represent diamond nuclei with an average diameter of ~ 4–10 nm, covered by a cluster shell of nondiamond carbon [1]. Such nanoparticles show weak luminescence in visible and near-UV spectral regions, and width of the forbidden zone of nondiamond carbon can decrease down to 2 eV with the increase of the part of "graphite-like" sp^2 bonds over "diamond-like" sp^3 bonds [2]. Due to high specific surface (more than 250 m^2/g [1]) and possibility of manipulation of the ratio between the indicated parts of carbon UDD are the interesting object for introduction into their cluster shell of efficiently luminescent activators and further preparation of luminophors with new spectral-luminescent properties.

In the first paper of such a kind [3] it has been shown that at impregnation of UDD cluster shell by the solution of europium salt and further thermal processing the formation of chemical bonds of Eu – O – C takes place. This causes an increase on the average in the degree of Eu – O chemical bond covalency and change of coordination polyhedron of the activator, the result of that is multiple increase of excitation efficiency of state $^5D_0$ of ions Eu^{3+} in a band of charge transfer. Later the possibility has been demonstrated of UDD activation by ions of Cr^{3+} [4]. The obtained Cr-containing powders at low temperature of annealing have been efficiently luminesced in a wide vibrational band $T_2 \rightarrow {}^4A_2$, and at a high – in a narrow spin-forbidden band $^2E \rightarrow {}^4A_2$.

In the present paper, except for the analysis of the existing achievements in this area, we also discuss the original results concerning structural and spectral properties of new luminescent compositions prepared using UDD. Particularly, it has been established that impregnation of these latter cluster shell by compounds of rare-earth activators (Ce^{3+} and Tb^{3+}) and some buffer elements with further thermal processing in air leads to formation on the surface of diamond nuclei of oxide film protecting it from burning-out, at least, up to T = 900°C. This film can efficiently luminesce, and its spectra differ from spectra of films and powders of identical content, but without diamond nanoinclusions (see Fig. 1). The peculiarity of activated UDD is increased intensity of excitation of luminescence in ultraviolet spectral region. Small size of individual grains of the obtained luminophors (Fig. 2) allows us to use them for introduction into various polymer and oxide films and also into gel-glasses. In the last case thanks to the absence of the melt stage, it is possible to avoid their dissolution in the glasses matrix.

This work was supported by the ISTC program (grant no. B-1988p).

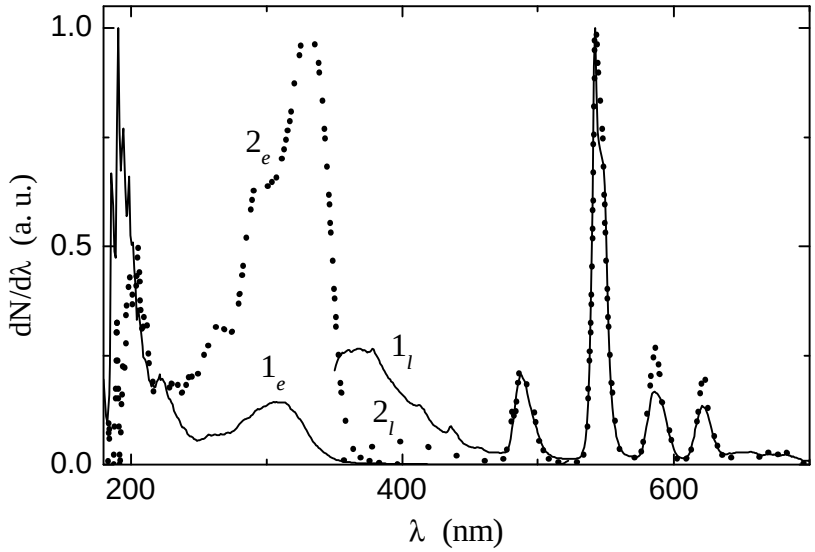

Fig. 1. Corrected and normalized luminescence (1_l, 2_l) and excitation (1_e, 2_e) spectra of Ce–Tb- containing luminophors with (1_l, 1_e) and without (2_l, 2_e) of UDD.

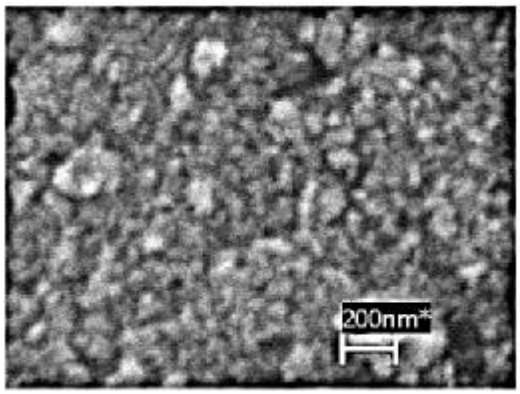

Fig. 2. Microphotography of activated UDD after thermal processing in air (T = 700°C) and in blend of 90Ar:10H_2 (T = 1000°C).

1. Aleksenskii A.E., Baidakova M.V., Vyl A.Ya., Siklitskii V.I. The structure of diamond nanoclusters // Physics of the Solid State. – 1999. – V. **41**, No. 4. – P. 668–671.
2. Kompan M.E., Terukov E.I., Gordeev S.K. et al. Photoluminescence spectra of ultradisperse diamond // Physics of the Solid State. – 1997. – V. **39**, No.12. – P. 1928–1929.
3. Malashkevich G.E., Lapina V.A., Semakova G.I. et al. Luminescence of Eu^{3+} ions in ultradisperse diamond powders // JETP Letters. – 2003. – V. **77**, No.6. – P. 291–294.
4. Malashkevich G.E., Lapina V.A., Pershukevich P.P. Luminescent powder on basis of ultradispersed diamond activated by Cr^{3+} ions // Bulletin of the Russian Academy of Sciences. Physics. – 2006. – V. **70**, No.11. – P. 1899–1901.

Physical Properties of Nanostructures with SiGe Solid Solution Thin Films

Matveeva L.A., Neluba P.L., Venger E.F.

V. Lashkaryov Institute of Semiconductor Physics NAS of Ukraine, Kyiv, Ukraine

Nanostructures with SiGe solid solution arise to a great scientific attention due to their practical application in novel technologies and researchers. Their physical properties determined by the composition of the films and the substrate material. During the manufacturing process heterosystems appears the the mechanical stresses due to the difference of lattice film and substrate periods and coefficients of thermal expansion. The appearance of internal mechanical stresses is usually accompanied by the structural defects at the interface film – substrate. They leads to bending of the heterosystems, deteriorate the characteristics and reduced reliability of the corresponding devices. An investigation of the physical properties of nanostructures with SiGe films is importance for the technology development and for the prediction of the devices properties based on them.

To reduce internal mechanical stresses the fitting of Ge film and GaAs substrate lattice parameters was used, by deposition of the solid solutions, the lattice parameters of witch may be regulated by the composition variation. To reduce these stresses was used too the extrinsic influence (γ - irradiation). In this work we presented the results investigation of mechanical stresses, electron and optical properties of nanostructures with Si_xGe_{1-x} thin films on GaAs and Si substrates, of the features of their electronic band structure, depending on the film composition, the substrate type and too on the influence on them γ – irradiation.

Si_xGe_{1-x}/GaAs heterosystems were obtained by thermal vacuum deposition Si_xGe_{1-x} solid alloys with x 0 to 4 at. % and $Si_{0.75}Ge_{0.25}$ heterosystema was obtained by CVD method. The films had a single crystal structures, their thickness was 0.1 to 1 μm. The composition, structure, electron and optical properties and the internal mechanical stresses of the heterosystems were studied by electroreflectance modulation spectroscopy, light absorption classical spectroscopy and measurements of the heterosystems bending. The electroreflectance spectra were measured by an electrolytic method [1] at the room temperature in 3 to 3.6 eV spectral range of direct electron transitions for GaAs (E_0), Ge (E_1) and Si_1 (E_0').

The important data were obtained concerning the film and interface film – substrate band structures, their structure perfection, presence of elastic stresses and charge scattering processes, as well as the effect of γ – irradiation on the heterostructures. The E_g forbidden gap width, the sign and the value of internal mechanical stresses σ, the conductivity type of the films and the substrate on the interface and parameter of charge scattering Γ (of spectral collision extension),

as well as the their mobility μ and time τ of the energy relaxation of exciting charge carries were obtained from the spectral location and from the electroreflectance signal value. The internal mechanical stresses in the films were studied too by profilometryl measuring of the heterosystems bending radius using the Stoney's equation [2]

$$\sigma = Ed^2[6Rt(1-\nu)]^{-1},$$

where R is the radius of the heterosysteme curvature, E the Joung's modulus, ν. Poisson' ratio of the substrate, and d and t the substrate and film thickness, respectively. Compressive stress is in the film, if it is on the convex side of the substrate.

The films Ge on GaAs at photon energy below E_g had an exponential course of the absorption coefficient k: $k = \exp(E_g-E)/\Delta$. The characteristic energy $\Delta = dE/d\ln(k)$ in the range of the density states tail in the energy gap characterizes the degree of film structural perfection. The characteristic energy Δ is independ of the temperature in the range 4 to 300 K. With increasing x the parameters Δ and Γ increased, τ and μ decreased as the addition of Si in the Ge film led to her disorder. At the same time, the parameter Γ in the GaAs substrate at the interface had a minimum value at x = 0.02. The sign and magnitude of heterosystems bending depend on the composition of the film. For x < 0.02, the film is compressed, and for x > 0.02 - stretched. The mechanical stresses in the heterosystem disappear at x = 0.02, and the generation of technological defects in interface is minimal.

To translate nanostructures $Si_{0.75}Ge_{0.25}/Si$ in a state of equilibrium, we used the γ-rays irradiation ^{60}Co. The film thickness was 100 nm, and the film was compressed. The magnitude of bending depend on the dose of γ – irradiation 10^6 to $1.9x10^7$ R. The mechanical stresses in the heterosystem disappear at the dose $1.5x10^7$ R. The signal of electroreflectance can was measure simultaneous from the film and the substrate. With increase in dose was manifested in the increase E_g of the substrate to a value 3.38 eV, which corresponds to the surface unstressed Si. The additional peaks appear in the spectra of the films. They correspond to the following values of x: 0.8, 0.67, 0.58 and 0.48.

Thus, it was established, that Si_xGe_{1-x} film can change composition with the formation of the other solid solution structure both in processes of the films deposition and by γ – irradiation of the heterosystem. The possibility was found to reduce the mechanical stresses, to improve electronic and optical parameters for the films and for the substrates on the interface, and to fabrication of the nanostructures with SiGe solid solution without the bending deformation.

1. M. Cardona, Modulation spectroscopy, Academic press, New York, 1969.
2. R.W.Hoffman, in Physics of Thin Films, ed. by G. Hass and R.E Thun, Academic press, New York and London, 1966.

Liquid-phase Synthesis of TiO_2 Crystalline Modifications

Myronyuk L.I.[1], Chelyadyn V.L.[2], Sachko V.M.[1], Myronyuk I.F.[1]

[1]*PreCarpathian Vasyl Stefanyk National University, Ivano-Frankivsk, Ukraine*
[2]*Public Company "Zhyvytsya", urban village Vygoda, Ukraine*

Titanium dioxide with nanometer particles exposes unique properties related to its catalytic and photocatalytic activity. Fine particles acquire this activity due to the large number of surface titanium atoms, which under the influence of external factors change their valence state and influence the course of chemical processes in substances in contact with oxide material.

The most promising precursor in gas-phase synthesis of TiO_2 is titanium tetrachloride. However, interaction of $TiCl_4$ with aqueous medium leads to formation of titanium-containing aqua-complex dilution $[Ti(OH_2)_6]^{3+}$ by reaction:

$$TiCl_4 + 8H_2O \rightarrow [Ti(OH_2)_6]^{3+} + 4HCl + O_2 . \quad (1)$$

Reduction of four-valence titanium atoms to the trivalent state in $[Ti(OH_2)_6]^{3+}$ ($pH \sim -3.3$) provides for water dissociation and formation of groupings $HO^{\bullet}$ and H_2O_2 molecules in the reaction medium:

$$H_2O - \bar{e} \rightarrow H^+ + HO^{\bullet} \quad (2)$$

$$H_2O + HO^{\bullet} \rightarrow H_2O_2 + H^+ \quad (3)$$

As a result, hydrogen peroxide degrades while H_2O and O_2 molecules are formed.

With increase of pH of reaction medium, Ti^{3+} atoms in aqua-complex spontaneously oxidize to Ti^{4+} due to electron transfer to one of the surrounding water molecules, which is also forced to dissociate. In this case, the process is accompanied by formation of molecular hydrogen and OH^- anions:

$$2H_2O + 2\bar{e} \rightarrow 2OH^- + H_2 \quad (4)$$

In aqua-complexes Ti^{4+} cations connect OH^- anions and form a chemical bond $\equiv Ti - OH$. As the pH increases, the hydroxylation degree of titanium atoms increases too and they transfor into hydroxo(aqua)complexes $[Ti(OH)_m(OH_2)_{6-m}]^{(4-m)+}$ ($1 \le m \le 6$) as follows:

$$[Ti(OH_2)_6]^{3+} \xrightarrow{pH:1.0} [Ti(OH)_2(OH_2)_4]^{2+} \xrightarrow{pH:6.7} [Ti(OH)_4(OH_2)_2]^0 \xrightarrow{pH:14.0} \xrightarrow{pH:14.0} [Ti(OH)_6]^{2-}$$

Heating of hydroxo(aqua)complexes solution at 40÷80°C results in condensation and formation TiO_2 nanocrystallites. In acidic reaction medium ($pH \sim 1.0 \div 2.5$), $[Ti(OH)_2(OH_2)_4]^{2+}$ condensation leads to formation of rutile particles in the form of rods with the diameter of $3 \div 6$ nm and the length of 6 – 13 nm. At the stage of hydrogel drying, they are united in associates size 100–500 nm (fig. 1a). In the environment with $pH \sim 3.0 \div 4.8$, hydroxo-(aqua)complexes $[Ti(OH)_3(OH_2)_3]^+$ delivers formation of spherical or ellipsoidal nanocrystallites with the diameter of $3 \div 7$ nm. Synthesized product contains 47% anatase and 53% brookite (fig. 1b). Weakly acidic and weakly alkaline

environment (pH ~ 5.5 ÷ 8.5) is favorable for formation of TiO_2 anatase. Anatase nanocrystallites with the diameter of 5 ÷ 8 nm coagulate and form aggregates of 20 – 50 nm (fig. 1c).

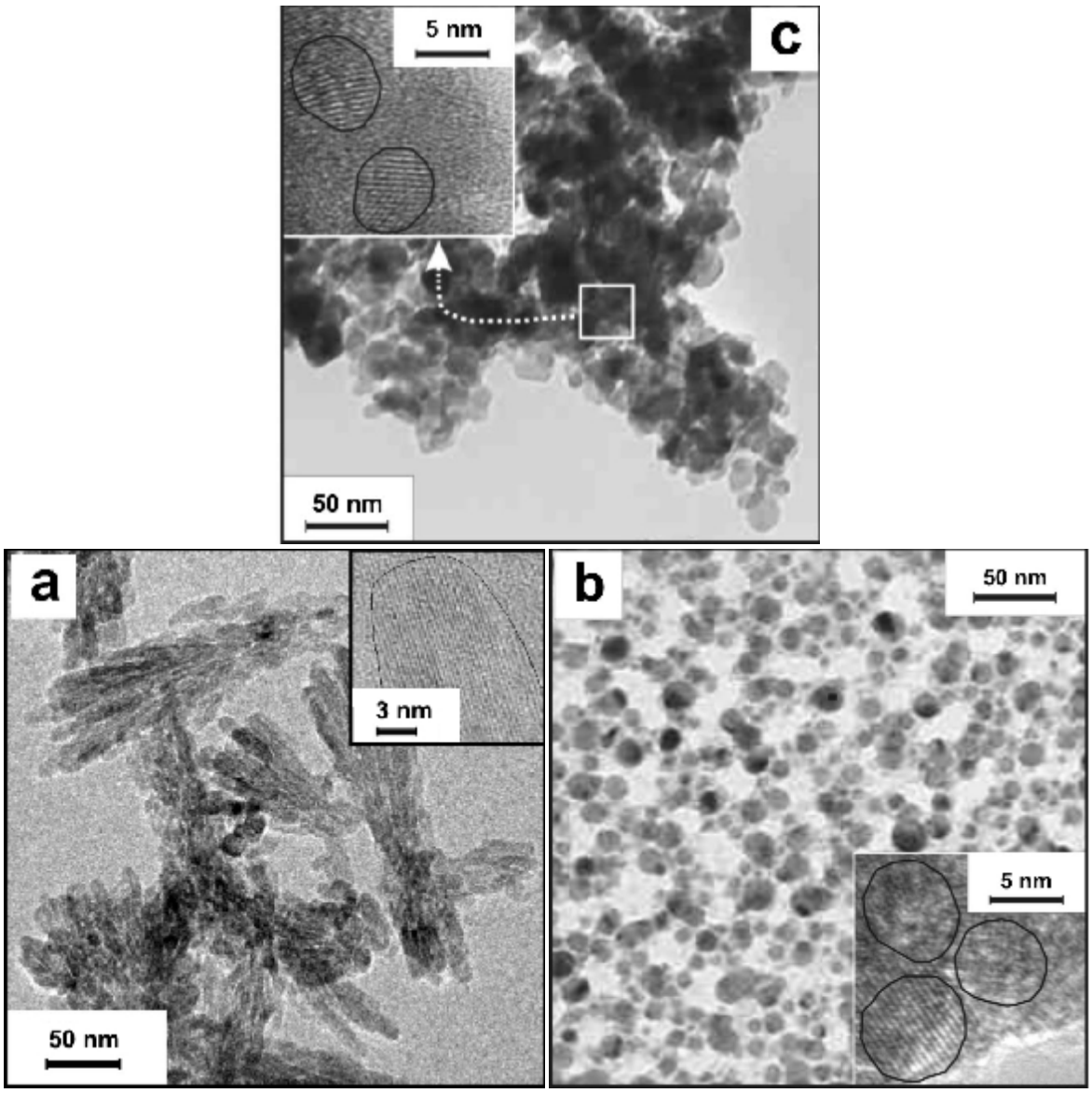

Figure 1. Photos of TiO_2 nanoparticles: rutile (a), anatase and brookite (B) and anatase (c).

The present studies have revealed a clear dependence of the crystal structure of the synthesized TiO_2 on the hydroxylation degree of titanium-containing precursor.

Photoinduced Effects in Ge(As)-Se Thin Films and Nanostructures

Nemec P.[1], Bacso J.[1,2], Makauz I.[3],Shipljak M.[3], Charnovich S.[2], Kokenyesi S.[2]

[1] *Univeristy of Pardubice, Pardubice, Czech Republic*
[2] *University of Debrecen, Debrecen, Hungary*
[3] *Uzhgorod NationalUniversity, Uzhgorod, Ukraine*

Photoinduced effects due to the laser illumination of thin amorphous layers are compared for compositions with the same Se contents from As-Se and Ge-Se systems of chalcogenide glasses with emphasis on the Se-enriched compositions. The influence of the technology on the measured transformations of optical and structural parameters of thin, 600 nm thick layers was investigated by optical spectroscopy, ellipsometry and SEM, AFM methods. Comparison of simple vacuum evaporation and pulsed laser deposition methods was made to establish the possible role of composition and structural stability deviations, especially for germanium-based glasses.

Further development of these investigations was made towards the new structures of amorphous Ge(As)-Se chalcogenides – gold nanoparticles based composite layers, with aim to establish the possible influence of localised plasmon fields on the stimulated structural transformations and optical or geometrical relief formation processes. The enhancing influence of a gold nanoparticle layer, deposited between the oxide glass substrate and the chalcogenide cover layer, on the amplitude-phase optical recording , optical and geometrical contrast formation was observed if the resonance excitation of localised plasmons occurs simultaneously with recording excitation.

The results are used for deeper understanding of the mechanism of stimulated structural transformation, selection of the best compositions and recording parameters for the technology of *in situ* prototyping photonic elements.

This work was supported by the TAMOP 4.2.2.A-11/1/KONV-2012-0036 project, which is co-financed by the European Union and European Social Fund. Bacso J. acknowledges the support of ERASMUS grant.

Contact Effects in a Heterostructure Metal-Semiconductor with the Built-in Layer of Quantum Dots

Peleshchak R.M.[1], Bachynsky I.Ya.[1], Doroshenko M.V.[1], Velchenko A.A.[2], Stanko M.H.[1], Shtym V.S.[1]

[1]*Drohobych Ivan Franko state pedagogical University, Drohobych, Ukraine*
[2] *Volodymyr Dahl East Ukrainian National University, Luhansk, Ukraine,*

At present, the study of electric properties of stressed heteroborder between a quantum dot(QD) (InAs, CdTe) and matrix (GaAs, ZnTe) is of great interest)[1]. Modern nanotechnology allows to grow up, both separate quantum dots (QD), and the whole layers of coherently-strained QDs, on which basis are created opto- and nanoelectronics devices (lasers, tunnel diodes, Shottky diodes). Construction of devices with use of QD layer (InAs/GaAs, CdTe/ZnTe) allows to operate effectively their electric and optical characteristics, thanks to predicted control of technological parametres such as density, distances from QD layer to contact metal-semiconductor, the sizes, the form, a spectrum of conditions of carriers of a charge. In particular, in the presence of built in QDs in area of a spatial charge of barrier structure of a kind of Shottky at certain technological parametres probably occurrence S-similar voltage-current characteristic of diodes Shottky which can be used in high-frequency electronics. Stresses that arise in nanoheterosystems with QDs both in processes of growth and temperature changes, and during fabrication on their basis of opto- and nanoelectronics devices, influence the shape and of potential barrier height on boundary a QD - a matrix, band-gap energy, a discrete spectrum of energy states of the electrons localised in a QD, charge emission from the QD into the corresponding bands of the semiconductor, the barrier capacity of the structure and the width of the space charge region.

In this article the topology of distribution of electrostatic potential $j(x, y)$ in barrier structure with the built in layer of QDs (InAs) in area of a spatial charge of a semi-conductor matrix n–GaAs is constructed within the framework of the self-consistent electron-deformation model. It is established that resulting electric field in Shottky barrier structure with built in QD layer is defined by superposition of two fields: the electric field $\vec{E}_{BS}$ created on border of contact metal - semiconductor and electric field $\vec{E}_{QD}$ of the section formed on border QD-semiconductor matrix. It is shown that the potential along a direction of placing Qd has oscillation character with the period h, and, the period of oscillations is defined by step of placing QDs. It is shown that to a direction perpendicular to border of contact metal-alloyed of n-type the semiconductor, the potential has descending exponential character.

1. S.D.Lin, V.V.Ilchenko, V.V.Marin// Appl. Phys. Lett., **90** (2007).

Stages of Low-Dimensional 3D Systems Formation at Condensation under Extremely Low Supersaturations

Perekrestov V.I., Davydenko T.A.

Sumy State University, Sumy, Ukraine

On the basis of large experimental data, mechanisms of nucleation and growth of metal, carbon and silicon layers under conditions of steady-state extremely low supersaturations have been systematized. To fabricate low-dimensional 3D structures we have used the technological system "plasma-condensate", in which sputtered substance is accumulated near growth surface. This feature of the technological system [1] has been realized by means of both increased pressure of highly purified working gas (Ar) and diffusive mass transfer of the sputtered atoms. Analysing large experimental material, it has been established that the nucleation kinetics can be represented as the following stages depending on the substrate type and structural state of its surface:

i) Nucleation of unconnected clusters on the substrate surface. Afterwards the clusters average their sizes by means of Ostwald ripening.

ii) Origination of aggregates of the clusters, which create fractal networks on the surface during mutual jointing.

iii) If the substrate surface has high density of active centres, a continuous layer of amorphous phase is formed at the initiation stage. During subsequent thickening the amorphous phase gradually transfers to crystalline state.

As a rule, during further deposition onto the base layer, which is formed directly on the substrate, structural and morphological characteristics of the layers undergo changes with increasing of the thickness. Thus, generalizing the experimental results, we have established the following variants of 3D systems:

i) The systems, possessing considerable amount of pores in the form of ellipsoids of revolution, major axes of which are oriented perpendicularly to the substrate surface.

ii) 3D nano- and microsystems in the form of weakly bound crystals or amorphous clusters of approximately the same habits and sizes.

iii) The systems of interconnected and randomly oriented whickers.

When reducing the supersaturation, that is usually observed at increasing of the layers thickness, the structural fragments become transformed according to the following scheme: *faceted crystals → round-shaped crystals → whickers*.

1. Perekrestov, V.I. Self-organization of quasi-equilibrium steady-state condensation in accumulative ion-plasma devices / V.I. Perekrestov, A.I. Olemskoi, Yu.O. Kosminska, A.A. Mokrenko // Physics Letters A. – 2009. – V.373, Is. 37. – P.3386-3391.

Modeling of Optical Processes in Silicon Nanocrystals

Poddubny A.N., Prokofiev A.A., Yassievich I.N.

Ioffe Physical-Technical Institute RAS, S.-Petersburg, Russia

The models for optical processes in silicon nanocrystals have been developed in two approaches: i) multi-band effective mass approximation, and ii) tight binding approach. They give the possibility to calculate wave functions and energy levels of carriers localized in silicon nanocrystals, the probability of optical emission and absorption as well as multiphonon relaxation processes. The modeling of the energy levels and wavefunctions localized in silicon nanocrystals embedded into dioxide thin films has been produced with taking into account the tunneling effect. The results of photoluminescence study has been demonstrated a good agreement between the theory and experiments [1].

It is shown in the framework of the tight binding approach that the carbon surface termination of silicon nanocrystals gives rise to drastic modification in the electron and hole wavefunctions and radiative transition rates between the lowest excited states of electron and hole attain ‘direct bandgap-like’ (phonon-less) character. This effect has been recently demonstrated in the optical spectroscopy investigations of the chemically synthesized alkyl-capped Si-QDs, which have shown photoluminescence tunable in the visible range with the nanosecond decay [2].

Two new phenomena – i) spaced-separated photon cutting by Si nanocrystals, and ii) red shift of hot photoluminescence with nanocrystal size decreasing – have been discovered in common work with the experimental group from the Amsterdam University [3, 4].

1. O. B. Gusev, A. N. Poddubny, A. A. Prokofiev, and I. N. Yassievich, Semiconductors **47**, p.183 (2013).
2. K. Dohnalova, A. N. Poddubny, A. A. Prokofiev, et al., Light: Science & Applications , to be published (in Febrary 2013).
3. D. Timmerman, I. Izeddin, P.Stallinga, I.N.Yassieviich, and T. Grekorkiewicz, Nature Photonics **2** , p. 105-109, 2008
4. W. D. A. M. de Boer, D. Timmerman, K. Dohnalova, I. N. Yassievich, et al., Nature Nanotechnol. **5**, p. 878 (2010).

The Double Role of NH_3 Molecules in Surface Doping of Si and GaAs *P-N* Junctions as Gas Sensors

Ptashchenko O.O.[1], Ptashchenko F.O.[2], Gilmutdinova V.R.[1], Dovganyuk G.V.[1]

[1]*Odessa National I. I. Mechnikov University, Odessa, Ukraine*
[2]*Odessa National Maritime Academy, Odessa,Ukraine*

The effect of prolonged exposure of Si and GaAs *p-n* junctions in moist ammonia vapors with a partial pressure of 12 kPa was studied on the characteristics of *p-n* structures as sensors of ammonia, water and ethanol vapors. Kinetics of forward and reverse currents in *p-n* junctions after a change in the ambient atmosphere composition was analyzed.

The presence of NH_3, H_2O and C_2H_5OH vapors in the ambient atmosphere strongly increased the direct and reverse currents in studied *p-n* junctions. The sensitivity of a *p-n* junction as gas sensor was defined as

$$S_I = \Delta I / \Delta P, \qquad (1)$$

where ΔI is the change in the current (at a fixed voltage) due to a change ΔP in the corresponding gas partial pressure.

The ammonia-sensitivity of GaAs *p-n* junctions at a forward bias voltage of 0,3 V was of 15 nA/Pa and 50 nA/Pa at a reverse bias voltage of 1 V. For the Si *p-n* junctions the sensitivity was some lower. The gas sensitivity of *p-n* junctions is due to action of adsorbed ammonia (water, ethanol) molecules as donors on the Si- and GaAs surface. The electric field of ionized donors forms a conducting channel on the p-region surface, which shorts the *p-n* junction.

The measured response time t_r and decay time t_d of the Si- and GaAs sensors were <50s. As the molecules adsorption time $t_A \le t_r$ and the desorption time $t_D \le t_d$, this means that $t_A, t_D < 50\,\text{s}$.

The treatment in NH_3 vapors of high concentration enhanced the ammonia-,water- and ethanol sensitivity of Si- and GaAs *p-n* junctions by a factor of 30. This effect can be explained by the forming of additional donor centers as a result of durable adsorption of NH_3 molecules from the atmosphere with a very high ammonia partial pressure.

A durable storage of the treated samples in a neutral atmosphere lowered their gas sensitivity. The characteristic time of this process in GaAs *p-n* junctions τ_2 is of $5\cdot10^5$ s and is of the same order of value in Si *p-n* junctions.

Thus, adsorption of NH_3 molecules from the ambient atmosphere forms two types of surface donors in GaAs with the desorption times τ_{D1}<50 s and τ_{D2} of $5\cdot10^5$ s. A similar effect was observed on Si *p-n* junctions. And the response time t_r and decay time t_d of the Si- and GaAs sensors were practically not changed by the treatment and the subsequent storage. This indicates that the two types of donors are independent.

Magnetic Structure of Subsurface Layers of Single Crystalline Yttrium-Iron Garnet Films Implanted with Si^+ Ions with Various Energies

Pylypiv V.M., Garpul O.Z.,

Vasyl Stefanyk Precarpathian National University, Ivano-Frankivsk, Ukraine

Findings from the investigation of subsurface layers of epitaxial single crystalline yttrium-iron garnet $Y_3Fe_5O_{12}$ films implanted with Si^+ ions with the dose of 5×10^{13} cm^{-2} and the energies of 100-150 keV using conversion electron Mossbauer spectroscopy are presented and the comparison with previously obtained results from simulations and x-ray diffractometry studies is carried out. The analysis of energy dependence of the components Mossbauer spectra, the integral intensity of the deformation profiles and the integral lattice disorder in the subsurface layers confirms the validity of theoretical models used in this work.

The integral lattice disorder in the 65 nm thick sub surface layer of YIG film decreases with the increase in the implant Si^+ ions energy, which is consistent with the energy dependence of the mean free path of implant ions in the crystals.

The presence of two octa-coordinated positions of Mossbauer cores comes from two possible orientations of the main axes of the electric field tensor relative to the magnetization direction [1].

The presence of two magneto-inequivalent tetra-coordinated positions is caused by the deviations in anion stoichiometry driven by the lack of equilibrium and introduction of dopant atoms in the final stages of epitaxial growth process.

The validity of the theoretical model is supported by the similarity in the energy dependences of the relative composition of the doublet component of Mossbauer spectrum acquired from (65 nm think) subsurface layer and the integral intensity of the deformation profile obtained from x-ray diffractometry studies correlated to the changes in the amount of integral lattice disorder in subsurface layer.

1. Ostafiychuk B. K., Fedoriv V. D., Kotsyubynsky V.O., Mokliak V.V. Mössbauer study of magnetic and electric interactions in ¬ thin epitaxial films $Y_3Fe_5O_{12}$ // Physics and Chemistry of Solids. — 2005. — T. 6, № 1. — P.60-64.

CVD Diamond Films and Single Crystals: Synthesis and Properties

Ralchenko V.G.

A.M. Prokhorov General Physics Institute RAS, Moscow, Russia

Diamond, the material combining a number of extreme physical properties, is of interest for applications in electronics, multispectral optics, micromechanics, biomedicine. In this talk it will be described how a microwave plasma assisted chemical vapor deposition is used to grow nanocrystalline (NCD), microcrystalline and single crystal (epitaxial) diamond films from CH_4-H_2 gas mixtures [1-3]. The film structure can be varied in a broad range using the same deposition apparatus simply by appropriate choice of process parameters.

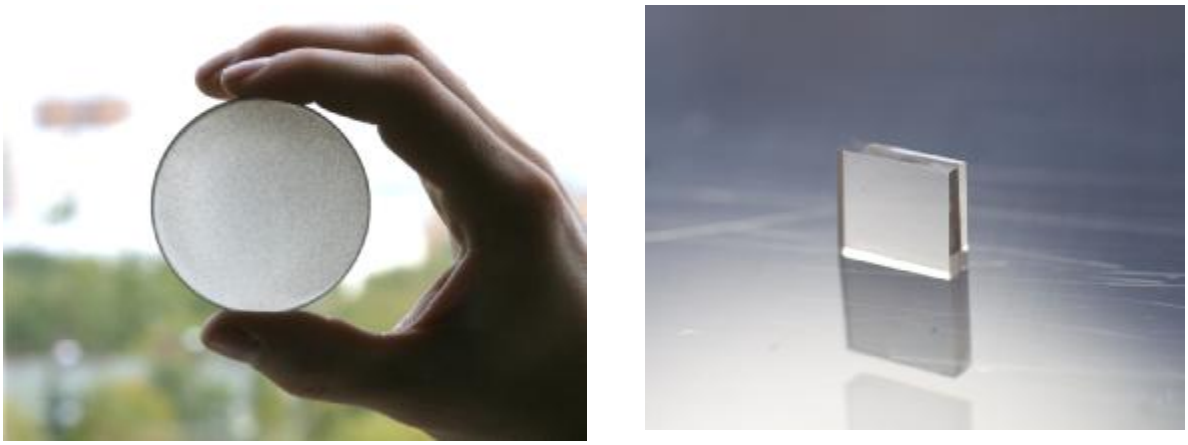

Polycrystalline samples (left) and single crystal (right) CVD-diamond

The data on structure, defects and impurities will be presented, and the effects of nitrogen doping of NCD films and isotopic modification of the diamond films and crystals will be demonstrated. Particularly, ~50% increase in thermal conductivity at room temperature, up to 3400 W/cmK, is measured for single crystal films with reduced (from 1.07% to 0.07%) ^{13}C carbon isotope content in diamond. Selected examples of applications of thick diamond films, such as UV and X-ray detectors, field effect transistors, heat spreaders, laser windows and Raman lasers will be discussed.

1. Bolshakov A.P., Ralchenko V.G., Polskyi A.V. et al. Growth of single-crystal diamonds in microwave plasma // Plasma physics reports. – 2012. – V. 38. – No. 13. – C. 1113.
2. Fodchuk, I.M., et al. Distribution in angular mismatch between crystallites in diamond films grown in microwave plasma // Diamond Relat. Mater. –2010. –V. 19, –P. 409.
3. Pleskov, Y.V., Krotova, M.D., Ralchenko, V.G., et al. Electrodes of strongly nitrogenated nanocrystalline diamond // Russian J. Electrochemistry. – 2010. – V. 46. –No. 9. –P. 1063.

Transport Properties of Bi - Based 2D-Structures and Size Effects

Rogacheva E.I.

National Technical University "Kharkov Polytechnic Institute", Kharkov, Ukraine

Bismuth and $Bi_{1-x}Sb_x$ solid solutions have for many years attracted much attention both as a fascinating material in solid state physics and as a promising thermoelectric material for refrigerating devices at temperatures below ~ 150 K [1]. Due to their unique electronic properties (extremely low effective electron masses, an anomalously high charge carrier mobility and mean free-path) and due to the possibility of a radical change in their band structure under changing composition in $Bi_{1-x}Sb_x$ solid solutions these materials are very convenient for observing quantum size effects and for studying what is special about electronic phase transitions. The development of nanotechnologies and the possibility of enhancing the dimensionless thermoelectric figure of merit ***ZT*** in low-dimensional structures have stimulated studies of $Bi_{1-x}Sb_x$ thin-film structures. Recently, interest in investigating the transport properties of Bi and $Bi_{1-x}Sb_x$ crystals and thin films has grown sharply due to the prediction and subsequent experimental observation of the special properties characteristic of topological insulators in $Bi_{1-x}Sb_x$ crystals. The first 3D topological insulator to be discovered experimentally was the semiconducting alloy $Bi_{0.9}Sb_{0.1}$.

An overview of the studies related to classical and quantum size effects in thin Bi and $Bi_{1-x}Sb_x$ films and Bi-based heterostructures conducted at National technical university "Kharkov polytechnic institute" is given.

Temperature and thickness dependences of electrical conductivity, Hall coefficient, charge carrier mobility, and Seebeck coefficient were obtained for Bi and $Bi_{1-x}Sb_x$ thin films and Bi-based heterostructures fabricated by the thermal evaporation of the crystals in vacuum and deposition on mica substrates at different temperatures. Thickness oscillations were observed and attributed to the quantization of the electron and hole energy spectrum. It was shown that with increasing substrate temperature the manifestation of oscillations becomes more distinct.

On the basis of experimental studies of the temperature and thickness dependences of the kinetic coefficients in thin Bi films and detailed theoretical analysis taking into consideration the presence of native charge carriers of *p*- and *n* - types as well as acceptor states, the conclusion regarding the existence of semimetal- semiconductor transition as a result of size quantization of energy spectrum of charge carriers was made. Using this assumption and taking into account the existence of surface states, for the first time it was shown that the gap between the valence and conduction bands in the semiconductor region increases with decreasing *d* which supports the idea as to the existence of a semimetal–semiconductor transition in Bi thin films [2].

An oscillatory behavior of the dependences of kinetic properties on the Bi layer thickness was also revealed in micaPbTe/Bi/Al_2O_3 heterostructures, which is indicative of size quantization of charge carrier energy spectrum. It was established that in the above mentioned heterostructures one can attain higher values of thermoelectric power factor in comparison with those in Bi films.

The dependences of the kinetic coefficients on the thickness of the thin $Bi_{1-x}Sb_x$ films were obtained. The influence of classical and quantum size effects was isolated. It was shown that the monotonic component of the thickness dependences of electrical conductivity can be satisfactorily approximated by theoretical calculations based on the classical Fuchs - Sondheimer theory. The theoretically estimated period of oscillations was in good agreement with the experimentally observed one. The influence of various factors, such as composition, substrate temperature and others, on the character of the manifestation of size effects was investigated.

In addition to the oscillations which are attributed to the quantization of the semiconductor electron energy spectrum, oscillations with a small period were also revealed in the $Bi_{1-x}Sb_x$ thin films. It is suggested that the existence of the high-frequency oscillations may be connected with the quantization of the metallic surface states energy spectrum [3].

The revealed nonmonotonic behavior of the dependences of the kinetic properties on the thickness of thin Bi and $Bi_{1-x}Sb_x$ layers should be taken into account when predicting properties of thin film structures and developing devices based on thin films for thermoelectric, microelectronic and other applications.

1. D.M. Rowe, *CRC Handbook of Thermoelectrics*, CRC Press, Boca Raton, London, New York, Washington, 1995,
2. E.I. Rogacheva, S.G. Lyubchenko, M.S. Dresselhaus: Semimetal-semiconductor transition in thin Bi films. *Thin Solid Films*, Vol. 516, № 10, pp. 3411-3415 (2008).
3. E.I. Rogacheva, D.S. Orlova, O.N. Nashchekina, M.S. Dresselhaus, S. Tang, Thickness dependence oscillations of transport properties in thin films of a topological insulator $Bi_{91}Sb_9$, Applied Physics Letters, 101, 023108 (2012).

Nanostructures with Ferroelectric Properties on the Glassy and Amorphous Chalcohalogenides Basis

Rubish V.M., Gasynets S.M., Gorina O.V., Guranich O.G.,
Rigan M.Yu., Shtets P.P.

Uzhgorod Scientific-Technological Center of the Institute for Information Recording, NASU, Uzhgorod Ukraine

Chalcogenide glasses and amorphous films on the basis of ferroelectrics $A^{V}B^{VI}C^{VII}$ group arouse scientific and practical interest, since in the matrix of such materials under certain correlations of components and conditions of heat treatment and lazer irradiation exists the possibility of formation crystalline inclusions various morphology with ferroelectric properties.

The present paper is devoted to studying of structure and properties of glasses, amorphous films and composities on their basis in the $A_2^{V}B_3^{VI}$ – $A^{V}B^{VI}C^{VII}$ (A^{V} – As, Sb; B^{VI} – S, Se; C^{VII} – I) system.

Glassy alloys were prepared by vacuum melting method of correspondent mixture of binary (for example, As_2S_3, As_2Se_3) and ternary (for example, SbSI, SbSeI) components followed by cooling of the melts on the air or into cold water. Thin films (1-2 μm) were deposited by vacuum thermal evaporation of glassy alloys from quasiclosed effusive cells on cold silica substrates. The structure of glasses, amorphous films and composites on their basis were studied by the methods of Raman spectroscopy and X-ray diffraction.

It was established that all investigated glasses and films have a nanoheterogeneous structure. Their matrix is formed by only binary structural groups $AX_{3/2}$ and AI_3 and also contain insufficiently amount molecular fragments with homopolar bonds A-A and X-X the concentration and morphology of which depend on chemical composition and technological conditions of obtaining.

The structural investigations have shown that the phase structure arising in matrix of glasses of As_2S_3–SbSI, As_2Se_3–SbSI, Sb_2S_3–AsSI partial systems during its crystallization, corresponds to the structure of crystalline SbSI. In matrix of glasses As_2Se_3–SbSeI system formation of needle-like nanocrystals SbSeI in glassy matrix on the As_2Se_3 basis occurs with their further growing. The mechanism of formation of nanocrystals SbSI and SbSeI in glassy matrix is discussed.

The influence of obtaining and crystallization conditions, electric field and laser irradiation on structure, optical and dielectric properties of glasses, amorphous films and composites on their basis in $A_2^{V}B_3^{VI}$–$A^{V}B^{VI}C^{VII}$ system is discussed.

Practical application possibilities of the studied materials are under discussion.

Synthesis and Optical Properties of Layered Diluted Magnetic Semiconductor based Nanoparticles

Savchuk A. I.[1], Stolyarchuk I. D.[1], Savchuk O. A.[1], Stefaniuk I.[2]

[1]*Chernivtsi National University, Chernivtsi, Ukraine*
[2]*University of Rzeszow, Rzeszow, Poland*

Diluted magnetic semiconductors (DMSs) are semiconductors for which a magnetic impurity is intentionally introduced – a small fraction of the native atoms in the hosting non-magnetic semiconductor material is replaced by magnetic atoms. The main characteristic of this class of materials is exhibition of an exchange interaction between the hosting electronic subsystem and electrons originating in the partially-filled d- or f- levels of the introduced magnetic atom. The low-dimensional structures of DMS materials on the basis of traditional II-VI and III-V compounds with magnetic component of Mn, partially in responce to demands coming from spintronics for new and improved materials, has extensively spread throughout several fields of science and technology [1,2]. On the other hand, the layered DMSs type of PbI_2: Me (Me: Fe, Co, Ni…) and related nanoparticles are insufficiently studied.

In this work, we report on fabrication and absorption, photoluminescence (PL) and electron paramagnetic resonance (EPR) studies of colloidal solutions of nanocrystals $Pb_{1-x}Me_xI_2$ (Me: Mn, Co) and the nanoparticles dispersed in the polymer matrix of polyvinylalcohol (PVA), polyvinylpyrrolidone (PVP) and gelatin. For the exciton structure of the absorption spectra of colloidal solutions of nanoparticles except blue shift due to quantum size effect has also been observed dependence of the maximum of the exciton absorption band in the direction of the light beam. The difference in the position of the maximum for orientation c | | z and c $\perp$ z is 5 - 7,5 nm. This behavior is caused by a form of plate-like nanoparticles, that is, the difference in their size relative to the z axis (fold thickness of one monoatomic layer I-Pb-I) and the plane XOY. The room temperature PL spectra of $Pb_{1-x}Co_xI_2$ nanocrystals with concentration of the magnetic component of up to 3% show an intense line at λ =527 nm (2.35 eV). This band can be interpreted by the presence of Co^{2+} ions in the matrix of PbI_2. The X-band EPR spectrum of $Pb_{1-x}Mn_xI_2$ nanoparticles consists of an intense broad line and several weak narrow lines which correspond to hyperfine spectra of Mn^{2+} ions.

1. D. D. Awschalom, D. Loss, N. Samarth Semiconductor Spintronics and Quantum Computation // Springer - Verlag, Berlin Heidelberg. – 2002. - p. 315.
2. R. Beaulac, L. Schneider, P. I. Archer, G. Bacher, and D. R. Gamelin Light-Induced Spontaneous Magnetization in Doped Colloidal Quantum Dots // Science. – 2009. – 325. - p. 973-976.

The Effect of Thin Film Thickness of the Metallic System on the Atomic Interactions and on the Shift of Phase Diagram Curves

Shirinyan A.S.[1], Makara V.A.[1,2], Bilogorodskyy Y.S.[3], Komisarenko O.S.[2]

[1] *"Physical-chemical materials science" center of Kiev Taras Shevchenko National University and National Academy of Sciences of Ukraine, Kyiv, Ukraine*
[2] *Department of metals physics, School of Physics of Kiev Taras Shevchenko National University, Kyiv, Ukraine*
[3] *Cherkasy regional ecological-naturalistic center, Minor Academy of Sciences, Cherkasy, Ukraine*

We investigate energy-related issues of nanosized materials concerning their stability and structure, specifically targeting nanocrystalline metallic thin nanofilms, offer the atomic hypothesis about the size dependence of nearest interactions and coordinated actions of atoms in such solid nanomaterials. The verification have been done for different metalic thin films on the basis of experimental results, theoretical approach and molecular static simulations.

From molecular static calculations we show that one can construct the nanophase diagrams for the case of thin films based on new concepts of size-dependent energies of atomic interaction. The results have been tested for the nanophase diagram construction of binary metallic thin Bi-Sn and Bi-Pb films.

It is shown that for the case of the solid thin films the effect of size on the energy of atomic interaction is found up to 20-30nm. Also, in the frame of the thermodynamic approach one can use the average potential energy of the atomic interaction in the form of a Taylor series and in the simplest case it has the following form: $F(L)=F_{\infty}\{1 - \varepsilon/L\}$. Here F_{∞} – potential energy of atom-atom interaction in a bulk phase and ε is the energy fitting parameter, L – is the thickness of a solid film.

One can formulate the modified atomic concept in the following simple form: "the atom-atom interactions and coordinated actions of atoms in the nanomaterial are different depending on the size of it".

1. Shirinyan A.S., Bilogorodskyy Y.S. Atom–Atom Interactions in Continuous Metallic Nanofilms // The Physics of Metals and Metallography. – 2012. – Vol. **113**, № 9. – pp. 823–830.
2. Ширінян А. С., Білгородський Ю. С. Оцінка впливу розміру металевої наносистеми на енергію міжатомної взаємодії // Вісник Київського національного університету імені Тараса Шевченка: Серія фізико-математичні науки. – 2011. – № **13**. – С. 34-37.

Thin Film of Fullerides: Preparation and Properties

Shpilevsky E.M.

A.V. Luikov of Heat and Mass Transfer Institute NAS Belarus, Minsk, Belarus

Fullerides are the chemical compounds of fullerenes with other chemical elements or their complexes. It is distinguished ekzofullerides (the compaunds with the formation of bonds on the outside of the spherical fullerene carcass) and endofullerides (the compaunds with the location of alien atoms inside of the spherical fullerene carcass). It is known ekzofullerides K3C60, Rb3C60, Cs3C60, Cu6C60, (OH)24C60 [1].

Much attention is paid to the synthesis and study of fullerene hydrides as with the external position of the hydrogen atoms HnC60, so with endohedral Hn@C60. The interest to these compounds is due to the fundamental possibility to use them for compact and safe storage of hydrogen. Studies of compounds (OH)nC60 resulted in a water-soluble forms of fullerenes. The variety of chemical compounds of fullerenes provides a wide diversity of their chemical and physical properties depending on the embedded metal or complex. That provokes a great interest to this compounds.

The obtaining of chemical compounds of fullerenes with the external arrangement of atoms of olien elements ekzofullerides is carried out on the usual way of chemical reactions: the bringing to the desired distance and the ensuring the required temperature, allowing to occupy a certain geometric and energy position. To formate endofullerides fthe olien atoms must overcome a higher energy barrier and penetrate into the carcass of the fullerene molecules. This can be achieved in two different ways:

1) the creation of such conditions when in the process of synthesis of fullerene molecules some part of fullerene molecules is filled with atoms or molecules of an alien element which is in the zone of synthesis;

2) the penetration of atoms or molecules into the carbon csrcassof ready fullerene molecules.

The educing of fullerides in both cases was carried out by extraction and chromatographic methods. The thin films jf fullerides were obtained by thetraditional method of evaporation and cjndensation in vacuum.

To realize the first method the arc electric method is most often applied. It produces endofullerides in macroquantity. For the second method the ion implantation is used.

However, the procedure of educing of endohedral fullerenes in pure statein macroscopic quantities is extremely labourious. Thus, to obtain10 mg of Y@C82 it is necessary to carry out 40 - 50 chromatographic loadings during 25 - 35 hours, requiring 30 -40 liters of toluene.

The phisic-chemical properties of endofullerides are determined by the features of their electron structure. Since the inner diameter of the fullerene shell is much larger than the diameter of encapsulated atom, during the transmission

of valence electrons onto the outer surface of the fullerene shell the displacement of the equilibrium position of the encapsulated atom relative by to the geometric center of the fullerene shell take place. That determines the significant permanent dipole moment of such molecules. In turn, the dipole moment of the molecules gives them the definite orientation in the crystal, providing a constant polarizability of such crystals. Endofullerides usually have highly anisotropic properties, many of them are segnetoelectric.

Rearrangement of the electronic structure of endohedral complex leads to the fact that the metal atoms are passed on their valence electrons in part or in full, on the outer part of the fullerene carcass, almost losing its chemical identity. The transition of valence electrons of the metal on the outer shell is reflected at the electronic properties of molecules such as its ionization potential, electron affinity, conductive capacity.

It is discovered superconductive properties of fullerides, it is found that the temperature of superconductive transition of alkali metal fullerides is linearly dependent on the lattice constant [2]. For fulleride of copper superconductive transition temperature is 120 K [3]. It is obtained a new substance Cu6C60 [4], which has a high emission properties [5].

To indicate endofullerides the formula used Mm@ Cn, where M - encapsulated atom or molecule, and the subscripts m and n show the number of such atoms and the carbon atoms in a fullerene molecule, respectively. For example, K@C60 is read: "fullerene60-incar-kalium". At present, a large variety of endofullerides is known: Li@C60, Na@C60, K@C60, N@C60, Pr@C60, Nd@C60, Gd@ C60,La@C60 and La2@C60, La@C82, Er@C82 etc. Depending on the type and number of atoms within a spherical carcass endofulleridy can have both acceptor and donor properties [6].

Thus, the films of fullerides are a new class of objects that have unique physical and chemical properties and are very promising for practical use.

1. Shpilevskii M. É., Shpilevskii É. M., Stel'makh V. F. // Journal of Engineering Physics and Thermophysics. 2001. V. 74. No 6. P. 1499—1508.
2. Markin A.V., Smirnova N.N., Bykova T.A., Ruchenin V.A., Titova S.N., Gorina E.A., Kalakutskaya L.V., Ob’edkov A.M., Ketkov S.Yu., Domrachev G.A.// J. of Chemical Thermodynamics. – 2007. V.39. No5. – P. 798-803.
3. Masterov V.F,.Popov B.P, Prihodko A.V.// FTT, -1995. V. 37. P.
4. Baran L.V. Shpilevsky E.M, Okatova G.P. // Advanced Materials. 2004., № 4, P. 76-81.
5. Shpilevsky E.M., Litovchenko V.G., Baran L.V., Evtukh A.A., LA Matveeva, Semenenko N.A// Fullerenes and fullerene-like structures. Minsk: Institute of Heat and Mass Transfer. NA of Belarus, 2005. – P. 22-31.
6. Popov M., Buga S., Vysikaylo Ph., Stepanov P., Tatyanin E., Medvedev V., Denisov V., Kirichenko A., Aksenenkov V., Skok V., Blank V. Phys. Status Solidi 2011.V. A 208. P. 2783–2789.

Electron Transport Phenomena in Ultra Thin Metal Films

Stasyuk Z.V., Bihun R.I.

Ivan Franco Lviv national university, Lviv, Ukraine.

Thin layers of substance are basic elements of many devices of modern electronic techniques. The further development of electronics is impossible without microminiaturisation of electronic systems by nanotechnology, in particular, by techniques of electrically stable ultrathin-thickness covering formation. Properties of ultrathin slabs can essentially differ from properties concerning thick layers which are used in nowadays engineering. This difference first of all is caused by prevailing influence of the surface phenomena on ultrathin layer structure and electric parameters.

The current theoretical and experimental researches on electron charge transport in ultrathin (layer thickness are 2-12 nm) electrically continuous metal films (temperature coefficient of resistance $\beta > 0$) under the condition of inequality realisation $d < l$ were analysed and reviewed. Here d is the film thickness, l is the charge mean free path. The peculiarities of film structure are meant as crystal lattice parametres and the crystalline average linear sizes.

The fabrication of ultrathin electrically continuous metal film on dielectric substrate surface is a problem of considerable difficulty due to the action of surface tension forces. These phenomena lead to coagulation of metal particles. As a result there is some critical thickness layer d_c at which current starts to flows (***percolation threshold*** is observed here). The technological features of film formation (the speed of material condensation, the substrate temperature at layer deposition, the modes of further heat treatment) defines the average of d_c as well as the properties of condensate material, in particular fusion temperature. Essential decrease d_c may be reached at epitaxial growth of metal film on the oriented substrate. The other effective way of d_c decrease is preliminary deposition of surfactant underlayers of superficially active substances of a subatom thickness on dielectric substrate wich preveling coagulation of metal condensates. This technique allowed the formation of ultrathin conductive coverings. In particular, the Hall voltage investigation on 1-3 nm thicknees chrome films deposited on surfactant germanium underlayer was performed in [1].

The electron transport phenomena are essentially influenced by electron scattering on film surface when the mean free path of electron becomes commensurable to the thickness of a metal film d. Thus the contribution of surface scattering in the total electron relaxation time is close to the contribution of bulk scattering. The thickness dependence of kinetic parameters of electrically continuous metal films is described within the framework of the classical and internal size effect theories [2].

With further reduction of metal layer thickness when the electron mean free path satisfies the condition $d < l$, the quasiballistic electron transport in a film (without changes of the power spectrum of electron in metal film) is presented. Thus charge carriers surface scattering in metal film becomes dominating. The contribution of surface scattering has essentially influenced the macroscopic surface inhomogeneity because the mean linear grain sizes are commensurable to

film thickness. The quasiballistic electron transport in metal films can be described by size dependencies of kinetic coefficients proposed in Namba theory and within the framework of polycrystalline layer heterogeneous cross section [2]. The treatment of experimental data by the mentioned theories allows the reliable calculation of the average amplitude of one-dimentional surface asperity h. The calculated values h well coordinate with experimental data of direct STM and AFM investigation.

When the film thickness does not exceed 5 - 8 nm the quantum effects which have influence on electron transport in film are possible. Existence of changes in the transport phenomena caused by dimensional quantization was predicted by I.M.Lifshitz and A.N.Kosevich [3]. Quantum size effects are most brightly displayed in semimetal films. The length of an electron de-Brogle wave length in these materials in 10 times exceeds interatomic distances and consequently the interference of electronic waves is influenced poorly by imperfections of film surface. In metal films the situation is essentially different as a de Brogle electron wave length is commensurable to interatomic distances. Therefore, to observe oscillation of the kinetic coefficients in thin metals layers it is necessary to provide high perfection surface structure. In the quantum electron transport range of films thickness the laws of residual conductivity size dependensis $\sigma_{res}=1/[\rho(d)-\rho_{\infty}]$ takes place. The theoretical expressions are most convenient for direct experimental comparison with theoretical data has been received by Fishman and Calecki [4]. The expression for residual conductivity may be written in form: $\sigma_{res} \sim d^{\alpha}$, where α are changing from 2,1 (pure metals) to 6 (semiconductors). Physical understanding of α parameter can be taken in the framework percolation theory. Electron transport in percolation metal films successfully can be treated with simple expression:

$$R \sim (d-d_c)^{-\gamma}.$$

where R – resistance of metal films, d – metal film thicknees, d_c – critical thickness corresponding to p_c (percolation threshold at which first ohm conduction channel appears), γ – percolation exponent. Analyzing the value of γ we can predict mechanism of metal film growth [5].

Modern theoretical approaches of quantum size effect in kinetic phenomena of metal films are based on assumption that the metal sample electronic structure is the same as in bulk materials. Quantum size effect in metal film is a consequence of electron system size limitation along Z axis in thin film thickness direction. Calculation of the electron band structure of metal film by various theoretical approaches well known in literature shows major distinction in electron structure parameters computed data. Therefore, it is very difficult to establish the precise criteria of quantum size effect models application region.

1. Schroder K., Zhang L. Phys. Stat. Sol. B.- 1994.- Vol.183.- P.k5-k8.
2. А.П. Шпак., Р.І. Бігун., З.В. Стасюк., Ю.А. Куницький. Наносистеми, наноматеріали та нанотехнології.– 2010.– Т. 8, № 2.– С. 1001-1050.
3. И.М. Лифшиц А.М. Косевич. Изв. АН СССР, сер.физ, 19, 395, (1955).
4. Calecki D., Fishman G., Phys.Rev.Lett.,62, 1302-1305, (1989).
5. Smilauer P. Thin metal films and percolation theory. Contemporary Physics, 1991, Vol. 32, N. 2, P. 89-102.

Photoluminescence Characterization of CdTe Polycrystalline Films

Tetyorkin V., Sukach A., Boiko V., Stariy S. and Tkachuk A.[1]

V. Lashkaryov Institute of Semiconductor Physics NAS of Ukraine
[1]V.Vinnichenko Kirovohrad State Pedagogical University

Photoluminescence spectra are investigated in polycrystalline CdTe films grown by a modified close-space sublimation technique on sapphire substrates. The mean grain size in the investigated films was ranged from ~10 to ~400 μm. The as-grown films had resistivity of the order of 10^5-10^6 Ω×cm at room temperature. They exhibited high photosensitivity and stable electrical parameters after multiple temperature cycling as well as during the long-term storage at ambient laboratory conditions. A number of the photoluminescence spectral bands associated with bound excitons, dislocations and deep impurities were observed at 77 K. Typical energies of these bands are as follows: 1.580, 1.440 and 0.85-1.05 eV, respectively. Their intensity is shown to depend strongly on the grain size. These experimental data were used to elucidate the spatial origin of the photoluminescence bands.

The most intensive luminescence lines were found to be centered at 1.580 and 1.440 eV. The spectral lines at higher energy is near the band gap of CdTe (1.590 eV at 77 K) and are usually ascribed to excitons localized at shallow donors or acceptors. This assumption was supported by measurements of photoluminescence intensity versus laser power in the films with different size of grains.

The intensity of the dislocation luminescence at 1.440 eV is found to be proportional to the density of grain boundaries. Thus, it has been concluded that dislocations are mainly located at the grain boundaries. A model of grain boundaries as dislocation networks is discussed in relation with the obtained experimental data.

By comparing the luminescence spectra measured for two excitation geometries (surface-side and substrate-side illumination), the nonuniform distribution of deep defects inside the grains is revealed.

Experimental results are analyzed in terms of possible improvements of solar cells based on CdTe polycrystalline films.

Synthesis and Characterization of Colloidal CdTe Nanocrystals

Tomashik V.M., Kapush O.A, Trishchuk L.I., Tomashyk Z.F.

V.Ye. Laskaryov Institute of Semiconductor Physics of NAS of Ukraine, Kyiv, Ukraine

The quantum dots of cadmium chalcogenides attract the great interest of researchers. Quantum size effects are observed more clearly in CdTe nanocrystals (NCs) than in CdS and CdSe because of a large exciton Bohr radius. Nevertheless, CdTe are the least investigated, which is due to the decomposition of some Te (II) compounds and their high toxicity.

The most popular methods of NCs obtaining now are the methods, based on the using of the self-organization phenomena, one of which is the method of colloidal chemistry. It is possible to synthesize nanocrystals with sizes in a few nanometers in a diameter (2-10 nm) using the last method. A bandgap and energy of luminescence of such NCs depends strongly on their sizes. Therefore the size, form and surface properties of nanosize materials must be adapted and optimize for the specialized application.

The physicochemical properties of nanosized systems based on CdTe, obtaining by mechanical milling and colloidal synthesis have been investigated.

We used highly dispersed CdTe, obtained by grinding of single crystal blocks grown by the Bridgman method. As a stabilizer of the particle surfaces thioglycolic acid was used, and as a dispersion medium deionized water, methanol, ethanol, propanol, isopropanol, butanol, isobutanol, pentanol, isopentanol, heptanol, nonanol were chosen. Our studies confirm the suggestion of a significant effect of solvent on the processes of stabilization of surface of CdTe low-dimensional particles. Analysis of the data allows to conclude that it should be better to carry out of stabilization of particles of CdTe in the high dispersed and nanosized systems by using methanol and ethnol as a solvent. These results can be used in the design and optimization techniques for obtaining of CdTe NCs by colloidal synthesis.

Colloidal synthesis was carried out by the use of ions of cadmium precipitated by ions of tellurium under an argon atmosphere in a three-necked flask equipped an electromagnetic mixer, thermometer, partitions and valves. Electrochemically obtained in a galvanostatic cell H_2Te was used as Te^{2-} source. Deionized water, aqueous solutions of 10-50 % ethylene glycol and 5-25 % glycerol have been used as the solvent. For stabilization of CdTe NCs surface during the synthesis tioglycol acid, oxyethylenediphosphonic acid, ethylenediaminetetraacetic acid, L-cysteine and thiourea were used. To reduce the influence of the nature and quantity of precursors on the optical properties of CdTe NCs we have also developed a method of post synthetic treatment of initial solution.

Near-Field Induced Nanostructuring of Amorphous Chalcogenides: Towards Optical Nanoimaging and Nanolithography

Trunov M.L.[1,2], Lytvyn P.M.[3], Nagy P.M.[4], Durkot M.O.[1], Dyachyns'ka O.M.[3], Rubish V.M. [1]

[1]*Uzhhorod Scientific-Technological Center of the Institute for IIR, Uzhhorod, Ukraine*
[2]*Uzhhorod National University, Uzhhorod, Ukraine*
[3]*V. Lashkaryov Institute of Semiconductors NAS Ukraine, Kiev, Ukraine*
[4]*Research Centre for Natural Science, Budapest, Hungary*

In this report we demonstrate how a surface plasmon generated near- field pattern in the vicinity of nano-scale gold particles (NGP) can be used to generate reversible topography changes in a photosensitive material layered over the nanoparticles. Appropriate light-sensitive layers of chalcogenide glasses (ChG), covering NGP as sublayer, previously arranged on the substrate, have been produced and used for direct all-optical surface relief fabrication.

Recently we detected that under the irradiation of the polarized light beam, giant surface relief happen due to the mass transport in some selected films of ChG [1]. Moreover, the photoinduced changes in surface relief are reversible and can be erased by polarized light [2]. These unique properties make the ChG a promising material for optical components that can be actively controlled. It was found that both in the NGP array/ChG and in the gold film with nanohole/nanoscratch array/ChG the plasmon fields, induced during the laser illumination of the structures, increase the efficiency of mass-transport and produce reversible surface nanostructuring. Using *in situ* recorded atomic force microscopy images of surface topography alterations during band-gap irradiation, we find that the response of the film differs for different compositions at similar geometries of the metal nanostructures. The maximum topography variation is higher for Se-reach film in As-Se system, whereas in the other material, the phenomenon is less visible and a variation in the opposite direction was revealed. The variation in the topography follows closely and permanently the underlying near field intensity pattern. The results, obtained for structures with $As_{20}Se_{80}$ amorphous layer, can be applied for other selected chalcogenide layers and fabrication of locally driven information recording media and mapping of surface plasmon intensity distribution.

1. M.L. Trunov, P.M. Lytvyn, P.M. Nagy et al. Real-time atomic force microscopy imaging of photoinduced surface deformation in As_xSe_{100-x} chalcogenide films // Appl. Phys. Lett. – 2010. – V. **96**, – P. 111908 (3 pages).
2. Yu. Kaganovskii, M.L.Trunov, Beke, S. Kökényesi. Mechanism of photo induced mass transfer in amorphous chalcogenide films // Materials Letters – 2011. –V. **66**, – P. 159–161.

Acknowledgements One of the authors, M.L.T. acknowledges support from International Visegrad Fund.

Preparation and Properties of Composite Coatings and Metal-Metalloid alloy Coatings for Different Applications

Tsydulskaya L.S., Gaevskaya T.V., Bekish Yu.N.

Research Institute for Physical Chemical Problems of the Belarusian State University, Minsk, Belarus

Functional metal-metalloid alloy coatings and nickel- and cobalt-based, composite coatings involving carbon nanomaterials (ultradispersed diamond particles, fullerenoles, etc.) have been prepared by electroplating from aqueous electrolytes. Incorporation of metalloids (boron, phosphorus) into the Ni and Co lattices as well as inclusion of nanosized carbon particles into the coatings leads to a significant improvement of their physical-mechanical, electrical properties and corrosion stability. The coatings have a thickness of 5-100 μm depending on the coating specifications.

Novelty of the proposed technology is in the following. We have developed new bath formulations, optimized the operating conditions, proposed several variants of the technology of Ni-B, Co-B, Ni-P, Co-P and composite Ni-carbon nanoparticles coating electroplating on different metal substrates (copper and its alloys, aluminum and its alloys, steel, titanium, etc.).

Organic boron compounds (belonging to the class of amine boranes and derivatives of higher boranes) were used as boron-containing additives; phosphoric acid was used as a phosphorus-containing additive.

Basing on the performed researches we have shown that the content of metalloid component in the alloy can be varied from 1.5 to 22.5 at. % by changing the concentration of boron- and phosphorus-containing additives in the electrolytes of Ni and Co electroplating, the current density and the pH of electrolyte. Transformation of the coating structure from polycrystalline to amorphous-polycrystalline and finally to amorphous (at the B or P content ≥ 15 at.%) occurs with increasing the boron or phosphorus content in the alloy. As the metalloid content increases, the Ni lattice parameter a and the α-Co lattice parameters a and c, the size of alloy crystallites and the average roughness coefficient decrease. With increasing the boron and phosphorus content the microhardness of the Ni-B, Co-B, Ni-P and Co-P coatings increases by 2.3-3.7 times as compared with Ni and Co coatings and the wear rate decreases by 20-160 times. Contact resistance for polycrystalline Ni-B coatings remains not high (3-5 mOhm) and is close to the values typical of nickel, gold and silver coatings. Electrochemically deposited Ni-B and Ni-P coatings are easily soldered using a low-active flux and a low-temperature solder. They are well welded by ultrasound with an aluminum conductor (the pullout force is 1,5-3 times higher than that for Ni coatings) and also have a high corrosion stability in chloride-containing medium [1].

1. Bekish, Yu. N. Poznyak S.K., Tsybulskaya L.S., Gaevskaya T.V. // lectrochim. Acta. 2010. V. 55. P. 2223-2231.

Optical Properties of ZnSe Crystals Doped with Transition Metal Elements

Vaksman Yu.F., Nitsuk Yu.A.

I.I. Mechnikov National University, Odessa, Ukraine

The interest in research of wide-gap semiconductor crystals doped with transition elements impurities has increased considerably during the past few years. This is due to wide application of such materials as active media and passive gates of lasers emitting in the mid-infrared (IR) spectral region.

In this case, there are actual problems of optimum technology for obtaining crystal elements doped by the transitional metals. The results of the past few years' research testify to the preference of diffusion doping methods. However, the parameters of transition metals impurities diffusion process are not certain. Information about absorption and luminescence spectra is represented for the IR-region, mainly. At the same time, the optical characteristic features in the absorption edge region were not examined.

In this study, ZnSe: Cr, Co, Ni, Fe crystals obtained by diffusion doping are investigated. We suggest a method for determining the indicated impurities diffusivities that is based on an analysis of crystals optical-absorption spectra[1]. The Cr, Co, Ni, Fe diffusivities (*D)* and diffusion process activation energy (E_D) of ZnSe crystals is determined for the first time (see table).

The optical absorption spectra and luminescence in the visible and near infrared wavelength regions are studied and identified. The agreement of the theory calculated energy spectra and experimentally obtained absorption and emission spectrum is established. The depth of the ground state levels (E_i) of the Cr, Co, Ni, Fe impurities in the ZnSe lattice is calculated. The visible region photoluminescence lines that are characteristic for these impurities, conditioned by intracentre optical transitions are found out.

Table. Diffusion and optical properties of investigated crystals

Impurity type	E_D, eV	D, sm^2/s	E_i, eV
Cr	4.45	$4\cdot10^{-9}$	0.3
Co	3.8	$5\cdot10^{-10}$	0.24
Ni	3.48	$5\cdot10^{-8}$	0.19
Fe	2.86	$3\cdot10^{-11}$	0.07

1. Ваксман Ю.Ф., Павлов В.В., Ницук Ю.А., Пуртов Ю.Н., Насибов А,С., Шапкин П.В. Оптическое поглощение и диффузия хрома в монокристаллах ZnSe// Физика и техника полупроводников.-2005.-Т.39,в.4.-С.401-404.

Surface Plasmon-Phonon Excitations in ZnO Films Placed on Optically Anisotropic Substrates

Venger E.F.[1], Melnichuk L.Yu.[2], Melnichuk O.V.[2]

[1]*Institute of Semiconductor Physics V. Lashkarev NAS Ukraine, Kyiv, Ukraine*
[2]*Nizhyn Gogol State University, Nizhyn, Ukraine*

Despite the large number of scientific papers, films of metal oxides placed on dielectric and semiconductive optically isotropic and optically anisotropic substrates retain till nowadays scientific and practical interest and are widely used in opto- and nanoelectronics.

The report highlights the results of surface excitations study in transparent, highly texturized ZnO single crystals placed on dielectric and semiconductive "semiinfinite" substrates Al_2O_3 and 6H-SiC with the thickness of 0,1 up to 1 μm and with concentration of electrons $n_0=(0,05\div5)\cdot10^{19}\,cm^{-3}$. The films were cultivated using low-temperature plasmochemical vapor deposition of doped In, Al, Ga.

Presented theoretical studies of surface plasmon-phonon excitations were obtained using highly oscillatory mathematical model with additive deposite of oscillators into permittivity of heavily doped ZnO films, placed on the indicated substrates, taking into account phonon and plasmon-phonon anisotropy in them.

Using the analysis of variance of attenuated total reflection of bilayer structures in the range of 400 ÷ 1000 cm^{-1} electrical characteristics of ZnO films placed on substrates Al_2O_3 and 6H-SiC were determined. It was specified that ZnO films' mobility remains within $m_L=10\div90\,cm^2/(V\cdot c)$ and conductivity $s_0=80\div220\,Om^{-1}\cdot cm^{-1}$, which is consistent with the data obtained using IR reflection spectroscopy and so on.

In heavily doped ZnO films, placed on optically anisotropic semiconductive 6H-SiC substrate with concentration of electrons $n_0=(0,5\div5)\cdot10^{19}\,cm^{-3}$ and orientation $K\perp C, xy\perp C$, the excitation of new dispersion branches in highly dispersive range of spectrum of 620÷800 cm^{-1} was observed, this was caused by plasmon-phonon anisotropy and its linkage to long-wave optical phonons in the film and the substrate. The criteria of their excitation and propagation were determined. It was detected that the number of dispersion branches in ZnO changed by changing the concentration of free charge carriers and that the maximum amount of dispersion branches is three. It is shown that surface plasmon-phonon polariton excitations of third and fourth types exist in the limited range of values of the wave vector.

It was established that with the decrease of ZnO film thickness, ZnO low-frequency dispesion branch shifted to short- and high-frequency branch and high-frequency branch shifted to long-frequency IR area. Increasing the thickness of ZnO film leads to the reduction of cutoff frequency of surface phonon polaritions of sapphire.

Impact the Sb-cup-Covering and Annealing Treatment on the Optical and Magnetic Properties as Well as on the Electronic and Band-Structure of the (Ga,Mn)As Epitaxial Layers

Yastrubchak O.[1], Żuk J.[1], Domagala J.Z. [2], Andrearczyk T.[2], Sadowski J.[2,3], and Wosinski T.[2]

[1]*Institute of Physics, Maria Curie-Skłodowska University, Lublin, Poland*
[2]*Institute of Physics, Polish Academy of Sciences, Warszawa, Poland;*
[3]*MAX-Lab, Lund University, Lund, Sweden*

The ternary III-V semiconductor (Ga,Mn)As has recently drawn a lot of attention as the model diluted ferromagnetic semiconductor, combining semiconducting properties with magnetism. (Ga,Mn)As layers are usually gown by the low-temperature molecular-beam epitaxy (LT-MBE) technique. Below a magnetic transition temperature, T_C, substitutional Mn^{2+} ions are ferromagnetically ordered owing to interaction with spin-polarized holes. However, the character of electronic states near the Fermi energy and the valence-band structure in ferromagnetic (Ga,Mn)As are still a matter of controversy.

There are two alternative models of the band structure in (Ga,Mn)As. The first one assumes mobile holes residing in the valence band of GaAs and the Fermi level position determined by the concentration of valence-band holes. The second one involves persistence of the narrow, Mn-related, impurity band in highly Mn-doped (Ga,Mn)As with metallic conduction. In this model the Fermi level exists in the impurity band within the band gap and the mobile holes retain the impurity band character.

The photoreflectance (PR) spectroscopy was applied to study the band-structure evolution in (Ga,Mn)As layers with increasing Mn content. We investigated (1000 - 700nm and 230 – 300nm) (Ga,Mn)As layers with Mn content in the range from 0.001% to 6% and, as a reference, undoped GaAs layer, grown by LT-MBE on semi-insulating (001) GaAs substrates. Photoreflectance studies were supported by Raman spectroscopy and high resolution X-ray diffractometry (XRD) measurements and magnetic properties of the (Ga,Mn)As films were characterized with a superconducting quantum interference device (SQUID) magnetometer. In addition, we investigated impact of the Sb cap-covering and annealing of thin (50 -250 nm) (Ga,Mn)As layers with 6% of the Mn content on the electronic and band structure as well as on the electrical and magnetic properties of these films. Our findings were interpreted in terms of the model, which assumes that the mobile holes residing in the valence band of GaAs and the Fermi level position determined by the concentration of valence-band holes [1].

1. O. Yastrubchak, J. Zuk, H.Krzyzanowska, J.Z. Domagala, T. Andrearczyk, J. Sadowski,T. Wosinski, **Physical Review B**, Volume 83, 245201, 2011.

Crystal-chemical dependence of energy redistribution of valence electrons in nanomaterials and increase of oxygen charge state at mechanochemical activation of oxide nanocomposites

Zaulychnyy Ya.

National Technical University of Ukraine "Kyiv Polytechnic Institute", Kyiv, Ukraine

Unique properties of nanomaterials are determined by energy contribution of surface atoms interaction in total energy of nanoparticles.

It has been revealed that energy redistribution of valence electrons after transition from bulk to nanosize state is a consequence of disappearance of energy splitting of levels and change of their location when bonds of surface atoms break.

Study of this effect in materials with different bond types and atomic-crystal structures has showed that in covalent crystals distribution become narrower due to dehybridization of sp^2– and sp^3–states and increase of level density in high-energy part of valence band. In covalent-ion crystals value of redistribution of electronic states is proportional to their occupation and in ion-covalent crystals density of occupied nonbinding O*p*-levels increases due to break of covalent-binding anion-anion states.

It has been found that redistribution of electronic states in high-energy region of valence bands in crystals causes increase of band energy $\int_{E_0}^{E_F} N(E)EdE$, where E_0 is the bottom of valence band, E_F is energy of Fermi level.

It has been showed that energy levels after disappearance of splitting shift towards the lower energies especially for nonbinding O*p*-states due to relaxation of broken bonds by means of appearance of π-binding orbitals between surface atoms of amorphous nanooxides and turbostratic BN_g.

Mechanochemical synthesis of x-Al_2O_3+y-SiO_2, x-SiO_2+y-TiO_2, x-Al_2O_3+y-TiO_2 and Al_2O_3-SiO_2-TiO_2 nanocomposites causes energy redistribution of Me*sd* and O*p*-states that leads to increase of oxygen charge state in composited in comparison with mixture of nanooxides.

Segregation of Rare-Earth Impurity of *Eu* in the *PbTe*:*Eu* Crystals Grown from Doped Melts

Zayachuk D.M.[1], Ilyina O.S.[1], Pashuk A.V.[1], Mikityuk V.I.[2], Shlemkevych V.V.[2], Ulyanitsky K.S.[2], Scik A.[3], and Kaczorowsky D.[4]

[1]*Lviv Polytechnic National University, Lviv, Ukraine*
[2]*Yuri Fedkovich Chernivtsy National University, Chernivtsy, Ukraine*
[3]*Institute of Nuclear Research, Hungarian Academy of Sciences, Debrecen, Hungary*
[4]*Institute of Low Temperature and Structure Research, Polish Academy of Sciences, Wroclaw, Poland*

The rare earth elements have been used for a long time for controlling of physical properties of the semiconductor crystals and films and for fabrication of the different electronics structures. The sizeable parts of the investigations of the semiconductors doped on the rare earth impurities have been carried out in the crystals grown from melt. The presented report is devoted to the further study of the problem of behavior of rare earth impurities in semiconductors and concentrates on the comparative investigation of the behavior of the *Eu* impurity into the surface and bulk layers of the doped *PbTe:Eu* crystals grown from melt.

The *PbTe:Eu* single crystals were grown by Bridgman method from the melt with different initial concentration of *Eu* impurity about $1\cdot10^{20}$ cm^{-3} and fewer and were investigated by the methods of X-ray fluorescent element analysis, secondary neutral mass spectroscopy, and magnetic measurements.

It is revealed that character of distribution of doping impurity into the doped crystal cardinally depends on the initial concentration of impurity in the melt. If the concentration is about $1\cdot10^{20}$ cm^{-3}, Europium is distributed over the entire cross section of the doped ingot. In this case, the concentration of doping impurity into the surface layers of doped ingot is somewhat larger than the concentration of *Eu* in the bulk of crystal. If the initial impurity concentration into the melt is very small, for example about 10^{19} cm^{-3}, practically all the impurities can be pushed out onto the lateral surface of the crystal ingot. Thickness of the doped surface layer to be estimated about several microns or slightly more. Also it is possible to establish specific conditions for the growth of a doped crystal under which the impurity behavior will be opposite to that described above, i.e., the impurity will not be pushed out onto the lateral surface, but conversely will be pulled into the bulk of the crystal spreading along the doped crystals farther than usually.

It is shown that both the longitudinal distribution of *Eu* impurity along of axis of doped ingot if the initial *Eu* concentration in the melt is about $1\cdot10^{20}$ cm^{-3} and the cross one in the surface layer where entire doping impurity is pushed out if the initial *Eu* concentration in the melt is about $1\cdot10^{19}$ cm^{-3} are significantly non-monotonic. Possible reasons for so unusual behavior of *Eu* doping impurity during the growth of *PbTe:Eu* crystals from the melt are analyzed.

Interaction in ZnS (ZnO) – Sb_2S_3 – Ge System and Parameters of Obtained Thin Films

Zinchenko V.F.[1], Mozkova O.V.[2], Chygrynov V.E.[2], Magunov I.R.[1]

[1]*A. V. Bogatsky Physico-Chemical Institute of NAS of Ukraine, Odessa, Ukraine*
[2]*State Enterprise for Special Instrument Making "Arsenal", Kyiv, Ukraine*

Zinc silfide, Antimony sulfide and Germanium are basic materials for IR-optics, in particular for night-vision techniques [1]. Oxide admixtures cause the decay of optical and technological parameters of above mentioned substances, especially in thin-film coatings. Besides, Sb_2S_3 forms a rather soft and in stable coating. The positive effect of the Ge additives on the characteristics of coatings from ZnS is reported earlier [2]. The Sb_2S_3 additive to ZnS is able to eliminate ZnO impurity almost entirely [3]. But the rest of additive results in a sharp decay in adhesion of coating to substrates from various materials. The problem is solved using an additive of Ge, which reacts with Sb_2S_3 through CVD mechanism. Zinc silfide purified from oxide admixtures in two-stage way exhibits good optical (scattering coefficient about 0.07%) and very high mechanical durability (30,000 rotations, ten times higher than required for group 0). It was wonder to learn does the additive of Ge affect optical and technological properties of Sb_2S_3, not only its volatility. Thermodynamic calculations show that the reaction of Sb_2S_3 with Ge volatizing, described by the scheme:

$$Sb_2S_3 + Ge \xleftrightarrow{t,vac.} 2SbS\uparrow + GeS\uparrow,$$

should be possible even at rather low temperatures (below 400°C, when evaporation of components becomes noticeable). The changes of composition are suggested by the XRPD data and IR transmittance spectra. Thin-film coatings obtained by the thermal evaporation of Sb_2S_3 – Ge sample in deep vacuum showed a significant enhancement of the adhesion to the substrates and mechanical durability (up to 4,000-4,500 rotations, i.e. to group 0) compared with pure Sb_2S_3 (1000 rotations, i.e. worse than group 3). Thus, materials based on the mentioned system may be regarded as very perspective ones for far IR interval of spectrum.

1. Справочник технолога-оптика / М.А. Окатов, Э.А. Антонов, А. Байгожин и др. Под ред. М.А. Окатова. 2-е изд., перераб. и доп.–СПб.: Политехника, 2004.–679 с.
2. Зінченко В.Ф., Кочерба Г.І., Магунов І.Р., Мозкова О.В., Соболь В.П., Бєлявіна Н.М. Оптичні властивості тонкоплівкових покриттів, одержаних з композитів ZnS-Ge методом CVD // Фізика і хімія. твердого тіла.–2011.–Т.**12**, №2.–С. 433-437.
3. Зинченко В.Ф., Магунов И.Р., Садковская Л.В., Стоянова И.В., Тимухин Е.В., Витюкова Е.О., Ковалевская И.П. Взаимодействие в системе ZnS-ZnO-Sb_2S_3 // Укр. хім. журнал.– 2011.–Т.**77**, №12.–С.78-82.

СЕКЦІЯ 1 (усні доповіді)
ТЕХНОЛОГІЯ ТОНКИХ ПЛІВОК (МЕТЕЛИ, НАПІВПРОВІДНИКИ, ДІЕЛЕКТРИКИ, ПРОВІДНІ ПОЛІМЕРИ) І МЕТОДИ ЇХ ДОСЛІДЖЕННЯ

21-24 травня 2013 р.

SESSION 1 (oral)
THIN FILMS TECHNOLOGY (METALS, SEMICONDUCTORS, DIELECTRICS, CONDUCTIVE POLYMERS) AND THEIR RESEARCH METHODS

May, 21-24, 2013

The features of Pd_2Si-n^+-Si Interface Formation in Au-Pt-Ti-Pd_2Si-n^+-Si Ohmic Contact

Belyaev A.E.[1], Pilipenko V.A.[2], Petlitskaya T.V.[2], Turtsevich A.S.[2], Sachenko A.V.[1], Konakova R.V.[1], Boltovets N.S.[3], Korostinskaya T.V.[3], Kudryk Ya.Ya.[1], Vinogradov A.O.[1], Sheremet V.N.[1]

[1]V. Lashkaryov Institute of Semiconductor Physics, NAS of Ukraine, Kyiv, Ukraine
[2]Public Corporation "Integral", Minsk, Belarus
[3]State Enterprise Research Institute "Orion", Kyiv, Ukraine

Anomalous temperature dependence of contact resistivity $\rho_c(T)$ (ρ_c grew with T) in ohmic contacts to semiconductors with high dislocation density was found and studied in [1-6]. The authors of [1, 2, 4] assumed metallic conduction through shunts of atomic sizes formed due to metal mass transport over dislocations that appeared in the near-contact region of semiconductor because of relaxation of intrinsic stresses. The calculations of $\rho_c(T)$ and experiments [5, 6] showed adequacy of the assumption [1]. We performed some experimental investigations to get direct proof of appearance of high dislocation density in that case, in particular, for Si.

The TLM (transmission line method) structures were prepared on heavily doped n^+-Si substrates to measure $\rho_c(T)$ in the 100-400 K temperature range, as well as test structures with continuous Au-Pt-Ti-Pd_2Si-n^+-Si metallization were made for structural and analytical studies. The metals were deposited in a single technological cycle using layer-by-layer thermal deposition in a vacuum onto a substrate heated to 350 °C. Some specimens were annealed in a vacuum at T = 450 °C for 10 min. A defect analysis of structures was made according to the conventional procedure. All the layers were removed from Si surface using hydrofluoric acid, aqua regia and hydrogen peroxide, with further etching in Wright etch at room temperature for 90 s.

The prepared contact-forming layer involved mainly Pd_2Si phase. After annealing structural defects (in particular, dislocation loops with density over 10^{10} cm^{-2}) were produced in a thin near-contact Si layer. A columnar structure (involving ~26% Si, 15% Au and 15% Pt) was observed at contact metallization cleavages. Judging from the $\rho_c(T)$ curve, such a spatially distributed configuration of the contact-forming layer led to ρ_c growth with temperature. Thus, the experimental results confirmed appearance of high dislocation density in the Si near-contact region in the course of ohmic contact formation due to annealing.

1. T.V. Blank et al. PZhTF 30(19), 17 (2004).
2. T.V. Blank et al. FTP 40(10), 1204 (2006).
3. Zhang Yeuzong et al. Chin. J. Semicond. 22(6), 984 (2007).
4. T.V. Blank et al. FTP 43(9), 1204 (2009).
5. A.E. Belyaev et al. SPQEO 13(4), 436 (2010).
6. A.V. Sachenko et al. J. Appl. Phys. 111(8), 083701 (2012)

Structural features of interfaces in AlInSb films grown on GaAs substrates determined by multibeam X-ray diffraction

Borcha M.D.[1], Fodchuk I.M.[1], Kshevetsky O.S.[2], Kroitor O.P.[1]

[1] *Yuriy Fedkovych Chernivtsi National University, Chernivtsi, Ukraine*
[2] *Chernivtsi Institute of Trade and Economics of Kyiv National University of Trade and Economics, Chernivtsi, Ukraine*

Films of the antimonides grown on the GaAs substrates are very appropriate for small band gap photovoltaics or thermophotovoltaics particularly for infrared detectors, magnetic-field sensors, light-emitting diodes, solar cells etc. [1]. However the large lattice mismatch ($\Delta a/a \approx 14.6\%$) is a reason of elastic strains and appearance of defects including interfacial misfit dislocations [1]. Elastic residual strains and inhomogeneous distortions caused by defects have an appreciable influence on properties and operation of microelectronic devices. The unique possibilities and effects of multi-beam X-ray diffraction (Renninger method) allow apply it for unambiguous analysis the structural imperfections on interfases between film and substrate as well as in various multilayer systems [2]. Since the analytical expressions for simulation of reflection intensity distribution at Renninger scanning using kinematical approach were obtain only for perfect crystals [3], we use numerical methods for solution of Takagi equation in the case of structural distortions of crystal lattice.

We present results of simulation of X-ray multi-beam diffraction in epitaxial layers InSb та AlInSb on the GaAs substrates. Changes of relative intensity and angle position of multi-beam maxima, their broadening and profile modification in dependence on structural distortions were researched. Various one-dimensional elastic strain fields as well as dislocations of different type and density were considered.

The optimal conditions for experimental investigations were proposed and quantitative relationships between structural imperfections of epilayers and characteristics of individual multi-beam reflections (asymmetry, broadening, maximal intensity, integral reflection coefficient) in research by means of simulation of X-ray multibeam Renninger scans and using various models of strains arising near interface.

[1]J. M. Ripalda, A. M. Sanchez, A. G. Taboada, A. Rivera, B. Alén et al. Appl. Phys. Lett. (2012) V.100, 012103
[2] E. Rossmanith, Acta Cryst. (2006). A62, p.174–177
[3] R. N. Kyutt. Technical Physics Letters (2012) V.38, No 1, p.38-41

Evidence of Oxidation System Ti/Si(001) by Ionization Spectroscopy

Butariev K.A., Koval I.P., Len Yu.A., Nakhodkin M.G.

Kiev Taras Shevchenko University, Kiev, Ukraine

Titanium silicide is one of the first few silicides considered for application in ultra-large-scale integrated circuits owing to its low resistivity, good thermal stability and compatibility with Si processes.

The effects of oxygen on silicide formation for titanium-silicon solid phase reactions are a key concern in device processing. Many transition metals can react with both Si and SiO_2. To successfully utilize metal silicides in device applications, a good understanding of their oxidation behaviours is required.

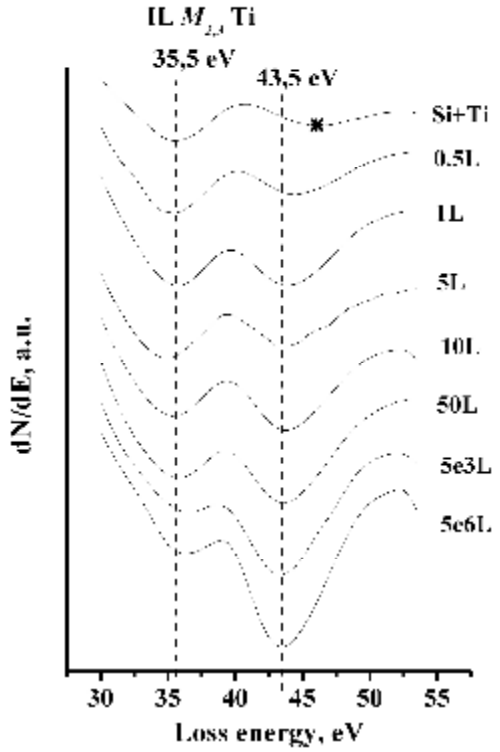

Fig.1. IL $M_{2,3}$ Ti of the system submonolayer Ti/Si(001) for various exposures of oxygen.

To investigate the chemical bonding character between Ti and the Si(001) surface it was applied ionization spectroscopy.

Ionization line (IL) of the Ti $M_{2,3}$ with energy loss 35,5 eV are shown in a Fig.1. It is clearly seen from Fig.1, that in the spectrum of the Ti+Si(001) system an additional IL having an energy loss of 46 eV is observed besides the ionization line of the pure titanium. This line is related to the satellite feature of Ti.

At the increase of an exposition (more than 1 L (1L = 10^{-6} Torr·s) was revealed, that after oxidation submonolayer Ti film in Ti/Si(001) system, changes the form and position IL $M_{2,3}$. It can see from Fig.1, in IL spectra having additional IL with energy loss 43,5 eV.

It testifies to formation of chemical bonding, therefore it is possible to make the suppositions, that Ti on a surface of silicon interacts with molecular oxygen and the oxide titanium is organized.

At the following exposition Ti/Si(001) system in molecular oxygen relative intensity of IL Ti with energy loss of 46 eV is increased.

It was concluded that the titanium oxide was formed.

Study of Ultrathin Metal Films Conductivity During Deposition

Grin I.P., Tomilin S.V., Yanovsky A.S.

Zaporizhzhya National University, Semiconductor Physics Department, Ukraine, Zaporizhzhya

Study of ultrathin metal films conductivity show the existence of the activation process of charge transfer [1]. This is due to the film's discrete structure (an island structure). It is known that at relatively high deposition rates the formation of island structure realized by the Stranski – Krastanov mechanism. In this case the conductivity of thin films has to change during the deposition.

This paper presents the experimental results of studies of ultrathin metal films conductivity during deposition. Conductivity measurement was carried out by double-probe scheme with a constant voltage. Metal films were deposited by thermal evaporation in vacuum ($P \approx 10^{-3}$ Pas). Substrates – polished Al_2O_3 plates with the Al contact metallization.

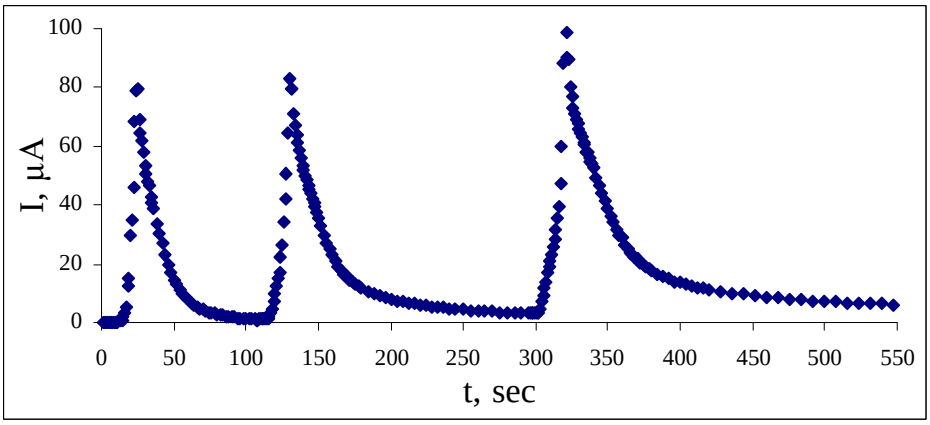

Fig. 1 – Current change in ultrathin Al films during deposition (U = 5 V)

In Fig. 1 presents the results of current measurement in ultrathin Al films during deposition process. Minima on the graph correspond to the vaporizer switching on time, maxima – to the vaporizer switching off time. The graph shows that after vaporizer stopping the current decreases monotonically and reaches saturation. After vaporizer restart situation does not change. Only the saturation current and the time to saturation change.

Such conductivity changes are probably connected with the restructuring of the deposited film. Changes in the structure are due to the energy relaxation of hot deposited atoms and results in the islands structure formation.

1. Loboda V.B., Hursenko S.N. Crystal structure and conductivity of Ni-Cu alloy ultrathin films // Journal of Experimental and Theoretical Physics (by russian). – 2006. – Vol. 130, № 5(11). – P. 911–916.

Mechanisms of Growth, Structure and Properties of thin Films and Nanostructures Pb-Sb-Te, Pb-Bi-Te Systems

Javorsky Ja.S.

Vasyl Stefanyk Precarpathian National University, Ivano-Frankivsk, Ukraine

Lead telluride is a perspective semiconductor material for infrared technology and in thermoelectric devices for high temperature range (200-500) °C. The doping of PbTe by heterovalence impurities leads to modification of its electronic and photonic subsystems.

Thin films and nanostructures have been obtained from the vapor phase by evaporation in an open vacuum advance synthesized compounds PbTe:Bi with 1 at.% of Bismuth and PbTe:Sb with 0.25 at.% of Antimony. As substrates are used ceramics and mica plates that were pre-chemical purification. Thickness of the condensate was determined by the interferometer MYY-4. Morphology of surface nanostructures was investigated by atomic force microscopy (AFM) Nanoscope 3a Dimention 3000 (Digital Instruments USA). Electrical parameters of the films were measured by installing UHV-1.

In this work, AFM images of nanostructures have been obtained by evaporation of an open sample synthesized compounds of various technological factors. It is shown that vapor-phase growth of nanostructures PbTe:Bi is the Folmera-Weber mechanism. Based on the analysis of growth mechanisms of PbTe:Sb nanostructures in Ostwald ripening representing have been established the dominance of diffusion processes in the formation of nanostructures. It has been found that the deposition of condensate complex influences the character of topological features: there is a multistage process comprising the steps of nucleation, aggregation and growth of individual nanocrystallites.

The distribution of the thickness and effective local values of electrical parameters for doped lead telluride films on various substrates has been investigated. Values of electrical parameters of surface layers and their dependence on exposure time in air have been calculated by the Petritz model. Thermoelectric properties of thin films of PbTe:Bi(Sb) on their thickness and exposure time of the air have been investigated.

Dependencies changes in linear dimensions of the crystallites annealing time for polycrystalline PbTe:Bi varying thickness have been determined with using electrical resistance of polycrystalline model. It is shown that the aging process can occur recrystallization associated with fragmentation of crystallites.

The work supported by an integrated project of MES of Ukraine (N 0113U000185) and by projects of FRSF State Agency for Innovation and Informatization of Ukraine. (Contracts: R54, F53, 3), NAS of Ukraine (N 0110U006281)

Electrodeposition of Thin Film Stacks for Precursors of Kesterite and Chalcopyrite Solar Cells

Klochko N.P.[1], Khrypunov G.S.[1],Volkova N.D.[2], Kopach V.R.[1], Momotenko O.V.[1], Lyubov V.M.[1]

[1]*National Technical University "Kharkiv Polytechnic Institute", Kharkiv, Ukraine*
[2] *National Aerospace University "Kharkiv Aviation Institute", Kharkiv, Ukraine*

With the prospect of large scale deployment of terrestrial photovoltaic (PV) becoming realistic, issues of sustainability and costs of raw materials for device manufacture are assuming greater importance. As some components for thin film PV technologies based on CdTe and chalcopyrite $CuInSe_2$ (CIS) or $Cu(Ga,In)(S,Se)_2$ (CIGS) can cause availability and toxicity problems, kesterites containing only abundant non-toxic elements, namely $Cu_2ZnSnSe_4$, Cu_2ZnSnS_4 and $Cu_2ZnSn(S,Se)_4$ (CZTS) should become promising candidates for solar cell base layers. These kesterites are p-type semiconductors with direct band gaps in the range 1.0 – 1.5 eV. Because of the complexity of single-stage three- or quaternary semiconductor compound deposition, most researchers use two stages: the production of films stack precursors and the following their conversion by the annealing into CIS or CZTS. Among all methods an electrodeposition technology best suits for creation of high quality, low cost and large area thin film precursors. Modern electrodeposition techniques allow a variety of direct or reverse pulse modes and an ultrasonic agitation of electrolytes, which are able to modify the structure and properties of the deposited layers. The aim of this work was a comparative analysis of structure and surface morphology of the individual metal film components and layered compositions (stacks) for CIS and CZTS precursors produced by different electrodeposition modes. In addition, we investigated the influence of electrolysis mode on the structure, optical properties and surface morphology of the selenium films.

A comparative analysis of structure by X-ray diffraction studies and of the surface morphology using scanning electron microscopy of copper, indium, tin, zinc films and film stacks made by electrochemical deposition in galvanostatic steady-state conditions, in galvanostatic mode with ultrasonic agitation of electrolytes, in the forward pulse and reverse pulse modes with rectangular pulses was performed. The influence of the modes of electrodeposition on the structure, optical properties and surface morphology of the amorphous and crystalline selenium films was investigated. By sequential electrochemical deposition the film stacks Cu/In/Se and Cu/Sn/Zn/Se were obtained, which are models of chalcopyrite $CuInSe_2$ and kesterite $Cu_2ZnSnSe_4$ precursors, respectively. These precursors after their conversion into $CuInSe_2$ and $Cu_2ZnSnSe_4$ by subsequent annealing will be used as base layers of cheap and efficient thin film solar cells of the new generation.

Internal Stresses, Thermodynamic Parameters and Adhesion in Metal Condensates on Single-Crystal Silicon.

Koman B.P.[1], Juzevych V.M.[2]

[1]*Ivan Franko Lviv National University, faculty of electronics, Lviv, Ukraine;*
[2]*Karpenko Physicomechanical Institute, National Acad. Science of Ukraine, Lviv, Ukraine*

Systems Si - metallic condensate are widely used as basic elements of modern micro- and nanoelectronics, as well as a number of sensory devices. But duration of their operation and stability parameters are determined by the existing mechanical stresses in the substrate-condensate, as well as the nature of interfacial interactions. Therefore, the formation of stable heterophase nanosystems for the needs of nanoelectronics requires specific information about the surface properties of interacting layers, as well as the values of their thermodynamic and adhesion parameters.

The aim of the work was to study the kinetics patterns of tension, interfacial interactions analysis and calculation of energy and adhesion parameters in systems of single-crystal silicon - metal condensate (Cr, Cu, Al, Au).

Based on the experimental dependence of the kinetics of internal stresses studied regularities of mechanical stresses in the system Si-substrate metallic condensate. Investigated the dimensional dependence of internal and thermal stresses and Young's modulus condensates on silicon. Established self-organizing role in the formation of Si substrate mechanical stresses. It is assumed that the degree of self-organizing role of the substrate in the formation of internal stresses is determined by the difference in electronegativity material substrate and condensate.

With the use of the thermodynamic approach to the study of the mehanoelektrychnyh processes in the nanolayers of the condensates at the interface metal-semiconductor is stated the value of the contact and contact-boundary value problem for determination of free electric charges in the metal and the semiconductor and related mechanical stresses. For systems Si-(Cr, Cu, Al, Au) the numerical value of the interfacial energy, interfacial tension, work of adhesion, adhesive bonds and interphase charge.

It is found that the most sensitive parameter during the analysis of interfacial interactions in the systems Si - metal is the interphase energy, which changed 4 times in the investigated number of metals.

The peculiarity of the studied systems is consistency of the interphase charge, because electronic structure of covalent bond formed in the interfacial layer.

Influence of Normal and Tangential Growth Mechanisms Onto Formation of Three-Dimensional Porous Copper Structures

Kosminska Yu.O., Latyshev V.M.

Sumy State University, Sumy, Ukraine

At present all well-studied variants of structures of layers, fabricated by means of ion-plasma sputtering, are systematized in the form of the structure zone models (SZM). Usually, the structures are divided into regions – zones – depending on temperature, working gas pressure and energy flux onto a substrate. Up to now a region of the layers with developed three-dimensional porosity, obtained during condensation of substance near equilibrium, i.e. at very low supersaturation, has not been considered within the framework of SZMs [1].

In the present work the formation regularities of porous three-dimensional copper structures has been investigated experimentally. In order to implement corresponding technological conditions of proximity to equilibrium we have used the accumulative ion-plasma system featuring both direct plasma influence onto growth surface during deposition and accumulation of deposited substance near the substrate. The system operates at such technological conditions as increased working gas pressure (Ar) 5-10 Pa and low discharge power ~7-30 W.

Generalizing the results obtained, it has been established that extremely developed porous labyrinth layer is formed after several hours of deposition. It is characterized by statistical homogeneity of its structural elements. All the obtained structures can be divided into two types: structures with rounded and faceted habit of the structural elements. Minimization of the surface energy during condensation results in formation of round-shaped crystals, which testifies prevalence of normal mechanism of crystal growth and atomically rough growth surface (Fig.1a). Corresponding change of the growth mechanism to tangential one originates well-defined faceting (Fig.1b). In the last case one can observe formation of whiskers (Fig.1c) and unusual whiskers-like structures (Fig.1d) during prolonged condensation.

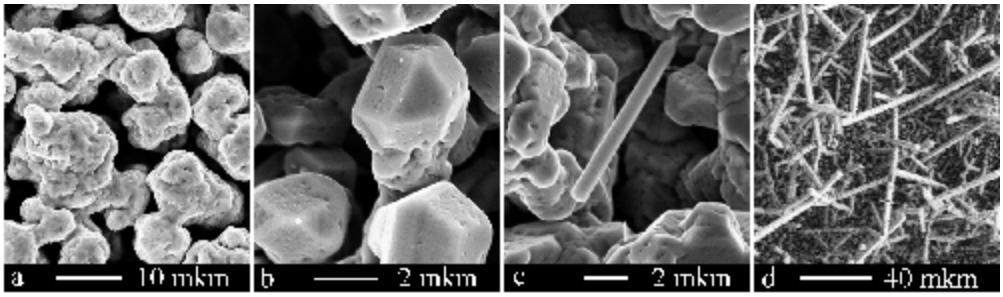

Figure 1 – SEM images of the fabricated copper structures

1. Perekrestov V.I. et al. Impact of selective processes on Al porous structures formation during self-organized quasi-equilibrium steady-state condensation // Journal of Porous Materials. doi:10.1007/s10934-013-9674-6.

Study of Ordered Oxide Patterns Got on the Dielectric Surfaces with the Combined Electronic Technology

Kovalenko Y.I.[1], Bondarenko M.A.[1], Vertsanova E.V.[2], Iatsenko I.V.[1], Andrienko V.A.[1], Bondarenko Y.Y.[1]

[1] *Cherkassy State Technological University, Cherkassy, Ukraine*
[2]*LLC "Melitek-Ukraine", Kiev, Ukraine*

The pprevious research of the team of the University Centre "Mikronanotehnologies and equipment", which demonstrated the possibility of producing of thin (up to 5 nm) oxide coatings with the thickness ordered structure formed on the surface of the dielectric (K8 optical glass) by the combined thermal vacuum deposition technology with the subsequent electronic surface modification. Further conditions optimization of this technology allowed to significantly improve the process of formation and increasing of the degree of order in these structures, which can be applied, for example, as anti-reflective coatings for optoelectronics or memory elements in nano-electronics.

In the course of the experiments it became clear that not the thickness of deposited coatings has a significant influence on the ordering of formed structures but the geometric characteristics and chemical purity of the material to be precipitated.

The research carried out by us with the scanning electron microscope Zeiss Ultra Plus company “Carl Zeiss” (Germany) showed a high order of structures (degree of order of 82 ... 85%, size 5 ... 8 mm), formed on the dielectric surfaces (in particular, on the technical and optical glass, quartz, piezoelectric ceramics, etc.) with the thermal vacuum deposition of fine high-purity oxide powders with their further modification by the electronic method, Figure 1.

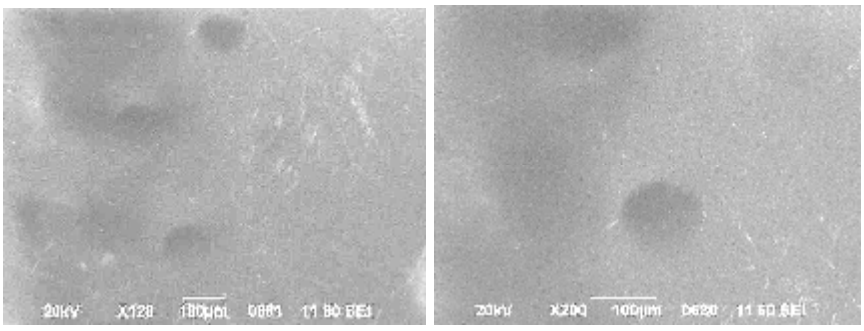

Fig.1. Micrograph of formed ordered structures of ZnO on the surface of the optical glass K8 (the average size of deposited particles is 2.6 ... 3.2 mkm, the manufacturer: LLC "Powder nanotechnologies", city Cherkassy, Ukraine).

These results are planned to be used to obtain nanostructured metal-dielectric coatings on the surfaces of the elements to create products of nanoelectronics nanooptoelectronics, micro-optics and informational medicine.

Peculiarities of the Morphology of GaAs(AlGaAs) Epitaxial Layers Grown on GaAs(111A) Substrates by Mocvd Epitaxy at Reduced Pressure

Larkin S.Y.[1], Avksentev S.Y.[1], Vakiv M.M.[2], Krukovsky S.I.[2], Kost Y.Y.[2], Krukovsky R.S.[1]

[1]SPC «Nauka» Ukraine, Kyiv;
[2]SRC «Carat» Ukraine, Lviv

Nowadays one of the most common methods of manufacturing heterostructural A_3B_5 junctions is the technology, of Metalorgenic Chemical Vapor Deposition from organometallic sources (MOCVD). However, the mechanisms of growth of GaAs (AlGaAs) epitaxial layers on (111A/B) substrates using this method at reduced pressures are not fully understood. Therefore, the exploration of the main factors which determine formation of the morphology of GaAs (AlGaAs) surface layers with (111A) crystallographic orientation is relevant.

The aim of the work is to study the influence of crystallization temperature, the ratio of number of fifth and third group's elements in the gas phase at the surface morphology of GaAs (AlGaAs) epitaxial layers grown on GaAs (111A) substrates by MOCVD at reduced pressure.

GaAs (111a) epitaxial layers and their solid solutions were grown at MOCVD Discovery 180LDM equipment with vertical reactor. Temperature of the substrates varied within 580-680°C. The pressure in the reactor was 70 Torr. As initial reagents were used trymetylgallium, trymetylaluminum and arsine AsH3.

Found that at temperatures higher than 680°C, in epitaxial layers with thickness of 0,4-1,0 microns appears a significant number of pyramidal shaped defects (triangle at the base). The concentration of the defects significantly diminishes as the temperature range reduces. At the same time the transformation of pyramidal shaped defects into hexagonal defects is observed. At crystallization temperatures lower than 590°C and V/III elements ratio equal to 180/190 in gas phase of the reactor and in effective flow of arsine equal to 410 sccm were obtained defect-free GaAs (AlGaAs) epitaxial layers, which appeared to have high structural perfection, as determined by high-resolution X-ray diffraction method.

Obtained results can be used to develop the technology of growing GaAs epitaxial structures on the substrates with (111) crystallographic orientation for different applications.

Technological Features of Reduction of Density of Dislocations in Epitaxial Layers of Arsenide of Gallium from a Liquid Phase when Using Isovalent Metal-Solvent

Lebed O.N.

Kherson state maritime academy, Kherson, Ukraine

Dislocations often are the reasons of the raised currents of leak, deterioration of electric characteristics and developments of processes of degradation in various semiconductor devices. One from ways of reduction of density of dislocations in the epitaxial layers (EL) is creation of methods of leaders to stabilization of the front of crystallization. EL cultivation in isovalent metal-solvent gives additional opportunity in management of semiconductor [1] structure.

In work mechanisms of decrease in density of dislocations in EL of arsenide of gallium on the basis of isothermal excerpts are investigated, and also when using isovalent metal-solvent of bismuth.

Epitaxial layers grew up by compulsory cooling of solution fusion, in the vertical reactor. As substrates single-crystal plates (100) with concentration of carriers of a charge of $n = 1 \cdot 10^{17}$ cm^3 were used.

The special mode of cooling was applied, at interruption of process of growth, at the expense of use of the phenomenon of natural convection.

Process of cultivation was carried out by means of the cyclic temperature and time scheme. The cycle represents: interval of homogenization of solution fusion at 850ºC, an interval of crystallization (cooling) to 830ºC, an interval of homogenization of solution fusion at 830ºC, a dissolution interval.

Application of a step mode of cooling of system allows to bring during annealing the crystallization front into a condition close to the equilibrium. It creates sufficient conditions for smoothing of consequences of change of the mechanism of growth of the layer, being shown in reorientation and annihilation of dislocations. Result of it is improvement of structure of a single-crystal layer. Respectively it brings to more uniform distribution of dislocations in EL and fall of their density.

These technological features in aggregate with use of bismuth as metal-solvent allowed to reduce density of dislocations in epitaxial layers of arsenide of gallium to value of $5 \cdot 10^2$ cm^{-2}.

1. Баганов Е.А.. Управление структурными свойствами GaAs при эпитаксии из жидкой фазы. / Баганов Е.А., Лебедь О.Н., Коваленко В.Ф., Шутов С.В.. // Вестник ХНТУ . – 2007. № 3(29). – С. 60 – 62.

Structural and electrical properties of the TiO_2 : Fe films obtained by electron - beam evaporation

Lorents V.M., Solovan M. N., Maryanchuk P. D., Fodchuk I.M.

Yuriy Fedkovych Chernivtsi National University, Chernivtsi, Ukraine

In this paper the research of effect of Fe on the structure and the electrical properties of TiO_2 thin films (Fe content is 1, 3, 5%) was carried out.

The TiO_2: Fe (0.1% Fe) thin films were grown on precleaned glass substrates in a Leybold Heraeus L560 vacuum deposition unit using electron beam evaporation of appropriate mixtures of TiO_2 and Fe powders pressed into 9-mm-diameter pellets [1]. The films are adhered well to the glass and did not peel off even when a mechanical load was applied. The pellets were placed in a water cooled copper crucible and gradually heated by an electron beam in a vacuum chamber, which was evacuated by a molecular pump to a pressure of $6 \cdot 10^{-3}$Pa. The electron beam power, deposition rate, and film thickness were controlled by an INFICON XTC thin film deposition controller.

Titanium dioxide and appropriate mixtures of titanium dioxide and iron were deposited onto precleaned glass substrates. The substrate temperature was monitored with a number of thermocouples in the vacuum chamber, and was maintained by a controller on a control board.

Investigation of the structure and the influence of annealing on it TiO_2: Fe thin films was carried out by X-ray high resolution diffractometer X'Pert PRO MRD, surface morphology and phase composition of the films were studied using scanning electron microscopy and atomic force microscopy.

To study the electrical properties of TiO_2 thin films by thermal deposition of indium at 150 ° C obtained ohmic contacts, as evidenced by the linear plots of I–V curves at room temperature. It was established that the resistance increased when studied films were heated. In the TiO_2: Fe films change in resistance is lower in comparison with pure TiO_2 films. It is known that the magnitude of the conductivity of titanium dioxide is determined mainly by native donors Heating in air reduces their concentration, which is responsible for the observed reduction in the resistance of the films. It explains the increase of resistance, besides the growth of this magnitude was observed due to annealing.

1. Solovana M. N., Maryanchuka P. D., Brusb V. V., and O. A. Parfenyuk Electrical and Optical Properties of TiO_2 and TiO_2:Fe Thin Films, Inorganic Materials, 2012, Vol. 48, No. 10, pp. 1026–1032. (Original Russian Text)

Transparent Silicon Film: Thickness Control

Maievska T.[1], Sharan V.[2]

[1] *«Polus» research center of radioelectronics, Vinnytsa, Ukraine*
[2] *Vinnytsia national technical university, Vinnytsa, Ukraine*

Micromechanical silicon devices contain membranes, torsions, suspensions, etc. Small linear dimensions of the latter exclude direct evaluation of their thickness: optical control methods are accepted.

Thickness evaluation of a thin silicon element through monotone correlation of the absorption (transmission) ratio of the light of a fixed wavelength revealed influence of the element surface condition on the measurement result: demonstration of silicon monocrystal defects in the etching process, evaporation of the condensed liquid inflects, diffuses and deflects a part of the light flux.

The paper presents a device developed for introduction of the technological control of transparent silicon element thickness by colorimetric method.

Pic. The silicon film thickness monitor:

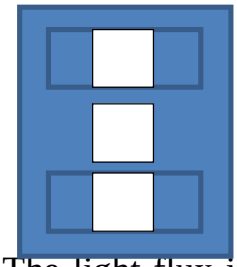

a microscope 2 for orientation at the control object is complemented with a monochromator 1 (movable optical grating located in the path of the light; its turn forms the light source of a certain wavelength) and a light receiver 3.

The light flux is not modulated in time: the monochromator is adjusted to the wavelength of 1 μm for predetermined calibration of 100% transmission of a certain detail part that is monitored; then - a cycle of decrease of the wavelength to 10% transmission conditioned by this silicon thickness. For each such measurement part the transfer from 100%) transmission to 10% for all wavelengths occurs under the same conditions.

Accuracy of the thickness evaluation - 0.1 μm within the thickness range of 5... 30 μm.

Research on the Processes Occurring in the 2D-Layers of Single and Polycrystalline Materials Under Cyclic Deformation

Oliynich-Lysyuk A.V., Taschuk A.Yu., Raransky N.D.

Yu. Fedkovych Chernivtsi National University, Chernivtsi, Ukraine

According to current concepts, any solid consists of two subsystems: a three-dimensional crystalline 3D-subsystem with a translational invariance and a planar 2D-subsystem (surface layers and all internal interfaces) with no translational invariance. Primary shifts are developed in a planar subsystem as flows of channeled local structural transformations of short-range type. They generate all types of deformation defects. Their emission into crystalline subsystem assures plastic change of material shape on a microscale level. The processes of local structural transformations in the 3D- and 2D-planar subsystems are interrelated. However, the processes occurring in a planar subsystem are always considered to be primary, since they are related to nanostructured states in solids. To confirm this assumption and to divide their contributions into the nonlinear behaviour of solids, special studies with a high structural selective sensitivity are required [1].

In this paper, the elastic and nonelastic properties of single (Si) and polycrystalline (Be condensate) layers ~100 μm thick were studied under microplastic deformation conditions with a view to divide the contributions of 2D- and 3D-subsystems to their nonlinear behaviour.

Use was made of low-frequency internal friction method and modulus of torsion behaviour at thermocycling of samples in the range of 20-450°C.

It was discovered that active contribution of planar subsystem to the investigated properties is recorded only with the first heating-cooling: a hysteresis maximum appears in the internal friction spectrum at 0.4 T_{melt} due to grain boundary sliding processes in nano macrocrystalline materials [2]. Further thermocycling is followed by nonlinear (hysteresis) changes only in the 3D-defective subsystem.

1. V.E. Panin, V.E. Yegorushkin, A.V. Panin. The role of local nanostructured states in plastic deformation and destruction of solids // Physical Mesomechanics. – 2012. – V. **15**, № 5. – P. 5–18.
2. M.Yu. Gryaznov, V.N. Chuvildeyev, A.N. Sysoyev, V.I. Kopylov. Grain boundary internal friction and superplasticity of nano- and microcrystalline metals and alloys // Bulletin of N.I. Lobachevsky State University of Nizhny Novgorod. – 2010. – № 5(2). – P. 147-158.

Novel Method of Producing Ultrablack Ni-P Coatings

Perevoznikov S.S., Poznyak S.K., Tsybulskaya L.S.

Research Institute for Physical Chemical Problems of the Belarusian State University, Minsk, Belarus

Ultrablack surfaces obtained after chemical blackening of electroless Ni–P coatings are of great interest because of their extremely low reflectance in visible and near IR regions. In particular, they can improve the absorbance of thermal detectors and reduce the effect of stray and scattered light in optical instruments.

The present work was focused on the replacement of expensive and poorly reproducible chemical Ni-P deposition with more controllable electrochemical deposition. The 50-μm thick Ni-P coatings were electrodeposited from the bath containing (g/l): 180 $NiSO_4 \cdot 7H_2O$, 10 $NiCl_2 \cdot 6H_2O$, 10 H_3PO_4, 28 KH_2PO_4, 1–18 H_3PO_3, 0–2 saccharine at a temperature of 65°C and pH 2.0. Increasing the H_3PO_3 concentration from 1 to 18 g/l was shown to result in an increase of the P content in the coatings from 3 to 13 wt. %.

As-deposited coatings were chemically blackened in 4.5 M HNO_3 solution for several minutes. This blackening process is similar to that described in the work [1]. We found that the reflectance of the blackened coatings depends strongly on the P content in Ni-P, and the coatings with 5 wt. % P exhibit the lowest reflectance values. Moreover, an addition of saccharine to the electrolyte for Ni-P electrodeposition was revealed to have a crucial effect on the optical properties of blackened coatings. The Ni-P coatings deposited with saccharine react vigorously when immersed in nitric acid solution producing uniform surfaces with regular microholes having a diameter of 1-3 μm (Fig.). Blackened samples prepared without saccharine demonstrate quite different morphology. They have no craters and pinholes at the etched surface. The surface is smooth and only deep narrow cracks at grain boundaries can be seen. This behavior of the Ni-P coatings electrodeposited with saccharine can be explained by their lower corrosion resistance. Saccharine provides incorporation of trace amounts of sulfur into the coatings which is a promoter of pitting corrosion. The blackened surfaces obtained exhibit the reflectance superior to that for the best samples of electroless Ni-P blacks.

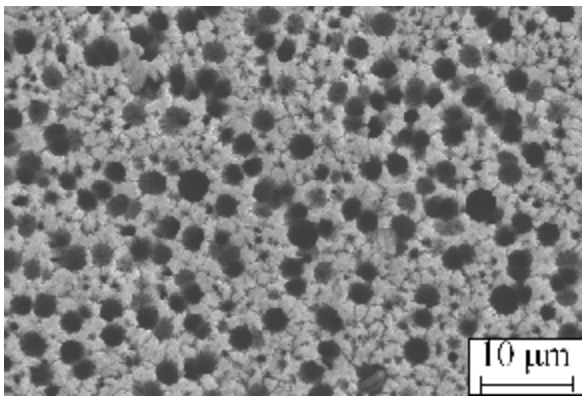

Fig. SEM image of etched Ni-P alloy electrodeposited with saccharine.

1. Johnson // Met. Finish. – 1980 – V. 78, – P. 21.

Catalytic systems for depolymerization of polydimethylsiloxanes

Protsak I.S.[1], Bolbukh Yu.N.[2], Tertykh V.A.[3]

Chuiko Institute of Surface Chemistry of National Academy of Sciences of Ukraine
Kyiv, Ukraine

Polydimethylsiloxanes have been applied for preparation hydrophobic nanomaterials, particularly fumed silicas, with high contents of grafted organic groups in the surface modifying layer. These products are widely used as active fillers for polymeric systems, effective thickeners of dispersive media and nanosized powders in modern materials science. However, chemisorption of polidymetylsiloxane chains on the silica surface require significant energy expenditure and modification processes are usually carried out at the relatively high temperatures (about 400 °C). Therefore, it is important to develop new approaches to modification processes using organosilicon polymers to create nanomaterials with desired surface characteristics.

Various catalytic systems for the process of depolymerization of linear polydimethylsiloxane (PMS-100) were investigated in this work. Reactions of heterolytic cleavage of siloxane linkages were performed by alcoholysis in the presence of inorganic salts and alkalis. Dimethyl carbonate (DMC) was added to the reaction system as an auxiliary reagent. The influence of the ratios of the components on the rate of organosiloxane depolymerization was determined. The depth of depolymerization process and effectiveness of the used catalytic systems has been characterized by changes in the molecular weight of the original polymer. The molecular weight was defined using data of viscosity measurements. Kinetic dependences of the degree of PMS-100 depolymerization after treatment by alkali (*1*) and DMC with NaCl (*2*) are represented in Fig.

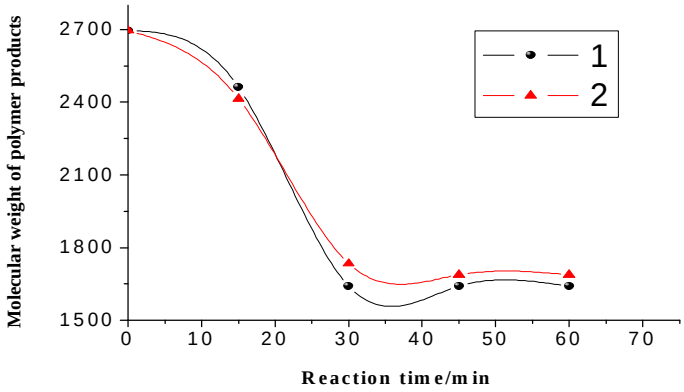

Fig. Kinetic curves of changes of molecular weight of PMS-100 after treatment by alkali (*1*) and DMC with NaCl (*2*).

Polymer degradation was shown to take place during the first 30 min. The further reaction has a little effect on the process of depolymerization.

Fabrication of Phosphorus Doped ZnO Thin Films

Rogozin I.V., Kotlyarevsky M.B.

Berdyansk State Pedagogical University,Berdyansk, Ukraine

Owing to its unique properties, ZnO is widely used in various optoelectronic devices, such as piezoelectric converters, varistors, optical waveguides, photodetectors, and solar cells. The large band gap of ZnO (E_g~3.37 eV) and the high exciton binding energy in it (~60 meV) allow one to obtain high-intensity ultraviolet radiation due to exciton recombination even at room temperature. In view of this, ZnO is thought to be an attractive material for the fabrication of ultraviolet light emitting diodes and lasers. At the same time, ZnO has a tendency toward monopolar (*n*-type) conduction, due to the high background concentration of native donor defects, such as zinc interstitials and oxygen vacancies, which impedes the preparation of *p*-type material.

ZnO:P films were grown at temperatures from 400 to 800°C by radical-beam gettering epitaxy [1]. As substrates, we used tetragonal (red) zinc diphosphide (ZnP_2) single crystals (Eg ~ 2.05 eV). The substrates were degassed in a vacuum of 5×10^{-3} Pa at 400°C for 30 s. Atomic oxygen was generated using a 100-W rf discharge at a pressure of 0.1 Pa. The thickness of the films determined on an MII-4 microscope was ~0.3 μm.

The structure and crystallographic orientation of the films were determined on an X-ray diffractometer with CuK_α radiation. Their surface morphology was examined with a Nanoscope IIIa Dimension 3000 SPM force microscope. The electrical properties of the ZnO:P films were inferred from room-temperature Hall effect measurements in the van der Pauw geometry at a current of 0.01 mA and magnetic induction of 0.5 T. Al and Au contacts to the *n*- and *p*-layers, respectively, were deposited at a substrate temperature of 200°C in a VUP-5 vacuum system. The elemental composition of the ZnO layers was determined by X-ray photoelectron spectroscopy. Photoluminescence (PL) spectra were measured at liquid-nitrogen temperature using a nitrogen laser as the excitation source.

The X-ray diffraction patterns of the films showed the 002 peak, indicating that their *c* axis was normal to the substrate surface. According to the Hall effect data, the layers were *p*-type, with a resistivity of ~20 Ω·cm, hole mobility of ~9 $cm^2/(V\cdot s)$, and hole concentration of $\sim7.8\times10^{17}$ cm^{-3}. The photoluminescence spectra of the ZnO:P films showed a peak at 3.356 eV (neutral acceptor bound exciton). Our results indicate that the ZnO:P films contain the P_{Zn}–$2V_{Zn}$ defect complex as a shallow acceptor responsible for their *p*-type conductivity.

1. Rogozin I.V. Nitrogen-doped p-type ZnO thin films and ZnO/ZnSe p-n heterojunctions grown on ZnSe substrate by radical beam gettering epitaxy // Thin Solid Films. – 2009. – T.517. – P. 4318-4321.

Mechanical Properties of Nanostructured Composite Coatings on the of Copper or Nickel Basis

Sakhnenko N.D, Lyabuk S.I., Bogoyavlenska E.V., Ovcharenko O.A., Tarnavska A.V.

National Technical University "Kharkiv Polytechnic Institute" Kharkiv, Ukraine

The development of many branches of modern technologies largely depends on the development and practical usage of different kinds of coatings. The analysis of a number of engineering products shows that there are numbers of them that are more cost-effective when produced with electrosynthesis. A coating can improve many functional properties and provide specific technological features for work surfaces of machine parts and tools.

The aim of this work was to study the mechanism and kinetics of electrodeposition of composite foils of copper or nickel reinforced by particles of nanoscale alumina with improved usage characteristics.

Composite foils of copper or nickel are synthesized from sulfate solutions containing nanoparticles of Al_2O_3 in different concentrations. The foil thickness was 10-100 μm depending on the time of electrolysis. The kinetics of the synthesis includes the following steps: delivery of dispersed particles to the cathode, their following adhesion to the surface. Particles initiate the nucleation once in contact with the cathode surface. The structure of the copper foil is unity with an average grain size of 10 μm. With the introduction of dispersed phase the structure of composite becomes more dispersed.

Deposit microhardness was 1200 MPa for copper based and 1600 MPa for nickel based composite foil exceeding those values for copper and nickel foils, namely 800 MPa and 1000 MPa, respectively.

Based on the results of the study the electrolyte composition for Cu-Al_2O_3 and Ni-Al_2O_3 electrodeposition from sulfate solutions was suggested. It was determined the effect of electrolyte composition and such electrolysis parameters as temperature, agitation, and cathode current density on current efficiency and quality of coatings. Also the conditions to synthesize foils with enhanced mechanical properties were developed.

When the concentration of Al_2O_3 increases the micro-hardness, liquid limit, the strength increase but the flexibility reduces accordingly. The Al_2O_3 particles are present as obstacles for dislocation which is characteristic to the dispersion hardening mechanism by Orovan. Nickel composites possess higher strength properties than copper ones.

Relaxation resistance measured by the reciprocal of the relative depth relaxation. With a minimum content of the hardening phase relaxation, resistance is low, due to a non-equilibrium state of the structure. With increased alumina content, the relaxation resistance rises due to higher density of barriers to dislocation (Al_2O_3).

Synthesis of Zirconium (IV) Oxide thin Films on VARIOUS Substrates

Sakhnenko N.D., Bykanova V.V., Proskurin N.N., Ved M.V.

National Technical University "Kharkiv Polytechnic Institute", Kharkov, Ukraine

The zirconium oxide thin films have high heat resistance, impact elasticity, chemical inertness, resistance to mechanical wear, catalytic activity. This allows to use their in various industries. It is known [1, 2] that the functional properties of ZrO_2 largely determined by the method of synthesis, so the actual problem is the ZrO_2 coatings synthesis on the substrates of different nature and the study of their physical and photocatalytic properties.

The ZrO_2 films were prepared by the chemical deposition at 50˚C in 60 minutes from the zirconium sulfate aqueous solution on a ceramic carrier (grog). Reagent precipitator is the ammonium persulfate. The precursors were mixed at the various ions' ratios Zr^{4+} / $S_2O_8^{2-}$: 0,25; 0,5; 1. The synthesized contact mass activity was analyzed in the photocatalytic oxidation model reaction by the ultraviolet irradiation of the methyl orange dye aqueous solution with the concentrations, g/dm^3: 0.02, 0.04, 0.06, 0.08, 0.1. The dye concentration was determined by the optical density solutions measuring using the fotokalorimeter.

The ferroelectric coatings doped with the zirconium oxide ($Ba_{0,75}Sr_{0,25}Ti_{0,5}Zr_{0,05}O_3$) were deposited by micro-arc oxidation (MAO) from the alkaline solution (KOH) on the aluminum alloy (A 99) substrate. Final molding voltage was 600 V, the electrolysis process time – 60 min., anode current density – 3-4 A/dm^2.

As the result of the studies it was found out that the chemically deposited ZrO_2 thin films on the grog exhibit photocatalytic activity in the model reaction. The highest degree of the methyl orange photodegradation is observed in ZrO_2 films, obtained from a solution with a ratio concentration Zr^{4+} / $S_2O_8^{2-} \approx 0,5$. It is shown that in the $Ba_{0,75}Sr_{0,25}Ti_{0,5}Zr_{0,05}O_3$ coatings increasing of the ZrO_2 concentration leads to the sample electrical resistance increase. Thus, the coatings based on zirconium oxide (IV) are promising as an independent photocatalyst and so as the high-voltage capacitors plates' structural material.

1. Reddy B.M., Khan A. Recent Advances on TiO_2-ZrO_2 Mixed Oxides as Catalysts and Catalyst Supports // Catalysis Reviews. – 2005. - №47. – P. 257-296.
2. Salami T.O., Yang Q., Chitre K. Toward a Better Understanding of Synthesis and Processing of Ceramic/Self-Assembled Monolayer Bilayer Coatings // J. of Electronic Materials. – 2005. – V. 34, №5. – P. 534-539.

Electrochemical Impedance Analysis of Anodic Aluminum Oxide Membrane

Semkina E.V., Bayrachniy B.I., Borzenko O.V., Kramarenko A.V.

National Technical University "Kharkiv Polytechnic Institute", Kharkov, Ukraine

In recent years, intensive studies of nanometer-scaled aluminum oxide films were carried out. These films are of interest, because they used to produce embedded grid structures of metals.

The anodizing of an aluminum thick-film under certain conditions leads to a complicated structure consisting of an aluminum base, the porous layer and the barrier layer separating them. The barrier layer is an insulator that prevents direct contact between the electrolyte and the cathode in the subsequent electrodeposition of metal into the pores. Thus, the properties of the barrier layer affect the uniformity and quality of the filling of the pores by AC electrodeposition.

The oxide Al_2O_3 layer properties were determined using the method of Electrochemical Impedance Spectroscopy (EIS). Samples for measurements were anodized at 60 V, with voltage decrease to 40 and 20 V in a solution of 0.5 M oxalic acid. The impedance of the cell was measured in the frequency range 0,021-100 kHz using an ac bridge P-5083 in phosphate buffer solution.

The data obtained was presented as Bode plots, from which calculated the frequency-independent barrier capacitance C_b and constant phase exponent α by the equation

$$Z = 1/(jw)^{a} C_b .$$

The results of calculation of the alumina barrier layer thickness using the values of C_b and formula for a plane-parallel capacitor are shown in Table.

The values of parameter for the barrier layer of aluminum oxide films obtained in 0.5 M $H_2C_2O_4$ at various finite voltage

U, V	C_b, μF cm^{-2}	α	d_b, nm
60	0,984	0,960	61,7
40	1,352	0,966	44,9
20	2,512	0,969	24,2

Calculation of the thickness of the barrier layer on the basis of information on the distance between the pores led to similar results.

The films with a decreased to 20 nm barrier layer has been filled with copper from the electrolyte of 0.9 M $CuSO_4$ + 0,6 M H_2SO_4 on AC current at 50 Hz. Scanning electron microscopy shows the presence of uniformly distributed copper nanowires 54 nm in diameter, embedded in a matrix of Al_2O_3.

Thermoelectric and Spectral Properties of Thin Films on the Basis of PbTe

Shimko A.N.[1], Malashkevich G.E.[1], Freik D.M.[2], Nykyruy L.I.[2], Svito I.A.[3]

[1]*B.I.Stepanov Institute of Physics of the National Academy of Sciences of Belarus, Minsk, Belarus*
[2]*Physical-chemical Institute at the Vasyl Stefanyk PreCarpathian National University, Ivano-Frankivsk, Ukraine*
[3]*Belarusian State University, Minsk, Belarus*

Lead chalcogenide films are actively investigated and applicated in thermoelectric devices which require enchanted sensitivity and response. However, there is lack of studies devoted to the search of correlations between thermoelectric and spectral preoperties of these compounds. In present study we have made an effort to reveal such correlations by investigation of FTIR spectra and thermoelectric figure of merit of doped and non-doped PbTe films. Such films were obtained by means of precipitation from the gas – dynamical steam. Glass and mica, including glass and mica containing surface Ag islets, were used as substrate materials.

Composition, evaporator (T_1) and subtrate (T_2) temperatures, sputtering time (t) and thermo-EMF coefficient (α), measured at $\Delta T \approx$ 21–33 °C between electrodes, are given in Table 1. The value of t for Ag films was 5 minutes. It is seen that non-doped films on glass substrate are characterised by maximum α value. The doping by Bi significantly lowers thermo-e.m.f. coefficient and the use of substrate with insular Ag film significantly echances thermo-EMF coefficient. It was discovered that α increases while absorbtion edge steepness icreases and absorption edge position shifts into longwave region of spectrum. The correlation observed can be attributed to the decrease in chalcogenide film defects concentration. The reasons of the described effect of Bi and Ag on spectral properties of investigated films as well as thermo-EMF sign change depending on preparation conditions of films are analyzed.

Table 1
Properties of films

No	Samples composition	T_1/T_2, °C/°C	t, min	α, μV/K
1	PbTe/glass	700/200	10	-317±30
2	PbTe/glass	700/200	20	-267±25
3	PbTe:Bi/glass	700/200	10	-87±9
4	Ag/PbTe:Bi/glass	700/200	10	-102±10
5	PbTe/mica	700/200	10	-81±8
6	PbTe:Bi/mica	700/200	10	-66±6
7	Ag/PbTe:Bi/mica	700/200	10	-69±7
8	Ag/PbTe/mica	700/200	10	-92±9
9	PbTe/glass	700/150	30	220±20

Prospects and Problems in Development of GUNN Diodes Made of Wide-Gap Semiconductors

Slipokurov V.S.

V. Lashkaryov Institute of Semiconductor Physics, NAS of Ukraine, Kyiv, Ukraine

We consider the state-of-the-art development of Gunn diodes (GDs) as well as calculated operating frequency and power limitations on the materials used for their production. Figure 1 presents the experimentally achieved values of operating frequency and power for GaAs- and InP-based GDs. An analysis of the structure of modern GDs is also discussed. Its choice depends on the device purpose (frequency and efficiency maximization, operation at the second harmonic) [1, 2].

The materials most often used now for GDs production are GaAs and InP. Besides, GaN as well as solid solutions $Ga_xIn_{1-x}As$ and GaP_xAs_{1-x} are considered as promising ones. The possibility of microwave generation using InN and AlN has been predicted. Figure 2 presents the calculated parameters of GaN-based GDs in comparison with similar GaAs- and InP-based models (continuous operation mode).

Fig. 1. Dependence $P_{max}(F)$ for InP- and GaAs-based GDs (experiment).

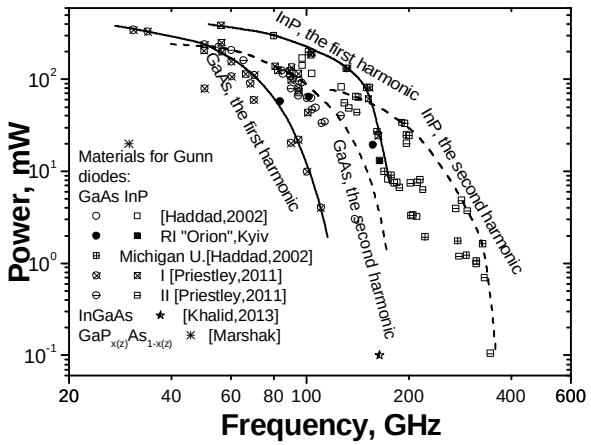

Fig. 2. Dependence $P_{max}(F)$ for GaAs-, GaN- and InP-based GDs (calculation).

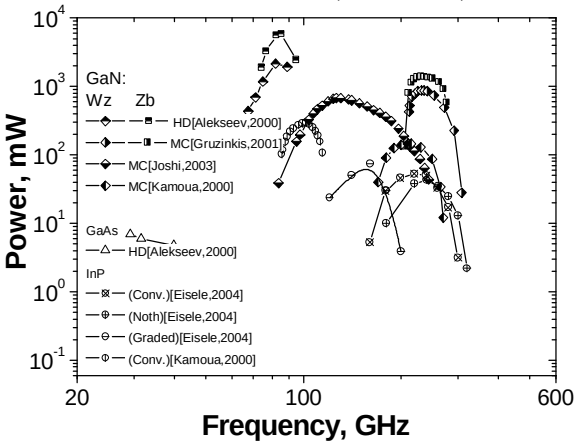

It is shown that GDs with Schottky barrier cathode contacts are quite competitive in frequency and power parameters with GDs of more complex geometry. The problem of making stable low-resistance ohmic contacts to GaN-based GDs is considered too.

1. Priestley N., Farrington N. Millimetre wave Gunn diode technology and applications / UK Automated RF & Microwave Measurement Society Conf.-2010 / ARMMS 2010 (Milton Hill House, Oxfordshire, 19-20 April 2010);
2. Haddad G.I., Trew R.J. Microwave Solid-State Active Devices. // IEEE MTT.- 2002.- V. 50. – N 3. p.760.

The Processes of Formation and Growth Mechanisms of Vapor-Phase Condensates CdTe

Sokolov O.L., Lishchynskyy I.M., Potyak V.Yu.

Vasyl Stefanyk Precarpathian National University, Ivano-Frankivsk, Ukraine

Cadmium telluride - wide-gap semiconductor from a group of compounds II-VI, which is widely used as active elements of nonlinear optics and optoelectronics [1,2]. In particular, thin film CdTe layers are the base of solar modules and in photovoltaic energy conversion [3]. Cadmium telluride in their physical characteristics and parameters has several advantages over other semiconductor compounds II-VI. These include a wide band gap, the ability to show both types of conductivity (n-, p-), their low concentration of charge carriers under normal conditions (2,0 • 10-16 cm-3 at 300 K), low coefficient of light absorption in the infrared region of the spectrum, high resistance to chemicals and humidity, relatively high mobility of charge carriers and not very stringent conditions of synthesis [4].

Film nanostructures CdTe obtained from the vapor phase by the method of hot wall. The process of deposition occurred on substrates of glass and ceramics. Temperature evaporation of the sample pre-synthesized compounds CdTe change within T_V = (400 - 500)°C. Chamber wall temperature T_S maintained at 50 K above the temperature of the evaporator T_V. Deposition on the substrate temperature change in the range T_S = (150 - 250) °C. The thickness of the condensate asked deposition time t = (0,3-5) min. These nanostructures were investigated by atomic force microscopy (AFM) in contact mode periodically.

Methods AFM studies revealed features of structure formation in thin film nanostructures of CdTe, grown from the vapor phase by the "hot wall" on substrates of glass and sital. It is shown that the mechanism Folmera-Weber on substrates of glass and ceramics formed single nanostructures mainly columnar or pyramidal shape, placed normal to the substrates.

1. С.А. Медведев. *Физика и химия соединений* $A^{II}B^{VI}$ / С.А. Медведев. Мир, М. 624 с. (1970).
2. А.Н. Георгобиани, М.К. Шейкман. *Физика соединений* $A^{II}B^{VI}$. Наука, М. (1986).
3. Ю.З. Бубнов, М.С. Лур'є, Ф.Г. Старос, Г.А. Филаретов. *Вакуумное нанесение пленок в квазизамкнутом объеме*. Энергия. Л. 161 с. (1975).
4. D. Nobel. Phase equilibria and semiconducting properties of cadmium telluride // ***Phil. Res. Repts.*, 14,** pp. 361-492 (1959).

The work supported by an integrated project of MES of Ukraine (N 0113U000185)

Optical Properties of Titanium Nitride Thin Films

Solovan M.N., Brus V.V., Maryanchuk P.D.

Yuriy Fedkovych Chernivtsi National University, Chernivtsi, Ukraine

Titanium nitride (TiN) is widely applied due to its good combination of physical-chemical properties: low specific resistance, relatively high transmittance within the visible spectral range, high hardness, high chemical and corrosion resistance.

Due to its physical properties TiN is a prospective material for the application in different photoelectrical devices. This work reports the results of optical and electrical properties of TiN thin films, prepared by the reactive magnetron sputtering method.

The deposition of the TiN thin films was carried out onto glass substrates by means of the reactive magnetron sputtering of a pure titanium target in the mixture of argon and nitrogen gasses at DC voltage. The partial pressures of argon and nitrogen were equal to 0.35 Pa and 0.7 Pa, respectively, at a constant magnetron power 120 W. The substrate temperature was equal to 473 K during the deoposition process.

The transmittance and reflectance spectra of the thin films were measured using a conventional spectrophotometer СФ-2000. The experimental points were measured within the wavelength range from 200 to 1000 nm with the step 1 nm.

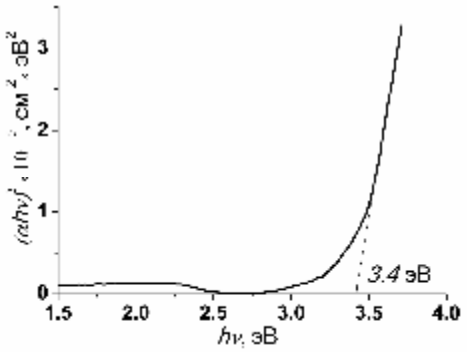

Fig.1 The plot of the dependence $(\alpha h\nu)^2 = f(h\nu)$ for the TiN thin films.

The main optical constants of the TiN thin films were determined from the measured transmittance and reflectance as well as the absorption coefficient of the TiN thin films is well governed by the following equation within the self-absorption region:

$$a(hn) = A(hn - E_g)^{1/2}, \qquad (1)$$

where A is the coefficient which is dependent on the ratio of the effective masses of charge carriers. This dependence of α(hν) provides evidence that the material of the TiN thin films deposited by means of the DC reactive magnetron sputtering is a direct band gap semiconductor. The value of the band gap of the TiN thin films (Eg = 3.4 eV) was determined by the extraopolation of the linear segment of the dependence $(\alpha h\nu)^2 = f(h\nu)$ toward the interception with the energy axis (figure 1).

1. Jeyachandran Y.L., Narayandass Sa.K., Mangalaraj D. Properties of titanium nitride films prepared by direct current magnetron sputtering // Materials Science and Engineering. –2007. – A 445–446. – P. 223–236.

Electrochemical Formation of Nanostructured Anodic Niobium Oxide

Tokareva I.A., Lyashok L.V., Bayrachniy B.I., Savitsky B.A., Leshenko S.A.

National Technical University "Kharkov Polytechnic Institute", Kharkov, Ukraine

Porous oxides valve metals (Al, Ti, Nb, Ta, Zr), obtained by anodic oxidation, attract researchers' attention because of their unique physical and chemical properties that allow them to form the basis of new functional materials with a wide range of applications.

This work aims at the complex study of the electrochemical synthesis of a self-organized porous niobium oxide (PNO) and the development of the theoretical bases of the processes during the synthesis.

The analysis of the theoretical regularities and experimental results of the formation of the anodic oxide film (AOF) on niobium made it possible to determine the sequence of the processes during the synthesis of the self-organized structure PNO: 1) the formation of a barrier film; 2) the thickening of the barrier layer and pore nucleation; 3) the growth of the porous layer, pore separation to form the self-ordered structure of PNO.

Using the method of linear volamperometriya and the processing of the obtained data, it was determined that the formation of the barrier AOF on niobium in solution of 1 M H_2SO_4 is a two-step mechanism, where the first step is the reaction of the electrochemical adsorption of hydroxyl ions, and the second one is the reaction of their recombination.

During the anodization in acid electrolyte in the presence of an activator (F^-) pores appear on niobium and the self-ordered structure PON is formed. The mechanism of porous oxidation is not certain yet. However, most scientists agree that on the anode several processes take place simultaneously: the growth of the oxide and the dissolution of the oxide film. The reactions taking place in the system can be described as follows:

$$10NbOH_{ads} = Nb_2O_5 + 8Nb + 5H_2O$$
$$Nb_2O_5 + 14HF = 2[NbF_7]^{2-} + 5H_2O + 4H^+$$

The formation of the self-organized structure of PNO is determined by the concentration of the activator, the oxidation regime and the hydrodynamics of the processes in the pores.

The results of scanning electron microscopy synthesized on niobium AOF in the solution of 1 M H_2SO_4 with the activator (0,5 M and 1 M HF) at 60 V indicate the origin and growth of the secondary structures, which completely cover the surface of PNO. The morphology of the films depends on the composition of the electrolyte, voltage and the time of anodizing.

Effect of the Ag Intermediate Layer on the Structure and Magnetic Properties of Annealed FePt/Ag/FePt Thin Films

Vladymyrskyi I.A.[1], Verbitska T.I.[1], Pavlova O.P.[1], Sidorenko S.I.[1], Katona G.L.[2], Beke. D.L.[2], Makogon I.M.[1]

[1]*National Technical University of Ukraine "KPI", Metal Physics Department, Kyiv, Ukraine*
[2] *University of Debrecen, Department of Solid State Physics, Debrecen, Hungary*

Chemically ordered $L1_0$-FePt films caused high interest as possible material for ultra high density information storage due to their large magnetic anisotropy of about 10^7 J/m^3. Typically *L10*-FePt phase forms at elevated temperatures due to thermally activated diffusion processes from the chemically-disordered *A1*-FePt phase. Reducing of the ordering temperature and magnetic properties improving are actual tasks for FePt thin films industrial application.

In this study, we prepared FePt(15 nm)/Ag(x)/FePt(15 nm) trilayers with various Ag interlayer thickness which were deposited at room temperature onto SiO_2(100 nm)/Si(001) substrates. These films were post-annealed at temperatures up to 900°C for 30 seconds. The influence of the Ag interlayer on the $L1_0$-FePt phase formation and its related magnetic properties were investigated by physical materials science methods. It was assumed that mechanical stresses at the layers interfaces could be additional driving force for diffusion processes resulting in ordering temperature reducing. Formation of isolated FePt grains was expected after annealing due to the limited solubility of Ag in FePt and its primary grain boundary diffusion mechanism, resulting in higher coercivity of the films.

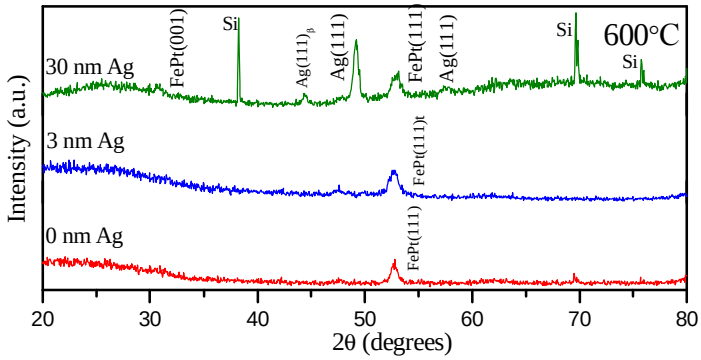

Fig. 1 XRD patterns of FePt/Ag(x)/FePt (x=0; 3; 30 nm) films after annealing at 600°C

XRD analysis indicates that annealing of the film samples up to 500°C does not significantly change the structure. The onset of chemical ordering in films with Ag layer thickness 0 nm or 3 nm is observed at annealing temperature 700°C. But film with 30 nm thick Ag interlayer shows small (001) superstructure reflection after annealing at 600°C (fig. 1), which indicates that Ag interlayer introduction can lead to the ordering temperature decreasing.

Research and Design of Iron Films, Electrodeposited Surge Current

V.O. Zabludovsky, R.P. Ganych, V.V. Artemchuk

Academician V. Lazaryan Dnepropetrovsk National University of Railway Transport
Dnipropetrovsk, Ukraine

At the present time, for non-equilibrium states in metal films, as well as the formation of their amorphous structure found widespread variety of methods superfast cooling melts and laser surface hardening of metals and alloys. However, these methods have recently become widely used electrolytic deposition of metals and alloys by pulse current, in which the role of superfast supercooling during crystallization of films from solutions of electrolytes takes cathode strain. The interest in this method caused not only by its relative simplicity and efficiency, but also its great potential in the management of the crystallization kinetics of metal films, which in turn allows them to influence the morphology, structure and physics-chemical properties.

Represents great practical interest the possibility of creating a mathematical model that would allow to establish a relationship between the magnitude of crystallization over potential at the cathode and structure (grain size) formed electrolyte films. For receiving films of iron sulphate salt used. Electrolyte had the following composition (gram/liter): $FeSO_4 \cdot 7H_2O - 220$; $H_3BO_3 - 20$. Correction acidity pH = 2 ... 2,5 performed by adding 5% solution. Deposition was carried out at 293 ... 298 K rectangular current pulses at 30 ... 1000 Hz and aperture pulses from 2 to 32 and an average current density of 1.5 ... 3 A/dm^2.

On the basis of these studies was proposed mathematical model that allows us to predict the grain size of crystals in electrolytic films formed on the surface and the mechanism of their growth, the value of crystallization polarization. In constructing a mathematical model used the results of the Kolmogorov AM for the case of two-dimensional growth of embryos and Chernoff AM of layered-spiral growth of crystals.

The experimental results of the size of crystals films when compared with the calculated by the model showed a high degree of overlap. Differences were observed only at very low supersaturation (630 nm and 820 nm, both theoretical and experimental, respectively), and at very high supersaturation (330 nm and 230 nm). In the first case, this is due to the passivation of the cathode surface at small polarizations, which makes the formation of a large number of embryos in the second - a significant discharge of hydrogen adsorption on the surface of the crystal which inhibits their growth. The results obtained studying the influence of pulsed current conditions of crystallization of metal films show that using this method can widely change the structure and growth kinetics of electrolytic metals and alloys, which in turn will allow manage their physical and chemical properties.

Technological Features of the Formation of Electronic Instrument Composition PcCu / por-Si / n-Si and PcAl / Por-Si / n-Si

Zubko E.I.

Zaporozhye State Engineering Academy, Zaporozhye, Ukraine

An important problem of modern electronics is to improve quality semiconductors, due to the extensive development of nanostructured materials. One of the areas which are electronic instrument composition that combine incorporates micro- and nanoparticles of various compounds and materials that have advanced the surface. The latter refers porous silicon (PS) formed by electrolytic anodizing floor which precipitated by spraying solutions of copper phthalocyanine (PcCu) or aluminum phthalocyanine (PcAl). Further samples saturated for 2 hours in a desiccator and dried. After this operation, structure annealed at 250 - 300 °C in air in a current of 5 - 10 minutes.

With the formation of surface films phtalocyanine (Pc) use solutions with concentration $C_{32}H_{16}N_8Cu : C_3H_6O : H_2O = 2 : 39 : 59$ wt. % and $C_{32}H_{16}N_8Al : C_2H_5OH : H_2O = 2 : 59 : 39$ wt. % That obumovlyuyesya creating structures with copper mesh size of 200 - 1000 nm or aluminum mesh with dimensions 500 - 1200 nm. Size of metal fibers in PcCu/por-Si/n-Si differs from fibers PcAl / por-Si / n-Si 1.5 times [1].

As a result of solvent evaporation and structuring compositions observed correlation of internal stresses arising in the structures. High values of internal stresses cause cracking along the border "monocrystalline silicon - porous silicon." Therefore it is necessary to use a solution with t_{sol} = 40 °C and the substrate with $t_{n\text{-}Si}$ = 45 °C.

In the study of multicomponent electronic instrument tracks were found dependence of physical effects (annealing) for electrical and electrical properties of compositions.

1. E. I. Zubko, Zaporozhye State Engineering Academy, Zaporozhye, UK, "A method for manufacturing a contact layer on the surface anti-reflective coating of the solar cell", Ukraine, patent for utility model 67830 Ukraine: IPC (2012.01) N 01 L 43/00, owner. — U 2011 08780, appl. 07/12/2011, publ. 12.03.2012, Bull. № 5, pp. 4.

СЕКЦІЯ 1 (стендові доповіді)
ТЕХНОЛОГІЯ ТОНКИХ ПЛІВОК (МЕТАЛИ, НАПІВПРОВІДНИКИ, ДІЕЛЕКТРИКИ, ПРОВІДНІ ПОЛІМЕРИ) І МЕТОДИ ЇХ ДОСЛІДЖЕННЯ

21 травня 2013 р.

SESSION 1 (poster)
THIN FILMS TECHNOLOGY (METALS, SEMICONDUCTORS, DIELECTRICS, CONDUCTIVE POLYMERS) AND THEIR RESEARCH METHODS

May, 21, 2013

The Creating Ordered of Nanostructure with Template Synthesis

Barabash M.Yu., Vlaykov G.G., Grynko D.A., Martynchuk E.L.

Technical Center of NAS of Ukraine, Kyiv, Ukraine

Template is a functionally organized in space mikroinstrument for guiding physical and chemical processes of nanoobjects selforganization in space and time by interaction with its surface via the local field. Strong, spatially organized electrostatic field of template influence the nucleation, adsorption and diffusion transport of nanoparticles.

Template is a tool which allows fabricating nanostructures, fig.1, 2, in non-lithographic process [1-5]. For the electrostatic template preparation authors suggest to apply photothermoplastic electrophotographic process with a free surface of the specific nanocomposite organic photoconductors [5]. The spatial resolution of template is determined by the larger of two factors: the diffusion length of components (molecules, nanoclusters, nanocrystals, etc., which essentially depends on the mass of nanoparticles and interaction with the surface topology) and the period of the field distribution.

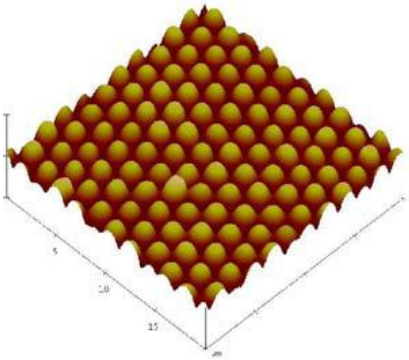

Fig.1. Gold nanoclusters organized by strong electric field of the template, AFM. Period 2μm, height 120 nm

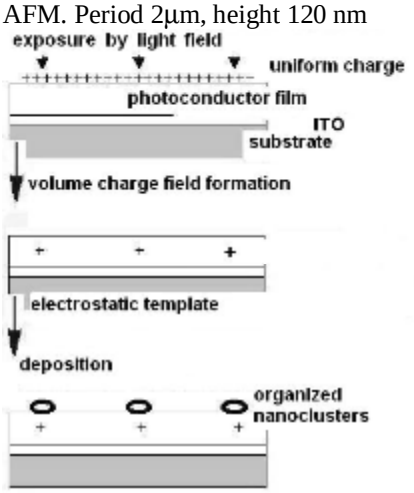

Fig.2. Nanstructure assembly on the template. Nanstructure topology controlled by topology of light field

Template-organized 2D optical nanostructures maked with organic dye and gold nanoclusters. Their optical resonances and template preparation technique presented in publications [5]. Nanocomposite Au- plymer (poly-N-vinyle-carbazole), co-deposited in vacuum on the surface of template, selforganised efficiently also. TEM investigation of nanocomposite gold clusters permit to find out nanoclusters size distribution and critical nuclear size. Shift of critical nuclear size in the electric field of template show the dramatic impact of local electric field on nucleation and critical nuclear size. Nucleation modeling in the thermodynamics approach yield estimation of local electric field. Estimated fields are: electric mean field 10^8 V/m and local field 10^9 V/m.

Conclusions

Manipulation with electric field of template allows controlling basic processes of condensed phase formation: adsorption, diffusion and nucleation and to assemble some nanostructures for nanophotonics and nanoplasmonics via guided selforganisation processes. Nucleation in the electric field of the template is the way to new phases formation.

[1] Patent of Ukraine №55127, 2010.

[2] Patent of Ukraine №58732, 2011.

[3] D.A. Grynko, Yu.M. Barabash, M.A. Zabolotny, I.E. Matash, M. Yu. Barabash, *Producing of surface periodic nanostructures by templates technique,* Nanosystems, nanomaterials, nanotechnologies 2008, Vo. 7, № 3, pp. 977-984.

[4] Yu.M. Barabash, M. A. Zabolotny, V.N. Kharkyanen,, *Holographic interferometry as a method to study conformational change in macromolecules,* Semiconductors physics, quantum electronics and optoelectronics, 2002, Vol. 5 ,№3 , pp.58 –63

[5] D.A. Grynko, Yu.M. Barabash, I.E.Matyash, B.K.Serdega, *e.a.,Modulation polarimetry of topological effects in films of gold-organic nanocomposites,* Physics of the Solid State, 2012, Vol. 54, №11, pp.146-153.

Strain determination in the area near the crack by Kikuchi line analysis

Borcha M.D.[1], Zvyagintseva A.V.[2], Tkach B.M.[3], Yushenko K.A.[2], Balovsyak S.V.[1], Fodchuk I.M.[1], Khomenko V.Yu.[1]

[1] *Yuriy Fedkovuch Chernivtsy National University, Chernivtsy, Ukraine*
[2] *E.O. Paton Electric Welding Institute of National academy of Science of Ukraine, Kyiv, Ukraine*
[3] *V.N.Bakul Institute of Superhard Materials of National academy of Science of Ukraine, Kyiv, Ukraine*

Electron backscatter diffraction method (Kikuchi method) allows us to investigate the local elastic lattice strains in single crystals, multilayer systems, films and on the interface between the nanoscale areas [1-2]. This method was used for studying the weld joint in nickel alloy near the crack arisen due to thermal influence (fig. 1a). Kikuchi patterns from the areas with minimal grain strains (clear, blur-free images of Kikuchi lines) and from the highly deformed areas (strongly blur patterns) were studied. Experimental patterns of Kikuchi lines were obtained by scanning electron microscope «Zeiss» EVO-50 with the CCD-detector.

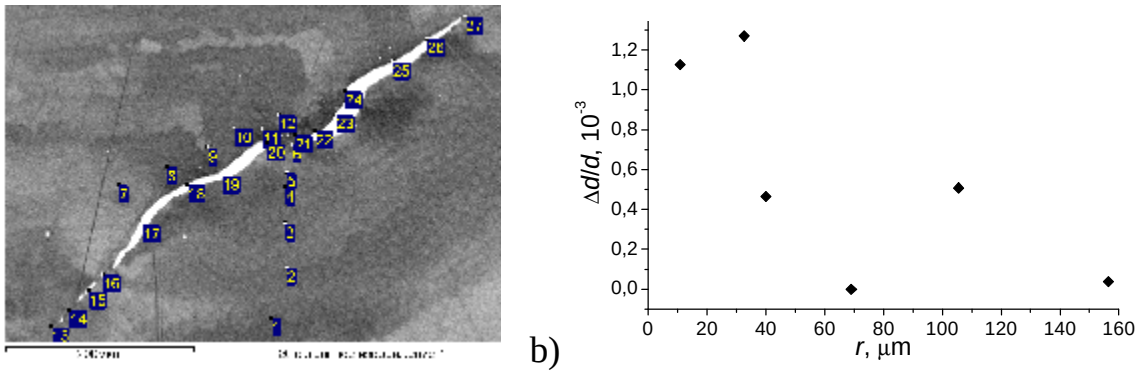

Fig.1. a) Fragment (600 × 450 μm) of specimen surface near the crack; numbers indicates subareas, from which Kikuchi patterns were obtained; b) values of the $\Delta d_{hkl}/d_{hkl}$ in local areas situated on the distance r from the crack.

To determine interplanar spacing the analysis of two dimensional Fourier spectrums of Kikuchi patterns was used. Analysis was carried out for spatial frequencies ν = 0 ... 150, because higher frequencies correspond to the noise. Dependence of harmonic amplitudes on spatial frequency ν forms curve, square S under which is proportional to level of pattern blur. Difference between this square and square that corresponds to perfect area (ΔS_f) is related with value of relative strain $\Delta d_{hkl}/d_{hkl}$ by empirical formulae $\Delta d_{hkl}/d_{hkl}=k\cdot dS_f$. So strain distribution in the area near the crack was determined from the analysis of ΔS_f and it shown on the fig.1b.

1. Borcha M., Fodchuk I., Balovsyak S., Garabazhiv Ya., Tkach V. // Phys. Status Solidi A, - 2011, 208, N 11, 2591–2596
2. Keller R.R., Roshko A., Geiss R.H., etc. // Microelectronic Engineering. V.75. N 1. 2004. P. 96.

Technological Modification of AS_2S_5 glass

Borkach E.I., Ivanytska G.M., Svatyuk O.Y.

Uzhgorod national university, Uzhgorod, Ukraine

We have studied the influence of synthesis on microstructure and parameters of the short order AS_2S_5 glass. For this aim the glasses was synthesized at different temperature isothermal exposure (T_1 =870 K; T_2 =1120 K; T_3 =1370 K) and at different cooling velocity (V_1 =10^{-2} K/s; V_2 =1,5 K/s; V_3 =1,5·10^2 K/s). Structural investigations of the obtained glasses were conducted with the use of electron diffraction and electron microscopy. For this from the massive specimen the cuts of 75-100 nm were produced.

In the investigation process we got the following results:

1. As_2S_5 glass microstructure synthesized at 870 K and melt cooling velocity 10^{-2} K/s is a homogeneous glassy matrix in which there are evenly placed some micro-disperse parts of another phase in the form of pseudo-grains no more then 1-2 nm. In some cuts of these glasses the big regions were found that were free from micro-disperse parts of another phase. The structural $AsS_{3/2}$ units create the main matrix of glass and micro-disperse phase is aggregation of S atoms that are situated among micro-regions created by structural $AsS_{3/2}$ units. Micro-disperse formation on some regions may create clusters of spherical form 50-100 nm in diameter.

2. As_2S_5 glasses that are synthesized at 1120 K and melt cooling velocity 1,5 K/s have homogeneous micro-dispersed structure. The size of micro-dispersed grains is 1-2 nm in diameter.

3. As_2S_5 glasses that are synthesized at 1370 K and melt cooling velocity 1,5·10^2 K/s are characterized by non-homogeneous two-phase structure, which is created by the mixture of micro-dispersed phase with the strong level of micro-dispersion and arbitrary scattered in them microcrystalline elements with 50-100 nm in diameter. The sharp peaks on electro diffraction patterns of such glasses correspond to the most intensive lines of S_α. It is evident that at high synthesis temperature As_2S_5 melting dissociation takes place.

4. Electron diffraction patterns of As_2S_5 (T_1V_1) and (T_2V_2) glasses do not differs from each other and they are very close to electro diffraction pattern of glassy As_2S_3. We can conclude that the main structural units in the both glasses are the same.

5. The further increase imbalance of synthesis process of $As_2S_{2/3}$ due to the laser melting of the components leads to realization of two-phase micro-disperse structure. That is manufactured by arbitrary mixture of micro-disperse parts 50-100 nm in diameter with dark diffraction contrast included into micro-disperse matrix that takes 60 % of the total specimen volume. The location of the sharp diffraction peaks of parts coincides with the lines of monoclinic S_β.

Influence of Laser Radiation on the Structure and Physical Properties of Proustite Ag_3AsS_3

Borovoy N.[1], Gololobov Y. [2], Salnik A. [1]

[1] *Taras Shevchenko National University of Kyiv, Kyiv, Ukraine*
[2] *Transport National University, Kyiv, Ukraine*

Proustite Ag_3AsS_3 crystals are promising materials for nonlinear optics, so its investigation is well-developed in a wide temperature range – from helium to 600 K. Decreasing of temperature of the proustite crystals accompanied by structural phase transitions (PT) at a temperature 56 K and 24 K. It is important to note that the situation changes in optical radiation of proustite.

The available data on the effect of optical illumination on physical properties of proustite crystals is rather contradictory. The temperature dependences of the unit cell parameter *a(T)* and *c(T)* of proustite crystal were obtained by X-ray dilatometry method with high precision in temperature range 100 to 300 K in dark mode and during laser irradiation. It was found increasing of the parameter *c* on the value of $\Delta c \approx (0{,}002 - 0{,}003)$ Å at temperature $T_p = (145 - 147)$ K for the sample that was exposed during the cooling of the laser radiation. This jump is typical for systems in which occurs a phase transition of the first order. The nature of the observed photoinduced change of the parameter *c* can be associated with direct photostimulated migration processes of the ion Ag^+ at affordable crystallographic positions in the unit cell. Also, there are anomalies of temperature dependences of longitudinal ultrasonic waves velocity along the main crystallographic directions of irradiated proustite crystals (emission of a helium-neon laser), which were observed only at the temperature 150 K.

1. K. A. Schonau, S. A. T. Derfern, High-temperature phase transitions, dielectric relaxation, and ionic mobility og proustite, Ag_3AsS_3, and pyrargyrite, Ag_3SbS_3 // Journal of applied physics. – 2002. – V. **92**, № 12. – C. 7415.
2. Г. А. Смоленский, И. Г. Синий, Е. Г. Кузьминов, А. А. Годовиков, Оптические фононы и мягкая мода в прустите при фазовых переходах // ФТТ. – 1979. – Т. **21**, № 8. – С. 2332.
3. Г. А. Смоленский, И. Г. Синий, С. Д. Прохорова, Е. Г. Кузьминов, А. В. Годовиков, Новый фазовый переход в прустите // Кристаллография. – 1982. – Т. **27**, № 1. – С. 140.
4. Л. А. Кот, С. Д. Прохорова, Ю.М. Сандлер, И.Г. Синий, И. Н. Флеров, Фотоиндуцированный фазовый переход в прустите // ФТТ. – 1983. – Т. **28**, № 5. – С. 1535.
5. Я. Шаурен, К. Н. Р. Тейлор, Исследование фотоиндуцированного фазового перехода в прустите Ag_3AsS_3 // ФТТ. –1986. – Т. **28**, № 9. – С. 2604.

The Processes of Formation and Thermoelectric Properties of Vapor-Phase Tin Telluride Structures

Chaviak I.I.

Ivano-Frankivsk National Medical University, Ivano-Frankivsk, Ukraine

The recent intensive development of nanophysics and nanotechnology stimulates theoretical and experimental studies of the specific properties of systems whose behavior can be described only in terms of quantum mechanics. Quantum size effects (QSE) belong to the group of phenomena reflecting the wave properties of electrons in solids.

IV–VI compounds are commonly considered to be promising materials for thermoelectric, optoelectronic and other applications and. Recently, interest in these materials has grown due to the observation of an increase in the thermoelectric figure of merit $Z = S2\sigma/\lambda$ (S is the Seebeck coefficient, σ is electrical conductivity, λ is thermal conductivity) in IV–VI superlattices. The interpretation and forecasting of the transport properties of IV–VI semiconducting multilayered structures are impossible without knowing the properties of a single QW.

Samples for the investigation were grown from the vapor open phase by evaporation under vacuum at fresh chips (001) mica-muscovite. Evaporator temperature during deposition was T_e = 700 °C, and the temperature substrates was varied T_s = (150-250) °C.

Measurement of electrical parameters investigate in air at room temperature, magnetic field constant. Measured sample four hall contact and two current contacts. In ohmic contacts were used as film silver. The current through the sample was ~ 4 mA. Magnetic field was perpendicular to the surface condensate in the induction of 1,4 Tesla.

Hall mobility was calculated $\mu=RH\cdot\sigma$. Carrier concentration p-type determined ratio $p=A/(R_H \cdot e)$, considering it corresponding actual concentration by significantly dominant one media type and taking Hall factor A=1. All have p-type conductivity.

It is shown that for SnTe nanostructures on mica dependence of conductivity, Hall coefficient, mobility, concentration and Seebeck coefficient the thickness of the thermoelectric power exhibit non-monotonic, oscillation behavior that is related to the dimension quantization of the energy spectrum of light holes quantum wells.

1. Чав’як І.І. Наноструктури станум телуриду на сколах слюди-мусковіт // Фізика і хімія твердого тіла. – 2012. – Т.**13,** №1. – С. 64-68.
2. І.К. Юрчишин, І.І. Чав’як, Ю.В. Лисюк, Л.Т. Харун. Розмірні ефекти термоелектричних параметрів у наноструктурах p-SnTe на слюді. // Фізика і хімія твердого тіла. – 2010. – Т.**11,** №4. – С. 898-903.

The work supported by projects of NAS of Ukraine (N 0110U006281)

Calculations of Interatomic Interaction Potential Parameters for Modelling of As-S Film's Condensation Processes and Structure

Demesh Sh.Sh., Dalekorey A.V., Opachko I.I.

Uzhhorod National University,
Uzhhorod, Ukraine

During the investigations of amorphous thin films of system As-S scientists had met with numerous interesting properties and physical-chemical phenomena, for example with photoinduced mass-transport and optical anisotropy. But the nature and the mechanisms of their manifestation on the disordered level of atomic network until this time haven't found exhaustive explanation. In our opinion, this would be done by building macromodels of As-S thin film's structures, which are consist of a few thousand atoms. These models must comply with real structure formation processes of disordered atomic systems during the condensation of vapor flows, which can be also successfully investigated by modern computational methods. Adequate way for such kinds of investigations is the application of modern approximational quantum-mechanical methods, which have shown their high efficiency in case of study large-scaled macrosystems: macromolecules, crystals, polymers, proteins and so on. Applying such kinds of computational approaches gives us opportunity to obtain results, which couldn't be obtained experimentally or which could be obtained only as results of very complicated experiments. However solutions to most problems of modelling with approximational methods are impossible without knowing the many-particle potentials, which could realistically describe interatomic interaction of atoms up to one nanometer. Finding the exact parameters for such kinds of potentials in case of disordered networks of As-S systems is devoted to this work.

Calculations were performed on the basis of density functional theory. All calculations were performed in the software environment called Quantum Espresso PWSCF, by the way of performing self-consistent calculations in order to achieve density functionals by expanding the investigated system to basis function using plane wave method. Basis functions with the exchange-correlation functionals using the software interface could be given in form of numerous different mathematical expressions – pseudopotentials. As initial structural and energetical quantities for the determination of the parameters of potentials we have used crystallographical and thermodynamical data for ten different crystal phase, which are realized in As-S systems: AsS, AsS-α, As_2S_3, As_2S_3-α, As_4S_3, As_4S_3-β, As_4S_4, As_4S_4-α, As_4S_4-β, As_4S_5. In order to check the reality of obtained potentials we have provided comparison of energy values of different molecules As_nS_m from 10-15 atoms, wchich were calculated using the potentials and ab initio quantum-mechanical calculations with unrestricted Hartree-Fock method using the GAMESS software.

Surface Structure of the Polymer Modified Materials

Domantsevich N.I., Yatsyshyn B. P., Martinyuk M.M.

Lviv Commercial Academy, Ukraine

Structural studies and mechanical tests of polymer materials, contained dyes and secondary raw materials from wastes, are done.

A polyethylene materials with brand of PE2NT22-12 with additions of secondary raw polymer material were obtained by force-feed casting. The surface structure investigations was studied with scanning electron microscope EVO 40XVP with high-resolution of objects.

It is discovered structure of the unmodified samples, close to structure thin polymer films, which were obtained by extrusion in ordinary technological terms (with small stretching and insignificant blowing) – the oriented structure formations that is determined by viscidity of fusion and direction of his exit from the head of extruder, that's mean gathers with direction of action of the stretchings and thermogradient fields. Quantity of crystals in such structures is insignificant, and their growth is unoriented, that masks characteristic crystalline diamond-shaped forms which is peculiarities of the polyethylene crystals. That's why sample surface acquires a scaly-kind nature with the insignificant hollows and cavities.

Partial substituting of initial polyethylene by secondary raw polymer material (up to 60 wt. %) and addition of the modifying components (silicon lubricant), that allows to facilitate technological processing, considerably change structure and properties of polymer material. Defection in matrix and size of cavities increase, only a partial orientation of structure in direction of operating technological deformation efforts observed.

The contaminations which entered in a matrix lead to increasing of quantity of crystallization centers, but do not influences on orientation of crystals, however in future results in enlargement of crystalline structure and, accordingly, leads to increasing defects concentration along lines "amorphous-crystalline boundary".

Grain growth in polymer samples, which fully made from secondary raw material, was more active. The crystallization of the sample grows. A structure acquires more defects that guide to disintegration and ramified of separate crystalline areas.

Properties and Structure of the Modified Polyethylene Films

Domantsevich N.I., Yatsyshyn B. P., Mykitiv N. S.

Lviv Commercial Academy, Ukraine

The application of polymer thin films for the necessities of food industry correlated in most cases with packing and storage of products. As a polymeric matrix low density polyethylene (LDPE with brand 15803-020) of not imported and foreign production granulate was choose. As additions-fillers, organic (Casein, up to 9 wt.%), mineral (Kredolen, up to 25 wt. %) and mixed (Vatpol 210, up to 30 wt/ %), were used.

Oxygene permeability determined with the help of oxygene depolarization gauges or thin film thermocouple, which were placed under polymer films.

The mineral fillers considerably diminish initial index of permeability. But high temporary dynamic of changes of permeability index in such films show activity of destructions process during short period. In the Casein contained films such tendency is not observed. The increasing of film thickness results in decline of diffusive transference through material in 1,2 – 1,4 times – from $P = 1{,}3515 \cdot 10^{-16} \ \frac{m^3 \cdot m}{m^2 \cdot s \cdot Pa}$ for a polyethylene film with thickness h = 50 μm up to $P = 1{,}0109 \cdot 10^{-16} \ \frac{m^3 \cdot m}{m^2 \cdot s \cdot Pa}$ for film with h = 150 μm.

The speed of diffusive transference diminished with strengthening of molecular interaction, degree of crystallization and orientation in matrix, which predetermined increase of density polyethylene objects. Samples with high density have greater strength, less creep, and less gas permeability, while objects with low density are more flexible and translucent. The uses of different fillers, paints, dyes, plasticizers, lubricants, glues, also as electromagnetic fields and ionizing radiations, changes diffusive characteristics of materials.

Insignificant defects of initial samples were ascertained by scanning electron-microscopy researches of surface. Such result contacts with technology of films manufacturing. Additions of casein change the structure of surface – the amount of crystalline formations diminishes, however their sizes grow.

Addition of inorganic fillers leads to specific structure of surface which has initial insignificant defects, micro- and nanoporous.

Optimization of Semiconductor $Hg_3In_2Te_6$ and $In_4(Se_3)_{1-x}Te_{3x}$ Telluride Single Crystals Surface

Dremlyuzhenko S.G., Rarenko I.M., Strebezhev V.V., Strebezhev V.N.

Yuriy Fedkovych Chernivtsi National University, Chernivtsi, Ukraine

Promising for sensor electronics compound semiconductor functional materials, such as $Hg_3In_2Te_6$ and $In_4(Se_3)_{1-x}Te_{3x}$ tellurides solid solutions, are currently the focus of intense research. Growing need for the design of radiation-resistant semiconductor Schottky diodes and epitaxial heterojunctions causes thorough study of $Hg_3In_2Te_6$ and $In_4(Se_3)_{1-x}Te_{3x}$ single crystals surface. $Hg_3In_2Te_6$ crystals have been grown by modified zone melting method. Studies of $Hg_3In_2Te_6$ samples resistivity and Hall effect in 80-420 K temperature range have shown that they have an electronic type of conductivity and high radial homogeneity of electrical and photovoltaic parameters.

Schottky diodes have been created by vacuum deposition of thin nickel films on the surface of grown crystals. Diodes are resistant to X, γ and β-radiation doses within 10^6–$4\cdot10^8$ rem and photosensitive in the important range of infrared spectrum 0.75–1.5 microns. $In_4(Se_3)_{1-x}Te_{3x}$ crystals have been grown by Czochralski method using the Peltier effect. Photosensitive In_4Se_3–$In_4(Se_3)_{1-x}Te_{3x}$ heterostructures are obtained by liquid-phase epitaxy.

Morphology and surface structure of $Hg_3In_2Te_6$ and $In_4(Se_3)_{1-x}Te_{3x}$ single crystals are studied by scanning electron microscopy at accelerating voltage of 30 kV. It is found that crystals surface with a minimum number of surface defects and etching tracks can be achieved by chemical etching and ion polishing treatment (Fig. 1). Applications of developed etchants and polishing modes improves parameters and characteristics of $Hg_3In_2Te_6$ and $In_4(Se_3)_{1-x}Te_{3x}$ based film structures.

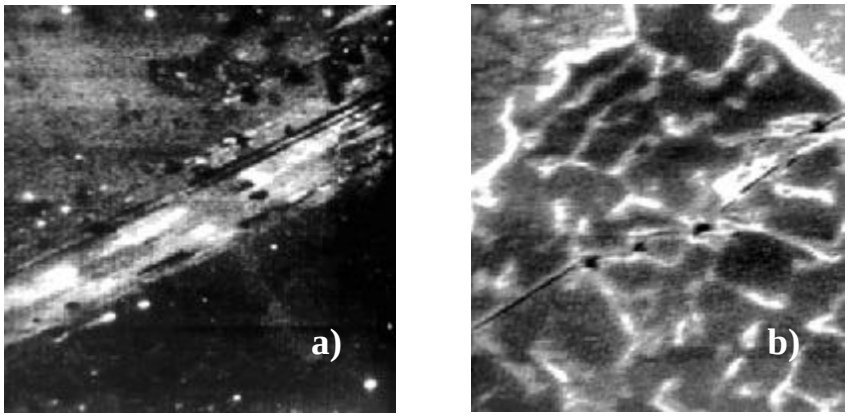

Fig. 1. Morphology of $Hg_3In_2Te_6$ crystal surface to (a) and after (b) chemical polishing.

Simulation of moiré patterns of silicon depending on the nature of arrangement of local concentrated forces in the series

Fodchuk I.M., Novikov S.M., Fesiv I.V., Struk Ya.M., Yaremchuk I.V.

Yuriy Fedkovych Chernivtsi National University, Chernivtsi, Ukraine

Today X-ray interferometry is a powerful tool for studying medical and biological objects in phase tomography [1]. In this case, structural defects and macrodeformation in plates of interferometer significantly affect on interference image. Therefore, the establishment of common principles and mechanisms of the formation of moiré intensity distributions has a great scientific and practical importance, because it allows much easier interpretation of the causes of the complex moiré patterns formation.

We have carried out simulation of moiré patterns in case of their formation from model scratches, formed by the action of evenly or unevenly distributed point forces. Such research should identify mechanisms of the formation of moiré images on the distance and in the immediate proximity to the source of strain.

So for example in Figure 1 increase in microscratches power *P* generally increases the number of moiré patterns and reduce their periods as well as it leads to a stronger bending of structural moiré bands. In particular, if at a relatively small power of scratches (*P*=48) the central band of structural moiré bifurcated and skirted the area of strain moiré appearing, then already at *P*=113 there left only six of 9 strips of structural moiré, but the area of strain moiré increased.

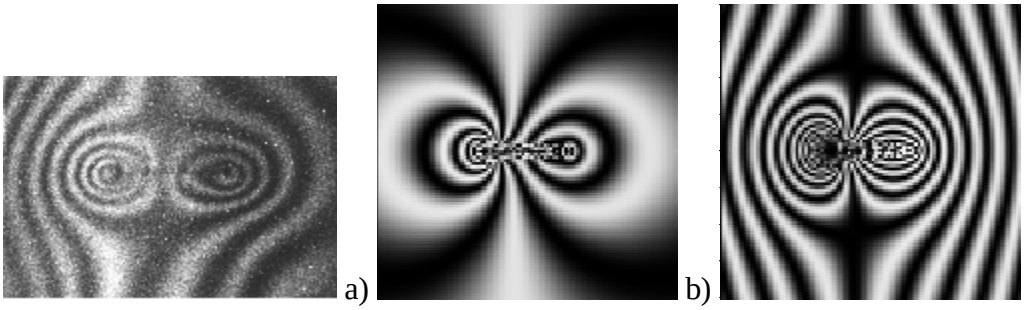

a) b) c)

Fig.1. (a) Experimental moiré images of scratch after scribing by indenter of the output surface (111) of the interferometer analyzer [2] (line of scratch is parallel to $\vec{H}_{220}$). (220) reflection for Cu$K_{\alpha 1}$-radiation.
(b, c) Theoretically calculated moiré patterns. The number of concentrated forces equals 7. The distance between them is uniform. Distribution of power is unequal (downward), i.e. tension is the greatest on the left end, the smaller – on the right. *P*=48 (b), *P*=113 (c). Cycle of structural moiré Λ = 1800 μm (d).

1. Raranskyy N., Shafranyuk V., Fodchuk I. *Metallofiz.*, **7**, №5: 63 (1985).
2. Fodchuk I., Novikov S., Struk Ja., Fesyv I. *Metallofiz. Noveishie Tekhnol*, **34**, №12: 1865 (2012).

The peculiarities of influence of high-dose implantation by N^+ ions on the $Y_{2.95}La_{0.05}Fe_5O_{12}$ crystal structure

Fodchuk I.M.[(a)], Gutsuliak I.I.[(a)], Zaplitnyy R.A.[(a)], Dovganiuk V.V.[(a)], Yaremiy I.P.[(b)], Bonchyk A.Yu.[(c)]

[(a)] Yuriy Fedkovych Chernivtsi National University, Chernivtsi, Ukraine
[(b)] Vasyl Stefanyk Prykarpatskyy University, Ivano-Frankivsk, Ukraine
[(c)] Institute for Applied Problems of Mechanics and Mathematics of NASU, Lviv, Ukraine

Structural changes in the surface layers of epitaxial films of lanthanum-substituted $Y_{2.95}La_{0.05}Fe_5O_{12}$ garnet before and after high-dose implantation by nitrogen ions (E=50 keV, D=0.5•10^{18} ions/cm^2, D=1.5•10^{18} ions/cm^2 and D=5.0•10^{18} ions/cm^2) was studied by X-ray diffraction methods. Ions N^+ introduced into the lattice and the resulting vacancies have Gaussian distribution, with 60% of knocked out oxygen atoms, 28% – Fe, 13% – Y, <1% – La [1]. The greatest changes in rocking curves and AFM images are observed at doses of $D\geq10^{17}$ cm^{-2}, thickness of atomized film layer ≥25 Å.

Statistical dynamical theory of X-ray diffraction [2] was used for the calculation of rocking curves and intensity maps near the node of reciprocal space. Various models containing several types of dominant microdefects were considered in study of possible scenarios of defects creation. For example, one of models used small and large dislocation loops as dominant types of microdefects.

The best agreement between theoretical and experimental curves was observed for next the size and concentration of microdefects: R_{1L}=68 nm, C_{1L}=6•10^7 cm^{-3} and R_{2L}=3.5 μm, C_{2L}=1•10^5 cm^{-3}, redistribution of the impurities from the surface layer into the film takes place at the same time as grinding of larger microdefects.

The both negative and positive areas are observed on the strain thickness distributions. For the positive strain fields the deformed layer is formed mainly by introduction of nitrogen ions of largest concentrations. The presence of negative strain is associated with the ejection of the oxygen ions from the surface of $Y_{2.95}La_{0.05}Fe_5O_{12}$ layers of the films and the formation of a significant concentration of vacancy-type defects. At the same time, reduction of the oxygen concentration, and consequently the increase of part of magnetic iron ions (Fe^{2+}) leads to improvement of the magnetic properties of the studied materials (almost twice).

1. N. Pashniak, **I. Fodchuk**, A. Davydok, A. Biermanns, U. Pietsch, S. Balovsyak, R. Zaplitniy, I. Gutsuliak, O. Bonchyk, G. Savitskiy, I. Vivorotka, I. Yaremiy. High-dose implantation of $Y_{2.95}La_{0.05}Fe_5O_{12}$ epitaxial films by nitrogen ions // **Proc. of SPIE – 2011. - V.7008, 7008(19-1-19-6)**

2. Y. I. Nesterets and V. I. Punegov. The statistical kinematical theory of X-ray diffraction as applied to reciprocal-space mapping // Acta Cryst. (2000). A56, p. 540-548.

Spectrum of Elementary Excitations in Strongly Anisotropic Ferromagnet with Mechanical Boundary Conditions

Gorelikov G.A., Fridman Yu.A.

V.I. Vernadskiy Taurida National university, Simferopol, Ukraine

In this research properties of strongly anisotoropic easy-plane ferromagnet with mechanical boundary conditions in external homogeneous magnetic field H (H||OZ) were studied. The spin of the magnetic ion is supposed to be equal to unity (S=1). We considered two cases - rigidly fixed in basal plane (XOY) and perpendicular to basal plane (XOZ) sample. Investigation was made using the rotationally-invariant theory of magneto-elastic (ME) coupling [1] in low-temperature ($T << T_C$) case. Considered system in fact is a model of thin magnetic film on nonmagnetic layer. Its Hamiltonian can be presented as follows:

$$H = -H\sum_n S_n^z - \frac{1}{2}\sum_{n,n'} J(n-n')\cdot \mathbf{S_n}\mathbf{S_{n'}} + \frac{b}{2}\sum_n (R_{zi}^{-1}S_n^i)^2 + n\sum_n (R_{if}^{-1}S_n^f)(R_{jg}^{-1}S_n^g)e_{ij}(n) +$$

$$+\int d\mathbf{r}\left\{\frac{(l+h)}{2}\left(e_{xx}^2+e_{yy}^2+e_{zz}^2\right)+h\left(e_{xy}^2+e_{xz}^2+e_{yz}^2\right)+l\left(e_{xx}e_{yy}+e_{xx}e_{zz}+e_{yy}e_{zz}\right)\right\},$$

where $J(n-n')$ is the constant of exchange interaction, S_n^i is the i-th component of the spin operator on the n-th site, $b>0$ is the constant of single-ion anisotropy, ν – ME-coupling constant, λ and η are elastic modules, $\hat{R}$ - operator of local rotations, e_{ij} - tensor of finite deformations.

In the considered system there are three possible phase states: ferromagnetic (FM) phase at $H>\beta>J$, quadrupolar (QU) phase at $\beta>J,H$ and quadrupolar-ferromagnetic (QFM) phase at $H\sim\beta$. Phase transitions proceeds along the transverse polarized quasi-phonon branch of excitations, and in critical point there is an gap in quasi-magnon spectra. Dynamic and static properties of the system essentially depends on symmetry of imposed boundary conditions. Resolved value of FM-QFM transition field is noticeably bigger than value, resolved in model without rotational invariance consideration [2]. In the case of rigidly fixed in XOZ-plane sample ME-coupling causes the appearance of orthorhombic anisotropy, which leads to compensation of quantum spin-reduced effect and, on the assumption of great value of ME-coupling constant - decreasing area of QU-phase existence.

1. V.G. Barjahtar E.A. Turov in *Electronic structure and electronic properties of metals and alloys*, Naukova dumka, Kiev (1988) p.39.
2. Yu.N. Mitsay, Yu.A. Fridman, Theor. Math. Phys., **81**, 263 (1989).

Interaction of CdTe, $Zn_xCd_{1-x}Te$ and $Cd_{0.2}Hg_{0.8}Te$ with HNO_3–HI–$C_3H_6O_3$ Iodine Evolving Etching Solutions

Gvozdiyevskyi Ye.Ye.[1], Tomashyk V.M.[2], Tomashyk Z.F.[2], Denysyuk R.O.[1], Zinkevych I.G.[1]

[1]*Ivan Franko Zhytomyr State University*
[2]*V.Ye. Lashkaryov Institute of Semiconductor Physics of NAS of Ukrane*

Semiconductor materials such as II-VI, especially cadmium telluride and solid solutions based on it are widely used for the manufacture of photodetectors that are sensitive in the infrared spectrum, radiation and X-ray radiation detectors, solar cells and other semiconductor devices and appliances. Therefore, the formation of high surface quality single-crystalline substrates of such semiconductor materials is of particular importance.

The kinetics of the physico-chemical interaction of CdTe and $Zn_xCd_{1-x}Te$ and $Cd_xHg_{1-x}Te$ solid solutions with iodine evolving aqueous solutions based on HNO_3–HI–lactic acid has been studied and the concentration limits of the etching compositions according to the quality of the semiconductor surface and the dissolution rate of the material have been developed and compositions of polishing solutions have been optimized.

For the experimental studies single crystal samples of *p*-type CdTe, $Cd_{0.2}Hg_{0.8}Te$, $Zn_{0.1}Cd_{0.9}Te$ and $Zn_{0.04}Cd_{0.96}Te$ plates with an area approximately 0.5 cm^2 and thickness of 1.5-2 mm have been used. For the preparation of the etchants the solutions of HNO_3 (70 %), HI (57 %) and lactic acid (80 %) were used. All reagents had the chemical grade. The study was conducted using the settings for chemical-dynamic polishing at T = 293 ± 0.5 K and speed of the disc rotation 80 min^{-1}.

Mixtures of HNO_3–HI–lactic acid have polishing properties at the etching of the CdTe and $Zn_xCd_{1-x}Te$ and $Cd_xHg_{1-x}Te$ solid solutions at the content of HNO_3 from 5 to 25 vol.%/ The rate of mentioned above semiconductors dissolution in the studied etchant varies from 2 to 14 mm/min. It was found that increasing of the zinc content in the solid solution leads to improving the quality of the semiconductor surface, and the best polished semiconductor is $Cd_{0.2}Hg_{0.8}Te$. From the kinetic dependences it was found that in all polishing iodine evolving solutions the dissolution occurs according to the diffusion mechanism as apparent activation energy, calculated from the temperature dependences, does not exceed 20 kJ/mol.

Polishing of CdTe and $Zn_xCd_{1-x}Te$ and $Cd_{0.2}Hg_{0.8}Te$ can be carried out with the solutions of composition (in vol. %) (5-25) HNO_3 : (40-95) HI : (0-55) $C_3H_6O_3$ with the polishing rate of 3-14 mm/min. After processing the samples must be washed in a 0.5 M solution of sodium thiosulfate and a large quantity of distilled water.

The CdTe Thin Films for Solar Cells Application Growing on Three Dimentional Substrates

Il'chuk G.[1], Kurilo I.[1], Petrus' R.[1], Kusnezh V.[1], Kogut I.[2]

[1]*Lviv Polytechnic National University, S. Bandera Str. 12, Lviv, 79013, Ukraine,*
[2]*Vasyl Stefanyk Precarpathian National University, Ivano-Frankivsk, Ukraine*

Solar cells (SC) based on CdTe films are an attractive alternative to Si and GaAs monocrystalline photoconverters. A new approach to improve SC efficiency is creation of three-dimensional substrates with enlarged surface and specified microtexture, to work effectively for different angles of incidence radiation.

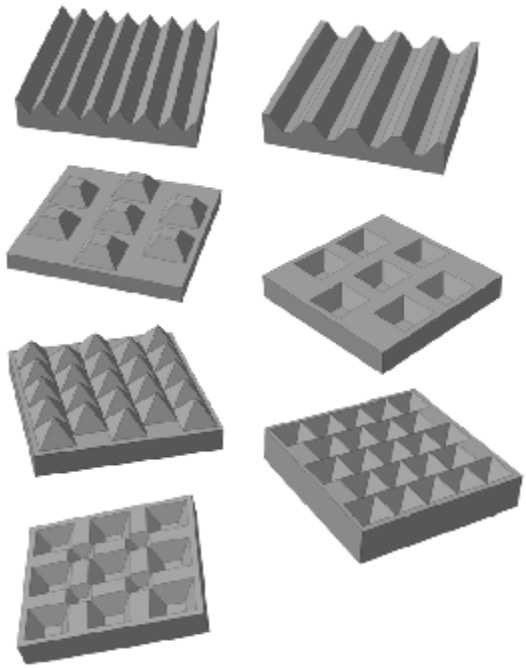

Figure. The Si substrate models of three-dimensional topography surface.

The seven models of three-dimensional surface of silicon wafers with a pyramids height of about 8 microns were developed. The modeling takes into account the technological possibilities of the photolithography and anisotropic etching of silicon wafers.

The CdTe films were deposited in quasi-closed volume on Ni layer, predeposited on the Si-substrate. Temperature conditions of growth ($T_{\text{deposition}}$ = 760–820 K, T_{source} = 860–900 K) were chosen on the basis of the thermodynamic analysis of the vapor phase composition and mass transfer.

The element composition of the CdTe films determined from the characteristic X-ray spectral dependence indicate that atomic ratio of the cadmium and the tellurium Cd/Te = 50,293/49,704 show minor excess the stoichiometry conditions for cadmium (0.293 at. %) and lack of tellurium (-0.296 at. %).

The mechanical stresses of double heterostructure are caused by the thermal linear expansion coefficients and the lattice mismatches of the conjugate layers difference were calculated. The stresses caused by the difference of the lattice parameters are much higher than the stresses caused by difference of thermal linear expansion coefficients.

Peculiarities of Clusters Parameters Calculations of As-S System Vapour Phase

Ivanitsky V.P., Kovtunenko V.S., Meshko R.O., Stojka M.V.

Uzhgorod National University, Uzhgorod, Ukraine,

Study of the structure and properties of atomic clusters of metallic and ionic chemical bond types is dedicated a lot of both theoretical and experimental works. For covalent materials such studies were only sporadically. At the same time, the structure and parameters of these clusters in a large extent determine the character passage of the technological processes formation of many semiconductor materials and nanosystems modern optics and electronics. Therefore, we conducted studies of features formation structure clusters of materials with covalent type of chemical bonds based on the system As-S.

To find the geometry and parameters of clusters As_nS_m we used the software package GAMESS (U.S.) first principle quantum chemical calculations. Since most of the examined clusters containing both closed and unclosed (free) electronic orbitals, then the first phase calculations should be used unrestricted Hartree-Fock method (UHF). Made by us comparative calculations show that using limited methods RHF and ROHF provides for clusters As_nS_m overstated values of energy and nontype settings of bonds (tab.).

In the second stage we used also multiconfiguration method of self-consistent field MCSCF (configuration interaction method), which reliably performs the calculations of clusters with open electronic shells. It was found that for clusters with the number of atoms is less than 15, this method gives the parameters are very similar to those obtained in the method of UHF.

The geometry optimization and calculation of As_nS_m clusters parameters should be in a broader valence-cleft basis 6-31G*, which contain both polarization wave functions of d-orbitals and diffuse f-functions external orbitals.

Clusters parameters	ROHF, 3-21G	ROHF, 6-31G	UHF 6-31G	UHF, 6-31G and d = 1	UHF, 6-31G and d = 1, f = 1	UHF, 6-31G and d = 3, f = 1
Energy, a.u.	-700,324	-701,537	-701,563	-701,762	-701,761	-701,764
r_{12}, nm	0,259	0,253	0,258	0,248	0,248	0,248
r_{13}, nm	0,259	0,253	0,250	0,235	0,235	0,235
r_{23}, nm	0,231	0,227	0,250	0,235	0,235	0,235
Angle, deg.	63,4	63,3	59,0	58,2	58,2	58,2
Total valency	3,17 and 3,37	2,80 and 2,92	2,92	2,95	2,90	2,58
Bonded valence	2,32 and 3,37	1,95 and 2,92	1,90	2,12 and 2,37	2,09 and 2,29	1,71 and 1,82
Free valence	0,85	0,85	1,02	0,82 and 0,62	0,81 and 0,62	0,87 and 0,73

Ion implantation of PMMA and characterization by SRIM simulation and PALS measurements

T.S. Kavetskyy[1], V.M. Tsmots[1], O. Šauša[2],
V.I. Nuzhdin[3], V.F. Valeev[3], A.L. Stepanov[3]

[1]*Solid-State Microelectronics Laboratory, Drohobych Ivan Franko State Pedagogical University, Drohobych 82100, Ukraine*
[2]*Institute of Physics, Slovak Academy of Sciences, Bratislava 84511, Slovakia*
[3]*Kazan Physical-Technical Institute RAS, Kazan 420029, Russia*

Ion implantation of polymers is attractive as the effective technological method to turn dielectric polymers into conducting semiconductors [1]. In the present work, as substrates for low energy ion implantation, 1.2-mm-thick polymethylmethacrylate (PMMA) plates were used [2]. Xe^+, He^+, and B^+ ion implantation (the energy of 30-40 keV, doses from 10^{14} to 10^{17} ion/cm^2, and ion current density < 2 μA/cm^2) was performed under a pressure of 10^{-5} Torr at room temperature on an ILU-3 ion accelerator at the Kazan Physical-Technical Institute (Russia) [2]. The Stopping and Range of Ions in Matter (SRIM) simulations were conducted using the software SRIM-2012 to obtain the depth profile of implanted ions and introduced vacancies during ion implantation of polymer (Fig. 1). Positron annihilation lifetime spectroscopy (PALS) measurements were carried out at the Institute of Physics of Slovak Academy of Sciences (Slovakia). Three component fitting procedure for PALS data treatment was applied and long-lived lifetime component t_3 and intensity I_3, showing positronium (Ps) formation (the metastable electron-positron bound state), were finally taken into account for analysis. It is found that t_3 is practically independent on the ion dose for Xe^+- and He^+-implanted PMMA within experimental uncertainties but t_3 is dependent on the ion dose for B^+-implanted PMMA. At the same time, I_3 shows changes in the dependence on the dose of ion irradiation for the investigated polymers.

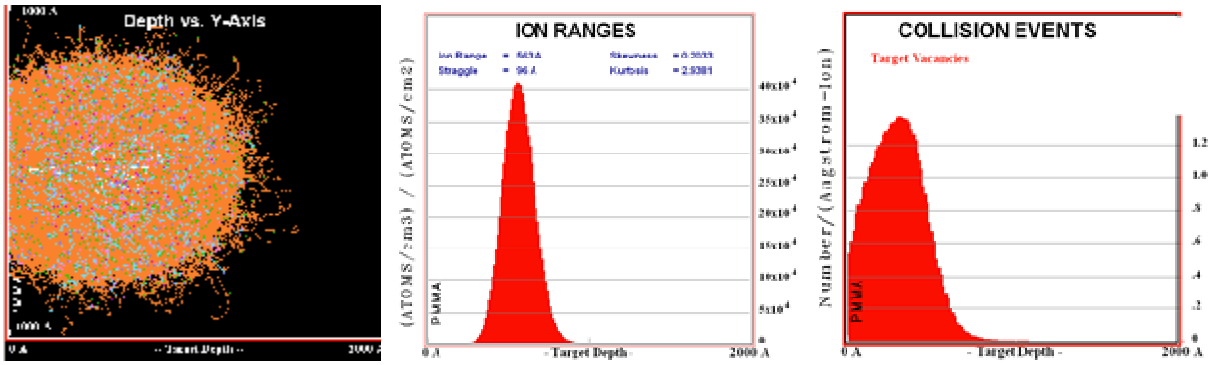

Fig. 1. SRIM sumulation for 40 keV Xe^+-implanted PMMA, shown as example.

[1] D.V. Sviridov, Russ. Chem. Rev. **71**, 315 (2002).
[2] A.L. Stepanov, Tech. Phys. **49**, 143 (2004).

Mathematical Simulation of the Growth of the Deposition Film From a Composite Beam-Atom Cluster

Keeprich V.I.[1], Kornich G.V.[1], Onikienko T.M.[1]

[1] *Zaporizhya National Technical University, Zaporizhya, Ukraine*

The latest technologies of the electronics industry often use a variety of complex surfaces - multi-coating, textured film, whiskers and other nanostructures. This allows obtaining of devices with unique physical properties and building of new-generation equipment. For complex surface nanostructures energy beams, consisting of different types of particles, are used often [1].

In the research film growth simulation, composed of a sputtered cluster-atom beam, was performed. Mathematical description of this process has a number of difficulties associated with a significant difference between the particle size in the beam and the other properties.

To describe the process within diffusion-like model the concept of volume-normalized concentration C_i was introduced:

$$C_i = \frac{N_i \cdot n_i}{N_n} \tag{1}$$

where N_i – concentration of i-th component; v_i – relative volume; N_v – the volume-normalized total concentration.

$$N_n = \sum_i N_i n_i . \tag{2}$$

In the presented model the deposition rate depends of sticking coefficients and sputtering yield of particles, as well as cluster ruin probability. Diffusion-like mass transfer equations, describing the evolution of the system components, were recorded with these elements.

The obtained model allows us to carry out numerical calculations of the characteristics (the distribution of surface and bulk concentration, growth rate, etc.) of the film depending on the deposition parameters (energy bombardment, the flux density of incident particles).

Different depending deposition films at the energy bombardment of 25 eV were obtained. The evolution of the profile of the bulk components with different initial conditions, the ratio of surface concentrations at different time points, the rate of growth of the film were received by this model.

1. Киприч В.И., Корнич Г.В., Бажин А.И., Сошников И.П. Моделирование роста нитевидных нанокристаллов TaB_2 // Поверхность. – 2010. – № 6. – С. 22 – 25.

Thick Films Based on Spinel Manganite Ceramics Testified by Pal Methods

Klym H.[1], Hadzaman I.[2], Ingram A.[3], Shpotyuk O.[4]

[1]*Lviv Polytechnic National University, Lviv, Ukraine*
[2]*Drohobych State Pedagogical Univ`ersity, Drohobych, Ukraine*
[3]*Opole University of Technology, Opole, Poland*
[4]*Scientific Research Company "Carat", Lviv, Ukraine*

Spinel-type ceramics are known to be widely used in industrial electronics and engineering for temperature measurement and control (temperature sensing arrangements), in-rush current limiting, liquid and gas sensing, flow rate monitoring and indication, etc. Because of significant complications in the structure of spinel-type $(Mn,Cu,Ni,Co)_3O_4$ ceramic materials revealed at the levels of individual grains, grain boundaries and pores, the further progress in this field is dependent to a great extent on the development of new characterization techniques, which can be used in addition to traditional ones.

This idea was successfully realized due to unique possibilities of positron annihilation technique in the variant of PAL spectroscopy – one of the most powerful experimental methods for studying of structurally intrinsic voids/pores in solids, which was effectively used earlier for investigation of vacancy-like defects and some of their extended modifications in "traditional" single-crystal semiconductors and insulators. Early we successful used this method for the characterization of bulk spinel-type ceramics. However, until now no attempts was done with respect to the research of structural peculiarities of thick-film elements. Basic difficulties were related to the thick-film elements obtained on Al_2O_3 substrate, not as the so-called "free" film that makes the study of this material separately from substrate impossible.

In this work, for the first time, grain-pore structural features of so-called "free" thick film structures based on transition-metal manganite $Cu_{0.1}Ni_{0.8}Co_{0.2}Mn_{1.9}O_4$ ceramics are studied using PAL spectroscopy.

It is shown that two-state positron trapping model is appropriate for an adequate description of changes caused by additional glass phase in these materials. The observed behaviour of defect-related component in the fit of the experimentally measured positron lifetime spectra for thick films in comparison with bulk ceramics testifies in a favour of agglomeration of free volume entities during technological process. Experimental PAL spectra, measured for the $Cu_{0.1}Ni_{0.1}Co_{1.6}Mn_{1.2}O_4$ (Co-enriched) bulk ceramics and multilayered thick films, are decomposed into two discrete components (t_1, I_1) and (t_2, I_2), showing no positronium formation. The observed components can be fully defined within the two-state positron trapping model. The positrons are trapped more strongly in thick films due to glass additives near grain boundaries in these materials and void agglomeration during technological process.

The Formation Methods for Ohmic Contacts to Silicon CARBIDE

Kudryk Ya. Ya.[1], Kudryk R.Ya.[2]

[1]*Lashkaryov Institute of Semiconductor Physics of NAS of Ukraine, Kiev, Ukraine*
[2]*Ivan Franko National University of Lviv, Lviv, Ukraine*

There are a number of experimental works reporting the results of investigation of contacts with different metallization to silicon carbide (fig.1, fig.2). However, a problem exists when comparing the results obtained by different authors who used different parameters of thermal treatment (time and temperature), different dopant concentrations and different contact formation technologies. As a result, at first, one has either to strongly restrict sampling and compare more or less uniform data only (which leads to loss of information) or generalize the results obtained by using additional calculations. In this work, we apply just the latter way. After this,we have to select a good quality contacts for analysis.

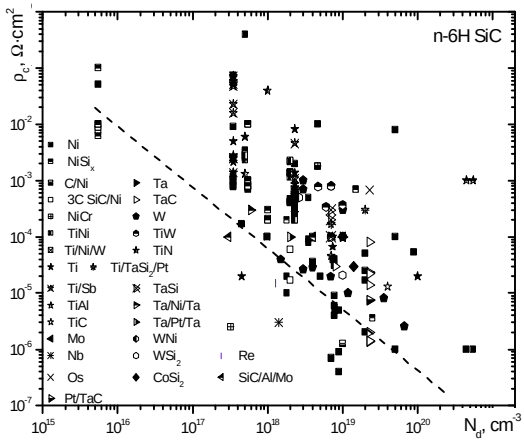

Fig. 1. Contact resistivity vs dopant concentration in *n*-6H SiC.

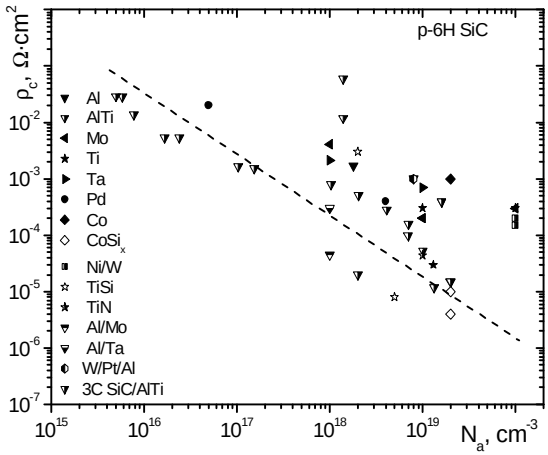

Fig. 2. Contact resistivity vs dopant concentration in *p*-6H SiC.

A typical ohmic contact resistance vs an annealing temperature curve has a minimum; usually an ohmic contact is burnt-in just at that temperature. Before that minimum, a thermally stable contact-forming phase appears. After that minimum, the contact is degrading, with formation of another (new) phase and diffusion smearing of the layer structure. Both above processes are of activation type. Under the assumption that the corresponding chemical reactions are of the first order, their kinetics (Fick law) are similar because in both cases the main factor that determines degradation time is diffusion. If one assumes that change of the contact electrical parameters depends on the percentage ratio of the two phases (contact forming and new), then similar dependence will be valid for the contact resistance too. Using the derived dependences, one can calculate two parameters, namely, the reduced contact resistance and reduced heat stability temperature. These parameters characterize the ohmic contact properties and are more convenient for comparison than such parameters as burn-in temperature and time, contact resistance and impurity concentration in the semiconductor.

Research on the Peculiarities of Dislocation Dynamics in Beryllium Condensate

E.I. Kurek, I.G. Kurek, A.V. Oliynych-Lysyuk, N.D. Raransky

Yu. Fedkovych Chernivtsi National University, Chernivtsi, Ukraine

Beryllium and its alloys is well-known structural material widely used in space and other branches of industry. However, increased brittleness of this material at near-room temperatures is a constant stimulus for research aimed at solving this problem [1].

This paper studies the elastic, nonelastic properties and dislocation motion velocities in polycrystalline layers of condensed Be ~100 μm thick at thermo-mechano-cycling in the range of 20 – 200 °C after a long natural ageing.

The main research results can be briefly summarized as follows.

- A nonlinear behavior of the modulus of torsion and the ratio of dislocation motion velocities at thermo-cycling (Fig.1a) – the temperature hysteresis of investigated properties – was established.
- On heating and cooling, dislocation motion velocities in Be condensate vary exponentially with temperature (Fig.1 b).

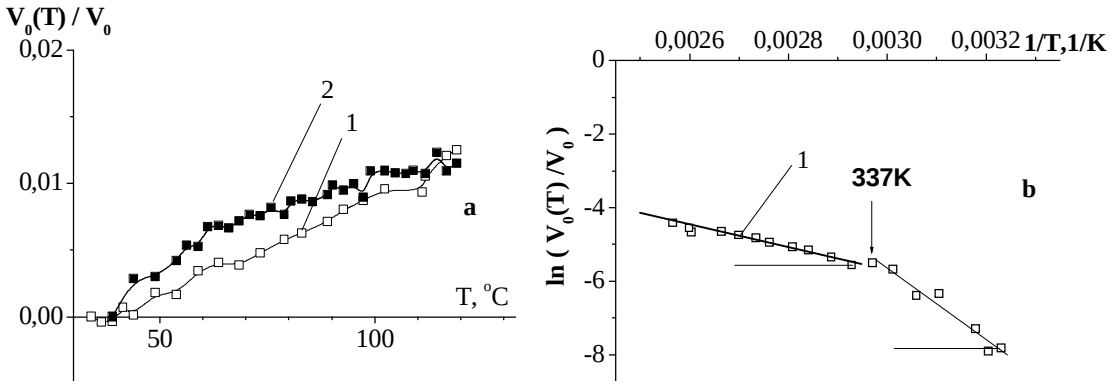

Fig. 1 Temperature dependences of the ratio of dislocation motion velocities $V(T)/V_0$ (a) in Be condensate and dependence $\ln(V_0(T)/V_0) = f(1/T)$ (b). Curve 1 – heating, 2 – cooling.

- In the region of 337 K a change in dislocation motion mechanism followed by a decrease in activation energy E_D from 0.77 to 0.24 eV was established.

1. S.S. Petrov. Kinetics of copper-beryllium alloys ageing in a constant magnetic field. Synopsis of a thesis for PhD in physics in mathematics. Samara 2011. P.1-20.

Formation of Films in the Nickel-Boron-Nitrogen System under Ion Implantation

Kuzey A. M., Taran I. I., Filimonov V. A., Yakubovskaya S. V.[1]

Physical-Technical Institute of NAS of Belarus,
[1]Belarussian National Engineering University

The effect of the nitrogen ion implantation on the structure of electrochemically deposited films of the nickel-boron system was investigated.

The films were produced from a boron-fluoride electrolyte at the temperature of 295 K and current density of 15-30 mA/cm^2. Borane-morpholine complex (BM) with boron concentration equal to 2-8×10^{-2} mass % was used as a boron-doping component. The thickness of films was 15-30 μm. The ion implantation of deposited films was performed using vacuum setup equipped with a nitrogen ion source. The nitrogen ion energy of a beam was 2.5 keV with the ion current density of 1.5 мA/cm^2. The duration of ion implantation was 2-4 hours.

The formation of electrochemical alloys of the Ni-B system occurs during chemical-catalytic reduction of boron on active surface. Depending on concentration of boron-containing compound of electrolyte and the compound structure the films are formed having either microcrystalline or X-ray amorphous structure. In this study the films had heterogeneous structure that represented itself a matrix based on solid solution of boron in nickel with the (0.3219 nm) parameter of lattice that contained dispersed (0.2–0.5 μm) and ultradispersed (10–80 nm) particles of nickel borides. The thermal stability of this structure is rather high.

The ion implantation of films transforms their heterogeneous structure into a quasi-homogeneous one. The observed increase in a corrosion resistance of films after implantation can be associated with changing their surface layer structure and composition as follows:

$$B_a \xrightarrow{N^+} BN \qquad Ni_xB_y \xrightarrow{N^+} BN + Ni \qquad Ni_xB_y \xrightarrow{N^+} Ni_xB_yN_z$$

where *x*, *y* and *z* are the stoichiometric coefficients and B_a is the solid solution of boron in nickel. The implantation of nitrogen ions in a film is accompanied by ablation of the latter material. When electrochemically deposited film is affected by the factors of ion flow (including chemical and thermal ones) the surface layer structure can be conditioned by a chemical action of nitrogen atoms to ultradispersed particles. The higher corrosion resistance, hardness and different structure of the layer should be attributed to the formation of ultradispersed particles of boron nitride and the composite material such as γ-BN + Ni having a nano-scale quasi-homogeneous structure. The thermal effect of ion implantation intensifies a chemical effect.

Thus, implantation of nitrogen ions in electrochemically deposited films of Ni-B system brings about changing the phase and chemical compositions which is mainly caused by the action of two factors such chemical and thermal ones.

Synthesis of **PbTe Nanoparticles, Thin Films and Nanorods**

Leontyev V. G.

A.A. Baikov Institute of Metallurgy and Material Science RAS, Moscow, Russia

We investigated the possibility of synthesizing nanoparticles, thin films and nanorods by thermal decomposition of salts containing lead. The starting material was used three water acetate of lead and tellurium powder with particle size of -56 μ. By methods of thermogravimetry and differential scanning calorimetric were investigated thermo-chemical reactions and phase transformations in mixtures of lead acetate - tellurium. We found that heating the mixture with a ratio of lead and tellurium 1:1 (Te with a slight excess) in a reduction atmosphere (H_2), may be described by the following processes: dehydration three water Pb acetate at temperatures up to 100 ° C, melting Pb acetate at 200 C, the chemical interaction molten lead acetate and elemental tellurium to form an intermediate unstable compound $PbTe(CH_3COO)_2$ and its subsequent decomposition with formation of lead telluride nanoparticles. The phenomena of melting and formation an intermediate compound together with wetting of oxide surfaces by molten mixed salt allowed to obtain by thermal decomposition the nanostructured thin film on the surface of glass and quartz substrates. Study of particles and films by scanning electron microscopy (SEM) and energy dispersive microanalysis (EDX) allowed to determine the chemical composition and morphology of the particles PbTe (Fig. 1a). Particle size and the thickness of the film depended on the mass of the mixture placed on the substrate and the synthesis temperature (250-350^{o}C).

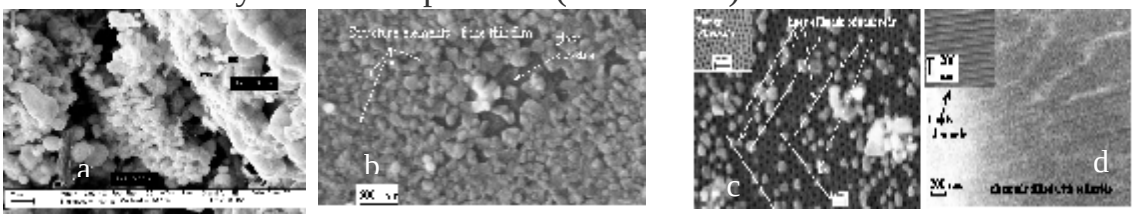

Fig.1.SEM images of PbTe particles (a), PbTe thin film on the surface of glass substrate (b), c - template surface with a heads of nanorods, d- cross-section of the template with nanorods. Synthesis temperature - 300^{o}C.

Carrying out the synthesis on the surface of Al-oxide template with nanoscale channels (with diameter 50 nm and length 5000nm) and capillary effects allowed to fill the channels by molten PbTe acetate, and after subsequent heating and decomposition to obtain the lead telluride nanorods inside of the channels (Fig.1 c,d). Filling the channels and the synthesis PbTe was carried out by heating of the template with initial mix in H_2 to 300°C at 2.5 °C/min and subsequent exposure for 1 hour. In the upper left corners fig.1 (c,d) shows SEM pictures of empty template. The reported study was partially supported by RFBR, research project No.13-03-00130a.

Conditions of Crystal Nucleation Processes Suppression at the Quenching from a Liquid State

Lysenko A.B., Zagorulko I.V., Kazantseva A.A., Kalinina T.V.

Dniprodzerzhinsk State Technical University,Dniprodzerzhinsk, Ukraine

Within the limits of the model which is proposed in the paper [1], the estimates of metal melts u_-^a cooling rate at which for transit time of a temperature interval from melting point T_m to glass-transition point T_g in the volume unit it is formed no more than one crystalline nucleus are performed. Numerical values of u_-^a was defined by means of a relation:

$$\left(u_-^a\right)^{-1}\int_{T_g}^{T_m}\frac{N_v kT}{3pa_0^3}\exp\left[-\frac{16pV_m^2 s^3}{3kT(\Delta G)^2}\right]\times\exp\left[-\frac{3p^2V_m h u_-^a}{RT(T_m-T)}\right]dT\le 1, \qquad (1)$$

where V_m is the molar volume; is the dynamic viscosity of melt; R is the gas constant; N_n is the number of atoms per unit volume; a_o - interphase boundary thickness ; - is the specific free energy of the interface crystal-melt; G is the molar free-energy difference of the liquid and crystal phases; k - Boltzmann constant.

Calculations carried out for materials with various glass-forming ability, notably, pure metals Al (1), Ni (2), alloy $Fe_{80}B_{20}$ (3), and also the bulk amorphized alloys $Mg_{65}Cu_{25}Y_{10}$ (4) and $Zr_{41.2}Ti_{13.8}Cu_{12.5}Ni_{10}Be_{22.5}$ (5). It is shown, that cooling rates u_-^a are necessary for damping of crystals nucleation processes in pure metal melts is ~ 10^{13} – 10^{14} К·s^{-1} which cannot be reached by modern methods of rapid quenching. For truly amorphous state fixing in alloys 3, 4 and 5, according to data of calculations, critical cooling rates u_-^a of melts should be, respectively, ~ $5\cdot10^{10}$, ~ 10^7, ~ $3\cdot10^4$ К·s^{-1}. The value u_-^a obtained estimates argues that truly amorphous structures can be obtained by the modern methods of the quenching from a liquid state only in alloys 4, 5 and other alloys with high glass-forming ability.

1 *Vreswijk J.C.A., Gossink R.G., Stevels J.M.* Nucleation kinetics and critical cooling rate of glass-forming liquids // J. Non-Cryst. Solids. – 1974. - № 16. – P. 15 – 26.

Prediction of Microstructure Parameters in Conditions of Quenching from Melt

Lysenko O.B., Kosynska O.L., Kravets O.L.

Dneprodzerzhinsk state technical university, Dneprodzerzhinsk, Ukraine

By method of mathematical modelling, with a joint numerical solution of thermal and kinetic problems, explored singularities of structure formation in thin layers of Al cooled on a massive heat-conducting substrate. The mathematical model of explored process is grounded on a heat conduction equation of Fourier (1) and the kinetic equation (2) which takes into account effect of nucleation processes deceleration at the expense of decrease of liquid phase volume and a reduction of crystals growth rate owing to the mutual blocking of the next grains:

$$cr\,\frac{\partial T_1(z,t)}{\partial t} = k\,\frac{\partial T_1(z,t)}{\partial z^2} + r\Delta H_m\,\frac{\partial x}{\partial t} \qquad (1)$$

$$x(t) = \frac{4}{3}p\int_0^t (1-x(t'))I(t')[R_c(t') + \int_{t'}^t (1-x(t''))u(t'')dt'']^3 dt' \qquad (2)$$

where T_1, t, z – accordingly, temperature, time and co-ordinate along the heat removing of layer; c, r, k – specific heat, density and thermal conductivity of explored metal; ΔH_m – crystallisation specific heat; x – fraction crystallized volume; t' и t'' – current moments of time ($0 \le t' \le t'' \le t$); I – nucleation rate; R_c – radius of a critical nucleus; u – linear growth rate of crystals.

The developed algorithm allows to calculate temperature of thin melt layers T_1, fraction crystallized volume x and number of crisallization centres N_S during cooling of melt from melting point of metal T_m to some given temperature $T_1 < T_m$.

By the presented mathematical model, exploration of thin layers crystallisation kinetics of melted aluminium which is cooled on the massive heat-conducting substrate is performed. It is shown, that on all explored interval of thickness aluminium films (from 20 to 200 μm) the full crystallisation of melt is observed. It is fixed, that medial sizes of crystals $\overline{R}$ significant depend on a quenching foils thickness l and vary over the range from 0,02 μm (for l=20 μm) to 8,1 μm (for l=200 μm).

Derived by calculation values of medium-sized crystals compared to microstructure parametres determined by measurements of the conditional grain size on foils photomicrographies in the thickness 110 μm. It is fixed, that experimentally estimated medium size of crystals amount to 3,7 μm while modelling calculations for foils of current thickness give value $\overline{R}$ =2,6 μm.

Results of reduced explorations show, that the given mathematical model allows to obtain results which correlated with experimental data and can be used for prediction of microstructural parametres of rapid quenched products.

Resonance Absorption of Granule Film AgAl Deposited on a Substrate with a Rough Sub-Layer ZnS

Makarovsky N.A., Letyago L.M.

V.S. Karazin Kharkov National University, Ukraine

Granulose silver, aluminum and AgAl (23% Ag) film resonance absorption of light precipitated on roughened surface ZnS has been observe. Granulose silver, aluminum and AgAl (23% Ag) films are occurred in roughened surface ZnS and have two absorption band. Mostly one absorption band can be observed in grain films. Band position is determinate free natural frequency electron in grain and dipole-dipole interaction between grains [1]. Two absorption band can be explained if we suppose that two grain film region are formed by different occupation factor and different effective ambient medium dielectric capacitivity. High frequency band position is produced by fundamental frequency free electron oscillation in discontinuous films [2]. We can define real part dielectric capacitivity ε_{1m} with is concerned with interzone crossover in metal films.

Function optical density-cyclic frequency spectrophotometric analyses has been done. Silver, aluminum and AlAg maximum absorption band frequency have been determinate. They are $\omega_{max}^{Ag} = 5.1\times10^{15}s^{-1}$, $\omega_{max}^{Al} = 5.54\times10^{15}s^{-1}$, $\omega_{max}^{AgAl} = 5.42\times10^{15}s^{-1}$. Relationship between alloy high frequency band and fine metal high frequency bands are determinate of concentration of fine metal in alloy. We calculated ε_{1m} and plasma frequency ω_p for alloy by knowing datum $\omega_{max}^{Ag}, \omega_{max}^{Al}, \omega_{max}^{AgAl}$. The value of this constant are $\varepsilon_{1m} = 2.1$ and $\omega_p = 11\times10^{15}s^{-1}$. This data are accorded with Hampe-Shkljarevsky theory.

1. Макаровский Н.А. Плазменный резонанс в гранулярных пленках сплавов Au-Al /Н.А. Макаровский, Л.М. Летяго// Вестник ХНУ, серия «Физика». – 2006. - №739. – С.138-140.
2. Шкляревский И.Н. Плазменный резонанс в гранулярных серебряных пленках, осажденных на шероховатые поверхности монокристаллов NaCl и KCl /И.Н. Шкляревский, Ю.С. Бондаренко, Н.А. Макаровский// Оптика и спектроскопия – 2002, Т.93. - №1. – С. 33-37.

Analysis of the Spectral Polarization Dependence of Internal Reflection in Ultrathin Gold Films.

Maksimenko L.S., Matyash I.E., Mishchuk O.N., Serdega B.K., Stetsenko M.A.

V.E. Lashkaryov Institute of Semiconductor Physics NAS of Ukraine, Kiev, Ukraine,

The polarization properties of nanoscale gold films fabricated by thermal spraying method were investigated by internal reflection method with using modulation polarimetry technique. Polarization characteristics of the parameters of internal reflection - angles at different wavelengths λ and spectral at different angles of incidence θ - were obtained. The dependences of the reflection coefficients of linearly polarized light for cases when an electric field of the wave is perpendicular R_s^2 and parallel R_p^2 to the plane of incidence, and the characteristic of the polarization difference $\rho = R_s^2 - R_p^2$, as the product of the modulation technique were measured.

Physical meaning of the parameter ρ consists in disappearing of the general particularities of functions after their subtraction. The residual result containing individual particularities of characteristics provides a hypersensitivity of the system for the change of polarization state and the physical causes leading to this. This parameter is the result of the physical subtracting and it is devoid of errors that accompany this operation at the mathematical operations. Also ρ is an element of an expression that identifies the mathematical derivative. The result of the subtraction is similar to the derivative of reflection by appropriate arguments that received from physical differentiation under the conditions $\rho << R_s^2$ and R_p^2.

It was found that the characteristics of the parameter $\rho(\lambda)$ have the form of complex, composite resonance in the appropriate range. The value of $\rho(\lambda)$ is independent of the incidence angle of probing radiation outside previously specified range and, therefore, is not a resonant component. The values of this component in the resonance range were determined from the angular characteristics of internal reflection at the corresponding wavelengths. The method of analyzing of the polarization difference spectra which includes their approximation of the Gaussian functions and takes into account the non-resonant component in reflection was developed. Several resonances were determined in the spectral characteristics $\rho(\lambda)$, their parameters (frequency, relaxation time) were identified and dispersion dependencies of these resonances were obtained. The type of surface resonances (plasmon-polariton or local) was defined from shape and location in the ω-k space of the dispersion characteristics.

Electrical Properties of Porous Silicon Layers Prepared by Etching of p-type c-Si(110) Wafers

Miroshnychenko A.I., Soloshenko V.I.

Odessa I.I.Mechnikov national university

Porous silicon (PS) is unique material that can find application in many areas of modern electronics. Despite of large number of publications on porous semiconductors, many issues, concerning the electrophysics of porous silicon and structures on his basis, are unsolved. A serious obstacle to understanding the overall picture of the electric properties of porous silicon are a variety of morphological features of the material and their dependence on the technological parameters of forming of porous structure. The features of the porous silicon prepared by etching c-Si(110) wafers are studied insufficiently. Therefore in order to the effective use of material it is necessary to study this dependence, in particular dependence on time of anodization.

The PS layers were formed by electrochemical anodization p-type c-Si (110) wafer of 10 Om·cm resistivity in a Teflon cell using HF and C_2H_5OH in 1:1 proportion by volume, as electrolyte and a platinum gauze as a counter electrode. The wafers were anodized at a constant current density of a bout 10 mA/cm^2 for time 5, 15, 30 minutes. For electrical measurements Al circle of ≈ 1,2 mm diameter were immediately thermally evaporeted on top of the porous layers in glancing geometry at on angle 30^0 between molecular beam and the sample in order to prevent shorting of contact between evaporated metal an the silicon crystal substrate. By means of the optical microscope a photographs of the surface samples were taked. The photos were processed on a computer in order to estimate the average size of the parts not etching silicon by using intensity of the reflected light. It was found that the number and average size of the parts decreases with increasing etching time. The computer treatment can be used for indirect estimation of porosity.

The conventional analysis of current-voltage (I-V) characteristics show rectifying behavior for all three groups samples. The forward bias I-V characteristics had two different parts with various dependencies on the voltage. The first length was characterized by a linear dependence of the current on the voltage, the second – a power dependence with an index of 2-2,6. We believe that the similar of type I-V characteristics is due to flow space-charge-limited currents in the layer of the porous silicon.

Multifractal Parametrization of Spatial Forms on the Surface of A2B6 Semiconductors Layers

Moskvin P.P., Kryzhanivskyi V.B., Lytvyn P.M.*, Rashkovetskyi L.V.*

[1]*Zhytomyr State Technological University, Zhytomyr, Ukraine*
[2]*Institute of Semiconductors Physics NAS Ukraine, Kiev, Ukraine*

Multifractal representations [1] have been applied to the description of the surface area of layers which are characterised by the difficult fractal structure on micro- or nano level. Application of the concept of multifractals, unlike monofractals approach, allows to use all spectrum of fractal parameters for the surface description .

As the initial data at the multifractal analysis application the data about the area of its surface has been used. This data has been obtained by processing AFM images of layers surfaces. Such method has allowed to obtain the information on the areas of the "elementary" surfaces for realization of the integration splitting method in calculations of multifractal spectra. The developed software was used for obtainment of multifractal parameters for distribution of the surface area of polycrystalline layers of solid solutions $Zn_X Cd_{1-X} Te$. Solid solution layers have been formed on substrates Si(111) by «hot wall» method. Quantitatively surfaces of layers were characterized by number of Renii D_0 and the order parameter: $\Delta_{q\to\infty} = D_1 - D_{q\to\infty}$ (q - factor of degree)

The multifractal spectra obtained for all analyzed samples corresponded to its canonical form [1]. Typical values of multifractal parameters depending on synthesis time and substrate temperature in the specified system changed in ranges D_0=2.15 - 2.22, Δ =0.50 - 0.70. Such values of Renii number corresponds to the surface with the developed relief which does not planar on nanolevel. Results of application of multifractal analysis to the description of a layer surface show the presence of the interrelation between parameters of multifractal spectrum of a layers surface both a properties of the solid solutions and conditions of its formations.

1. Moskvin P. P, Rashkovetskij L.V., Vujchik N.V., Litvin P.M. Multiracial parametrization of a heterocompositions layers on the basis of A^2B^6 semiconductors. // Actual problems of applied physics (APAP-2012). Mater. of 1 –th. Internation. Science - practical conference. Sevastopol, Ukraine, 2012, p. 119-120.

LED Research System

Mukha I.V.

Національний технічний університет України "Київський політехнічний інститут", Kyiv, Ukraine

Currently the world LED (light-emitting diode) production grows intensively. Both designing and development of novel types of LEDs as well as improvement of parameters of the existing LEDs require comprehensive analysis of LED characteristics and processes occurring in them. The setup proposed in this work makes it possible to take and study the LED photometric, spectral, electrical and thermodynamic parameters and characteristics as well as investigate the processes occurring in LEDs. For today the LEDs on GaN heterojunctions based some of the most popular on the world market. [1] Creation of such LEDs based on thin film technology.

The main unsolved problem is their intense degradation resulting from violation of the temperature condition of LED operation.[2] From above written is clear that to solve this problem, need to investigate the processes taking place inside the thin-film structures.

System is developed on the basis of a monochromator "Ум-2" and microcontroller ATMegaA4. Compared with other spectrophotometric system like HAAS-2000 or Beckman DU-640 my system has the best integration features. Several tens of nanoseconds versus tens of microseconds. Of features can be noted integration at a single wavelength against integration of the whole spectrum. That allows for repeated measurements were not only for the full spectrum, but also the necessary parts of the spectrum. This ability is an important element of the research process optimization.

An analysis of current state standards of LED quality control was performed. On the basis of obtained data an original method on enhanced examination and analysis of thermal and light characteristics powerful LEDs. On the basis of modern microelectronics the system was created allowing to examine characteristics of powerful LEDs in more detail. Created analytical system that allows, on basis of the obtained characteristics, observe the processes taking place in the thin-film elements of power LEDs.

1. http://www.isuppli.com
2. A. Polischuk. Degradation of semiconductor light-emitting diodes based on gallium nitride and its solid solutions. Components and Technologies no 2, 2008 (in Russian).

Sol-gel Synthesis of Thin Films on the Basis of Sulfocontaining Polymer

Demchyna O.I. [1], Yevchuk I.Y. [1], Semenyuk I.V. [2], Syrotyuk S.V. [3], Galchak V.P. [3], Musiy R.Y. [1]

[1] *L.M. Lytvynenko Institute of Physico-organic Chemistry and Coal Chemistry NAS of Ukraine Lviv, Ukraine*
[2] *Lviv scientific-research institute of polygrafic industry, Lviv, Ukraine*
[3] *Lviv National State Agricultural Institute, Lviv-Dublyany, Ukraine*

The increasing number of research papers are devoted to synthesis of novel materials for application in microelectronics, in electrochemical and solar energy devices, in separation processes *etc.* Sol-gel technology, which allows to obtain nanostructured materials and organic-inorganic composites, is one of the prospective methods for obtaining of materials for different functional applications.

We obtain thin films of organic-inorganic composites with high ion-exchange and proton-conductive properties. Sol-gel synthesis was conducted as follows: sol-gel system (SGS) tetraethoxysilane-ethanol-water in appropriate proportions was added to the mixture of comonomers: acrylamide, acrylonitrile and 3-sulphopropylacrylate potassium salt. Then polymerization composition was exposed for UV irradiation. As a result of the reaction of photoinitiated polymerization and simultaneous sol-gel transformation of sol-gel system the organic-inorganic network was formed. The obtained thin films have high ion-exchange capacity (0,38 mg-eq./g) and proton conductivity (10^{-4} Sm/cm).

Spectral-selective composite coatings for solar collectors were synthesized using sol-gel method. The coatings contain carbon nanoparticles dispersed in dielectric SiO_2 or NiO matrices. The compositions were applied on Al and Cu plates (40 x 40 mm) by spin-coating or by dipping of the plates with following drying at different temperatures. For evaluation of the effectiveness of the synthesized materials maximal temperature of heating of the plates with investigated coatings applied on them were determined at irradiation by natural solar irradiation as well as at irradiation by the imitator of solar spectrum. Comparative investigation of the synthesized coatings with the sample from SunSelect (Germany), prepared by expensive technology – vacuum evaporation, were conducted. Experimental results indicated that synthesized coatings are of the same effectiveness of solar energy absorption as the known analogue and can be used as selective coatings for solar collectors.

Physical and Technological Features of the Formation of Submicron Metallization GaAs Structures LSI ion Milling.

Novosyadlyy S.P, Kindrat T.P, Melnyk L.V, Varvaruk V.V., Voznyak Yu.V.

Carpathian National University V.Stefanyk, Ivano-Frankivsk, Ukraine

This article describes research conducted over the process brings images of elements in the functional layer by ion-beam etching, also called ion milling. It focuses on the basics of physical ion etching, the advantages and disadvantages of this method in comparison with our methods and outlines the features of this process in the formation of sub-micron VLSI structures. Ion-beam etching is seen as a slow sputtering surface under ion bombardment of high flow. Of course, this process has a physical rather than chemical nature, as built on the momentum transfer from incident ions surface atoms, causing the latter receive enough momentum to leave the surface.

To use ion-beam etching (IPT) has several important reasons. Firstly, IPT is a universal method by which you can etch beloved material (eg permaloy) or multilayer metallization of *Ti-Pt-Au* or *GeAu* which practically impossible to liquid chemical or plasma methods. Chemical etching is usually highly selective, while speed ion etching of various substances differ by no more than an order of magnitude. So complex multilayer structures can be etched in a single technological cycle. Second, IPT has the best of all methods of etching resolution and its application can receive items with size <10 nm.

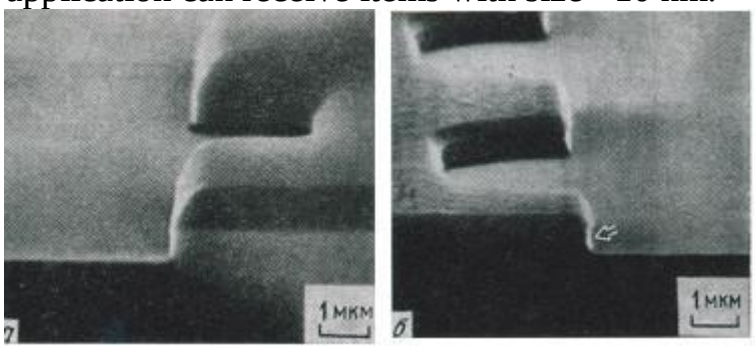

b a

Fig.1. Relief etching of polysilicon through a lot of photoresist a) and through the mass of SiO2 b).

1. Novosyadlyy SP Sub-nanomikron technology and VLSI structures. // Ivano-Frankivsk City NV, 2010 - 254 p.
2. M. Shur. Modern instrumentation for Gaul arsenic. // M. Peace. 1991-628p.
3. V.A. Afanas'ev., M.P. Duhnovskyy. T.A. Krisev. Machinery for pulsed curing. // PD neutron Technology August 1. // Microwave Electronics - 1984 - Vol 12 p.24-29.

The features of X-ray topographic images of dislocations in Si

Novikov S.M., Fodchuk I.M., Fedortsov D.G., Struk A.Ya.

Yuriy Fedkovych Chernivtsi National University, Chernivtsi, Ukraine

For more complete interpretation of experimental topograms it is necessary to conduct theoretical researches of mechanisms of diffraction images of different structural defects.

In general case simple photo-electric absorption does not influence on a contrast of image. However there is a reason as a result of that the increase of thickness of the sample influences on an image contrast of dislocation on topograms. With the removal of dislocation from the exit surface image of dislocation broadens due to divergence of rays within the limits of Borman's tent and as a result – the contrast of image relaxes.

In case of weak absorption the zone of strong positive contrast round dislocation begins wherein noticeable "dispersion between branches" of Bloch's waves takes place, but nature of the deformation field of dislocation is such, that it is expediently to use criterion of inclination of crystalline planes near-by distribution for the foresight of width of dislocation image. In obedience to this criterion, distortioned areas of grid in relation to a perfect matrix on a corner that corresponds the parameter of rejection of $w \approx 2$, give large surplus of the diffracted intensity. Interference stripes can have a various form in dependence on geometry of location of dislocation and its orientation descriptions. An a few another situation is observed for the case. Character image of 60°-dislocation substantially depends on that, where is the dislocation placed : near-by an entrance, in a center or in close to the entrance surface of crystal. Thus, character of dispersion between branches depends substantialy on orientation of dislocation.

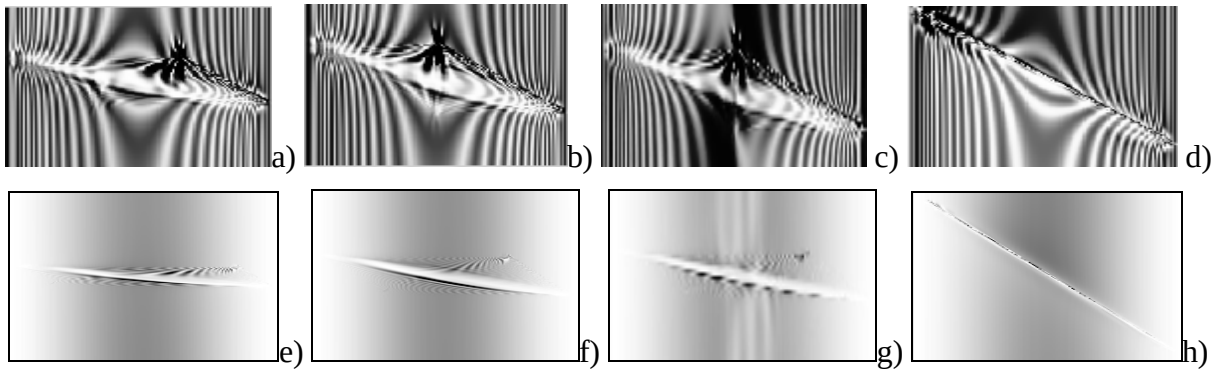

Fig.1. Simulated section topograms of 60° dislocations, which are parallel to the exit surface. Si, MoK_α, (220): μt=1 (a-d), μt=6 (e-h). The depth of location : a) z=240, b, c) 360, d) 500, e) 1000, f, g) 2000, h) 4000 μm. Influence of acoustic deformations U_0=0,01 Å (c,g).

1. Novikov S., Fodchuk I., Fedortsov D., Struk A. *Phys. stat. sol. (a).* A**206**, №8: 1820 (2009).
2. Fodchuk I.M., Novikov S.M., Struk A.Ya. *Metallofiz. Noveishie Tekhnol,* **32**, №9: 1198 (2010).

CdZnS Films Grown by Spray-Pyrolysis and their Properties

Orletsky I.G., Frasunyak V.M., Chupyra S.M.

Yuri Fed'kovych Chernivtsi National University, Chernivtsi, Ukraine

The common design of a thin-film solar cell includes a wide-band window layer through which light enters the cell. It is useful to move the area of intensive photo-generation from upper contact to reduce surface recombination losses of non-equilibrium carries. A wide-band semiconductor – for example, cadmium sulfide with Eg ≈ 2.4 eV – is a good option for the window layer. Ternary solid solutions $Cd_{1-x}Zn_xS$ may also function well for semiconductors such as CdTe, minimizing conduction band mismatch and defect concentration at the interface, also enhancing layer transmission for the incident light. Other benefit of simple deposition techniques consists in their low production cost that may help to achieve cost reduction for the entire photovoltaic device.

In this paper we studied the properties of $Cd_{1-x}Zn_xS$ ($0 \le x \le 0.8$) obtained by spray pyrolysis method under different conditions. We used sital and quartz substrates depending on the physical properties we wanted to study. All spraying solutions were water based. For example, $Cd_{0.9}Zn_{0.1}S$ solution was composed of 1 ml of zinc acetate $Zn(CH_3COO)_2 \cdot 2H_2O$ solution in water (0.1M), 9 ml of cadmium chloride $CdCl_2$ solution in water (0.1M) and 15 ml of thiourea $(NH_2)_2CS$ solution (0.1M as well). The order in which the components are mixed had no apparent influence on the quality of the films. All solutions were filtered before the pyrolysis. The growth of the films was significantly dependent on the surface quality. The best films were obtained under pyrolysis temperatures 390-420ºC. The film thickness was estimated by Linnick interferometer MII-4. As it was found from electro-physical studies, the increasing zinc contents varied specific resistivity of $Zn_xCd_{1-x}S$ films within the ranges of $10^4 \div 10^6$ Ohm·cm, also modifying band gap and carrier concentration. Using proper thermal treatment it became possible to reduce series resistivity of solar cell for about two orders of magnitudes at low composition $x<0.4$. However, for high composition values $x > 0.6$ not much progress was achieved.

Transmission spectra of thin $Zn_xCd_{1-x}S$ films produced by spray-pyrolysis were investigated for wavelength range $\lambda = 200 \div 800$ nm with spectrophotometer SF-2000. We studied films deposited on mirror-smooth quartz substrates at pyrolysis temperature $T = 390^oC$. All samples had the same thickness $d = 0.27$ μm, featuring a fixed shift of their interference peaks. The films of $Zn_xCd_{1-x}S$ for the ranges of zinc contents studied were characterized with high transmission $T = 55 \div 70\%$ in the visible and infrared spectra. Linear dependence of $\alpha^2 = f(h\nu)$ suggests that light absorption triggers direct band transitions. The band gap of $Zn_xCd_{1-x}S$ films for $0 < x < 0.8$ varied in ranges $2.4 \div 3.27$ eV. This method to control $Zn_xCd_{1-x}S$ film parameters has good perspectives for improvement window part in heterojunction solar cells.

Growt and the Properties of Nanostructured CdZnTe Films, Deposited by Method of "Hot Wall" Epitaxy

Rashkovetskyi L.V., Vuichyk M.V., Lytvyn P.M., Gudymenko O.J., Sizov F.F.

V.Lashkaryov Institute of Semiconductors Physics of NAS of Ukraine, Kyiv, Ukraine

The influence of technological factors on the formation of thin films based on CdZnTe grown by method of "hot wall" epitaxy is studied. Substrate's temperature (T_{sub}), temperature of evaporation source material (T_{sou}) and wall's temperature (T_w) varied within: T_{sub}: 100°C - 400°C, T_{sou}: 350°C – 600°C, T_w: 380°C – 650°C.

As a substrates were used the chemically polished monocrystalline wafers Si (111). As a source of evaporation were used monocrystalline grains $Cd_{1-x}Zn_xTe$ containing zinc (0.04 -0.1 mol.%), synthesized in advance. Deposition time of films was 1-120 min.

The thicknesses of the obtained films were determined using ALPHA STEP 100 and "MICRON-ALPHA" profilometers. The morphology and composition of the obtained nanostructures were investigated by methods of atomic force microscopy (AFM) (Nanoscope Dimention 3000, Digital Instruments, USA) and scanning electron microscopy JXA-8200 (JEOL). From these investigations growth mechanisms films, their composition, size nanocrystallites, surface roughness, thickness of the films have been determined.

Analysis of the image of surface of nanostructured films of CdZnTe obtained at different technological factors confirmed that Folmer-Weber mechanism should be considered as the dominant mechanism. This mechanism is characterized by the initial formation of separate three-dimensional nuclei (islands) condensation on the substrate surface, followed by their growth and the growth of a continuous film. Found that the thickness of grown films increases from 0.1 microns (deposition time 1 min) to 2.6 microns (deposition time 120 min). With increasing of deposition time nanocrystallites dimensions (lateral and height) increased from 0.04 microns to 0.5 microns and have a distinct form of truncated hexagonal pyramid. This trend is explained by the increase in the flow, and hence increases the deposition rate of atoms (molecules) of condensate. Also found that with increasing of substrate temperature at constant temperature evaporation and deposition time the thickness of the grown film decreases. This can be explained as possible effect of re-evaporation of components of the film surface and decrease in the flow of condensate due to reduced gradient substrate temperature - temperature evaporation.

X-ray diffractometry studies showed that the films follow the orientation of the substrate and have polycrystalline structure and crystallize in the cubic form.

Vacuum Deposition of the thin Layers of ZnCdTe Solid Solutions on Nonoriented Substrates

Rudnitskyi V. A.[1], Rashkovetskyi L.V.[2], Moskvin P.P.[1], Lytvyn O.S.[2], Stronski O.V.[2]

[1]*Zhytomyr State Technological UniversityZhytomyr, Ukraine*
[2]*Institute of Semiconductors Physics NAS Ukraine, Kiev, Ukraine.*

Composite structures with participation of semiconductor glasses and ultrathin layers of A^2B^6 semiconductors solid solutions are perspective systems of nonlinear optical elements. In this work we report about the development of technology and realization of deposition regimes of ZnCdTe solid solution layers on glass substrates. The typical thickness of the deposition layers was at level of a tenth fraction of micron.

Films were obtained on the modernized standard equipment for a vacuum deposition which provided possibility of work with uncongruent evaporating compounds. The basic piece of equipment which has been subjected modernizations and which provided possibility of work with uncongruent evaporating compounds was the evaporator of initial substance. The evaporator with electronic bombardment of the anode was used in equipment. As a source of thermo electrons the ring tungsten cathode was used. The developed design of the evaporator at the expense of change of mutual orientation of the cathode and the anode allowed realizing of a regime of indirect heating of evaporated substance or a regime of a direct electronic warming up of substance-source. Also thermal evaporation was used.

The typical operating regime of equipment provided process of deposition of a layer in a free electronic regime at which the thermo issue current exceeds an anode current. It allowed to reduce considerably level of ionic bombardment of the cathode and by that to eliminate undesirable currents in system. The modernized equipment allowed to carry out clearing of a substrate by argon ions.

Anode evaporation was carried out from quartz crucible, as a source of substance the ZnCdTe solid solution was used. As a substrates were used a traditional glass with specially prepared surface, and chalcogenide glass of GeAsS system. Time-temperature regime of a deposition, as well as a relative positioning of electrodes, a substrate and a source varied in enough wide ranges.

The morphology of the obtained layers was investigated by AFM measurements, Their composition was estimated by a X-ray method. Correlations between the layers parameters and of their synthesis conditions are found.

An Influence of pH on the Contact Deposition of Copper on the CdSb Surface

Sema O. V., Woloschuk A. G., Kobasa I. M.

Yu. Fedkovych National University, Chernivtsi, Ukraine

An influence of pH on the contact deposition of copper on the CdSb surface has been investigated by the methods of potentiometry, thermodynamic analysis and scanning electron microscopy. It was found that an ionic exchange in the system CdSb–Cu^{2+}–H_2O depends on the crystal-chemical state of the semiconductor's surface and the chemical state of Cu^{2+} ions in the solution. The contact deposition runs according to the reaction $CdSb + x\ Cu^{2+} \leftrightarrow Cd_{(1-x)}\ Sb + x\ Cd^{2+}$.

An optimal deposition can be achieved for the nearly atomic-clean surface. The Pourbe diagram for the **CdSb–H_2O** system proves that the CdSb surface can be either active or passive depending on the pH value. The active state is caused by dissolution of the semiconductor's surface in the strong-acid solutions (pH<2). A complex composition of the oxide and hydroxide compounds ($Sb(OH)_3$, $HSbO_2$, Sb_2O_3, $Cd(OH)_2$, depending on the pH value and the oxidizing agent's potential) can be formed on the CdSb monocrystals surface in the subacid solutions. Since the contact deposition of metals involves surface atoms of cadmium, the chemical condition of the semiconductor's surface will make a considerable influence on this process.

Different forms of copper can be found in the solution depending on its pH: Cu^{2+}, $CuOH^+$, $Cu(OH)_2°$, $Cu(OH)_3^-$ and $Cu(OH)_4^{2-}$. Certainly, different ionic forms of the metal will exert an influence on the kinetics and mechanism of the ion-exchange processes in the system CdSb–Cu^{2+}–H_2O.

The analysis of the experimental data reveals some special characteristics of the electrode behaviour of CdSb-monocrystals in the solutions. The increase in concentration of the Cu^{2+} ions results in positive shifting of the CdSb electrode's potential while the increase in pH switches the electrode's potential negative at pH>6.

A specific composition of the dependencies E = f(pH), which have two separate linear parts with different signs and values of the angular coefficient ($\Delta E/\Delta pH$) is their characteristic trait. These two parts indicate the fact that the contact exchange in the CdSb–Cu^{2+} systems can involve different forms of the reagents. Changes in the reagents concentrations can also influence the equilibrium $H_2O \leftrightarrow H^+ + OH^-$. At the same time, the chemical condition of the surface also exerts a significant influence on the contact deposition, which is also proven by E = f(pH) curves having a well noticeable break at pH>4 for both systems.

Definition of a Complex Refractive Index by Results of Reflection Measurement at two Angles of Incidence.

Shkaleto V.I., Kopach G.I.

National technical university «Kharkov polytechnic institute», Kharkiv, Ukraine

One of main not destroying methods of control with purpose of definition of physical parameters of materials is the carrying out optical researches. The decision of a back task of optics allows determining thickness and complex refractive index by results of measurements coefficients of reflection and transmission of researched objects. For this purpose it is necessary to execute as a minimum three various measurements: coefficients of transmission of film system and coefficients of reflection at two various incidence angles. Therefore were designed and fabricate the attachments to spectrophotometer SF-46 for measurement reflection coefficients at angles of incidence: 30° and 60°.

With the purpose of definition of a complex refractive index by results of measurements reflection coefficients from massive or film object at two various incidence angles the algorithm and program «Back Task Optic» in language VB6 was developed.

The basis of algorithm and program is the principle of minimization of criterion function, which represents the sum of squares of differences of the experimentally measured coefficients of reflection and calculated theoretically. The search of a minimum of criterion function by a method of the least squares results to necessity of the decision of nonlinear system of the equations by the Nelder-Mid method in the closed area of a plane of values of a complex refractive index. In a case, when the search of the decision make go out borders of area, the program allows to construct a map of criterion function, with which help is possible manually to choose the localization area of minimum required function. Further search of a minimum proceeds in an automatic mode.

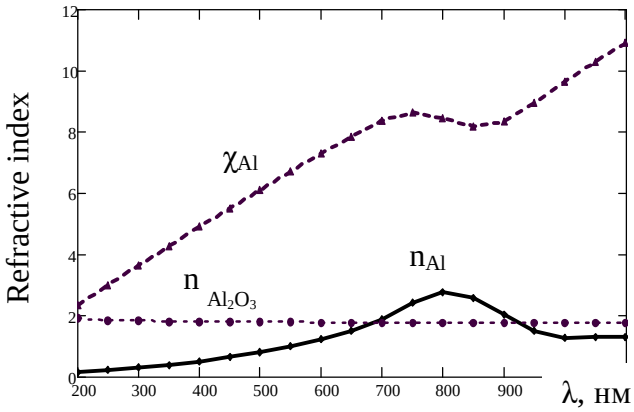

The check of program work was carried out by results of modeling spectral dependences of reflection coefficients from massive Al at two angles of incidence: 30º and 60º. The results of program work check are given in figure for system: a film alumina (Al_2O_3) on a mirror aluminum (Al) surface. The good agreement of the program work results and initial data for modeling is observed.

Time-Resolved Photoluminescence Study of $Zn_{1-x}Cd_xO$ ($0.051 \leq x \leq 0.086$) Ternary Alloys Grown by the dc Magnetron Sputtering

Shtepliuk I.[1], Khranovskyy V.[1], Lashkarev G.[1], Khomyak V.[3], Lazorenko V.[1], and Yakimova R.[2]

[1] *I. Frantsevich Institute for Problems of Material Science, NASU, Kiev, Ukraine*
[2] *Department of Physics, Chemistry and Biology (IFM), Linköping University, Linköping, Sweden*
[3] *Chernivtsi National University, Chernivtsi, Ukraine*

There is worldwide interest in the use of ZnCdO-based semiconductors for optoelectronic devices such as light-emitting diodes (LEDs) and lasers. It is due to possibility to control of the band-gap and color of the emission of ZnO by the change of Cd content. In spite of the impressive progress made in recent years in the development of heterostructures, significant work needs to be done to further optimize device performance. In order to achieve this goal, the physics underlying the operation of these devices must be better understood. It is important to understand the fundamental properties of the optical process and emission mechanism in ZnCdO alloys, especially for Cd-rich ZnCdO films.

Here we present the results of micro-photoluminescence (μ-PL) and time-resolved photoluminescence (TRPL) measurements (Fig.1) on three ZnCdO films grown by the dc magnetron sputtering. The decay curves can be fitted by the sum of two exponential functions. Therefore, PL in ZnCdO consists of two independent components. The faster (τ_1) and slower (τ_2) time constants correspond to the lifetime of the nonradiative and radiative recombination, respectively. The results of a bi-exponential fit to the TRPL intensity decay (Fig. 1) show the carrier lifetimes τ_2 is nearly 2 times longer in the samples with higher Cd content in comparison to the Cd-poor one. Additionally, it should be noted that the τ_1 constant has been elongated when the Cd content is increased. Thus, the longer τ_1 lifetime observed in the samples with Cd content of 6.3-8.6 at.% is most likely the result of a reduction in non-radiative recombination rate by strong carrier localization, since carriers are trapped by the potential minima and confined away from the non-radiative recombination centers. Effect of cadmium content on the internal quantum efficiency of ZnCdO luminescence is also studied and discussed.

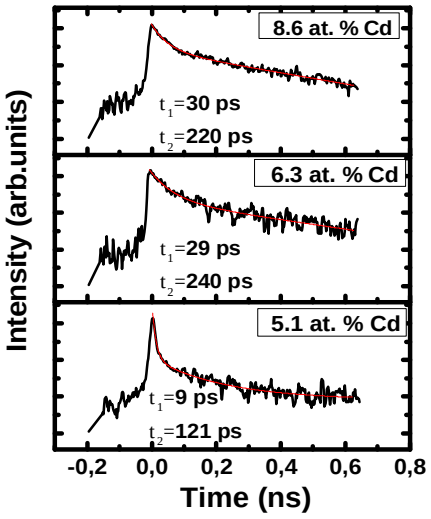

Fig. 1. PL decay curves for ZnCdO films.

Crystallization of High – Voltage p-i-n Si Epitaxial Structures with Liquid – Phase Epitaxy Method.

Vakiv M.[1], Tymchyshyn V.[2]

[1]*SPE " Karat", Ukraine, Lviv*
[2]*NU "Lviv Politechnic",Ukraine, Lviv*

The singularity of p – i – n Si epitaxial structures is presence of thick high – resistance *i* – region, on the both sides of which contact layers of p – and n – type are forming. As a rule, crystallization of p – i – n Si structures is realized with liquid - phase epitaxy (LPE) method in two steps. In the first step on the one side of underlayer crystallizes n – layer, and in the second step crystallizes p – layer on the other side of underlayer. This technological approach to forming two – side epitaxial layers is complicated, and in case of forming high – voltage epitaxial layers we can see significant deterioration of their parameters as a result of long thermal treatment of active high – resistance layer. LPE process takes place at temperatures higher than 800 – 900 ^{0}C. When temperature is so high, we can observe degradation of electrophysical propeties of underlayer (decreasing of ρ). Degree of degradation of underlayer depends on absolute temperature of heat treatment and on its duration. Improvement of the situation in this case can be achieved by decreasing time of thermal treatment. This can be achieved by joining two technological processes of crystallization n – and p – layers Si in one.

Solution of this problem is in developing construction of cassette for incremention of epitaxial layers on the both sides of underlayer during one technological process. In this work we present results of investigation of forming p – i – n Si epitaxial structures grown in developed graphite cassette.

Crystallization of layers took place in temperature range 860 – 650 ^{0}C. In this range also grown of n – Si epitaxial layer from solution – fusion based on Tin (Sn) was realized. In temperature range 740 – 650 ^{0}C realized crystallization of p – Si from Ga solution – fusion, alloyed with Antimony (Sb) and Itterbium (Yb). I.e., crystallization of epitaxial layers takes place at the same time on both sides of underlayer. As a result we get p –i– n Si epitaxial structures with such electrophysical parameters: thickness of n – layer – (3,1 – 4,1) μm, electron concentration - $(1,1 – 1,9)\times10^{19}$ cm^{-3} , thickness of p – layer - (5,1 – 7,1) μm, hole concentration - $(1,5 – 3,7)\times10^{19}$ cm^{-3} . Specific resistance of i – Si region stays constant, and this fact gives us an ability of creation p-i-n Si - based epitaxial structures high – voltage diodes with piercing strain over 1000 V.

Thus, we worked on the technology of obtaining high – voltage two – side p – i – n Si epitaxial structures by LPE method with ability of growing n – and p – layers in one technological process, which gives an opportunity to get structures with improved parameters.

The Properties of PbTe, PbSe and PbS thin Films, Prepared by Pulsed Laser Deposition Method

Virt I. S.[2], Rudyj I.O.[1], Kurilo I.V.[1], Lopatynskyi I.Ye.[1], Frugynskyi M.S.[1]

[1]National University "Lviv Polytechnic", Lviv, Ukraine
[2]Drogobych State Pedagogical University, Drogobych, Ukraine

Connections of semiconductors of type IV–VI it is enough widespread materials for the thermoelectric devices through their high coefficient of thermoelectric transformation *Z*. In particular, material PbTe known, presently, how the best thermoelectric material is [1]. That to get a still higher coefficient mixes PbTe up with PbSe, or PbS which is also other IV–VI connections with high transformation. Thanks to the tendency of miniature of thermo-electric devices, it is necessary to study not only properties of massive standards but also properties of thin films of these materials.

The films of PbTe, PbSe and PbS of different thickness were obtained on Al_2O_3, glass and KCl substrates in vacuum of 1×10^{-5} Torr by the pulsed laser deposition method. The samples were obtained under the substrate temperature 300–473 K. A thickness of films was in the range of 40–1500 nm depending on the number of laser pulses. The structure of target bulk materials was investigated by X-ray diffraction method. A structure of laser deposited films was investigated by the transmission high-energy electron diffraction (HEED) method. The electric resistivity was measured in the temperature range 77–450 K. It is conducted electric measuring of specific resistance and also analyses structure of thin films using HEED and scanning electron microscopy.

The PC kinetics under LED pulse illumination at different temperatures and pulse durations is presented in work. The estimations show that for the beginning of relaxation the characteristic time 10^{-6} s at 300 K. So the rapid relaxation time appears to be by at least two orders of magnitude larger than the characteristic times of optical band-to-band recombination in PbTe.

1. D.M. Freik, R.I. Zapukhlyak, M.A. Lopjanka, G.D. Mateik, R.Ya. Mikhajlonka Thermoelectric property features of PbTe monocrystalline and polycrystalline films // Semiconductor Physics, Quantum Electronics & Optoelectronics. – 1999. – Vol. 2, № 3. – P. 62–65.

Vacuum Vapor-Phase Heaters for Vapor-Phase Condensates

Ja.S. Javorsky, Lopjanko M.A., Pavljuk M.F., Javorsky R.S., Lysyuk Yu.V.

Vasyl Stefanyk Precarpathian National University,
Ivano-Frankivsk, Ukraine

Semiconductor's thin films and nanostructures have a wide range of effective use as active elements in the sources and detectors of electromagnetic radiation at different wavelengths, filters and reflective surfaces, etc. [1]. For the getting of semiconductor films and nanomaterials are used the molecular beam epitaxy (MBE), metaloorganic vapor-phase epitaxy (MOVPE), and others [1].

This paper are presented improved design previously developed vacuum heaters [2], which allow to obtain a series of vapor-phase condensates in a single cycle for various technological factors: different thickness h = (0,1-5) mm at constant temperature deposition T_n = (300-570) K, the same thickness h for different T_n in the above-mentioned limits. We are described the procedures to ensure the receipt of condensates of different thicknesses at constant temperature substrates and the same thickness at different deposition temperatures. The possibility of use the proposed vacuum heaters for double-layer nanostructures have been examined.

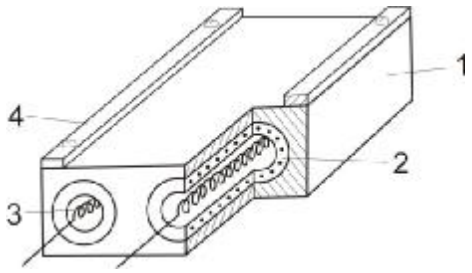

Figure 1 Structural diagram of vacuum microfurnace.

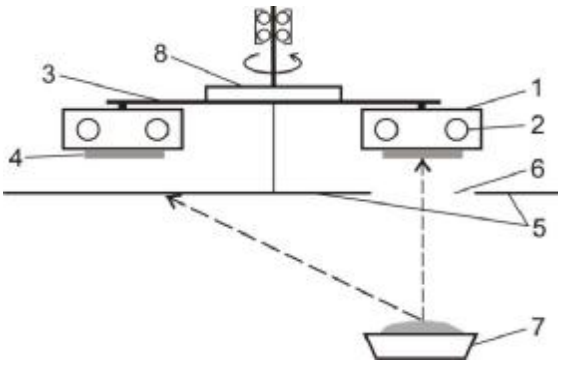

Figure. 2. Structural diagram of the device for films and nanostructures.

1. Freik D.M., Galushchak M.O., Mezhylovskaya L.Jo.. Physics and Technology of semiconductor films. High School. Lions. 152 p. (1988).
2. Bjelavski V.N. The Physics Basis of Semiconductor Nanotechnologies // Sorosovsky Education Journal, 10, pp. 92-98. (1996).

The work supported by an integrated project of MES of Ukraine (N 0113U000185) and by projects of FRSF State Agency for Innovation and Informatization of Ukraine. (Contracts: R54, F53, 3); NAS of Ukraine (N 0110U006281).

Optical Properties of Thin Polymer Films Obtained by Deposition in a Vacuum

Zadorozhniy V.G., Polishchuk S.G., Keybal E. A., Kobrin V.L.

Odessa National Academy of Food Technologies, Odessa, Ukraine

The influence of the deposition conditions of thin polymer films in a vacuum on their optical properties were studied. The effect of crystallinity, structure and thickness on optical transmission, refractive index, and radiation resistance were investigated. A new technique has been proposed for determining the degree of crystallinity during the X-ray analysis of ultrathin polymer coatings.

The effectiveness of the grain size was examined using the formula of Selyakov depending on the conditions of condensation. It slightly changed (in the range of 9 - 15 mm) on the rate of deposition. Since for all modes of deposition the same grain size was observed, it can be concluded that the increase in the degree of crystallinity with increasing the rate of evaporation (V_e) is higher than 0.3 mg/cm^2 mainly due to the decrease of the disordered regions in the coating, and not due to proliferation of the crystallinity centers.

It has been found that the films obtained without initiating of the secondary polymerization during the condensation process, contain the higher number of chromophoric groups, which significantly absorb radiation in the visible and UV regions.

Presence near the chromophore groups, other groups, such as OH, NH_2, OCH_3, increases the wavelength of the absorption band. A definite role in the long-wave range plays the conjugation. It has been found that by changing the conditions of formation of the film, one can minimize the number of chromophore groups and maximize the light transmission.

Significant impact on the optical transmission has the presence of spherulites with dimensions of the same order as the wavelength of light. Scattered intensity is defined as the size of the spherulite and the perfection of its structure. Choice of the electron beam irradiation regimes in the making of the film managed to destroy spherulitic order and significantly increase their transparency.

Annealing of films decreases transmission. Annealing in vacuum leads to decrease of the light transmission by 2 to 3%, in the air up to 15% due to the formation of carbonyl and carboxyl groups. It is possible that in this case recrystallization occurs in the films, but it has smaller impact on the light transmission.

Peculiarity of the Formation of Composite Device Based on Porous Silicon Coated by Metallophthalocyanine

Zubko E.I.,

Zaporizhia State Engineering Academy, Zaporizhia, Ukraine,

It was shown that porous silicon (PS) can be used as a base material for passive or active optical devices. Due to porous nature, the effective refractive index of PS is lower than that of bulk silicon and can varied with porosity value. This allows many optical applications of this material. Recently, PS discussed as a novel material for chemical sensors and biosensor. Phthalocyanines (PCs) possess a wide range of chemical and physical properties that make them interesting as building blocks for a number of applications as well as for obtaining new material. One of the important applications emerging in recent years includes their use as chemically sensitive films.

In the present study, soluble MPCs (M=Al, Cu) was used for formation of the active layer and deposited on a large surface area device consisting of PS. Samples of n-type silicon wafers were having electrochemically etched in HF/ C_2H_5OH, according to known methods. The samples were deposited with MPCs by pulverisation method, sustained 2h in a desiccator for saturation and annealed in air at the 250-300C 5-10 min.

At formation of PCs coating, we used solutions with concentration $C_{32}H_{16}N_8Cu$: C_3H_6O: H2O = 2:39:59wt.% and $C_{32}H_{16}N_8Al$: C_2H_5OH:H_2O = 2:59:39 wt. %. In this case, we observed creation on the surface of PS of Cu and Al network. Size of metal fibers 200 - 1000 nm and 500-1500 nm for Cuprum and Aluminium respectively. As a result of solvent evaporation and ordering of PS/ PCs composite device, we observed correlation of internal stresses arising in the structures.

In our investigation, we also noticed that structural features of the interface formed between the metal-PCs on the PS could be determined of the temperature of solution and substrate. In this case optimal will be 40 °C and 45 °C respectively.

In the study of peculiarity formation of metallophthalocyanine coated porous silicon composite device the dependence of electrical properties of compositions from physical effects (annealing) was found**.**

СЕКЦІЯ 2 (усні)
НАНОТЕХНОЛОГІЇ, НАНОМАТЕРІАЛИ І КВАНТОВО-РОЗМІРНІ СТРУКТУРИ

21-24 травня 2013 р.

SESSION 2 (oral)
NANOTECHNOLOGIES AND NANOMATERIALS, QUANTUM-SIZE STRUCTURES

May, 21-24, 2013

The Destruction of the Ceramic Probe of an Atomic-Force Microscope in the Study of Dielectric Materials

Bilokon S.A.

Cherkassy State Technological University, Cherkassy, Ukraine

The atomic-force microscope is one of the most promising and versatile research methods of study of micro-geometry and of surface mechanical properties of nano-materials. The main disadvantage of AFM is the fragility of the probe. One of the reasons for the destruction of the silicon probe can be electrostatic discharge in dielectric surfaces scanning. Let us consider the mechanism of interaction between the silicon probe with dielectric surfaces and define the materials of these surfaces, at the interaction of which there is a risk of electrostatic discharge.

According to the terms of the sliding contact between the probe and the sample surface, we take the value of the charge Δq, acquired by the probe after each step of the scan. The scanning speed is *n* steps per a unit of time. Therefore, the charge current:

$$i_c = n \cdot \Delta q \quad (1)$$

Increasing of the voltage ΔU with each step will be:

$$\Delta U = \frac{\Delta q}{\tilde{N}} \quad (2)$$

where *C* is the probe capacitance ($\tilde{N} = 4 \cdot \pi \cdot \varepsilon_0 \cdot \varepsilon \cdot r$ = 1,29 10^{-17} F).

The maximum value of the charge Δ q_{max}, accumulated by the probe at a given step:

$$\Delta q_{\max} = e_0 \cdot E_b \cdot A \quad (3)$$

Here ε_0 is the dielectric capacity of the air (8,85 10^{-12} F / m);
E_b is field density of breakdown in the air between the electrodes (2,8 10^6 .. 3,2 · 10^6 V / m), and A is the area of the dielectric, contacting with the probe (6,28 10^{-16} m^2).

We take the maximum voltage possible to charge probe U, then the resistance of the "run-off" charge must satisfy the condition:

$$R \le \frac{U}{n \cdot \Delta q_{\max}} \quad (4)$$

Therefore, through a series of calculations it has been shown that for the majority of the dielectrics the electrostatic breakdown does not occur in the process of scanning. This is due to lack of time of the breakdown charge accumulation and its run-off on the layer of moisture absorbed on the surface of the dielectric.

Therewith, the materials, the scanning of which can cause danger of the accumulation of the electrostatic charge during the research conducted by the silicon probe will be the materials with an electrical resistivity from 1.8 10^{14} ohm m to 1.16 10^{16} ohm m. Such materials correspond to these values: paper, quartz glass, wax, polystyrene, mica, porcelain, hard rubber, etc.

Absorption and Photoluminescence Intensity of Semiconductor Quantum Dots

Boichuk V.I., Bilyns'kyi I.V., Shevchuk I.S., Hols'kyi V.B.

Drohobych Ivan Franko State Pedagogical University, Drohobych, Ukraine

In recent years quantum dots as well as other nanoscale heterostructures have attracted growing attention of many investigators – both experimentalists and theoreticians. Remarkable progress has been observed in the study of absorption and photoluminescence spectra of quantum dots. Great success has been achieved in understanding of optical properties and theoretical research of physical processes in quantum dots.

We have considered absorption and photoluminescence intensities of spherical quantum-dot systems. The numerical calculations of absorption and photoluminescence intensities have to take into account the real band structure of nanocrystals, since it effects the values of optical transition energies and leads to the change of optical selection rules.

To describe quantitatively absorption and photoluminescence intensities of quantum dots, electron-hole pairs (EHPs) are considered with regard of the exchange interaction, size distribution of quantum dots, and phonon spectrum. Optical absorption of quantum dots is studied using the adiabatic approach. The interaction between the electron-hole pair and longitudinal optical phonons has been described with the Fröhlich-type Hamiltonian taking into account the valence band degeneracy.

The photoluminescence spectral line shape resembles that obtained from the experiment in [1] and supports the formation of the EPH-polaron. The numerical calculations are carried out for quantum dots of different sizes and the absorption intensity is found as a function of quantum-dot radii values.

The model of the electron-hole pair with finite barrier potentials, in case when nonadiabatic effects can be neglected, proves to be useful to describe the absorption and photoluminescence spectra of small spherical quantum dots. The analysis is performed for the CdTe/HgTe quantum-dot system.

1. M. Bissiri, M. Capizzi, V.M.Fomin, V.N. Gladilin, J.T. Devreese, Phys. Stat. Sol.(b) 224 (2001) 639.

Interband Absorption Coefficient in Quantum Dots of Different Shapes

Boichuk V.I., Bilynskyi I.V., Sokolnyk O.A., Shakleina I.O.

Ivan Franko Drohobych State Pedagogical University, Drohobych, Ukraine

In modern semiconductor optoelectronics manufacturing of sources and receivers in the range of average infrared emission is one of important directions of investigations. For this purpose it is necessary to study interband optical transitions of charge carries taking place due to absorption of polarized light.

The effect of quantum-dot (QD) shape of the GaAs/AlAs heterostructure on the frequency of interband absorption of polarized light is considered. The calculations have been carried out in the adiabatic approach for a cubic, ellipsoidal, cylindrical and tetrahedral shapes by changing the quantum-dot volume.

The Hamiltonian describing the interaction of the electron-hole pair (EHP) and phonons takes into account the interaction of charged particles with polarization oscillations.

Interband light absorption in semiconductor nanoheterosystem is considered within the modal of quasi-zero-dimensional structure in the dipole approximation where absorption wavelength is large in comparison with quantum-dot size. The interband absorption coefficient caused by transition of a charge between optically active QD states has been calculated according to the equation

$$a(w) = \frac{4p^2 e^2}{ncm_0^2 \mathbf{h} w V_0} \sum_{f \neq 0} \left\{ D_f \exp\left[-g_f \left(2\bar{N}+1\right)\right] \sum_{n=-\infty}^{\infty} I_n \left(g_f \sqrt{\bar{N}\left(\bar{N}+1\right)} \right) \right.$$
$$\left. \times \exp\left(nb\mathbf{h}w_0 / 2\right) d\left(w - w_0 + \Delta_f - nw_0\right) \right\}. \quad (1)$$

The effect of quantum-dot shape on the EHP-phonon interaction and interband absorption spectrum is discussed. Particularly, the dependence of Huang-Rhys factor which determines the electron-phonon interaction in heterosystems is analyzed. The absorption coefficient caused by transitions of charge carriers between optically active levels in QDs under the influence of linearly-polarized light is calculated.

The information obtained in the study can be used to establish GaAs quantum-dot shape in the AlAs matrix.

Aspects of Growing III-V Compounds and Their Solid Solutions by «Ostwald Ripening» of Nanowires

Bolshakova I., Kost Ya., Makido O., Stetsko R., Shurygin F.

Magnetic Sensor Laboratory, Lviv Polytechnic National University, Lviv, Ukraine

Semiconductor micro- and nanocrystals have attracted great interest in recent years in connection with their unique properties relating both to minimal number of inherent structural defects and to size effects. Microcrystals of binary compounds such as GaAs, InAs, InSb and their solid solutions InSb-InAs, GaAs-InAs form the basis for creating sensing elements for sensors of physical quantities.

Growth of such whiskers is carried out in closed reactors from vapour phase following the method of chemical transport reactions (CTR) by the vapour-liquid-crystal mechanism (VLC mechanism). Effectiveness of the mechanism depends upon the choice of metal catalyst, which has to satisfy the requirement of ensuring easy transportation to growth zone and possessing low-temperature eutectics of InSb-metal alloy. The catalyst used for growing GaAs, InAs crystals and their solid solutions GaAs-InAs is gold, while nickel is used for InSb crystals and solid solutions InSb-InAs.

The method of microcrystal growth consists of several stages. In the first stage clusters of nanowires are formed following the VLC mechanism. Nanowires grow in the kinetic region in a definite crystallographic direction. In the second stage conditions for the so-called «Ostwald ripening» of nanowires are created [1]. Its essence is the following: as a result of competitive growth of nanowires a substantial part of these nanowires becomes a source of energy for the vapour phase, out of which nanowires of bigger diameters are then grown. This self-consistent process results in simultaneous decrease in the number of nanowires and in increase of their sizes to microns. In the third stage microcrystals are further grown until they reach the sizes required for the crystals to be used in sensors. This process, which resembles epitaxial growth, takes place in the diffusion area. Duration of this stage determines the dimensions of final semiconductor microcrystals.

Semiconductor microcrystals obtained in this way are applied for production of sensing elements for sensors of physical quantities: magnetic field, temperature, deformation, pressure.

1. J. B. Hannon et al. Nature Lett. Vol. 440(2). March (2006).

Properties of the Silicon Enriched SiO_xN_y Films

Bratus O., Evtukh A., Voitovych M., Lisovskii I.

V. Lashkaryov Institute of Semiconductor Physics, Kiev, Ukraine

The intensive development of micro- and nanoelectronics requires new types of dielectrics with unique properties. Nowadays, the multi-layered dielectrics (SiO_2-Si_3N_4-SiO_2) and dielectrics with silicon nanocrystals (Si-NCs) in insulating matrix are widely investigated and used in nonvolatile memory. The aim of our research is to obtain Si-NCs in silicon oxynitride (SiO_xN_y) matrix. In this work the first results on properties of silicon enriched silicon oxynitride films and their changing after temperature annealing due to transformation of the SiO_xN_y film into nanocomposite SiO_2N_y (Si) film are presented.

SiO_xN_y films were deposited by ion-plasma sputtering of the silicon target in a vacuum on c-Si (p - type) substrate at different ratios of working gases Ar / (O_2/N_2).

The broad band with two characteristic peaks (positions of the maxima ~ 750 and ~ 1020 cm^{-1}) is observed in IR-spectra of initial SiO_xN_y film. The peaks are located in the areas of stretching vibration of Si-N and Si-O bonds. High temperature annealing resulted in significantly different IR spectra, especially in high-frequency region. The significant shift of the absorption band caused by Si-O bonds (from 1020 to 1075 cm^{-1}) and the increase (almost in 4 times) its integrated intensity is observed. High temperature annealing led to some changes in low-frequency absorption bands: (i) halved the component at ~ 660 cm^{-1} corresponding to Si-H bonds, and (ii) redistributed the intensity of the profiles that are related to the Si-N bonds in different structural configurations. It is important that the main characteristics of the mentioned profiles (position of the maxima and half-width) remained unchanged. These facts indicate that the structure of silicon nitride phase does not change during heat treatment. There is only transformation of vibration frequencies of Si-N bonds that is likely related to changes in local concentrations of hydrogen and oxygen surrounded by nitrogen atoms.

I-V characteristics of the initial silicon oxynitride SiO_xN_y film and nanocomposite SiO_2N_y (Si) film show that the high temperature annealing (T = 1100 °C) decreases the electrical conductivity of the initial oxynitride film by several orders of magnitude. During the high temperature annealing the transformation of SiO_xN_y into SiO_2N_y matrix is performed. That leads to the increase in the bandgap and reduce the density of electron and hole traps. To clarify the conductivity mechanisms of silicon oxynitride films the measurements of I-V characteristics at different temperatures were performed. The analysis of temperature dependences of the conductivity of silicon oxynitride films indicates the realization of variable range hopping conductivity mechanism through localized states near Fermi level.

Ostwald Maturation Processes in Lead Telluride Nanostructures

Chobanyuk V.M., Bylina I.S.

Vasyl Stefanyk Precarpathian National University, Ivano-Frankivsk, Ukraine

The processes of cross-sructurization in vapor-phase condensates cadmium telluride attract considerable attention of researchers due to wide possibilities of their using in opto-and nanoelectronics, such as detectors and radiation hard and LEDs in the visible part of optical spectrum [1-4]. New physical methods like as atomic power microscopy (AFM), give the possibility to learn the morphological peculiarities of the nanoformations on diffferent stages of inception and growth.

Thin film nanostructures CdTe got from the vapor phase, using the "hot wall" method. The glass, glass ceramic, fresh chips (0001), muscovite mica were using as wafers. Obtained thin film structures were explored by methods of atomic power microscopy (AFM) Nanoscope 3a Dimention 3000 (Digital Instruments USA) in the periodic contact. Measurements, which were carried out in the central part of the samples with using serial silicon probes NSG-11 with a nominal radius of runding of the tip to 10 nm. According to the results of AFM investigations, except morphology of surface and profilohram in the program Gwyddion the sizes of nanocrystals are determined in the lateral direction and their height.

It has been shown that through the Folmer-Weber's engine on substrates of glass and glass ceramic, individual nanostructures principally column or pyramid shapes,which are located to the substrate normally are forming . The regularities in changing of the heights of nanostructures on the surface of condensates,the most likely heights for them and also the size of roughness and the lateral sizes on the temperature and time of vapor deposition on the substrates and temperatures of exhalation of sample .It is shown that the predominant is Wagner's mechanism of growth of nanostructures for the dominance of the formation of chemical bonding in the "vapor-condensate" system.

1. С.А. Медведев. *Физика и химия соединений $A^{II}B^{VI}$*. Мир, М. 624 с. (1970).
2. С.А. Колосов, Ю.В. Клевков, А.Ф. Плотников. Транспортные явления в крупнозернистых поликристаллах CdTe // *Физика и техника полупроводников,* 38(3), сс. 305-309(2004).
3. И.П. Калинкин, В.Б. Алесковский, А.В. Симашкевич. *Эпитаксиальные слои соединений $A^{II}B^{VI}$*. Изд-во ЛГУ, Л. (1978).
4. А.П. Беляев, В.П. Рубец, М.Ю. Нуждин, И.П. Калинкин. Механизми гетероєпитаксиального роста тонких пленок теллурида кадмия в тепловом поле градиента температуры // *Физика твердого тела*, **43**(4), сс. 745-748 (2001).

The work supported by an integrated project of MES of Ukraine (N 0113U000185) and by projects of FRSF State Agency for Innovation and Informatization of Ukraine. (Contracts: R54, F53, 3); NAS of Ukraine (N 0110U006281)

Optical and Sensing Properties of Planar Arrays of Silver Nanoparticles

Dmitruk N.L., Malynych S.Z.

V. Lashkarev Institute of Semiconductor Physics NAS Ukraine, Kyiv, Ukraine

Silver nanoparticles possess unique optical properties due to the excitation of collective oscillations of the electronic density by impinged electromagnetic radiation termed localized surface plasmon resonances (LSPR). LSPR frequency for silver nanoparticles occurs in the visible spectral range and can be tuned by varying particles' size and shape. This opens new perspectives of using Ag nanoparticles as building blocks for optical and optoelectronic devices.

In this work we present synthesis procedure of an aqueous suspension of silver nanoparticles as well as fabrication of planar arrays of nanoparticles. Single crystal, monodispersed Ag particles in the size range from 10 to 200 nm were synthesized using chemical reduction technique and self-assembled into planar 2D arrays. Prior to the self-assembly, the particles were characterized with a variety of techniques including measurements of the absorption and scattering cross sections. Scattering (extinction) spectra of isolated Ag nanoparticles can be calculated within a framework of Mie theory. The spectra comprised from broad bands associated with dipole and quadrupole LSPR modes. At the same time the arrays of Ag nanoparticles exhibit plasmon coupling characterized by the formation of an extremely sharp plasmon mode in the blue spectral range. The spectral width of this mode was at least one order of magnitude smaller than the resonance of the same but uncoupled particles. The studies revealed the coherent quadrupole nature of the coupling that takes place by means of the overlapping local fields associated with the electron oscillations in individual particles. The effect of the interparticle distance and dielectric medium on the plasmon coupling was studied for different polarizations and incidence angles of light beam. It is experimentally demonstrated that planar arrays of 100 nm Ag nanoparticles are extremely sensitive to the dielectric environment and can be used as refractive index sensors.

Electrical properties of silicon oxide films containing nanocrystals

A.A. Evtukh[1,2], A. Yu. Kizjak[1], Yu. M. Pedchenko[1], O.V. Steblova[2]

[1]*V. Lashkaryov Institute of Semiconductor Physics, Ukraine*
[2] *Institute of High Technology, Taras Shevchenko National University of Kyiv, , Kyiv, Ukraine*

Preparation and investigation of electrical properties of the films containing nanocrystals in a dielectric matrix are extensively studied for their applications in nanoelectronics and optoelectronics. A promising approach in this case is to obtain a structure with the required electrophysical parameters by self-organization.

The aim of this study was to investigate the electrical properties of thin nanocomposite films SiO_2(Si) containing silicon nanocrystals in a dielectric matrix of silicon dioxide and to determine the mechanisms of electrical conductivity of the films. The films under investigation were formed from silicon enriched SiOx films obtained by low pressure chemical vapor deposition (LP CVD) at T = 640 °C, followed by high-temperature annealing at T = 1100 °C to obtain nanocomposite SiO_2(Si)films. The film thickness (deposition time) and excess silicon content (ratio of working gas SiH_4/N_2O) were as variables. As a result, after the high-temperature annealing SiO_2(Si) film with the thickness in the range of 15 - 22 nm, and the refractive index 1,45-1,9 were obtained.

The electrophysical properties of nanocomposite SiO_2(Si) films were characterized by measurement of I-V characteristics at different temperatures (T=153-293 K) (Fig.1), as well as the high-frequency C-V characteristics. There is the significant difference in the value of the current through the nanocomposite films. Analysis of the data shows the unhomogeneous distribution of nanocrystals both in area and thickness of the film. The great influence of temperature on the electrical conductivity of SiO_2(Si) films has been shown, especially at low voltages (up to ~ 1 V). The main reason for this change in the electrical conductivity is a change of size and the concentration of silicon inclusions in SiO_2 matrix. Based on analysis of I-V and C-V characteristics the mechanisms of electrical conductivity in nanocomposite films, in which a significant role play the processes of tunneling through the dielectric layer between the nanocrystals and electron traps in the band gap of the dielectric.

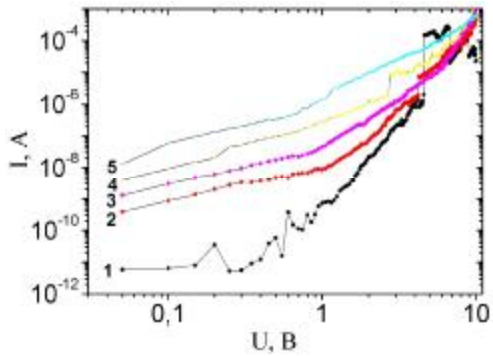

Fig.1. I-V characteristics of n-Si – SiO_2(Si) – Al structures with the temperature as a parameter: 1- T=(149 -153) K; 2- T=(198 - 199,2) K; 3- T=(229 -233) K; 4- T=277 K; 5- T=(320 -315) K, $d_{SiO2(Si)}$ = 22 нм.

Thermoelectric Composites with Nanoinclusion Based on Lead Telluride

Freik D.M.[1], Gorichok I.V.[1], Krynytskyi O.S.[2], Matkivskyi O.M.[1], Ralchenko V.H.[3]

[1]*Physico-Chemical Institute of Precarpathian National University named after V.Stefanyk, Ivano-Frankivsk, Ukraine*
[2]*Ivano-Frankivsk National Technical University of Oil and Gas, Ivano-Frankivsk, Ukraine*
[3]*Institute of General Physics named after A.M. Prokhorov, Moscow, Russian Federation*

A new stage in improving the value of dimensionless thermoelectric figure of merit ZT materials ($Z = S^2\sigma/\chi$) should be considered as an innovation associated with the formation nanoinclusion in composite structures. It was found that blocking fonon-electron conductivity at the interface nanoinclusion leads to a significant reduction in thermal conductivity (χ) and increase ZT, respectively[1]. For PbTe nanocomposites with combined nanoinclusion Ag and Sb and Pb and Sb is a filtration carriers that causes the growth of the Seebeck coefficient (S) and increases the value of ZT = 1.4 at (650-700) K compared with ZT = 0.8-1.0 for pure PbTe [2]. There is an interesting fact about the inclusion of PbTe PbS matrix without the formation of solid solutions can effectively reduced lattice thermal conductivity without significant effect on the electronic subsystem. The last thing ist that the interface grains PbS and PbTe crystal structure is completely ordered by introducing dislocations inconsistencies. This idea is widely used for the creation of nanocomposites type of PbTe-SnTe and other so-called layered structures in the system PbTe-Sb_2Te_3 that are similar to the superlattices. The distances between the superlattice that modifies it's fonon subsystem can be changed depending on the technological regime and in such a way it modifies it's phonon subsystem. Such structures obtained ZT = 1,5 at 650K.

We have shown that the most promising are the researches related to the modification of composites based on PbTe with nanoinclusion of refractory oxides TiO_2 and ZnO, and diamond and graphite nanopowders.

1. D.M. Freik, M.O. Galuschak, O.S Krynytcky New nanocomposite thermoelectric materials (review) // Physics and chemistry of solid state **14** (1) pp.300 -316 (2013).
2. Ma Y., Heijl R., Palmqvist A. E. C. Composite thermoelectric materials with embedded nanoparticles // J Mater Sci 48:2767–2778 (2013).

This work is performed under the Project DFFD State Agency of Science and Innovation Information of Ukraine (F54, F53.1).

Influence of Cobalt Acetylacetonate (3 +) and the Time of Formation the Films Based on it on the Structuring of Polyurethane Networks

Gagolkina Z.O., Lobko E.V., Kozak N.V., Gomza Y.P., Nesin S.D., Klepko V.V.

Institute of Macromolecular Chemistry NAS of Ukraine, Kyiv, Ukraine

The immobilization *in situ* of nanoscale metal complexes in polymer matrix, variation of the complex amount and selection of the formation time of the polymer allows create nanostructured systems with an expected range of properties [1].

Structure of the cross-linked polyurethanes (CPU) with 1 and 5% of cobalt acetylacetonate was investigated by wide-angle (WAXS) and small-angle (SAXS) X-ray scattering. Time of the film formation essentially depends on solvent amount.

It was shown (Fig. 1), that cobalt-containing CPUs are amorphous. The mean Bragg's period is of 0.44 nm. On the WAXS curves of the 5% cobalt-containing CPU crystalline maxima at 10 and 13 ^{o} were observed (Fig.1). This effect was caused by segregation of the metal complexes from CPU matrix [1,2]. The most intensive crystalline maxima were observed for the systems with longest formation time.

The presence of diffraction maxima on the SAXS curves (Fig. 2) indicates forming of the space-ordered structures with periodicity from 2.9 to 3.9 nm. It was indicated, that the heterogeneity of the modified systems increases comparing with CPU without modifier (CPU-0). In addition, the intensity of the maximum for the film with longer formation time decreased. The maxima positions for the CPU-Co shifted to higher values for samples with longer formation time. It was shown, that the periodicity of CPU with space-ordered structures lowered.

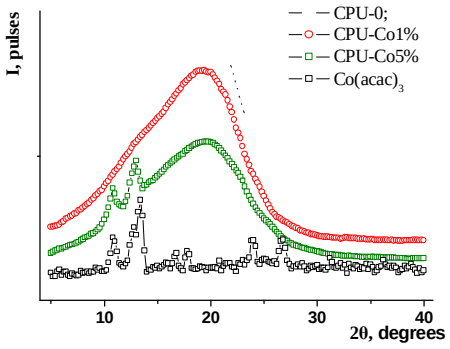

Fig. 1. The WAXS curves for CPU with various amount of $Co(acac)_3$.

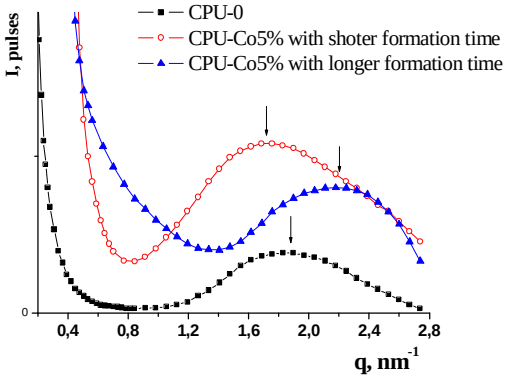

Fig. 2. The SAXS curves for CPU with various formation time.

1. Nizelskii Yu., Kozak N. In situ nanostructured polyurethanes with immobilized transition metal coordination complexes // Macromolecular Sci. Part B: Phys. 2006. V.46. - P.97-110.
2. The influence of cooper (2+) chelate compounds on the short-range order structure in polyurethanes / Lobko Eu. V., Gagolkina Z.O. Hubina A.V., Kozak N.V., Klepko V.V. // 12th Eurasia Conference on Chemical Sciences. 16-21 April 2012. Corfu, Greece. – S11-PP9.

Effect of Impurities on the Crystallization of Amorphous Calcium Phosphate with Different Ca/P Ratios

Goncharenko A., Rokhmistrov D., Zyman Z.

V.N. Karazin Kharkiv National University, Kharkiv, Ukraine;

Amorphous calcium phosphate (ACP) is known as a precursor in the crystallization of hydroxyapatite (HA), the main inorganic constituent of hard tissues [1]. However, recent studies have revealed that ACPs also occur at the early stage of precipitation of calcium phosphates with a Ca/P ratio differing from that of HA [2]. Besides, the crystallization temperature of a powder prepared of the ACPs and the phase composition formed as a result are highly influenced by the impurity state of the powder [3, 4]. Though ACP powders have progressively been used in bone cements and the nanoparticles of the powders are considered as a prospective agent in nanomedicine, there are little data on the effect of impurities on the crystallization, thermal behavior and phase composition in ACPs under various conditions, and the results are contradictory.

ACP powders with different Ca/P values were prepared by the nitrous synthesis [1]. Various initial proportions of the reactants resulted in different total Ca/P ratios in the ACPs. The synthesis temperature 5 ^{0}C, the reaction time was restricted to a few minutes. The separated precipitates were immediately filtered and then dried by lyophilization or in vacua after multiple washing.

All the powders were amorphous according to XRD-examination. However, they revealed very different thermal behavior. Powders with Ca/P=1 and 1.5 manifested an exothermic peak in DTA curve at about 670 ^{0}C. The intensity of the peak was inversely proportional to the Ca/P value. No peak was found for powders with Ca/P ratios of 1.67 and 2.1. Some by-products and remnants of the initial reactants were detected in the powders by TG and IR-examinations. The thermal behavior of the powders was associated with different amounts of these phases and the superimposition of the exothermic and endothermic reactions caused by the crystallization of the ACPs and thermal decomposition of the impurity phases. In case of an ACP powder free of any contaminating phase, a strong exothermic peak was present.

1. E.D. Eanes, I.H. Gillesen, A.S. Posner, Nature, 1965, 208, 365-367.
2. Y. Li, W. Weng, J. Mater. Med., 2007, 18, 2303-2308.
3. R.Z. Le Geros, D. Mijiares, J. Park, X.F. Chang, I. Kijkowska, R.Dias, J.P. Le Geros, Key Eng. Mater., 2005, 284-286, 7-10.
4. Y. Li, F. Kong, W. Weng, J. Biomed. Mater. Res. Part B: Appl. Biomat., 2009, 89B: 508-517.

Scanning Probe Microscopy Investigation of Bi Film Surfaces on Ge(111) Substrate

Goriachko A., Popova O., Sydorov R., Kulyk S., Melnik P., Nakhodkin M.

Department of Radiophysics, Taras Shevchenko National University of Kyiv
Kyiv, Ukraine

The surfaces of bismuth (Bi) are a model system to study the Rashba effect, namely the electron spin splitting in the absence of external magnetic field. Consequently, thin Bi films on top of semiconductor substrates are excellent candidates to study a phenomenon of spin-polarized current injection into the semiconductors.

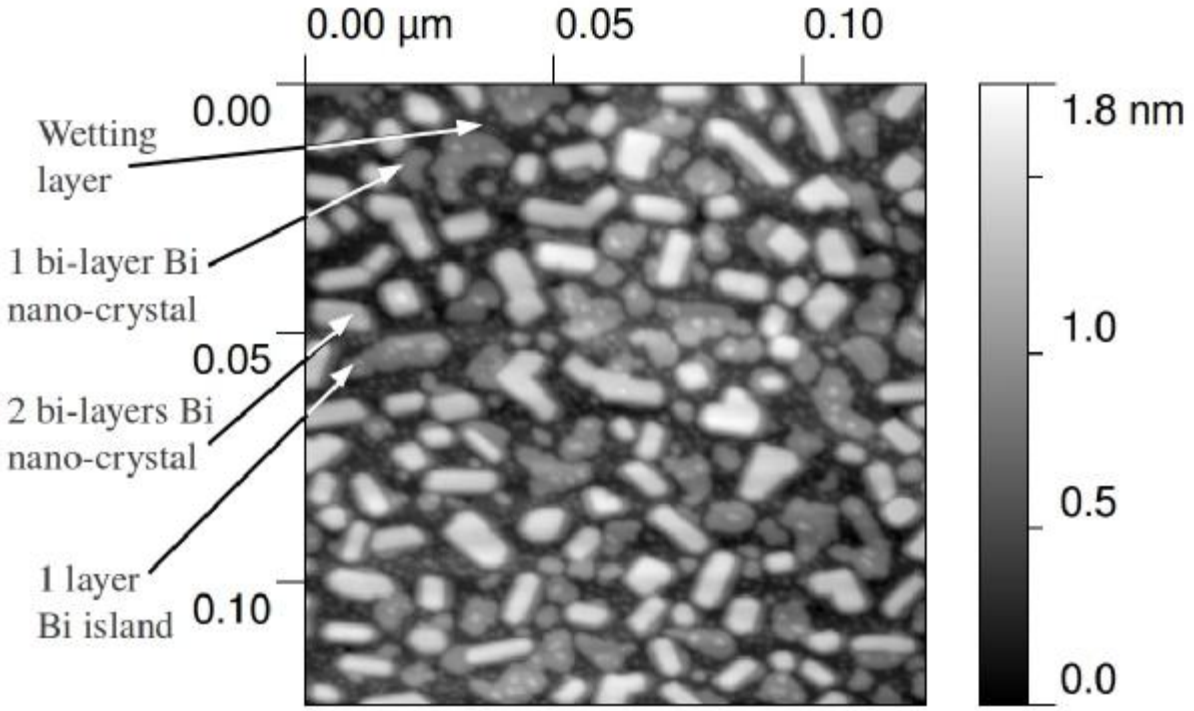

We have employed the scanning probe microscopy (SPM) techniques to study the growth of ultra-thin Bi films evaporated onto atomically clean Ge(111)-c(2×8) substrates at 300 K in ultra-high vacuum (UHV) environment. The following stages of Bi film growth were observed: initial wetting layer formation, isolated nanocrystals growth with atomically flat topmost surfaces, coalescence of nanocrystals and continuous film formation. The nanocrystals' thickness of 2 and 4 bismuth atomic layers and also their shapes are strongly indicative of a pseudo-cubic bismuth allotrope, similar to the one observed in the Bi/Si(111) system. Annealing the as-grown Bi films at 450 K in UHV causes thermally activated transport of the deposited material in the surface plane, resulting in formation of nanocrystals with increased lateral sizes. In conclusion, Bi films up to 15 atomic layers thickness were investigated with SPM.

On the Possibility of Using Powders of Variable Grain-Size Composition for Preparation of Thermoelectric Materials

Gorsky P.V.

Institute of Thermoelectricity of NASU and MESJSU, Chernivtsi, Ukraine

For the purpose of improving the thermoelectric figure of merit and efficiency of thermoelectric modules based on single crystals, the latter are doped with various impurities. But with the use of materials prepared by hot pressing, extrusion or SPS methods based on powders there appears another opportunity for control of the figure of merit and efficiency of thermoelectric modules. It consists in using size effects for figure of merit improvement of thermoelectric materials. This paper deals solely with classical size effects due to boundary scattering. By the example of *n*-type Bi_2Te_3 it is shown that in the approximation of constant mean free paths of charge carriers and phonons, transition from a single crystal to pressed, extruded or SPS-material based on powder yields no gain in thermoelectric figure of merit. However, in the temperature region relevant for thermoelectric applications predominant in thermoelectric material are N- and U-processes of phonon-phonon scattering, caused by the anharmonicity of lattice thermal vibrations, when the respective relaxation times are functions of frequency. These processes can modify phonon scattering on the boundaries. However, for electrons the approximation of mean free path constant with respect to energy is valid, since in the temperature region relevant for thermoelectric applications electron scattering on the deformation potential of acoustic phonons is predominant. Electron and phonon scattering on the boundaries of shape-forming elements is taken into account by method of summation of the inverse mean free paths. With account of frequency dependence of phonon mean free path it is demonstrated that for each temperature in the region of 75-600K there is the optimal radius spherical powder particle whereby the thermoelectric figure of merit of material is maximum. The respective dependences for *n*-type Bi_2Te_3 are depicted in Fig.1.

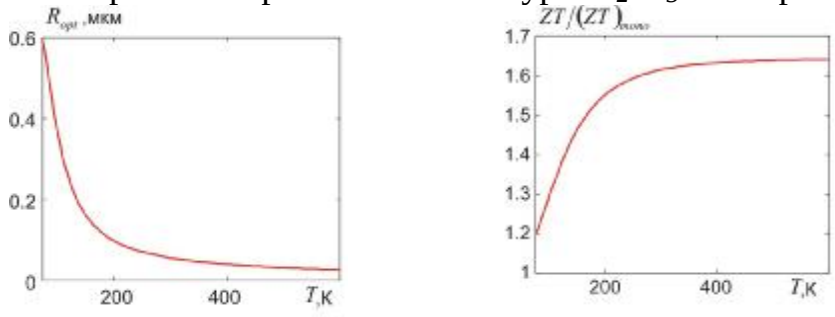

a) b)

Fig.1. Temperature dependences: a) of the optimal radius of spherical powder particle; b) of thermoelectric figure of merit of material with respect to single crystal

With a change in temperature from 75 to 600K, the optimal radius of spherical powder particle decreases from 0.574μm to 0.026μm, and maximum thermoelectric figure of merit with respect to single crystal increases from 1.2 to 1.65.

Au (Ag) Nanoparticle Arrays Produced by Pulsed Laser Deposition

Kaganovich E.B., Kravchenko S.A., Krishchenko I.M., Manoilov E.G.

V. Lashkaryov Institute of Semiconductor Physics, NAS of Ukraine, Kyiv, Ukraine

The aim of this work is to obtain porous gold (silver) films with developed PLD method [1, 2] for surface enhanced Raman spectroscopy . In our work PLD method from backward low-energy cluster flow was used. Glass and silicon substrates were located in the target plane. YAG:Nd^{3+} laser beam (wavelength 1.06 μm, pulse energy 0,2 J, pulse duration 10 ns, pulse frequency 25 Hz) scanned the target in a vacuum chamber with the argon pressure 10 to 100 Pa. The energy density for illumination of the target was varied from 5 up to 20 j/cm^2, the laser shot number – from 4500 up to 45000.

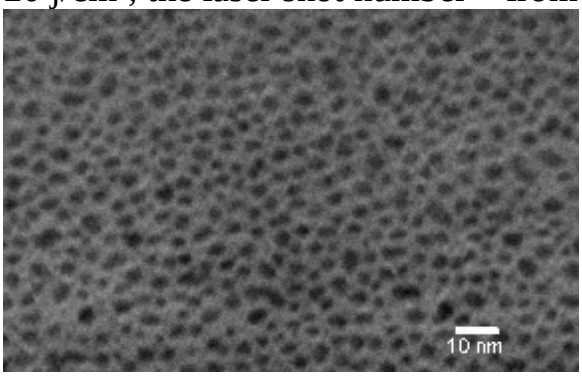

Fig.1 TEM image of por-Au film grown with 4500 laser pulses at 13,5 Pa of Ar.

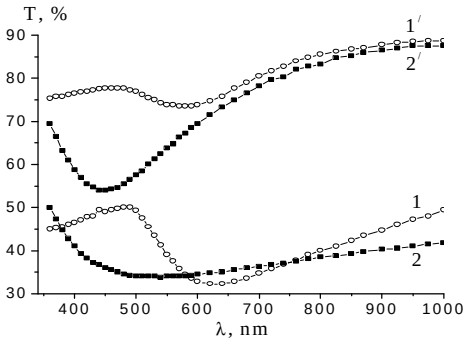

Fig.2 T(λ): 1, 1′ – por-Au, P_{Ar}=35 Pa; 2, 2′ – por-Ag, P_{Ar}=13,5 Pa. 1, 2 – l=5 mm, 1′, 2′ – l=15 mm.

The characterization of the surface morphologies of the deposited films with Au (Ag) nanoparticles (NPs) was done by AFM, SEM, TEM and by UV-visible spectroscopy. We studied the influence of formation condition on their structural and optical properties. Deposition from backward cluster flow leads to the formation porous films (Fig.1). The film morphology and NP spatial density, their size, form depend on Ar pressure, number of laser pulses, location point of the film on the substrate (l). Ascertained are the conditions of PLD method providing creation of porous films with Au (Ag) NPs arrays, in extinction spectra of which one can observe a resonance band related with local surface plasmons (Fig.2).

1. Manoilov E.G. Optical and photoluminescent properties of Ag/Al_2O_3 nanocomposite films obtained by pulsed laser deposition // SPQE&O – 2009. – V. 12, № 2. – P. 298-301.
2. Kaganovich E.B., Kizyak I.M., Kudryavtsev A.A., Manoilov E.G. Optical properties of gold nanostructures obtained with laser methods // ibid. – 2009. – V. 12, № 1. – P. 8-11.

Phase States of Spin-1 Ising-Like Antiferromagnetic With Strong Easy-Plane Single-Ion Anisotropy in an External Magnetic Field

Klevets Ph.N.[1, 2], Kosmachev O.A.[1], Fridman Yu.A.[1]

[1]*V.I. Vernadsky Taurida national university, Simferopol, Ukraine;*
[2]*Institut für Physik, Universität Augsburg, Augsburg, Germany*

Nowadays frustrated magnets attract considerable attention, related with the search for new quantum states. Generally, frustrated magnets are systems in which localized magnetic moments (or spins) interact via competing exchange interactions, giving rise to various types of degeneracy of the ground state. At certain circumstances, this can result in the formation of spin liquid states, or in the realization of the rather new quantum state – supersolid magnetic phase (it is also called the intermediate or biconical phase) [1-3].

We investigated the phases and phase transitions in two-sublattice S=1 antiferromagnet with Ising-like exchange interaction and strong easy-plane single-ion anisotropy in the external magnetic field perpendicular to the basal plane. Although Ising-like exchange interaction depends only on the S^z component of spin operator, the spin operator itself has all three components, $\mathbf{r}$ $\vec{S} = \left(S^x, S^y, S^z\right)$. We consider the low temperature case ($T << T_N$, T_N is the Neel temperature).

Carried out investigations shows that, depending on the value of the external magnetic field, three phases can realize in antiferromagnet with Ising-like exchange interaction and strong easy-plane single-ion anisotropy: the ferromagnetic phase, the supersolid phase, and the quadrupolar phase. It was shown [4] that the same phases realize in strongly anisotropic Heisenberg antiferromagnet; however, the antiferromagnet with Ising-like exchange interaction, considered in the present work, exhibits some peculiarities. We have obtained spectra in these phases and have analyzed the free-energy density which allowed us to determine the types of the phase transitions and to construct the phase diagram of the system.

1. L. Balents, Nature (London) 464 (2010) 199.
2. D. Peters, I.P. McCulloch, W. Selke, Phys. Rev. B 79 (2009) 132406.
3. Judit Romhányi, Frank Pollmann, and Karlo Penc, Phys. Rev. B 84 (2011) 184427.
4. Y.A. Fridman, O.A. Kosmachev and P.N. Klevets, Eur. Phys. J. B 81 (2011) 185.

Semibounded Metal in External Electric Field

Kostrobij P. P., Markovych B. M.

Lviv Polytechnic National University,
Department of Applied Mathematics,
S. Bandera str., 12, Lviv 79013, Ukraine

Due to the intensive experimental research of surface by scanning tunneling microscopy, scanning tunneling spectroscopy, field ion microscopy and their modifications [1,2] researching of electron density in semibounded metal in external electric field is actual. Density functional theory (DFT) is widely used for the theoretical study of these and many other problems of condensed matter physics. DFT allows sufficient accuracy to calculate the characteristics determined by the behavior of the electron density. The local density approximation (LDA) are commonly used for taking into account exchange-correlation effects. However, LDA is based on the results that were obtained for uniform electron gas. Theory with account of the many-body effects of semibounded metal is developed in [3-6].

Influence of external homogeneous electric field on the electronic subsystem semibounded metal is investigated. It was found that the applied field causes the change of the effective electron-electron interaction, even in the direction perpendicular to the field. Influence of external electric field on the electron density of semibounded metal is investigated.

1. Van de Leemput L. E. C, van Kempen H. Rep. Prog. Phys. –1992. –Vol.55. –P.1165.
2. Moriarty P. Repts. Prog. Phys. –2001. –Vol.64. –P.297.
3. Kostrobij P. P., Markovych B. M. Condens. Matter Phys. –2006. –Vol.9, No.4(48). –P.747–756.
4. Kostrobiy P. P., Markovych B. M., Suchorski Yu. Solid State Phenomena. – 2007. –Vol.128. –P.219.
5. Holst B., Piskur J., Kostrobiy P. P., Markovych B. M., Suchorski Yu. Ultramicroscopy. –2009. –Vol.109, N.5. –P.413.
6. Kostrobij P. P., Markovych B. M. Condens. Matter Phys. –2008. –Vol.11, N.4(56). –P.641.

Researches of Nanostructured Porous Silicon Passivation Properties

Kostylyov V.P.[1], SachenkoA.V.[1], Serba O.A.[1],
Slusar T.V.[1], Chernenko V.V.[1]

*[1]V.E. Lashkarev Institute of Semiconductor Physics,
Nat. Acad. of Sci. of Ukraine Kyiv, Ukraine*

In order to reduce the recombination and optical losses in silicon solar cells special passivation layers are applied on their front surface. These layers reduce the effective surface recombination velocity S_{ef} and the light reflection coefficient. In the work the passivation properties of microporous silicon films were experimentally investigated. The porous films were formed on the front surface of back-contact back-junction silicon solar cells also called interdigitated back contact (IBC) using alcohol solutions of hydrofluoric acid. IBC experimental samples were manufactured on *n*-type float-zone silicon wafers with resistivity of 2 Ω·cm. Initially the front surface of the samples was protected and passivated by a thermal SiO_2 layer with thickness of 110 nm.

The illuminated current-voltage characteristics at standard test conditions AM1,5 and photocurrent spectral dependencies at constant monochromatic power mode in the wavelength range 400...1200 nm were measured on the IBC experimental samples. The effective thickness and refractive index of formed porous layer were determined by ellipsometry.

It was experimentally shown that the effective surface recombination velocity S_{ef} on silicon surface coated with thermal SiO_2 film is high enough and this causing significant recombination loss of light generated electron-hole pairs. Removing SiO_2 film in an aqueous HF solution does not affect significantly on the value of S_{ef}, although the short-circuit current I_{sc} of IBC solar cells decreases by increasing the light reflection coefficient.

Formation of microporous silicon films on the front surface of IBC solar cells results in surface recombination velocity decreasing due to the surface recombination-active centers neutralization by hydrogen atoms released during the electrochemical reaction. The neutralization effect becomes more pronounced with increasing of micropores depth, reducing their diameter, as well as reducing the time interval between the electrochemical formation process and photoelectric measurements. On the other hand, on the IBC surface with microporous silicon film the depletion layer with reduced majority carrier's concentration is formed, where in case of small radiation powers the recombination velocity is significantly increased. Increasing of the light intensity leads to the recombination velocity in space charge region decreases and to the corresponding I_{sc} increasing. Thus, applying the nanoporous silicon films as passivation layers can only be effective for IBC solar cells operating at medium and high irradiation levels.

Photoelectrochemical Properties of Electrodeposited Nanocrystalline ZnO Films Sensitized with $Cd_xZn_{1-x}S$ Nanoparticles

Kozytskiy A.V., Stroyuk O.L., Kuchmiy S.Ya.

Institute of Physical Chemistry of National Academy of Sciences of Ukraine, Kiev, Ukraine

Nanocrystalline zinc oxide films composed of porous ZnO micro-platelets 1–3 μm in size and 100–200 nm in thickness formed by loosely aggregated 30–50-nm crystallites were electrodeposited onto ITO substrates. The ITO/ZnO films were sensitized to visible light via deposition of $Cd_xZn_{1-x}S$ nanocrystals using the SILAR method. Fig. 1a shows typical SEM image of an ITO/ZnO/CdS film.

Photovoltage observed at illumination of the ITO/ZnO/$Cd_xZn_{1-x}S$ films by white light ($\lambda > 400$ nm) in aqueous Na_2S solutions increases at a decrease in the molar Cd (II) fraction *x* proportionally to an increase of the conduction band potential of $Cd_xZn_{1-x}S$ nanocrystals. The maximal photovoltage increment achieved in the systems studied at a decrease of *x* from 1,0 to 0,62–0,67 (280 mV) is close to the increment of the conduction band potential of $Cd_xZn_{1-x}S$ nanocrystals (220 mV) caused by the increase of molar Zn (II) fraction. The photocurrent density generated by the ITO/ZnO/$Cd_xZn_{1-x}S$ films at illumination with white light increases by a factor or around 4 at a decrease of *x* from 1,0 to 0,62–0,67 and corresponding augmentation of the conduction band potential of $Cd_xZn_{1-x}S$ nanocrystals (Fig. 1b). Dependence between the photocurrent density normalized to the light absorbance of the sensitizer and an increment of the conduction band potential caused by the decrease of *x* obeys the Tafel equation.

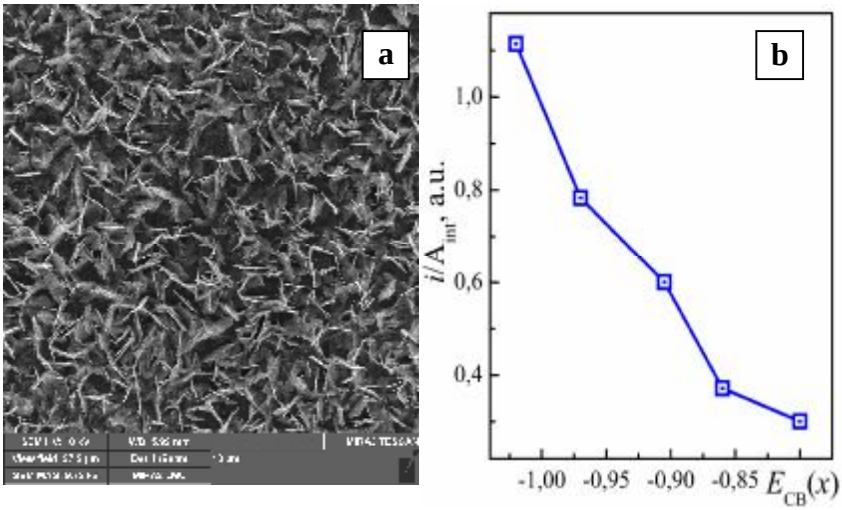

Fig. 1. (a) Scanning electron microphotograph of an ITO/ZnO/CdS film. (b) Photocurrent density *i* normalized to the integrated absorbance A_{int} of ITO/ZnO/$Cd_xZn_{1-x}S$ films as a function of the conduction band potential $E_{CB}(x)$ of $Cd_xZn_{1-x}S$ nanocrystals.

Methods of Forming Nanocomposite's Thermoelectric Materials

Krynytsky O.S.

Ivano-Frankivsk National Technical University Oil and Gas

For nanocomposites, thermoelectric nanoparticles usually first prepared and then compacted in three-dimensional solids. The most common methods of obtaining thermoelectric nanoparticles are: ball millg, mechanical abrasion, hydrothermal synthesis, sol-gel synthesis, electrochemical deposition, condensation in the inert gas, sonochemical synthesis, chemical vapor deposition, and their compaction - cold pressing, hot pressing, spark-plasma sintering [1].

In particular, ball mills are effective for large quantities of thermoelectric nanoparticles from one to several micrometers from ingots in a short time. It is important that the thermoelectric nanoparticles compounds can also be obtained by this method directly from the individual elements. For example, crystalline nano powder Bi_2Te_3 can be directly synthesized from the elements Bi and Te through mechanical alloying. In hydrothermal method by dissolving in a suitable solvent inorganic precursors at elevated temperatures produced pressure in an autoclave, followed by crystallization of dissolved substances in the form of individual nanostructures. The essence of the chemical vapor deposition (CVD) is the end product formed on the substrate target (located in the most heated zone), resulting from the interaction of gaseous precursors in a hot area or thermolysis vapor precursor.

What pertains compaction nanostructures, it should be noted promising methods of hot pressing and spark plasma sintering, by which are well sealed Composites with a total value of thermoelectric figure of merit (ZT = 1,2).

1. D.M. Freik, M.O. Galuschak, O.S Krynytcky New nanocomposite thermoelectric materials (review) // Physics and chemistry of solid state **14** (1), pp.300 -316 (2013).

The work supported by projects of FRSF State Agency for Innovation and Informatization of Ukraine. (Contracts: R54, F53, 3); NAS of Ukraine (N 0110U006281)

Controlled Synthesis of Silver Nanoparticles in Aqueous Solution

Kytsya A. R., Bazylyak L. I., Hrynda Yu. M., Medvedevskikh Yu. G.

Physical Chemistry of Combustible Minerals Department
Institute of Physical-Organic Chemistry & Coal Chemistry named after L. M. Lytvynenko
National Academy of Sciences of Ukraine, Lviv, Ukraine

In spite of the fact that the properties of silver nanoparticles and also the conditions and methods of their obtaining are sufficiently well described in references [1], however the research of their kinetics of synthesis has enough episodical character [2]. In particular, the stages of the silver nanoparticles nuclear centers formation and their growing are not described, and also the influence of kinetic factors on the form and the size of obtained nanoclusters is not investigated. That is why the aim of this work was to study the influence of the synthesis conditions on kinetic parameters of a process, and also on the form and the size of obtained silver nanoparticles.

Silver nanoparticles have been obtained via reaction of the silver nitrate reduction with hydrazine in alkaline medium in the presence of the sodium citrate. The kinetic regularities of reaction depending on the initial concentrations of the reagents and temperature have been studied with the use of the potentiometry method. The reaction orders for every reagent, the effective constants rate of new phase nucleation and its growing and also their activation parameters were determined.

In order to identify the obtained silver nanoparticles it were investigated the optical properties of their aqueous sols. The all electronic spectra are characterized by single maximum that is definitely evidence of the spherical form of the nanoparticles [**1**]. On the basis of a wave length into the adsorption maximum of the superficial plasmous resonance it were calculated the values of their average diameter *d* [**3**]. Under analysis of the experimental data it was determined that the values of the average diameter of the obtained silver nanoparticles is a function on the new phase nucleation rate (W_0) and new phase growing (W_{max}) $d = f(W_0/W_{max})$. Such dependence, and also the all set of the obtained kinetic data permits to obtain the nanoparticles with given and defined form and sizes.

1. Krutyakov Yu. A., Kudrinsky A. A., Olenin A. Yu., Lisichkin G. V. Synthesis and properties of silver nanoparticles: advances and perspectives // *«Uspiekhi khimiji»*. – 2008. –т. 77. – № 3. – p. p. 242–269 *(in Russian).*
2. Chou K. S, Lu Yu. Ch., Lee H. H. Effect of alkaline ion on the mechanism and kinetics of chemical reduction of silver // *«Materials Chemistry and Physics»*. – 2005. – v. 94. – p. p. 429–433.
3. David D., Evanoff Jr., Chumanov G. Synthesis and Optical Properties of Silver Nanoparticles and Arrays // «Chem. Phys. Chem.». – 2005. – v. 6. – p. p. 1221–1231.

Peculiarities of Interaction of Nanostructured and Fine-Grained Modifiers with Aluminum Alloys

Levchenko J., Verkhovluk A., Bezpaly A., Zheleznyak O.

Phisico-Technological Institute of Metals and Alloys National Academy of Science of Ukraine, Kyiv, Ukraine

Aluminum alloys castings are widely used in different branches of industry. It is very important task to develop the new methods of production of high-quality metal castings. It is known, that a refinement of castings structure affects positively on the mechanical characteristics of cast and deformed alloys.

For improvement of cast metal quality the modern development of science and technologies proposes new special modifiers on the basis of nanostructured and fine-grained metallic materials. After insertion of such type modifiers into a liquid metal, ones distribute uniformly in the volume of metal and act as heterogeneous nucleus of crystallization.

One of the conditions of modifiers production in nanostructured and fine-grained state is a uniformity of output liquid metal. In the course of modifiers preparation there are some difficulties for the choice of refractory material for a melting crucible. These difficulties come from the using of chemically active elements which are used in the modifiers alloys. In this connection we investigated the interphase interaction in the systems of refractory material and melt alloys (47% Al – 40% Cu – 13% Zr and 47% Al – 40% Cu – 10% Zr – 3% Ni).

Investigations were conducted by the method of lying drop in the temperatures interval from 1333 K to 1523 K in vacuum ($P = 1{,}0 \cdot 10^{-2}$ Pa). The electrode graphite, fine-grained graphite, fine-grained dense graphite, black lead and alundum were used as the materials for substrates. Experiments showed that the contact angle of wetting had value less than 90 degree for all systems at temperature of 1453 K (and this is the beginning of interaction in this system). Exception is the system of molten alloy 47% Al – 40% Cu – 13% Zr and fine-grained dense graphite, where the contact angle of wetting is higher than 90 degree and equal to 140 degree. Fine-grained dense graphite substrates become wetted at temperature about 1500 K.

Same results were obtained during investigation of interphase interaction in the system of molten alloy 47% Al – 40% Cu – 10 % Zr – 3% Ni and alundum. Molten alloy begins to spread about the surface of alundum substrate at temperatures higher than 1453 K. Obtained data allowed to select the refractory materials for melting crucibles. The selected refractory materials are inert towards the molten alloys in the specified temperature regimes of melting.

On development of modification technology of different alloys it is necessary to have information about the interaction of modification additives with molten alloys. It is known that such type modifiers present itself the binary

or multicomponent systems, therefore its dissolution in molten metal can be described as a process of interaction of separate components with melt. Because the process of interaction occurs at the interphase boundary it is necessary to take into account the role of surface properties, especially liquid phase and diffusive layer.

Modifiers obtained from a fine-grained powder by a pressing method have high porosity and nonuniformity of macro- and microstructure and so it distributed on separate elements in the volume of metal on dissolution in melt.

In this connection we investigated the kinetics of dissolution of the fine-grained modifiers of different systems Al – 2,5 % Zr and Al – 40 %Cu – 10 % Zr – 3% Ni and its separate elements (Zr, Cu, Ti) in melts on the basis of aluminium of B95. The chemical composition of B95 in % mass is Zn – 5,98; Mg – 2,42; Cu – 1,80; Si – 0,40; Mn – 0,36; Fe – 0,33; Cr – 0,15; Ti – 0,10.

Experiments were conducted by the method of rotating disk with an equally accessible surface in the atmosphere of inert gas at temperature of 1073 K and speed of disk rotation 600 rpm. Pure zirconium, copper and titanium cylindrical specimens 10 mm in diameter were machined on a lathe. Complex modifiers were casted in graphite shells.

Specific speed of dissolution of pure Cu, Zr and Ti equals to 18,60 $kg/m^2 \cdot s$, 0,17 $kg/m^2 \cdot s$ and 0,10 $kg/m^2 \cdot s$, respectively. Specific speed of dissolution of alloys (Al – 2,5 % Zr) and (Al – 2,5 % Zr and Al – 40 %Cu – 10 % Zr – 3% Ni) is 17,27 $kg/m^2 \cdot s$ and 13,80 $kg/m^2 \cdot s$, respectively. Thus the specific speeds of dissolution of alloy systems of Al – Zr and Al – Cu – Zr – Ni near to one of pure copper, that is during 10 seconds solid alloys transfer to the liquid state.

Thus, obtained results of interphase interaction of the molten alloy systems 47% Al – 40% Cu – 13% Zr and 47% Al – 40% Cu – 10% Zr – 3% Ni with the refractories allowed to choose materials and adjust the temperature regimes of melting and modifiers preparation. Kinetics data of dissolution allowed defining the conditions of modification process.

Gas-Dynamical Stream of Steam for Reception of Cd, Pb, and Zn Sulphides

Lopyanko M.A., Nykyruy R.I., Seniv M.S.

Vasyl Stefanyk Precarpathian National University, Ivano-Frankivsk, Ukraine

The vacuum vapor deposition methods are most widely used for reception of the films of II-VI and IV-VI compounds [1,2]. The special attention have a methods with the possibility of predictable properties. This perspectives opens the method of gas-dynamic stream of steam. Therefore, a study of this method of synthesis and study the deposition mechanisms of PbS, CdS and ZnS nanocrystalline films has scientific and applied interest.

It is shown that with increasing of dimensionless coordinates ξ re-evaporation contribution decreases rapidly and at $\xi \geq 0.6$ the condensation coefficient is close to 1. The gas-dynamic stream of steam parameters depend primarily due temperature evaporation T_e, temperature gradient along the walls dT/dx, and define locations substrate coupling ξ. On the section $\xi = 0$ there is no condensation (condensation coefficient $\alpha = 0$). The sharp growth rate of condensation ($0 \leq \alpha \leq 0.9$) is at $0 \leq \xi \leq 0.3$ for CdS and PbS and at $0 \leq \xi \leq 0.4$ for ZnS.

It is shown, that the length of the substrate coupling x_{cr} where no condensate layer increases as the temperature evaporation T_S increases and temperature gradient dT/dx decreasing. Reducing the absolute value of the gradient contributes to a sharp rise x_{cr} than increasing of evaporation temperature.

Optimal physical and chemical conditions of films growth meet low values of the degree of supersaturation of the vapor phase ψ and significant speed of condensation ω^* in heavy re-evaporation. For lead sulfide these requirements are best satisfied the change interval dimensionless coordinates $0.18 \leq \xi \leq 0.25$. For temperature gradient dT/dx = 30 K/cm the distance from the evaporator, which corresponds to the most improved deposition layers on substrates is x 1.6 cm. Similarly, for cadmium sulfide, these values are: $0.22 \leq \xi \leq 0.35$ and 2.0 cm, and for zinc sulfide, these values are: $0.11 \leq \xi \leq 0.14$ and 1.1 cm, respectively.

1. Zhengbang Pi, Xiaolu Su, Chao Yang, Xike Tian, Fang Pei, Suxin Zhang, Jianhua Zheng. Chemical vapor deposition synthesis and photoluminescence properties of ZnS hollow microspheres // Materials Research Bulletin – 2008. - Vol. 43. - P. 1966–1970.
2. Bubnov Y.Z., Lurje M.S., Staros F.G., Filaretov G.A. Vacuum deposition of films in quasi-closed volume. L. (1975).

The work supported by projects of FRSF State Agency for Innovation and Informatization of Ukraine. (Contracts: R54, F53, 3) and NAS of Ukraine (N 0110U006281).

Influence of Deposition Conditions and Thermal Treatment on Phase Formation in Nanoscaled $CoSb_x$(30 nm) (2<x<4.5) Films

Makogon Iu.M.[1], Pavlova O.P.[1], Sidorenko S.I.[1], Shkarban R.A.[1], Figurna O.V., Csik A.[2], Beke D.L.[2], Beddies G.[3], Daniel M.[3], Albrecht M.[3]

[1] *Kyiv Polytechnic Institute, National Technical University of Ukraine, Kyiv, Ukraine;*
[2] *University of Debrecen, Department of Solid State Physics, Debrecen, Hungary;*
[3] *Institute of Physics, Chemnitz University of Technology, Chemnitz, Germany*

$CoSb_3$-based skutterudites are perspective materials for application as thermoelectric materials due to electrical properties [1]. It was investigated the influence of deposition conditions and annealing in vacuum on phase formation processes in $CoSb_X$(30 nm) (2<x<4,5) films obtained by method of molecular-beam epitaxy in ultra high vacuum of ~10^{-8}Pa on SiO_2(100 nm)/Si(001) substrates at temperatures of 20°C and 200°C. Heat treatment was carried out in vacuum of $1.3 \cdot 10^{-3}$Pa in temperature range of (400-700)°C for 30 s, 30 min, 1 h, 1.5 h and 2 h.

It was established that in $CoSb_x$ (2.4<x<4.07) films deposited on substrate at room temperature is observed x-ray amorphous state. Crystallization of amorphous films occurs during heating in temperature range of (140-200)°C. At increase in substrate temperature to 200°C in $CoSb_x$ (2<x<4.5) films at deposition it is formed polycrystalline state without texture. With increase in Sb content the formation of phase composition occurs along the same lines sequence as it is shown on phase diagram for Co-Sb system bulk.

Thermal stability of crystalline $CoSb_{4.16}$ film preserves at thermal treatment to 400°C. At temperature higher (450-500)°C it is occurred sublimation of Sb that is reflected in change of phase composition: amount of $CoSb_2$ phase increases and amount of $CoSb_3$ phase decreases due to chemical reactions: $CoSb_2 \xrightarrow{600^\circ C} Sb\uparrow + CoSb$, $CoSb_3 \xrightarrow{600^\circ C} Sb\uparrow + CoSb_2$.

In x-ray amorphous films contained more 75 at.% Sb it isn't observed crystalline Sb phase and Sb evaporation occurs more intensively.

1. G.A. Slack, in CRC Handbook of Thermoelectrics, edited by D.M. Rowe (CRC, Boca Ration, 1995), p. 407.

Flicker-Noise Spectroscopy as a Monitoring Instrument of Defect-Impurity Engineering

Makoviychuk M.I.

Yaroslavl Branch of the Institute of Physics and Technology of RAS, Yaroslavl, Russia

The method of flicker-noise noise spectroscopy of structure-disordered semiconductors finds more and more broad application both in physical researches and in the analysis of different processes of micro- and nanotechnology. The practical realization of this method as a monitoring instrument of defect-impurity engineering for to solve the technological problems of silicon electronics are presented and discussed.

In presented activity the experimental results on analysis of flicker noise processes in disordered semiconductors on an example of designed production process of flicker noise gas sensor of a new generation are classified.

Studies concerned with the design of new approach for gas sensors based on ion-implanted silicon structures are analyzed. The influence of adsorbed molecules on the electronic state, electrical conductivity and flicker noise of the surface and inner interfaces in disordered silicon structures are discussed. The sensor properties of disordered silicon structures in the detection of various adsorbed molecules are described.

The special role of defect-impurity flicker-noise spectroscopy (DIFNS) - in its application for information express-analysis of defect - impurity interaction at implementation of methods of defect - impurity engineering, namely methods of depressing of formation of residual disturbance, decrease of diffusion coefficients of impurity in ion-implanted silicon and gettering of metallic impurities.

The application DIFNS of silicon structures as the diagnostic tool of microtechnology is demonstrated at design of flicker - noise gas sensors of new generations tendered as the constituent of microanalytical systems [1]

The tendered method adsorption–desorption flicker-noise spectroscopy (ADFNS) will use process of an adsorption and desorption of adsorbed particles from surface of the semiconductor for realization of the full electrophysical analysis of connection an adsorbate - adsorbent. Thus it is possible to receive also information about composition of a surface.

ADFNS - highly sensitive method of testing of surface phenomena in gas sensitivity semiconducting structures. The relation of flickers-noise performances to a structure of a gas phase can be utilized for essential sensitization both selectivity of detecting of gases and steams [1].

1. Makoviychuk M.I., Chapkevich A.L., Chapkevich A.A., Vinokurov V.A. Flicker-noise gas sensor. // Biomedical Engineering. - 2009. - V 43, No 3. - P. 109-113.

Nano-Silicon Thin Films Producing by Thermal Spray in a Vacuum.

Neimash V.[1], Shepelyaviy P.[2], Yuhymchuk V.[2], Popov V.[3], Makara V.[4]

[1]*Institute of Physics NAN of Ukraine, Kyiv. Ukraine.*
[2]*Institute of Semiconductors Physics NAN of Ukraine, Kyiv. Ukraine.*
[3]*Institute of Micro-devices NAN of Ukraine, Kyiv. Ukraine.*
[4]*Shevchenko National University, Kyiv. Ukraine.*

Nanocrystalline silicon thin films are one of the most promising materials for photovoltaic solar energy. This work is devoted to developing a method for fast and cheap production of films of nano-silicon on doping an amorphous Si by IV-grupe elements C, Sn and Pb. This work is dedicated to the development of methods for the rapid and low-cost production of nano-silicon films by use C, Sn and Pb doping of amorphous silicon alloy.

A method of producing thin films of amorphous and amorphous-crystalline alloy Si-C-Sn and Si-C-Pb based on the thermal spray of powders in a vacuum have representing. Several experimental series of films with thickness 200-600 nm make. The influence of technology conditions and composition of the alloy on the films microstructure have been investigated by Auger and Raman spectroscopy, X-ray fluorescence analysis and electron microscopy. The method of generating photocurrent in Schottky barrier based on these films was used for study of photosensitivity, as well as means of electron microscopy in the mode of induced current - for study of charge carriers diffusion length.

The main result is the creation of a new silicon nanocomposite material that consists of crystal size of 3-6 nm in amorphous matrix. Its recombination and photovoltaic parameters is in some times better then amorphous silicon. This is made possible through the study and use of influence of impurities C, Sn and Pb on the processes of silicon transformation from amorphous to crystal state during the alloy film formation. It is shown that the impurity Sn and Pb can serve as embryos for silicon crystallization and as factor of restricting the size of crystallites. The increasing of Sn and Pb solubility in amorphous Si as result carbon doping is found. Raman peak amplitude in the range 515-520 cm^{-1} correlates with an impurity content of tin and lead in alloy. Electron microscopic pictures of tin clusters surrounded by silicon crystals on the background of the amorphous matrix demonstrated.

The possibility of producing amorphous-crystalline silicon nanocomposite as a film with structured in scale 100 nm relief surface demonstrated. The prospect of using the created material for solar cell production analyzed.

Optical Characteristics of Nonsplit Narrowband Frustrated Total Internal Reflection Filter

Ovcharenko A. P.[1], Bilozertseva V. I.[2], Gaman D .A.[2], Guseynova I. Ya.[1], Fin'ko A. Yu.[1]

[1]V.N. Karazin Kharkiv National University, Kharkiv, Ukraine
[2]National Technical University "Kharkiv Polytechnic Institute", Kharkiv, Ukraine

Completely non-absorbing films in their place would give pass bands with 100% transmission. At the same time the film would need to be highly reflecting to obtain narrow half width. Frustrated total reflection (FTR) films satisfy these requirements. Frustrated total reflection occurs at a low index film imbedded in a high index material and inclined so that the angle of incidence exceeds the critical. If the film is very thick, total reflection occurs. But as the film becomes thinner, the reflection is no longer total, it becomes "frustrated" so to speak, and some light "leaks" through the film. Any reflectance to transmittance ratio can be obtained by adjusting the film thickness. Since the FTR film is made of non-absorbing material, no light energy is lost in the process.

An all-transparent symmetric three-layer structure, which consists of a high-index center layer coated on both sides by a low-index film (FTR layer) and embedded in a high-index prism, can function as an efficient narrowband interference filter under conditions of frustrated total internal reflection over a wide range of incidence angles [1].

The thickness of the middle spacer film controls the wavelength position of the pass band. When the total phase angle between multiple reflections is a whole multiple of 2π a pass band occurs. The phase angle results from the effective optical thickness of the spacer for the angle of incidence used, plus the phase retardation of the FTR films. As the s-component is retarded more than the p-component, the pass bands of FTR interference filters are doublets. Each component of the doublet transmits only linearly polarized light, the directions of polarization in the two components being at right angles to each other. The half widths of FTR filters may be decreased by going to higher order spacers or by increasing the thickness of the FTR layer.

In this paper the five-layer narrowband FTR filter having identical positions of s- and p- component pass bands have been considered. It was shown, that such filter properties are achieved by a special selection of middle FTR layer thickness.

1. Turner A. F. Some current developments in multilayer optical films // Le Journal De Physique Et Le Radium. – 1950. – V. 11, № 7. – P. 444-460.

Control of an Energy Spectrum of Charge Carriers in Stressed Heterosystems by Means of Nanocluster

Peleshchak R.M., Kuzyk O.V., Dan'kiv O.O., Uhryn Y.O., Shuptar D.D.

Drohobych Ivan Franko State Pedagogical University, Drohobych, Ukraine

The interaction between point defects and the self-consistent deformation field, which can arise owing to the very existence of those defects and to the crystal system inhomogeneity (e.g., a heterointerfase), gives rise to a spatial redistribution of defects and, under certain conditions, results in the formation of self-organized defect-deformation structures.

A non-uniform deformation induced in heterostructures by defect clusters owing to the self-consistent electron-deformation coupling results in a local change of the energy gap width and. accordingly, in a variation of the charge-carrier potential energy. In this work, the regularities in the reconstruction of localized electron levels in three-layer heterosystems under the influence of a deformation induced by the presence of a point-defect cluster in a quantum well are established. The electron-deformation interaction distorts the potential well, and the latter acquires a complicated shape with an additional dip (barrier) induced by the point defect cluster, in a vicinity of which a non-uniform tensile (compressive) deformation arises. The potential well with such a profile is used in resonant-tunneling diodes. The current-voltage characteristics (CVC) of such a resonant-tunneling diode are more contrast, i.e. the ratio between the maximum and minimum current values is higher, than the corresponding characteristics of a resonant-tunneling diode with a simple well.

We have derived the equations, which allow the energy spectrum of election in a three-layer heterostructure containing a cluster of point defects in a quantum well to be calculated.

The dependence of the difference between the electron energies in the first excited and ground states on the average point defect concentration is studied for various values of effective electron mass in the nanocluster material. The examined difference was shown to be larger than the corresponding value in the structure free of the defect cluster, if the effective mass of the electron in the nanocluster is less than that in the quantum well.

The difference between the electron energies in the first excited and ground states *DE* is important parameter for CVCs of resonant-tunneling diodes. Namely, the quantity *DE* determines the current magnitude at the CVC minimum. The increase of *DE* leads to a reduction of the minimum current magnitude and, accordingly, to the growth of the CVC contrast for resonant-tunneling structures.

Formation of Three-Dimensional Zinc Oxide Nanosystems by Low-Temperature Zinc Oxidation

Perekrestov V.I., Kornyushchenko A.S., Latyshev V.M.

Sumy State University, Sumy, Ukraine

ZnO is one of the most promising materials for applications in UV emitters, detectors, solar cells, piezoelectric transducers, transparent electronics, gas sensors etc. Therefore, development of technology that allows formation of porous ZnO nanostructures is of great interest nowadays. To obtain highly porous metal structures we have developed novel technological approach basing on deposition of ion-sputtered substance onto negatively based substrates in vicinity to thermodynamical equilibrium in plasma-condensate system [1]. On the example of Ni, Al, Cu, Cr, Ti it has been shown that above conditions provide effective formation of metal three-dimensional nanosystems [2].

In this work two-stage technology of porous ZnO formation is proposed. On the first stage highly porous Zn nanostructures with different morphologies have been obtained using quasi-equilibrium condensation in plasma-condensate system. It should be noted that structural and morphological conditions of the condensates are easily controlled by varying such technological parameters of the experiment as working gas pressure and power of discharge. On the second stage Zn samples were oxidized during one hour in 99,9% pure oxygen atmosphere under pressure 800 mbar and at temperatures 200, 350 and 400^0 C. The results of SEM and X-ray diffraction investigations have shown that the most effective mode of oxidation corresponds to temperature 350^0 C, because in this case the full transformation of Zn into ZnO occurs without changes in the condensates morphology.

The photoluminescence properties of ZnO nanostructures have been investigated in the work. The spectra obtained have narrow pick in UV spectrum range and broad green pick. The spectra analysis has shown that optical properties of the nanostructures depend both on ZnO morphology and oxidation temperature. In the case of oxidation at 350^0 C the maximum of luminescence intensity corresponds to UV range. Oxidation at 400^0 C leads to decrease in UV pick intensity, and green pick become dominant. For some morphologies UV pick completely disappears. Thus, proposed technological approach allows formation of highly porous ZnO nanostructures with different morphologies and physical properties.

1. Perekrestov V.I., Olemskoi A.I., Kosminska Yu.O. , Mokrenko A.A. Self-organization of quasi-equilibrium steady-state condensation in accumulative ion-plasma devices // Physics Letters A. – 2009. – V. 373, N7. – P. 3386-3391.
2. Perekrestov V.I., Kosminska Yu.O., Mokrenko A.A., Kononenko I.N., Kornyushchenko A.S. Structure formation mechanisms of low-dimensional porous titanium systems condensed under quasi-equilibrium steady-state conditions// Vacuum. – 2011. – V. 86, N1. – P. 111-118.

Photo- and Electroluminescent Properties of Ultra-Small CdS Quantum Dots Stabilized With N_2H_4 and Mercaptoacetic Acid

Rayevska O.Ye., Solonenko D.I., Grodzyuk G.Ya., Stroyuk O.L., Kuchmiy S.Ya.

L.V. Pysarzhevsky Institute of Physical Chemistry of National Academy of Sciences of Ukraine Kiev, Ukraine,

A new method of producing ultrasmall colloidal CdS nanoparticles (quantum dots, QDs) in water by using a combination of hydrazine and mercaptoacetic acid (MAA) is introduced. The N_2H_4/MAA-stabilized CdS QDs exhibit a sharp absorption peak at 360 nm and an absorption edge at 410 nm (Fig. 1a). Large "blue" shift of the absorption band edge of QDs relative to bulk CdS (517 nm) indicates strong exciton confinement due to very small size of the CdS QDs. The average QD size *d* estimated from the absorption edge was found to be ~2,5 nm which is in good correspondence with the average hydrodynamic size (2–3 nm) measure by dynamic light scattering and the size determined by transmission electron microscopy (TEM), 3 nm (Fig. 1b). The CdS QDs emit photoluminescence (PL) in a broad range of 400–700 nm with the relative quantum yield of ~5%. Being introduced into a model four-layer LED (Al – CdS QDs – PEDOT:PSS – ITO) CdS QDs emit electroluminescence (EL) in the range of 400–600 nm. The N_2H_4/MAA-stabilized CdS QDs exhibit unusually strong and reversable temperature dependence of PL intensity in the range of

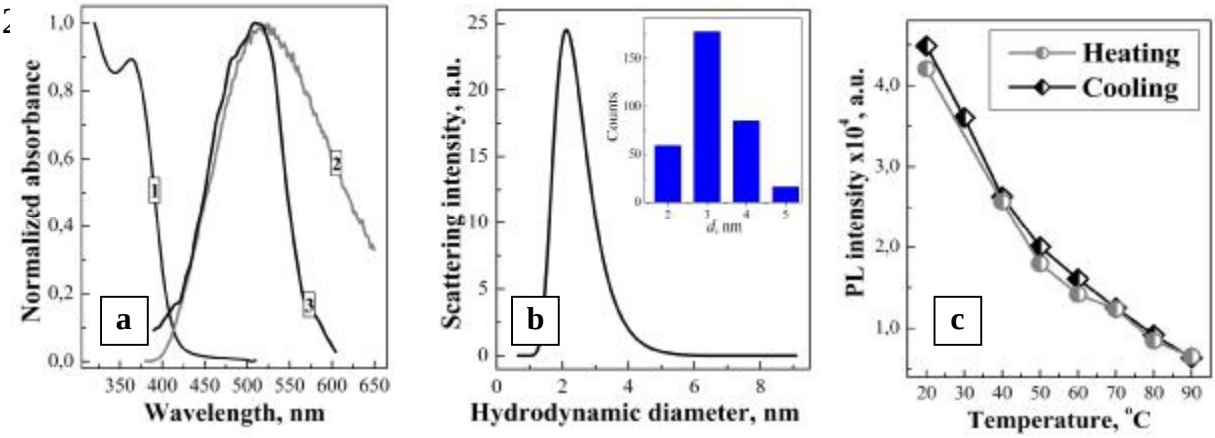

Fig. 1. (a) Normalized absorption (curve 1), PL (2) and EL spectra (3) of N_2H_4/MAA-stabilized CdS QDs. (b) Distribution of CdS QDs by the hydrodynamic diameter (main figure) and by the size according to TEM results (inset). (c) Temperature dependence of the integral PL intensity of N_2H_4/MAA-stabilized CdS QDs in a heating-cooling cycle.

The work is supported by the Collaborative research project # 07–03–12(У) by NASU and Siberian branch of Russian Academy of Sciences.

Structure, Phase Composition and Functional Characteristics of Calcium Phosphates Synthesized by the Step-Crystallization Method From the Aqueous Solutions

Rokhmistrov D.V. , Goncharenko A.V. , Zyman Z.Z. , Maklakov Y.A.

V.N. Karazin Kharkiv National University, Kharkiv, Ukraine

Hydroxyapatite (HA) is widely used in medicine as an implant [1]. It is commonly produced by the precipitation from the aqueous solutions. This route of the synthesis is also extremely important for understanding the crystallization process in hard tissues of human and animals. Despite the numerous researches which were carried out over the past few decades, this question is still not clear.

The aim of this work was to study structure, phase composition and functional characteristics of calcium phosphates synthesized by at different stages of HA synthesis by step-crystallization method from aqueous solutions.

HA was synthesized by the precipitation method [2] from $Ca(NO_3)_2$ and $(NH_4)_2HPO_4$ solutions at 19^oC. The reagents were chosen in the proportion to get the product with Ca/P ratio equal 1.67. The phosphate solution was divided into quarters. The first step of the synthesis was performed by the addition of the one-fourth fraction of $(NH_4)_2HPO_4$ into $Ca(NO_3)_2$ solution dropwise during 10 min. Then the reacted solution was aged 3 days. It was divided into two parts: first was left untreated, the second was remixed during 30 min at 200 rpm. The second step of the synthesis was made by the addition the second part of phosphate solution in the reacted solution. The last two steps of the synthesis were made the same route. The precipitates were dried at room temperature during 3days and then were fired at 1150^oC during 1h. The obtained samples were studied by XRD, IR analysis. The linear shrinkage and Vickers microhardness were measured on the cylindrical samples.

The results of the studies have shown that the remixing of the precipitates sufficiently impact on the phase composition at the initial and the final stages of the crystallization. However microhardness of the samples obtained at the middle step of the synthesis is in two times higher as at the initial and final stages. This route of the synthesis opens the ways to produce the biphasic calcium phosphate ceramics with definite phase composition.

1. L. L. Hench, Bioceramics, J. Am. Ceram. Soc., 1998, 81, 1705.
2. M. Jarcho, C. H. Bolen, M. B. Thomas et al., J Mater Sci, 1976, 11, 2027.

Methods of Nanotechnology Application to the Prevention and Elimination of Emergency Situations

Rudyk Yu.I, Lavrivska O.Z.

Lviv State University of Life Safety, Lviv, Ukraine

National programs in the field of nanotechnology postindustrial countries are oriented not only to the scientific or military spheres, but also in social, economic and technological trends.

Most experts believe that advanced line of XXI century in the development of science and technology is nanotechnology. Obviously, the development of this area requires making radical changes in the activities of the national security and will push to increase the level of life safety [1].

Nanotechnologies become a revolutionary foundation of society development. Unfold opportunities synthesis unknown in nature systems not only in composition but also in structure and, above all, the properties, and hence, by functional abilities.

It is known that with every exhalation person produces at atmosphere set certain chemicals. They can reveal at considerable distance. Earlier this were only able to specially trained dogs. However, scientists from the Leibniz Institute in Dortmund (Germany) designed a mobile device that a few minutes can determine the presence of a living person within tens of meters.

Using this device in the public service of emergency situations when you want to find survivors under the rubble or in a burning building, including people who have lost consciousness is expedient. Ion mobility spectrometer (Ion-mobility spectrometry, IMS), together with chromatograph can quickly determine the chemical composition of the gas, in that case, air. Scientists previously tested and determined 12 chemicals that people constantly provide the atmosphere. It is assumed that a pile of wreckage can propel the hose and take air samples. If it has a high concentration of 12 elementary "Human" substances, it is next to a live person. Spectral analysis takes three minutes. The device showed itself during laboratory experiments [2].

The need arises to develop methods of use of nanomaterials and quantum-dimensional structures to prevent technogenic emergency situations (electrical, hazardous technology processes, transport, etc.) and adaptation means to perform of tasks to rescue people and elimination emergency and their consequences.

1. Nanotechnology [Electronic resource]. – Available with http://nano-info.ru.
2. Finding Signs Of Life With Ion Mobility Spectrometry [Electronic resource]. – Available with http://cen.acs.org/articles/91/web/2013/01/Finding-Signs-Life-Ion-Mobility.html.

Dynamic Conductivity in Doped Graphene Beyond Linear Response

Ruvinskii B.M.[1], Ruvinskii M.A.[2]

[1] *Ivano-Frankivsk National Technical University of Oil and Gas, Ivano-Frankivsk, Ukraine*
[2] *Vasyl Stefanyk Precarpathian National University, Ivano-Frankivsk, Ukraine*
bruvinsky@gmail.com

A number of theoretical works revealed universal behavior of low-temperature dynamic conductivity and optical transparency of graphene monolayer as a linear response of Dirac fermions to alternating electric field and incident electromagnetic wave. This behavior is mainly determined by universal physical constants and fine structure constant, it was experimentally confirmed in the infrared and visible spectral region. The letter [1] spread beyond the linear response theory in relation to interband clean intrinsic conductivity (at zero values of absolute temperature and chemical potential).

The present work contains another method of consideration for the interband and intraband conductivity of doped graphene in post-linear response at arbitrary temperature and chemical potential. The dependences of induced currents on frequency and amplitude of external electric fields, the graphene temperature and chemical potential were determined for sufficiently strong electric fields. The nonlinear effects of saturation of both dissipative and non-dissipative parts of induced current were obtained under general conditions, as well as relevant "nonuniversal" features from effects of doping, finite temperature, interband and intraband transitions for the graphene transparency behavior at sufficiently large intensity of incident radiation. The research of the interband and intraband currents of doped graphene showed significant deviations from the linear response theory in the strong electric fields and at low frequencies. The saturation was defined for all amplitudes of induced currents, as well as for nonlinear increase of appropriate transparency of suspended graphene with intensity growth of incident radiation. The intraband transmission coefficient decreases with chemical potential and temperature rise, while the interband transmission coefficient increases under the same conditions.

1. Mishchenko E.G. //*Phys. Rev. Lett.* – 2009 – **V.103**, P.246802-1 – 246802-4.

The work supported by projects of FRSF State Agency for Innovation and Informatization of Ukraine. (Contracts: R54, F53, 3)

Classical and Quantum Dimensional Effects in Dynamic Interband Conductivity of Straight-Line Graphene Ribbon

Ruvinskii M.A.[1], Ruvinskii B.M.[2]

[1] Vasyl Stefanyk Precarpathian National University, Ivano-Frankivsk, Ukraine
[2] *Ivano-Frankivsk National Technical University of Oil and Gas, Ivano-Frankivsk, Ukraine*
bruvinsky@gmail.com

The aim of this work is the theoretical determination of interband conductivity of limited graphene on the example of plane straight-line graphene ribbon with taking into account the classical and quantum dimensional effects. If the linear sizes of the system exceed the average "thermal" de Broglie wavelength of current carriers, the quantum dimensional effects can be neglected and the classical dimensional effects should be considered. In this case the dependences of integral interband conductivity on field frequency, wire size and free length of Dirac electrons within different parameters' values of diffuse-specular mechanism for electron scattering from the lateral wire bonders were calculated. The influence of classical dimensional effects for the interband current has been revealed in the cubic approximation on amplitude of the alternating voltage (the wire length is much greater than its width).

The quantum effects of the interband conductivity have been studied for the narrow graphene ribbons ("nanoribbons"). The electronic states of graphene nanoribbons depend strongly on their size and geometry [1]. In the nanoribbons with zigzag edges ("zigzag ribbons") the boundary conditions for the wave function are vanishing on a single sublattice at each edge, and the Dirac valleys **K**, **K'** do not mix. For armchair edges ("armchair ribbons") the boundary conditions for the wave function are vanishing on both sublattices at the edges, and two valleys mix. The armchair ribbons are metallic under the critical widths and insulating otherwise. The dissipative parts of interband currents for the zigzag and armchair nanoribbons have been obtained in our work.

1. Brey L., Fertig H.A. // *Phys. Rev. B.* – 2006 – V.**73** – P.235411-235415.

The work supported by projects of FRSF State Agency for Innovation and Informatization of Ukraine. (Contracts: R54, F53, 3)

Field Induced Chirality in Magnetic Multilayers

Salyuk O.Y.[1], Golub V.O.[1], Tartakovskaya E.V.[1], Lott D.[2] Schreyer A.[2]

[1]*Institute of Magnetism, National Academy of Sciences of Ukraine, Kiev, Ukraine*
[2]*Helmholtz-Zentrum Geesthacht, Germany*

Breaking chiral symmetry is a common subject of biology, chemistry and physics [1]. How to produce chiral materials with predicted handedness and to change this parameter for practical usage? This question is under massive investigations in chiral magnets, which are solid candidates for use as elements in spintronic devices [2,3].

The physical origin of the field-induced chirality experimentally observed in rare earth multilayers [4] is determined here. The role of Dzyaloshinsky-Moriya, RKKY and Zeeman interactions causing the magnetic structures with non-zero chirality is analyzed. The agreement between theoretical and experimental temperature dependencies of the chirality factor proves a physical relevance of the presented theory.

1. E. Edlund, O. Lindgren, and M. Nilsson Jacobi, Phys. Rev. Lett. 108, 165502 (2012)
2. Y. Togawa, T. Koyama, K. Takayanagi, S. Mori, Y. Kousaka, J. Akimitsu, S. Nishihara, K. Inoue, A. S. Ovchinnikov, and J. Kishine, Phys. Rev. Lett. **108**, 107202 (2012).
3. A.T.D. Grünwald, A.R. Wildes, W. Schmidt, E.V. Tartakovskaya, J. Kwo, C. Majkrzak, R.C.C. Ward, and A. Schreyer, Phys. Rev. B **82**, 014426 (2010).
4. S. V. Grigoriev, Yu. O. Chetverikov, D. Lott, and A. Schreyer, Phys. Rev. Lett. 100, 197203 (2008).

Current-Voltage Characteristic of Nano-Diode in Strong Electromagnetic Field

Seti Ju.O., Tkach M.V., Matijek V.O., Grynyshyn Yu.B.

Chernivtsi National University, Chernivtsi, Ukraine

The rapid development of nano-physics caused the appearance of new fundamental knowledge and the creation of unique nano-devices – nano-diodes, quantum cascade lasers, quantum cascade detectors and so on. The majority of nano-devices operate at the base of phenomenon of electronic transport through the multi-layer open resonance tunnel structures driven by the electric, magnetic or high-frequency electromagnetic fields.

In the majority of theoretical papers the theory of ballistic transport of electrons through the multi-layer open resonance tunnel structures was developed for the condition of weak electromagnetic field [1, 2]. Therefore, the quasi-stationary states of the system were the “pure” electronic ones. The problem of electronic transport, in this case, became simplified and the complete Schrodinger equation was solved within the method of time-dependent perturbation theory. The results obtained for the transmitting coefficient of the resonance tunnel structure proved the existing of the resonance transmitting canals only.

The perturbation theory can not be used for the case when the electronic currents transport through the resonance tunnel structure placed into the constant electric field or interact with the strong electromagnetic field [3].

In the proposed paper the transport properties of two-barrier resonance tunnel structure in electric and strong electromagnetic field are studied using the expand of the exact solution of one-dimensional time-dependent Schrodinger equation into Fourier ranges. The results of calculations performed for the experimentally studied two-barrier resonance tunnel structures prove the existence of non-resonance transmitting canals of nano-system. These canals cause the double-peak curve for the current-voltage characteristic of two-barrier resonance tunnel structure driven by the strong electromagnetic field.

1. Belyaeva I.V. Resonant interaction of electrons with a high frequency electric field in two-barrier structures / I.V. Belyaeva, E.I. Golant, A.B. Pashkovski // Semiconductors – 1997. – T. 31, № 2. – C. 103 – 109.
2. Remnev M.A. Effect of spacer layers on current-voltage characteristics of resonant-tunneling diode/ M.A. Remnev, I.Yu. Kateev, V.F. Elesin// Semiconductors – 2010. – V. 44, № 8. – P. 1034 - 1039.
3. Tkach N.V. Nonresonant transparency channels of a two barrier nanosystem in an electromagnetic field with an arbitrary strength/ N.V. Tkach and Yu.A. Seti// JETP Letters – 2012. – V. 95, № 5. – P. 271 - 276.

Photocatalytic Properties of Rutile Nanocrystals Obtained Via an Original Low-Temperature Route From Titanate Nanotubes

Shvalagin V.V. [1], Andryushina N.S. [1], Stroyuk O.L. [1], Bavykin D.V. [2]

[1] *L.V. Pysarzhevsky Institute of Physical Chemistry, Kiev, Ukraine*
[2] *University of Southampton, Southampton , United Kingdom*

Acid treatment of titanate nanotubes (TNT, Fig. 1a) with diluted H_2SO_4 results in their transformation into various forms of nanostructured TiO_2 with the shape and size depending on temperature and duration of treatment. Transformation at 25 °C yields rutile nanocrystals (NCs, Fig. 1b) with high crystallinity, the specific surface area of around 250 $m^2 \times g^{-1}$ and small average diameter of particles, ca. 3 nm. The mechanism of acid-assisted TNT transformation into rutile NCs includes dissolution of nanotubes, release of soluble forms of Ti(IV), and crystallization of dissolved Ti(IV) to TiO_2. Studies of photochemical properties of rutile NCs revealed their uncharacteristically high photocatalytic activity in gas-phase ethanol vapor oxidation by O_2 and hydrogen evolution from water/ethanol mixtures as compared to original TNT and to a well-known reference photocatalyst – Degussa/Evonik P25 (Fig. 1c). High photoactivity of nanocrystalline rutile, which is typically inert in the microcrystalline state is probably connected with mild synthesis conditions preserving the NC size below 3 nm and NC surface in a highly hydroxylated state which benefits to fast migration of the photoelectrons to the surface and capture of the photoholes with the surface hydroxyl groups.

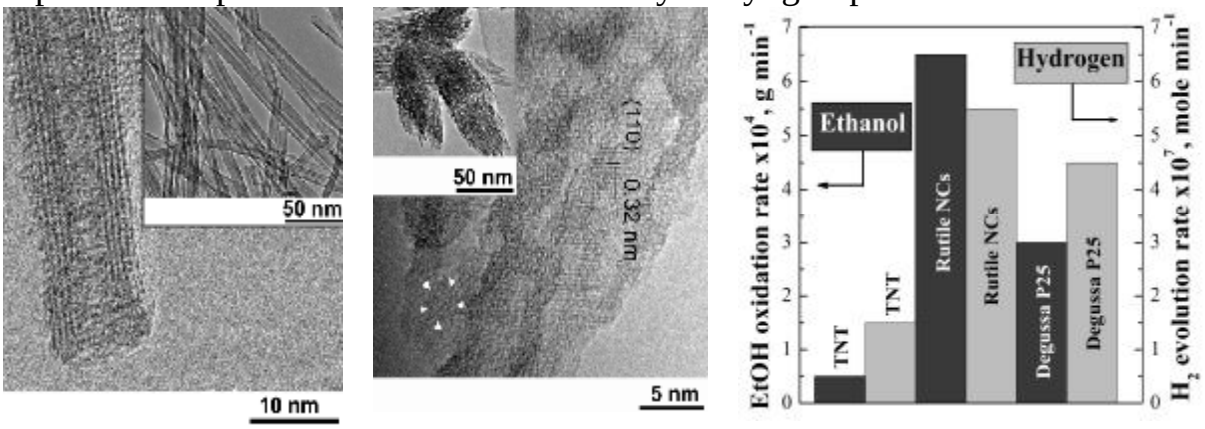

a **b** **c**

Fig. 1. TEM images of TNT (a) and rutile NCs (b) as well as rates of photocatalytic oxidation of ethanol and evolution of H_2 in the presence of TNT, rutile NCs and Degussa/Evonik P25 in identical conditions (UV light, λ = 300–400 nm).

Raman Scattering From Pulsed Laser Deposited Si Nanocrystals Embedded in Alumina Matrix

Strelchuk V.V., Nikolenko A.S., Kaganovich E.B., Krishchenko I.M., Manoilov E.G.

V. Lashkaryov Institute of Semiconductor Physics, NAS of Ukraine, Kyiv, Ukraine

Thin films were deposited by pulsed laser ablation of silicon and aluminium in argon atmosphere from backward low energy cluster flow of an erosion torch using YAG:Nd^{3+} laser beam (λ=1.06 μm, E_p=0,2 J, t_p=10 ns, f_p=25 Hz). Micro-Raman spectra were taken in backscattering geometry at room temperature using Horiba Jobin–Yvon T64000 Raman spectrometer. The 488.0 nm line of an Ar–Kr ion laser with power densities on the sample surface in the range P=0,01 – 20 mW/μm^2 was used for excitation. Obtained Si quantum dots (QD) in alumina have exciton photoluminescence in visible range of spectra at room temperature. Stokes and anti-Stokes components of the Raman spectra were analyzed (Fig.1). At P<0,2 mW/μm^2 spectra display two components of Si Raman peak at ~520,4 and 525,8 cm^{-1}, the first one – due to phonon confinement in Si QD and the second one – due to compressive strain as result of the lattice mismatch of Si and Al_2O_3 (Fig.2). Fitting of calculated curve in RWL confinement model [1] to experimental curve at P=0,1 mW/μm^2 with subtraction of high frequency peak gives $\Delta\omega$=2,5 cm^{-1}, FWHM=7,7 cm^{-1} and the average Si QD size 6,5 nm. Upon increasing the laser power density a shift of Raman peak to lower wave numbers, line broadening and intensity ratio $I_S/I_{a\text{-}S}$ decreasing are observed due to laser heating. At P>5 mW/μm^2 temperature estimation gives T>1000 K.

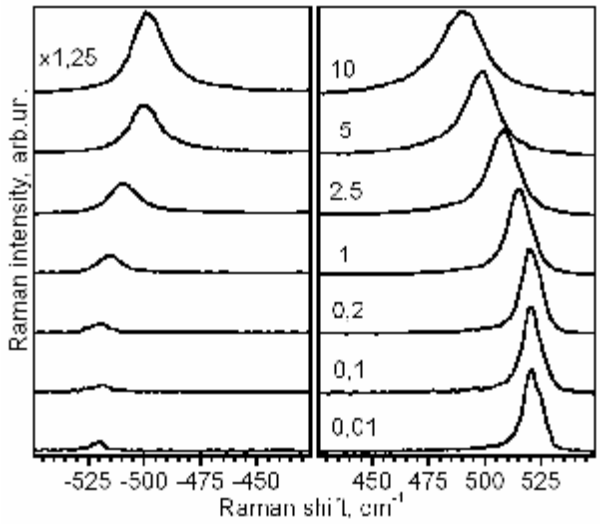

Fig.1.

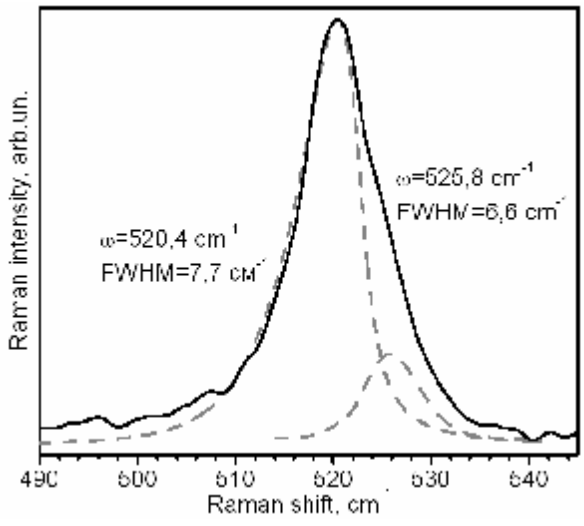

Fig.2.

1. Richter H., Wang Z.P., Ley L. The one phonon Raman spectrum in microcrystalline silicon // Solid State Commun. – 1981. –V.39. – P.625 – 629.

Formation of Porous Structure of Indium Phosphide

Suchikova Y.A.

Berdyansk State Pedagogical University, Berdyansk, Ukraine

Porous indium phosphide - a promising material in microelectronics, which is prepared by electrochemical etching. Despite the simplicity of the method, still remain unresolved questions about the influence of current density on pore formation. Experimental way was established the following facts: 1) the microstructure of porous-InP layer correlates with the current formation. The thickness of the layer of porous indium phosphide increases from 15 m at a current density of the formation 30mA/sm^2 to 60mkm at 80mA/sm^2. In this case, the morphology of porous-InP transferred from weakly ordered a clearly elongated (columnar) normal to the surface of the plate; 2) A layer of porous indium phosphide should be formed at the highest current density (~ 100 mA/cm^2). In this case, reached a maximum growth rate of the layer and the optimum flatness of the boundary porous-InP - monocrystalline InP;3) At low current densities (j <25 mA/cm^2) forming a porous layer is observed. At current densities in the range from 30 mA/cm^2 to 200 mA/cm^2, the electrochemical etching occurs with the active formation of pores, which, depending on the applied current anodization have different diameter and depth of germination; 4) At the critical current density (~ 170 mA/cm^2), a porous layer is separated from the substrate. The surface of indium phosphide wafer has an uneven structure with multiple mounds and pits.

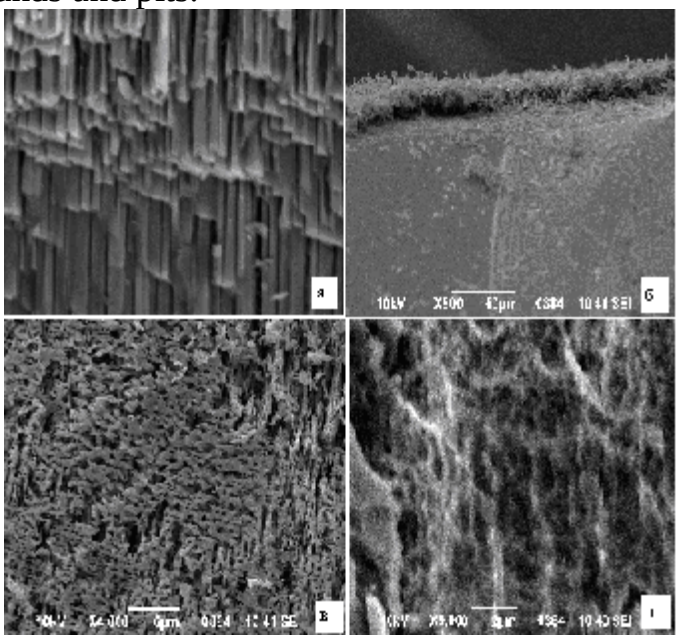

Figure 1. Different images of the porous surface of indium phosphide: a) cleavage, showing a columnar structure, and b) chips, showing the flatness of the boundary porous-InP / InP, a) the surface of porous-InP, d) surface of indium phosphide with the "cut" a porous layer.

Preparation and Mesoscopic Ordering of the Casted Hybrid Photonic Nanomaterials

Telbiz G., Leonenko E., Stronski A.[1]

L.Pizharzhevski Institute of Physical Chemistry NASU, Kiev, Ukraine
[1]V.Lashkaryov Institute of Semiconductor Physics NASU, Kiev, Ukraine

Materials science has made significant advances in understanding and identifying of the fundamental mechanisms that control the behavior of nanoscale structured materials: control of material heterogeneity, interfacial topology and chemistry, as well as designing films with different functions. Building on recent advances in nanomaterial science, we have the opportunity to design new materials for energy efficiency and high energy environments. The specific property under consideration, mesoscopic materials can described in terms of continuous, homogeneous media on scales less than that of the nanostructure. With other sides, controlled assembly of mesoscale heterostructures allow to produce materials with new functionality not available in bulk with enhanced ionic and electronic conductivity, ferroelectrics, and novel catalytic and photonic materials.

The synthesis of surfactant-templated mesoporous silica triggered an explosive technological development in mesoscopic materials. Mesoscopic films have submicrometer thicknesses but macroscopic lengths and widths and are composed of mesoscopic subunits with unit cells in the size range of micelles. Interfacial confinement, in combination with externally applied fields, has led to important advances in mesoscopic materials. Such films can used as nanoreactor device where the mesoscopic ordered dye molecules or semiconductor nanoparticles can be transformed, for instance, as sensors or mesoscopic waveguides for mirrorles lasing. The efficient energy transfer processes can be also indicative in case of the formation of tightly coupled to dye/acceptor complexes. The excellent optical properties, along with the ultrafast optical responses of the intercalated dye/acceptor complexes, can make these composite films ideally suited for use as the photonic layer in an all-optical ultrafast switching device.

Here we review the technological development of these materials containing columnar pores normal to the film plane and arranged in a lattice. We highlight results of monitoring of optical and FL spectra of laser dyes encapsulated in mesoscopic silica films. Unusual spatial localization of the dye dimers and rise of the concentration limit of the fluorescence of laser dye in micellar space deliberated in the body of mesostructured silica was shown, that is accompanied by the increasing changes of absorption and fluorescence spectra [1, 2]. The observed manifold of the optical and fluorescence spectra shows the ability of dispersity and controlled aggregation of dye molecules (such as Rh6G) owing to time-delay of their spontaneous transformation during the process of

formation of mesostructured hybrid sol-gel films. Emission in films received by the pre-doping method, observed even at high dye concentrations and characterize of long-term stability. A distribution of dye molecules in a body of film corresponded to three extreme configurations, which we attribute to monomers, sandwich H-type dimers and head-to tail J-type aggregates. The formation of fluorescent aggregates most probably can promoted of the amphiphilic triblock copolymers that favor the formation hybrid micelles and the excited state CT complex between dye and surrounding Pluronic molecules. Variation of values of refractive index, absorption coefficient and optical conductivity can be evidence of various spatial organizations of dye molecules within the body of generated films, subject to method of deposition on substrates. We are considered also the mesoscopic formation of uniform sized Ag nanostructures within the nanowire structure dye to the self-assembly of biochemical based nanoparticles. These nanocomposite showed attractive electronic and photocatalytic properties, in particular, in the hydrogen energetics, photochemistry, is can be promising for application in SERS.

Nanocrystalline metal chalcogenide semiconductors make great sense in the photoelectric applications. Since the size and shape of the materials have a strong influence on their properties, new methods with high feasibility are always expected for the synthesis of chalcogenides with different dimension and morphology. We suppose that the mesoscopic morphology of the semiconductor, including also chalcogenide glasses obtained in mesoscopic composite films will allow us to produce materials with intriguing optoelectronic properties. It is known that introduction of different dopants into chalcogenide glasses changes their optical, electronics and magnetic properties [3]. Therefore, we believe that new glass morphology will be a supplementary way of properties' control, besides concentration of dopant, due to influence of confinement inside mesoscopic structures.

1. Telbiz G., Dementjev A., Kiskis J., Gulbinas V., Valkunas L. Phys. Status Solidi A.-2010.-**207.-**P.2174.
2. Tikhonov E., Telbiz G. Molecular Crystals and Liquid Crystals.-2011.-**535**.-P.82.
3. A.P. Paiuk, A.V.Stronski, P.F.Oleksenko, M.Vlček, Proc. SPIE 8306 Non-Linear Materials, Devices, and Applications, 830617 (2011) August 2011 Photonics, Devices, and Systems V Eds.

Electronic Transport in Injectorless Quantum Cascade Lasers

Tkach M.V., Seti Ju.O., Boyko I.V., Voitsekhivska O.M.

Chernivtsi National University, Chernivtsi, Ukraine

The majority of functioning quantum cascade lasers is constructed in such a way that every separate cascade contains the active band consisting of several wells and respective number of barriers and injector also consisting of wells and barriers. This injector plays the role of energy relaxation and transferor between the neighbor cascades. It also synchronizes the operation of cascades. The sizes of the injector in quantum cascade laser operating in infrared range are, as a rule, at least two times bigger than the sizes of active band. Due to this, the number of cascades inside of quantum cascade laser is strongly confined. This problem is solved in the so called injectorless quantum cascade lasers, already produced experimentally [1]. Its principle of operation is the following: the separate cascade is used as an active band, being in its turn the open three-barrier RTS driven by the electric field. The sizes of wells and barriers and the intensity of the electric field would be such that in each cascade there would be three quasi-stationary states. Their energies would be such that the electronic current falling at nano-system with the energy E_3 radiates the electromagnetic field with the energy $\Omega=E_3-E_2$ in the demanded spectrum range due to the transition into the state with energy E_2. The difference of energies E_2-E_1 has the order of the energy of confined and interface phonons, thus, due to the electron-phonon interaction, the electrons perform the radiationless quantum transition into the first quasi-stationary state, from which further tunnel at the third quasi-stationary state of the next cascade.

In the proposed paper we develop the quantum theory of the electron quasi-stationary states and dynamic conductivity of separate cascade of the injectorless quantum cascade laser using the model of rectangular potentials and different effective masses in the layers of three-barrier RTS. The theory opens perspectives to optimize the geometrical design of active band in such a way that nano-devices operate in optimal regime.

The performed theoretical calculations perfectly correlate with the results of experimental paper [1].

1. Kumar S. Two-well terahertz quantum-cascade laser with direct intrawell-phonon depopulation / S. Kumar, C. W. I. Chan, Q. Hu and J. L. Reno // Appl. Phys. Lett. – 2009. – V. 95, № 14. – P. 141110-1 - 141110 -3.

Strain Effect in Magnetooptical Properties of Film System Fe/Pt/S and $[Fe/Pt]_8/S$

Velykodnyi D.V.[1], Cheshko I.V.[1], Makukha Z.M.[1], Panchal C.J.[2], Protsenko I.Yu.[1]

[1] *Sumy State University, Sumy, Ukraine,*
[2] *University of Baroda, Vadodara, India,*

The results of the study magneto-optical properties (MOKE) bilayer film systems Fe(32 nm)/Pt(3 nm)/S (S - substrate) and multilayer $[Fe(3)/Pt(3)]_8/S$ in longitudinal deformation conditions ε_l=0-10 %, that includes the elastic (up to $\varepsilon_l \approx 0{,}4$ %) and plastic deformation. The external magnetic field (50 mT) had two orientation - along and perpendicular to the direction of deformation. Setting the experiment in this version is a complete analog strain effect, which is characterized by the longitudinal strain coefficient $g_l = \frac{1}{R} \cdot \frac{\Delta R}{\Delta e_l}$ (R і ΔR – the initial resistance and its change during deformation). In the case MOKE deformation dependence can be described by MOKE strain coefficient $g_l^{KE} = \frac{1}{j} \cdot \frac{\Delta j}{\Delta e_l}$.

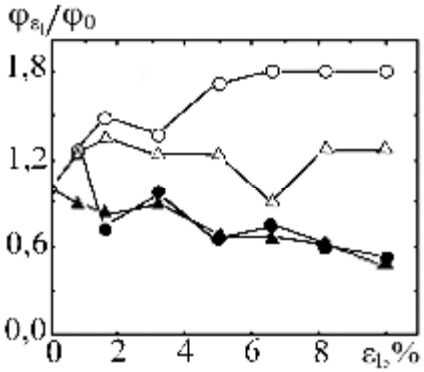

Fig.1. The dependence of the ratio of the polarization plane rotation angle φ_{ε_l} the longitudinal strain to the rotation angle φ_0 at ε_l=0 % for film samples Fe(32)/Pt(3)/S (●, ○) and $[Fe(3)/Pt(3)]_8/S$ (▲, Δ). The orientation of the external magnetic field: longitudinal (●, ▲) and perpendicular (○, Δ) to plane of sample

On Fig.1 the experimental dependence of the rotation angle the polarization plane φ_{ε_l} in the deformation process. The increase of φ_{ε_l} compared with φ_0 can be explained based on the well-known [1] value for the Faraday effect:

$$\frac{j_{e_l}}{j_0} = \frac{(l-\Delta l)}{l} \cdot \frac{(\partial n/\partial w)e_l}{(\partial n/\partial w)_0},$$

where l і Δl – traversed path of electromagnetic waves in the region of the magnetic field and its variation, respectively; n - refractive index.

Since the first factor $(l-\Delta l)/l$ varies within 1.0 – 0.9, the dependence j_{e_l} from ε_l can be explained by amplification dispersion relations $n(\omega)$ in the elongation of magnetic domains.

This work was performed by the joint project №M/362-2012 between Sumy State University (Ukraine) and University Baroda (Vadodara, India).

1. Белюстин С.В. Классическая электронная теория. – М.: Высшая школа, 1971. – 352 с.

Thermoelectricity of Nanostructures Based on Compounds IV-VI

Yurchyshyn I.K.

Vasyl Stefanyk Precarpathian National University, Ivano-Frankivsk, Ukraine

Recently, the process of creating of highly efficient thermoelectric materials the research activities in the field of low-dimensional structures were intensified [1,2]. Decreasing the dimension of the material creates the conditions for observing the phenomenon of quantum size effect, which leads to an increase in the density of states near the Fermi energy. This allows to keep the high conductivity at relatively low Fermi energy, where there are high values of the Seebeck coefficient S. Tangible impact of quantum effects on the thermoelectric properties is possible only if the size of the structure in the direction of limitation is comparable to the de Broglie wavelength of carriers. This condition is satisfied for the structures in the form of quantum wells, quantum wires and quantum dots, which create the dimensional confinement in one, two and three dimensions, respectively. Also, the electronic density of states shows a marked deviation from the usual parabolic law in bulk materials.

The paper presents an analysis of new approaches to improve the thermoelectric parameters of nanostructures based compounds IV-VI.

We found that the thermoelectric figure of merit of materials based on quantum dot superlattices reaches ZT = 2 at 300 K due to the sharp decrease in the lattice thermal conductivity of more than 4 times compared to solid materials of the same composition.

The optimum parameters of the segment length and orientation of the superlattice nanowires based on lead chalcogenides were established.

Oscillation character of the thickness dependences of kinetic parameters quantum wells superlattices suggests that this behavior is due to quantum size effects associated with the restriction of movement of the main type carrier. Definition of oscillation period yielded the energy parameters of corresponding nanostructures.

1. Davies J.H. The physics of low-dimensional semiconductors. An introduction. – Cambridge university press. – 1998. – 451 p.

2. Dresselhaus M.S., Ghen G., Rang M.I., Yang R., Lee H., Wang D., Ren Z., Fleurial J-P., Gogna P. New Directions for Low-Dimensional Thermoelectric Materials // Adv. Mater. - 2007. - № 19. - P. 1043-1053.

The work supported by an integrated project of MES of Ukraine (N 0113U000185) and by projects of FRSF State Agency for Innovation and Informatization of Ukraine. (Contracts: R54, F53, 3), NAS of Ukraine (N 0110U006281)

Investigation of photoluminescence features of metal oxide nanopowders during adsorption of gases

Ostafiychuk B.K.[1], Pawluk V.S.[2], Popovych D.I.[2,3], Serednytski A.S.[2], Zhyrovetsky V.M.[2]

[1]*Vasyl Stefanyk Precarpathian National University*
[2] *Pidstryhach Institute for Applied Problems of Mechanics and Mathematics NASU*
3b, Naukova Str., Lviv 79060, Ukraine
[3] *Lviv Polytechnic National University 2 St. Bandera St., 79013 Lviv, Ukraine*

In the present study the investigation of photoluminescence features of ZnO and TiO_2 (anatase) nanopowders during adsorption of gases has been presented. Nanopowders produced by pulsed reactive laser ablation [1]. According to electron microscopy and X-ray diffraction analysis the size of nanogranules were 60-80 nm.

It is established that photoluminescence of ZnO and especially TiO_2 nanopowders strongly depends on the previous history of the samples, excitation conditions and ambient gases. Comparison of the photoluminescence spectra of nanopowders in air and vacuum (P~3Pa), has allowed to establish that for ZnO in air take place increase (40%) of intensity of the main peak and decrease in intensity of the accompanying peak which probably corresponds to defects caused by interstitial atom of zinc. At the same time for TiO_2 observed photoluminescence quenching in air.

With the purpose of modifying the intrinsic defect structure of nanopowders was conducted pulse laser annealing (λ=1.06 μm, τ=10 ns, E=0.3 J/cm^2) in air. It is established that the laser annealing of ZnO leads to decrease (30%) the intensity of luminescence main peak (λ=515 nm) and it small shifts to long wavelength side, intensity of accompanying peak (λ=430 nm) is increasing. On the other side, laser annealing of TiO_2 leads to increase adsorption capacity and the significant increase of luminescence intensity main peak (λ=510 nm). For the laser modified the intrinsic defect structures of nanopowders established correlation between changes in concentration of adsorption centres, which can interact with centres of luminescence or carry out their function and intensity of the photoluminescence.

Investigations of processes of the temperature quenching of ZnO nanopowders photoluminescence in the field of temperatures 300-530 K in vacuum (P=0.1 Pa) are conducted. It is established the mechanism of thermal quenching and found effect of emission sensitization in the short-wave region of the luminescence spectra. The obtained results can be effectively used in the construction of optical gas sensors.

1. Gafiychuk V.V., Ostafiychuk B.K., Popovych D.I., Popovych I.D., Serednytski A.S. ZnO nanoparticles produced by reactive laser ablation // Applied Surface Science. – 2011 – V.**257**, #20. – P. 8396–8401.

СЕКЦІЯ 2 (стендові доповіді)
НАНОТЕХНОЛОГІЇ, НАНОМАТЕРІАЛИ І КВАНТОВО-РОЗМІРНІ СТРУКТУРИ

24 травня 2013 р.

SESSION 2 (poster)
NANOTECHNOLOGIES AND NANOMATERIALS, QUANTUM-SIZE STRUCTURES

May, 24, 2013

Identification of Individual Gas Molecules Chemisorbed on Graphene

Ananina O., Fefelova N.

Zaporozhye National University, Department of Semiconductors Physics, Zaporozhye, Ukraine

Study of carbon nanoclusters is a fundamental problem of a present-day nano-material science. Graphite and it's two-dimensional form - graphene - is of great interest today [1]. In this paper we simulated physical and chemical adsorption of CH_4, PH_3 and NH_3 molecules on graphene. The goal of this work is to study the changes in the energy difference between the HOMO (highest occupied molecular orbital) and LUMO (lowest unoccupied molecular orbital) in graphene as a result of molecules adsorption on graphene. The dependence of HOMO-LUMO energy (E_{HL}) of graphenes as a function of number of carbon atoms in the graphene cluster and type of adsorbed gas molecule have been studied.

Simulation of graphenes was carried out by a group of methods: semi-empirical MNDO, MINDO/3, AM1 and PM3 methods of MOPAC software, and also ab-initio Hartry-Fock methods of PC GAMESS program. Cluster geometric parameters, cluster energy, HOMO-LUMO energy, bond orders of atoms, orbital population, molecular and localized orbitals and density of states were calculated.

Initially, we investigate the dependence of the energy difference E_{HL} from the size of graphene, i.e. the number of carbon atoms in the cluster. Energy difference E_{HL} for graphenes of different size tends to decrease with increasing number of carbon atoms in the cluster (Fig. 1).

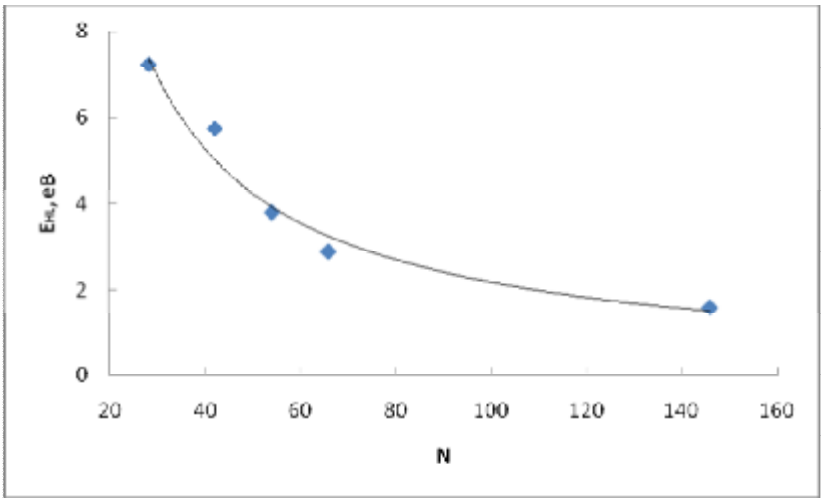

Fig.1. The dependence of HOMO-LUMO energy (E_{HL}) of graphenes as a function of number of carbon atoms in the graphene cluster ($E_{HL}=179,7N^{-0,95}$)

Ideally, when a number of carbon atoms tend to infinity, the value of E_{HL} will be 0. Graphic dependence (Fig. 1) can be approximately described averaged curve corresponding function $E_{HL}=A\cdot N^{-x}$.

Table 1. The adsorption energy (E), the charge transfer from the molecules to graphene, the distance from P(N, C) atom to graphene surface (d) for physical adsorption.

molecule	E, meV	ΔQ, e	d, Å
PH_3	48	0	3.65
NH_3	54	-0,03	3.56
CH_4	56	0	3.78

Table 2. The energy E_{HL} dependence from a number of carbon atoms in a graphene for physical adsorption of gas molecules.

graphene cluster	E_{HL}, eV			
	pure cluster	PH_3	NH_3	CH_4
$C_{28}H_{14}$	7,25	7,22	7,3	8,95
$C_{42}H_{18}$	5,74	5,42	5,73	5,73
$C_{54}H_{20}$	3,79	3,79	3,8	3,79
$C_{66}H_{22}$	2,19	2,88	2,19	2,19
$C_{146}H_{34}$	1,89	1,8	1,8	1,8

Table 3. The energy E_{HL} dependence from a number of carbon atoms in a graphene for chemisorption of gas molecules.

graphene cluster	E_{HL}, эВ			
	pure cluster	PH_2+H	NH_2+H	CH_3+H
$C_{28}H_{14}$	7,25	9,46	3,89	9,88
$C_{42}H_{18}$	5,74	8,22	8,69	8,76
$C_{54}H_{20}$	3,79	5,01	4,47	6,65
$C_{66}H_{22}$	2,19	3,98	3,67	4,02
$C_{146}H_{34}$	1,89	2,18	2,49	3,92

So, with increasing the number of carbon atoms in the graphene nanocluster the energy difference E_{HL} tends to zero. The molecules presence on graphene surface affects the energy spectrum of electrons, but in the case of physical adsorption - not much (tab. 2). The chemisorptions of gas molecules on graphene leads to a change the energy difference E_{HL}, and the E_{HL} energy dependence from molecules type can be used to create a gas sensor (tab. 3).

1. Novoselov K.S., Geim A.K. Morozov S.V., Jiang D., Katsnelson M. I., Grigorieva I.V. et al. Two-dimensional gas of massless Dirac fermions in graphene // Nature. – 2005. 438. - P. 197-200.

Platinum-Nickel Layer Catalysts for Fuel Cells

Balabai R., Chernikova E.

Kryvyi Rih National University, Kryvyi Rih, Ukraine

One appealing aspect of bimetallic catalysts is the possibility of rationally designing the catalytic properties of the material by changing the layer elements and composition. For example, a catalytic process in which the use of bimetallic catalysts could provide a significant benefit is fuel oxidation [1]. The mechanism of this catalytic reaction can be strongly influenced by the atomistic details of the surface, by the formation of surface oxides and mechanical strain in layers. This work is dedicated to the first-principle investigations of the electronic structure of the Pt–Ni catalyst with variable composition under varying oxygen pressure on its surface and with the effect of the presence of other reactants such as methanol. All the calculations are performed using the author program code. We use slab geometry to model the layer catalyst, using Pt layers, Ni layers for the (100) epitaxial heterostructure with mechanical strain or Pt-Ni alloy, on surface of which the adsorption structures are created, on two side on the slab. Pt lattice compression can be induced by layer formation during epitaxial growth of Pt layers on Ni substrate. A Pt f-band center can be altered by orbital overlap, resulting in a change in the surface activity of the Pt sites. Our calculations confirmed that compression of the Pt lattice in Pt-Ni heterostructure could downshift the energy of the f-band center. Pt lattice compression can thus enhance the catalyzed methanol oxidation via reaction $CH_3OH+O_2 \rightarrow CO_2+H_2O$. Decomposition of the molecule is seen from drawing.

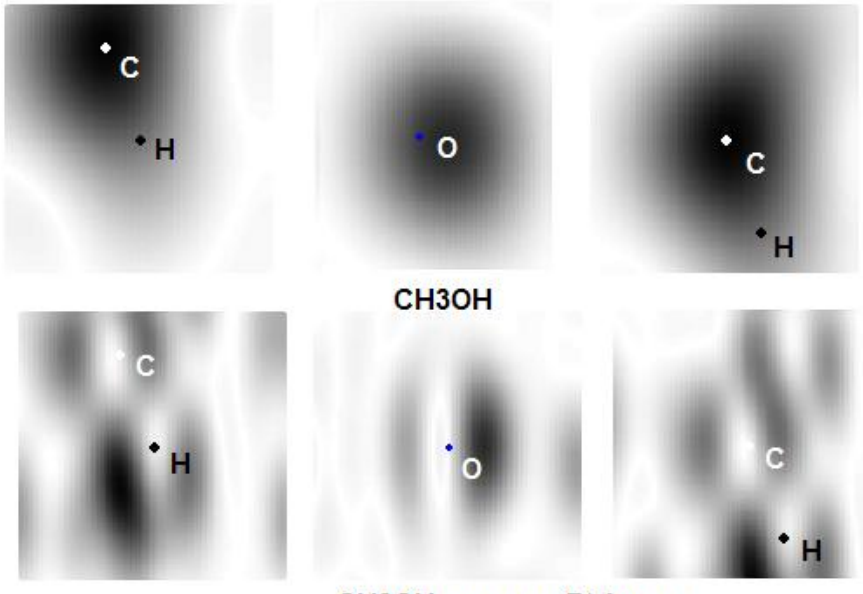

CH3OH on press Pt layers

1. Frolova L.A., Dobrovolsky Yu.A. Platinum-based alloy catalysts for low-temperature fuel cells // International Scientific Journal for Alternative Energy and Ecology. – Vol.76. – №8. – 2009. – P.10-24.

Selection of Silicon Based Nanostructure for CH_4 Detection

Balabai R., Merzlikin P.

Kryvyi Rih National University, Kryvyi Rih, Ukraine

The operational principle of a gas sensor is based on transformation of the value of adsorbed on semiconductor surface gas directly into an electrical signal associated with the conductance changes. Having established the potential of the material as the basis of a gas sensor, device fabrication can then be undertaken in order to establish its feasibility. CH_4 detection systems have gained special focus due to their extreme importance for safety reasons in oil and coal industries. The structural symmetry and high temperature firing nature of CH_4 molecules determine its low reactivity and response. This work aims at the first-principle investigations enhancing the CH_4 response through using nanostructured Si for sensor chips. The crystallite size reduction is one of the main factors enhancing the sensitivity of semiconductor sensors, but using standard silicon technology for sensor chips is guarantee of the success.

All the calculations have been performed using the auctorial program code [1]. We researched changes to sharing the electronic states of atomic complexes in consequence of adsorption of methane molecules on Si nanowires, Si thin film or porous Si to find the most sensitive nanoforms. An analysis of density of states shows that for all nanostructures widening of valence band is observed. Also we can see an appearance of local states near the upper part of valence band as a result of molecule adsorption (Fig.1). The most sensitive nanostructure amongst other examined structures is nanosized Si film.

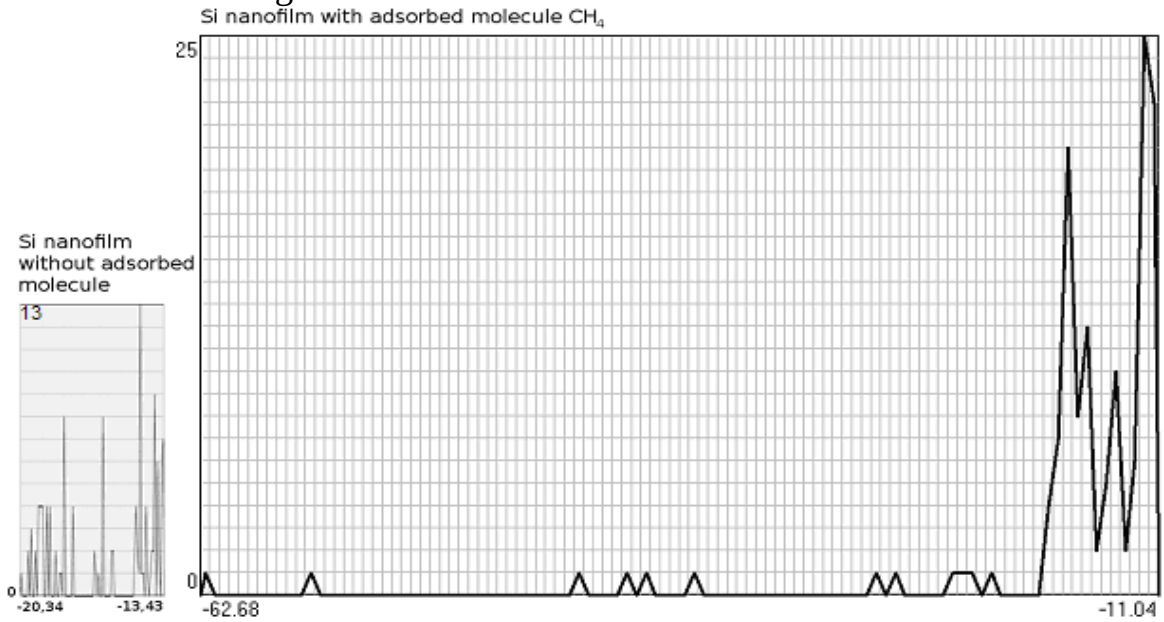

Fig. 1. Valence electron density of states of silicon nanofilm

1. Балабай Р.М. Обчислювальні методи із перших принципів у фізиці твердого тіла: квантово–механічна молекулярна динаміка. – Кривий Ріг: Видавничий дім, 2009. – 123 с.

Structural Properties of Zinc Oxide Thin Films Obtained by Chemical Bath Deposition

Berestok T.O.[1], Kurbatov D.I.[1], Opanasyuk N.M.[1], Manzhos O.P.[1], Kuznetsov V.M.[2]

[1] *Sumy State University, Sumy, Ukraine*
[2] *Applied Physics Institute NAS of Ukraine, Petropavlovskaya, Sumy, Ukraine*

Due to high radiation, chemical and thermal stability zinc oxide is widely used for fabrication of light-emitting diodes, cathode-ray tubes, thin film electroluminescence, gas sensors and etc. Chemically deposited ZnO thin films are perspective material for creation of conductive and optical cover layers of large area solar cells based on Si, CdTe, CIGS and CZTSe abrorber layer. Compared to the other techniques of obtaining condensates chemical bath deposition is generally economical, simple, doesn't require high temperature and pressure during the deposition.

In the work we investigated ZnO thin films obtained by chemical bath deposition from zinc nitrate and hexamethylene tetramine solution on glass substrate. The temperature of initial solution was 368 K. Duration of the deposition was equal (60-180) min. After the deposition the substrates were rinsed in distilled water in order to clean condensate from unnecessary sediment.

Structural investigations were carried out with using X-ray diffractometer DRON 4-07 (Ni-filtered K_α – radiation of Cu-anode). The phase analysis was carried out by comparing interplane distances and specific intensities of diffraction patterns from the investigated samples and JCPDS etalon. The quality of the film texture had been estimated by the Harris method. The XRD results were also used for the description of the coherent scattering domain (CSD) size in the films. Moreover we have applied the Nelson–Riley extrapolation method for more precise determination of the parameters a and c for both phases [1].

These researches allow us to study dependence of obtaining films parameters (such as phase analysis, texture quality, lattice constants, grain size, coherent scattering domain size (CSD), concentration of dislocations) on physical and chemical condition of samples deposition.

It is found that the films have a hexagonal structure ZnO. Obtaining films are textured with growth texture [100]. The values of CSD were equal to $L_{(100)}$ = (40.19-82.83) nm, $L_{(101)}$ = (30.64-70.11) nm. Lattice constants were equal a=0.33895 nm, c=0.51446 nm. Furthermore optimal deposition conditions of uniform single-phase films with controllable composition were found.

1. Opanasyuk A.S. Characteristics of structure formation in zinc and cadmium chalcogenide films deposited on nonorienting substrates / A.S. Opanasyuk, D.I. Kurbatov, V.V. Kosyak, S.I. Kshniakina, S.N. Danilchenko // Crystallography Reports. – 2012. – V.57, №7. – P. 927-933.

Optical Properties of Semiconductor Nanoheterostructures

Boichuk V.I.

Drohobych Ivan Franko State Pedagogical University, Drohobych, Ukraine

The investigation of optical properties of quantum-dot nanoheterostructures makes it possible to determine specific features of interactions between particles and physical conditions at the separation boundaries of the media.

The effect of quantum-dot shape on interlevel and interband absorption of electro-magnetic waves is considered. Absorption and photoluminescence intensities of different semiconductor heterosystems are calculated taking into account polarization vibrations and the real band structure of semiconductors.

Impurities are an important factor that enables one to change optical spectra of quantum-dot heterosystems. The properties of heterosystems when each quantum dot of the heterosystem contains one or two impurities is discussed. The dependence of optical absorption coefficient on the frequency of light dependent on the type of impurity in quantum dots is analyzed.

In case of a superlattice of spherical quantum dots the excitonic spectrum for quantum dots of various sizes and different distances between them is analysed. The change of the excitonic spectrum due to the change of dimensionality of the superlattice is researched.

Investigation of a Surface Morphology of Structures with Open Quantum Dots Obtained by a Liquid Phase Epitaxy

Bondarets S., Bykovsky S., Maronchuk I., Petrash A., Sanikovich D.

Sevastopol National University of Nuclear Energy and Industry

Recently a rapid growth of investigations of an obtaining and a determining of properties of low dimensional nanostructures are observed that connected with perspectives of developing of different devices with improved properties on a base of such structures.

Despite of achieved successes in a technology of a quantum dots obtaining by methods of a molecular beam and MOS-hydride epitaxy there are a number of problems that connected with both a high cost of equipment and defects in obtained structures. As an alternative, for a obtaining of nanoheteropitaxial structures we use method of a liquid phase epitaxy (LPE) with a pulse cooling of a substrate (PCS) [1]. A growing of such quantum sized structures requires not only high technological equipment but also a creation of new methodologies and devices for a supervision of a quality of manufacturing structures on different stages of production.

The main purpose of the work was an evaluation by methods of an atomic-force microscopy a quality of a surface morphology of InAs quantum dots in a matrix (a buffer layer) of GaP grown on silicon substrates with a different orientation by the method of a LPE with PCS.

Investigations of a surface morphology of samples of obtained structures with open quantum dots on a SMM-2000 microscope are carried out. Sizes of quantum dots under a forming them under same technological conditions of a growing are found. The seeding density of quantum dots on a silicon substrate with the orientation (111) disoriented on 4 degrees was established to be higher than on a substrate without any disorientation. In our opinion this is due to a presence of stairs on a disoriented substrate. The same is caused a presence of various sizes of quantum dots: big ones with a width about 150 nm and a height up to 70 nm and small ones (that presented on stairs situated under sum angle) with a width up to 120 nm and a height up to 40 nm.

The work was performed under support of State Agency on Problems of Science, Innovations and Informatization of Ukraine, St. Reg. No. NII 0112U004939.

1. Patent of Ukraine UA № 94699 Cl. C 30B 19/00, C 30B 29/00, H 01L 21/20 A process of a growing of epitaxial nanoheterostructues with arrays of quantum dots / I.E. Maronchuk, T.F. Kulyutkina, I.I. Maronchuk; the customer and the owner I.E. Maronchuk, T.F. Kulyutkina, I.I. Maronchuk; Ordered 20.09.2010; Published 10.06.2011, Bul. №5.

Optical Properties of Nanometer Thickness Ag Films

Borodchook A.V., Gavrelookh V. M.

Ivan Franko national university , Lviv, Ukraine

Ultrathin metal films with before percolation structure contain conductive (metal) and non conductive (dielectric) phase can be considered as nature objects, in which on the metal clusters with localized plasmons and plasmons associated with the oscillations of the electrons on the inner surfaces can co-exist. In percolation films the delocalized surface plasmon modes can be occured. The possibility of metal films fabrication with varying degrees of metal phase make them promising for the study of mechanisms of light interaction with free carriers in metal-dielectric nanocomposites [1].

We investigate the optical transmission and reflection spectra of Ag films with thickness of 1 – 20 nm deposited on glass substrates with thermal evaporation of the metal. Optical transmission and reflection spectra of films in the spectral range 350 – 1650 nm were studied. It was shown, that the transmission spectrum of Ag films have a minimum of 510-860 nm, the spectral position of which with increasing thickness of the film shifts to longer wavelengths. In particular, the Ag film thickness d = 2,2 nm has a maximum transmission at λ = 345 nm and a minimum at λ = 510 nm. In the transmission of the film a gradual increase at λ > 600 nm, which is as high as 92% at λ > 1300 nm. The reflection spectra of the spectral position of the minimum at λ = 310 nm is independent of film thickness, the more the intensity of the reflection at the minimum also varies slightly with thickness, where at λ > 350 nm reflection intensity increases dramatically. The absorption spectra of the films in which there is an intense absorption band with a peak position of which also depends on the thickness of the film was calculated. The investigation of size dependences of electrical resistivity shows that the percolation threshold for Ag films appears at 15 nm.

Linear dependence of the spectral position of the minimum bandwidth of the mass thickness of the film, based on which you can offer a relatively simple method for determining the thickness of the Ag film thickness in the nanometer range of their passing.

1. Є.Ф Венгер., А.В. Гончаренко, М.Л. Дмитрук. Оптика малих частинок і дисперсних середовищ. // НАН України, Ін-т фіз. напівпровідників.- К.: Наук. думка, 1999.- 347 с.

Effect of phonons on the position and shape of the exciton absorption band in semiconductor nanofilm

Derevyanchuk A.V., Pugantseva O.V., Kramar N.K., Kramar V.M.

Yuriy Fed'kovych Chernivtsi National University, Chernivtsi, Ukraine

The method of theoretical studying of the exciton absorption band characteristics in a flat double nanoheterostructure with single quantum well (QW) – nanofilm, is proposed. The method is based on the using of Feynman-Pines diagram technique [1], adapted for the studying of exciton-phonon interaction in nanofilm [2], and the effective mass approximation for carriers and model of dielectric continuum [3] – for phonon subsystem. Its use allows make the calculation of temperature changes of the position and shape of the exciton absorption band in nanofilms of different thickness.

Explicit form of the exciton-phonon coupling function, the mass operator of the Green's function of exciton-phonon system and the absorption band shape function with considering self-polarization effects and exciton-phonon interaction were found.

Concrete calculations were performed by using models of rectangular QW with finite ($Ga_{1-x}Al_xAs/GaAs/Ga_{1-x}Al_xAs$) and infinite (E-MAA/$PbI_2$/E-MAA) depth. Interactions with the longitudinal polarization optical (LO) and interface (I) phonons at different temperatures are taken in consideration.

The growth of half-width and long-wave shift of the main exciton line with temperature increasing was shown. Speed and absolute value of specified changes depends on the thickness of nanofilm by cause of different contributions of LO- and I-phonons in magnitude of the shift.

1. Tkach M.V. *Quasiparticles in Nanoheterosystems. Quantum Dots and Wires*. – Chernivtsi: Yu. Fed'kovych Chernivtsi National Univ., 2003. – 311 p. (in Ukrainian).
2. Kramar V.M., Tkach M.V. Exciton-phonon interaction and exciton energy in semiconductor nanofilms // Ukr. J. Phys. – 2009. – V. 54, № 10. – P. 1027-1035.
3. Huang K., Zhu B.F. Dielectric Continuum Model and Fröhlich Interaction in Superlattices // Phys. Rev. B. – 1988. – V. 38, № 18. – P. 13377-13386.

Structure of Surface Layer on Al-Be Alloy after Treatment in Electrolytic Plasma

Fedorenkova L.

Dnepropetrovsk National University, Dnepropetrovsk, Ukraine

Alloys of the system Al-Be-B, containing to 1% boron, in that a beryllium boride, being situated both on the beryllium grain boundary and crystallized with a phase on basis of aluminium, promotes alloy hardening without the relative lengthening reduction [1]. The hardening of binary Al - Be alloy by the borating in electrolytic plasma [2], in fact, can be an alternative to Al-Be-B alloy preparation.

The results of metallographic, X-ray structural and spectral analyses show the increase of microhardness and strength of the diffusive layer on Al-Be alloy (3,6%Be) after treatment in electrolytic plasma, takes place due to formation of nanosize structures of beryllium borides, concentrated mainly on the grain boundary and phases. According the X-ray structural analysis, the phases of Be_2B and Be_4B are mainly identified in a diffusive layer obtained after treatment in electrolytic plasma. The presence of high-boron compound BeB_6 is conditioned, evidently, by boron segregation at the local temperature action.

The compound of Be_2B is unstable and eutectoid decomposed on Be_4B and Be_2B_3 at a temperature below 985 °C [3]. However, in the non-equilibrium conditions of the electrolytic plasma with cooling and heating high-rates the Be_2B decomposition does not have time to result.

Accoding data of spectroscopic analysis the boron microalloying is no more than 1 %. The beryllium borides formation prevails over aluminum borides formation.

Microhardness of Al – Be alloy surface is in 2 - 3 times higher, than untreated surface and substantially depends on a Al - Be phases arrangement and size.

Hard strengthening beryllium particles in composition with the plastic aluminium matrix are barriers at motion of dislocations and resulted to diffusion reduction of dislocations and boron particles moving with them. All of it, in final analysis reduces the microhardness of layer.

1. Novoselova A.V., Molchanova L. V. and others. Research of Al - Be - B subsystem and boron influence on ABM-1 alloy properties. // Metallurgy and heat treatment of metals. – 1989. – №2. – P. 9-11.
2. Fedorenkova L. I., Spyridonova I.M. Features of saturation at treatment of aluminium and his alloys in electrolytic plasma. // Reports of NAS Ukraine. – 2002. – №11. – P. 71-75.
3. State diagrams of the double metallic systems. Edited by Lyakyshev N.P., M.: Engineering. – 1996-2000.

Study of Nanostructures on (100) Surface of In_4Se_3 Silver Intercalated Crystals by STM/STS and Auger Electron Spectroscopy

Galiy P.V.[1], Nenchuk T.M.[1], Mazur P.[2], Poplavskyy O.P.[3], Buzhuk Ya.M.[1], Yarovets' I.R.[1]

[1] *Electronics Department, Ivan Franko Lviv National University, Lviv, Ukraine*
[2] *Institute of Experimental Physics, University of Wroclaw, Wroclaw, Poland*
[3] *Chair of Life Safety, Vasyl Stefanyk PreCarpatian National University Ivano-Frankivs'k, Ukraine*

Study of In_4Se_3 layered semiconductor crystals, intercalated by metals, are promising due to the natural formation of nanostructures, in particular nanowires, which can be easy identified and studied with such research methods of the surface as STM / STS. Due to cleaving of In_4Se_3 crystals with the van der Waals interlayer interactions in ultra-high vacuum, the bulk metal nanostructures, which are formed in the process of intercalation, become surface ones.

The studied Ag intercalated In_4Se_3 layered crystals have been grown by the Czochralski method from the melt, containing silver up to 35 at.%. Further thermo treatment of In_4Se_3 crystals with silver impurity in evacuated quartz ampoules during 30 h at 540 K leads to Ag intercalation. The 09IOS-2 Auger spectrometer was applied for elemental analysis. Despite a high amount of silver in the melt, the Auger quantity analysis shows its (100) In_4Se_3 surface's averaged concentration less than 2.5–3 at.%. X–ray analysis of In_4Se_3(Ag) crystals reveals their well-layered structure. STM/STS data were obtained by a Omicron Nano-Technology STM/AFM System (Germany). The experiments were performed in UHV with base pressures less than $1 \cdot 10^{-10}$ Torr at room temperature. In_4Se_3(Ag) (100) surface was obtained by cleavage with stainless steel tip *in situ*.

Comparison of STM images for non and intentionally intercalated crystals' surface areas, obtained with the same resolution and bias, suggests about the nature of the nanostructures formation on (100) In_4Se_3 surfaces. For both surfaces we observed periodicity along directions ***b*** and ***c***, which doesn't differ from the received by X-ray diffraction for bulk (12.3 and 4.08 Å, respectively).

However, for In_4Se_3(Ag) also there are observed noisy areas without any periodicity with bright and dark patches which can be associated with the presence or lack of intercalate. Height differences for such patches don't exceed 15 Å, that corresponds to the thickness of crystal monolayer. Thus, STM reveals non uniform distribution of intercalated Ag on the cleavages in the nanoscale.

The presence of silver on the surface is also confirmed in the STS spectra, where along with the donor impurity states, originating from unintentionally doped In in In_4Se_3(Ag) crystals, appears the density of states corresponding to silver acceptor impurity.

Formation of High-Ordered Anodic Aluminum Oxide Films

Gasenkova I.V., Mazurenko N.I., Ostapenco E.V.

Institute of Physics, National Academy of Sciences of Belarus, Minsk, Belarus

This paper presents the results on the formation and investigation of high-ordered anodic aluminum oxide (AAO) films, obtained in a complex electrolyte on the basis of oxalic and phosphoric acids mixture.

Samples of AAO were obtained by two-step anodizing of aluminum foil grade A99 in a complex electrolyte under potentiostatic conditions at the various voltages. On the first step anodizing voltage was 90 V. The 30 micron thick layer was then removed in etching solution. The second anodizing step was carried out at the voltages of 100, 140 and 150 V and electrolyte temperature 2 ^{o}C with constant stirring.

The main morphological parameters (cell diameter, pore diameter) and the degree of order of the samples obtained were identified by scanning electron microscopy (SEM). Significant differences in surface morphology and cell size of anodic aluminum oxide obtained at various voltages has been established. Found that the greatest degree of order has the sample obtained at 150 V. Sample obtained at 100 V has a disordered structure. Cell diameter both pore diameter increases with increasing anodizing voltage. Cell diameters are 200, 280 and 300 nm and pore diameters are 70, 80 and 100 nm for samples prepared at 100, 140 and 150 V, respectively.

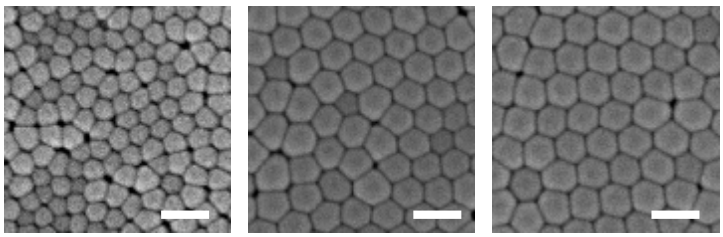

a) b) c)

Fig. 1 – SEM image of bottom surface of AAO, demonstrating different degree of order for samples obtained at 100 (a), 140 (b) and 150 V (c). Bar size is 400 nm.

The Surface Morphology of Nanoscale tin Dioxide Films Influenced by Precursor Properties

Grinevych V.S., Serdega B.K., Smyntyna V.A., Filevska L.M.

Odessa I. I. Mechnikov National University,Odessa, Ukraine

Thin films of oxide materials with nano-sized grains are widely used as sensors in modern gas analyzers, the transparent electrodes for solar cells, catalysts of the oxidation processes. The well-known production methods for nanosize tin dioxide, as well as other metal oxides, for sensitive elements of sensors are liquid-phase chemical methods: sol-gel method, chemical precipitation from solution, etc. The basic process for such technologies is the decomposition of thermally unstable tin compounds to form tin dioxide as the final product. The small number of such compounds, as well as limited and contradictory literature data on their physical and chemical properties causes the necessity for selection of a suitable precursor for nanosized tin dioxide.

We have proposed a technique for obtaining SnO_2 films based on the method of chemical precipitation from solution using polyvinyl acetate (PVA) as structuring agents. Supposedly the different drying processes determine conservation of water molecules in the precursor complex which influences the structure and morphology of the resulting film. The principal goal of the present work is the investigation of the mentioned precursor's peculiarities influence on the surface morphology of the obtained tin dioxide films.

The studies of tin dioxide films' surface morphology obtained from two different precursor complexes had established a significant effect of even small differences in the process of obtaining of tin dioxide precursor on the morphology of the surface and structure.

It was found that differences in the drying process used in the production of precursor complexes' films are the significant factor in the topological features of the films. The main feature which defines this influence is the bound water in the precursor's composition.

At the complex thermal decomposition the water, which is in its composition acts as a loosener, which allows to obtain tin dioxide films with nanograins of different sizes, depending on the precursor's type. Consequently, the use of a complex containing a hydrated precursor should be preferable in obtaining nano-sized tin dioxide films with a well-developed surface, thus providing high sensitivity of its physical parameters to the environmental changes and, and therefore, widely used as sensors. In the tin dioxide films obtained by the proposed technology the plasmons effects, investigated in [1] were registered. These investigations gave the possibility to determine optical parameters and structural peculiarities of the films.

1. V.S. Grinevich, L.M. Filevska, I.E. Matyash, L.S. Maximenko, O.N. Mischuk, S.P. Rudenko, B.K. Serdega, V.A. Smyntyna, B. Ulug. Thin Solid Films 522 (2012) 452–456.

Kinetics Doping Quantum Dots InAs with Bi Impurity by Low-Temperature CVD-Metods

Guba S.K.[1], Petrovich R.Y.[2]

[1]Lviv Polytechnic National University, Semiconductor Electronics Department,
[2]Lviv Polytechnic National University, Computational Mathematics and Programming Department, Lviv, Ukraine

Growth of $In_xGa_{1-x}As/GaAs$ heterostructures with embedded arrays of quantum dots (QD) InAs CVD-metods at low temperatures is actual to the needs of nanoelectronics.

QD InAs in GaAs matrix is formed by Stranskij-Krastanow mechanism. Growth kinetics and stress distribution in the QD matrix affects the size, shape and location in the matrix [2]. Features of the electronic structure of QDs depends not only from final dimension and form, but also from the influence of internal elastic deformations [3]. One of the management practices of forming homogeneous coherently deformation InAs QDs is their isovalent impurity doping Bi [4]. Therefore creation of model concepts of formating mechanism of of InAs QDs in GaAs matrix in their isovalent impurity doping Bi at low temperature CVD-metods is scientific novelty.

On the basis of model representations described [5] the growth model of GaAs / InAs (Bi) is constructed for a low temperature CVD-metods. In the result the simple description of gas dynamics system is obtained. From the analysis of surface kinetics processes, the expressions that bind growth rate and concentration of Bi isovalent impurities with local concentrations are received in the gas phase and growth temperature CVD-metods. Using these expressions could quantitatively describe the isovalent doping of InAs QDs Bi isovalent impurity, find the change in growth rate and concentration of impurities along the GaAs substrate in direct-flow horizontal reactor.

The influence of input concentration of a component in the gas phase, the flow rate propellants and distribution of temperature field along the GaAs substrate for the growth rate and concentration of isovalent impurity Bi in InAs quantum dot are investigated.

1. С.К. Губа. Технология и конструирование в электронной аппаратуре. 1998. **2**. 40-43.
2. В.Г. Дубровский. ФТП. 2006. **40**. 1153-1160.
1. Б.В. Новиков, Г.Г. Зегря, Р.М. Пелещак, О.О. Данькив, В.А. Гайсин, В.Г. Талалаев, И.В.Штром, Г.Э. Цирлин. ФТП. 2008. **42.** 1094-1101 .
4. Р.М. Пелещак, С.К. Губа, О.В. Кузык, И.В. Курило И.В., О.О. Данькив. ФТП. 2013. **47**. 324-328.
5. С.К. Губа, Р.Й. Петрович. Нові технології. **2**. 2008. 230 –235.

The Compositional Material SiO_2 - C as Cathode for Lithium Power Sources

Gumenyak V.V., Myronyuk I.F., Mandzyuk V.I.

Vasyl Stefanyk Precarpathian National University, Ivano-Frankivsk, Ukraine

The modern achievements in area of inorganic chemistry, which touch the receipt of materials with the particles of nanometric scale, give a hope, that new electrode materials for lithium electrochemical power sources with high power capacity will be created on their basis in the near time. The materials with a channel or layered structure are most suitable for the intercalation processes of current formation in such sources. Electrode materials must have high conductivity, sorption capacity accordingly to the lithium ions, their structure must provide the rapid transport of lithium to the place of their localization.

The fumed silica has an amorphous structure and can be applied as electrode material for the lithium power sources. A basic problem for such application is low conductivity of aerosil (according to data of impedance spectrometry it makes 0,14 $mkOm^{-1} \cdot m^{-1}$ for aerosil A-300). Therefore it is necessary to apply current-conducting additions at forming of electrode mixture.

In order to increase a conductivity of aerosil and give up application of current-conducting addition at forming of cathode material, we got an electrode material by gas-phase deposition of two-dimensional graphite layers (graphene) on the SiO_2 particles surface. The content of graphene in composite made $16 \div 20$ weight %. This material owns greater specific conductivity in comparison with initial material (49 $Ohm^{-1} \cdot м^{-1}$).

An electrochemical element was formed on the basis of composite got. Metallic lithium was used as anode, 1 M solution of $LiBF_4$ in γ-butirolactone was as electrolyte. Electrochemical introduction of lithium ions was conducted in the galvanostatic mode at the current density of 40 mkA/sm^2. Using dependence of voltage of element from discharge time, the values of the specific capacity C_{sp} and the specific energy E_{sp} were calculated. According to the experimental data, electrochemical element on the basis of SiO_2 – C composite possesses very high specific capacity which makes 3272 mA·h/g. Specific energy calculated as an area under discharge curve $U = f(C_{sp})$ makes 6334 W·h/kg.

X-ray Spectral Investigation of Electronic Structure Peculiarities of Graphite Nanosheets

Ilkiv B.[1], Foya O.[1], Petovska S.[1], Sergiienko R.[2], Vasylyna O.[3]

[1]*Frantsevich Institute for Problems of Materials Science of NASU, Kyiv, Ukraine;*
[2]*Physics-Technological Institute of Metals and Alloys of NASU,Kyiv, Ukraine*
[3]*National Technical University of Ukraine "Kyiv Polytechnic Institute",Kyiv, Ukraine*

Graphite nanosheets electronic structure was investigated by using the ultrasoft X-ray emission spectroscopy (USXES) method. The x-ray emission C$K\alpha$ ($K \rightarrow L_{II,III}$ transition) bands reflecting the energy distribution of the C2p-like states were obtained for graphite nanosheets and (CNCs)@(FePt) carbon nanocapsules and graphite nanosheets mixture. X-ray diffraction, scanning and transmission electron microscopy investigations were used in addition to USXES.

Comparison of emission spectra of (CNCs)@(FePt) carbon nanocapsules and graphite nanosheets mixture and carbon onions showed that binding energy of electrons providing sp^n ($2<n<3$) σ-bonds in carbon layers of (CNCs)@(FePt) nanocapsules is greater than that in carbon onions.

It was revealed that after magnetic separation of metal cores of (CNCs)@(FePt) nanocapsules overlapping of the $p\pi$–orbitals over the surface of graphite nanosheets increases approaching to that in graphite.

It was found that in graphite nanosheets smaller mixing of σ+π states occurs in comparison to (CNCs)@(FePt) nanocapsules and graphite nanosheets mixture since nanosheets after magnetic separation became flat and $p\pi$-orbitals overlap less with sp^2–orbitals of σ-type.

Synthesis of CdS Nanocrystal using Ultrasonic Bath

Kapush O.A, Trishchuk L.I., Mazarchuk I.O., Tomashyk V.M., Tomashyk Z.F., Kuryk A.O., Budzulyak S.I.

V.Ye. Laskaryov Institute of Semiconductor Physics of NAS of Ukraine, Kyiv, Ukraine

Semiconductor nanocrystals (NCs) exhibit unique size and shape-dependent optical properties due to the quantum confinement effects and thus may find a wide range of applications in optoelectronic devices, photocatalysis, solar energy conversion and biological imaging and labelling. The NCs of CdS, CdSe and CdTe are the group of nanostructures that have been mostly investigated because of their high luminescence efficiency and easily adjustable luminescence from ultraviolet to near infrared region depending on NCs sizes. Such nanostructures are perspective for optoelectronic devices and biological imaging as well as labelling applications. As a direct wide bandgap (2.42 eV) semiconductor, CdS NCs may be potentially used in optoelectronics of nonlinear optics and light emitting diodes.

Currently, there are many different methods of colloidal NCs obtaining for using in various fields of science and technology. Physical methods provide a high degree of control system parameters, but they are quite complicated in implementation and require bulky and expensive equipment. Chemical methods are simple and economical, more profitable than the others methods, thus they allow to obtain the CdS NCs of small sizes, even to several nanometres.

The purpose of this work is the experimental study of synthesis of CdS NCs. The CdS NCs were prepared via sulphide ion precipitation by cadmium ions under an argon atmosphere in an ultrasonic bath. CdI_2 and $Na_2S_2O_3$, L-cysteine ($HOOC–CHNH_2–CH_2–SH$), and deionized water were used as starting chemicals, a stabilizer of the particle surfaces, a dispersion medium, respectively. The obtained solutions were irradiated at 20 KHz frequency for 3 hours in an ultrasonic bath.

The photoluminescence characteristics of solutions were studied in detail. Investigations of optical properties of solutions have been performed in the quartz and polystyrene cuvettes using the dispersion environment for comparison. The photoluminescence spectra have been measured at room temperature.

The CdS NCs obtained by this method are not limited by any solid surface, thus they can be produced in large quantities in the reaction chamber with the further inclusion in the polymer matrix. This allows use of these systems for the manufacture of various components of working microelectronic and optoelectronic devices.

Preparation and Investigation of the Properties of Porous Ge

Kidalov V., Demyanenko-Mamonova V.

Berdyansk State Pedagogical University

To date, the Ge semiconductor technology plays a major role, and is used for the manufacture of sensors or special filters. The literature on the electrochemistry describes the preparation of porous germanium [2,3], but the process of pore formation is not studied enough.

Germany has traditionally applied in various fields of technology, and in recent years have increasingly used and nanostructures based on it. In the last few years successfully developed techniques to obtain different nano-objects, which include electrochemical etching.

Porous germanium was obtained earlier by electrochemical etching in [1, 4-5]. But the difference is to obtain test sample has closed.

Micrograph of the etched sample (Fig. 1) was obtained with a scanning electron microscope JSM-6490. It presents the pores closed, which were obtained after etching of the germanium crystal in a solution C2H5OH: HNO3: HF = 1:1:0,4 for 20 minutes. Clearly seen on the entire surface of the crystal formation and pore distribution.

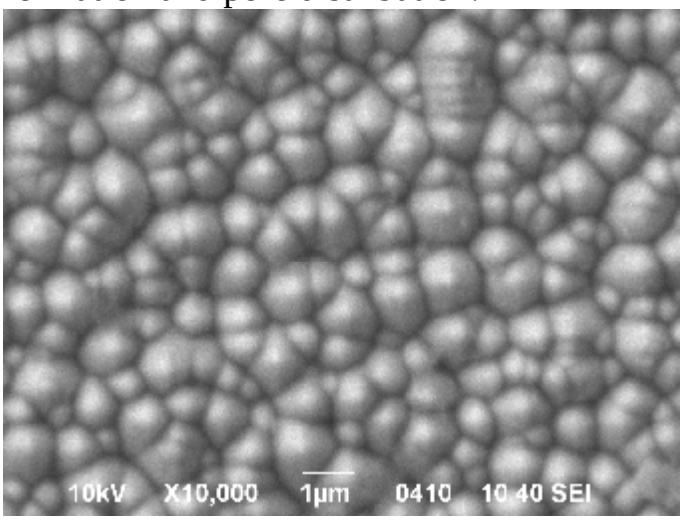

Fig. 1. SEM image of the surface of the porous n-Ge, the etching time t = 20 min, the electrolyte C2H5OH: HNO3: HF = 1:1:0,4, cavitation voltage 16-17 V, current density of a porous structure j = 5,4 ÷ 100 mA.

1. Porous III-V Semiconductors: online book. Porous III-V Semiconductors by I. Tiginyanu, S. Langa, H. Foell and V. Ursachi

2. А. И. Чукавин, Р. Г. Валеев, А. Н. Бельтюков. Синтез наноразмерных структур на основе германия в матрице пористого оксида алюминия. Вестник удмуртского университета. 2011. Вып. 2

3. S. Langa, J. Carstensen, M. Christophersen, K. Steen, S. Frey, I. M. Tiginyanu, and H. Föll. Uniform and nonuniform nucleation of pores during the anodization of Si, Ge, and III-V Semiconductors

4. S.-S.Chang,R.E.Hummel. Comparison of photoluminescence behavior of porous germanium ands park-processed Ge. Journal of Luminescence86(2000)33}38

5. S. Langa, M. Christophersen, J. Carstensen, I. M. Tiginyanu and H. Föll. Electrochemical pore etching in Ge. Rapid Research Note

The Electrical Conductivity and Thermoelectrical Power of Nanometer Thickness Palladium Films

Kravchenko O. E.

"Ivan Franko" Lviv National University, Lviv, Ukraine

The investigation of kinetic size phenomena in thin metal films allow to obtain useful information about the electronic structure of limited size samples and the charge scattering mechanisms on static defects. It is interesting to ascertain the minimum thickness of film layers in the framework of classic and internal size effects in which the electronic structure of sample are identical of bulk metal electronic structure. Setting the limits of theoretical models suitability which describe size kinetic phenomena in metal film thermoelectric power allow to estimate the critical films thicknesses at which electronic structure of the samples are changed. The investigation of palladium films electrical conductivity and thermoelectric power size dependence allowed us to obtain information about minimum film thickness at which the energy band structure became similar to electronic structure of bulk films.

The production and investigation of metal films was conducted under ultrahigh vacuum conditions (residual gas pressure ~ 10^{-7} Pa) in glass experimental devices. The technique used in this work is similar to the method [2]. Palladium films deposited on glass substrate cooled to 78 K (clear or coated germanium underlayers mass thickness of 1-2 atomic layers) with speed deposition 0,1-0,2 nm/s by condensation of thermally evaporated metal. The control of germanium underlayers and metal film thickness was performed by shift of quartz vibrator resonance frequency placed in the metal vapor flux (Ge or Pd). Palladium films were annealed for stabilization structure and electrical properties during one hour at a temperature of 370 K. Palladium films of growing thickness were obtained by additional metal applying.

The experimental dependence of the resistivity $\rho = \rho(d)$ and temperature coefficient of resistance $\beta = \beta(d)$ can be quantitatively described by polycrystalline inhomogeneous layer thickness model [3, 4], which combines theory impact of surface (Fuchs-Sondheimer and Namba) and grain-boundary (Mayadasa-Shatskesa, Telle-Tosse-Pishara) charge carriers scattering on the kinetic coefficients and parameters of charge transport in films of metals. It was shown that germanium sublayers reduce average of crystallites linear dimensions in palladium films and contribute the electrically continuous film thickness formation of 3 nm in comparison with the films grown on clean glass substrate. Analysis of palladium films resistivity and thermoelectric power size dependence deposited on germanium sublayers show that the dimensional dependence well described by a model of two independent groups of current carriers with different effective masses. It was shown that in the film of palladium with average linear dimensions of crystallites D = 10 nm, the ratio between the conductivity of different groups of charge carriers is $\sigma^+/\sigma^- = 0{,}8$, and for palladium films deposited on germanium sublayers with mass thickness of 0,5 nm; $\sigma^+/\sigma^- = 0{,}75$. The formation of the electronic structure which identical to bulk metal electron structure is compiled in electrically continuous palladium films close to 5 nm.

1. Г.А. Катрич, В.В. Климов, Л.С. Мирошниченко, Свойства малых частиц и островковых металлических пленок (Киев: Наукова думка: 1985).
2. А. П. Шпак, Р. І. Бігун, З. В. Стасюк, Ю. А. Куницький, Наносистеми, наноматеріали, нанотехнології, 8, вып. 2: 1001 (2010).
3. З.В. Стасюк, А. І. Лопатинський, Фізика і хімія твердого тіла, 2, № 4: 521 (2001).
4. Z.V. Stasyuk, Journ. Phys. Studies, 3, 102 (1999).

Absorption of electromagnetic irradiation by aqueous suspensions of noble metal particles

Kryvoruchko Ya.S.[1], Lerman L.B.[2]

[1]*National University of Bioresources and Nature Management of Ukraine, 15, Heroes of Defence Str., Kyiv-41, 0341, Ukraine*
[2]*Chuyko Institute of Surface Chemistry National Academy of Sciences of Ukraine, 17, General Naumov Str., Kyiv, 03164, Ukraine*

Aqueous suspensions of nanoparticles, pure precious metals, particularly gold and silver or their mixtures, are widely used in medicine as diagnostic products for certain types of diseases. Effectiveness of their use is largely determined by the distribution of particles relative to the composition, shape and size, as defined by traditional chemical methods is very complicated. Therefore, the search for natural non-destructive methods of identifying the parameters of nanoparticles of noble metals is of great practical importance. Among these methods, the method stipulates of measurement of their optical properties, including absorption and reflection coefficients, and surface plasmon resonance frequency. Using the Drude model to describe the frequency-dependent dielectric functions of metals, calculated absorption coefficients of aqueous suspensions of binary, ternary (Fig. 1), and four-component mixtures (Fig. 2) of nanoparticles of noble metals.

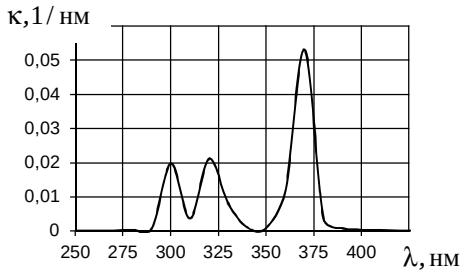

Fig.1. Absorption in suspension of three-component mixtures of gold, silver, and mixed nanoparticles

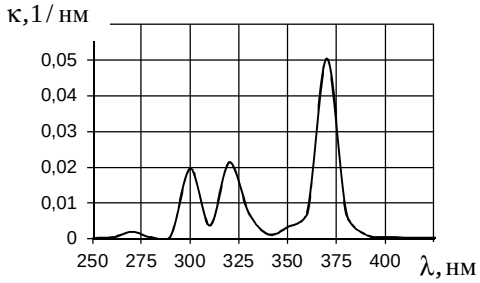

Fig. 2. Absorption in suspension of quadruple mixture of gold, silver, mixed nanoparticles and gold particles covered silver

Calculations have shown that aqueous suspensions of several types includeing gold and silver nanoparticles (dispersed matrix system with two types of inclusions), for a matrix disperse system with three types of inclusions of gold, silver and mixed (gold + silver) nanoparticles, as well as for matrix disperse system formed by gold, silver, mixed (gold + silver) nanoparticles and particles of gold core and silver shell, the number of extrema in the absorption spectra relates to the number of fractions. For one type of inclusions single maximum is present for inclusions of two types - two for three types - three, to four types - four. The extrema points determine the frequency of surface plasmons for each faction.

Synthesis and Anticorrosion Activity of the Zinc Phosphate Nanoparticles

Kytsya A. R.[1], Bazylyak L. I.[1], Zin' I. M.[2], Korniy S. A.[2]

[1]*Physical Chemistry of Combustible Minerals Department*
Institute of Physical-Organic Chemistry & Coal Chemistry named after L. M. Lytvynenko
National Academy of Sciences of Ukraine, Lviv, Ukraine
[2]*Physical-Mechanical Institute named after G. V. Karpenko*
National Academy of Sciences of Ukraine, Lviv, Ukraine

Using of the protective coatings having the different pigments as the corrosion inhibitors has a much wide application among the different protective methods of the fabricated metals from the corrosion. Taking into account the ecological safety and also modern demands to such coatings, zinc *ortho*–phosphate and also the compositions on its basis have a much wide application as the corrosion inhibitors, though the anticorrosion activity of the zinc *ortho*–phosphate on the initial stages is some lesser, than in a case of the conventional plumbum– and chromium–containing pigments using. This fact is caused by a low solubility of zinc *ortho*–phosphate in water. An improvement of the anticorrosion activity of zinc *ortho*–phosphate can be achieved at the expense of its particles sizes diminishing to the nano–level. In such a way, its solubility is increased, the content of a pigment into the composition is decreased, and its sedimentation stability is also increased.

We have developed the method of the zinc phosphate nanoplates (by thickness 20 *nm*) obtaining [**1-2**]. Proposed by us technique is energy–efficient and doesn't require the complicated instrumental equipment. That is why it can be realized into industrial scale under the minimal expenditures.

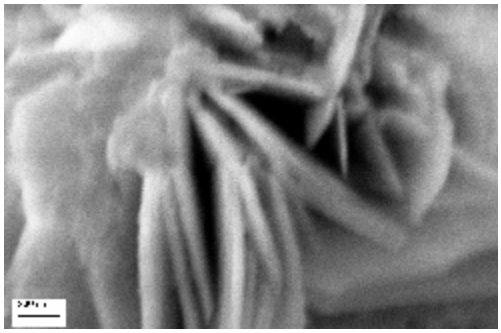

With the use of impedance method the anticorrosion activity of the obtained pigment has been investigated. It was determined that the addition of the nanosized zinc *ortho*–phosphate to the corrosion medium considerably decreases the corrosion current of alloy material D16 in comparison with the industrial pigment *Novinox PZ02*.

1. Pokhmurskyj V. I., Kytsya A. R., Bazylyak L. I., Zin' I. M., Korniy S. A., Hrynda Yu. M. Method of Zinc Phosphate Nanoparticles Obtaining // *Application for a patent of Ukraine obtaining №* U 2012 09848. – 14. 08. 2012.
2. Pokhmurskyj V. I., Zin' I. M., Kytsya A. R., Bilyj L. M., Korniy S. A., Zin' Ya. I., Khlopyk O. P. Undercoat composition for anticorrosive coating // *Application for a patent of Ukraine obtaining №* U 2012 09348. – 30. 07. 2012.

***Financial support**: grant №* 4.11.1.42–12/K–2 *«Nanotechnologies & Nanomaterials» (National Academy of Sciences of Ukraine).*

The Application of Nanotechnologies and Nanomaterials for Improvement of Ceramic Implants

Lashneva V.V., Shevchenko A.V., Dudnik E.V., Tsukrenko V.V., Ruban A.K., Matveeva L.A.[1)], Nelyuba P.L.[1]

I.N.Frantsevich Institute for Problems of Materials Science of NASU, Kiev, Ukraine
[1]*V.E. Lashkaryov Institute of Semiconductors Physics of NASU, Kiev,Ukraine*

Ceramic implants are widely used for restoration of dysfunction of a living organism in traumatology and orthopedics oral surgery, dental and other medicine. As compared with metal implants they have a wider range of chemical, mechanical and other properties and the possibility to regulate wide-range functionality and life time in the body. Ceramic implants completely exclude the possibility of galvanoza fenomena.

Ceramic implants are inserted into the body for a long time (about 20-30 years). They must work stably and reliably in a biologically aggressive multifactorial media often under the considerable stress. A high level of physical and chemical characteristics of the ceramic implants can be achieved only through using nanocrystalline powders and new technologies.

A new zirconia-based ceramic material was designed for production ceramic implants with composition ZrO_2 (4,5-5,4% Y_2O_3, 2-3% CeO_2)+10% Al_2O_3. They are characterized by high strength, optimal microstructure and increased low-temperature stability in wet environment due to combined stabilization of ZrO_2 by yttria, ceria and the addition of alumina.

The developed material demonstrates flexural strength above 600 MPa, density over $5.8 \cdot 10^{-3}$ kg/m^3, the average grain size – not more than 0.4 μm, the phase composition – tetragonal solid solution with traces (below 3%) of monoclinic ZrO_2-based phase.

The wear properties of high-molecular polyethylene "Chirulen", which is currently used in mobility junctions almost in all hip joint construction, with a friction pair of developed ceramic is compared with the friction wear of ceramics based on alumina and CoCrMo alloy.

The low-temperature stability of the material determined by the method of "accelerated ageing" showed that phase composition and strength did not vary significantly after samples ageing under hydrothermal conditions of 7 h at 140 °C.

This suggests that the physical and chemical properties of the developed material will remain stable for at least 20 years in the human body.

Dental implants, artificial tooth roots and ball elements (heads) of hip joint were produced from developed material.

Nanostructure of Chalcogenide Amorphous Thin Films

Lykah V., Dyakonenko N.

National Technical University "Kharkov Polytechnic Institute", Kharkov, Ukraine

It is shown experimentally that the chalcogenide films based on bismuth have an amorphous nanocluster structure. The interaction energy of atoms in a disordered state was calculated, the order parameters were entered. The equations for the boundaries of clusters were obtained. The order parameters dependences of the coordinate at the boundary of the clusters were found.

The resistive evaporation method of A^1BiC^{V1} (A^1-Li, K, Na, Rb, C^{V1} -S, Se, Te) powder compounds was used to obtain the samples. The films were condensed on glass substrates at a temperature T_s = 300 K at a rate 0.1-0.5 nm/s in a vacuum 1mPa. The thickness of the samples was 40-80 nm. The structure was investigated by transmission electron microscopy. It is shown that an inhomogeneous (clusters) of size 5 to 10 nm appeared in the amorphous film as the result of statistically homogeneous atoms distribution transforming. These structures are characterized not only neighbors, but also the intermediate-range order in the arrangement of the atoms. The emergence of nanoclusters in amorphous chalcogenide films due to partial self-organization of matter under the influence of forces of the chemical bond.

Two interacting order parameters have been chosen for theoretical description of film structure: the mean square deviation of angle from optimal average value in covalent bond and the average interatomic distance. The free energy functional has some local minima on the plane of order parameters. The minima correspond to high density state with optimal angle and optimal interatomic distance. Different minima correspond to different mutual orientation of atoms in covalent bond. The initial distribution of angles and distances disorientation between randomly deposited atoms in the film corresponds to the minima in the plane between the order parameter and has a relatively high energy. The energy optimization under the high temperatures leads to changes in the position of the atom and the crystallization. But at low temperatures redistribution of atoms is difficult, leading to local optimization of energy. This streamlined site or cluster can match the domain (analogue of magnetic one). The area may not be large, since the optimization angle accompanied by an increase in bond length. Areas of low density between clusters corresponding to the boundaries of areas are the topological defects. On the plane of order parameters was selected trajectory of the cluster boundary. For the interatomic potential model the energy of the bond and the size of the clusters were calculated. Cluster boundary gives a positive contribution to the total energy; the clusters give a negative contribution to the energy of the system: a general decrease in energy level is due to the establishment of the reorientation of the links and change of their length.

The Thermal Activation Effect of Porous Carbon Material on Capacity Parameters of Lithium Power Sources on its Basis

Mandzyuk V.I.[1], Budzulyak I.M.[1], Nagirna N.I.[2], Rachiy B.I.[1]

[1]*Vasyl Stefanyk Precarpathian National University, Ivano-Frankivsk, Ukraine*
[2]*The College of Electronic Devices, Ivano-Frankivsk, Ukraine*

One of basic ways of improvement of existing electrochemical technologies and creation new ones is development of new electrode materials which own necessary properties – high electro-catalytic activity, stability and cheapness of initial components [1]. The given requirements can be well-to-do at creation of electrodes on the basis of porous carbon materials (PCM), which are actively used as electrode materials for the primary and second chemical power sources [2] and supercapacitors [3].

We have shown earlier that the specific energy parameters of lithium power sources on the PCM basis carbonised by hydrothermal method depend substantially on the carbonisation temperature, which effect on forming of material porous structure. The most value of capacity was got for an element on the basis of material carbonised at a temperature 750°C (C_{sp} = 1138 mA·h/g). For the increasing of capacity characteristics we conducted the thermal activating of given standard at temperatures 300, 400, 500, and 600°C at different times of activating in air atmosphere. The cathodes of electrochemical power sources of PCM : teflon = 96 % : 4% composition were formed on the basis of got materials. Lithium foil was as a counter electrode, 1 M solution of $LiBF_4$ in γ-butirolactone – as an electrolyte. Specific capacity was calculated according a formula $C_n = It/m$, where I – discharge current, t – discharge time, m – mass of cathode active material. As results of researches showed, the electrochemical system on the basis of PCM activated during 2,5 h at temperatures of 400 and 500°C owns the most specific capacity: C_{sp} = 1511 mA·h/g (400°C) and C_{sp} = 1500 mA·h/g (500°C). Thus, an application of the thermal activating of PCM gave the possibility to increase a discharge capacity on 32 % comparatively with initial material.

1. Tarasevych M.R. Electrochemistry of carbon materials. – M.: Nauka, 1984. – 253 p.
2. P. Novak, D. Goers, M.E. Spahr. Carbon materials in lithium-ion batteries / in *Carbons for* Electrochemical Energy Storage Systems (F. Béguin and E. Frackowiak, Eds.), CRC Press - Taylor and Francis Group, Boca Raton-New York, 2002. – P. 263-328.
3. B.E. Conway. Electrochemical supercapacitors. Scientific fundamentals and technological applications. – New York: Kluwer Academic Plenum Publishers, 1999. – 698 p.

Studies of ZrO_2 Electrolyte Thin Film Thickness on the All-Solid-Thin Film Electrochromic Devices

Patel K.J.[1], Desai M.S.[2], Panchal C.J.[2], Mehta P. K.[3], Odnodvorets L.V.[4], Velykodnyi D.V.[4], Protsenko S.I.[4]

[1] *BITS Education campus, Gujarat, India*
[2] *The M.S. University of Baroda, Gujarat, India*
[3] *The M.S. University of Baroda, Gujarat, India*
[4] *Sumy State University, Sumy, Ukraine*

The electrochromic device (ECD) controls the optical properties such as optical transmission, absorption, reflectance, and/or emittance in a continual but reversible manner on application of a voltage. This property enables the ECD to be used for numerous applications like smart-window, EC mirror, and EC display. The basic structure of solid-state thin film ECD consists of glass substrate / transparent conducting electrode (TCO) / ion-storage layer (IS) / solid-electrolyte / EC layer / TCO. In solid-state ECD the electrolyte is the most important layer for ion transport between EC layer and ion-storage layer. We have prepared an all solid-thin film ECD structure in our laboratory consisting of layers ITO/NiO/ZrO_2/WO_3/ITO on a glass substrate. The device performance includes transmittance modulation and open circuit memory effect, which is affected by the thickness of the electrolyte used in the devices. In the present paper, the optimization condition of the ECD performance as a function of variations in the ZrO_2 electrolyte thin film thickness is discussed. The indigenously developed devices' characteristics like optical modulation and memory effect with different ZrO_2 thickness are also been presented. The transmittance modulation and memory effect was found to improve with increases of ZrO_2 electrolyte. The photograph for bleached state and colored state of ECD present in Fig. 1.

Fig.1. The picture of ECD in colored and bleached state

The device having 5000Å ZrO_2 thickness shows good transmittance modulation (56 %) in wavelength range of 450 - 1000 nm with good open-circuit memory effect of 170 min.

Hydrothermal Synthesis of Nanostructured Zirconia of Predetermined Modification

Pavlenko T.V., Rudkovska L.M., Omelchuk A.O.

V.I.Vernadskii Institute of General & Inorganic Chemistry, Kyiv, Ukraine

This paper presents results of studies on the synthesis of nanostructured zirconia from zircon concentrate decomposition products. Concentrate was decomposed with alkaline solutions under hydrothermal conditions in the presence of calcium fluoride to form zirconium-containing compounds of different chemical and phase composition (sodium fluorozirconates, zirconia or their mixture) and calcium silicates. It has been found that depending on the chemical and phase composition of decomposition products, predetermined modifications of nanoscale zirconia can be obtained by hydrothermal synthesis. Unlike the known methods for the preparation of zirconia, the method developed makes it possible to use calcium ions that are present in zircon concentrate decomposition products as a tetragonal modification stabilizer. In the samples synthesized, specific surface areas and their porosity as a function of synthesis conditions have been studied. Specific surface area was measured by the BET method, nitrogen sorption-desorption method.

Porosity and specific surface area of nanostructured ZrO_2 samples

ZrO_2 modification	monoclinic		tetragonal	
Synthesis conditions (250°C)	6 h	8 h	6 h	8 h
Specific surface area (BET), m^2/g	38,5	31,3	91,9	44,6
Specific mesopore volume, cm^3/g	0,17	0,16	0,23	0,17
Mean mesopore radius, Å	89,7	102,1	49,3	74,9

The fractal structure of samples was investigated by the small-angle X-ray scattering (SAXS) method.

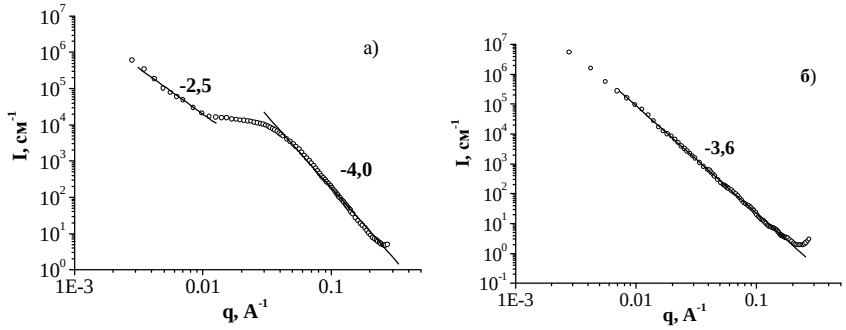

Fig.1. SAXS curves for samples: t – ZrO_2 (a), m – ZrO_2 (b).

Analysis of the data obtained (Fig.1(a)) shows that primary particles aggregate to form mass fractals of the same size with the mean diameter d_s =19,6 nm and undeveloped surface. The order of the types of fractal aggregation of the sample t – ZrO_2 is S → M (primary particle → aggregate). The curve (b) in Fig.1 has one straight line portion, indicating that there is no fractal aggregation in m – ZrO_2.

Temperature Dependence of Electron's Ground-State Energy in E-MAA/PbI_2/E-MAA Nanofilms

Pugantseva O.V., Kramar V.M.

Yuriy Fed'kovych Chernivtsi National University, Chernivtsi, Ukraine

Within the effective mass approximation for the electrons and dielectric continuum model – for phonons, the calculations of temperature changes of the ground subband bottom of the electron energy spectra in a flat double nanoheterostructures with quantum well (QW) – nanofilms (NF), where performed. Methods of the Green's function theory in the Feynman-Pines technique [1], adapted for the studying of electron-phonon interaction (EPI) in NF [2] had been used.

The analytical expression of the ground-state energy of the electron and the mass operator of electron-phonon system's Green's function in the infinitely deep QW considering the self-polarization effects and EPI with longitudinal (LO) and interface (I) phonons are obtained. Numerical calculation is also performed for the lead iodide NF embedded in organic medium – ethylene-methacrylic acid (E-MAA) copolymer.

It is shown that temperature growth causes nonlinearly increasing of the absolute value of long-wavelength shift displacement (Δ) of the ground subband. Velocity of such growth depends on the thickness of NF (Fig. 1), because the contributions from LO- and I-phonons in the magnitudes of Δ are different.

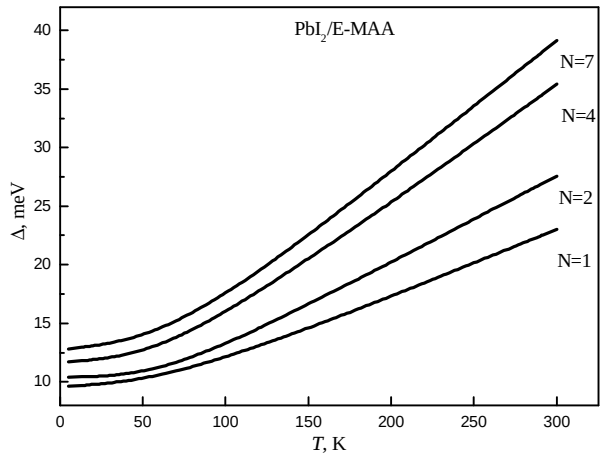

Fig. 1. Temperature dependence of electron's ground-state energy long-wave shift (Δ) in E-MAA/PbI_2/E-MAA nanofilms (*N* is number of PbI_2 layers)

1. Tkach M.V. *Quasiparticles in Nanoheterosystems. Quantum Dots and Wires*. – Chernivtsi: Yu. Fed'kovych Chernivtsi National Univ., 2003. – 311 p. (in Ukrainian).
2. Tkach M.V., Kramar V.M. Thermal genesis of bottom of main electron's energy band in a flat nanofilm // Ukr. J. Phys. – 2008. – V. 53, № 11. – P. 1110-1118.

Carbon Nitride Nanostructed Films Doped with Europium Oxide

Shemchenko E.I., Varyukhin V.N., Shalaev R.V., Proskurenko M.V., Prudnikov A.M.

Donetsk Institute for Physics and Engineering of Ukrainian Academy of Sciences, Donetsk, Ukraine.

In the hydrogenated diamond-like carbon films doped with rare earth, annealing method is used for creating of the optimal ligand structure of the luminescent center. Annealing in oxygen worsens the film structure, which leads to great losses in the transmission of excitation energy from the matrix to the rare earth ion [1,2]. The magnetron sputtering used to obtain of nanostructured carbon nitride films, consist of the arrays of nanocolums [3]. These structures allow the material doping no metal, but its oxide, thus avoiding annealing and provided the optimal ligand environment REM ion during film growth.

The goal of this work was to obtain luminescent nanostructured carbon-nitrogen films with optimal ligand environment for the REM ion. The films doped with europium oxide in the growth process, were obtained by magnetron ion plasma coscattering ot the combined target on GGG single crystal substrates.

The luminescence spectra of the samples were measured on the spectrofluorometer, which was assembled on the basis of monochromators «МЗД -2».

It was found luminescence in the obtained films, with transitions $^5D_0$-$^7F_1$ (595 nm) and $^5D_0$-$^7F_2$ (617 nm) of the ion Eu^{3+}. Excitation mechanism was implemented in the matrix, followed by non-radiative energy transfer to the ion Eu^{3+}.

In addition, it was found by elementwise control impurities in the films with the aid of a scanning electron microscope, an abnormally high amount of oxygen at magnetron current values from 38 to 55 mA.

1. Ястребов С.Г., Аллен Т., Иванов-Омский В.И., Чан В., Жукотински С. Оптические свойства плёнок аморфного гидрированного углерода, осаждённых из плазмы тлеющего разряда // Письма в ЖТФ. – 2003. – Т.**29**, №20. – С.49–57.
2. Иванов-Омский В.И., Матвеев Б.А. Отрицательная люминесценция и приборы на её основе. Обзор // Физика и техника полупроводников. – 2007. – Т.**46**, №3. – С.257–268.
3. Shalaev R.V., Ulyanov A.N., Prudnikov A.M. et al. Noncatalytic synthesis of carbonnitride nanocolumns by dc magnetron sputtering // Phys. Status Solidi. – 2010. – A **207**, №.10. – P.2300–2302.

Mass Transport in Nanoscale Metals Films under the Influence of Plasma Discharge

Sidorenko S.I., Voloshko S.M., Kotenko I.E., Basyh V.A.

National Technical University of Ukraine "Kyiv Polytechnic Institute", Kyiv, Ukraine.

Plasma technologies based on gas discharge plasma interaction with thin-film materials gained widespread aplication in modern micro-and nanoelectronics. These technologies are used to condense, to etch, to modificate the surface of films by ion implantation and as compared with traditional ones have significant advantages, namely less energy consummation, high sustainability and easy to control process.

However, physical and chemical processes of gas discharge plasma interaction with a solid surface are not well established at present time. The optimal treatment regimes for the production of thin-film devices with predetermined properties are not finally determined. This is especially true for nanoscale multilayered compositions that consist of elements with different degrees of mutual solubility. Therefore, further experimental researches in this area are the issue of significant practical interest.

The purpose of this paper is to study changes in chemical composition and microstructure of the Cu/Ni and Cr/Cu/ Ni nanoscale films surface layers under argon plasma glow discharge.

Samples were obtained in vacuum 10^{-2} Pa by resistive evaporation. Each layers thickness was about of 40 nm. Sytal wafers were used as substrates. Cr or Cu films were used as underlayrs. Plasma treatments were done during 20 and 60 minutes in side VUP-5M unit, discharge current was maintained within 30μA. In-depth chemical composition analysis was performed by secondary ions mass spectrometry unit MS 7201. Studies of the microstructure evolution (in different areas of the crater) was done by SEM - REMMA 2 101 unit.

Time dependence of the main elements secondary ion currents shows up that the plasma treatment in Ar atmosphere intensifies the process of mass transfer of the components and leads to the surface segregation of Cu atoms. The concentration of nickel in the surface layer decreases. This effect is observed for both two-and three-layer systems and is more significantly observed with increasing of treatment duration up to one hour. The lateral size of the microrelief elements for initial sample is larger than this size after treatment in plasma. The density of structural imperfections increases across the thickness of the film, which is due to radiation defects saturation. Vacancy generation in the surface area under the influence of charged plasma particles causes diffusion of atoms of one of the matrix elements (Cu) from the depth of the sample that is opposite to the upstream of vacancies and is realized in the opposite Kirkendal effect.

Physical daMages of Electron Transport Chain of Mitochondrions of Cages with Electromagnetic Radiation of Superhigh Frequency

Stadnik Irina[1], Burlaka Anatoliy[2]

[1]Taras Shevchenko National University of Kyiv, Physics Dept., Kyiv, Ukraine;
[2]R. E. Kavetsky Institute of Experimental Pathology, Oncology and Radiobiology of National Academy of Sciences of Ukraine, Kyiv, Ukraine

A research aim was to learn the consequences of influence of electromagnetic radiation of superhigh frequency (EMR SHF) on the system of electron transport chain (ETC) of mitochondrions of cages. Researches were spent on 80 rats-males breeds of Wistar(middle mass of animals is 0,20±0,02 kg) who have been irradiated EMR SHF not thermal range with pulse and continuous influence, fluence of energy - 6±2,4 mW/sm2 (equivalent to the maximally possible power loading of workers of the radiolocation stations). The state of components of electron transport chain of mitochondrions in a liver, heart and aorta cages was estimated through 1, 7 and a 28 days from the moment of irradiation of EMR SHF after the followings paramagnetic centers: with g-factors 1,94 – the intensity of EPR signal, which characterizes the state of FeS-protein N2 ETC of mitochondrions; 2,00 – levels of ubisemiquinone (USQ) in ETC of mitochondrions; 2,03 – contents of complexes non heme NO-FeS-protein in ETC of mitochondrions; 2,07 – restructuring ETC of mitochondrions.

The animals found in violation of the complexes of heme and non heme of iron proteins tissues of liver, heart and aorta, changed amplitude signals EPR complexes of FeS-protein N2, USQ and complexes of non heme NO-FeS-proteins in ETC of mitochondrions been registered deformation of EPR signal with g = 2 , 07. The changes are not renewed during the period of observation. The results indicate a damaging influence on EMR SHF electron transport system of mitochondrions and increase the speed of generation of superoxide radicals.

Key words: electromagnetic radiation of superhigh frequency (EMR SHF), electronic paramagnetic resonance (EPR), electron transport chain (ETC) of mitochondrions cages, liver, heart, aorta;

Nanocomposites Materials Based on Organic-Inorganic Interpenetrating Polymer Networks

Alekseeva T.T., Martyniuk I.S., Gomza Yu.P., Klepko V.V., Nesin S.D.

Institute of Macromolecular Chemistry NAS of Ukraine, Kiev, Ukraine

In the last decade scientific and practical interest is caused by the problem of creation of organic-inorganic hybrid materials with the use sol-gel of synthesis. The special attention is attracted by interpenetrating polymeric networks (IPN) based on different modifications of poly(titanium oxide) in connection with their unique electric, optical and chemical properties.

Structure peculiarities of simultaneous IPNs based on crosslinked polyurethane (PU) and organic-inorganic copolymer based on 2-Hydroxyethylmethacrylate (HEMA) and titanium-tetraisopropoxide ($Ti(OPr^i)_4$) have been studied by SAXS method. The ratio polymer components PU/PHEMA in the initial and organic-inorganic IPN was 50/50 mass % and the molar ratio HEMA/ $Ti(OPr^i)_4$ – 4/1, 8/1, 12/1.

In SAXS curve of initial IPN (Fig., curve 1) is not observed any interference effects. Introduction of the minimal amount of $Ti(OPr^i)_4$ leads to rise of interference peak corresponding of spatial periodicity at 9.7 nm in curve SAXS (curve 2). It is in agreement with the model of structure, where separate ($–TiO_2–$) fragments were uniformly distributed on polymer matrix with formation of the space-ordered structure.

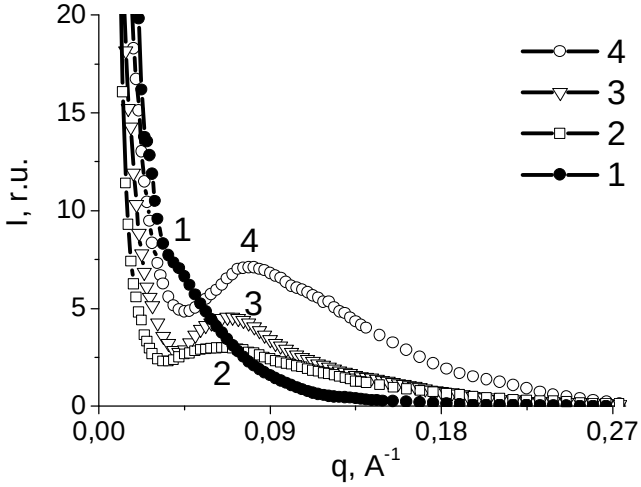

Fig. Scattered intensity *I* vs *q* for organic-inorganic IPN at variation of TiO_2 content

Increasing of the Ti-component content (TiO_2 – 3.4 mass %) (curve 3) caused its partially segregation, that lead to decrease spatial periodicity to 9.0 nm. At the molar ratio HEMA/ $Ti(OPr^i)_4$ – 4/1 (TiO_2 – 5.6 mass %) (curve 4) enhanced the segregation processes of the ($–TiO_2–$) fragments in a polymeric chain of PHEMA. As a result the spatial periodicity decrease to 7.9 nm and total level of scattered intensity rise. Such structure peculiarities are connected with crosslinking effect of the ($–TiO_2–$) fragments in polymer system.

This have been confirmed by the methods of dynamic mechanical analysis and thermogravimetric analysis.

Dimensional Effects of Ultrasound Treatment on the Thermodynamic and Kinetic Parameters of Li-Intercalation Current formation in the Talc

Balaban O.V., Grygorchak I.I.

Lviv Polytechnic National University, Lviv, Ukraine

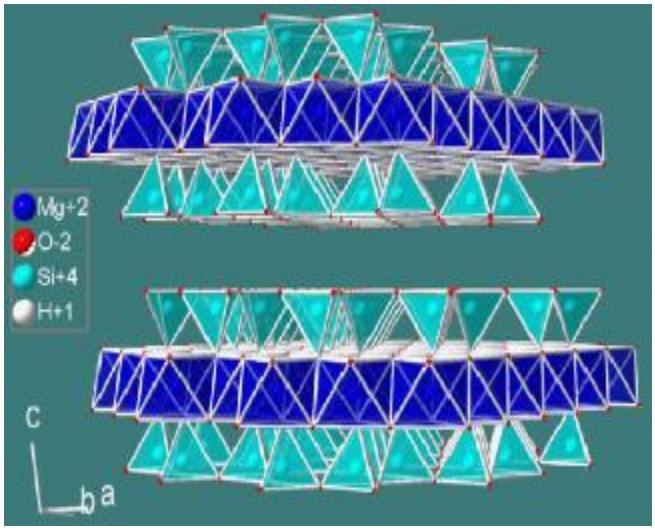

Fig.1 Talc structure.

It is known wide class of cathode materials for devices of generation, storage and energy conversion. However, they are unable to meet modern, increasingly functional requirements for such devices, conjugated with cheapness and environmental safety. Therefore today the task of the mentioned problem overcoming became a dominant aim. One of the solution ways is application of natural mineral – talc ($Mg_3Si_4O_{10}(OH)_2$) in the cathode lithium intercalation process. Its structure is shown in Fig. 1. In order to improve functional capabilities, talc was subjected to ultrasonic modification in 1 M solution of $LiBF_4$ in γ-butyrolactone.

In this work multiplicity of ultrasound using was analyzed in terms of it's influence on properties of the solid, including the fractal structure of the guest subsystem and electronic spectrum. In Fig. 2 the change of the Gibbs free energy of lithium intercalation for different size talc particles: 1 μm (curve 1) and 0.5 μm (curve 2) is presented. It was discovered the extraordinary fact of higher value for diffusion coefficient of lithium as the guest in large size particles and it's explanation was proposed.

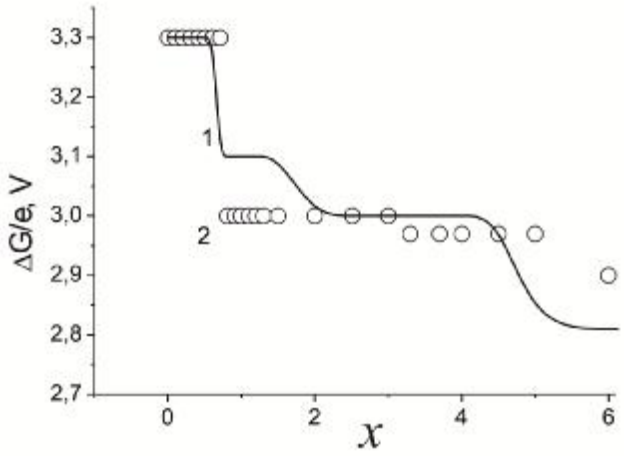

Fig.2 Change of the Gibbs energy of lithium intercalation for different size talc particles: 1 μm (curve 1) and 0.5 μm (curve 2)

Influence of Thermo-Mechanical Annealing on Nanocrystallization Process in FeCuNbSiB Wires

Bashev V., Derun A., Kovalenko V., Kutseva N.

Dnipropetrovsk National University, Dnipropetrovsk, Ukraine

Nanocrystalline glass-coated microwires (MW) become very promising for applications due to their excellent combination of soft magnetic properties, stability of nanocrystalline state with small dimensions and insulating glass coating. The great internal stresses (~1GPa) are occurred during the fabrication due to difference in the thermal expansion coefficients of the metallic core and glass insulation. The presence of such a residual stresses forms a complex domain structure of initial MW. The enhanced softness is usually achieved by appropriate treatments. It is connected with the formation of nanocrystalline structure. The aim of this work is to investigate the effect of thermal treatments such as conventional annealing and annealing after tensile stress on the structure and magnetic properties of MW.

Initial $Fe_{70.8}Cu_1Nb_{3.1}Si_{14.5}B_{10.6}$ amorphous MW with metallic nucleus diameter 16 μm and total diameter 26 μm were obtained by the Taylor-Ulitovski technique. The structure functions and the functions of radial distribution were calculated to describe short-range order of atoms in initial and treated MW(fig.1). From these data it was found that the average distance between atoms and coordination number are approx. 0.258 nm and 12, respectively.

Annealing of MW at the temperature range from 500 ^oC to 550 ^oC leads to the formation of the nanograins α-Fe(Si). The grain size of the crystals formed is derived from Scherrer's equation, the relative content of phase is evaluated from the area of the crystalline peak normalized to the total area of peak. The α-Fe(Si) grain size and the their relative content are increased from 17 nm to 21 nm and from 40% to 45 % , respectively, in this temperature range. It should be noticed annealing under tensile stress accelerates the crystallization processes, the grain size is increased from 17 nm to 24 nm and from 40% to 45 % , respectively. (fig.2). Optimal magnetic properties are achieved at the annealing at 520 ^oC.

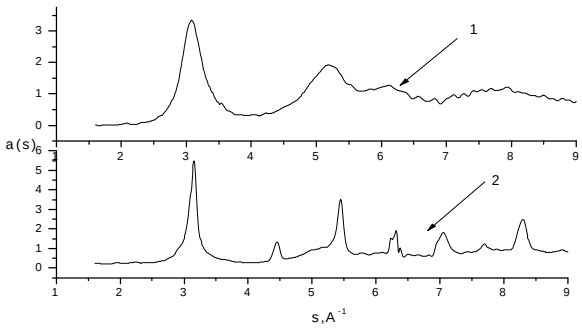

Fig.1 Structure function
1- intial MW ; 2 - annealing at 520 ^oC

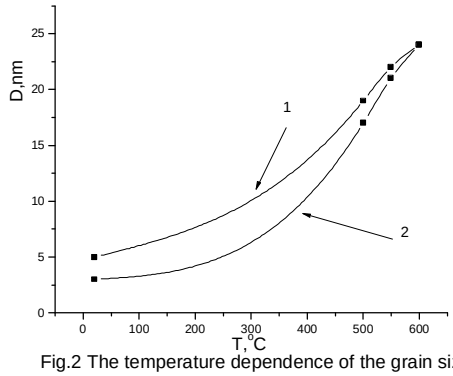

Fig.2 The temperature dependence of the grain size
1-annealing under tensile stress 185 MPa;
2-conventional annealing

Modeling and Investigation of Anodic Oxidation and Etching Processes of Al/Nanoporous Alumina Structures

Bednov M., Lebyedyeva T., Shpylovy P.

V.M. Glushkov Institute of Cybernetics, Kyiv, Ukraine

Nanostructured aluminum/porous anodic alumina films can be used as a base for metal clad waveguide (MCWG) biosensors. Fabrication of such sensors requires anodic oxidation of aluminum film and chemical etching of porous anodic alumina (PAA) layer for widening of pores. We built a theoretical model that describes anodization and etching processes. This model calculates dependence of porosity of PAA upon the etching time, effective index of refraction of the porous layer within the framework of Bruggeman effective medium theory and reflectivity curves with the help of Fresnel equations (Figure 1). Good correlation between theoretical and experimental dates was obtained.

Theoretical modeling revealed optimal manufacturing conditions that lead to highest sensitivity of the proposed sensor.

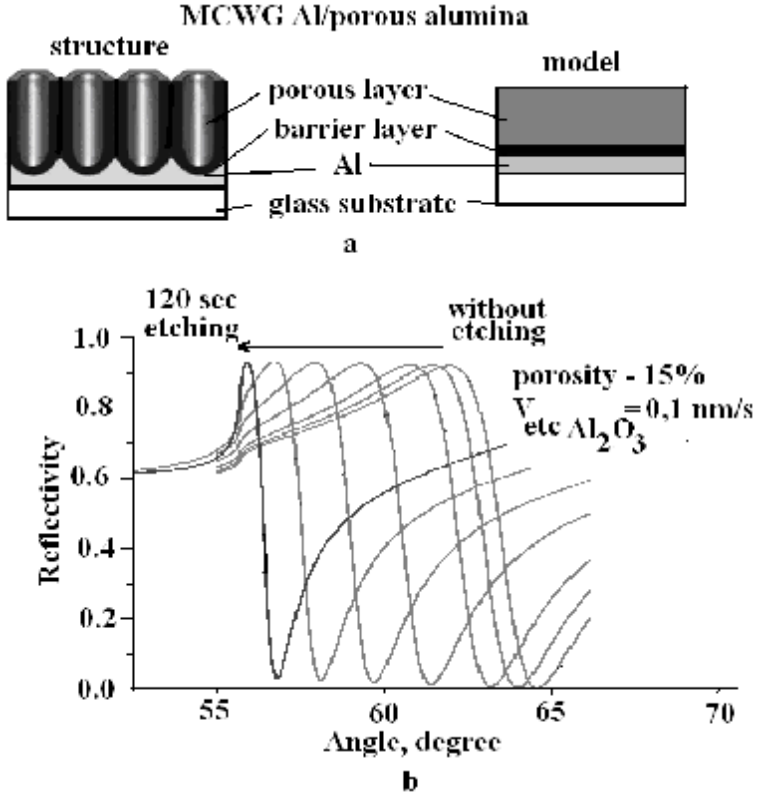

Figure 1. Model of MCWG Al/porous PAA (a) and calculation of reflective curves under widening of pores by etching (b). Initial thickness of porous layer is 400 nm, barrier oxide layer -50 nm, Al – 15 nm.

Quantum-Chemical Simulation of Hydrophobic Nano-Silica Particles

Bezruka N.A.[1], Lobanov V.V.[2]

[1]*V. Stefanik Precarpathian National University, Ivano-Frankivsk, Ukraine*
[2] *Chuiko Institute of Surface Chemistry of NAS of Ukraine*

Unmodified silica nanoparticles have a pronounced hydrophility due to the presence of hydroxyl groups on their surface. In many practical applications of nano-sized silica such as inert filler polymer materials, a necessity avises in a surface with hydrophobic properties, which can be obtained by treating the silica samples with different silanes. In the surface layer, a sequence of bonds ≡Si–O–Si–CR_3 is formed with high resistance against elevated temperatures and water. However, according to the experimental data, even when functional groups (R) of hydrocarbon radicals with different length and structure are used, complete blocking of silica surface can not be achieved from the access of water molecules.

In this report, the results of calculations (DFT method, B3LYP, 6-31 G**) on the electrostatic potential distribution (r) for a series of globular clusters derived from the cluster of adamantan-like structure (gross formula $Si_{10}O_{28}H_{16}$ (Fig. 1)) via sequential replacement of the hydrogen atoms of isolated silanol groups by trimethylsilyl ones. An advantage of this model compared to that of (111) β-cristobalite is the absence of dangling bonds.

Fig. 1. Cluster model of silica nanoparticle

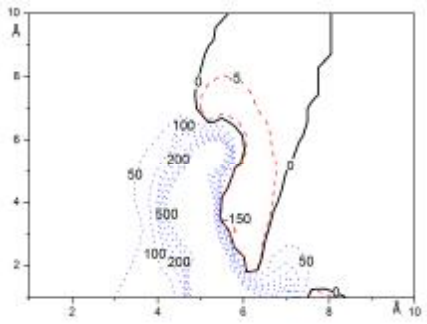

Fig. 2. Distribution of r due to total hydrophobization of initial particle

It is seen from Fig. 2 that there is an extended area of negative r values in the vicinity of trimethylsilyl group providing an access of water molecules siloxane bonds what indicates hydrophilic properties of completely hydrophobic particles.

The Effect of Stibium Underlayers on Percolation Threshold in Copper Film

Bihun R.I., Buchkovska M.D.

Ivan Franko's Lviv National University Lviv, Ukraine

Preparation of ultrathin electrically continuous metal films with metallic charge transport at the surface of the dielectric substrate, is rather difficult technological task due to coagulation of metal particles during it's condensation. Therefore, there is a threshold above which the current flow appear (percolation threshold), which corresponds to the minimum thickness d_c of metal layer, in which first channel of conductivity appears. It was emerged that surfactant under layer have an significant influence on polycrystalline metal film formation [1].

The influence of stibium underlayers with thickness of 2 nm on the appearance ohm conductivity in as deposited copper films were investigated.

The experiment was conducted under ultrahigh vacuum conditions (residual gas pressure during the preparation and study of films was lower than 10^{-7} Pa) in unsoldered glass devices. Asdeposited films by condensing steam thermally heated material into cooled to T = 78 K substrate were investigated. Mass thickness of films was monitored with quarts oscillator. Measuring the resistance of the films was carried out with ohmmeter. Sublayers stibium deposited on the substrate immediately before applying the copper film.

Found that, the conductivity of copper films, which was deposited on stibium substrate, occurs at a thickness less than the thickness at which the conductivity is recorded in similar films, which was deposited on a clean glass surface. Resistivity of the films of equal thickness, which was deposited on a clean glass surface in the region of thicknesses in excess of 10-15 nm, was smaller than the resistivity of deposited films on stibium sublayers. The results were analyzed in the framework of percolation model. Plot of experimental size dependence $R = R(d)$ can be represented as linear in a double logarithmic scale: $\ln R \sim \gamma \ln (d-d_c)$. Linearization of function for usdeposited films on a clean glass surface is obtained by d_c = 6,8 nm, while for similar copper films, which was deposited on stibium sublayers with thickness 2 nm, dc = 3,8 nm. Relationship was founded out between d_c and parameter average amplitude of surface inhomogeneities h within the framework of Namba [2]. The values of the exponent γ respectively equal to 1.3 and 1.2. Arguably, 2D percolation mechanism sold in usdeposited copper films, since the value of γ close to 1,3, according percolation model.

1. Бігун Р.І. Вплив підшару германію на процес перколяції в тонких плівках паладію / Р.І. Бігун, М.Д. Бучковська, Б.Р. Пенюх, З.В. Стасюк, Д.С. Леонов // Наносистеми, наноматеріали, нанотехнології.– 2012.– Т.10, №3.– С. 505-512.
2. Бучковська М.Д. Вплив підшарів сурми на поріг протікання струму в тонких плівках міді / М.Д. Бучковська, // Фізика та хімія поверхні. – 2012. – Т.13, №4. – С. 916-920.

A-site and B-Site Doped $LaNbO_4$ Electrolyte for Proton Conducting Fuel Cells Formed by E-Beam Technique

Bockute Kristina, Virbukas Darius, Laukaitis Giedrius, Dudonis Julius

Kaunas University of Technology, Kaunas, Lithuania

Among different kinds of fuel cells, high temperature proton conducting fuel cells (PCFC) become more and more studied due to their low activation energy, high energy efficiency and for the mobility of protons means they can operate in a wide range of temperature [1, 2].

Acceptor-doped rare-earth ortho-niobates (ABO_4-type, e.g. $LaNbO_4$), have been investigated as promising proton conductor materials for PCFC because of high chemical stability in CO_2 environment. The partial substitution of La^{+3} or Nb^{5+} by lower valence elements introduces a negative charge that may be compensated by the formation of oxygen vacancies and this contributes to the improvement of the ionic conductivity [3].

This work presents a systematic investigation of A-site and B-site acceptor-doped $LaNbO_4$ thin films formed using e-beam physical vapor deposition (EB-PVD) method. The influence of different dopants, their concentrations, deposition parameters, substrate and temperature on thin films microstructure, chemical composition, electrochemical properties and homogeneity were studied. The possible reasons for such dependencies are also discussed.

Acknowledgements

This research is funded by the European Social Fund under the Global Grant measure.

1. A.K. Demin, P. E. Tsiakaras, V.A. Sobyanin, S.Y. Hramova, Solid State Ionics 152–153 (2002) 555.
2. Francesco Bozza, Nikolaos Bonanos, Solid State Ionics 213 (2012) 98–102.
3. T. Mokkelbost, I. Kaus, R. Haugsrud, T. Norby, T. Grande, M.A. Einarsrud, J. Am. Ceram. Soc. 91 (2008) 879–886.

Collective Magnonic Modes in 2D Arrays of Planar Magnetized Nano-Elements

Bondarenko P. V.[1], Dvornik M.[2], Ivanov B. A.[1] and Kruglyak V. V.[2]

[1]*Institute of Magnetism, NASU and MESYSU, Kiev, Ukraine*
[2]*University of Exeter, Exeter, United Kingdom*

As the packing fraction of magnetic arrays increases, the magneto-dipolar coupling between elements also increases. In particular, the magnetization dynamics are no longer described by precessional modes of individual elements. Instead, collective normal modes of precession are formed. This behavior is common to all systems of coupled oscillators, while its understanding forms fundamental basis of any field of modern solid state physics.

Theoretical study of collective magnonic modes in finite arrays of dipolarly coupled magnetic nano-elements with quasi-uniform magnetization are perfomed. The mode spectrum and character are numerically computed for an individual isolated nano-element and then used to calculate analytically the splitting of the modes due to the inter-element magneto-dipole interaction using strong coupling approximation.

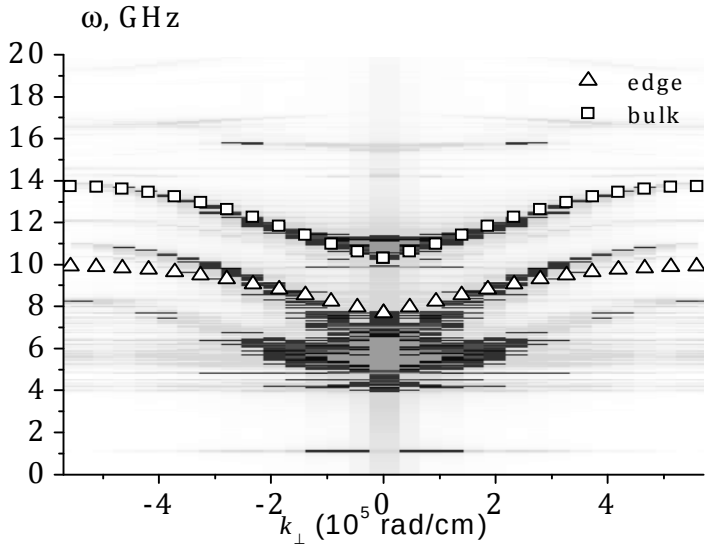

Magnonic dispersion in the 30x30 array with the edge-to-edge separaton of 5 nm

The results are compared with those obtained using direct simulations for the arrays of the elements. A generally good agreement between the two methods has been found [1]. For the edge mode, the interaction between the edges of the neighboring elements can exceed that between the edges of the same element, leading to violation of the assumptions of the analytical approach.

1. Dvornik M. Collective magnonic modes of pairs of closely spaced magnetic nano-elements / M. Dvornik, P. V. Bondarenko, B. A. Ivanov, V. V. Kruglyak // J. Appl. Phys. – 2011. – Vol. 109, Iss. 7. – P. 07B912 (1-3).

Luminescence Centers in Thin Films of $ZnGa_2O_4$

Bordun O.M., Bihday V.G., Kukharsky I.Yo

Ivan Franko National University of L'viv,Ukraine,79005, Lviv, Dragomanova str. 50.
e-mail: bordun@electronics.wups.lviv.ua

Zinc gallate is among the materials that find the widest application in microelectronics. Optoelectronics and information display devices. Properties of $ZnGa_2O_4$ films strongly depend on the choice of deposition technique and process parameters. In this work we presented a detailed comparison of $ZnGa_2O_4$ films produced by RF magnetron sputtering. After obtained films carry out thermoprocessing in air or argon at 1000–1100°C. A number of films after thermoprocessing experience recovery in hydrogen atmosphere at 600°C. Based on X-ray diffraction analysis it has been ascertained that after heat treatment crystalline structure of films $ZnGa_2O_4$ is considerably improved and meets space group Fd3m with crystal lattice parameter a=8.32–8.33 Å.

Photoexcitation spectra and luminescence of thin films of $ZnGa_2O_4$ under photo-, cathode and X-ray excitation were investigated. Luminescence spectra were factorized on ultimate constituents using Alentsev-Fock method. It is established that the spectra of luminescence of thin films $ZnGa_2O_4$ consist elementary bands with maxima at 3.35, 2.85, 2.50, 2.38 and 1.75 eV.

Emission bands with maxima at 3.35, 2.85, 2.50 and 2.38 eV were referred to the luminescence at the expence of electronic transitions between $^4T_2$, $^4T_1$, ^2E and $^4A_2$ terms in octahedral complexes $(GaO_6)^{9-}$. Based on energetical levels terms of octahedral structure $(GaO_6)^{9-}$ proposed diagram of energetical levels in such structure and corresponding luminescent transitions, selected in thin films $ZnGa_2O_4$. Luminescence band with maximum at 1.75 eV is attributed to oxygen vacancies.

Photoluminescence of CdS Quantum Dots in Polymer Matrices

Budzulyak S.I.[1], Kuryk A.O.[1], Korbutyak D.V.[1], Melnychuk O.V.[2], Shevchuk O.M.[3], Tokarev S.V.[3].

[1] V.E. Lashkarev Institute of Semiconductor Physics, National Academy of Sciences, Kyiv, Ukraine
[2]Mykola Gogol Nizhyn State University, Nizhyn, Ukraine
[3] National University Lviv Polytechnic, Lviv, Ukraine

Formation of the thin polymeric films with the embedded nanoclusters doped on the basis of CdS/ZnS and CdS/CuS was performed via several stages: At the first stage a solution of the polyfunctional copolymer (PFC) poly[(butyl acrylate)-*co*-(5-tert-butylperoxy-5-methylhex-1-en-3-yne)-*co*-(maleic anhydride)] modified dimethylaminoethanol, polyethylene glycol PEG-200 (taken in the amount of 10% respectively to PFK) and a mixture of two salts Cadmium Acetate $Cd(Ac)_2$ with either $Cu(Ac)_2$ or $Zn(Ac)_2$ in dimethylformamide at their ratio as $[Cd(Ac)_2]:[Me(Ac)_2]=99:1\div90:10$. Theoretical content of MeS in the film was of 20%.

On glass plates from the obtained solutions were spin-coated the thin polymeric films containing metal ions bonded with polymeric matrix due to formation of both ionic and coordinate bonds. The film thickness was in average of ≈ 20 nm. Crosslinking of the films obtained occurred at their heating ($T=100\div120^{\circ}C$) as results of an esterification reaction between hydroxyl groups of bifunctional PEG-200 and the maleic anhydride moieties in PFC. At the final stage the CdS nanoclusters doped were formed by treatment of the films by Hydrogen Sulfide in gas phase.

Absorption maxima in the area of 2.6-2.85 eV depending on the nature and concentration of doping metal cations were observed in the UV-vis spectra of obtained thin films.

In the spectra of photoluminescence (PL) of the samples were observed two broad bands: one in the spectral region (1,6 - 2,3) eV, the second - in the (2,4 - 3,4) eV. The first is caused by structural defects in QDs CdS, the second (high-energy, with energy quanta greater than band gap of bulk CdS) related to the radiative annihilation of excitons. Characteristically, the introduction of Cu impurities in CdS QDs led to the quenching of "defect" PL band (1,6 - 2,3) eV while increasing the intensity of high-energy (2,4 - 3,4) eV PL band. This means that Cu enhances structural perfection CdS QDs. Introduction Zn impurities in QDs CdS, in contrast, did not lead to improved structural characteristics of QDs, as evidenced by the increase in the intensity of "defect" PL band with increasing zinc content of impurities.

Influence of Temperature on the Electrical Properties of (1-*x*)$MgFe_2O_4$ – *x*$BaTiO_3$ Composites

Bushkova V.S., Kopayev A.V.

Vasyl Stefanyk Pre-Carpathian National University, Ivano-Frankivsk, Ukraine

In the last few years, multiferroic materials which combine ferroelectric and ferromagnetic properties have attracted a great deal of attention thanks to their scientific significance and technological applications. In particular, the coexistence of electric and magnetic orderings makes it possible to manipulate the magnetic state of a multiferroic material through an electrical field, or vice versa. The recent interest in magnetoelectric (ME) materials is stimulated by their significant technological potential. Multiferroic composite systems could be potentially used in multifunctional devices, such as magnetic field sensors, transducers, actuators, memories, and spintronics. The existence of a connection between the magnetic and electric parameters of a substance demands a study of all the possible mechanisms of influence an electric field has on the magnetic characteristics of such substances.

Multiferroic materials can be realized in single phase and composite forms. Single phase multiferroic materials are still unable to produce a suitable value of ME coupling coefficient. The composite multiferroic systems with magnetostrictive and piezoelectric phases are a better alternative to single phase multiferroic materials, because they have the potential of showing larger ME effects.

The aim of this paper is synthesis and study of composites with the general formula (1-*x*)$MgFe_2O_4$ – *x*$BaTiO_3$, where *x* = 0.0, 12.5, 25.0, 37.5, 50.0, 62.5 vol.%. The ferrite phase, $MgFe_2O_4$ with spinel structure is well known for its soft magnetic properties. In addition $MgFe_2O_4$ has high specific resistance. Magnesium ferrite was prepared by the sol-gel method with participation of auto-combustion. Barium titanate with perovskite type structure is an extensively studied ferroelectric material from the past few decades for its electromechanical properties. The ferroelectric $BaTiO_3$ was prepared by means of ceramic technology. Then composites with different volume percents were mixed and pressed into briquettes with diameter 1.7 cm approximately at a pressure of 35 MPa and thermally annealed at 1320 °C for about 7 h in air.

The measurement of the total complex impedance was carried out on Autolab PGSTAT 12/FRA-2 spectrometer in the frequency range of 0,01 Hz - 100 kHz in the temperature range of 20 - 450 °C in increments of 50 °C. The study of dielectric properties obtained from the analysis of impedance spectra allowed to determine the regularities of their changes depending on the temperature, frequency and composition.

Entropic Stabilization of Phases and Ultrafast Diffusion of Guest Lithium Intercalated into PYROPHYLLITE

Bishchaniuk T.M., Grygorchak I.I., Pokladok N.T.

National University Lviv Politechnik, Lviv, Ukraine

The vast majority of the presently known electrochemical systems of generation and Faraday energy storage contain cathode and anode materials which are at a stage of exhaustion. Thus the task of search of low-cost, widespread and ecologically safe natural resources, capable to be applied in portable devices, becomes of great interest.

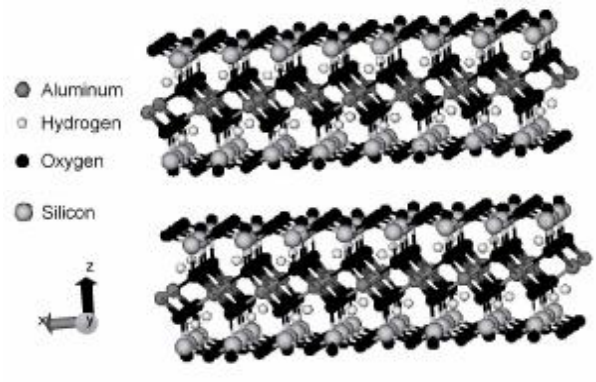

Figure 1. Pyrophyllite structure

The possibility of lithium – cation current forming reaction in natural mineral pyrophyllite $Al_2(OH)_2[Si_2O_5]_2$ is shown. The crystal structure of this mineral is pictured in Figure 1. The dependence of change in free energy and entropy of intercalation reaction on lithium guest load degree is analyzed in Figure 2. The effect of entropic stabilization of intercalated phases was revealed. This effect provides a horizontal view of chronopotentiogramm at relevant x values.

The distinctive feature of intercalation kinetics in $Li_xAl_2(OH)_2[Si_2O_5]_2$ is of anomalously high values of the diffusion coefficient of lithium cations at x>0,3.

A microscopic model which explains the results is proposed.

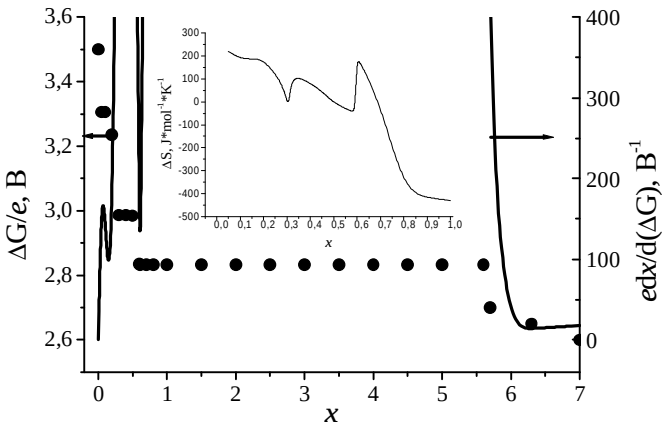

Figure 2. Change in Gibbs energy of lithium intercalation process Li_xPPh - (point) and in differential capacitance as functions of the guest load degree - (solid curve). In the Box - change in entropy of the process, determined from the temperature studies.

Nanoindentation Study of Lithium Tetraborate

Chobal O.[1, 3], Rizak I.[2], Chobal I.[1], Kováč F.[3], Gavendová P.[3], Petryshynets I.[3], Holovey V.[4], Rizak V.[1]

[1]*Uzhhorod National University, Uzhhorod, Ukraine*
[2]*National Aerospace University of "KhAI," Kharkov, Ukraine*
[3]*Institute of Materials Research, Košice, Slovakia*
[4]*Institute of Electron Physics, Uzhgorod, Ukraine*

Lithium tetraborate ($Li_2B_4O_7$) is a promising material for application in non-linear optical and surface acoustic wave devices. The doped $Li_2B_4O_7$ is used in a thermoluminescent dosimetry. The present work is devoted to experimental measurement of mechanical properties of the lithium tetraborate in glass and crystal phases by means of nanoindentation.

The indentation tests were performed on „Nanoindenter G 200", using a pyramidal diamond Berkovich indenter tip, to determine the mechanical properties. The samples were measured with a maximum force of 50, 100, 150, 200, 250, 300, 350, 400, 450, 500 mN. The calculation was done according to the standard ISO 14577.

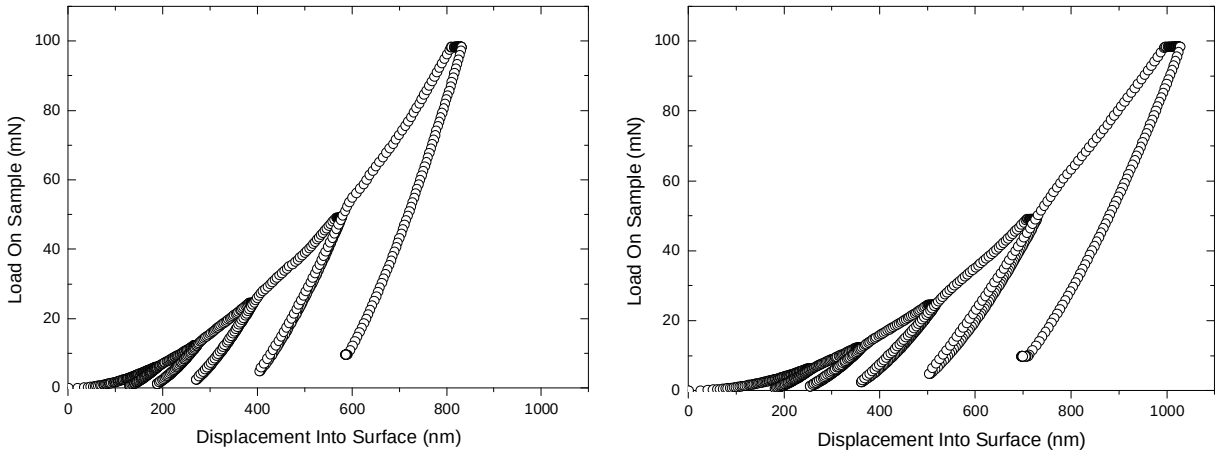

(a) (b)

Fig. 1. Load–displacement curves for the $Li_2B_4O_7$ single crystal (100) face (*a*) and lithium tetraborate glasses (*b*)

From the resulting load- displacement curve (Fig. 1), the elastic modulus and hardness of the $Li_2B_4O_7$ material have been calculated. The differences in the Young's modulus and the hardness for the crystallographically unequal planes of the $Li_2B_4O_7$ crystal and glasses are related to the difference in the elastic and plastic deformation mechanisms.

Acknowledgement

O. Chobal is grateful to the International Visegrad Fund for the support of his research at Institute of Materials Research of SAS.

Heat Capacity of $Sn_2P_2S_6$ Ferroelectric Nanocrystals

Chobal O.[1,6], Rizak I.[2], Iľkovič S.[3], Reiffers M.[3,5], Šebeň V.[3], Baláž P.[4], Timko M.[5], Kováč F.[6], Petryshynets I.[6], Rizak V.[1]

[1]*Uzhhorod National University, Uzhhorod, Ukraine*
[2]*National Aerospace University of "KhAI," Kharkov, Ukraine*
[3]*University of Prelov in Prelov, Prelov, Slovakia*
[4]*Institute of Geotechnics, Kolice, Slovakia*
[5]*Institute of Experimental Physics, Kolice, Slovakia*
[6]*Institute of Materials Research, Kolice, Slovakia*

Multicritical points on the phase diagram $Sn_2P_2S_6$ crystals were found, what make them attractive for basic research. In particular, recent studies of the thermal properties of crystals $Sn_2P_2S_6$ under pressure showed unusual behavior of thermal conductivity in the vicinity of the phase transition (PT), as well as the presence of tricritical Lifshitz Point (TCLP) on *p-T* diagram of solid solutions $(Pb_ySn_{1-y})_2P_2(Se_xS_{1-x})_6$. Actual continuation of this work is study of size effects influence on the heat capacity of $Sn_2P_2S_6$ nanocrystals with PT close to TCLP.

For preparation of the $Sn_2P_2S_6$ nanocrystal powder were used the method of high-energy milling of the starting material using a Pulverisette 6 planetary mill (Fritch, Germany). Particle size measurements have been performed using Nanophox apparatus (Sympatech, Germany). To study the heat capacity of $Sn_2P_2S_6$ nanocrystals at low temperatures was performed *ab initio* calculation of thermodynamic properties.

We showed that mechanical milling leads to a decreasing of average particle size, and the obtained powders are characterized by a bimodal or polymodal size distribution. Analysis of the specific heat anomaly at the PT shows a decline phase transition temperatures and the heat capacity anomaly of the $Sn_2P_2S_6$ powders smears with decreasing average particle size. Comparison of experimental data with the calculation results using of phenomenological model developed for the ferroelectric nanoparticles with PT close to TCLP revealed, that smearing of the phase transition in $Sn_2P_2S_6$ nanocrystals was caused by the size effects and a large concentration of defects.

Acknowledgement

This work has been supported by the Agency of the Ministry of Education of the Slovak Republic for the Structural Funds of the EU ITMS No 26220220003; and partly by projects of Slovak Grant Agency VEGA 2/0070/12 and Slovak Research and Development Agency APVV-0189-10, by the CEX NANOFLUID and CEX CFNT MVEP as the Centers of Excelence SAS. The first author is grateful to the Institute of Materials Research of SAS for its hospitality and to the International Visegrad Fund for financial support.

Effect of Isovalent Substitution on the Physical Properties of Nanoclusters of Lithium Tetraborate

Chobal O.[1,3], Rizak I.[2], Chobal I.[1], Kováč F.[3], Petryshynets I.[3], Rizak V.[1]

[1]*Uzhhorod National University, Uzhhorod, Ukraine*
[2]*National Aerospace University of "KhAI," Kharkov, Ukraine*
[3]*Institute of Materials Research, Kolice, Slovakia*

Numerous works on different physical properties of lithium tetraborate ($Li_2B_4O_7$) crystals point to promising possibilities for applications of these materials in acoustoelectronic devices, ultra-violet solid state lasers and dosimetry. At the same time, atomic clusters are building blocks of new nanostructured materials and, consequently, are of interest for intensive investigations with the prospect for applications in future nanotechnologies. The aim of the present work is to perform a theoretical ***ab initio*** investigation of the optimized geometric configuration and electronic structure, as well as the effect of isovalent substitution on the investigated physical properties of the $Li_2B_4O_7$ nanoclusters.

The optimized configuration and electronic structure of the investigated nanoclusters containing 1–8 formula units of the $Me_2B_4O_7$ (Me=Li, Na, K) compound, were calculated from first principles. All calculations were performed with the GAMESS (US) quantum-chemistry package. The calculations of the total energy and equilibrium geometric structure were performed by the spin-restricted Hartree–Fock method (RHF) with the 6-31G split-valence basis set.

It has been shown that the clusters of lithium tetraborate are stable and retain the topology of the simulated crystal. However, the spatial structure of the clusters deviates slightly from the true geometric configuration of the crystal and they acquire a rounded shape, which is characteristic of nanoobjects. The isovalent substitution of Na (K) for Li in the $Li_2B_4O_7$ nanoclusters reduces the HOMO–LUMO band gap where the average Me-O distance increases. The calculated results are compared with available experimental data from the literature. The influence of the isovalent substitution on the physical properties under investigation has been analyzed.

Acknowledgement

O. Chobal is grateful to the International Visegrad Fund for the support of his research at Institute of Materials Research of SAS.

Synthesis and Luminescence Characterization of Nanosized Luminescent Material for Temperature Distribution Monitoring

Chornii V.[1], Nedilko S.[1], Hizhnyi Yu.[1], Terebilenko K.[1], Slobodyanik M.[1], Boyko V.[2], Aigouy L.[3], Sheludko V.[4]

[1] Taras Shevchenko National University of Kyiv, Kyiv, Ukraine
[2] National University of Life and Environmental Sciences of Ukraine, Kyiv, Ukraine
[3]UMR 8213 Institut de Physique, Laboratoire de Physique et d'Etude des Matériaux, France
[4] Oleksandr Dovzhenko Hlukhiv National Pedagogical University, Glukhiv, Ukraine

It is well-known that some branches of technology and medicine require the measuring with high spatial resolution the temperature field distribution on various surfaces. It is possible to use for this issue a dependence on temperature of photoluminescence intensity of some polycrystalline luminescent material. Obvious, that spatial resolution in such case depends on a size of luminescent particle. We investigate submicron particles of molybdates $NaAl(MoO_4)_2:Cr^{3+}$ as perspective luminescent probes for measuring of the temperature field distribution.

The investigated compound was obtained during slow cooling of a high-temperature melts from Na-Al -Mo-O system containing 0.1% Cr. The samples were prepared using $Al(OH)_3$, Na_2CO_3 and MoO_3 (analytical purity) as an initial reagents, which were heated up to 950°C and then cooled down to 620°C at a rate of 30-10° per hour.

The phase composition was determined using Shimadzu XRD-6000 ($Cu_{K\alpha}$-radiation) diffractometers. The microstructure of the compounds obtained was studied with a scanning electron microscope (SEM) Hitachi S - 2400.

During investigation of the synthesized compound its composite structure $Al_2O_3:Cr^{3+}/NaAl(MoO_4)_2:Cr^{3+}$ was established. The samples consist of layers of polycrystalline $NaAl(MoO_4)_2:Cr^{3+}$ with nano/microsized Al_2O_3 grains (size 80-220 nm) incorporated into molybdate crystals or on it's surface.

Photoluminescence and PL excitation spectra in UV and visible regions were recorded using MDR-23 spectrometer. The N_2 laser (λ_{exc} = 337.1 nm) and two diode-pumped lasers (λ_{exc} = 473 and 532 nm respectively) were used as sources of PL excitation.The VUV-excited luminescence was studied on SUPERLUMI station at HASYLAB (DESY), Hamburg, Germany in 3.7 – 14 eV region of excitation energies and T = 8 K.

The results of syntesis and luminescence characterization of probes are presented. Possibility of usage $Al_2O_3:Cr^{3+}/NaAl(MoO_4)_2:Cr^{3+}$ composit for measurements of the temperature field distribution on surfaces of various materials is shown.

Effect of Ag Thin Films on Photoluminescence of Silicon Nanoclusters in SiO_x Matrix

Dan'ko V.A., Michailovska K.V., Indutnyi I.Z., Shepeliavyi P.E.

V. Lashkaryov Institute of Semiconductor Physics, NAS of Ukraine, Kyiv, Ukraine

Surface plasmon polariton (SPP) optic is a potentially attractive approach to photonic integration. In thin metallic films, containing nanoscale surface feature, a giant enchancement of optical responses are observed. The enchancement is associated with surface plasmon (SP) or (SPP) modes, whose characteristics are strongly dependent on the geometric structure of the metallic component of the medium. Luminescence can be modified by altering the photonic density of states due to resonantly coupling light to a structure such as a metallic film, which exhibits surface plasmon resonance (SPR). Such a system can be realized by a quantum dot located near a thin metal film.

In this report time-resolved photoluminescence (PL) measurments of silver coated nc-Si-SiO_x structures were studied using N_2 laser excitation at 3,68eV. Investigated samples were produced by thermal obliquely evaporation of SiO with the following annealing at 975^0C in vacuum and treating in the HF vapor. Polished Si wafers were used as a substrates. The obtained column-like porous films containing Si nanoparticle (nc-Si) exhibit strong PL emission with a peak near 1,88eV (660nm), which can be attributed to exciton recombination in nc-Si embedded into SiO_x matrix. To modify the exciton recombination rate in quantum dots (nc-Si) by means of SP coupling some samples of the nc-Si-SiO_x structures were coated with a ultrathin nanoisland-like Ag film (with effective thickness near 5nm) using thermal vapor deposition. The red-shift of PL emission peak to 1,77eV (700nm) was observed in the Ag coated samples. We believe that these experimental results can be explained by assuming that at the interface Ag/nc-Si-SiO_x the binding of nc-Si emission with surface plasmon modes of Ag nanoparticles takes place.

More direct demonstration of exciton recombination modification is comparative measurments of the PL decay rate from the photoexcited nc-Si on the silvered and unsilvered samples. The PL decay curves were fitted with the stretched exponential function to determinate the PL decay rate. It was found that the PL of Ag coated part of nc-Si-SiO_x structure decayed faster than of uncoated one. For example, at PL photon energy of 1,75eV (wavelengths = 710nm) experimental decay times were equal to 5,9 and 11,7μs, respectively. A similar result was observed for other emission wavelengths, and reducing of the decay times depends on the emission energy and silver thickness. Thus the present results demonstrate that recombination rate in nc-Si-SiO_x structures were enhanced when the emission from silicon nanoparticles was resonantly coupled with a metal surface plasmon modes, especially in red wavelength range where nanoisland of Ag films show SPR.

Effective Medium Approximation for Photo-Induced Processes Explanation in Chalcogenide glass As_2S_3-gold Nanopaticle Composite

Dmitruk N.[1], Romanyuk V.[1], Taborska M.[1], Charnovych S.[2], Kokenyesi S.[2], Yurkovich N.[3]

[1]*Institute for Physics of Semiconductors NAS of Ukraine, Kyiv, Ukraine*
[2]*University of Debrecen, Debrecen, Hungary*
[3]*Institute of Solid State Physics, Uzhgorod National University, Uzhgorod, Ukraine*

Chalcogenide glasses display the highest photoinduced effects among other materials and their photosensitivity does not involve chemical reactions. Refractive-index changes of $\Delta n \sim 0.1$ can be produced by band-gap illumination. Photo-induced transformation processes (PhTP), as some laser-stimulated changes of optical parameters in amorphous chalcogenide films (As_2S_3, As_2Se_3 etc.), are used for optical memory and recording, fabrication of photonics elements, integrated optics, direct laser writing of buried optical waveguides etc. Because of excitation of localized (surface) plasmons (SP) in metal nanoparticles is used for enhancement of various photophysical phenomena, it can be assumed that PhTP in chalcogenides also can be influenced this way. Near coincidence of both energies generation of SP and nonequilibrium electron-hole pair generation in chalcogenides allows to hope for enhancement of PhTP rate.

We have fabricated single and multicomponent layered structures, which consist of granular (gold) nanoparticle (GNP) film and light-sensitive chalcogenide layers on a glass substrate, measured their optical spectra before and after the laser irradiation. Experimental spectra of optical transmittance/reflectance of these composite structures have been modeled and described by the effective medium approximation. Using these modeling procedures the enhancement of transformation rate of the refractive index and of the extinction coefficient change in the presence of GNP layer were established and related to the influence of local (surface) plasmon fields. Results obtained enable further selection of optimized structures for optical recording, direct fabrication of plasmonic structures with suitable lasers.

Essential enhancement of the absorption coefficient near both the fundamental edge and the interference mode of chalcogenide film has been observed and explained quantitatively.

Quantum Chemical Study of the Spherical Silica Molecules Formation in Silicic acid Condensation

Filonenko O.V.

Chuiko Institute of Surface Chemistry of the NAS of Ukraine, Kyiv, Ukraine

Polycondensation of silicic acid molecules is a key stage of hydrothermal and sol-gel syntheses of nano- and mesoporous systems based on silica and aluminosilicates.

Significant progress in identifying of the peculiarities of some polycondensation stages is reached from analysis of the NMR spectroscopy and scattering of electromagnetic radiation data. Nevertheless the mechanism of particles condensation throughout the whole process has not been fully clarified yet. Thereby, elucidation of its features is necessary for further improvement of methods for synthesis of new materials based on silica.

Possibility of formation of fullerene-like molecules of polysilicic acids $[HOSiO_{1.5}]_n \equiv ((SiO_2)_n(H_2O)_{n/2})$ (figure) during polycondensation of monosilicic acid is analyzed by means of DFT/B3LYP, 6-31 ++G(d,p) (to take into account the influence of the solvent we used polarizable continuum model (PCM)). Data about the structure features of the considered fullerene-like molecules are also presented in this study.

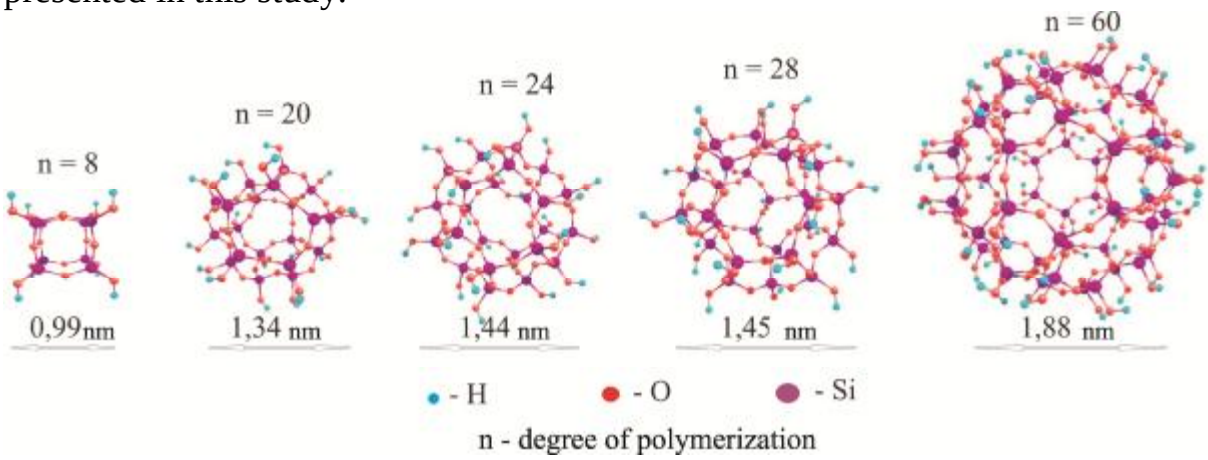

Figure. The equilibrium spatial structure of polysilicic acids

It is shown that formation of the hollow spherical silica molecules is energetically favorable, in contrast to its reverse reaction of hydrolysis. During the transition from $Si_8O_{20}H_8$ molecule to $Si_{20}O_{50}H_{20}$ molecule, its stability in solution increases due to reducing the curvature of the surface with silicon atoms, thus indicating the possibility of its presence as an intermediate in the synthesis process.

Simulation of Thermal Diffusion in Multilayered Structures Irradiated by Two Interfering Laser Beams

Gatskevich E.I., Ivakin E.V., Kisialiou I.G.

B.I. Stepanov Insitute of Physics of NAS of Belarus, Minsk, Belarus

Method of thermal transient gratings is widely used for thermal characterization of large variety of materials. However the interpretation of diffraction efficiency signals decay experimentally obtained under excitation of multilayered systems or thin film deposited on substrate appears to be rather complicated and ambiguous.

In this paper we carried out the simulation of the thermal diffusion in layered system irradiated by two interfering laser beams. The distribution of intensity of laser radiation is periodic along the x-axis $Q(x,t)= Q_0h(t)[1-\cos(gx)]$, where x is the coordinate in plane, $h(t)$ is the temporal shape of laser pulse, $g=2p/L$, L is the gratings period. The absorption of laser radiation gives rise the spatially periodic heating (thermal grating). Choosing the solution in the form $T(x,z,t) = T(x,t)T(z,t)$ we simplify our problem by separation of variables. The solution for $T(x,t)$ is found analytically taking into account periodical boundary conditions. The dependence $T(z,t)$ describing the depth depended temperature distribution is found by numerical solution of heat transfer equation in finite differences. The density, thermal parameters of each layer as well as heat transfer at the layer interface are taken into account.

The calculated data concerning relaxation of thermal gratings are shown to be in reasonable compliance with experimental results.

Using Atomic-Force Probe Technique in Ab-initio Study of Graphene Surface Reactivity

Gorbenko V.I.

Classical Private University, Zaporizhzhya, Ukraine

The main aim of this work was to define the potential-energy parameters of interaction of the H, O and C atoms with graphene sheet. The atomic-force probe technique has been used in ab initio calculations performed by GAMESS quantum chemistry software package. All ab initio calculations reported in this work were carried out using the Hartree-Fock method and was run on computers cluster of V.M.Glushkov Institute of Cybernetics of NAS of Ukraine. The graphene sheet has been presented by cluster model with 96 carbon atoms in the hexagonal cells and 24 hydrogen atoms on the cluster perimeter. In the atomic-force probe technique the atom-probe is moving above the surface on fixed distance without any optimization of its geometry. As a result the potential-energy (PE) profiles of interaction of the various atoms-probe with graphene sheet have been obtained.

The calculation results for hydrogen atom-probe are shown on the fig.1. Minima on the curve (a) are corresponding exactly to the positions of the H-atom probe above middle of the C-C bonds and maxima are to the site above center of hexagonal cell. The calculation results for hydrogen atom-probe are shown on the fig.1. Minima on the curve (a) are corresponding exactly to the positions of the H-atom probe above middle of the C-C bonds and maxima are to the site above center of hexagonal cell. The curve (b) is corresponding to the moving of the H-atom probe above C-atoms of graphene. For H-atom probe the site above middle of the C-C bonds is like to a saddle point. On fig.2 the result of atomic-force probe calculations for C-atom probe is shown. Its has been found the small local maximum of PE-profiles in the centre of hexagonal cell.

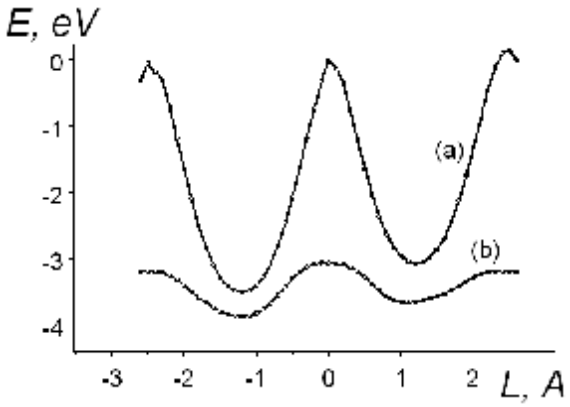

Fig.1. PE-profiles for H-atom probe/

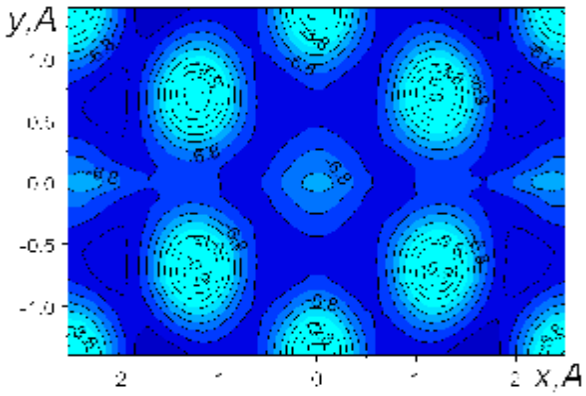

Fig.2. PE-contours for C-atom probe/

Dynamics of Spin-Crossover Materials Driven by Multiplicative Colour Noise Action

Gudyma Iu.V., Maksymov A.Iu.

Chernivtsi National University, Chernivtsi, Ukraine

The exhaustive capabilities of existing informational technologies cause the problem of finding new classes of the nanomaterials with much better characteristics for data storage and processing system. The spin-crossover compounds are the class of magnetic macromolecules characterized by ligand environment which form the crystal field with octahedral symmetry and the central situated transition metal ion with $d^4 - d^7$ electronic configuration. Depending on spin orientation of electrons on outer orbital of the ion is possible two configurations: the stable low-spin (LS) and metastable high-spin (HS) configuration with diamagnetic and paramagnetic properties. The mechanism of functioning of spin-crossover solids are based on interconversion between LS and HS spin-states induced by external physical fields (light irradiation, temperature, magnetic fields and other).

We studied the effect of fluctuation on the transition between LS and HS states. The fluctuations are described by multiplicative colour noise partially using the mathematical tools from the work [1] where the spin-crossover system with additive colour noise action was investigated. The additive and multiplicative Gaussian white noise action on system behaviour was studied in our previous works. Here the stochastic dynamics of spin-crossover system is studied in framework of Langevin macroscopic equation with multiplicative Ornstein–Uhlenbeck process:

$$\frac{dn_{HS}}{dt} = b\left(1-n_{HS}\right) - n_{HS}\exp\left[-an_{HS}\right] + \left(1-n_{HS}\right)x(t). \qquad (1)$$

Here b is light intensity (control parameter), n_{HS} – HS fraction, a – self-acceleration factor, $x(t)$ is colour noise term. From stationary solution of corresponding Fokker-Planck equation is defined the probability distribution function which describes the system behaviour under multiplicative noise. From probability distribution of system states it is easy to find the spinodals separating bistable and monostable regions. These results were used to obtain the ratio of passage times from metastable state and backwards in framework of Mean First Passage Time technique with Kramers-like approximation. The time characteristic of system states qualitatively differ for additive and multiplicative noise action. For the both cases the system shows different sensitivity to change of additive and multiplicative colour noise.

1. Gudyma Iu., Maksymov A., Enachescu C. Decay of a metastable high-spin state in spin-crossover compounds: mean first passage time analysis // Eur. Phys. J. B. – 2010. – V.78. – P.167–172.

Influence of Magnetic field on Electron Energy Spectrum in Complicated Cylindrical Semiconductor Nanotube

Gutsul V.I., Makhanets O.M., Tsiupak N.R.

Chernivtsi National University, Chernivtsi, Ukraine

The intensive development of nanotechnologies gives opportunity to create the new nano-systems with clear-cut shapes. In particular, in paper [1] the authors have been obtained the arrays of complicated semiconductor nano-tubes and investigated the respective radiation spectra. The unique properties of quasi-particles in nano-tubes allow their utilization as the basic elements of tunnel nano-diodes, nano-transistors with the high mobility of electrons, efficient light emitting devices, photo electric transformers, nano-sensors for the diagnostics of different biological and chemical compounds.

Under the influence of outer magnetic field the electron energy spectrum in nano-tube is now formed not only due to the spatial confinement of the charge carriers but due to the Landau magnetic quantization as well. Taking into account the both reasons brings to the new and interesting peculiarities in electron energy spectra and its dependence on geometrical parameters of nano-system and magnitude of magnetic field induction.

In the proposed paper we study the nano-system consisting of the cylindrical quantum wire, semiconductor barrier-shell and nano-tube embedded into the outer medium. The constant magnetic field with the induction $\vec{B}$ is directed along the axial axis of nano-system.

The calibrating relationship for the vector potential considering the cylindrical symmetry and constant magnetic field is conveniently taken as $\mathrm{A}(\vec{r}) = \frac{1}{2}[\vec{B}\times\vec{r}]$. In this case the stationary Schrodinger equation is exactly solved for the each part of complicated nano-tube. The electron wave functions are obtained as linear combinations of the degenerated hyper geometrical functions and generalized Legendre polynomials. The dispersion equation defining the electron energies is obtained from the normality condition and the continuity of wave functions and their densities of currents at all semiconductor media interfaces of nano-system.

In the paper we study the dependences of electron energy spectrum on the geometrical parameters of nano-tube and the magnitude of magnetic field induction.

1. Fontcuberta i Morral, D. Spirkoska, J. Arbiol, M. Heigoldt, J. R. Morante, G. Abstreiter Prismatic quantum heterostructures synthesized on molecular-beam epitaxy GaAs nanowires // Small. – 2008. – V.**4**. – P.899–903.

Influence of Nanostructurization on Superficial Activity of Amorphous Metallic Alloys

Hertsyk O.M., Kovbuz M.O., Pereverzeva T.G., Bojchyshyn L.M.

Ivan Franko Lviv National University, Lviv, Ukraine

Forming superficial films on the amorphous metallic alloys (AMA) $Fe_{78.5}Ni_{1.0}Mo_{0.5}Si_{6.0}B_{14.0}$ (AMA-1) and $Fe_{73.1}Cu_{1.0}Nb_{3.0}Si_{6.5}B_{7.4}$ (AMA-2) from (0,5÷5,0)mM aqueous-ammoniac solutions of oligoperoxide (OP) based on vinyl acetate, 2-tert-butylperoxy-2-methyl-5-hexene-3-yne and maleic anhydride, obviously depends on element composition and structure of the surface. Values of coordinating numbers, expected from a curve of radial distribution of atoms (Z_s) and selected after minimum (Z_m) for AMA-2 differ (table), that specifies on its partial nanostructurization.

By potentiometric investigation (Jaissle Potentiostat-Halvanostat IMR 88 PCR) of adgesive firmness of the films inflicted on the contact (c) and external (e) surfaces of AMA, wich have different degree of crystalline, it has been shown that for AMA-2 in all cases under shielded films corrosive firmness of metal surface increases, but on AMA-1 steady films formes only from 0,5% oligoperoxide solution during 10 minutes (τ), what resulted in positive potentials of the electrode only for this case. Results of electrochemical impedance spectroscopy (Autolab®/PGSTAT-20) of AMA samples with OP films got after ($R_1(Q_{dl}R_2)$) scheme (R_1-resistance of electrolyte, 51,5 Om, R_2 – resistance of charge transfer, Q_{dl} – capacitance of double electric layer) (table) confirmed higher cognation of investigated oligoperoxide to AMA-2 surface, what resulted in higher values of R_2 and notably lower values of surface asperity (R_f).

Comparison of structural and electrochemical characteristics of AMA surface, preliminary caused by OP films

AMA	Z_s	Z_m	τ, min	Side	R_2, Om·cm^2	Q_{dl} ·10^4, F·cm^{-2}	R_f
AMA-1	11,8	11,4	-	c	2370	10,12	50,6
				e	5950	7,82	39,1
			10	c	870	18,28	91,4
				e	3220	4,52	22,6
AMA-2	11,4	12,1	-	c	3180	0,54	2,72
				e	6640	0,15	0,75
			10	c	1920	0,53	2,63
				e	9230	0,25	1,23

Partial structurization of AMA-1 after heat treatment also promotes its surface activity. Thus, nanostructurization of amorphous metallic alloys based on ferrum caused increasing of surface activity.

Oscillator Strengths of Quantum Transitions in Spherical Core/Shell/Well/Shell Quantum Dot with Donor Impurity

Holovatsky V.A., Bernik I.B.

Chernivtsi National University, Chernivtsi, Ukraine

The semiconductor low-dimensional quantum heterostructures (i.e. quantum wells, wires and dots) are conspicuous in many technological applications such as infrared photo detectors, lasers, light-emitting diodes, single electron transistor, etc. The modern advances in semiconductor technology allow the produce of more complex structures than the simple quantum wells, wires or dots. These structures, such as multiple quantum rings, complex quantum wires and the quantum-dot-quantum-well (QDQW) structures [1], are extensively studied. QDQW are the multi-layered quantum dots, composed of two semiconductor materials, the one with the smaller bulk band gap is sandwiched between a core and an outer shell of the material with larger bulk band gap and embedded into the matrix. QDQW structures can be applied for the creation of white-light emission sources [2].

The energies of carriers mainly depend on the core radius and shells sizes of the QDQW. An impurity realizes the important effect on the electronic and optical properties of QDs. The presence of charged impurity in QD changes the potential of size quantization, affecting both the quasi-particles energy spectra and oscillator strengths of radiation transitions.

In this study, we have performed an investigation of the electron and hole energies, wave functions and probability distribution for the cases with and without the donor hydrogen-like impurity in the centre of QDQW structures with different thicknesses of layers. On the base of this investigation the oscillator strengths of intra- and inter-band quantum transitions were estimated. The dependencies of 1s-1p and 1s-2p intra-band electron quantum transitions and intra-band electron-hole quantum transitions were obtained as functions of geometrical parameters of QDQW. It was established that oscillator strengths of the quantum transitions non-monotonously depend on the layers thicknesses due to the different carriers localization.

1. Tyagi P. and Kambhampati P. Independent Control of Electron and Hole Localization in Core/Barrier/Shell Nanostructures // J.Phys.Chem.C. – 2012. – V.116, №14. – P. 8154–8160.
2. Nizamoğlu S., Mutlugün E., Ozel T., Demir H., Sapra S., Gaponik N., Eychmuller A. Dual-color emitting quantum-dot-quantum-well CdSe-ZnS heteronanocrystals hybridized on InGaN/GaN light emitting diodes for high-quality white light generation // Appl. Phys. Let. – 2008. – V.92, P.113110.

Heterostructures of TiO_2 with Various Polymethine Dyes

Husyak N.B., Kobasa I.M.

Yu. Fedkovych National University of Chernivtsi, Ukraine

Designing and development of new highly active photocatalytic systems for various important applications is one of high-priority issues in modern photocatalysis. As proved by a series of investigations, high prospects are expected in designing of structurally ordered photocatalytic blocks, which contain a semiconductor's nanoparticle and the dye-sensitizer, applied and fixed on the surface with the electron-conducting film. The kinetic complications are eliminated because of the tight contact between the photocatalyst and photosensitizer, which ensures better light absorption because an effect of the inner light filtration does not act in this case. However, only preliminary assumptions were made about a chemical form of the dye applied on the semiconductor while no information about a character of the dark-phase interaction between the photocatalytic block's components is available. The information related to the concentration dependencies of the block's activity should also be supplemented as well as checking of possible utilization of various dyes as sensitizing agents.

The cationic polymethine dyes with indolyne cycles with 2-4 methine groups were used to design the TiO_2-based heterostructures.

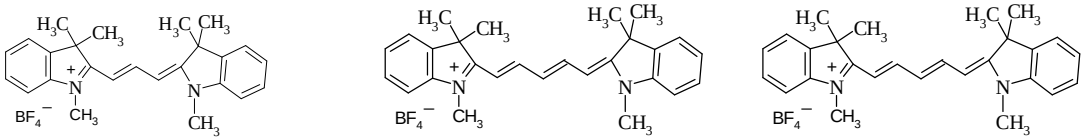

New materials with extended light sensitivity range have been synthesized.

We also determined a character of relations between the composite photocatalyst's activity and its quantitative composition. The energy parameters of the photocatalytic systems were estimated and possible mechanism of the photocatalysis was considered.

Analysis of the results proves that the above mentioned approach to designing of the light sensitive materials, which includes construction of the single block from the semiconducting photocatalyst and sensitizer (the polymer film should be applied to protect the latter component from dissolution), can generally be used for different semiconductors and sensitizers.

The Gold Nanoparticles Arrays on Glass Slides Fabrication and Properties

Il'chuk G., Kusnezh V., Petrus' R.

Lviv Polytechnic National University, Lviv, Ukraine

The further increase efficiency of CdS/CdTe thin film solar cells (SC) requires the use of new approaches. In particular thin-film SC performance can be significantly improved by using metal nanoparticles (NPs) deposited on top of the photoactive layer.

The arrays of gold nanoparticles on glass substrates were fabricated by thermal annealing (400 º C, 120 min.) in vacuum (P ~ 1,3 Pa) of gold thin films with 6-7 nm nominal thickness obtained by magnetron sputtering (Neo Coater MP-19020 NCTR, Jeol, Japan) on pretreated glass substrates (16×16 mm^2). The surface morphology using an atomic force microscope and optical absorption α(λ) using fiber optic spectrophotometer (AvaSpec-ULS2048-UA-50, Avantes, Netherlands) were investigated, fig.1.

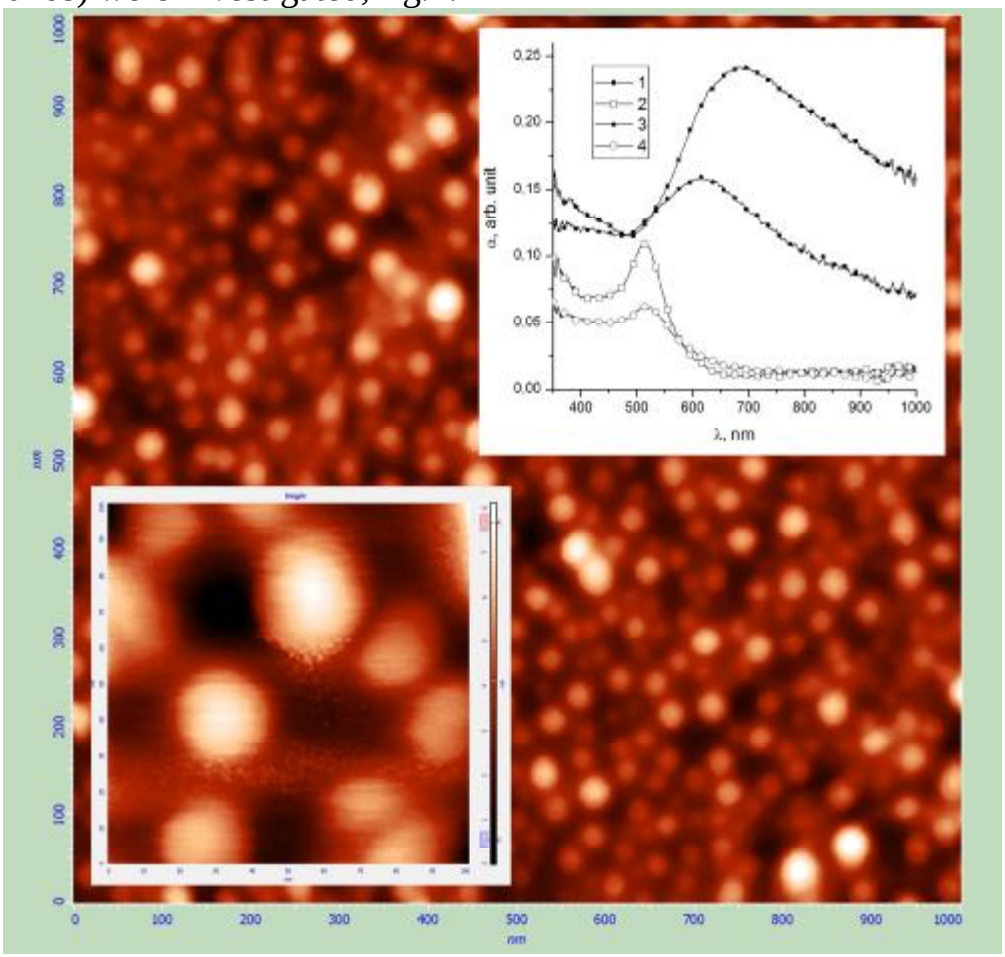

Fig.1. The surface morphology of gold films with 6-7 nm nominal thickness after thermal annealing, on top inset the absorption spectra of gold films as deposited (1, 3) and after thermal annealing (2, 4) for different samples.

Optical Diagnostics of Heating and Melting Processes in Cadmium and Lead Tellurides under Pulsed Laser Irradiation

Ivlev G.D.[1], Gatskevich E.I.[2], Malevich V.L.[2], Malashkevich G.E.[2], Shimko A.N.[2], Freik D.M.[3], Nykyruy L.I.[3], Yavorski Ya.S.[3]

[1]*Belarusian State University, Minsk, Belarus*
[2]*B. I. Stepanov Institute of Physics, Minsk, Belarus*
[3]*Physics and Chemistry Institute of V.Stefanik Pre-Carpathian National University, Ivano-Frankivsk, Ukraine*

The *in-situ* monitoring of laser-induced processes in CdTe and PbTe has been carried out by using optical probing method. The method is based on the registration of the changes in reflectivity under transformation from solid to liquid phase.

The samples were irradiated by single pulses of a ruby laser (wavelength 694 nm, pulse duration 80 ns at FWHM). The energy densities varied from 0.1 to 0.35 J/cm^2. The laser optical scheme ensured the high homogeneity of irradiation in cross-section. The optical probing was realized by using a non-spiking pulsed Nd:Glass laser. The wavelength of probing beam was 1.06 μm, that corresponds to photon energy density 1.2 eV.

It is found that in both semiconductors the dynamics of reflectivity depends on irradiation energy density, but their time dependences differ essentially. In CdTe at irradiation energy density E about 0.1 J/cm^2 we observe the increase in reflectivity. With increase in E up to 0.14 J/cm^2 a small valley between two peaks appears in reflectivity time dependence. The further increase in E up to 0.3 J/cm^2 leads to the prolongation of the distance between the peaks. At E exceeding 0.35 J/cm^2 the destruction of samples is observed. In contrast to CdTe, we observe the decrease in reflectivity of PbTe at irradiation with E=0.1 J/cm^2. The increase in E up to 0.14 J/cm^2 leads to prolongation of the phase of decreased reflectivity. This situation is observed up to the irradiation energy density corresponding to destruction of PbTe samples.

This distinction reflectivity dynamics can be explained by the different dependences of energy gap on temperature in semiconductors. In CdTe band gap E_g =1.49 eV at 300K. With temperature increase the band gap is constricted and at the melting temperature it is 1.05 eV that is less than the photon energy of the probing beam. This leads to an increase in reflectivity and complicated dynamics observed can be explained by interference effects taking place in liquid layer on semiconductor surface. As for PbTe its energy gap increases from 0.3 up to 0.36 eV with temperature rise from 300 K up to 450 K and then it does not change. Because of this, the refraction index and reflectivity of PbTe decreases with increasing temperature. The reflectivity dependences studied indicate also that the melting of both CdTe and PbTe is patterned after “semiconductor- semiconductor” transition.

Synthesis and Properties of Porous ZnSe

Kidalov V.V., Dyadenchuk A.F.

Berdyansk State Pedagogical University

The recent increased interest in porous semiconductors. They are used in the manufacture of optoelectronic devices-infrared, anti-reflection coatings as solar cells, sensors and microelectronics, etc. This makes the actual task study data properties of semiconductor materials.

The traditional way of producing porous semiconductors is electrochemical etching. Of these structures to now the most detailed study of binary compounds A^3B^5 [1].

A large number of publications devoted to the study of the properties of these compounds. However, studies to elucidate the mechanism of formation of porous semiconductor compounds A^2B^6 are still poorly understood [2-3]. Among the most promising materials such as wide-A^2B^6 belongs zinc selenide. ZnSe – binary compound, so we picked up a solution of acids, which poisons both sublattices.

In Fig. 1 (electrolyte $HF:HNO_3:HCl$ = 2:3:3, the etching time was 20 min) a micrograph of porous layers of processed crystal ZnSe (100) orientation. Clearly visible on the surface of pore formation and they are distributed more or less regularly over the entire surface of the crystal. Photos morphology of the porous layer of zinc selenide obtained with a scanning electron microscope JSM-6490. The method of energy dispersive X-ray analysis (EDAX) was established chemical composition of elements on the surface of the sample which demonstrates the stoichiometry of the surface.

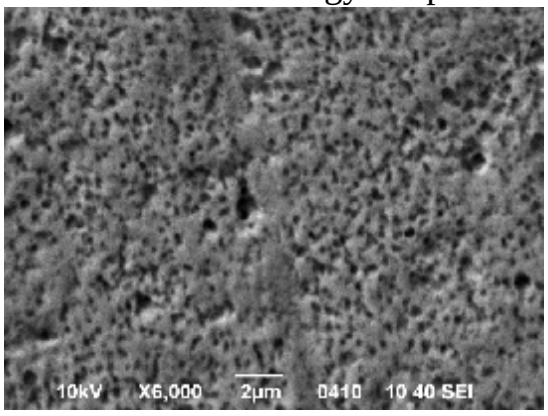

Fig. 1. SEM image of the surface of the porous n-ZnSe, the etching time t=20 min, the electrolyte of $HF:HNO_3:HCl$ = 2:3:3, cavitation voltage 16-17 V, current density of a porous structure j=80 mA/cm.

1. Kang Y. and Jorne J. Porous silicon formation: Morphological stability analysis // J. Electrochem. Soc. – 1993. – V. 140. – pp.2258.

2. S. Zimin, V. Vasin, E. Gorlachev, Ed. Buchin, V. Naumov. Investigations of PbSe layers after anodic electrochemical etching by scanning electron microscopy // Phys. Status Solidi. – V. 8, № 6. – 2011. – pp. 1918–1922.

3. Ed. Monaico, A. Ubrieta, P. Fernandez, J. Piqueras, I.M. Tiginyanu, V.V. Ursaki, and R.W. Boyd. Intense luminescence from porous ZnSe layers // Moldavian Journal of the Physical Sciences. – Vol.6, №2. – 2007. – pp. 129-134

Electric Voltage Driven Dynamic Properties of Multiferroic Nanoparticles with Antiferromagnetic Layer

Kondovych S.V., Gomonay H.V.

National Technical University of Ukraine "KPI", Kyiv, Ukraine

To drive and control the state of a magnetic nanoparticle, we can use not only intrinsic properties of magnetic material, but also shape and size of the sample. As for ferromagnetic particles, shape effects allow to set and control the parameters of the sample during production. Recent experiments [1–3] with nano-sized samples show that shape can affect also the properties of antiferromagnetic (AFM) materials, though theoretical interpretation of these effects is under discussion.

In the present work we study theoretically the shape-induced dynamic properties of synthetic multiferroic particle (AFM nanopillar on the piezoelectric (PE) substrate). Alternative electric voltage applied to the sample induces the tensile mechanical stress that changes shape of AFM layer and produces oscillation of AFM vector. We model shape-induced anisotropic effect on magnetic state of AFM layer according to the concept of the destressing energy [4], which depends both on volume-average AFM vector components and geometry of the sample.

In the framework of the Lagrange technique we calculate the oscillations spectra of AFM vector in the AFM/PE nanoparticle of the elliptic shape in the presence of the external magnetic field. We also discuss the conditions under which a) resonance and b) parametric resonance occurs.

1. Folven E. Antiferromagnetic domain reconfiguration in embedded $LaFeO_3$ thin film nanostructures / E. Folven, T. Tybell, A. Scholl, A. Young *et al.* // Nano Lett. – 2010. – Vol. **10**. – P. 4578-4583.
2. Folven E. Effects of nanostructuring and substrate symmetry on antiferromagnetic domain structure in $LaFeO_3$ thin films / E. Folven, A. Scholl, A. Young, S. T. Retterer *et al.* // Phys. Rev. B. – 2011. – Vol. **84**. – P. 220410(5).
3. Folven E. Crossover from spin-flop coupling to collinear spin alignment in antiferromagnetic/ferromagnetic nanostructures / E. Folven, A. Scholl, A. Young, S. T. Retterer *et al.* // Nano Lett. – 2012. – Vol. **12**. – P. 2386-2390.
4. Gomonay H. V. Shape-induced phenomena in finite-size antiferromagnets / H. V. Gomonay, V. M. Loktev // Phys. Rev. B. – 2007. – Vol. **75**. – P. 174439(6).

Synthesis and Optical Properties of Semiconductor Heterostructures with Dye-Sensitizers

Kondratyeva I.V., Kobasa I.M.

Yu. Fedkovych Chernivtsi National University, Chernivtsi, Ukraine

Titanium dioxide and cadmium sulfide are important semiconductor materials of the modern technique. Photochemical interaction involving semiconductor and a dye is very dynamic field of modern photochemistry and nanotechnology. Many investigations are being conducted in this field in relation to the solar energy utilization, transformation and toxic wastes treatment. Designing of new photoactive heterostructures, which contain some amount of photocatalytic heterostructures, dye-sensitizer and some other substances is quite a promising direction.

We have synthesized some examples of such heterostructures containing cyanine dye and TiO_2 or CdS. Absorption spectra of heterostructures have been analyzed and their photocatalytic activity in the reaction of methylene blue reduction was determined.

Special heterostructures comprising titanium dioxide or cadmium sulfide were synthesized using experimental method to determine sensitizing activity of the cyanine dye. This method includes treatment of the dispersions comprising a semiconductor with the ethanol solution of the dye. Further drying of the heterostructures at the room temperature followed by treatment in the benzene solution of polyepoxipropylcarbazole removed traces of the solvent and formed thin polymer film on the heterostructures surface. This film prevents dissolution of the heterostructures but does not impede any external electron interaction. It was found that 0.2 mg/g polyepoxipropylcarbazole in the heterostructures ensures best result.

Analysis of changes in the spectral parameters proved that decrease of the photocatalytic activity on increasing content of dye can be caused by decreasing interaction between the dye and semiconductor. Wavelength band of the TiO_2 comprising heterostructure spectra is wider than the same band for the solution spectra. Absorption spectra of the CdS comprising heterostructure are more informative. Positions of both bands depends on the dye content. Heterostructure shows much wider absorption bands comparing to the ones for the corresponding solutions. This widening results in more significant overlapping of the bands.

Interactions between the heterostructure components and their activity in the reaction of methylene blue reduction under irradiation of various spectral zones have been investigated. Some characteristics of these processes have been found and explained.

Theoretical Study of Carbon Monoxide Interaction with Platinum Binary Nanoclusters $Pt_{42}Me_{13}$ (Me – Fe, Co, Ni)

Korniy S., Pokhmurskii V., Kopylets V.

Karpenko Physico-Mechanical Institute of the NAS of Ukraine, Lviv, Ukraine

In frames of quantum-chemical method of density functional theory DFT a model was proposed to study poisoning of platinum binary nanoclusters $Pt_{42}Me_{13}$ (where Me – transition metals Fe, Co, Ni) of shell structure by carbon monoxide, which is an active component of fuel cell environment. The model is based on calculations of adsorption behaviors of CO interaction with nanocluster surfaces. In the sequence an ability of nanoclusters to form strong chemical bond with carbon monoxide in dependence on the core type of our nanoclusters and adsorption sites on their surface.

The electronic structure of optimized nanoclusters was calculated in the Stobe 2011 [1] program code by DFT method in generalized gradient approximation (GGA) for exchange-correlation functional B88-LYP and basis set double- ζ with valence polarization DZVP. For oxygen and carbon we used standard valence-splitted basis set 6-31G (d) with polarized 3*d*-orbitals.

The results indicate that binary nanocluster core influence sufficiently on geometry and energy parameters of platinum surface atom interaction with the molecule of CO. Thus, the adsorption heat or strength of CO bonding with the surface increases in the series $Pt_{55} \leq Pt_{42}Ni_{13} < Pt_{42}Co_{13} < Pt_{42}Fe_{13}$. Activity growth of nanoclusters to bind CO is determinate by electron density of the 5*d*-orbital, which in great degree depends on dimension surface forces (dimension effects) and electron interaction between platinum layer on the surface and the core it self as a ligand effect.

The presence of nickel in under layer of binary nanoclusters insufficiently influences on platinum properties, whereas iron and cobalt in the core vise versa – decreases the stability of platinum to poisoning by carbon monoxide. Such behavior of $Pt_{42}Ni_{13}$ nanoclusters during the interaction with CO would be described according to ligand mechanism of nickel influence on bonding Pt-CO through its action on electronic structure of surface platinum atoms.

Thus, received results may be used during preparation, component optimization and production of nano-dimension binary nanoclusters, based on platinum, in low temperature fuel cells.

1. Hermann, K.; Pettersson, L. G. M.; Casida, M. E. et al. StoBe 2011, Version 3.1, 2011.

Optical Properties of Ultrafine γ-Fe_2O_3

Kotsyubynsky V.O., Moklyak V.V., Hrubiak A.B.

Vasyl Stefanyk Precarpathian national university, Ivano-Frankivsk, Ukraine

Optical properties of ultrafine powdersγ-Fe_2O_3 synthesized by a modified liquid-phase method were investigated. Aqueous solutions of $Fe(NO_3)_3 \cdot 9H_2O$ and $C_6H_8O_7 \cdot H_2O$ in molar ratio of 1:1 were used as a base precursors. Two systems of hydratediron citrate gels with different molar concentrations of precursors weresynthesized. Molar concentrations of solution were 0.3 M and 0.5 M. Two series of ultrafine γ-Fe_2O_3 samples (named 0,3 Mand 0,5 M)were obtained by gels annealing at temperatures of 125, 150, 175, 200, 225 and 250°C during 1 hour. The sizes of coherent scattering regions (calculated by the Scherer formula)were7-10 nm for samples of 0,3M and 10-11 nm for 0,5M series respectively. The investigations of γ-Fe_2O_3 were carried out by optical spectroscopy methods in the visible and infrared regions of the spectrum. Accordinglyto IR spectroscopy data for all samplesthe presence of the surface molecular water and structurallybondedhydroxyl groups is typical what is proved by broad regions of absorption at 3100-3600 cm^{-1} and peaksat 1600-1650 cm^{-1}. Another typical feature is the absorption band at 1400-1480 cm^{-1}which correspondsto the stretching vibration surface adsorbed COO^-.

As a result of UV-VIS photometry data treatment the dependencies $ln(ahn) = f(hn)$ were formed (α – optical absorption coefficient). On the differential curves $\frac{d(ln(ahn))}{d(hn)} = f(hn)$ for all samples of both series two additional peaks that correspond to the band gap about 1.46and1.58eVfor materials of 0.3 M series and also 1.50and1.58eVfor a samples 0.5 M (Fig.1). The band gap for a bulk γ-$Fe_2O_3$is 2.06eV; this value is corresponded for the core parts of the nanoparticles. Band gap decreasing for ultrafine γ-Fe_2O_3 compared with the bulk samples was associated with the reconstruction effects on the nanoparticles surface. Minimizing energy of particle shells defect structure involves the formation of intermediate phase with the presence of impurity atoms (carbon) that lead to size effects and deformation of material electronic structure. Non-equabilityof ultrafine γ-Fe_2O_3 formation processes also make contribution. Ultrafine γ-$Fe_2O_3$with the modified band structure is a promising.

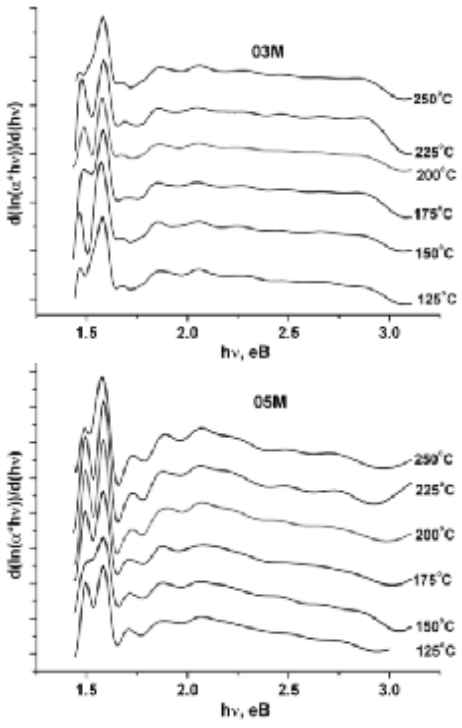

Fig.1

The Features of Magnetic Properties of Ferromagnetic Nanocomposites of Different Composition

Lashkarev G.V.[1], Radchenko M.V.[1], Bugaiova M.E.[1], Lazorenko V.I.[1], Pavliuk M.M.[1], Krushynskaya L.A.[2],Stelmakh Y.A.[2], Knoff W.[3], Story T.[3], Dumont Y.[4]

[1]*I.M. Frantsevych Institute for Problems of Material Science, National Academy of Sciences of Ukraine, Kyiv, Ukraine*
[2]*Electric Welding Institute, Academy of Sciences of Ukraine, Kyiv, Ukraine*
[3]*Institute of Physics, Polish Academy of Sciences, Warsaw, Poland*
[4]*Laboratoire GEMaC, University of Versailles St Quentin en Yvelines, Versailles, France*

The ferromagnetic nanocomposites (FMNC) as spintronic materials for magnetic sensors and magnetic memory are characterized by technologically controlled inclusions of transition metals (TM) or their alloys in the form of nanoparticles (NPs) in dielectric matrix with required dimensions and shape.

Electron beam evaporation of Co and Al_2O_3 from two crucibles was used for deposition of FMNC granular layers [1]. The transition temperature (TT) from spin-glass to superparamagnetic state (SPS) is ~ 200K at NPs dimensions d~10÷20nm, 50K at d~3÷5nm and 12K at d<3nm. It is shown that the transition from FM to SPS state due to magnetostatic interaction between FMNPs (appearance of hysteresis loop) occurs at increased temperatures for higher dimensions of Co NPs.

Firstly for FMNC Co/Al_2O_3, grown by mentioned technology, "magnetic exchange bias" (MEB) was observed. Its nature is associated with the magnetic exchange interaction between a ferromagnetic metal core NPs Co with an antiferromagnetic (AFM) CoO layer on the surface of NPs. Its magnitude is 60 Oe when the content of Co 42.8 at.%. With the reduction of the Co NPs size MBE decreases due to lowering of the magnetic anisotropy, which depends on the thickness of the AFM shell.Small magnetic shift (60 Oe) in FMNC Co/Al_2O_3 appeared significantly lower than in the case of Co NPs oxidized at high temperature ~ 1000 ° C (-9.5 kOe). This means that in samples grown by electron beam technology the energy of the exchange magnetic anisotropy, which decreases with lowering of the thickness for the AFM CoO layer is not sufficient to increase the coercive force in the opposite magnetic field direction relatively to the first applied one. It is due to the small thickness of CoO.

1. M.V.Radchenko, G.V.Lashkarev, M.E.Bugaiova et al. Phys. Stat. Sol. (b), **248**, 1619 (2011).

Fabrication of Anodic Porous Alumina Films for Biosensors

Lebyedyeva T., Shpylovyy P.

V.M. Glushkov Institute of Cybernetics, Kyiv, Ukraine

Metal clad waveguide (MCWG) is a transparent plate whereon there is a semitransparent film through which light goes in the transparent dielectric film of a relevant thickness which is a flat waveguide. Waveguide modes are seen as the minimums on reflectance curve, observation angles of which depend on thickness of dielectric film and on optical characteristics of the system [1]. MCWG sensor with porous anodic alumina (PAA) waveguiding layer is advantageous in sensing of biomolecules because of a high surface area of nanopores and a sharp dip in the reflection curve (Fig.1).

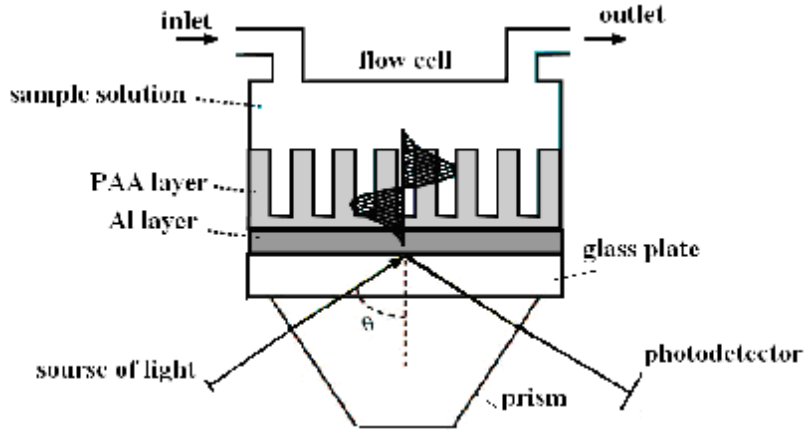

Figure 1. Scheme of MCWG Al - porous Al_2O_3 sensor setup and field distribution of a single guided mode.

The work is devoted to creation of technology of Al - porous Al_2O_3 sensor substrates. Fabrication of multilayer include magnetron sputtering for deposition of Al film and Nb adhesion layer, anodic oxidation of Al for formation of nanoporous alumina layer and chemical etching for widening of pores. Special device for providing and control regimes of anodization was developed. Formation of porous anode oxide and expansion of pores was controlled by monitoring appearance and changes of the waveguide mode on means of “Plasmontest” device, developed in Institute of Cybernetics. Preliminary immunosensor investigations on the “Plasmontest” employing standard couple protein A-IgG were carried out successfully.

The work was supported by State Scientific and Technical Program "Nanotechnologies and Nanomaterials" in 2010-2014, № 5.20.3.34.

1. Lebyedyeva T.S., Shpylovyy P.B. et.al. Modelling and Data Processing for Thin-Film Optical Sensors // Proc. of 6-th IEEE Intern. Conf. on Intelligent Data Acquisition and Advance Computing System: Technology and Application, Praga-2011.- Vol. 1.- P.119-124

Nanostructured Catalytic Hpa-Materials for Convertion Biomass Processes

Molodyy D.V., Tkachenko T.V., Melnichuk O.V., Povazhny V.A., Golovko L.V.

Institute of Bioorganic Chemistry and Petrochemistry, Kiyv, Ukraine

Promising use of biomass is the production of synthetic fuels [1]. To increase the efficiency of transformation of a biomass into biofuel recently nanoporous structured catalysts with strong acidic Brønsted centers on their surface often are used [2, 3].

Nanostructured heteropolyacid silicate composites (HPA) with controlled content $H_3PW_{12}O_{40}$ by simultaneous hydrolysis and condensation tetraethoxisilane (TEOS) of $H_3PW_{12}O_{40}$ in the presence of surface-active template Pluronic P123 ($EO_{20}PO_{70}EO_{20}$; EO-ethylene oxide; PO-propylene oxide) with followed hydrothermal treatment and template removal were obtained. Nanoporous hybrid catalysts had specific surface area of 650-700 m^2/g and a total pore volume of 0.5 - 1.2 cm^3/g. TPD method of ammonia desorption from the surface of the synthesized catalysts confirmed superacid level of catalytic centers (energy desorption of ammonia at 650^oC is 134 J/mol). By wide-angle scattering of X-rays method amorphous structure of the newly hybrid materials with strong interaction with silica of fine dispersed HPA were confirmed. By help of infrared spectroscopy Keggin structure of HPA inside hybrid catalyst was acknowledged.

An optimal concentration of $H_3PW_{12}O_{40}$ in the hybrid catalyst was established at the level about 17%. It is shown that the catalytic activity of hybrid catalysts $H_3PW_{12}O_{40}/SiO_2$ in 2.5-3 times more of the activity of pure $H_3PW_{12}O_{40}$. As a result of acid hydrolysis a high yield of hydroximethylfurfural and furfural derivatives were reached. It is prospective for obtaining high-energy biofuels. The obtained results have showed high promise of new hybrid catalysts for producing of biofuel components from renewable raw materials.

1. Kuznetsov B.N., Kuznetsova S.A., Danilov V.G., etc. // Catalysis Today. – 2002. – V.75. – P. 211-217.
2. Suganuma S., Nakajima K., Kitano M., etc. // J. Am. Chem. Soc. – 2008. – V. 130. – P. 12787-12793.
3. Hegner J., Pereira K.C., DeBoef B., Lucht B. // Tetrahedron Lett. – 2010.

Electrochemical Properties of Composite TiS_2<C> in Aqueous Electrolyte

Morushko O. V., Yablon L. S., Hemiy O. M., Rachiy B. I., Kuzyshyn M. M., Budzulyak I. M.

Vasyl Stefanyk Precarpathian National University, Ivano-Frankivsk, Ukraine

The hybrid condenser system, which combines the electrodes of battery and capacitor type, has several advantages over conventional supercapacitors, and therefore there is an intensive search for materials, electrodes from which will function in such systems. We have researched the use of titanium disulfide and composites TiS_2<C> as electrodes for hybrid supercapacitors. Composites TiS_2<C> with different carbon content (5, 10, 20, 30%) were formed. We have used the origin and the laser-irradiated TiS_2. Electrochemical studies of composites were carried out in galvanostatic mode by three electrodes scheme in 30% aqueous solution of KOH. Chlorine-silver electrode was the reference electrode. Opposite electrode was a platinum electrode. The working electrode was prepared from composite material TiS_2 and conductive additive in a ratio of 75:25.

Obtained energy parameters of composites are shown in Table. 1. As you can see, maximum capacity is reached at low discharge currents, because TiS_2 provides high electronic conductivity. Further increase in current causes the potential jump (IR-drop), because titanium disulfide restricts access of electrolyte ions, and therefore ion resistanceincreases and thus capacity reduces.

Thus, the laser modification allows to increase capacity by 15%, since in this case the change in resistance in the range of currents does not exceed 20%, while the change in resistance of unirradiated sample is 45%.

Table1

Parameters of composition materials

Sample*	I, mA	IR_{drop}, V	C_{sp}, F/g
TiS_2<C> – 0	1	0,03	47,0
	2,5	0,1	32,0
	5	0,2	26,5
	7,5	0,34	22,2
	10	0,48	18,1
TiS_2<C> – 1	1	0,03	65,9
	2,5	0,05	38,2
	5	0,11	34,2
	7,5	0,16	31,8
	10	0,22	30,5

*TiS_2<C> – 0 – not modified by laser radiation; TiS_2<C> – 1–modified by laser radiation.

Short range Order Change at Structural Relaxation in $Fe_{75}Si_6B_{14}Mo_5$ Amorphous Alloy

Mudry S., Kulyk Yu., Zhovneruk S.

Ivan Franko National University of Lviv, Lviv, Ukraine

Structural relaxation in amorphous alloys is related with changes of properties, most of which are important at practical application those materials. It is clear that such changes of properties should be analyzed with considering a short range order structure. It is known that heating of amorphous alloys is accompanied by two main processes: structure relaxation and crystallization. There are two kinds of structural relaxation – low- temperature relaxation and high-temperature one. In this work we represent the results on structure changes at high-temperature relaxation in $Fe_{75}Si_6B_{14}Mo_5$ amorphous alloy.

The structure changes in $Fe_{75}Si_6B_{14}Mo_5$ amorphous alloy at heating within temperature range 383-683 have been studied by means of X-ray diffraction method. Analysis of structure factors showed the variation of their parameters especially in the region of the second maximum. Its subpeak is most sensitive to annealing temperature and becomes most pronounced at annealing within temperature range 598-673 K. The similar behavior was observed early in other amorphous alloys and on that reason in general it is the most important characteristic of structural relaxation process. In order to have a more knowledge the detailed analysis of submaxima profile evolution should be carried out. We have analyzed the half height width at different annealing temperatures that is related with such structural parameter as cluster size. Experimental data shown that temperature dependence of this parameter has a maximum at temperature about 550 K. This maximum has no symmetric profile and shows the flat left hand side, whereas its right one reveals the drastic decrease at temperature increasing. Such behavior allows us to suppose that within observed temperature range the rearrangement of structural units (clusters) occurs.

Similar dependence was observed in the plot of half height peak width of pair correlation functions, calculated from structure factors, but in this case the maximum has a symmetric profile contrary to one in structure factor. It is clear that increase of maxima width height, observed in structure factors and pair correlation functions is related with decrease of structural units size. Thus, the structure relaxation is accompanied by formation the clusters of less size due to which an atomic distribution becomes more close to perfect amorphous structure.

Liquid-Solid Reactions at Formation of Nanocomposite Materials on the Base of Low-Melting Point Metallic Matrix

Mydry S., Shtablavyi I., Kovalskyi O.

Ivan Franko National University of Lviv, Lviv, Ukraine

Various composite materials attract the attention of researchers because their application in industry is rapidly developing. In order to obtain the nanocomposite materials with metallic matrix the improving of properties can be attained by combining the properties of liquid metals with other properties of solid materials. On that reason it is of importance to have knowledge on physical properties and structure of such systems especially at the boundaries between liquid and solid phase. A low melting point metals and eutectic alloys are commonly used as matrix and on that reason it is important to study the interaction at boundary between liquid metal and solid particle.

Small solid sphere like particles of Ni of about 3 μm of diameter were mixed with liquid gallium and maintained at 20; 50 and 500 K over 15 min. Content of Ni- powder was equal 20 at.%. Phase analysis was carried out by means of X-ray diffraction method with use STOE STADI P diffractometer ($Cu-K_\alpha$ radiation, Bragg- Brentano focusing geometry, graphite single crystal monochromatic).

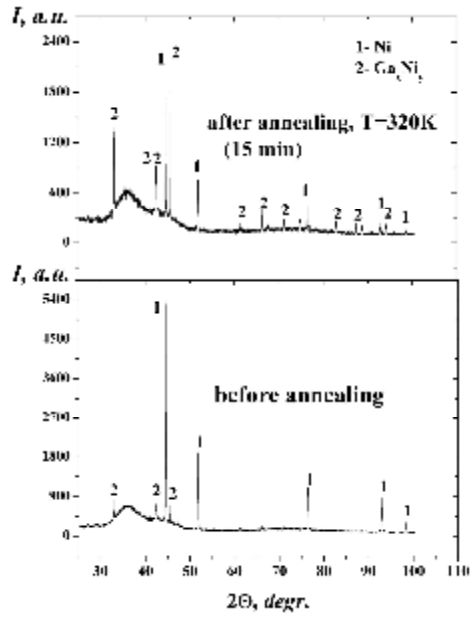

Fig. 1. Intensity curves for Ga-Ni alloys

Intensity curves (Fig.1) show the peaks, which suggest the formation of phases, corresponding to pure liquid Ga, solid Ni and intermetalic phase, which was identified to be close to stoichiometric Ga_4Ni compound. Notably that peak positions for obtained phase are slightly shifted in respect to ones for Ga_4Ni. Peak profile was analyzed in order to estimate the size of crystallites for earch phase before and after solid-liquid reaction at different temperatures.

Inelastic Tunneling Excitation of Tip-Induced Photon Emission on Au Nanoparticles

Nepijko S. [1], Schönhense G.[1], Shumakova N.[2], Yarmak A.[2], Shapko D.[2]

[1]Johannes Gutenberg-Universität, Institut für Physik, Mainz, Germany
[2]Sumy State University, Sumy, Ukraine

In the scanning tunneling microscope can be realized the spectroscopic measurements that can simultaneously with the characterization of nanoparticles to carry out research of the electronic structure (electron density of states at the Fermi level). Another possibility to study the electronic structure associated with the emission of photons in conducting such experiments. Light emission is due to the fact that some of the electrons tunneling between the tip and the sample inelastic manner. This radiation is characterized by a spectrum, the structure of which is due mainly to inter band transitions and plasmon decay. However, the plasmon frequency is determined by the material, size, shape of nanoparticles and the distances between them, as well as the dielectric environment. The electronic structure is also deformed by particle size. Thus, measurements of the light emission in research nanoparticles (nanoobjects) in a scanning tunneling microscope with extremely high information content. In our case studies have been performed on the Au nanoparticle film. Specifically, two-dimensional ensemble of tunnel-coupled Au particles were prepared by thermal evaporation on a dielectric (quartz glass) substrate. Preparation of samples and measurements were performed in ultrahigh vacuum (10^{-9} mbar).

X-ray Diffractometry Diagnostic Technology Sub-Micron and Nano Structures LSI

Novosyadlyy S.P, Kindrat T.P, Melnyk L.V, Varvaruk V.V.

Carpathian National University V.Stefanyk, Ivano-Frankivsk, Ukraine

For electro-physical diagnostics submicron layers x-ray diffractometry proposed methods in the surface layers of the structure of LSI based on using moving diffraction patterns and can be implemented on commercially produced diffractometer. These methods of diagnosis can be applied to determine the thickness of the oxide film on the silicon surface, the parameters of the transition layer film-substrate, detecting the topography of the oxide layer, as well as for the study of superlattices in *GaAs-AlAs* resonant tunneling transistors.

X-ray diffractometry and topography - is now highly effective methods for the analysis of structural defects in crystals of the high degree of perfection, which in comparison with other methods of diagnosis have a high accuracy of the crystal lattice parameters. ($\Delta d / d \leq 10^5$), non-destructive nature of the measurements and high speed, especially when using the powerful X-ray diffractometry.

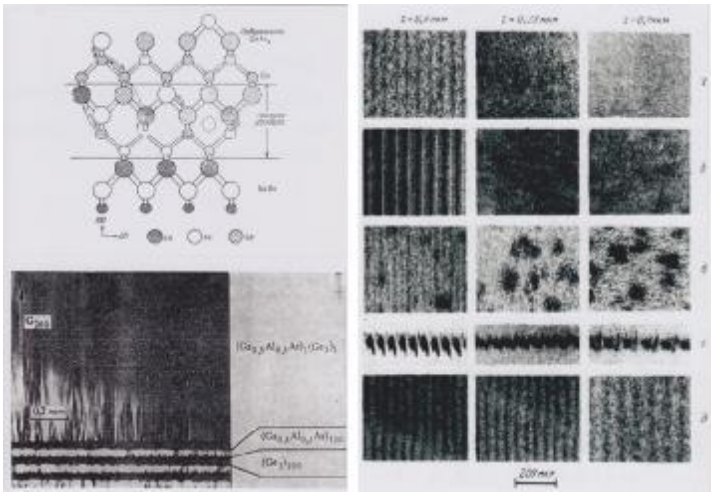

b a

Fig.1. Layered structure $GaAlAs - Ge$, showing the alignment of arrays. a) Samples topograms 3 shaped test structures of crystals with sharp relief depth b)

1. Novosyadlyy S.P. Sub-nanomikron technology and VLSI structures. // Ivano-Frankivsk City NV, 2010 - 254 p.
2. Imamov R.M, Novakov D.V, Melokov A.N. New methods of X-ray diffraction and topography in the study of the surface layers of single crystals. // Electronic industry № 5, 1990-49-52p.

Strain Properties of Granular Film Alloys

Odnodvorets L.V., Shumakova M.O., Shabel'nyk Yu.M.,
Protsenko I.Yu., Shumakova N.I.

Sumy State University, Sumy, Ukraine

In the work [1] the results of research thermoresistive properties of film materials in the form of multilayer film systems, where contain identity of the individual layers; the formation of solid solutions (s.s.) near interfaces or across the sample volume and based on s.s. formed granular state. In all four cases, there is satisfactory agreement of experimental results and semiphenomenological model for thermal coefficient of resistance, which proposed in the works [1,2]. In work [2] also performed approbation of semiphenomenological models for the strain coefficient of film systems for the first three types. Along with this at the moment there is no any theoretical model of strain coefficient for granular s.s.

Purpose of the work was to use a specified semiphenomenological models for longitudinal strain coefficient (γ_l). As in work [1], film granular s.s. modeled as a layered structure in which the tube current is modeled as a serial connection nanohranul (radius r_0) and fragments s.s. (Δl). After derivation equation for the resistivity of a layered system (for more details see [3]) to strain ε_l we received equation for the strain coefficient $g_l = \frac{1}{R} \cdot \frac{\partial R}{\partial e_l}$ (R - resistance of the sample) for the three limiting cases: $\Delta l / r_0 << 1$; $\Delta l / r_0$ **;** 1 and $\Delta l / r_0 << 1$. In all cases received that $g_l \cong g_l^{r_{ss}} + 1 + m_f$.

This suggests that the contribution of Co granules in the total value of γ_l is much smaller compared to the contribution of solid solution.

1. Kondrakhova D.M., Shabel'nyk Yu.M., Synashenko O.V., Protsenko I.Yu. Structure and phase state, electrophysical and magnetoresistive properties of solid solutions in film systems based on Co and Cu or Ag, Fe and Cr or Cu // Usp. Fiz. Met. - 2012. - V.**13**. – P. 1001 - 1027.
2. Protsenko S.I., Cheshko I.V., Velykodnyi D.V., Pazukha I.V., Odnodvorets L.V., Protsenko I.Yu., Synashenko O.V. Structure and phase state, stability of interfaces and electrophysical properties of double-layer film systems // Usp. Fiz. Met. - 2007. - V.**8**. – P. 247 - 278.
3. Protsenko S.I., Odnodvorets L.V., Cheshko I.V. Phenomenological model of electrophysical properties of granular film alloys // Visnyk SSU. Seria: Physic, Mathematic, Mechanic. – 2008. - №1. – P. 22 – 27.

Photocatalytic Activity of the TiO_2-Based Heterostructures with Polymethine Dyes

Odosiy L.I., Kobasa I.M.

Yu. Fedkovych National University of Chernivtsi, Ukraine

Selective sensitizing of photocatalytic systems promotes its activity within some wavelength region and this is one of important fields in the photocatalytic systems design and development. Some photocatalytic systems can be suitable for use in the visible and infrared solar energy transformation and accumulation equipment, which is very promising direction. Previous investigations proved that the systems combining photoactive oxide (TiO_2) with dye-sensitizer or other long wave sensitizing compound can be effectively used as photocatalysts.

Here we describe a method of design of solid and structurally oriented photosensitive heterostructures (the blocks). The required amount of the dye should be applied on the semiconductor's surface and then protected from dissolution by the polymer film, though any component should not be prevented from taking part in the electron transferring processes occurring on the interfacial bound. Heterostructures (HS) of this class revealed high activity in some redox process, *e.g.* photocatalytic decomposition of water. It should be determined if this method of design can be used as a universal tool for synthesis of other photocatalytic materials for the other redox processes. It is also interesting if the other dyes and semiconductors can be used as source materials for the photocatalytic blocks.

We have synthesized a series of new HSs based on titanium dioxide and polymethine dye. Then activity of the heterostructures has been measured in the test photocatalytic reaction of methylene blue (MB) reduction.

The following components were used to synthesize the light sensitive heterostructures: TiO_2 produced by $TiCl_4$ vapors hydrolysis in the air-hydrogen flame at 1170-1370 K (S_{spec}=50 m^2/g), polymethine dye N-[α-(coumarinyloxo-)-n-dimethylaminostyril]-4-n-dimethylaminostyrilquinolinium bromide and polyepoxypropylcarbazole.

Analysis of the absorption spectra of HS proves that TiO_2 makes a significant influence on the dye's electrons configuration. A degree of the conformation changes is in opposite relation to the content of the dye in HS. This means that increase of the dye concentration results in the weaker interaction with the semiconductor. On the other hand, this result clarifies a drop in the photosensitivity registered for high concentrations of the sensitizer.

It can be concluded that new light sensitive HSs based on TiO_2 and polymethine dye were synthesized and their photocatalytic activity has been measured in the reaction of methylene blue reduction under irradiation of the light that can be absorbed by both semiconductor and dye. A scheme of the photoelectric transformation was proposed on the basis of analysis of the electronic processes energy profiles.

Physical-Chemical Model of Nanostructured Silicon Formation by Metal-Assisted Chemical Etching

Pavlenko N.N., Iatsunskyi I.R., Smyntyna V.A., Myndrul V.B., Kanevska O.S.

Odessa I.I.Mechnikov National University,
Department of Experimental Physics, Odessa, Ukraine

This research presents an overview of fabrication the nanostructured silicon formation and physical-chemical features of the metal-assisted chemical etching method. Also, introduced the basic mechanism and process of metal-assisted chemical etching.

In a typical metal-assisted chemical etching procedure, a Si substrate partly covered by a noble metal is subjected to an etchant composed of HF and an oxidative agent. Typically, the Si beneath the noble metal is etched much faster than the Si without noble metal coverage. As a result, the noble metal sinks into the Si substrate, generating pores in the Si substrate or, additionally, Si wires. The detailed geometries of the resulting Si structures depend mostly on the initial morphology of the noble metal coverage. A pore induced directly by the sinking in of a noble metal particle is sometimes surrounded by a micro-porous structure (Fig.1). There are many phenomena in the metal-assisted chemical etching method can be qualitatively explained by hole injection from the noble metal into the Si substrate and the diffusion of holes within the Si substrate. As result of etching features, forming the nanostructured silicon formation (Fig. 2) which characteristics can be operate by etching conditions.

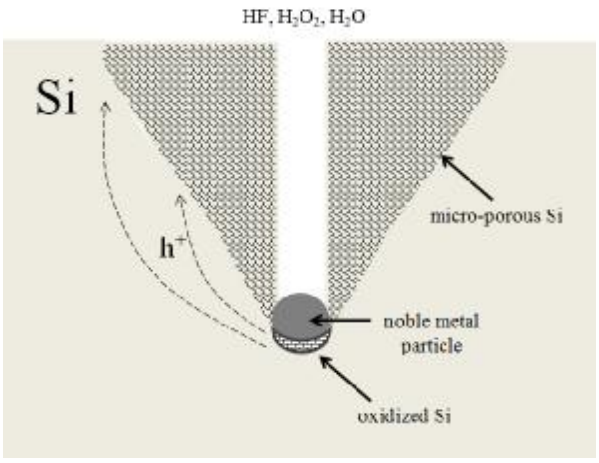

Fig. 1. Schema of the mechanism proposed for the formation of cone-shaped pores.

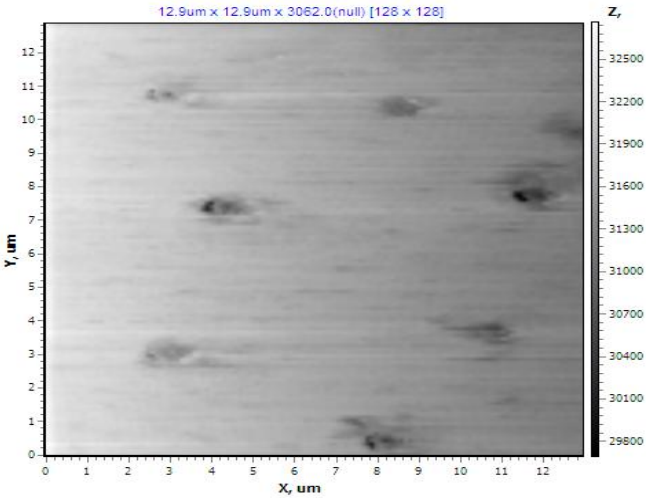

Fig. 2. Nanostructured porous silicon formation obtained by metal-assisted chemical etching in $HF–H_2O_2$ solutions.

Derivation and Characteristics of Composition Electrolitic Depositions Based on ni with Carbon Nanomaterials

Polishchuk Yu.V., Nefedov V.G., Butova E.A.

Ukrainian state chemical-technology university , Dniepropetrovsk, Ukraine

The producing of the composition electrochemical depositions (CED), when dispersed fractions of different sizes and types deposit together with the main metal on the details, is one of the most promising tendencies in electroplating. The inclusion of dispersed materials in metal matrix considerably improves depositions qualities, but what is most importantly – it increases their wear resistance, antifriction characteristics, thermal and corrosion stability by a factor of tens. The properties of CED depend on nature and size of the dispersed particles and their quantity in the deposition. Such “fillers” may serve graphite, silicon oxides, borides, amorphous carbon and metal nitrides. They are solid particles whose sizes are from 0,01 to 50 μm. However, CED modified by nanodimensional particles are researched more actively recently.

In the work were used the samples of CNM synthesized in Vladimir State University (Russia) in the form of tubes (CNT) and pinnate nano fibres (CNF). Deposition of CED carried out in two nickel-plating electrolytes by adding carbon materials in quantity from 1 to 20 g CNM per liter of solution. The time of electrolysis were calculated basing on the condition to receive the layer not less than 20 μm.

By producing CED with CNT, depositions have highly-developed surface, what is affirmed by S-form of the volt-ampere curves. And insertion surface active compaunds in ectrolyte favours more essential development of this effect at that.

For received samples the XRD analysis was carried out. There are clear peaks of metal nickel on XRD-diagrams while the peaks characterizing graphite or nickel carbide are absent. The essential difference in form and quantity of peaks underneath content of CNM in electrolyte is not discovered.

The Photoemission Investigations of Sb_2S_3 Nanolayers

Popovych N.[1], Kondrat O.[1], Holomb R.[1], Mitsa V. [1], Tsud N.[2], Matolín V.[2], Vondraček M. [4], Prince K.C.[4]

[1]*Uzhgorod National University, Institute for Solid State Physics and Chemistry, Uzhgorod, Ukraine*
[2] *Charles University, Faculty of Mathematics and Physics, Prague, Czech Republic*
[4]*Synchrotron Trieste S.C.p.A., Basovizza, Trieste, Italy*

Amorphous chalcogenides is a class of materials with a wide range of potential applications in modern nanotechnology [1]. In addition these materials show a number of interesting peculiarities in their electronic and optical properties that is, first of all, related to their geometrical structure at the nanoscale. Therefore, they are interesting as model objects too, intensively studied for better understanding of ordering and self-organization in amorphous materials. The structural information that could be obtained by experimental diffraction methods on these materials is limited due to absence of long-range ordering [2]. Theoretical and experimental investigations in the last years shown that two- and three-components chalcogenide glassy semiconductors are formed in a considerably wider variety of basic structural units than their crystal analogs. The majorities consist of the middle-range ordered groups (clusters) with different geometry, depending on stoichiometry and producing technology [3]. The ordering geometry of these groups in bulk glasses and films determines its physical properties.

The influence of the thermal annealing and laser illumination on the structure of amorphous Sb2S3 was investigated by synchrotron radiation photoelectron spectroscopy. It was observed that the laser illumination modify the surface structure of our samples what lead to the changes of the intensity, shape and positions of the Sb 3d, 4d and S 2p peaks. Similar changes were also observed in the spectra of thermally annealed samples. It is known that the deviation from the ideal covalently bonded network (i.e. different cluster formations) may influence the structural transformation due to laser induced photo-structural changes. The observed effects will promote the widespread use of these amorphous layers in nanotechnology and nanoelectronics.

1. A.V.Kolobov, J.Tominaga, J. Mater. Sci.:Mater.Electron.14 (2003) 677.
2. R. Holomb, V. Mitsa, Solid. St. Commun. 129 (2004) 655.
3. O.Kondrat, N.Popovich, R.Holomb, V.Mitsa, O.Petrachenkov, M.Koós, M.Veres, Phys. Stat. Sol. C 7, 3–4, (2010) 893.

Growth Kinetics of Nanocrystal in the Supercooled $Al_{50}Ni_{50}$ Alloy. Results of Simulations

Prokhoda A.S.

Dnipropetrovs'k National Oles Gochar University, Dnipropetrovs'k, Ukraine

The dynamics of solidification controls the microstructure development of materials. It is therefore essential to have detailed understanding of surface processes and knowledge of the kinetics parameters during solidification in order to improve production processes and the design of metallic materials. In some experimental work, an electromagnetic levitation is applied to containerlessly undercool and solidify melts in different conditions – an intensive convection or small convection at reduced gravity (a facility TEMPUS integrated into Airbus A300). The goal of these studies is to match the value of the surface kinetics coefficient for correct modeling of crystal growth in different conditions.

The MD simulations were fulfilled using our new program for parallel computing. Our programs for MD simulations [1,2] allow to analyze local structure of clusters and small crystallization centers, nucleation kinetics, mechanism and kinetics of nanocrystal growth.

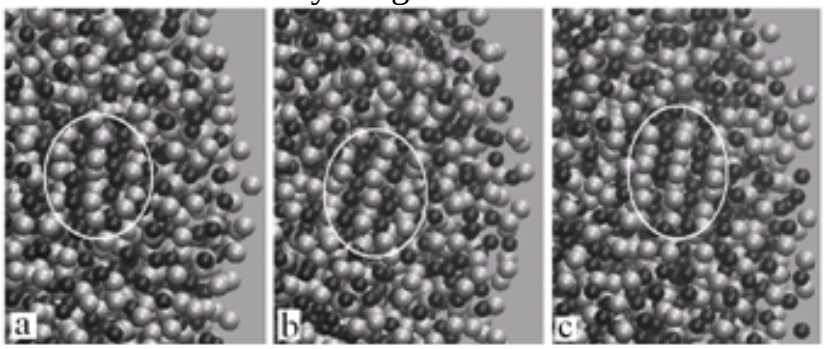

Fig. 1. Successive images of the model section, which show the consecutive stages of forming and growth of the crystallization center (coordinates of atoms were averaged during 1 ps); T=1000 K, times of annealing: a – 77 b – 87, c – 107 ps; atoms Al are light.

After detecting of growing crystallization centers, we studied changes of their structure during growth and changes of the structure of supercooled models in the past before their formation in the places where they will appear. The imperfect "non-critical" nucleus of finite size (~ 1 nm) is formed comparatively quickly (2–4 ps), after long annealing, in result of coordinated moving of several atoms. Then its structure improves gradually without growth practically (Fig. 1) or it can disappear. Sometimes we see side-by-side two or three distorted bcc-clusters as a nucleus; in spite of we did not see any bcc-cluster in this place 2 ps earlier. Sometimes the nucleus arises near the complex of several other clusters, where parallel rows exist. If there are icosahedral clusters from every side of the nucleus, it is not transformed into the crystallization center. Those groups of

bcc-clusters are transformed into the crystallization centers of the *B*2-phase, in which atoms of Ni and Al are mainly placed in right positions. Otherwise, they disappear with the time.

The degree of order in atom disposition varied at first gradually in the areas, where crystallization centers (CCs) will be formed – the curved rows of Al or Ni atoms are straightened slowly at first (Fig. 1,a). After straightening of the rows and formation of planes, the nucleus begins to grow, very slowly at the beginning. I.e. the crystallization center capable to the further growth (Fig. 1,c) is already formed. However, transformation of the nucleus into the crystallization center occurs practically without increase of its size. Thus, the crystallization center is not formed by means of addition of atoms but by means of gradual improving of the structure in some area with a short-range order corresponding to the structure of crystal phase.

If the supercooling is not small and the growth velocity becomes high enough with increase of the crystal size, the new parts of the crystal have no good superstructure order as at beginning of growth. Fig. 2 shows growth of a nanocrystal, which had an ideal structure at initial conditions, at two different temperatures. The superstructure ordering is not perfect in new parts of the growing crystal. Whereas there is a limited number of defects at comparatively small supercooling (Fig. 2,a), the ordering is bad at the large supercooling (Fig. 2,b) and larger growth velocity. This is obviously connected with that the time of growth is small in comparison with the time that is necessary for separation diffusion. There is the new CC at the bottom of Fig. 2,b with the better ordering because its growth velocity, which is size dependent, was smaller. The superstructure order is being improved in nucleus shown in Fig. 1, which practically does not grow yet.

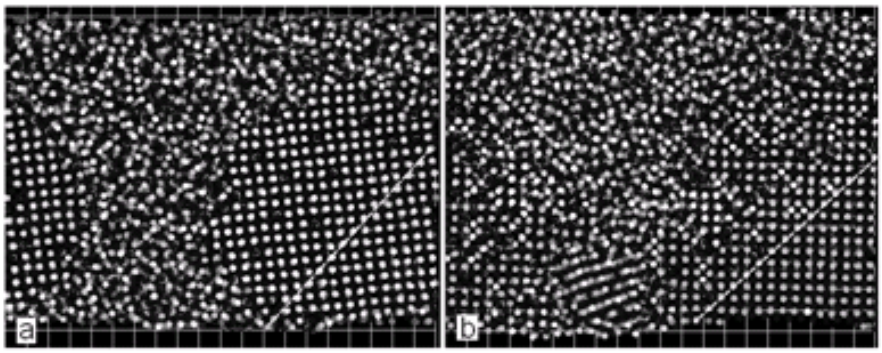

Fig. 2. Sections of the models with growing nanocrystals of *B*2-phase, white dotted lines indicate the initial interfaces, atoms of Ni are dark, a – T=1670 K, time of annealing t=875 ps; b – T=1100 K, t=390 ps.

1. Ovrutsky A. M. Peculiarities of Crystallization at High Underrcooling: Analysis of the Simulation Data for Aluminum / A. M. Ovrutsky, A. S. Prokhoda // Journal of Crystal Growth. –2011. –V. 314. – P. 258–263.
2. Ovrutsky A. M. Modeling of Initial Crystallization in the Alloys Al-10Ni and Al-5Ni-2.7Y at High Undercoolings / A. M. Ovrutsky, V. F. Bashev, A. S. Prokhoda // Computational Materials Science. –2011. –V. 50, №6. –P. 1937–1943.

The Singularity of Magnetic State of Pnanocompound $Ba_6Mn_{24}O_{48}$

Rykova A.I. , Cherny A.S. , Kalinin P.S. , Khatsko E.N.

B.I.Verkin Institute for Low Temperature Phys. & Engineering of NAS of Ukraine, Kharkov, Ukraine

The results of detailed studies of complex magnetic properties of the pnanocompound $Ba_6Mn_{24}O_{48}$ in the temperature range 4.2–300 K in magnetic fields up to 10 kOe are presented.

We investigated two samples $Ba_6Mn_{24}O_{48}$ (pressed powder and powder). The temperature dependences of magnetization M(T) are characterized by presence of anomaly in area 40 K for both samples. There is anomaly typical for the phase transition to a magnetically ordered state.

The temperature dependence of a *dc* magnetization M in external magnetic fields were measured using the different regimes of cooling (ZFC and FC regimes). There is clear-cut distinguishes between $M_{ZFC}(T)$ and $M_{FC}(T)$ curves at all fields. This is indicative of phase separation and presence of a condition like a spin glass [1, 2]. The temperature of splitting between temperature dependences of M_{ZFC} and M_{FC} weakly depend from the external magnetic field for both samples, it does not contradict with results of job [3]. It is necessary to note presence of appreciable difference in behaviour of curve temperature dependence static magnetization M_{ZFC}, $_{FC}$ (T) for a samples. Conducted study of the temperature dependence of the dynamic magnetization of pressed powder $Ba_6Mn_{24}O_{48}$ in the frequency range 10 - 10 000 Hz allowed to determine the frequency dependence of the freezing temperature T_f.

Based on these data determined the rate of frequency shift of the freezing temperature T_f $dT_f = \frac{\partial \ln T_f}{\partial \log_{10} w} \approx 0.013$, the resulting value is consistent with similar estimates for the spin - glass systems [2].

1. K. Binder, A.P. Young, *Rev. Mod. Phys*. **58**, p.801 (1986).
2. S. Sullow, G.J. Neiuwenhuys, A.A. Menovsky, J.A. Mydosh, S.A.M. Mentink, T. E. Mason, W.J.L. Buyers, *Phys. Rev.Lett*. **78**, p.354 (1997)
3. L.F. Cugliandolo, J. Kurchan, P. Le Doussal and L. Peliti, Phys. Rev.Lett., 78, p.350 (1997).

Synthesis and Application of Nanostructured Palladium

Saldan I.V.[1], Semenyuk Yu.Ya.[1], Pereviznyk O.B.[1], Reshetnyak O.V.[1,2]

[1]Ivan Franko National University of Lviv, L'viv, Ukraine
[2]Army Academy named after Hetman Petro Sahaydachnyi, L'viv, Ukraine

Today palladium nanostructures have a lot of applications in different types of physical and chemical processes. Therefore the material needs to be introduced in manifold nanoobjects at the certain surfaces of the special substrate [1]. There are many methods of palladium syntheses that are quite often typical to the others noble metals. Therefore a selective appearance of palladium nanoparticles or thin films needs to be developed. On the other hand many preparative procedures are proposed on multimetallic nanosystems [2] where palladium together with another noble or transition metal plays additional function.

In this work the general review on synthesis of palladium nanostructures are present. The main methods and approaches to obtain different nanoobjects are summarized. In addition to that a few specific syntheses are proposed and their outlooks are discussed. Nucleation and growth of nanopalladium in the colloidal solutions and on the solid surface are compared. Physical and chemical analyses of the prepared nanoobjects are proposed based on the modern techniques of nanoscience.

Using the potentiodynamic mode the metal-polymer nanocomposites based on polyaniline and palladium particles were synthesized. Their morphology, structure and electrocatalytic properties regards to oxidation of C_1–C_2 alcohols and their derivatives were studied. Obtained results confirm the availability of the use of these materials as electrodes in fuel cells and sensor devices.

1. Volkov S.V., Kovalchuk E.P., Ogenko V.M., Reshetnyak O.V. Nano-chemistry, Nanosystems, Nanomaterials // Kyiv: Naukova Dumka, 2008. – 422 p. (in Ukrainian).
2. Toshima N., Yonezawa T. Bimetallic nanoparticles – novel materials for physical and chemical applications // New J. Chem. – 1998. – Vol. 22, Is. 11. – P. 1172–1201.

Influence of pH on Optical Properties of CdS Colloidal Nanocrystals

Savchuk A.I., Stolyarchuk I.D., Shporta O.A, Makoviy V.V.

Yuriy Fedkovich Chernivtsi National University, Chernivtsi, Ukraine

During last decades semiconductor nanocrystals have been intensively studied owing to their unique size-dependent optical properties and different kinds of applications. In particular, potential applications include fluorescent probes, light emitting diodes, electroluminescent devices, optical coatings, solar cells, lasers and new devices like single electron transistors [1]. The most investigated are II-VI semiconductor based nanocrystals type of CdS, CdSe and CdTe. Tremendous efforts have been performed to develop synthetic methods for high-quality CdS nanocrystals, for example, the colloidal chemistry method, the controlled precipitation reaction, the thermolysis of single-source precursor at relatively high temperatures, and the rapid hot-injection based synthesis [2]. Comparatively, the colloidal chemistry method with using ultrasound transducer is the most successful one for high-quality nanocrystal growth due to the effective separation of the nucleation and growth stages.

In this work, the nanocrystals of CdS were synthesized in aqueous medium by the colloidal chemistry method using cadmium chloride $CdCl_2$ and sodium sulfide Na_2S in the presence of natural polymer - gelatin (H_2N-R_1-COOH, where R_1 – acid groups) as the capping agent. The concentrations of precursors were 10^{-3} mol/L. As it is known, gelatin may acquire positive and negative charge due to its acid-alkaline properties. For example, by increasing pH of aqueous medium the dissociation of COOH – group on H^+ and COO^- is occurred, thus gelatin become negatively charged and significantly influence on emitting characteristics of the nanocrystals.

To illustrate the influence of medium alkalinity on the photoluminescence properties of the CdS nanocrystals the pH value was changed from 5,5 to 8. It was revealed decrease in the photoluminescence intensity with increasing of pH value in the solution. The best luminescent properties have revealed for CdS nanocrystals synthesized in medium where pH value is equal 5,5.

1. Nogriya V. Electro- and photo-luminescence studies of CdS nanocrystals prepared by organometallic precursor //Chalcogenide Letters.-2008.-V5.-No.12.-pp.365-373.
2. Savchuk A.I. Evolution of CdS:Mn nanoparticle properties caused by pH of colloid solution and ultrasound irradiation //Phys. Status Solidi.- 2010.-C 7.-No.6.- pp. 1510-1512.

Macroscopic Quantum Bloch Point Reflection above – a – Barrier in Uniaxial Ferromagnetic Film with Strong Magnetic Anisotropy

Shevchenko A.B.[1], Barabash M.Yu.[2], Sperkach S.O.[2]

[1]*G.V. Kurdymov Institute of Metal Physics, National Academy of Science of Ukraine, Kyiv, Ukraine*
[2]*Technical Centre of National Academy of Science of Ukraine, Kyiv, Ukraine*

The physical properties of domain wall (DW) substructural nanosized elements (vertical Bloch lines (VBLs) and Bloch points (BPs)) in uniaxial ferromagnetic films with strong magnetic anisotropy are of great interest both fundamental and practical point of view. Vertical Bloch lines and BPs are nonlinear wave formations (solitons), which besides dynamical properties have also topological features. One of such features is a chirality, which characterizes a direction of magnetization reversal within substructural elements.

It is note, that in the subhelium temperature range VBLs and BPs reveal the quantum depinning property [1,2]. In this context quantum BP reflection above – a – barrier is an actual problem of nanosized materials physics.

Let us consider BP in an isolated DW containing pair VBLs with alternating chyralities. Bloch point gives to defect, which is within domain wall, under action of an external pulse magnetic field. To describe the BP dynamics we will use the Lagrangian formalism and WKB formalism to investigate of BP reflection from potential barrier created by defect. Analysis obtained of BP reflection above – a – barrier exponent expression for typical uniaxial ferromagnetic films parameters indicates the possibility of realization of this quantum phenomenon. The dissipation effect and validity of WKB formalism on BP reflection above – a – barrier are estimated.

The critical temperature T_c corresponding to reflection process is determined. It is established that T_c is in the same subhelium temperature range with appropriate values for quantum depinning VBLs and BPs [1,2]. The given fact specifies importance of the account of BP reflection above – a – barrier at studying quantum effects of DW substructural elements. The practical realization of considered phenomenon can serve by basis for a new precisions investigation methodics of DW interior structure in uniaxial ferromagnetic films.

1. A.B. Shevchenko, *Zh. Tekh. Fiz*. **77**, 128 (2007).
2. A.B. Shevchenko, M.Yu. Barabash, *Low Temp. Phys*. **37**, 690 (2011).

Specifics of Creating Nanoporous Structure of GaAs

Simchenko S.V., Kirilash A.I., Kidalov V.V.

Berdyansk State Pedagogical University, Berdyansk, Ukraine

Obtain high-quality three-dimensional porous structure today is an important scientific and technical challenge. These structures and devices based on them can be used to create devices of electronics, light-emitting elements, sensors, etc. The most convenient method of producing porous semiconductors is by electrochemical etching [1].

For experiments using single-crystal plates n-GaAs (111) orientation, thickness 100mkm doped with silicon (N = 10^{15}-10^{18}cm^{-3}). Electrochemical etching was carried in a cell with a platinum electrode at current densities j = 10-150mA/sm^2. On the back side of the plate GaAs was applied ohmic contact. The electrolyte used alcohol solutions on the basis of hydrofluoric and nitric acids. Etching parameters regulated automatically. The obtained surface morphology were investigated by scanning electron microscope JSM-6490. The chemical composition of elements on the surface of the samples was investigated by energy dispersive X-ray analysis (EDAX).

The influence of etching conditions on the types produced pore "srysto" pores - appear irregularly along the crystallographic plane and "surro" pores - pore thin parallel lines are perpendicular ekvipotentsial current [2]. Optimal quality of the structures was pulsed etching pulse duration and duty cycle 0.5s and 4 in solution HF: HNO3: C2H5OH = 2:1:1 (Figure 1).

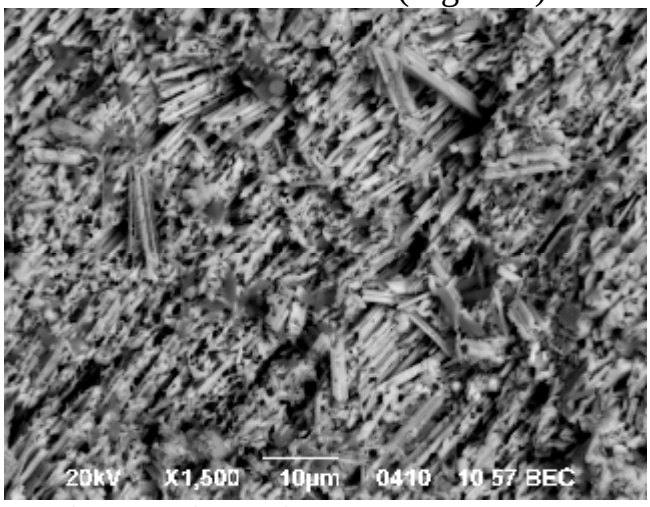

Fig.1. SEM image of the surface of the porous n-GaAs, the etching time t = 15 min, the electrolyte of HF: HNO_3: C_2H_5OH = 2:1:1, primary density of the current j = 70mA/sm^2.

1. Kang Y. and Jorne J., J. Electrochem. Soc., 1993, V. 140, pp.2258.
2. S. Langa, J. Carstensen, M. Christophersen, at all// Journal of the Electrochemical Society, 152, No. 8: 525 (2005).

Platinized Carbon Nanotubes for Oxygen-Hydrogen Membrane Fuel Cell

Smyrnova E.V., Dubovyk T.N.

Ukrainian State University of Chemical Technology, Dnepropetrovsk, Ukraine

The characteristics of fuel cells (FC) are highly dependent on catalyst support quality. Historically, the most common catalyst carriers in fuel cells are carbon materials - various types of graphite and carbon-black. In recent years, a new promising material - carbon nanotubes (CNTs) was developed. It has high electrical conductivity, corrosion resistance, and the most important possibility of producing fine-grained catalysts [1].

In present work it was studied the characteristics of fuel cells with electrodes which are produced from platinum activated carbon nanotubes, graphite powder and their mixtures.

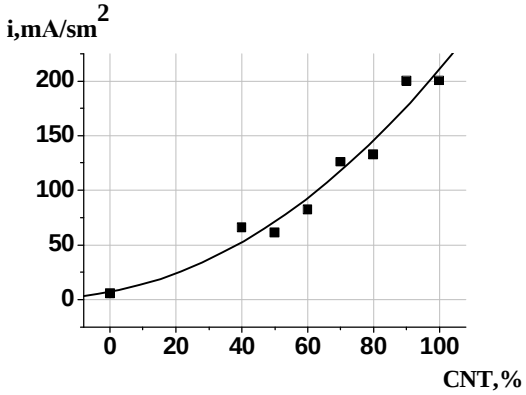

Figure. The influence of the relative content of CNTs in the active layers on the current density of membrane-electrode assembly (MEA).

It is shown that the increase of CNTs portion in the active layers of the MEA leads to higher current densities. It can be caused, apparently, by two mechanisms.

Firstly, the amount of platinum catalyst increases since only CNTs were Pt-contained component. Secondly, due to hydrophobic properties of CNTs that increases gas transportation in the reaction zone.

1. Mayorov N.A., Tuseeva E.V., Sosenkin V.E. Influence functionals lizations of carbon nanotubes on the structure and catalytic properties of electrodeposited catalysts / N.A. Mayorov, E.V. Tuseeva, V.E. Sosenkin // Electrochemistry. – 2009. – № 9. – p. 1168-1177.

Viscoelastic Properties of Nanofilled Epoxyurethane Polymers

Tereshchenko V.N., Yashchenko L.N., Todosiychuk T.T., Babkina N.V.

Institute of Macromolecular Chemistry NAS of Ukraine

Recently the development of work related to the synthesis of polymers containing nano-sized fragments and characterized by a new set of chemical and physico-chemical properties. These include nanofilled epoxyurethane polymers (nEU), in which the organic and inorganic elements of the structure are combined on a molecular level.

In this report the results of investigation on the effect of the content of polysiloxane particles on the viscoelastic properties of the filled epoxyurethane polymers which obtained by sol-gel method.

The hardener used iso-methyltetrahydrophtalyc anhydride (iso-MTHFA). Curing compositions carryed uot on stage regime , raising the temperature from 80 ^{o}C to 125 ^{o}C for 5 hours.

By dynamic mechanical analysis shows the changes in the viscoelastic properties of nEU reflecting structural changes that occur during the formation of EU in the presence of nanofillers.

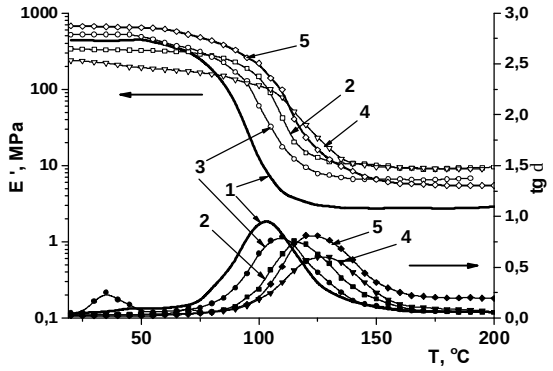

Рис.1 Temperature dependence of the mechanical loss (tgδ) and dynamic modulus of elasticity (E') of nEU containing of SiO_2% wt.: 1-0; 2-0,001;3-0,01; 4-0,5; 5-2,0

Table 1. Relaxation parameters and M_c of nEU

w(SiO_2) wt.%	tgδ (T)		$E_{v.e.}$, MPa	M_c
	T_c, ^{o}C	max tgδ		
0	103	0.94	2.78	4300
0,001	115	0.73	9.00	1350
0,01	110	0.79	6.45	1880
0,5	128	0.60	9.26	1300
2,0	123	0.81	5.68	2140

Studies have shown a significant increase in the density of the network (M_c), which occurs at the minimum concentrations of SiO_2 (up to 2.0% wt.) (Fig. 1, Table 1.) and T_c , which may evidented the formation of the spatial network of inorganic polysiloxane particles in the structure of the epoxyurethane matrix supported of strengthening effect on the polymer as a whole.

Adsorption States of Ge Dimers on Si (001) Face

Tkachuk O.I., Terebinska M.I., Lobanov V.V.

Chuiko Institute of Surface Chemistry of National Academy of Sciences of Ukraine, Kyiv, Ukraine

The state of the art in natural sciences is characterized by a booming interest in nanosize structures technology of their production, physical and chemical properties and prospects for practical use. Such structures are called quantum-dimensional and may be quantum-size layers, quantum strings and quantum dots, among them the most important are the Ge quantum dots on the Si(001) face, despite the difference in lattice constants of 4%.

Calculations have been performed by DFT method (B3LYP, 3-21G) on equilibrium spatial structure and formation energies of adsorption complexes of Ge dimers on buckling face Si(001) reconstructed to the (4×2) structure. We consider four different types of adsorption sites for Ge dimer on the substrate surface: perpendicular buckling =Si–Si–Si= bridges (1); bridges between rows perpendicular to lathers (2); bridges between rows parallel to them (3); over dimers parallel to them (4). The most stable has been found to be thet structure formed by adsorption of Ge dimer at type (4) the active site (see Figure). A growth of interatomic Ge–Ge distances from the equilibrium value for the dimer (2.24) to 2.74 Å is characteristic of such a structure. It can be a proof that the structure of the adsorption complex is "adapted" by the structure of Si(001) faces what is essential for the formation of epitaxial structures.

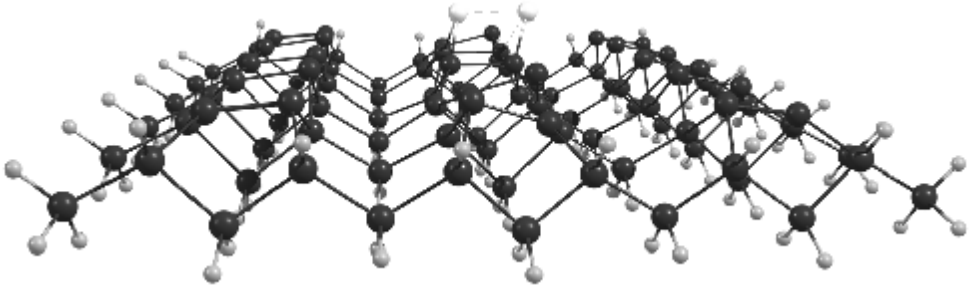

Figure – Structure of adsorption complex of Ge–Ge dimer on surfaces Si (001)

"Adapted" of dimer for lattice structure of substrate contributes to the subsequent replacement of Si atoms on of Ge on the surface of Si(001) face of mixed dimers of different ordering of the atoms relative to the substrate arrayed. Estimates of the energy of mixed dimers led to the conclusion on their distribution on the of Si(001) face, which is important to determine the mechanism of the subsequent growth of the adsorbed layer.

Size-effect Impact on the ZnO Gas Sensors Characteristics

Turko B.I.[1], Stanko O.P.[2], Kulyk B.Y.[2], Kapustianyk V.B.[1,2] and Serkiz R.Y.[1]

[1]Scientific-Technical and Educational Center of Low Temperature Studies, Ivan Franko National University of Lviv, Lviv, Ukraine
[2]Solid State Physics Chair, Physics Department, Ivan Franko National University of Lviv, Lviv, Ukraine

Sensor sensitivity dependence for the samples based on ZnO thin film, micro- and nanostructures on their active area was investigated under the influence of ethanol, ammonia and acetone vapors. The impact of the morphology type and the size effects on the main characteristics of the ZnO resistive sensor elements was studied. It was shown that the nanostructured samples possess significantly better characteristics comparing to the thin film ones.

Table 1. *Structural parameters of the sensing elements.*

	AFM-data			SEM-data
ZnO structure Type	Root mean square (nm)	Aver. grain size or the structure element diameter (nm)	Ratio of the surface to the projection area	Structural parameters
Film	6	28	1.07	-
micro-structure	73	2000	1.36	hexagonal vertical tightly packed rods of 2 мм average diameter
Nano-structure	102	216	1.45	nanowires with the length of about 1.5 мм, and diameter of about 0.1 мм

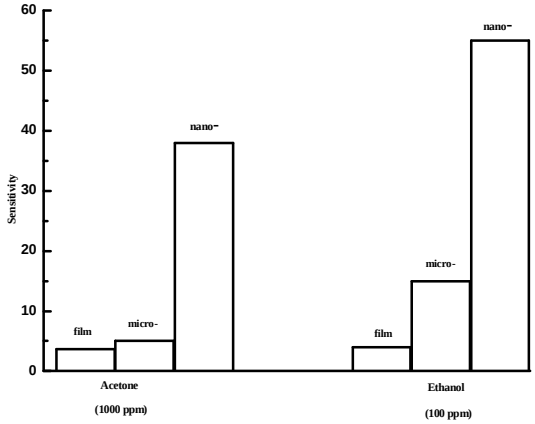

Fig. 1. Diagram displaying the sensitivity dependence to the ethanol and acetone vapor of the sensors with ZnO elements of different dimensionality at 400°C.

Percolation in Polymer/Carbon Nanotubes Systems

Yakovlev Yu.V.[1], Lysenkov E.A.[2], KlepkoV.V.[1]

[1]*Institute of Macromolecular Chemistry, Kyiv, Ukraine*
[2]*Mykolaiv National University, Mykolaiv, Ukraine*

Recently the question of percolation transitions in polymer composites filled with carbon nanotubes (CNT) is widely probed.These researches cause the both applied and fundamental interest. A large part of these nanotube-based polymer composites will exploit carbon nanotubes as conductive filler for applications ranging from the electronics to aerospace sector. In these materials highly conductive filler is added to the polymer matrix to provide a threedimensional network of filler particles through the component. This situation is known as percolation and the percolation threshold is characterised by a sharp drop of several orders of magnitude in resistivity.

In this work the polymer/multi-wall carbon nanotubes composites based on poly (ethylene glycol) and poly (propylene glycol) were produced. The dielectric properties and conductivity were studied by *ac* impedance spectroscopy. It was shown? That the composite conductivity σ follows a percolation scaling law $s \sim (c - c_c)^t$ with the critical concentration to form a conductive network c_c of 0.3-0.6 % and an exponent *t of* 1.2-1.8. The results are compared for amorphous and crystalline polymers, for polymer with different molecular weight and for nanotubes with various aspect ratios. The effect of the temperature and additives on the percolation properties was also studied.

Synthesis of Doped Nanosized tin (IV) Oxide by Sol-Gel Method

Yarotskiy O.M., Ivanenko I.M., Dontsova T.A.

National Technical University of Ukraine «KPI», Kyiv, Ukraine

It is known that the stability, sensitivity, selectivity and response time gas sensors can be significantly improved by not only reducing of the particles size SnO_2 to nanometer but also adding doping agents. Sol-gel method is one common technique of synthesis of the smallest powders, whose effectiveness was assessed by crystallite size and specific surface area of the synthesized samples.

Tin(IV) oxide doped Ag was synthesized in this work. For this purpose to intermediate product of sol-gel synthesis – α-tin acid (Fig. curve 1) was added 20% solution of argentum (I) nitrate, which volume depends on the required calculated Ag content in the final SnO_2.

X-ray diffraction patterns for three synthesized samples with argentum 3, 6 and 9 mol. % present in Fig. The presence of crystalline SnO_2 cassiterite type, as well as significant peaks Ag_3Sn and AgO with intensity proportional to the content argentums was found.

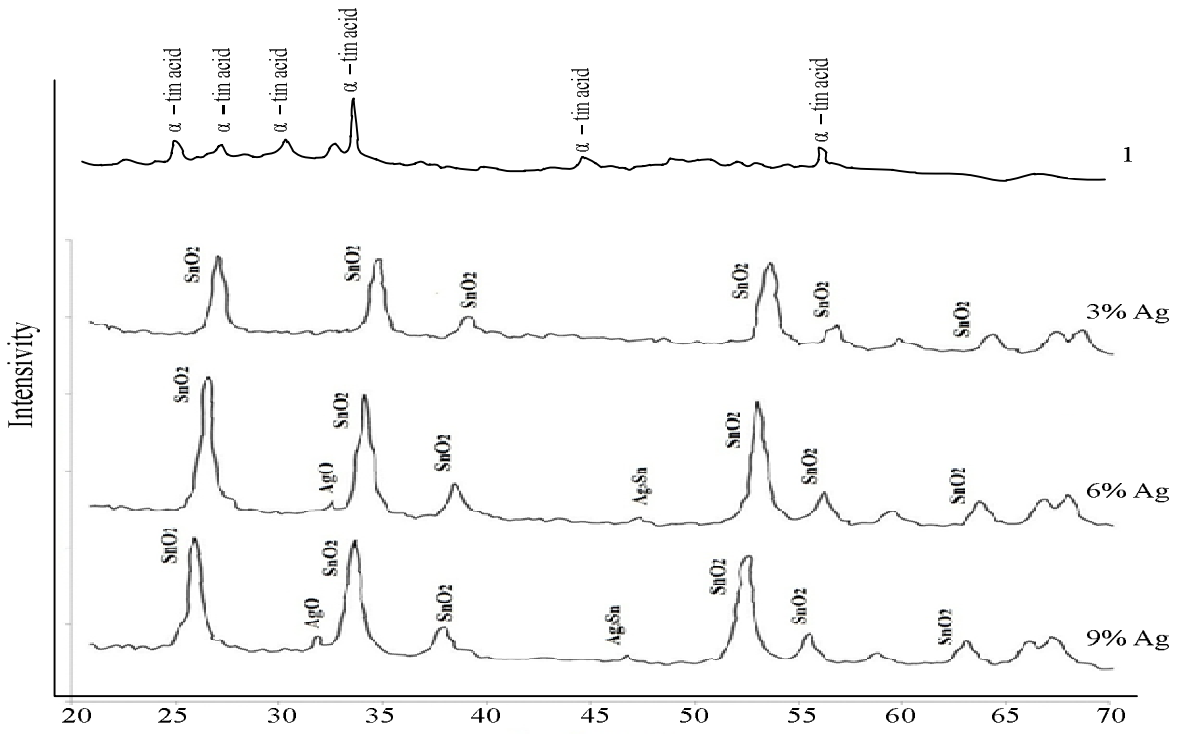

Figure. X-ray diffraction patterns for α-tin acid and doped Ag samples SnO_2.

Lattice parameters of pure and doped SnO_2 are 10x9x10 nm. The surface area of synthesized SnO_2 powders as a result of doping increases from 100 to 180 m^2/g.

Structure of the Polyaniline Films Electrodeposited on the $Al_{87}Ni_8(REE)_5$ Amorphous Metallic Alloys Electrodes

Yatsyshyn M.M.[1], Demchyna I.I.[1], [1,2]Reshetnyak O.V.,
Kulyk Yu.O[1], Pandyak N.L.[3]

[1]*Ivan Franko National University of L'viv, L'viv, Ukrainee*
[2]*Army Academy named after Hetman Petro Sahaydachnyi, L'viv 79012, Ukraine*
[3]*National Forestry Engineering University of Ukraine, L'viv 79057, Ukraine*

Both thin films and more thick layers of electroconductive polymers on the metallic substrates uses widely as a sensitive elements of sensors with different application, anticorrosive coverings, electromagnetic radiation absorbing screens, etc. The important representative of this class of the polymer is polyaniline (PAn) – organic metal, which can be deposited electrochemically with comparative ease on the different metallic electrodes, including aluminium and its alloys, amorphous specifically [1]. The ability of PAn to the change of the polymeric chains conformation under the variation of electrical potential uses today successfully during design of microdrives (artificial muscles), whereas nano- and microstructurized polyaniline layers with well-developed morphology found an application in chemo- and biosensors or in the supercapacitors.

It was determined that the electrochemical deposition in the potentiodynamic mode during potential cyclic scanning in the (–200)–(+1200) mV interval in the H_2SO_4 aqueous solutions is effective method of the formation of the high-conductive PAn films and layers on the surface of the $Al_{87}Ni_8(REE)_5$ (where *REE* – Y, Ce, Gd, and Dy) amorphous metallic alloys (AMA) electrodes. The structure, features of morphology and composition of synthesized polyaniline deposits were studied with use by scanning electron microscopy and energy dispersive X-ray spectroscopy (PEMMA-102-02 electron microscope-microanalyzer), X-ray phase analysis (DRON-3 diffractometer) and FTIR spectroscopy (NICOLET IS 10 spectrometer) methods. Experimental results indicated that the use of AMA as the electrode materials permits to produce, in comparison with polycrystalline active metals and Al-based alloys electrodes, of the PAn films with essentially differing morphology and structure. It was shown that obtained on the surface of AMA-electrodes polymeric films have the amorphous-crystalline structure where the PAn is in the emeraldine base and leucoemeraldine salt forms. The morphology of deposited PAn layers determine the state of AMA-electrodes surface, nature of amorphizing addition (*REE*) in AMA and also the electrode side (structures with developed surface forms on the contact side of electrode while the smooth film produces on the outer side).

1. Yatsyshyn M.N., Boichyshyn L.M., Demchyna I.I., Nosenko V.K. Electrochemical oxidation of aniline on the surface of an amorphous metal alloy $Al_{87}Ni_8Y_5$ // Russ. J. Electrochem.– 2012. – Vol. **48**, Is. 5. – P. 552–558.

Electronic Structure Peculiarities of Nanosize Al_2O_3 Depending on Sizes and Phase

Zaulychnyy Ya.V.[1], Ilkiv V.Ya.[1], Gun'ko V.M.[2], Zarko V.I.[2]

[1]*National Technical University of Ukraine "Kyiv Polytechnic Institute", Kyiv, Ukraine,*
[2]*Chuiko Institute of Surface Chemistry of NASU, Kyiv, Ukraine*

Al_2O_3 nanopowders electronic structure was investigated by using the ultrasoft X-ray emission spectroscopy method. The x-ray emission OK_α- and AlL_α-bands reflecting the energy distribution of the O*p*- and Al*sd*-electrons in valence band were measured.

Comparison of the OK_α-bands of fumed sample (coherent-scattering region CSR 20 nm) where no amorphous component was revealed and fumed sample θ-Al_2O_3+50 % amorphous component (CSR=17 nm) has showed that the OK_α-band of sample θ+50 % amorphous phase is much narrower than that of θ-Al_2O_3 with CSR=20 nm. Such difference in width of the OK_α-emission bands is possibly due to great amount of broken bonds in amorphous nanoparticles.

Comparison of the OK_α-emission bands of powders with different CSR has showed that bands with similar sizes of 11 nm and 13 nm almost coincide, whereas the OK_α-band of sample with CSR=20 nm is wider. Narrowing of the OK_α-band indicates decrease of oxygen charge state that is a consequence of the fact that electrons yielded to oxygen in massive crystals return to Al when Al-O bonds in nanoparticles break. Moreover narrowing of the OK_α-band is a consequence of disappearance of levels splitting when covalent constituent of Al-O and O-O–bonds breaks. The later is a consequence of overlapping of O*p*-states since in θ–phase a number of distances between oxygen ions O-O=2,6154 Å and O-O=2,6369 Å, which are shorter than double radius of oxygen ions $2r_{O^{-2}}$=2,66 Å, occurs.

Narrowing of the OK_α-band of δ–phase with specific surface of 140 m^2/g and CSR=7 nm in comparison with band of θ–phase with specific surface of 81 m^2/g and CSR=20 nm has been revealed due to return of electrons on aluminum ions when Al-O bonds break.

It has been revealed that decrease of Al-O distances in δ-phase leads to increase of overlapping of Al*sd*+O*p*-covalent-binding states that indicate the strengthening of Al-O-bonds and formation of O-O–bonds. As a result δ–phase of Al_2O_3 becomes stable in nanosize state when CSR reaches 7 nm.

Technology and Orientation Features in PbTe, PbTe:Sb(Bi) Nanostructures on Substrates of Mica and Ceramics

Lishchynsky I.M., Javorsky Ja.S., Bylina I.S., Klanichka Yu.V., Marusyak V.B.

Vasyl Stefanyk Precarpathian National University, Ivano-Frankivsk, Ukraine

Thin films and low-dimensional condensates of lead chalcogenides are promising semiconductor structures for making active elements of micro and nanoelectronics (detectors and sources of radiation in the infrared light spectrum and thermoelectric energy converters for temperatures (500-850) K). The performance and specific areas of application of thin film and nanosized condensates which based on PbTe is largely determined by the state of the surface morphology and topology formed separate nanocrystals, which in turn are dependent on technological factors of their production [1,2].

Thin films and nanostructures have been obtained from the vapor phase by evaporation in a vacuum of open pre-synthesized PbTe, PbTe:Sb, PbTe:Bi compounds. Deposition was carried out on substrates of mica and ceramics. Topological characteristics and orientation of nanostructures in the condensates have been investigated by atomic force microscopy (AFM) Nanoscope 3a Dimention 3000 (Digital Instruments USA). According to the AFM studies in addition to surface topology and its profilogram with the program Gwyddion have been defined orientation features, the size of nanocrystals, roughness, and other characteristics of the condensates.

The results of AFM studies of topological features of PbTe, PbTe:Sb and PbTe:Bi (Sital, mica) nanostructures received by open-evaporation sample synthesized compounds in an open vacuum for various technological factors have been presented. The kinetics of vapor-phase self-assembled structures is the complex multistage process which includes the steps of nucleation, aggregation and coalescence of nanostructures. As for orientation features, we have found some formed PbTe, PbTe:Sb nanocrystallites on (0001), muscovite-mica and ceramics have a pyramidal shape with the side faces {100} and the basis of (111) oriented parallel to the substrate surface.

1. D.M. Freik, M.O. Galushchak, L.I. Mezhilovska. Physics and Technology of Semiconductor Films. High School, Lviv. 152 (1988).
2. Zimin. S.P. Nanostructuring Lead Chalcogenides: Monograph / S.P. Zimin, E.S. Gorlachev; Yarosl. State. Univ., Demidov, -232 (2011).

The work supported by an integrated project of MES of Ukraine (N 0113U000185) and by projects of FRSF State Agency for Innovation and Informatization of Ukraine. (Contracts: R54, F53, 3).

Structure and Optical Properties of Vapor-Phase Lead Telluride Nanostructure

Malashkevych. H.E.[1], Mezhylovska L.Yo. [2], Freik D.M.[2], Chavjak I.I. [2], Javorsky Ya.S.[2]

[1]*Instytut of Molecular and Atomic Physics, NASB of Belarus, Minsk, Belarus*
[2]*Vasyl Stefanyk Precarpathian National University, Ivano-Frankivsk, Ukraine*

Lead telluride as a typical representative of semiconductor IV-VI compounds is characterized by a number of specific physical and chemical properties and it is a promising material for producing active elements of optoelectronic devices (photodiodes, photoresistors, injection lasers) in the infrared region of optical spectrum and for thermoelectric converters of thermal energy in the temperature range (600-750) K.

For the research we used PbTe-based nanostructures prepared by deposition of vapor phase synthesized on substrates of different nature. The microstructure of the synthesized films and the percentage ratio between lead and tellurium has been investigated with scanning electron microscope LEO-1420REM (Carl Zeiss, Germany). Absorption and reflection spectra were recorded using a Cary-500 spectrophotometer and FTIR Spectrometer Nexus (Thermo Nicolet, USA).

The surface morphology and the formation of vapor-phase topology PbTe nanostructures on single crystal substrates (111) Si, (111) Ge, (0001) mica and polished glass, fused silica, coated with SiO_2, GeO_2 and HfO_2 gel films with and without nanoparticles Ag and Au is mainly due to differences in thermal properties of these substrates. The difference of supramolecular structure condensates PbTe, deposited a gel-film SiO_2, GeO_2, HfO_2 on a quartz substrate has been experimentally determined. The correlation between the changes of the structure of the course of the temperature dependence of conductivity gel films has been observed. It is shown that the presence of gel film SiO_2 silver nanoparticles significantly alters the structure of supramolecular structures deposited PbTe at low (~ 150° C) substrate temperature.

It is shown that laser monoimpulse irradiation PbTe films can create local melted area, resulting in stationary heating of these films may shift a significant edge interband absorption, which correlates with the magnitude of atomic ratio Pb / Te. Moreover, the slope of the land decreases in shear maximum absorption in the high-frequency region and increases in shear at low frequency.

The work supported by an integrated project of MES of Ukraine (N 0113U000185) and by projects of FRSF State Agency for Innovation and Informatization of Ukraine. (Contracts: R54, F53, 3); NAS of Ukraine (N 0110U006281).

Features of the Size Dependences of Thermoelectric Parameters of Lead Chalcogenides Nanostructures

Freik D.M., Yurchyshyn I.K., Potyak V.Yu., Mateik G.D., Nadraga O.R.

Vasyl Stefanyk Precarpathian National University, Ivano-Frankivsk, Ukraine

The aim of this work was the theoretical explanation of the behavior of a number of thermoelectric (TE) parameters on the width of quantum wells (QW) for lead chalcogenides (PbS, PbSe, PbTe).

Consideration of *d*-dependence of the Fermi energy E_F and *z*-component of the effective mass allowed us to obtain the corresponding dependences of the Seebeck coefficient S and electrical conductivity σ on the well width for nanofilms of lead chalcogenides (Fig. 1).

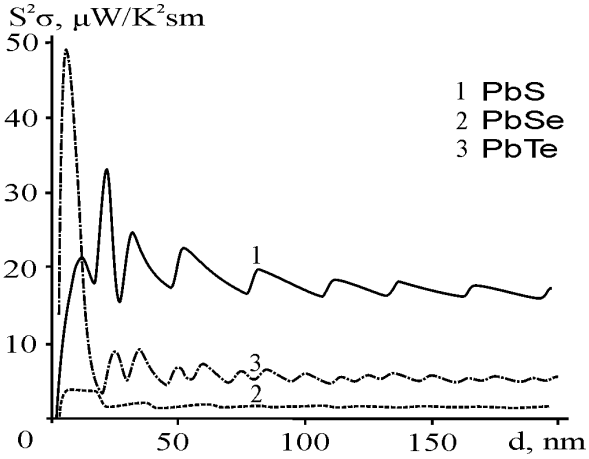

Fig. 1 – Theoretical dependences of the TE power factor $S^2\sigma$ on the width of QW for films PbS (1), PbSe (2), PbTe (3) in the model of infinitely deep potential well at T = 300 K.

The number of levels below the Fermi energy is determined by *d*-dependence of the effective mass and actually by E_F, as well as by the well width *d*. The calculations take into account the change of the Fermi energy, and the change of the number of levels below it, depending on the well width. Calculating the electrical conductivity σ it was assumed that $m_x^* = m_y^*$. In the theoretical model the quantum well width was considered to be equal to the thickness of the condensate in the experimental dependences of relevant parameters. The calculation was carried out in the approximation of constant concentration and carrier mobility across all the range of well width. The values of the last were selected basing on the relevant experimental measurements. The resulting dependences of TE coefficients on the width of lead chalcogenides QW are characterized by nonmonotonic oscillating behavior (Fig. 1), what is in a good coordination with the experimental results.

The work supported by projects of FRSF State Agency for Innovation and Informatization of Ukraine. (Contracts: R54, F53, 3) and by projects of NAS of Ukraine (N 0110U006281)

Laser Shockwave Treatment Impact on ZnO Photoluminescence

Zhurovetski V.M., Kovalyuk B.P., Mocharskyi V.S., Nikiforov Yu.,
Onisimchuk V.V., Popovych D.I., Serednytski A.S.

Institute of Applied Problems of Mechanics and Mathematics NASU,
Lviv, Ukraine

Investigation of structure and photoluminescence of ZnO that we made helped us to detect changes in defect structure after laser shockwave treatment [1]. In laser treatment we used energies E_{av}=5-12 J/pulse, with an average power density P=5.8*10^8 W/sm^2 and following diameter of the treated surface D=4mm^2. In this work we used ZnO nanopowder obtained by pulsed laser reactive technology [2]. Treated ZnO sample was purchased between copper plate (d=100μm) and steel plate (d=4.51 mm). ZnO nanopowders was treated in three stages wich differs by energy applied and quantity of laser pulses for each sample (sample 1: 7 pulses, E_{av}=8 J/pulse; sample 2: 14 pulses, E_{av}=8.5 J/pulse; sample 3: 21 pulses, E_{av}=9.3 J/pulse). Photoluminescence experiments was held in vacuum (P=10 Pa). After laser treatment we have noticed significant changes in photoluminescence properties of the treated ZnO samples. Other interesting feature we have been observing intensity growth of photoluminescence peak (λ=430nm) and weak decreasing of intensity of the main peak (λ=510 nm). Further treatment energy growth revealed photoluminescence intensity decreasing for both peaks in comparison with ZnO samples without laser shockwave treatment.

Intensity growth of the photoluminescence peak (λ=430nm) can be connected with releasing of large amount of defects created by laser shockwave treatment. We assumed that such defects witch induced by laser shockwave treatment are acceptor oxygen vacancies V_O. As we have seen in our previous work [3], intensity growth of photoluminescence peak (λ=430nm) can be induced by laser annealing on the sample of ZnO nanopowder in nanosecond pulsed mode. Laser shockwave treatment of ZnO nanopowder can used as simple and convenient method of obtaining structures with controllable features.

1. V.M. Zhurovetski, B.P. Kovalyuk, V.S. Mocharskyi, Yu. Nikiforov, V.V. Onisimchuk, D.I. Popovych, A.S. Serednytski, Structure and Photoluminescence Modification of ZnO Nanopowders by the Laser Shockwave Treatment. *Physics and Chemistry of Solid State.* vol.13, 4 (2012).
2. B. Kotlyarchuk, I. Myronyuk, D. Popovych, A. Serednytski, *Phys. and Chem. of Solid State*, 7, pp. 490-494 (2006).
3. V.V.Gafiychuk, B.K.Ostafiychuk, D.I.Popovych, I.D.Popovych, A.S.Serednytski, *Appl. Surface Science*, vol.257, 2011.

СЕКЦІЯ 3 (усні доповіді)
ФІЗИКО-ХІМІЧНІ ВЛАСТИВОСТІ ТОНКИХ ПЛІВОК
21-24 травня 2013 р.

SESSION 3 (oral)
PHYSICAL-CHEMICAL PROPERTIES OF THE THIN FILMS
May, 21-24, 2013

Design and Realization of Microcavity One-Dimensional Magnetophotonic Crystals with Double Layer Iron Garnet

Berzhansky V. N.[1], Shaposhnikov A.N.[1], Mikhailova T.V. [1], Karavainikov A.V.[1], Prokopov A. R.[1], Kharchenko M.F.[2], Lukienko I.M.[2], Kharchenko Y.N.[2], Miloslavskaya O.V.[2]

[1]*Taurida National V. I. Vernadsky University, Simferopol, Ukraine*
[2] *Institute for Low Temperature Physics and Engineering of the NASU, Kharkiv, Ukraine*

Microcavity one-dimensional magnetophotonic crystals (1D-MPC) based on oxide mirrors are perspective for application in magneto-optics. The use of a double-layer magneto-active (MA) film in such structures allows to increase the Faraday rotation (FR) and magneto-optical figure of merit Q [1, 2]. In this work the results of design and realization of six microcavity 1D-MPC of general structure "fused quartz/$(TiO_2/SiO_2)^4$/M1/M2/$(SiO_2/TiO_2)^4$" are presented. Here M1 and M2 are sub-layer of composition $Bi_{1.0}Y_{0.5}Gd_{1.5}Fe_{4.2}Al_{0.8}O_{12}$ with optical thickness $l_1 = \lambda_R/4$ and the main MA layer of composition $Bi_{2.8}Y_{0.2}Fe_5O_{12}$ with $l_2 = \lambda_R/4$ or $3\lambda_R/4$, respectively. λ_R is resonant wavelength. 1D-MPCs were fabricated by reactive ion beam sputtering of corresponding targets in argon-oxygen mixture [1]. Fig. 1 shows measured (symbols) and calculated (solid lines) FR and transmittance spectra of 1D-MPC with $l_1 + l_2 = \lambda_R/4 + 3\lambda_R/4$. The best values of 1D-MPC parameters that we have achieved are: for the long-wave peak at λ_R = 760 nm enhancement factor t = 10.5, Q = 10.3º, FR = 4.74º and for the shot-wave peak at λ_R = 623 nm t = 11.3, Q = 15.1º, FR = 13.6º.

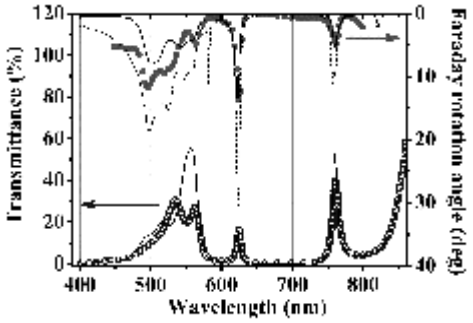

Figure 1

Based on the determined properties of MA layers some variants of 1D-MPC that provide higher values of Q are proposed. For example, 1D-MPC with 4x2 pairs of TiO_2/SiO_2 mirrors including two identical microcavities, with thicknesses of MA layers $l_1 + l_2 = \lambda_R/4 + 3\lambda_R/4$ and SiO_2 phase adjustment layer with $l_{SiO2} = \lambda_R/4$ allows to increase FR and Q at λ_R = 760 nm to 11º and 20.9º, respectively, and at λ_R = 623 nm FR and Q are 31º and 17.7º, respectively (Fig. 1, dashed line).

1. One-dimensional magnetophotonic crystals based on double-layer Bi-substituted iron garnet films / V. N. Berzhansky, A.N. Shaposhnikov, A. R. Prokopov [et al.] // Mat.-wiss. u. Werkstofftech. – 2011. – Vol 42, No 1. – P. 19.
2. Microcavity One-Dimensional Magnetophotonic Crystals with Double Layer Iron Garnet / V. N. Berzhansky, T. V. Mikhailova, A. V. Karavainikov [et al.] // J. Magn. Soc. Jpn. – 2012. – Vol 36, No 1_2. – P. 42-45.

Formation of Through Pores in Condensed Film of Lead, Tin and Indium

Churilov I.G., Dukarov S.V., Kravchenko S.G., Petrushenko S.I., Sukhov V.N.

V.N. Karazin Kharkiv National University, Kharkov, Ukraine

Studies of temperature influence on morphology and continuity of thin film systems are of great importance both for understanding of the fundamental processes occurring in thin films and for various applied uses. This work studies formation of through pores by heating and annealing of continuous polycrystalline films of lead, tin and indium 200-2,000 nm thick. The film under study was condensed by vacuum thermal evaporation on the extended glass plates on which amorphous carbon underlayer was pre-deposited. The temperature gradient (about 10 K/mm) was created along the substrate, a resulting in a series of samples being formed. They were obtained the under identical conditions and annealed to different temperatures during the same time.

According to electron microscopic research, the morphology of the film is different in the areas corresponding to different temperatures. Where the annealing temperature of the material under study exceeded the melting point of bulk samples, the film was individual spherical droplets solidified. The film remained solid and polycrystalline in the area with the substrate temperature below the melting point of bulk samples. Through pores were formed in this area during the condensation and growth, the size and area of which varied depending on the annealing temperature.

While analyzing the electron microscope images it was established that the increase in temperature resulted in an increase in the average pore size by the exponential law, and the extent to which the substrate was covered with the film tends to a small constant value attainable at the melting point.

In the assumption of the diffusion mechanism of pore formation the activation energy of the surface self-diffusion equaling 1.22, 1.62 and 1.70 eV for lead, tin and indium accordingly was obtained based on the data on the temperature dependence of the average pore size. During the analysis of electron microscopic images it was also discovered that the density of through pores (number per unit surface) does not increase with temperature. This indicates that annealing only increases the size of pores formed during the film deposition, but does not lead to the formation of new pores.

Hysteresis of Melting-Crystallization in Multilayer Film Systems

Churilov I.G., Dukarov S.V., Nevgasimov A.O., Petrushenko S.I., Sukhov V.N.

V.N. Karazin Kharkiv National University, Kharkov, Ukraine

Today researchers and technologists take steady interest in nanocomposite structures that are nanosized objects embedded in the solid matrix of another substance. It is convenient to use, as a model for studying thermodynamic and structural properties, vacuum-deposited multilayer films that can be studied by standard methods of electron diffraction and microscopy.

This work is devoted to studying phase transitions in multilayer films, in which the thin layer of fusible component (In, Sn, Bi, Pb) modeling the embedded particles is between the layers of the refractory material acting as a solid matrix (Cu, Mo, C).

The samples were prepared by sequential condensation of the test substances in vacuum 10^{-4}-10^{-5} Pa onto a substrate with pre-deposited electrical contacts, which allowed measure electrical resistance of system under study without depressurization. Phase transition temperatures were registered by electrical resistance jumps accompanying melting and crystallization of the fusible component when heated and cooled. Similar samples of the Cu-Bi-Cu system were studied by the electron diffraction methods when heated and cooled directly in the electron diffraction camera. The temperatures of phase transitions were registered on appearance and disappearance of diffraction reflections of the fusible component. The supercooling values obtained during the crystallization in the liquid phase of the fusible component located between the layers of the refractory component are presented in the table below.

System	ΔT, K	ΔT/Ts
Cu-Bi-Cu	64	0.12
Mo-Bi-Mo	52	0.09
Cu-In-Cu	9	0.023
C-Pb-C	138	0.23
C-Sn-C	140	0.29
C-Bi-C	102	0.19

It's observed that with the refractory component being carbon that is almost non-interacting with melts of the selected metals (130-140º edge contact angles) the relative supercooling value is maximal. Relative supercooling is significantly lower for the metal matrix well wettable by the fusible substance. The results obtained are consistent the existing views on the solid component influence on supercooling during the crystallization of the melt in contact with it.

Effect of the Grain Size on the Melting of the Polycrystalline Metal Films

Churilov I.G., Dukarov S.V., Petrushenko S.I., Sukhov V.N.

V.N. Karazin Kharkiv National University, Kharkov, Ukraine

Phase transitions in the finely dispersed polycrystalline metal films due to the large number of grain boundaries possessing excessible energy, have specific properties that distinguish them both from the bulk materials and from isolated micro particles This work studies melting polycrystalline films fusible metals 500-2,000nm thick. Films under study were deposited on glass or polikor plate in vacuum, with a pre-condensed sub-layer of amorphous carbon. After the completion of the condensation along the substrate with the deposited film a temperature gradient was created, which the same experiment, and under the same conditions, helped to register a set of states for samples obtained under the same conditions, meeting the requirements of heating, and annealing to different temperatures for the same time. According to our electron microscopic research the films above the melting point consist of islands of regular spherical shape typical for the liquid state. The film is polycrystalline and solid on low temperature substrates. Between these states there is a region of finite width, where an increase in temperature causes formation of discontinuities in the film afterwards turning into a labyrinth-shaped structure, and resulting in appearance of fused crystallites, which indicates the presence of a liquid phase below the equilibrium melting point.

The films condensed at a temperature much lower the melting temperature of the precipitants materials are finely dispersed polycrystalline and their area of grain boundaries is extremely high. Individual crystallite melting leads to disappearance of intercrystalline boundaries and allocation of the related cross-border energy, which stimulates further melting of the film and makes it possible to lower the equilibrium melting point. In this case, each grain of the polycrystal has its melting point, which depends on its size and orientation relative to other grains, that is why polycrystal melting occurs at a certain temperature interval, determined by the energy of the grain boundaries and grain size distribution.

The work has assessed the average energy of the grain boundaries by the rate of temperature width of the transition region and the average crystallite size for films of lead and tin, which turned out to be 0.27 and 0.14 J/m^2, accordingly which is consistent with the specific data. The work has also discovered an increase in temperature range in the transition area with an increase in dispersion of lead films.

Studying of Multicomponent Materials With the Using of Analytical Electron Microscopy

Danylenko M.

*Institute for problems of Materials Science NAS of Ukraine, Kyiv,*Ukraine

The method of analytical electronic microscopy was used for the study of interfaces between heterogeneous elements. High locality of quantitative x-ray microanalyse is achieved by studying of thin foils (thickness about 100 nm) and fine electron beam (0,5-1,5 nm). Analysis, carried out on an analytical complex JEM-2100F of thin foils shows that for a small step between analyzed points (5-10 nm) the transitional area of layered composite Cu-Nb is ~3-5 nm.

In powder composites of 80Ni –20Mo and 50Fe – 50Cr the abnormal high diffusion was detected. Both pairs are characterized unidirectional diffusion, and more refractory component has considerably higher diffusive mobility than low-melt one. The results indicate that interface of contacting elements is an essential in the mechanism of alloy formation under the effect of high deformations.

Studying of structural and chemical microinhomogeneity of high entropy alloy Ti-V-Zr-Nb-Hf-Ta was carried out. In spite of considerable deviations in the chemical composition of high entropy alloy (Fig.1), the deviations of the calculated average atomic radius of the lattice not exceed 1.5 %.

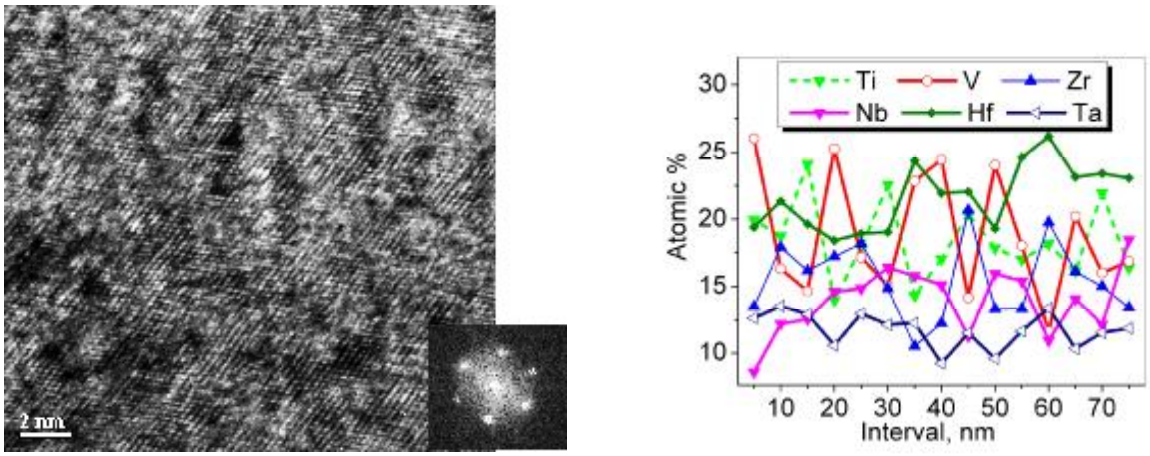

a b

Fig.1. Structure (a) and chemical composition (b) of high entropy alloy.

Results which will be presented show that precision studying of interfaces and grains with the use of analytical electron microscopy allow not only increase locality of the quantitative analysis of distributing of elements but also considerably to advance in understanding of mechanisms of contact formation and alloy formation in multicomponent materials.

An Automated System for Measuring Parameters of Thermoelectric Semiconductor Films

Dzundza B.S.

Vasyl Stefanyk Precarpathian National University, Ivano-Frankivsk, Ukraine

In this paper, electric circuits and the current unit of measurement of electrical parameters of semiconductor films constructed. The computer program that provides automated measurement and recording primary data processing, with the possibility of plotting time and temperature dependencies has been created.

Measurement of electrical parameters of semiconductor films - type of conductivity, electrical resistivity, carrier concentration, mobility, Seebeck coefficient have been performed at constant magnetic field magnitude (1.5-2) T. During measuring film samples were placed in the holder type design with six measuring probes, two thermocouples, internal (gradient) i outside heaters. The accuracy of temperature measurement was 0.5-1.0 K and magnetic fields of ±3%. Cryostat to generate low temperatures were a quartz Dewar vessel filled with liquid nitrogen and placed in the magnet gap. The intermediate temperature between nitric i potted achieved by heating of electrospiral, which was bifilar wound on tubular core sample holder. Use impermeable cell allows measurements in vacuum (10-3-10-4) Pa. Production of reliable ohmic contacts that do not destroy the film i meet all the necessary requirements, were methods of deposition of silver in combination with gold-plated contacts clamping or soldering at T <400 K the conductivity type was determined by the sign of the Seebeck.

Functional diagram of the setup is shown in Fig. 1. The basis for measuring complex is a digital multimeter UNI-T UT804 that supports output data to a computer and using a voltmeter DC voltage provides a resolution of 0.01 mV with an accuracy of 0.05% and has an automatic choice of the measuring range.

As a control device selected microcontroller ATMega16. The program is written in C in a medium CodeWizardAVR. Connectivity is provided at the hardware level converter USB-UART, and on the software using text command interpreter that provides two-way communication between the control program on the computer and microcontroller installation.

Switching voltmeter and removal of voltage drop on the resistor reference, sample current and Hall contact pairs sequentially have been used by six reed mikro relay block commutation. .

The work supported by an integrated project of MES of Ukraine (N 0113U000185) The work supported by projects of NAS of Ukraine (N 0110U006281)

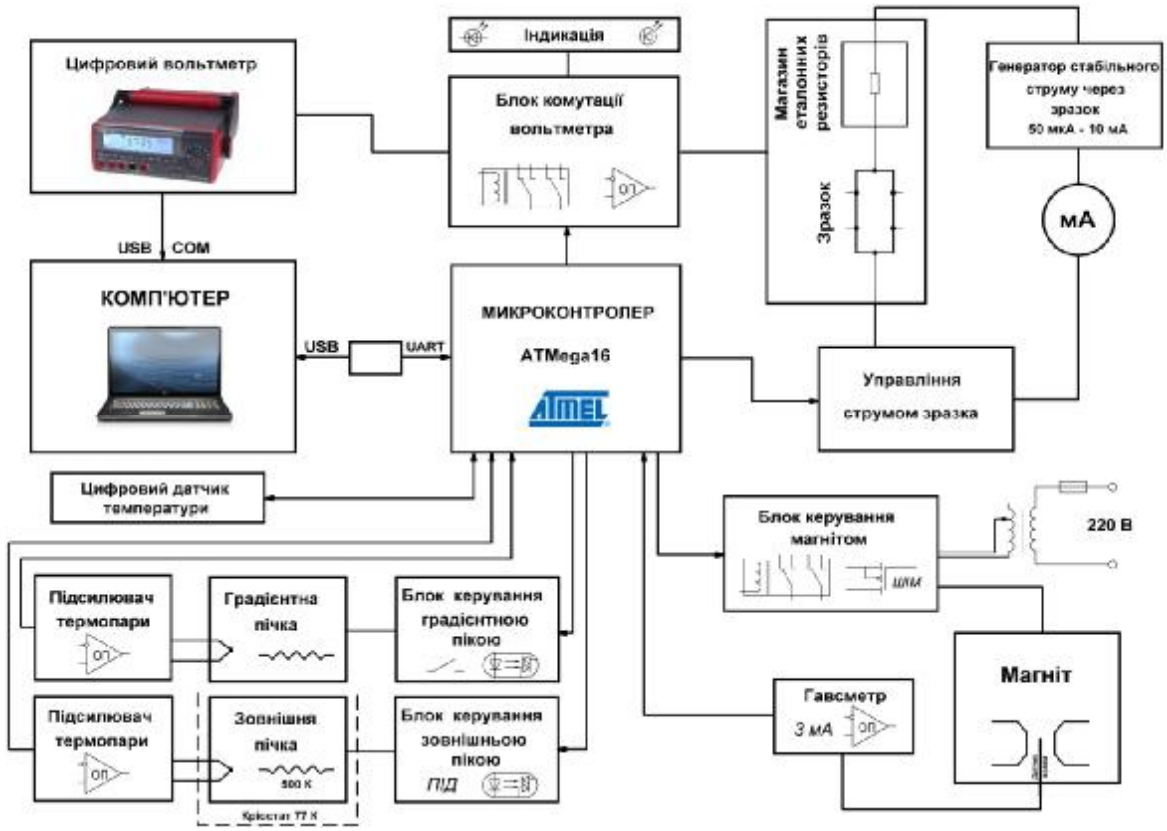

Fig. 1. A functional block diagram of the installation of automated measurement of electrical parameters of semiconductor films.

Generator stable current through the sample collected on the LM234 chip and has 12 discrete values of current are selected using wafer switcher and controlled ammeter. Turn the magnet and the magnetic field polarity change is implemented on electromechanical relays, current through the magnet is given laboratory autotransformer is switched to the rectifier bridge. Continuously increasing the current through the magnet to the nominal and when the smooth decrease to zero at shutdown by using pulse width modulation (PWM). Measurements of the magnetic field is realized on the hall sensor is placed on the outflow dipstick in the working area magnet.

The program has written in Delphi and provides registration information from a digital voltmeter, manual and automated process control measurements, pre-processing and visualization of data. The results of measurements of each sample save in a separate file with the possibility of continuing the experiment. The users can select specific data to be exported to MS Exel for further processing.

Work is executed according complex scientific project MES of Ukraine (hosudarstvennыy a registration number 0113U000185).

Mechanisms of Growth, Topology and Electrical Properties of Thin Films and Nanostructures of Lead Telluride

Freik D.M., Saliy Ya.P., Lopjanko M.A., Bachuk V.V., Myhajluk V.V.

Vasvl Stefanyk Precarpathian National University, Ivano-Frankivsk, Ukraine

The analysis of the topology of lead telluride vapor-phase nanostructures by surface condensates modeling methods on the mode of atomic force microscopy and cellular automata executed at first in thesis. The proposed geometric model of the terrain allows to describe all stages of nanostructures formation in axiomatic form depending on the both the conditions growth and physical parameters of the system.

At first established that the growth processes of nanostructures of lead telluride on monocrystalline substrates PbTe/(0001) mica, and PbTe/(111) BaF_2 have activated character, and kinetics of their formation exponentially dependent to the deposition time of vapor on substrate. And, this deposition time is the exponent of substrate temperature. Was define the spatial forms of nanocrystallines, their mutual orientation, and orientation relative to the substrates in heterostructures. It is shown that investigated values of technological factors is implemented in all cases the Folmer-Weber mechanism taking into account the orientation and energy influencing.

Was proposed and implemented distribution histograms represent of height of nanoformations on their superposition of three Gaussian functions. It is shown, that the size of individual nanoislands defined processes of Ostvald maturation provided simultaneous action the diffusion and Wagner mass transfer mechanisms, whose contribution depends on technological factors and evaporation temperature deposition.

It is shown, that in the thickness d-dependences of conductivity (σ), Seebeck coefficient (S), and thermoelectric power ($S^2\sigma$) of thin films (with micron thickness) occur classical size effects, and in nanostructures (nano-size thickness) - the quantum oscillation related to the quantization of energy spectrum of charge carriers in quantum wells formed barriers at the boundaries of the substrate and the surface.

The work supported by an integrated project of MES of Ukraine (N 0113U000185) and by projects of FRSF State Agency for Innovation and Informatization of Ukraine. (Contracts: R54, F53, 3)

Trapping Centers in CdI_2 Crystals Doped with PbI_2

Galchynsky O.V.[1], Gloskovska N.V.[2], Yarytska L.I.[3]

[1]*Lviv Medical Institute, Lviv, Ukraine*
[2]*Bogolyubov Institute for Theoretical Physics, Kyiv, Ukraine*
[3]*Lviv State University of Vital Activity Safety, Lviv, Ukraine*

Cadmium and lead iodide crystals are good X-ray adsorbers and can be used as ionizing-radiation detectors. Hexagonal structures of these layered compounds have similar lattice parameters: a=4.24 Å, c=6.84 Å for CdI_2 and a=4.56 Å, c=6.98 Å for PbI_2. In the PbI_2-containing CdI_2 crystals grown by the Bridgman-Stockbarger method the impurity is incorporated into the host crystal lattice in the form of Pb^+ isolated ions and PbI_2 nanocrystals as well [1].

Trapping centers were studied by the thermally stimulated depolarization method in the temperature range 80-300 K. Depolarization peaks at 112 and 158 K are related to Pb^+ isolated ions in the different hexagonal environment in 4H-CdI_2; peaks at higher temperatures are assigned to the nanocrystalline inclusions.

Electron trapping at the Pb^{2+}- centers is accompanied by the photoluminescence which intensity peaks lie in the range 120-150 K. Under excitation in 3.23 eV band activation energies of photoconductivity (T>140 K) and photoluminescence (T<170 K) coincide and amount to 0.18 eV, therefore, these processes are determined by the same factor. Within 140-240 K the process of delocalization of charge carriers in the crystal system is mainly contributed by the high-energy cationic excitons of PbI_2 nanocrystals [2].

Thus, at 120<T<170 K mechanisms of radiative annihilation of cationic excitons and recombination of charge carriers at the trapping centers coexist. At the same time the release of electrons from attachment levels occurs with a predominance of the recombination processes over re-trapping.

1. Bolesta I.M., Vistovskii V.V., Gloskovskaya N.V., Panasyuk M.R. and Yaritskaya L.I. High-energy Frenkel cation exciton and specific features of its self-trapping in the CdI_2-PbI_2 crystal system // Physics of the Solid State. – 2011. - V.**53**, №4. - P.799-803.
2. Gal'chinskii A.V., Gloskovskaya N.V. and Yaritskaya L.I. Carrier trapping and delocalization in PbI_2-containing CdI_2 crystals // Inorganic Materials. - 2012. - V.**48**, №4. - P.423-427.

Self-Trapped Exciton at Silicon Nanocrystal Surface.

Gert A.V., Yassievich I.N.

Ioffe Physical-Technical Institute RAS, S.-Petersburg, Russia

The intensive research of the silicon nanocrystals optical properties has been stimulated by its potential applications in optoelectronics, photovoltaic and medicine. The start of these investigations was initiated by the discovery of porous silicon effective photoluminescence in the visible range at room temperature [1]. In one of the first works on the porous silicon radiation the idea about surface self-trapped exciton (STE) was suggested [2]. The idea emerged due to the two facts: i) the large Stockes shift, 1 eV, between the threshold energy of absorption and quantum energy of the radiation for nanocrystals of sizes < 1.5nm, and ii) lack of the blue shift in the luminescence spectrum for the nanocrystals of diameters < 2.1nm. The experimental data recently obtained by the femtosecond pump-probe spectroscopy technique have shown that capture at the metastable self-trapped state, i.e. STE state, plays a key role in the dynamics of hot excitons in the photoexcited silicon nanocrystals embedded in the SiO_2 matrix [3].

We present the theoretical model of STE and the modeling of hot free exciton capture from the nanocrystal at the STE state and the reverse process. In additional, we consider radiative and nonradiative multiphonon recombination of STE. The ratio of the multiphonon STE recombination probability to the probability of the radiative self-trapped exciton recombination is estimated [4].

The modeling is based on the one mode Huang and Rhys model, in which vibration of oxygen on silicon nanocrystal surface is considered as this mode. The comparison of the experimental data and the theory lets us to determine theory parameters: i) the energy of electron-phonon binding, and ii) the STE energy position.

We demonstrate that the capture at the STE state decreases quantum efficiency of the photoluminescence for small nanocrystals (of diameter < 3 nm) in silicon dioxide matrix.

1. L.T. Canham, Appl. Phys. Lett. **57**, 1046 (1990).
2. F. Koch, V. Petrova-Koch, T. Muschik, J. Luminesc. **57**, 271 (1993).
3. W. D. A. M. de Boer, H. Zhang, A. N. Poddubny, Phys. Rev. B **85**, 161409 (2012).
4. A.V. Gert, I.N. Yassievch, JETP Letters (to be published in February 2013).

X-rays Diffractometry Methods for Polymer-Containing Nanocomposites Investigations

Gomza Yu.P., Klepko V.V., Nesin S.D.

Institute of Macromolecular Chemistry NAS of Ukraine, Kiev, Ukraine

The method of interpreting the X-ray scattering data is based on the analysis of the scattering curve, which shows the dependence of the scattering intensity, I, on the scattering angle, θ, or the wave vector, q. The experimental X-rays data obtained from the nanocomposites contain a large amount of information hidden in the structure of measured X-ray spectra. We developed the experimental approach for obtaining, processing and interpretation of wide-angles (WAXS) and small-angles (SAXS) X-rays scattering in terms of peculiarities of short-range ordering and nanoscale aggregations of weak-ordered polymer-containing nanocomposites determination. Wide-angle X-rays scattering (WAXS) was used mainly for primary estimation of short-ordering character – i.e. are the investigated material amorphous or partial crystalline. The another application of WAXS for nanocomposites is the establishing of different stages of organoclay dispersion in polymeric matrix – i.e. differentiated the three canonical variants of structure: i)phase separation; ii) intercalation, iii) exfoliation of primary inorganic sheets in polymeric matrix. The most informative for nanocompozite structure peculiarities determination in the range of sizes from 1-2 to 100-200 nm is small-angle X-rays scattering (SAXS). The overall SAXS intensity level is the measure of degree of microphase separation of investigated material at nanoscale level, and the character of scattering curve enables us to differentiated the nanoscale space-ordered structures (the presence of discrete maxima) from disordered (diffuse character of scattering) ones. The next stage of diffuse SAXS curves analysis is representation of scattering data in *log-log* coordinates. The scattering profiles exhibit a straight-line behaviour over a range of q indicating fractal nature of the structure of the samples. Also, profiles in the entire q-range may be divided into few (2-3) regions each with a different slope for the lines. This indicates different nature of structural features on different length-scales of observation. For the slope values determined the fractal type (mass of surphace ones) and the fractal dimension values. The intermediate regions between rectilinear parts of the curves are used for R_{gi} (the average radius of gyration of the structure elements) calculations.

This approach has been successfully used for studying the structures peculiarities of the nano-sized powders-, clay minerals- and carbon nanotubes and polymer-based nanocomposites filled by them. It was established the correlation of functional characteristics of such materials (i.e. ionic conductivity and cathalitic activity levels ets) and their structure peculiarities.

Electro-Physical Features of Thin Layers of Porous Silicon with Embedded Copper Oxide Nanoclusters During Adsorption of Organic Molecules

Gorbanyuk T.I.[1], Lytovchenko V.G.[1], Solntsev V.S.[1], Demin I.S.[2]

[1]*V.Lashkaryov Institute of Semiconductor Physics of NAS Ukraine, Kyiv, Ukraine,*
[2]*Kyiv National Taras Shevchenko University, Kyiv, Ukraine*

PL spectra and I-V characteristics of porous silicon with adsorbed molecules of aminoacids (methionine and glycine) were investigated at room temperature. It was found that the layers of porous silicon (PSi) with porosity about 40 % have more intensive photoluminescence (PL) than that with porosity in range of 50-80 % (Fig. 1). A short-wave shift of PL spectra under methionine adsorption was observed. This PL shift was accompanied by a decrease in the size of nc-Si due to the local oxidation of Si nanocrystals (nc-Si) during the interaction with adsorbed methionine molecules. In contrast to these phenomena, the adsorption of glycine leads to increase of PL intensity almost two times and to shift of the PL peak to the long-wave region (from 660 nm to 700 nm) caused by an increase in the average size of nc-Si as a result of the recovery process on PSi surface by glycine molecules. So the observed features of these spectra and their evolution can be interpreted not only in the framework of the quantum confinement model. It is necessary to take into account the influence of the electrochemical etching products of monocrystalline Si and/or adsorbed organic compounds with another dielectric constants embedded into the pores and/or surrounding its.

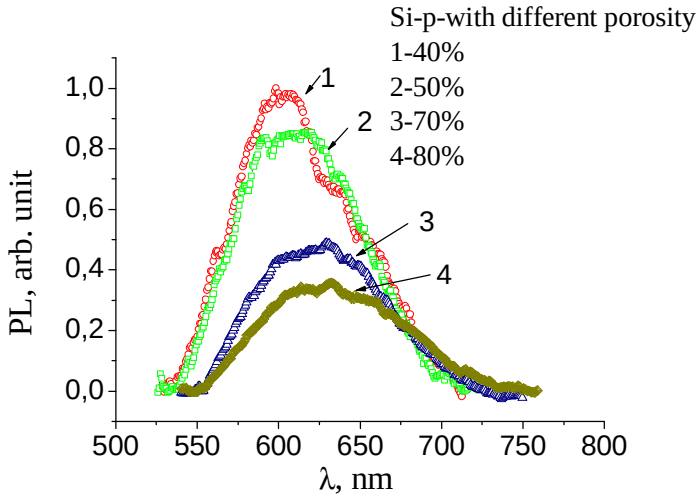

Fig. 1. Room temperature photoluminescence spectra PSi for four different of porosity levels all the curves normalized to the maximum PL for 40% porosity.

Effect of Weak Magnetic Field Treatment on the Photoluminescence and Absorption of GaN/Al_2O_3

Konakova R.V.[1], Milenin V.V.[1], Red'ko R.A.[1], Shvalagin V.V.[2], Red'ko S.M.[1]

[1]V. Lashkaryov Institute of Semiconductor Physics of the National Academy of Sciences of Ukraine, Kyiv, Ukraine,
[2]L. Pysarzhevskiy Institute of Physical Chemistry, National Academy of Science of Ukraine, Kyiv, Ukraine,

Gallium nitride epitaxial structures with a thickness of 2-2.5 μ, grown on Al_2O_3 substrate (430 μ), by MOCVD method and *n*-type doped with Si ($1{,}6\cdot10^{19}$ cm^{-3}) were objects of the investigation. The main goal of this study is to determine a physical processes, occurred in semiconductor material after weak magnetic field (WMF) treatment (B=60 mT). The photoluminescence (PL) and absorption spectrum of studied structures were measured during a month at 300 K in the 350–650 nm and 350-1100 nm wavelength range, respectively.

The initial spectrum of PL exhibits a sharp peak at 363 nm and non-elemental band ~530 nm. The first related with band-to-band emission, but the second – with donor-acceptor pairs, which consists V_{Ga}. The most efficiency changes after WMF treatment was detected for near-edge emission. The increase of its intensity (I/I_0) was more than 20%. The spectrum of absorption consisted two regions: a typical linear, related with absorption edge and the second (400-1100 nm) – oscillatory, attributed to a clear inner boundary between GaN and Al_2O_3. The last resulted to appearing interference. The estimated thickness of the layer, which forms interference, was d~2.2 μ and was changing during the experiment. Analyzing dependences $d(t)$ and $I/I_0(t)$ one can see, that the maximum of intensity coincide (time shift was 4-5 days) with minimum of effective thickness of layer, formed interference. At the end of research spectrum returned to initial position.

We can assume that in the semiconductor due to WMF action metastable complexes have destructed. Then parts of complexes can diffuse to the natural gate – a semiconductor surface, and can take part in the formation of different defect complexes. This depends from initial impurity-defect composition of semiconductor material. At first, optical absorption reacted to occurring processes because all volume of semiconductor forms this signal. The transformation of radiative recombination spectra was detected when the changes of microstructure were reached to region, which formed PL. Unfortunately, these changes are not stable and the return to initial state is observed after one month.

Synthesis and Spectral-Luminescent Properties of the $(Yb_{1-x}Er_x)_2O_3$–SiO_2 Films

Kouhar V.V.[1], Khodasevich I.A.[1], Pestryakov E.V.[2]

[1]*B.I.Stepanov Institute of Physics of the NAS of Belarus, Minsk, Belarus*
[2]*Institute of Laser Physics of the SB RAS, Novosibirsk, Russia*

In present work we synthesized by the sol-gel method Yb–Er-containing silica films and investigated their permolecular structure and spectral-luminescent properties.

Microscopic examination of the surface of experimental samples showed that they have a mosaic structure with inhomogeneities which have a mean size ~ 20 μm, and the size increases with rise of annealing temperature. Fluorination of the films increases the inhomogeneities. It should be noted that prepared films are characterized with a high adhesion to silica substrate and can contain up to 20 mass % of the Ln_2O_3.

Figure demonstrates anti-Stokes luminescence spectra of Yb–Er-containing films obtained at excitation by radiation of a semiconductor CW laser with a different specific power (P). It is seen that the luminescence spectrum of film after annealing in air at T_{air}=1200°C (curve *1*) with $P = 7\times10^5$ W/cm^2 is characterized by three relative intensity of the $^2H_{11/2} \rightarrow {}^4I_{15/2}$ ($\lambda \approx 522$ nm), $^4S_{3/2} \rightarrow {}^4I_{15/2}$ ($\lambda \approx 547$ nm) and $^4F_{9/2} \rightarrow {}^4I_{15/2}$ ($\lambda \approx 660$ nm) luminescence bands of Er^{3+} ions. The relatively high intense of luminescence from the $^2H_{11/2}$ level of Er^{3+} ions which is located on ~ 800 cm^{-1} above the $^4S_{3/2}$ one is a worth argument in favour of nanocrystalline $(Yb_{1-x}Er_x)_2O_3$ particles formation. It should be noted that relative intensity of the band at $\lambda \approx 522$ nm increases with lowering P to 3.5×10^5 W/cm^2 (curve *2*). This fact can be attributed by the decrease of cross relaxation loss in the $^2H_{11/2} \rightarrow {}^4I_{11/2}$: $^4I_{13/2} \rightarrow {}^4F_{9/2}$ channel. After fluorination at T_F=800°C (curve *3*) the relative intensity of the band $^4S_{3/2} \rightarrow {}^4I_{15/2}$ decreases. It may be explained by energy dumping from the $^2H_{11/2}$ state to the $^4F_{9/2}$ one through the above indicated channel due to the lower frequency vibrations of the Ln–F bond in comparison with Ln–O one.

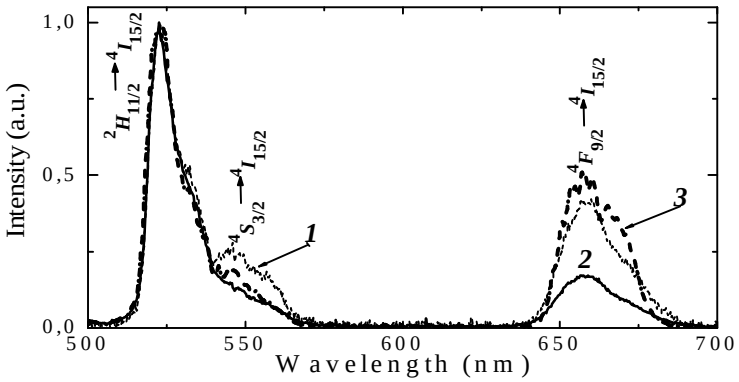

Fig. Visible anti-Stokes luminescence spectra of films after (*1*, *2*) annealing in air and (*3*) fluorination at l_{exc}=980 nm with specific power (*1*) 7×10^5, (*2*) 3.5×10^5 and (*3*) 1.7×10^5 W/cm^2. T_{air}=1200°C and T_F=800°C.

Ellipsometric study of thermally induced transformations in amorphous chalcogenide films

Kozak M.[1]*, Loya V.[2], Kozak O.[1], Fedelesh V.[1], Zhickarev V.[1], Puga P.[2]

[1]*Uzhgorod National University, Uzhgorod, Ukraine*
[2]*Institute of Electron Physics, Ukr. Nat. Acad. Sci., Uzhgorod, Ukraine*
**E-mail: kozakmi@ukr.net*

It is believed that after the deposition of thin films of glassy chalcogenide enough annealed at the glass transition temperature of bulk glasses, so they got all the properties of bulk glass. However, the transfer of "amorphous state - glass" is not so elementary. It has long been observed that between these states is to crystalline phase [1]. But since we heat the film to a temperature well below the melting point of the crystalline phase, the question “what do we get after annealing?”. In this report on the basis of the ellipsometric studies of glassy chalcogenide films discusses the possible situations that, from our point of view, may be the case.

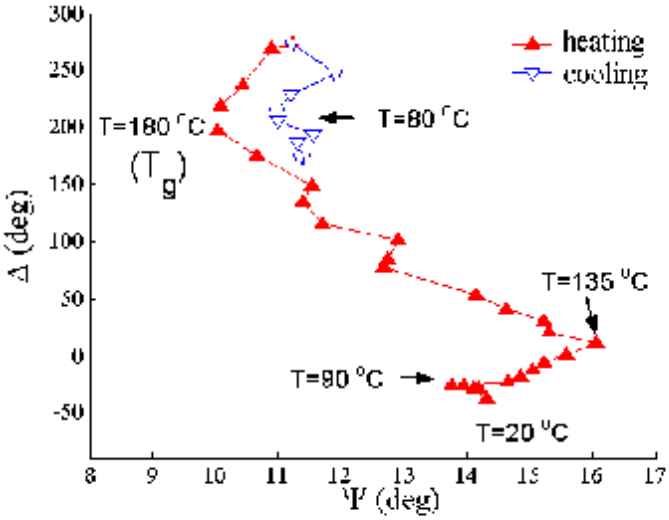

Fig.1. The plot of the ellipsometric angles during heating and cooling of the film As_2S_3 on a substrate KCl.

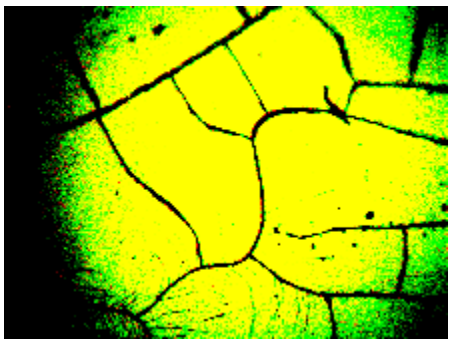

Fig.2. Photo images of the film As_2S_3|KCl after the heating-cooling in an optical microscope.

As a result, noted two critical points, except T_g course. As can be seen from Figure 1, the temperature is 80-90 °C and 135 °C. Last we associate with a second glass transition temperature T_2 of the Gibbs and DiMarzio and the presence of the first to be steadfast debate. It is also interesting to look at the kind of film after heating in an optical microscope (figure 2) – it is covered with characteristic grooves T-shape.

1. Курнаков Н.С. *Введение в физико-химический анализ.* – М.-Л.: Изд. Акад. наук СССР. – 1940. – 553 с.
2. Kozak M.I., Zhickarev V.N., Studenyak I.P. et al. // Opt.&Spectr. – 2006. – Vol. 101. – P. 568-570.

Reversible Swelling of a Calcein Film Under Humidity Exposure

Kruglenko I.[1], Burlachenko J.[1], Kravchenko S.[1], Slabkovska M.[2]

[1]*V. Lashkaryov Institute of Semiconductor Physics NAS of Ukraine, Kyiv, Ukraine*
[2]*V.Glushkov Institute of Cybernetics NAS of Ukraine, Kyiv, Ukraine*

The adsorption properties of calcein were investigated. Quartz crystal microbalance sensor with calcein thin film has demonstrated unusual response on the water vapor: the adsorption curve first went down up to - 6000 Hz (that is extremely high response value for such kind of sensor) and then went up to a saturation level. AFM measurements and ellipsometry data have shown that this effect is concerned with film swelling.

Fig. 1 demonstrates ellipsometry data for 30 nm film thickness changes after 20 min exposure in water vapor (point 2) with following drying (points 3-5). Film thickness increases more than two times. Moreover, these drastic changes are reversible.

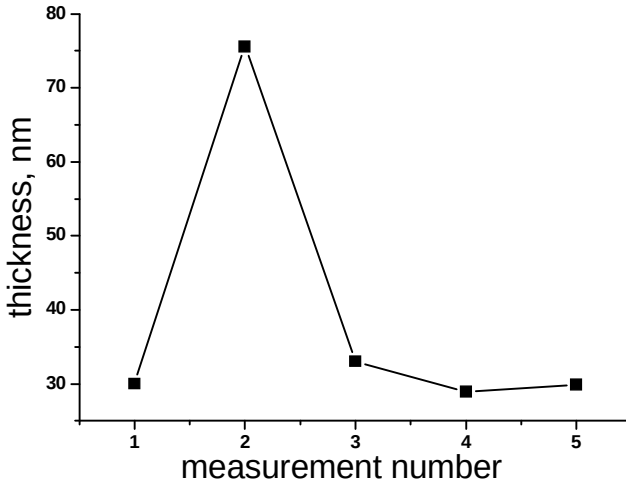

Fig. 1 – 30 nm calcein film thickness changes under water vapor exposure: 1 – initial state, 2 – after 20 min water exposure; 3-5 – desorption of water molecules during 10, 20 and 30 min respectively.

Apart from thickness changes the significant film restructuring under vapor exposure is observed. In the course of water molecules adsorption, nonuniform surface with a developed relief gradually transforms into smooth uniform one. And, again, after drying the surface returnes to its initial state.

Restructuring of the film surface in the course of adsorption–desorption is quite possible for molecular crystals where intermolecular bonding is relatively weak, and interaction with adsorbate may be of the same order as in between the molecules of material. We believe, however, that such essential changes (with further material returning to its original state) are a unique phenomenon.

The effect of reversible film swelling and restructuring under humidity exposure may be used for the development of nanoactuator transforming humidity pulses into mechanical shifts.

1. I. Kruglenko, Yu. Shirshov, J. Burlachenko, A. Savchenko, S. Kravchenko, Sensitive coating for vapors detection based on thermally sputtered calcein thin films.// Talanta -2010.- 82.- №4.-pp.1392-1396.

Infrared Transmittance of Pb Nanofilms

Kurbatsky V.P.[1], Babchenko I.A.[2]

[1]*Zaporozhye National Technical University, Zaporozhye, Ukraine*
[2]*Zaporozhye Hydraulic Power Engineering College, Zaporozhye, Ukraine*

Technologies of fabrication of several nanometers thickness metallic films were advanced during last ten years and methods of optical study of their properties were developed [1–3]. Interpreting results, experimentalists used the Drude theory with two fit parameters (the plasma frequency and the relaxation rate). A purpose of the work was to derive an analytical expression for transmittance of a metallic nanofilm suitable for discussing experimental results in words used by experimentalists. We suppose that we succeeded in representing simple free electrons-in a box-model as still valid for analyzing results of experiments.

Under normal incidence of radiation onto a film, as it took place in the experiments, dielectric function of a nanofilm is described in the first approximation by the Drude expression [4]. We obtained a formula for transmittance by solving Maxwell equations and compared results of calculation by the formula with measured transmittance of lead films of several nanometers thickness [3]. Analysis of the formula showed that transmittance is sensitive to a change in thickness of a film just like to a change in value of the plasma frequency or the relaxation rate. Accuracy of measurements of thickness is an important factor since the method of determination of the average film thickness from mass of deposited metal leads to a big systematical error when film is of several nanometers thickness.

1. G. Fahsold, A. Bartel, O. Klauth, N. Magg, A. Pucci. Phys. Rev. B 61, 14108 (2000).
2. J.J. Tu, C.C. Homes, M. Strongin. Phys. Rev. Let. 90, 17402 (2003).
3. A. Pucci, F. Kost, G. Fahsold. Phys. Rev. B 74, 125428 (2006).
4. V.P. Kurbatsky, V.V. Pogosov. Phys. Rev. B 81, 155404 (2010).

Modification of Thermoelectric Properties of Bulk, Thin and Nanoscale Structures of Lead Telluride

Lysyuk Yu.V.

Vasyl Stefanyk Precarpathian National University, Ivano-Frankivsk, Ukraine

In this work, through experimental studies of thermoelectric materials n- and p-PbTe, n-PbTe:Bi (Sb) and theoretical calculations using the method of thermodynamic potentials, crystal and variational method for solving the Boltzmann equation optimum technological factors and their synthesis briquetting.

Given the comprehensive experimental study within the law Mattisen for the independent contribution of different scattering mechanisms, models Thaler to change the resistivity and the thickness of the bilayer model Petritz calculated the mean free path of carriers, their mobility, size of grains in the films of PbTe, PbTe:Bi and shown that thermoelectric parameters determined by diffuse scattering at the surface and within Intergrain. The combination of the two carriers model with diffusion processes of oxygen and vacancies of lead appreciated contribution to the thermoelectric parameters of thin films of lead telluride electrons and holes in their endurance in the air. It is shown that the dominant process is the diffusion of oxygen in the volume of condensate and lead vacancies to its surface.

For the proposed models of quantum wells in nanostructures p-PbTe/PM-1and n-PbTe:Bi/Sutal calculated Fermi energy, effective mass and density of states of carriers that define quantum-dimensional non-monotonic oscillatory character thickness dependence of Seebek (S), electrical conductivity (σ), thermoelectric power ($S^2\sigma$) and well explain the experimental results.

The work supported by an integrated project of MES of Ukraine (N 0113U000185) and by projects of FRSF State Agency for Innovation and Informatization of Ukraine. (Contracts: R54, F53, 3); NAS of Ukraine (N 0110U006281).

Local Electrostatic Field and Carrier Density in the Heat-Resistant Metals with the Regular Matrix of Volume -Filling Nano-Defects

Marenkov V.I.

Odessa I.I. Mechnikov National University, Odessa, Ukraine

Research and development of the perspective high-temperature elements of the electronic circuits with the aim of their application at the diagnostic complexes and plasma-chemical sensors with the high specific energy contributions to the working medium is one of the most important tendencies in the modern nanophysics [1]. High temperatures and pressures that accompany such processes impose special requirements on the strength and electronic properties of the materials. Traditional semiconductors are not heat-resistant, so the materials with the possibility of the control of electronic characteristics by means of the changes in the microstructure of the material have to be made. In the line of this research the use of the branched structures of the volume filling nanodefects (VFND) in the matrix of base material is promising. In the known approaches, theoretical description of the electronic properties of the samples with the manifold volume nanodefects is based on the complex quantum mechanical calculations of the energy spectrum of the carriers on the specified defect. Plenty of adjustable parameters and usage of the previously known value of the Fermi level for the carriers usually makes impossible the application if such methods to the determination of the electronic characteristics of the samples with the specified structure of VFND.

In the present work the technique of calculation of the electrophysical properties of metallic samples with the planar gap in the volume based on the statistical approach [2] is generalized to the problems of the materials with the complex geometry of the VFND matrix. Statistical average “on the ensemble of cells” gives the possibility to calculate the effective parameters of the inhomogeneous materials with the VFND and “removes” the complexity of calculation of electrophysical properties for the micro-inhomogeneous materials. At the same time, the solution of the boundary electrostatic problem involves the minimization of the Helmholtz free energy functional on the parameters if the charge density distribution. After the averaging on the space and time, the electrostatic contribution of the neutral cells to the Helmholtz functional is additive and depends on the structure of the distribution of the local charge density and the self-consistent electric field at the neutral cells containing the

VFND. In the framework of the "cellular" approach the distribution is determined from the joint solution of the inner and outer problems for the potential and the conjugation condition on the boundary with the requirement of the minima of correlation energy of the cell charges. The spatial dependence of the local electric field and the electron density in the samples of tungsten, which contain VFND in the form of nano-cylinders with the size of the (r, x L)=(50 nm)x(400 nm) and the concentration of $n_d=10^{12}$ cm^{-3} were determined at a temperature of T=3200 K and are shown in figures 1 and 2 .

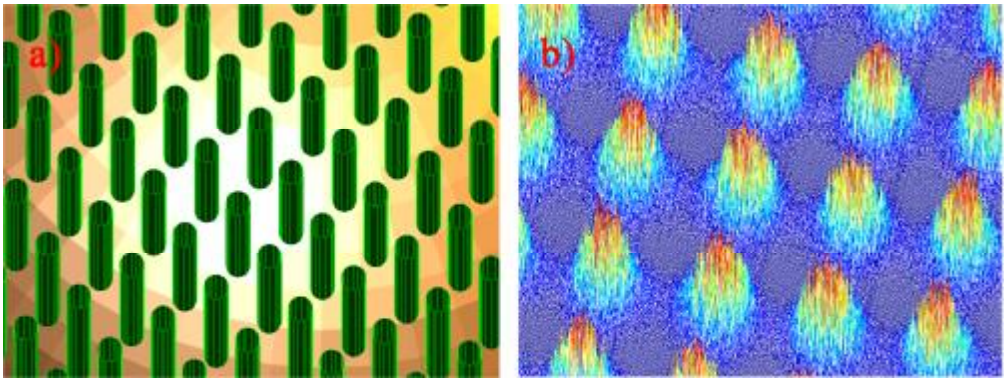

Fig.1. Local instantaneous electrostatic potential distribution in the tungsten sample with a regular structure cylindrical defects. Qualitative picture for VFND - (a); and for instantaneous potencial - b).

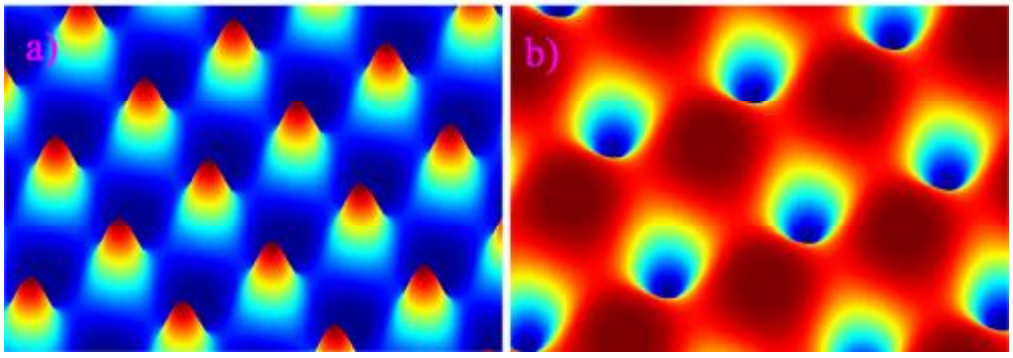

Fig. 2. 3D-graphics distributions of local self-consistent electrostatic potential - a) ; and the local density of carriers (electrons) - b).

There is good coordination of electrophysical characteristics of nanostructured samples of heat-resistant metals with VFND in the field of $T \in [1000, 3500]$ K.

1. Tappan B. C., Steiner S. A., Luther E. P. Nanoporous Metal Foams.- Angewandte Chemie.- Internat. Edition.- 2010, Vol. 49, Iss. 27, P. 4544–4565.
2. Marenkov V.I. The Fermi level of carriers and Coulomb inhomogeneities structure in metal and semiconductors with volume-filling nano-defects. – SEMST-5, Odesa , Ukraine, June 2 - 8, 2012. – Book of Absracts. – P. 62-63.

Chalcogenide Amorphous Materials with Phase Transitions

Maryan V.M.[1], Kyrylenko V.K.[1], Kozusenok A.V.[2], Pisak R.P.[1], Rubish V.M.[1], Horvat Yu.A.[1]

[1]Uzhgorod Scientific-Technological Center of the Institute for Information Recording, NASU, Uzhgorod Ukraine
[2]Uzhgorod National University, Uzhgorod, Ukraine

Recently, considerable interest is arousing work towards creating PCM (Phase Change Memory) devices working on the principle of reversible phase transition "crystalline ↔ amorphous" state. Local structural transformations in nanoscale layer of material are being carried out by an electrical pulse or pulse of light. Studies have shown that potentially suitable for the manufacture of these devices are chalcogenide vutreous semiconductors (ChVC). The majority of research in this direction is made for ternary ChVC.

The results of phase transition "amorphous phase → crystalline phase" studies in thin films of Sb-Se, Ge-Se, Sb-Te, Ge-Sb-Te systems are presented in this paper.

Amorphous films (thickness 0.2-0.4 μm) were obtained by vacuum evaporation of alloys of corresponding compositions from quasiclosed effusion cells onto unheated glass substrates. Research of film crystallization was carried out in the temperature range of 290-550 K by optical (λ = 0,85 and 0.90 μm) and electrical methods.

It was found that crystallization of amorphous films of mentioned systems is accompanied by a sharp decrease in optical transmission. The temperature and value of the temperature interval of phase transition from amorphous into crystalline state depends on the chemical composition of films and their heating rate. With increasing heating rate, these parameters are shifted into the region of higher temperatures. On the temperature dependences of transmission of some films in Sb-Se system before a sharp decrease in transmittance, peculiarities connected probably with structural relaxation in the "glassforming temperature – crystallization temperature" region are observed.

It was established that in films of Sb-Se and Ge-Sb-Te systems, phase transition "amorphous state → crystalline state" is accompanied by a sharp decrease in electrical resistance – by 1.5-2 orders for Sb_3Te and $Ge_2Sb_2Te_5$ films and more than 2 orders of value – for the film $Sb_{65}Se_{35}$. The temperature range of transition for the films of given compositions is 3-5 K. These materials can be used as recording media for systems of fast information recording.

On the Mutual Solubility in Ag/Ge Nanosized Binary Alloys

Minenkov A.A., Bogatyrenko S.I., Sukhov R.V., Kryshtal A.P.

Karazin Kharkov National University, Kharkov, Ukraine

In recent years, the problems of nanotechnology, micro- and nanoelectronics have motivated numerous investigations of phase transformations in binary alloys, including those the components of which form an eutectic-type phase diagram. This attention is primarily due to the fact that the reproducibility of the properties of these objects and materials on their basis are mainly determined by the interaction between the components.

In this work we present the results of experimental studies of solid-state solubility of Ge in nanosize Ag films of various thicknesses.

Nanosized Ag/Ge film system was chosen as the object of study. The components of this binary system form the phase diagram of simple eutectic type with a rather restricted solubility in a solid state and unlimited solubility in liquid one. The eutectic point lies at 24.5 at.% Ge and 651^0C. The terminal solubility of germanium in solid-state silver reaches 9.6 at.% at eutectic point while at room temperature it does not exceed 0.1 at.%. The solubility of silver in solid-state germanium is negligible [1].

The layered film systems were prepared by means of electron-beam evaporation of 99.99% pure silver and germanium from independent guns. Film systems were formed by sequential condensation of components. The process was performed in a high vacuum chamber at residual gas pressure less than 10^{-7} mbar. The mass thickness of each component in the films was measured by means of quartz crystal resonator. Experiments were carried out for sample series with 100, 50 and 25 nm thick silver layer. The concentration of Ge in the alloys was varied in 1-10 at.% range.

The method of electrical resistance measurement was used as an experimental basis for studying of the formation of homogeneous solid solution during heating – cooling cycles. The change of slope of the temperature dependence of electrical resistance during annealing of alloy film enables us to register the termination temperature of formation of solid solution in the system under study.

The measured equilibrium solubility values for samples with 100nm thick Ag film agrees with the available data for bulk samples [1]. The increase of equilibrium solubility of Ge with reduction of Ag film thickness has been measured. The observed effect is explained by the increased contribution of the surface energy into the total free energy of the system.

1. H. Okamoto. Phase Diagrams for Binary Alloys // ASM International, the United States of America. - 2000.

Ellipsometric studies of the porous silicon films structure

Odarych V., Rudenko O.
Kyiv National Taras Shevchenko University, Department of Physics, Glushkov Avenue 2, Block 1, Kyiv, Ukraine, 03022, e-mail: wladodarych@narod.ru

A measurement of ellipsometric parameters of light reflected from the porous silicon surface at wavelengths of the visible range are conducted. PC Samples obtained by electrochemical etching. PC Layers were formed on the surface of crystalline Si p-type by passing a few minutes an electric current with density of 10-40 mA/sm^2 through the electrolyte, which was a mixture of 48% aqueous HF and acetone in equal proportions. Acetone used as solvent. Samples aged in air for a long time up to a year. Phase difference Δ between p-and s-components of the electric vector of the light wave and the ratio of reflection coefficients tgψ in p-and s-planes of the sample at different angles of incidence φ and different wavelengths of the visible range was measured. Measurements are executed both before, and after surface treatment with ethanol. The treatment was performed by applying 96% ethanol to the surface of the samples. Measuring was executed after drying of surface out. The considerable sensitivity to surface treatment of ellipsometric parameter tgψ on one of wave lengths is observed. The parameter Δ shows much less sensitivity to ethanol. On figure the exposed effect is given as dependence of parameter tgψ on the angle of incidence of light on the explored sample, measured on a wave-length 579 nm. The experimental curve tgψ, obtained before treatment, it is possible approximately to describe in the model of single-layer film with refractive index 1.5 and thickness of 135 nm. The proper curve after treatment did not succeed to be described in the model of a single-layer film. After measurements of the week – 10 days is relaxation effect – tgψ curve returns to the state, which were before to the contact with an ethanol. The data can be explained if we assume that the film porous silicon have voids that are in contact with ethanol filled him and thus decorated that layer of porous silicon, that these cavities has.

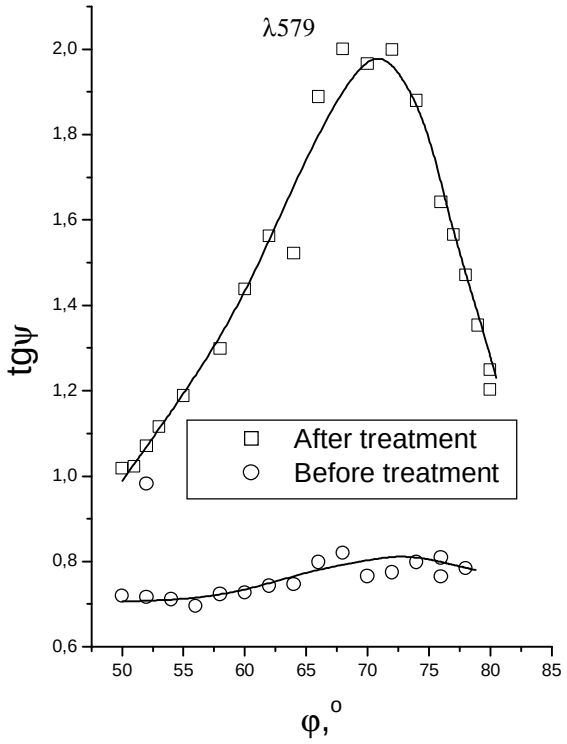

Reversible Alteration of Reverse Current in Mo/n-Si Structures Under Ultrasound Loading

Olikh O.Ya.[1], Olikh Ya.M.[2]

[1]*Taras Shevchenko National University of Kyiv, Kyiv, Ukraine*
[2]*Lashkaryov's Institute of Semiconductor Physics of NAS of Ukraine, Kyiv, Ukraine*

It is known, that controlled modification of the defect subsystem, so-called the "defect engineering" is one of methods of semiconductor structure and device performance improvement. Certainly, irradiation and thermal treating are the commonly used for achieving of these goals. The alternative ways of influencing on defects is the use of ultrasound (US) waves [1]. Thus potentialities of US treatment were shown to impact on the semiconductor material defect subsystem as well as to change integrally the properties of semiconductor barrier structures [2]. At the same time the effects appearing under US loading and vanishing after elastic oscillations turn off, are poorly investigated, although it should be of interest; in particular, such dynamic phenomena might be used to create a new class of acoustodriven devices.

The results of the experimental investigations of the reverse current-voltage characteristics of the Mo/*n*-n^+-Si Schottky structures are presented. We used the structures of n-Si:P epitaxial layer (0.2 μm thick) on n^+-Si:Sb. The thickness and the free carriers concentration of the substrate were 250 μm and 4.2×10^{22} m^{-3} respectively. A molybdenum Schottky contact, 2 mm in diameter, was fabricated on the epi-layer surface. The structures were irradiated by γ-rays ^{60}Co, the cumulative doses were equal to 0, 10, and 100 kGy. The investigation has been carried out in the temperature range 120–330 K and for the ultrasound loading condition (vibration frequency was 9.6 MHz, intensity of the longitudinal wave was up to 1.3 W/cm^2). The forward and reverse *I-V* characteristics were measured in the dc current range from 10^{-9} to 2×10^{-2} A.

It was established that the main charge transport mechanisms are the thermionic emission, the direct tunneling through deep center and the tunneling stimulated by phonons; the last one appeared after irradiation only. For the first time the acousto-stimulated reversible increase (up to 50%) of the reverse current has been revealed. The possibility of a creation of a γ-irradiation sensor based on this effect was considered. It was shown that effect's features can be explained by an ionization of the interface defects due to an interaction between ultrasound and dislocations or point radiation defects in the non-irradiated or irradiated structures respectively.

1. Olikh Ja.and Olikh O. Active ultrasound effects in the future usage in sensor electronics // Sensor Electronics and Microsystem Technolog. - 2004, **1,** 19-29.
2. Davletova A. and Karazhanov S. J. Phys. D: Appl. Phys. 2008, **41,** 165107.

Dynamic Wetting of Diamond Films and Crystals

Ostrovskaya L.Yu.[1], Boinovich L.B.[2], Pashinin A.S.[2], Ralchenko V.G.[3], Tkach V.N.[4]

[1] *Research Center for Studying Surface and Vacuum Properties, Moscow, Russia*
[2] *A.M.Frumkin Institute of Physical Chemistry and Electrochemistry RAS, Moscow, Russia*
[3] *A.M. Prokhorov General Physics Institute RAS, Moscow, Russia*
[4] *V.N. Bakul Institute of Superhard Materials, NAS of Ukraine, Kyiv, Ukraine*

For a number of applications in optics, electronics, chemical and biosensors, microfluidic systems it is important to fabricate diamond films with wettability variable in a wide range, from complete wetting to complete nonwetting [1]. Moreover the wetting properties should be highly durable. Here we report on the first investigation of the evolution of wetting behavior of diamond film using a sessile drop method [2].

Single crystal diamond plates and polycrystalline CVD diamond films with grain size of to 100 μm have been grown in microwave plasma. The samples have been characterized with Raman spectroscopy, AFM, SEM. Analysis of grain size and texture was performed by electron backscattered diffraction (Fig.1). It was shown, that dynamic contact angle is extremely sensitive to even minor variations in the diamond surface state: heterogeneity, roughness, chemistry. Depending on those features it took from a few minutes to several hours to approach the equilibrium wetting angle (Fig.2). Oxidized and ozonized diamonds reveal very fast dynamics of water contact angle equilibration in comparison with that for hydrogenated diamond.

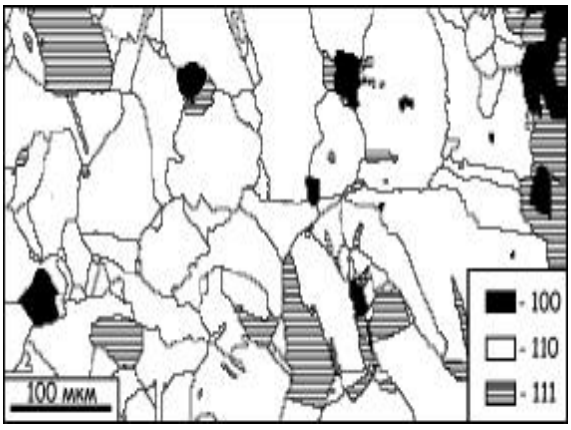

Fig.1 Map of grain orientations on the polished surface of polycrystalline CVD diamond film.

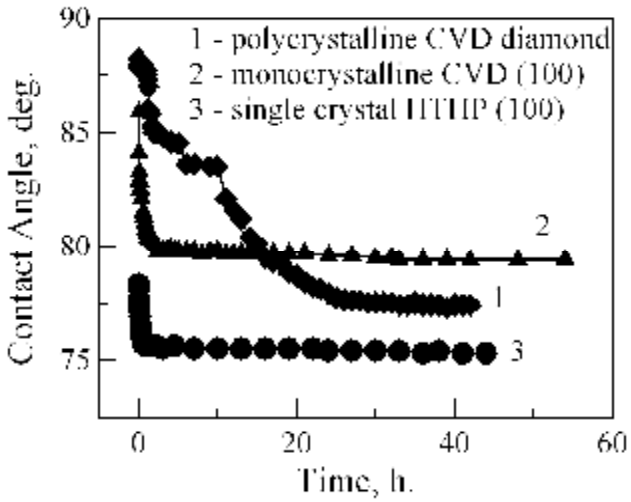

Fig.2: Evolution of water contact angle on mono- and polycrystalline diamonds in a saturated vapor atmosphere for prolonged time.

1. Ostrovskaya L., Ralchenko V. et al. *Protection of Metals and Physical Chemistry of Surfaces*, **2013**, Vol. *49*, No. 3, 1–8.
2. Boinovich L., Emelyanenko, A. *Adv. Colloid Interface Sci.* **2012**, *179*, 133–141.

Crystal Chemistry of Point Defects and Their Complexes in Cadmium, Stanum and Lead Telluride Thin Films

Prokopiv V.V., Prokopiv V.V (jr.), Strutynsky O.R.

Vasyl Stefanyk Precarpathian National University, Ivano-Frankivsk, Ukraine

Performance device structures are largely determined by the defect subsystem of the using material. The purpose of this study was to analyze the defective condition in Cadmium, Tin, Lead Telluride films grown from the vapor phase to choose the optimal conditions of the process.

The quasichemical reactions models of intrinsic point defects in the Cadmium, Tin, Lead Telluride films which were growing from the vapor phase by hot wall have been given. The analytical expressions for determining the concentration of free charge carriers and the prevailing point defects due to the equilibrium constant K quasichemistry reactions defect and partial vapor pressure of Tellurium P_{Te_2} have been received.

It is shown that Cadmium Telluride films at high temperatures, evaporation T_E receive only the n-type conductivity for the whole area of change of substrate temperature T_S. However, with increasing substrate temperature T_S, at a constant temperature evaporation T_E, the electron concentrations is decreased and if T_E <900 K conductivity inversion from n-to p-type have been occurred.

In tin telluride films grown at low substrate temperature T_S and high values of the partial vapor pressure of an additional source of tellurium P_{Te_2} predominant defects are doubly ionized vacancies Tin $\left[V_{Sn}^{2-}\right]$, and in the films grown at other values of these technological factors will prevail fourfold ionised vacancies Tin$\left[V_{Sn}^{4-}\right]$.

It was founded that PbTe films have complex disordering of Frenkel defect subsystem in cationic sublattice with the predominance of doubly charged vacancies and interstitial Lead, and increasing the temperature of deposition $420\,K \le T_D \le 620\,K$ and the partial vapor pressure of 1 Pa < P_{Te_2} <10^3 Pa leads to decrease in the concentration of electrons, inversion of conductivity from n-to p-type and the continued growth of concentration of holes.

During the growing of SnTe, PbTe films the changing of tellurium vapor partial pressure at constant temperature and substrate temperature TS TV evaporation at low pressure values tellurium (P_{Te_2} <10^{-3} Pa) does not affect the concentration of free charge carriers and defects due to the fact that at low additional source of tellurium pressures, the pressure of tellurium in the system is determined by the temperature of evaporation T_E.

The work supported by project of MES of Ukraine (N 0107U006768)

Crystallography of Formations on the Epitaxial Films Surface with NaCl I ZnS Srtructures

Saliy Ya.P., Freik I.N.

Vasyl Stefanyk Precarpatian National University, Ivano-Frankivsk, Ukraine

The thin-film CdTe and PbTe nanostructures on (0001) substrates of mica-muscovite are obtained in quasi-closed volume by hot wall technique. The analysis of atomic – force microscopy results are based on modeling surface of the film. Symmetry of nanoobject is lowered with increasing temperature evaporation and time of deposition. The PbTe nanoclusters at deposition temperature 350…630 K are formed by overlapping trigonal pyramides with facets of {100} are parallel to a plane (0001) of mica-muscovite. The activation energy of monomolecular mechanism growth is determined.

These orientational effects, namely, reducing the symmetry of formation as the evaporation temperature increases and time vapor deposition on a substrate associated with the increase in weight of the condensed material. The growth of crystallites limit the formation of perfect morphological forms.

Found that the experimental values of gains height Δh between adjacent points on the AFM image of the surface for a series of samples with temperature evaporator and with the change of the deposition time at fixed other parameters straighten in the coordinates lnN - Δh, where N - number of increments, and Δh - the boost.

The angular coefficient value of the first series (the variable temperature evaporator) and the second series (of alternating deposition time) are placed on the exponential dependence.

From the first, we have the characteristic energy dependence of growth patterns activation 0.9 eV, which is comparable to the binding energy of the molecules on the surface of CdTe condensate. Since the second - get the characteristic deposition time ~ 9 min, that determined the time interval of the formation of the given structures.

Density of islands increases and their size decreases with increasing substrate temperatures and deposition rates. In this step height distribution changes its shape by moving the most likely height towards higher elevations and the maximum height pyramids remains unchanged. Scatter pyramid height remains constant with temperature and deposition rate. In a typical hot wall method totally condensing mode most of the height of the pyramids increases in proportion to the time $t^{1/2}$. At high temperatures the process of filling layers

periodically repeated. The average height of the condensate grows linearly with time, the maximum height of the pyramids and the most likely is a periodic function of time. Set out in the geometric model of the formation of condensate can be described as axiomatic in all stages of its formation, depending on growing conditions and the physical parameters of the system.

On the basis of modeling the surface of epitaxial structures analyzed the results of studies of atomic force microscopy, surface topology of the films PbTe and CdTe, grown from the vapor phase by the hot wall on chips (0001) Mica - muscovite.

It is established that the growth process of the surface of objects PbTe at deposition temperatures 350 ... 630 K are carried out applying trigonal pyramids with facets of {100} planes are oriented (111) parallel to the (0001) plane of mica. The activation energy of the growth mechanism of monomolecular surface structures is 0.06 eV.

The features of the orientation of symmetry formation of condensation CdTe are established. It is shown that with increasing temperature and time of sample evaporation deposition of condensate symmetry of the crystallites decreases. The activation energy of the growth of surface structures and the characteristic time of their formation are determined.

The work supported by an integrated project of MES of Ukraine (N 0113U000185) and by projects of FRSF State Agency for Innovation and Informatization of Ukraine. (Contracts: R54, F53, 3)

Synergetics of Superlattice Formation in Films of Binary Compounds with non-Stoichiometric Composition

Saliy Ya.P.

Vasyl Stefanyk Precarpatian National University, Ivano-Frankivsk, Ukraine

A mechanism of formation of inhomogeneities in the alloy PbTe during either post-growth cooling or low-temperature precipitation is proposed, based on a diffusion instability in the interacting system which includes cations in lattice sites, interstitials and cation vacancies. The principal points of the mechanism are: vacancies follow local variations of alloy composition, being always in local equilibrium: their concentration depends exponentially on local composition. The uniform distribution of composition and the native dopants becomes unstable under a condition that is likely to be satisfied at low temperatures in samples enriched with lead interstitials. We show that the instability should result in the formation of a layered doping profile where the concentration of mercury interstitials varies by a factor of 2 while the variation of composition is of the order of 0,1. Possible consequences of this effect for the electrophysical properties of the alloy are discussed.

We have studied the diffusion instability of a homogeneous Te distribution in PbTe. A model for Te diffusion has been proposed which assumes two fluxes (fast interstitial and slow substitutional with conservation of lattice sites) interacting nonlinearly through cation vacancies. The vacancies are supplied, for instance, from the surface so that their local concentration is always adjusted to local composition. We have shown that for a exponential dependence of the vacancy concentration on composition the homogeneous distribution may become unstable and transform into some non-uniform structure. With the available data on the diffusion constants, we have found that the instability produces a layered structure with the concentration of Te interstitials varying from the initial value by up to 0,5**.** Because of the presence of acceptor cation vacancies, this may lead to the formation of internal p - n junctions.

The work supported by an integrated project of MES of Ukraine (N 0113U000185) and by projects of FRSF State Agency for Innovation and Informatization of Ukraine. (Contracts: R54, F53, 3)

Spin-Wave Spectra of Perpendicularly Magnetized FePd Thin Films and Circular Dot Arrays.

Salyuk O.Y.[1], Golub V.O.[1], Tartakovskaya E.V.[1], Kakazei G.N.[2], Östman E.[3], Hjörvarsson B.[3]

[1]*Institute of Magnetism, National Academy of Sciences of Ukraine, Kiev, Ukraine*
[2]*IFIMUP-IN (Institute for Nanoscience and Nanotechnology) and Departamento de F´ısica, Universidade do Porto, Porto, Portugal*
[3]*Uppsala University, Department of Physics and Astronomy, Sweden*

Magnetization dynamics of magnetic materials where the magnetic moments are not well-localized, namely FePt and FePd ferromagnetic shape memory alloys, has attracted a lot of attention as materials for ultrahigh density magnetic recording media [1]. Temperature dependence of spin wave spectra in perpendicularly magnetized ultra-thin FePd film as well as in arrays of thin circular FePd dots were studied using ferromagnetic resonance (FMR) technique. The dots and film thickness was fixed at 10 nm. The dot of the diameter 450 nm formed square arrays with the interdot distance of 62 nm. Quantitative description of the observed FMR spectra was given using the modified phenomenological model of dipole-exchange spin wave modes proposed in [2]. The obtained results clearly show the influence of interdot dipolar interaction in such close packed arrays on the shape of standing spin wave modes as well as on their energy. The specific structure of multiresonance FMR spectra both in the film and dot arrays suppose an arising of additional spin wave modes due to the magnetic polarization of Pd atoms in FePd alloy.

1. David Sellmyer and Ralph Skomski, Advanced Magnetic Nanostructures, Springer Science + Business Media Inc: USA. ,2006. — 497 p.
2. G. N. Kakazei, P. E. Wigen, K. Yu. Guslienko, [*et al*] Appl. Phys. Lett., — 2004. — Vol. 85, N3. — P.443-446.

Determination Methods of Thermal Conductivity of Thin Films

Tkachuk A.I.

Vasyl Stefanyk Precarpatian National University, Ivano-Frankivsk, Ukraine

Measurement of thermal conductivity of thin films is important for design elements of microelectronic circuits and film radiation receivers, etc., and for investigating the physical characteristics of the film. We describe the features of determining the thermal conductivity of thin films.

First of all, consider the absolute method of measuring thermal conductivity [1]. On the measured sample, which is a non-conductive film layer is applied auxiliary S-shaped metal or semiconductor. At admission is current through the strip it heating, which depends on the fed electric power and heat flux, which extends from the stripes to the insulated electrodes.

Measurements conducted in the isothermal chamber of evacuated cryostat. Where the we deposition of metallic and semiconductor films in vacuum 10^{-7} Pa.

Three omega [1] is a second method for measuring thermoelectric parameters of thin-film condensates. It is obtained by passing an alternating current with a frequency w through the metal line heater that was directly deposited on insulating sample. This current heats the sample with a frequency of $2w$ by Joule's heat, producing variations in temperature and at a frequency of $2w$ with an amplitude ΔT_{2w} and phase difference. The resistance of pure metals increases linearly with temperature, fluctuations in temperature creates oscillations in the resistance of metal lines with frequency $2w$. Oscillation resistance at $2w$, with a current source with frequency w, creating a small oscillating voltage signal on line metals with a frequency $3w$ [1].

The third laser flash method is based on measuring time propagation of thermal waves, wich created by a laser pulse to the opposite side of the film. Using a theory based on the one-dimensional model of heat distribution in a semibounded state, with relatively small heating, we can determine the thermal conductivity of the sample [1].

1. Галущак М.О., Ральченко В.Г., Фреїк Д.М., Ткачук А.І. Аналіз методів визначення теплопровідності тонких плівок // Методи та прилади контролю якості – 2012. – №1(28). – С. 162-167.

The work supported by projects of FRSF State Agency for Innovation and Informatization of Ukraine. (Contracts: R54, F53, 3); of NAS of Ukraine (N 0110U006281)

Multilayer Plasmonic Absorbing Nanocomposites

Zamkovets A.D., Ponyavina A.N.

B.I .Stepanov Institute of Physics of the NAS of Belarus, Minsk, Belarus

Last decades the plasmonic nanocomposites are studied more and more actively. They are already widely adopted in optics and electronics, at developing high sensitive biological and biomedicine sensors. As a rule, metal nanoparticles are distributed in a matrix volume randomly. At the same time, when forming the composites of partially-ordered structures, the new additional opportunities appear for controlling their optical properties.

In this paper we present the results of our investigations of spectral-selective properties of multilayer plasmonic nanocomposites Ag - Na_3AlF_6, which were fabricated with the use of a thermal vacuum evaporation. We studied the transmission and reflectance spectra for samples with different numbers of layers, values of an overlap factor of the silver nanoparticles monolayer, thicknesses of separating Na_3AlF_6 films, and substrate types.

Application of thin-film substrates from a poly(ethylene terephthalate), polyethylene, polyimide allowed us raising the total layer number in a composite with the use of elementary systems of a fixed layer number formed at a thermal evaporation process. In this case a polymer film due to its physical properties serves as a glued joint which creates an optical contact between a polymer surface and a thermal evaporated plasmonic coating. Formation of a multilayer hybrid nanocomposite was made at the definite controlled thermo-baric conditions from elementary nanostructures deposited on thin-film polymer substrates.

As a result, it was shown that on the base of layer-periodic photonic-plasmonic structures Ag-Na_3AlF_6 one can produce optical coatings characterized by a high absorption of electromagnetic waves and a low reflectance coefficient (less than 1%) in the visible region. Depending on a coating construction a spectral width of the high-absorptance range is about 100–300 nm and a residual transmission is less than 0,05%. Besides it was shown that on the base of layered plasmonic nanostructures Ag-Na_3AlF_6 one can produce the near infrared cut-off filters absorbing the visible radiation. Filter transmission in the range of transparency is of 60 – 80% depending on a width of a suppression zone. For optimization of filter and coating spectral properties the plasmonic layer-gradient structures were used.

Proposed plasmonic filters and coatings are considered as promising spectral elements in nanophotonics and optoelectronics.

Thermo-Optical Phenomena in Conducting Polymers Doped by $K_3[Fe(CN)_6]$ Complex

Zayarnyuk T.[1], Konopelnyk O.[2], Aksimentyeva O.[2], Dyakonov V.P.[1], Piechota S.[1], Horbenko Yu.[2]

[1]*Institute of Physics of Polish Academy of Science, Warsaw, Poland*
[2]*Ivan Franko National University of Lviv, Ukraine*

Great attentions now attract the conjugated polymers with intrinsic electron conductivity such as polyaniline and polythiophene derivatives because of their environmental stability, electro-optical properties and high conductivity. A subject of specific interest are optical phenomena in conjugated polymer layers, particularly, thermochromic effects. Thermo-induced changes of color are the most commonly used for various applications (sensors, smart windows, etc.) because conjugated polymers may exhibit the properties similar to liquid crystalline. Generally the color change is based on alteration of the electron states of molecules, especially the π- or d-electron state induced by temperature.

The temperature dependence of optical transmittance spectra of the conducting polymer films – polyaniline (PANI) and poly-3,4- ethylenedioxy-thiophene (PEDOT) obtained by electrochemical polymerization and doped with potassium ferricyanide has been studied in the interval of T = 80 – 380 K. It has shown that doping of polymers by $K_3[Fe(CN)_6]$ leads to increasing in optical transmittance of PANI films in the range of λ = 380 – 500 nm and of PEDOT films in the range of 670 – 780 nm. Temperature rising causes a decrease in optical transmittance in all temperature range, however characteristics of thermo-optical changes depends of polymer nature and time of doping. From the study of absorption spectra it found that under temperature change the variations in the color of polymer films are observed. In the optical spectra it's developed in the "blue shift" of absorption maximums and in the changing of their intensity. It is suggested that in result of polymer's doping by ferricyanide complex the thermo-induced variation in optical spectra of polymers may be connected both with conformation rotation of segments in polymer chain and changes in electronic properties of conjugated polymer system [1, 2]. Doping of PEDOT and PANI by ferricyanide complex causes a more strong dependence of the optical transition on temperature in comparison with non-doped polymers.

Acknowledgments: This work was partially supported by the Ministry of Science and Higher Education (Poland), Grant N 507 492438.

1. Konopelnik O.I., Aksimentyeva O.I., Martynyuk G.V. Effect of temperature on the optical properties of conducting polyaminoarenes and their composites with elastic polymer matrix // Molec.Cryst.Liq.Cryst. – 2005. – Vol. **427**. – P. 35 - 46.
2. Konopelnyk O.I., Aksimentyeva O.I. Thermochromic effect in conducting polyaminoarenes // Photoelectronics. – 2011. – Vol. **20**. – P. 18 - 22.

СЕКЦІЯ 3 (стендові доповіді)
ФІЗИКО-ХІМІЧНІ ВЛАСТИВОСТІ ТОНКИХ ПЛІВОК
23 травня 2013 р.

SESSION 3 (poster)
PHYSICAL-CHEMICAL PROPERTIES OF THE THIN FILMS
May, 23, 2013

Electronic Density of States of Hydrogenated Graphene

Artemenko O.S., Kardashev D.L.

Odessa National Maritime Academy, Odessa, Ukraine

Recently, much attention has been given to experimental and theoretical research of hydrogenated graphene – a hexagonal monolayer of carbon atoms. There were predicted and synthesized: graphane – saturated by hydrogen graphene monolayer with hydrogen atoms adsorbed on a different sub-lattices and situated on a different sides from the monolayer; graphone – graphene monolayer with hydrogen atoms adsorbed on one of the sub-lattices from one single side, and, also, diaman – a diamond-like double-layer graphene with hydrogen atoms adsorbed on its external surfaces. The electrical properties of these materials are rather different of electrical properties of graphene, which is a zero-gap, nonmagnetic semiconductor. Graphane, for instance, is a wide-band insulator with a $E_g \approx 5$ eV energy gap, and graphone is a magnetic semiconductor. Such unusual properties make these materialse very interesting for different applications in carbon nanoelectronics.

A short time ago there was predicted another modification of graphene - single-side-hydrogenated graphene(SSHG). In SSHG, as in graphone, the hydrogen atoms situated only from one side of graphene monolayer, but, instead of graphone, where they adsorbed on every other atom, in SSHG they adsorbed on each atom of carbon.

For calculation of local density of states of hydrogenated graphene we used Green's function method. The matrix elements of tight-binding Hamiltonian were chosen according to Sletter-Coster notation and included only most significant interatomic interactions. Graphene was modeled by two dimensional hexagonal Bethe lattice. Green's function of hydrogenated graphene was found from Dyson's equation. The local density of states of electrons in conductivity and valence band was determined by imaginary part of Green's function.

It is shown that hydrogenization of graphene leads to appearance of a gap in density of states. We obtained $E_g \approx 3.5$eV width of this gap for single-sided hydrogenization of grapheme.

On the Analytical Parameterization of Photoinduced Darkening in Amorphous Chalcogenide Films

Balitska V.O.[1] and Shpotyuk O.I.[2,3]

[1]Lviv State University of Vital Activity Safety, Lviv, Ukraine
[2] Institute of Materials of Scientific Research Company "Carat", Lviv, Ukraine
[3]Institute of Physics of Jan Dlugosz University, Czestochowa, Poland

Despite recently achieved progress in phenomenological description, some peculiarities of photoinduced effects in thin chalcogenide films need a deeper understanding. This concerns, in part, kinetics behavior observed in the change of optical properties of amorphous films caused by activated light of different penetration ability. In this research, we deal with both thickness and compositional trends in the photodarkening kinetics by testing films of different thicknesses, thermal pre-history and chemical compositions ($As_{40}Se_{60}$, $As_{50}Se_{50}$ and $As_{60}Se_{40}$) in terms of photon-assisted site switching (PASS) facilitating percolative growth of atomic clusters at ground state.

Within this formalism, the final photodarkened sites (independently on their population and origin), having higher energy, are supposed to be formed from original sites, giving a dynamic interbalance owing to straightforward (production) and backward (relaxation) activation reactions. These photoinduced production-relaxation processes terminated by corresponding initial and boundary conditions can be conveniently presented via a set of first- or second-order differential rate equations.

In the framework of this scheme, it was established that photodarkening itself in the studied arsenoselenide films is non-dispersive in nature, its kinetics description being first-order and governed by penetration depth of pumping light (the inverse value to the absorption coefficient). In the case of films thicker than a penetration depth, the photodarkening kinetics attained a character stretched exponential behavior, while in thinner films (with thickness less than a penetration depth) the stretched exponential relaxation tented to be single exponential. With illumination by over-bandgap photons effectively absorbed by amorphous chalcogenide film, more photostructural processes proceed simultaneously giving resulting stretched exponential kinetics, while low-absorbed light causes nearly ideal single exponential darkening kinetics.

Emf arising in Contact oxide Aluminum Films with Electrolyte

Burlak G.M., Vilinskaya L.N.

The Odessa State Academy of Building and Architecture, Odessa, Ukraine

Previously, we have shown the formation of space charge and EMF in the structures of Al-Al_2O_3-SnO_2 in an atmosphere of water vapor [1]. Such structures were created by electrochemical oxiding of aluminum foil in water solution of sorrel acid with the following deposit SnO_2 layer an oxide film by pyrolysis method. The oxide aluminum surface is catalitically active and so dissociation of adsorbent moleculs takes place. EMF is the result of the dissociation of water molecules adsorbed on the surface of microporous oxide and space separation of the charge on the film thickness due to the difference in the values of the diffusion coefficient of the dissociation products.

Occurrence of EMF should expect and then when the dissociation of the film surface is not obtained and charged ions coming from the external environment, such as the electrolyte. To confirm that the EMF in the films of aluminum oxide occurs in contact with the electrolyte, we measured the power at test films dipped in a 3% solution of ammonium sulphate. The second contact used graphite rod. The resulting system thus Al-Al_2O_3-electrolyte watching EMF whose magnitude was 0,1-0,6 V.

The appearance of EMF and steady current in the system Al-Al_2O_3-electrolyte occurs in following way. Reports from the positively charged ions of the electrolyte lead to charging of the surface adjacent to the electrolyte film. Negatively charged ions provide a flow of electrons to the film, which then diffuses to the aluminum electrode, causing it to acquire a negative potential. Neutral radicals formed in this case, leave the surface of the film, making it possible for her receipt of other ions, which provides steady-state current flow by closing the circuit through the load resistance. In addition, the recombination of ions coming from the electrolyte to the surface of the oxide film leads to the luminescence intensity of which depends on the concentration of certain substances in the electrolyte.

1. Burlak G.M., Vilinskaya L.N. Sensors on the basis of aluminum metaloxide films. Photoelectronics № 18, 2009, p.92-94.

Dispersion of Gold Nanoparticles in Silica-Methacrylate Composites

Burunkova Julia[1], Denisiuk Igor[1], Vorzobova Nadezda[1], Kokenyesi Sandor[2], Charnovich Stepan[2], Daroczi Lajos[2]

[1] National Research University of Information Technologies, Mechanics and Optics, St.Petersburg, Russia,
[2]University of Debrecen, Debecen, Hungary

Polymer composite nanomaterials containing metal nanoparticles (NPs) are widely investigated due to the basic scientific and applied interest. Gold is one of the most preferred metals which is used in glass and polymer nanocomposites (NC) due to its exceptional stability, biocompatibility and, not at last, because of the plasmon resonance effects, which are easily observed in 500 – 700 nm spectral range in dependence of the size and shape of the gold NPs (GNP). Plasmon fields can essentially influence the interaction of photons with the given composite materials, so it is a challenge to create new materials with optically guided parameters. Various techniques permit the fabrication of NC either by in situ synthesis of GNPs, or by introduction of preformed ones with a given geometry. Sometimes the last is a big problem because of the low compatibility of GNP and polymer matrix.

The aim of our work was to develop applicable direct physical method to produce necessary gold-polymer nanocomposite with plasmonic effects. The failure of direct introduction of GNPs to methacrylate was overcame by introduction of GNPs (up to 0,5 wt%) in the form of solution in toluene to a monomer mixture with SiO_2 NPs (up to 26 wt %). Optical properties, TEM characterization of obtained NCs were investigated. Effect of the GNPs on the monomer photopolymerization was investigated by analyzing the Raman spectra changes. The first criteria of good nanocomposite formation was the presence of plasmon resonance peak in the optical transmission spectrum. Plasmon resonance was detected in the vicinity of 520 nm for composites with SiO_2 NPs in a monomer solution and in the polymerized layer as well. It was found that in nanocomposite the AuNPs are uniformely distributed in the regions, which are modified with SiO_2 NPs. The investigated NCs was used as light-sensitive media for holographic recording of diffraction gratings with increased diffraction efficiency and are promising for plasmonic structures as well.

This work was partially supported by the TAMOP 4.2.2.A-11/1/KONV-2012-0036 project, which is co-financed by the European Union and European Social Fund.

Chalcogenide Glass Layer with Gold Nanoparticles: Fabrication and Optical Properties

Voynarovych I[1]., Shyplyak M[1]., Makauz I[1]., Kokenyesi S[2]., Charnovich S.[2]

[1]*Uzhgorod National University, Uzhgorod , Ukraine*
[2]*University of Debrecen, Debrecen, Hungary*

Incorporation of nanoparticles into a matrix can essentially change the properties of both the particle and the host, as well as the characteristics of different processes in the composite. Glass/metal nanocomposites are known among a wide number of composites. In particular, gold nanoparticles may be incorporated into a matrix due to the inertness and plasmon resonance effects, which are easily observable in the visible spectral range. Dielectric/metal nanocomposites have been exploited in improved photocatalysts, photochromic and electrochromic film, non-linear optical materials and devices

Amorphous chalcogenide semiconductors are widely investigated and applied in optics and photonics due to the number of unique characteristic and peculiar effects: wide range of optical transparency, especially in the infrared region, high optical nonlinearity, photoinduced change of optical parameters. This transformation occurs first of all due to excitation of electron-hole pairs which stimulate further bound switching. That is why plasmon field of gold nanoparticle can stimulate this process.

One possible method of preparation of metal-chalcogenide nanocomposites consists in the fabrication of gold nanoparticles (islands) array on the surface of glass substrate and subsequent covering it by the same glass layer or by other. The simplest way is the thermal annealing, rapture of nanometer thin gold layer and subsequent Ostwald ripening of nanoparticles on the surface. But the influence of localized plasmon fields extends only to the comparatively short distances, i.e. thin cover films can be influenced.

In our work we compare such samples of chalcogenide/gold particle layer composite with samples which contain gold nanoparticles in the volume and focuses our investigations on the fabrication and properties of the last ones. For investigation we used $Ge_{20}As_{20}S_{60}$ chalcogenide glass because of the comparatively high softening temperature, which allows annealing of the layers at temperatures up to $270^{o}C$, where the diffusion of Au atoms appeared sufficient for clustering in a glass matrix of the second type samples.

Structural and Magnetic Properties, and Electronic Structures of Fe-Mn-Ga Alloys

Dubowik J.[1], Kudryavtsev Y. V.[2], Uvarov N. V.[2], Iermolenko V. N.[2], Rhee J. Y.[3], Yoo Y. J.[5] and Lee Y. P.[5]

[1]*Institute of Molecular Physics, Polish Academy of sciences, Poznań, Poland*
[2]*Institute of Metal Physics NAS of Ukraine, Kiev, Ukraine*
[3]*Sunkyunkwan University, Suwon, Korea*
[4]*q-psi and Department of Physics, Hanyang University, Seoul, 133-791 Korea*

We report the structural and the magnetic investigations on bulk Fe-Mn-Ga alloy and the films with a stoichiometry of 1:1:1. Both the alloy and the films reveal an unstable crystallographic structure. The first-principle calculations of electronic structure and the magnetic properties of FeMnGa alloy for hexagonal and for cubic C1*b* structures suggest that the hexagonal structure with ferromagnetic (FM) order is energetically more preferable. While experimentally the bulk alloy appears to possess a mixed FM hexagonal structure with the presence of a $(Mn/Fe)_9Ga_5$ ζ-phase, the films have FM cubic phases in various types of structural ordering that depend on the deposition and the annealing conditions (see Fig. 1).

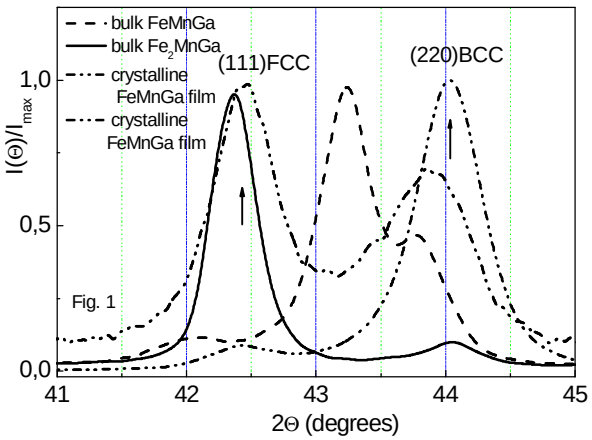

FeMnGa thin films with the high exchange anisotropy might be useful as pinning layer for spintronic applications. Exchange bias and enhanced coercivity occur simultaneously in B2-type ordered FeMnGa films, revealing an exchange coupling between coexisting AFM and FM phases.

The FeMnGa films exhibit an inhomogeneous magnetic structure that is the most remarkable for the B2-type ordered crystalline FeMnGa films deposited at 720 K. They show a complicated behavior with the presence of strong antiferromagnetic (AFM) and FM interactions, resulting in a high exchange bias (see Fig.2).

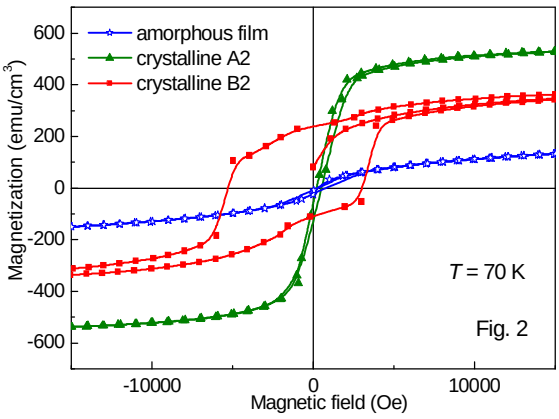

Own point Defects in the Layers of CdTe:Ca

German I.I.[1], Stets E.V.[2], Chernyh E.I.[1]

1 Yuri Fedkovych Chernivtsi National University, Chernivtsi, Ukraine
2 National Technical University KPI, Kyiv, Ukraine

CdTe is one of the most promising materials solar energy. This study is aimed at finding physical and technological principles to improve the parameters of the material and diode structures based on it. Important for this compound is the possibility of obtaining bipolar conduction. However, solar cells with pn-homoperehodom not use both crystalline and thin film in performance. Basically, this is due to lack of technologies obtained of CdTe thin layers with high hole conductivity.

Analysis of the literature shows that the typical impurities have low solubility and diffusion coefficients even at high temperatures, as well as very large ionization energy ($E_a \geq 40$ meV). Doping CdTe by isovalence impurities is one of the important ways to solve this problem. Impurities of this type is stimulated the generation of intrinsic point defects (IPD) acceptor type.

In IPD, in particular, the single-charged cadmium vacancies and atoms in VCd between atoms of crystal lattice. The ionization energy of their levels of ~ 15 meV.

This paper studies the possibility of obtaining thin layers of p-CdTe substrates due to annealing of cadmium telluride in the solution of its salts.

In this case the composition of the dominant IPD must be determined by the ratio of effective charges CdTe Q^*_{CdTe} and binary compound which comprising isovalent impurity Ca, ie Q^*_{CaTe}. As your know, $Q^*_{CdTe} > Q^*_{CaTe}$. Respectively of thermodynamic theory the isovalent doping must to take place additional generation V_{Cd} and Te_i. They are form the acceptor centers. Correctly to assume that Ca, included in cationic sublattice and partially "healed" vacancies cadmium.

This causes the dominance shallow acceptor centers a formed by atoms tellurium in layers CdTe: Ca in the internodes. These layers which includes by Ca should be pronounced hole conductivity .

This is confirmed by studies of thermoelectric properties. The value of thermoelectric coefficient is positive, corresponding to p-type surface layers annealed samples regardless of the type of conductivity. Note that doping does not lead to the formation of new chemical compounds. Appropriate optical reflectance spectra of basic and annealed substrates have a clear peak with a maximum at 1.5 eV. Its provisions agrees with a band gap of CdTe at 300K.

Electron Processes in Forming of Thread-Like Nanocrystals on Semiconductors

Grankin M.V., Bazhin A.I.

Azov State Technical University, Ukraine
Donetsk National University, Ukraine

Thread-like nanocrystals (TNC) made of semiconductor materials are promising in applications of opto- and microelectronics, designing emissive cathodes, chemical sensors etc. Fiend-effect transistors and nano-lasers were produced on the basis of TNC. However, only few papers are dedicated to investigation of processes of the TNC formation. Therefore mechanisms of the TNC growth are not fully realized.

Formation of the TNC can occur either by vapor-liquid-crystal mechanism or by diffusion mechanism i.e. as a result of surface diffusion and embedding of component atoms at the boundary of blob catalyst and TNC. As a rule, in order to stimulate the TNC growth, the surface of semiconductor is activated by metallic blobs of growth catalysts (e.g. Au). Diffusion models of the TNC growth assume equilibrium diffusion of adatoms on the substrate and side surface. Current models do not take into account processes of creation of hot atoms in the adsorption event and their movement on the surface to track length L until relaxation and also processes of the hot atoms' energy accommodation (via different channels).

The goal of this research is to design a mechanism of the TNC growth which accounts the processes of non-equilibrium diffusion of the hot adatoms created in adsorption events on the surface of substrate and TNCs, as well as accommodation of reaction heat via electron channel on the catalytic nanoblobs. Electron accommodation becomes apparent experimentally and it lies in the foundation of such phenomena as heterogeneous chemoluminescence (HCL) and chemoemission of electrons and ions from surface.

A model that describes growth of TNC was developed. The model takes into account spatial heterogeneity of the surface related to the fact that a process of atoms adoption runs on the substrate and relaxation of hot adatoms takes place on the catalyst blobs because of movement of the hot atom from formation point to the accommodation center of adsorption heat. We designed an algorithm and subsequently a computer program based on Monte-Carlo method for numerical simulation of the TNC growth. It was found that the TNC growth rate increases proportionally to $1/d$ with decrease of diameter d of the catalyst blob and increase of track length of the hot adatom on substrate. On the contrary, increase of phonon relaxation rate relative to electron relaxation rate leads to decrease of the TNC growth rate.

Photoluminescence of Thin Films of Amorphous Hydrogenized Silicon with Silicon Nanocrystals

Gusev O.B., Kukin A.B., Terukov E.I., Belolipetskiy A.B., Dmitriev A.P.

Ioffe Physical-Technical Institute RAS, S.-Petersburg, Russia

Amorphous silicon is widely spread as a solar cell material. The quantum efficiency of the solar cells formed on the basic of the amorphous silicon films is lower than that of crystal silicon cells. In spite of this fact the industrial production of amorphous silicon cells is going to grow, primarily because of low price. The defect density of hydrogenated amorphous silicon (a-Si:H) increases with light exposure, causing an increase in the recombination current and reducing the efficiency of the conversion of sunlight into electricity (Staebler–Wronski effect). Silicon nanocrystals are embedded in a-Si:H films to suppress the Staebler–Wronski effect.

In the present work the experimental results of the study of photoluminescence (PL) of the a-Si:H with silicon nanocrystals are reported. The thin films of the a-Si:H 200 nm thick with silicon nanocrystals of diameters $2 \div 3$ nm have been obtained by the decomposition of silane (SiH_4), diluted with hydrogen (H_2) in the glow discharge plasma. The temperature of the substrates has been maintained at 210 ^{0}C in the processes of the thin films deposition.

The photoluminescence spectra obtained are presented in Fig. The sharp PL pick at the energy 1.17 eV, which is equal the energy gap in the bulk crystal silicon has been observed.

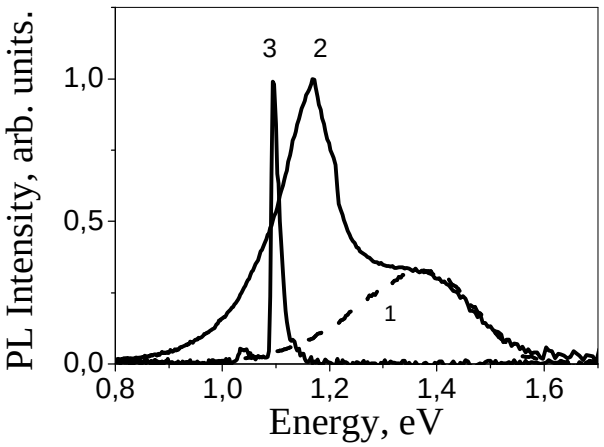

The PL spectra of a-Si:H *films without nanocrystals (1), with nanocrystals (2) and PL spectra of the bulk crystal silicon (3), T=77 K.*

Theoretical modeling has shown that PL pick observed is the result of radiative recombination that takes place, when one electron and two holes are localized in a Si nanocrystal. In this case radiative recombination of the electron-hole pairs is assisted by outcoming of one hole.

Differential thermal analysis during heating compounds Ge-S-Bi and Ge-S-In

Horvat H.T.[1], Hasynets M.S[2], Makauz I.I.[1], Loya V.Yu.[3], Rizak V.M.[1]

[1]*Uzhhorodskyy National University, Uzhgorod, Ukraine*
[2]*Uzhgorod Scientific-Technological Center of optical media of IIR Ukraine, Uzhgorod, Ukraine*
[3]*Institute of Electron Physics, National Academy of Sciences of Ukraine, Ukraine*

Despite of the rapid development of technology of plastic industries glassy materials are widely investigated and used in production till this time because of their low cost and good optical and mechanical properties. Development of new technologies for special glasses for different applications received a great impetus through the creation of new types of glassy matrices or modification of long known glasses new components. Glassy chalcogenide materials are interesting because they control the physical properties and phase transitions due to changes in ordering the local structure of atoms.

In this thesis was studied by differential thermal analysis the phenomenon of phase and structural transformations that occur during heating synthesized glasses systems Ge-S-Bi (Ge-S-In). Bulk glass compositions were synthesized of component elements of 5N purity common method of hardening melt. The amorphous nature of the samples confirmed by X-ray analysis using X-ray diffractometer DRON-3 with CuKα-radiation.

For comparison and identification of thermal phenomen that occur under thermal heating of the samples $(Ge_{40}S_{60})_{100-x}Bi_x$ $(Ge_{40}S_{60})_{100-x}In_x$ also performed differential thermal analysis of binary compounds of Ge-S. Found that with increasing number of additives (In and Bi) to some extent contributes to the formation of crystalline nanoclusters, ie the formation of new nanoscale structural phases are clearly evident on the thermograms. The process of phase transition enthalpy of formation were identified. That is to stimulate crystallization processes in this alloy and the formation of new compounds.

Electronic Density of States in Epitaxial Graphene

Kardashev D.L.[1] , Kardashev K.D.[2]

[1] *Odessa National Maritime Academy, Odessa, Ukraine;*
[2] *A.S. Popov Odessa National Academy of Telecommunications, Odessa, Ukraine*

At present time, the uniqueness of properties of graphene is well known and has its basic theoretical explanations. Graphene formed on a substrate and tied with it, called epitaxial. As a substrates it is often used crystals 6H-SiC{0001} and 4H-SiC{0001}. This is because graphene film can be created while thermal desorption of atoms of silicon from the surfaces of these crystals. The result of such process depends on which face (Si- or C-face) of silicon carbide crystal the removal of silicon atoms took place. If silicon carbide used as Si-face, the graphene monolayer separated from a substrate with a layer, covalently bonded to the substrate. It is often obtained graphene monolayer, weakly bonded to C-face of the substrate. One of the modifications of epitaxial graphene is, so called, quasi-free standing graphene. For its creation it's often used an intercalation of foreign atoms (atomic hydrogen, for instance) under external carbon monolayer. These foreign atoms break covalent bounds between first and second layers.

Thus, problems of interaction of epitaxial graphene with a substrate are extremely important as they determine characteristics of graphene sheet. One of such important characteristics is presence (or absence) of energy gap in electron specter of single-sheet graphene.

We used next trick: first, we considered a set of isolated carbon adatoms under SiC substrate, and then we built a graphene lattice from these adatoms.
Obtained analytical expressions for local densities of states of electrons in epitaxial graphene synthesized on a SiC substrate. It is shown that in a case of tight-binding (interaction of carbon atoms of graphene with substrate is in many times greater than interatomic bound) local density of states of graphene is approximate to density of states of isolated adatom of carbon on a semiconductive substrate.

A Nanoporous Zeolite Cathode Gas Discharge Electronic Devices For Plasma Light Source Applications

Koseoglu K.[1], Ozturk S.[1], Karaduman I.[1], Acar S.[1], Salamov B. G.[1,2]

[1]*Physics Department, Faculty of Sciences, Gazi University, Ankara, Turkey,*
[2]*National Academy of Science, Institute of Physics, AZ-1143 Baku Baku, Azerbaijan*

Abstract: The stabilization of glow discharges in a dc air plasma is studied functions of pressure (4-760 Torr), discharge gap (50-250 μm), and diameter *D* (5-25 mm) of the cathode areas in the gas discharge electronic devices (GDED) with nanoporous zeolite cathode (NZC) for the first time. Comparision of current from GDED is used for the determination of the stabilization under low- and atmospheric pressure (AP) glow microdischarges conditions. It is found that the gas in zeolite pores ionizes and, accordingly, the number of electrons in the pores grows. It is shown that breakdown voltage is reduced significantly at AP when the *D* of NZC is increased. It is established that the effect of various *D* on the clinoptilolite cathode area to the discharge are provided stable, homogeneous, nonthermal and controllable operation up to the AP as well. The cell optimization is realized by constructing the Paschen curves for each cell parameters. It is of importance to have knowledge in peculiarities of operation of GDED. It can be supposed that cheap natural zeolite will be effective in low-power GDED [1,2].

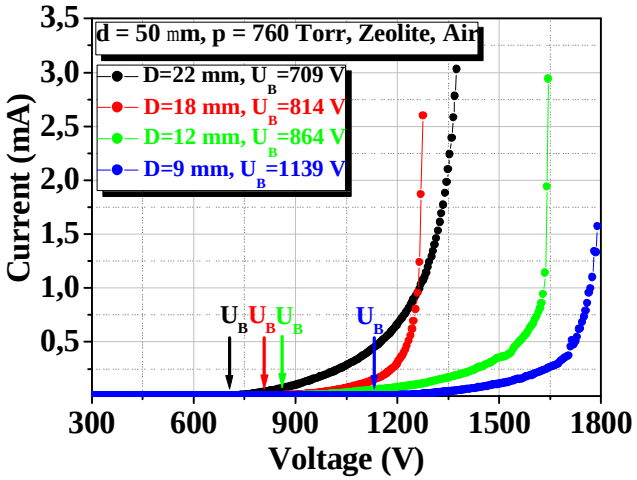

Fig.1. Current-voltage characteristics of a gas discharge cell with different *D* of the zeolite electrode area.

1. V.I. Orbukh, N.N. Lebedeva, S. Ozturk, Ş. Uğur and B.G. Salamov. Gas discharge electronic device based on the porous zeolite // *Optoelectron. Adv. Mat.*, **6**(11, 12), pp. 947-952 (2012).
2. R. Rosen, W. Simendinger, C. Debbault, H. Shimoda, L. Fleming, B. Stoner and O. Zhou. Application of carbon nanotubes as electrodes in gas discharge tubes // *Appl. Phys. Lett.*, **76**(13), pp. 1668 (2000).

Spectra of EPR and Photoluminescence Microcrystals of ZnS:Mn

Morozov A.S., Bulaniy M.F., Kovalenko A.V., Omelchuk A.R., Skuratovskaya O.V.

Oles Gonchar National University of Dnepropetrovsk, Dnepropetrovsk, Ukraine

Grinding of microcrystals solids (dispergation) by the modern planetary mills - is effective mean of receipt of nanomaterials. Even without the use of cryomechanical grinding at room temperature the dispergation significantly influence on the physical properties of the microcrystals. Processes that occur during the mechanical grinding can not be reduced to the normal decrease in the size of the microcrystals. Dispergation is accompanied by additional concurrent processes: defects in the volume of microcrystals, changes in internal stress and deformation of the crystal structure, local selection of heat, chemical reactions, acceleration of thermal diffusion, phase transformations, the formation of active sites on the newly created surfaces, and the like.

Changes of properties and EPR spectra of the microcrystals ZnS: Mn in their dispergation have been researched. Self-activated ZnS microcrystals were mixed with $MnCl_2$ powder (manganese concentration was 1.1 weight percent). To doping ZnS microcrystals by Mn^{2+} ions was carried out joke powder mixture at a temperature T = 950 ° C for 3.5 hours. The presence of Mn^{2+} ions in the ZnS matrix stimulated bright photoluminescence (PL) microcrystals ZnS:Mn near λ_{max} = 580 - 590 nm. Size of the individual microcrystals ZnS: Mn was ~ 25 μm. The regularities of modification processes of a structure and the local symmetry of Mn^{2+} ions at the dispergation samples was studied.

The X-ray diffraction analysis shown that is present phase ternary compound $Mn_{0.75}Zn_{0.25}S$ in microcrystals ZnS:Mn. Dispergation the basic samples during 10 and 20 min., significantly reduces the size of the microcrystals, respectively, to 10 and 5 μm, while the PL intensity decreased respectively by 6.5 and 10 times. With the increase in the proportion of time dispergation phase $Mn_{0.75}Zn_{0.25}S$ reduced and by dispersing 20 min. it disappears.

The decrease of the PL intensity in powdered samples, in our opinion, can not be explained only by the decrease in the size of the microcrystals and to increase of the scattering exciting light. When PL excited by light with λ_{exc} = 365 nm excitation mechanism main centers PL is the resonance energy transfer from the centers of sensitization to the ions Mn^{2+}. After dispertion the excitation mechanism is weakened. You also need to consider the possibility of the formation the amount of some additional centers of nonradiative recombination in microcrystals. The general action of these factors may explain the significant decrease of PL in ZnS:Mn microcrystals.

Selective Optical CO Gas Sensor Based on NiO/Al_2O_3 Structure

Kudanovich A.M., Filimonenko D.S., Parchomenko I.N.

Institute of Physics, National Academy of Sciences of Belarus, Minsk, Belarus

Resistive chemical sensors on the basis of metal oxides have high sensitivity at detecting gases in various analyzed atmospheres, but their selectivity is not enough for wide application of such type of devices. For increasing selectivity the method is proposed of diffusive reflection of structures on the basis of semiconducting oxides of p- and n-type. The structure of WO_3/Al_2O_3 NiO/Al_2O_3 has been tested as sensitive elements for optical gases of sensors. The tests have been conducted in the medium of different gases. As a sensitive element of the parameter the absorption and diffusive reflection have been studied. The investigations showed that WO_3/Al_2O_3 cannot be used as a sensitive element at such approach, because neither of the investigated characteristics showed any noticeable change at varying the content of gas medium. In a case of nickel oxide the diffusive reflection within the wavelengths range of 325 - 400 nm by one of sides of the investigated structure of NiO/Al_2O_3 after influences of gases exceeds the diffusive reflection by the other side approximately in 3.5 times independently on the quantity of influences; and before the influence this ratio was equal to 1. Thus, the detecting parameter of carbon monoxide influence on the sensitive element of NiO/Al_2O_3 can be used for multitude detection of carbon monoxide.

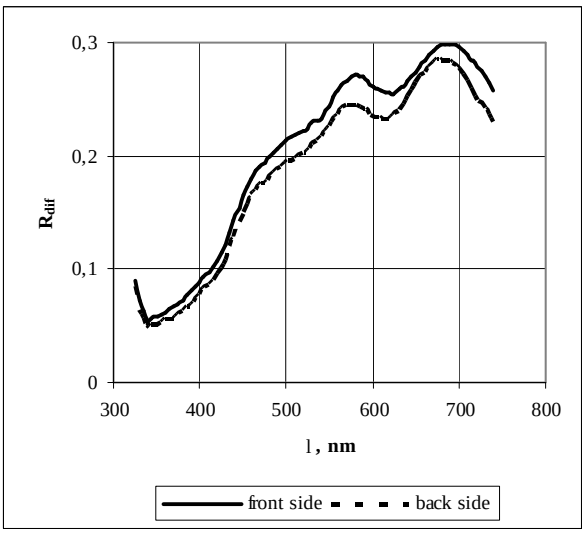

Picture 1 – Diffuse reflection of front and back sides of NiO/Al_2O_3 before gas exposure

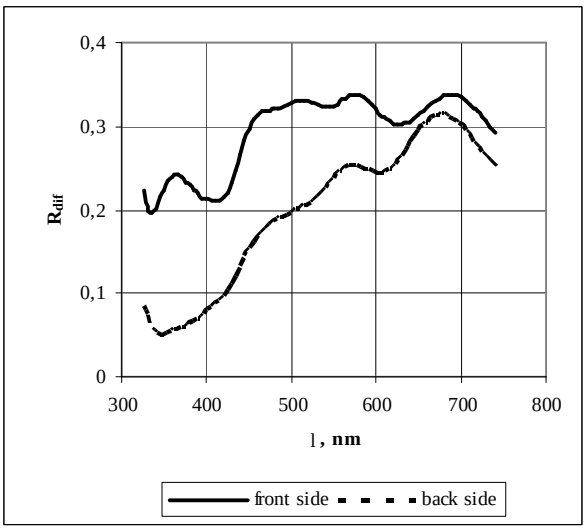

Picture 2 – Diffuse reflection of front and back sides NiO/Al_2O_3 after gas exposure

Electronic Structure, Optical and Magnetic Properties of Co_2FeGe Heusler Alloy Films

Kudryavtsev Y. V.[1], Uvarov N. V.[1], Kravets A. F.[2,3], Vovk A. Ya.[4], Borges R. P.[4], Godinho[4], and Korenivski V.[2]

[1]*Institute of Metal Physics, National Academy of Sciences of Ukraine, Kiev, Ukraine*
[2]*Nanostructure Physics, Royal Institute of Technology, Stockholm, Sweden*
[3]*Institute of Magnetism, National Academy of Sciences of Ukraine, Kiev, Ukraine*
[4]*CFMC, Department of Physics, University of Lisbon, Campo Grande, Lisbon, Lisbon, Portugal*

Optical properties of ferromagnetic half-metallic full-Heusler Co_2FeGe alloy are investigated experimentally and theoretically. Co_2FeGe thin films were obtained by DC magnetron sputtering and show the saturation magnetization at T=10 K of m =5.6 μ_B/f.u., close to the value predicted by the Slater-Pauling rule. First-principles calculations of the electronic structure and the dielectric tensor are performed using the full-potential linearized-augmented-plane-wave method in the generalized gradient approximation (GGA) and GGA+U approximation (see Fig. 1). Taking into account that the magnetic moment of Co_2FeGe obtained using the GGA+U approach fits better the Slater-Pailing rule than does the moment in the GGA approximation, we calculate the optical properties of Co_2FeGe using GGA+U.

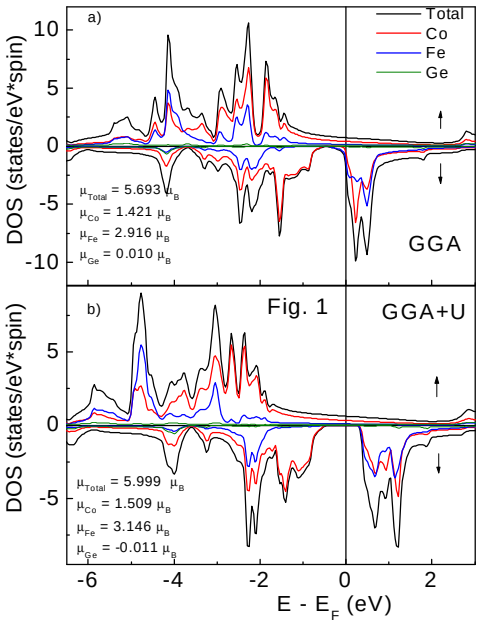

Fig. 1

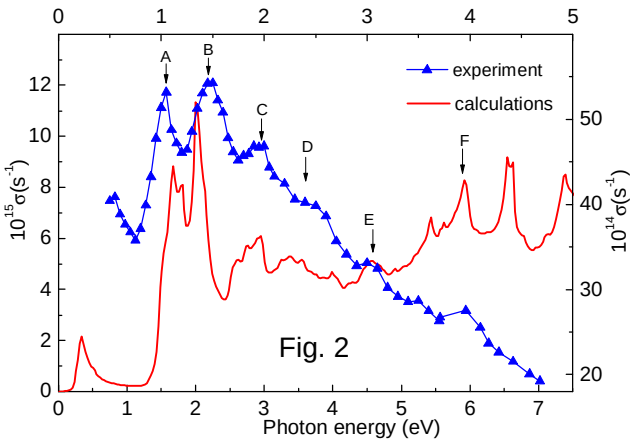

Fig. 2

The measured interband optical conductivity spectrum for (see Fig. 2) exhibits a strong absorption band in the 1–4 eV energy range with pronounced fine structure, which nicely agrees well with the calculated half-metallic spectrum of the system, suggesting a near perfect spin-polarization in the material. Interband absorption peaks marked by A, B, C, D and E are discussed in terms of band structure of alloy.

Simulation of Doping with Indium of Plumbum Telluride Thin Films Vapour Phase Method Grown

Kushnir A.I., Lishchynskyy I.M., Vasylyshyn I.D.

Vasyl Stefanyk Precarpathian National University Ivano-Frankivsk, Ukraine

Doping of semiconductors of group $A^{IV}B^{VI}$ the elements of the third group, allowes a wide range, to predict the properties and implement new methods of managing them. Specifically doped *In* crystals obtained with spatial uniformity of carrier concentration, provide stable properties and a weaken their sensitivity to the effects their mechanical of impurities and defects. However, in the literature there is no consensus on the mechanism of entry into the structure of indium doping of semiconductors of groups $A^{IV}B^{VI}$, its charging state.

We studied formation the mechanisms of atomic defects in thin films of PbTe, doped indium, which are based on crystal chemistry of model of quasi-chemical reactions of growth. Films precipitated from the vapor phase by hot wall on single-crystal substrates – chips (111) BaF_2. Other than that, we used two complementary sources of couples: the first with tellurium, the second with the doping impurity *In.*

A thermodynamic calculation was made of equilibrium atomic's own defects in thin films of lead telluride doped indium at pair-phase epitaxy for different condensation of temperatures and partial vapor pressure of tellurium and indium. We detected the equilibrium constant quasichemistry substitution reactions of indium atoms nodular lead. Dependence of vacancy concentration of the metal content of the doping impurity was calculated.

To describe the physical and chemical processes of growing films of lead telluride from the vapor phase and their doping during growth the quasychemical method was used.

Approximation of the experimental results the theoretical dependences based on the smallest scatter of constants quasychemical reactions found the best model of the alloying indium cluster In^+.

Charge state and cluster dimension of indium impurity in the lead telluride have been obtained by approximation experimental results of theoretical equations.

Structural transformations in GaSb based thin films

Lutsyk N.Yu, Mykolaychuk O.G.

Ivan Franko National University of L'viv, Physical Faculty, Chair of Physics of Metals

Structure, substructure, concentration areas of existence of metastable solid solutions and an amorphous state and kinetics of structural transformations depending on technological conditions of evaporation of thin films of systems GaSb-Ge and GaSb-Sn were studied by methods of electronography and transmission electron microscopy. Films with the thickness near 500A were prepared using method of a flash vacuum evaporation. Ceramic, glass and spallings NaCl monocrystals were served as substrates. The temperature of a substrate supported in a precipitation process of films has dominant effect on structure formation of explored films. Films of all explored GaSb-Ge compositions, precipitated on substrates at room temperature, were amorphous. In amorphous films GaSb threefold coordination in distribution of the proximate atoms is observed. At concentrations Ge_2 about 20 % transferring from threefold coordination to tetrahedral is observed. Amorphous films at heat crystallized, but phases of a solid solution it is not observed. Initial crystallization phases are crystal grains GaSb. The growth of crystallite sizes of GaSb takes place with the temperature increase. A speed of continuous heating has essential influence on the density and sizes of crystallites of GaSb formed in the amorphous semiconductor matrix based on Ge. With an increase of temperature of a substrate there is a forming the nonuniform amorphous films. With the further increase of temperature of substrates on the isotropic substrates polycrystalline films of a metastable solid solution of substitution are formed, and on spallings NaCl monocrystals are formed textured and epitaxial films.

Equilibrium of system GaSb-Sn in a massive state is featured by the diagram of the eutectic type. Films precipitated on substrates at room temperature were amorphous up to 60% of Sn atom concentration. Two-phase polycrystalline films (b-Sn and GaSb) are formed at higher concentrations of Sn. With the increase of temperature of a substrate there is a forming the nonuniform amorphous films. Amorphous films at heat crystallized, but phases of a solid solution it is not observed. Initial crystallization phases are crystal grains b-Sn. The growth of crystallite sizes of b-Sn takes place with the temperature increase. A speed of continuous heating has essential influence on the density and sizes of metallic crystallites of b-Sn formed in the amorphous semiconductor matrix based on GaSb. With the further increase of temperature of substrates on the isotropic substrates, polycrystalline films of a metastable solid solution of substitution are formed for the concentration up to 20% of Sn_2, and on spallings NaCl monocrystals textured and epitaxial films are formed.

Luminescence of ZnSe Heterolayers, Synthesized on ZnS Substrates

Makhniy V.P.[1], Gavaleshko A.S.[1], Slyotov M.M.[1], Horley P.P.[2], Slyotov A.M.[1]

[1]*Yu.Fedkovych Chernivtsi National University, Chernivtsi, Ukraine*
[2]*Centro de Investigation on Materials Avanzados (CIMAV) Chihuahua-Monterrey, Chihuahua, Mexico*

Due to the large band gap ($E_g \approx 2{,}7$ eV at 300 K) and by direct optical transitions, zinc selenide is one of the most promising semiconductor to create a blue injection light-emitting diodes (LED). The bases of LED are different types of the rectifying structures – p–n-homo- and heterojunctions, Schottky diodes, MOS structures, etc. For them, the general is the presence of a thin (a few micrometers) region in which the radiative recombination takes place. The main requirement to material of this area is a presence in the spectrums of luminescence of dominant blue band of radiation. This is achieved by using the appropriate dopants and technologies doping. In this paper, such a problem can be solved by annealing ZnS single crystal substrates in saturated vapors of Se. As a result the new compound of ZnSe appears on their surface. This is confirmed by differential transmission and reflection spectra. They contain bands with maximum near 2.7 eV, which corresponds with a zinc selenide band gap E_g. While the remaining (not fully substituted) S atoms of the base substrate are present in the heterolayers ZnSe as isovalent impurities (IVP). Their concentration can be up to 10^{19} cm^{-3}. According to the theory, these impurities IVP must contribute to the effectiveness of edge emission, which is confirmed by experiment. Emission spectrum in the visible region consists of very effective (~ 20% at 300K) blue band with a maximum near 2.68 eV, picture. However, the presence of photons with energies $> E_g$ is due to interband transitions. It is confirmed by the theoretical curve (dashed line) for this type of transition. The main emission band is formed by the exciton annihilation at their inelastic scattering on the major carriers. In this case, they are holes, as synthesized heterolayers have p-type conductivity. Methods to increase the radiation effectiveness and the practical use of research facilities are discussed.

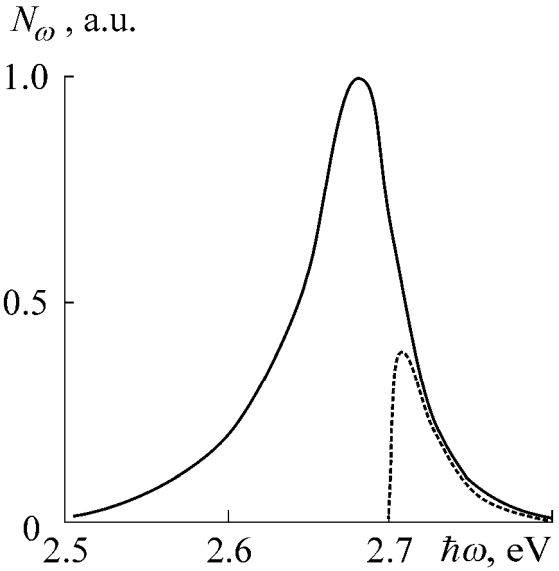

Emission spectrum of ZnSe heterolayers. T = 300 K.

Influence of Preparation on Optical Properties Heterostructures CdTe / CdS

Makhniy V.P.[1], Pavljuk M.Ph.[2], Slyotov M.M.[1], Slyotov A.M.[1], Yljanitzkij K.S.[1]
[1]*Yu.Fedkovych Chernivtsi National University, Chernivtsi, Ukraine*
[2]*Vasyl Stefanyk' Precarpathian National University, Ivano-Frankivsk, Ukraine*

Heterostructures (HS) with photoactive region on the CdTe can be the basis of solar energy converters into electricity. Among the most intensively studied HS system is telluride-cadmium sulphide, whose theoretical efficiency is about ~ 28%. However, the real value of solar cells based on these structures in the crystal and the film state is much lower. This is caused by defects in the interface due to the mismatch of the lattice parameters of HS component. The influence of this factor can be reduced by creating a graded-gap layer $CdS_{1-x}Te_x$. This can be done by selecting the method and mode of preparation of the heterostructure. Previously [1] reported on the possibility of obtaining HS telluride-cadmium sulphide by isovalent substitution. In this paper, the influence of ingredients and temperature T_a annealing on the optical properties of the CdTe/CdS structures is investigated. Heterolayers CdTe created by isothermal annealing of single crystal n-CdS plates in an evacuated quartz ampoule in the presence of the mixture. It's used as an elementary Te, CdTe ground or its components mixture. After annealing, the surface layers change color from yellow to black. Investigations have shown that at low annealing temperatures HS look like islet formation, which turn into a uniform film at $T_a \geq 800$ °C. We point out that the most advanced layers of CdTe obtained by using as a mixture CdT + Te. Transmission spectrum T_w of the structure obtained at $T_a \approx 820$ °C presents by curve 1 with a maximum at $\mathbf{h}w_{\max} \approx 1.64$ eV. Its value is consistent with a band gap of hexagonal CdTe. Further increase of T_a causes the displacement of the $\mathbf{h}w_{\max}$ to the value of 1.6 eV. It is caused by an increase in the thickness of the solid solutions $CdS_{1-x}Te_x$ which have a nonlinear dependence of $E_g(x)$. Relative amount of pure CdTe in a total heterolayers thickness then becomes smaller, which is confirmed by a weak peak at 1.64 eV in curve 2.

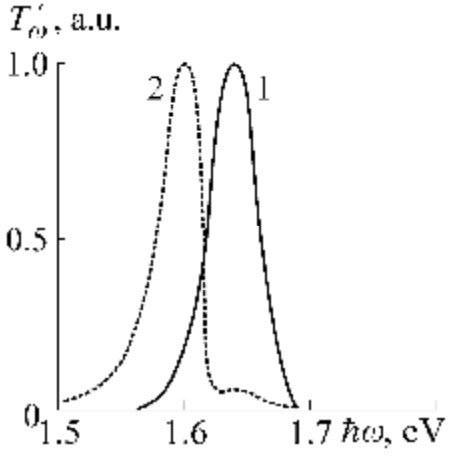

Transmission spectrum of CdTe heterolayers obtained at 820 °C (1) and 920 °C (2).

1. V.P. Makhniy, M.M. Slyotov, E.I. Chernykh, K.S. Yljanitzkij The obtaining and properties of CdTe/CdS heterostructures // Thesis 5th International Scientific and Technical Conference SEMST-5, 2012, June 4-8, Odessa, p. 247.

Self-Organizing Processes of the Dissipative Structures in Gradient non-Crystalline Materials of the Systems As(Ge)-S

Mar'yan M.I., Yurkovych N.V.

Uzhgorod National University, Uzhgorod, Ukraine

The investigation of the self-organizing processes at transition to the non-crystalline state and under the influence of external fields (electromagnetic adiation, temperature field) in non-crystalline materials is devoted. It was shown that such a dissipative structure with the hyper sensibility dis formed under influence of electromagnetic radiation ($l = 0.63\mu m$) at density $P \geq P = 1\ mW / sm^2$ in amorphous materials of $As - S$ systems. The nature of the bifurcation process of transition to a non-crystalline state on the basis of the theory of neural networks of Kohonen and Hebb are analysed at influence of velocity cooling. The structure bifurcation process of transition and functional dependence of structural-sensitive parameters f on velocity of cooling q in the form $f \approx q^{d_f}$ ($d_f = 0.631$ is fractal dimension of Kantor) are identificated [1].

Theoretical and experimental researches of dissipative structures are presented consisting of non-crystalline semiconductors with the set division of concentration of modifier on the thickness of tape on the basis of glassy Ge_2S_3. The dynamics of running the number of particles is considered component of modifier of the system N_{mod} at the action of source G of atomic stream in the process of during time t_p . The atomic stream of particles changes in course of time after a certain law which can be varied (the exponential law of change is examined in this case): $G = g_{source} \cdot \exp(-mz)$, where g_{source}, m are constants of source of particles. The technological parameters of receipt of the modified structures (speed of condensation, temperature of evaporation, thickness) are certain. This approach enables, being based on the unique physical principle, to describe forming of non-crystalline materials, their structure and features of co-operating with external factors at presence of self-organizing processes. Grounded possibility of receipt of hyper sensibility of dissipative structures of non-crystalline materials, got through the self-organizing processes, and development on the indicated phenomenon of new approach to forming of recordings environments, developments sensory devices.

1. Yurkovych N.V., Mar'yan M.I. Dissipative Structures And Self-Organizing Processes In Non-Crystalline Materials. Uzhhorod University Scientific Herald. Series Physics. Issue 29. – 2011.-P.79-86.

Diffusion in Cu/Ni Nanosize Layered Film System

Minenkov A.A., Bogatyrenko S.I., Sukhov R.V., Kryshtal A.P.

Karazin Kharkov National University, Kharkov, Ukraine

Under transition to nanoscale objects the properties of materials begin to significantly differ from the properties of macroscopic objects. One can observe the change of thermal, structural, optical, magnetic, etc. properties with a decrease of the characteristic size. Furthermore, the diffusion processes are considerably accelerated in such systems [1]. This fact drastically affects the stability of nanoscale systems, and, eventually, the durability of the equipment and devices based on them. One of the major problems arising during investigation of the diffusion processes in condensed films is the complexity of separation of contributions from different processes occurring in such systems, both during their formation and thermal annealing. In this work we present the results of experimental studies of the influence of characteristic size on the diffusion rate in nanoscale film systems.

Nanosized Cu/Ni multilayered film system was chosen as the object of studies. The choice of Cu-Ni system has been specified, first of all, by the fact, that copper and nickel exhibit unlimited mutual solubility in the liquid and in the solid states, thus forming the phase diagram of “cigar” type.

The layered film systems were prepared by means of successive condensation of Cu (99.99%) and of Ni (99.99%) being evaporated from independent sources. The experiments were conducted in a high vacuum chamber at residual gas pressure less than 5×10^{-7} mm Hg. The mass thickness of each layer was measured by means of quartz crystal resonator and was varied in 5-100 nm range. The mass ratio of the components in the film system was equal to unity.

The method of electrical resistance measurement was used as an experimental basis for studying of the diffusion processes during heating – cooling cycles. The relative change of the electrical resistance during annealing of film system enables us to register onset and termination temperatures of the homogenization process in the system under study and, thereby, to determine the activation energy of processes occurring therein.

It was shown that the activation energy of diffusion in Cu-Ni system decreases with decreasing of film thickness. The measured dependence has been constructed in a wide range of sizes. The observed effects are discussed in the framework of size reduction of the vacancy formation energy in nanomaterials.

1. S. I. Bogatyrenko, N. T. Gladkikh, A. P. Kryshtal, A. L. Samsonik, and V. N. Sukhov. Diffusion in Nanodisperse Layered Film Systems // The Physics of Metals and Metallography. - 2010. - Vol. 109, No. 3. - pp. 255–260.

Formation of Grain Boundary Joints in Nanocrystalline Silicon Films

Nakhodkin N.G., Kulish N.P., Rodionova T.V., Sutyagina A. S.

Taras Shevchenko National University of Kyiv, Ukraine,

Nanocrystalline silicon films are an attractive material for solar energy - electricity conversion [1]. Electrical properties in films are affected by crystal defects such as dislocations, twins, grain boundaries and grain boundary joints.

Joints of grain boundaries are characteristic feature of nanocrystalline film structure and are defined as peculiar kind of linear defects. It is evident that the joints influence the film structure formation and properties of the films. This effect is different for various joints and is structure-dependent.

The aim of this work is to study of grain boundary joints in undoped nanocrystalline silicon films depending of film thickness.

Silicon films were prepared by low-pressure chemical vapour deposition from a silane/argon mixture. Films were deposited on thermally oxidized (100) single-crystal silicon wafers. The deposition temperature was equal to 630^0C. The film thickness was ranged from 3 to 100 nm.

The microstructure of nanosilicon films has been investigated by transmission electron microscope (TEM). Specimens for TEM were prepared by chemical etching. Atomic force microscope (AFM) has been used to obtain a set of statistical data in studies of grain boundary joints.

Both AFM and TEM studies have shown that triple grain boundary joints dominate throughout the entire examined films. However, at film thickness increases up to ~ 70 nm the number of triple joints decreases and the number of multiple (special) joints increases. This behavior correlates with changing of film structure from equiaxial to fibrous (at thickness ≥ 70 nm [2]), appearance of preferred orientation [110] and drastically increasing of surface roughness.

There are several formation mechanisms of special grain boundary joints in nanocrystalline films. Splitting of grain boundaries is the most probable mechanism of special joint formation in nanosilicon films of equiaxial structure. In fibrous films, special joints are a result of multiple twinning that occurs during the film formation.

1. Mukhopadhyay S., Chowdhury A. Nanocrystalline silicon: A material for thin film solar cells with better stability // Thin Solid Films. – 2008. – Vol. **516**, - P. 6824-6828.
2. Nakhodkin N.G., Rodionova T.V. Formation of different types of polysilicon film structures and their grain growth under annealing // Phys. Status Solidi A. – 1991. – Vol. **123**, № 2. - P. 431-439.

Optical Properties of Densely Packed Plasmonic Nanocomposites

Ponyavina A N., Tselesh E.E., Zamkovets A.D.

B.I .Stepanov Institute of Physics of the NAS of Belarus, Minsk, Belarus

Plasmonic nanocomposites are promising materials for optics and nanoelectronic due to their unique properties connected with surface plasmon resonances of absorption (SPRA) which are high sensitive to the microphysical parameters and topology of these nanostructures. Modeling of their optical and electrical characteristics is an important step at the development of new functional plasmonic elements. The established way is the effective medium approximations, the most known of which are the Maxwell Garnett (MG) and Bruggeman theories. However their application to plasmonic nanocomposites in the concentration range of the matrix inversion is not quite successful [1].

Here we study the SPRA concentration dependence of planar nanocomposites Ag-LiF and Ag-KCl which are fabricated by the thermal vacuum evaporation and characterized by a high volume part of a metal phase. In order to analyze the optical properties of the metal-dielectric systems we use the combined model (CM) of efficient medium based on the probabilistic approach to the description of a nanocomposite structure at comparable concentrations of phases contained into the composite [2]. The CM leads to the following formula for the effective permittivity ε_{eff} :

$$e^{CM}eff = w_1 \frac{2e_2(e_1-e_2)p_1+e_2(e_1+2e_2)}{(e_1+2e_2)-(e_1-e_2)p_1} + w_2 \frac{2e_1(e_2-e_1)(1-p_1)+e_1(e_2+2e_1)}{(e_2+2e_1)-(e_2-e_1)(1-p_1)}.$$

Here $w_1=(1-p_1^{1/3})^3/[(1-p_1^{1/3})^3+(1-p_2^{1/3})^3]$, $w_2= (1- p_2^{1/3})^3/[(1-p_1^{1/3})^3+(1- p_2^{1/3})^3]$, p_1 and p_2– macroscopic volume concentrations of substances 1 and 2, respectively, e_1 and e_2 - their permittivities. Then effective complex index of refraction $m_{eff} = n_{eff} - ik_{eff.}$ may be found from the known relation $e_{eff} = (m_{eff})^2$.

The CM ensures much better coincidence with the experiment data at a high concentration of the metallic phase (p = 0,4-0,8) than the MG. It concerns both to the quantitative values of the optical density in the SPRA maximums and the half-widths of these bands. Some differences in the spectral position of the CM-calculated and measured bands might be associated with a layered structure of fabricated composites. Besides experimental samples have additional heterogeneities, since contacting the neighboring metal layers may give rise to the formation of nanoparticle chains and even a grid metal structure in composites.

1. Ping Sheng.// Phys. Rev. Lett.- 1980.- Vol. 45, № 1.- P. 60-63.
2. A. N. Ponyavina, S.M. Kachan, and E.E. Tselesh.// Journ. Appl. Spectr.- 2012.-Vol.79. - P. 765-773.

Applicability of the Superposition Principle During Poling of Thin Polymer Ferroelectric Films

Revenyuk T.A., Ignatenko V.S., Sergeeva A.E.

Department of Physics, Odessa National Academy of Food Technologies

Polyvinylidene fluoride (PVDF) and other ferroelectric polymers films are extensively studied as new materials for producing piezo- and pyroelectric sensors and actuators. In such devices, the ferroelectric films are initially poled, or charged with the purpose of obtaining the high and stable residual polarization. Such poling is a complex phenomenon consisting of several reversible and irreversible processes that should be separated in order to analyze which of them influence the final value and stability of the polarization.

The superposition principle consists in the statement that the response to any number of individual actions is equal to the sum of the individual responses to each separate action. It is known that this principle is applicable only to linear systems and, in general, the principle of superposition is just the criterion of the system linearity.

During formation of polarization in polymer ferroelectrics, the effect is the applied voltage and the response is the measured current or the electrical displacement. Study the applicability of the superposition principle in this case is of interest, because in the measured values contribute the reversible processes and the ferroelectric polarization, as well as the finite conductivity of the samples. Therefore, the separation of the completely reversible components, for which the superposition principle is valid, is quite important.

Comparison of theoretical and experimental currents and displacements has showed that during the initial electrification of polyvinylidene fluoride (PVDF), the superposition principle does not hold, as well as during the polarization switching. However, if the voltage is applied to the polarized sample for short periods of time, the duration of which is much shorter than the Maxwell relaxation time, only reversible processes take place. For the case in question, as we have found, the superposition principle is hold with a high accuracy of 99.3%.

These data indicate that a part of the developed polarization in PVDF is linear, while the ferroelectric component is essentially nonlinear and does not follow the superposition principle. The proposed methodology of measurements and calculations allows to determine during the study of a ferroelectric whether the total electric displacement has a contribution due to only the ferroelectric polarization, or the reversible component is also present.

Polarization During Initial Poling and Switching of Ferroelectric Polymer Thin Films

Sergeeva A. E.

Department of Physics, Odessa National Academy of Food Technologies, Odessa, Ukraine

It is known that the uniformity of polarization in ferroelectric polymer thin films can be affected by a space charge. Measurements of the spatial distribution of the polarization are usually performed on poled samples, thus reflecting only the final polarization state. However, it is interesting to study evolution of polarization profiles obtained by *'in situ*' measurements on thin films poled and switched at room temperature either in a 'low' field, or in a 'high' field. We performed experiments of 20 μm-thick PVDF and P(VDF-TFE) films at 60 and 180 MV/m, while the coercive field for the films was of the order of 50-80 MV/m.

The piezoelectrically induced pressure step method was used to measure the polarization profiles about 100 times per second with resolution of 2 μm. At low fields, growth of two symmetrical polarization peaks were observed in PVDF, while only one peak near the positive electrode appeared in P(VDF-TFE) under the same conditions. Subsequent switching by changing polarity of the field led to formation of the bimorph structure, because polarization near the positive electrode was not entirely switched, but its value was only reduced. The equilibrium state after short-circuiting was reached in about 1 min, in accord with the value of Maxwell's relaxation time. Under high poling fields, polarization was uniform during both original poling and switching, except for narrow (2-3 μm-thick) near-to-electrode layers where polarization dropped down to zero. Attempts to improve the uniformity of polarization in originally non-uniformly poled samples by applying the higher field were not successful.

We explained the observed phenomenon by the effect of injected and deeply trapped negative charges that prevent broadening of the polarized zone. A model has been developed assuming interdependence of the space charge and the polarization, as stipulated by Poisson’s equation. The space charge stabilizes the polarized state compensating the depolarization field. However, it causes also a non-uniformity of the polarization. It has been proved that the space charge is localized in transition zones by which polarized regions are separated from non-polarized ones. Thus, the depolarizing field is compensated not inside the individual crystallites, but in the whole region. It is believed that depending on the poling conditions, the charge is trapped either near surfaces (at high fields), or in the bulk (at low fields). One can assume that the observed features are common for the whole class of the ferroelectric polymers thin films.

Model of the Polarization Profil Formation in Thin Polymer Ferroelectric Films at a Constant Applied Field

Sergeeva A.E., Shul'gin I.A., Revenyuk T.A.

Odessa National Academy of Food Technologies

Uniformity of the ferroelectric polarization in polymer films is very important for proper operation these films in a new generation of piezoelectric and pyroelectric sensors and actuators.

Our measurements by the method of the piezoelectrically generated pressure step (PGPS) of the polarization profile in polyvilylidene fluoride (PVDF) films, electrified under the continuous field strength of 60 MV/m, which is close to the coercive value, have showed that the polarization after 8 sec of the field application is uniform, but it is only 0.5 mC/cm^2 and does not contain the ferroelectric component.

During the further application of the same field, the polarization profile becomes highly non-uniform with a maximum always near the positive electrode. It has been found that the subsequent increase of the field even by 3 times does not improve the already formed non-uniformity of the polarization.

To explain the observed phenomenon, a model has been developed suggesting an important role of the negative charge injected from the electrode, which forms a space-charge layer in the area of the inhomogeneous polarization.

In accordance with the Poisson equation, this layer compensates the depolarizing field and forms the stable system with zero field with the inhomogeneous polarization, which is formed after the completion of the electrification and the short-circuiting of the sample.

Solution of differential equations describing the process of the formation of the polarized state, as well as the transfer and accumulation of the charges has showed that with time there is an acceleration of the front of the injected charges causing a sharp increase in the field strength near the positive electrode.

The proposed model allows to analyze the evolution of the polarization profile after switching off the applied constant voltage and the short-circuiting of the sample and to prove the impossibility to improve the uniformity of the already formed non-uniform polarization profile by subsequent increasing the applied field strength.

Thus, we have showed that for obtaining the uniform and high residual polarization in the ferroelectric polymer like PVDF it is necessary to perform initial poling of a virgin sample using the high field, at least 3-4 times higher than the coercive value of the field for this ferroelectric polymer film.

Effect of Cd^{2+} and S^{2-} Ions Concentration on Optical Properties of CdS Chemical Bath Deposited Thin Films

Shcherbak L. and Krupko O.

Yuriy Fedkovych Chernivtsi National University, Ukraine

CdS nanoparticles (NP) have very high photosensitivity that makes them a promising candidate for the detection of visible radiations, as photoconductor in optoelectronic devices and a number of biological applications. CdS chemical bath deposited films are now being developed to be utilized in converting solar radiation into electricity.

This work deals with the preparation of CdS thin films by chemical bath deposition from CdS/L-cysteine colloid solutions previously prepared at pH = 11 similar to those described in [1]. Cadmium chloride and sodium sulfide was used as a source of cadmium and sulfide ions and L-cysteine as capping agent. The films were deposited onto well-cleaned glass substrates at room temperatures using a special automatic apparatus [2]. It was used a 2% aqua solution of polydialyldymethylammonium chloride (PDDA) with molar mass M = 200000 as layer forming polymer. The process of the substrate dip into solution was repeated for 30 times. So formed CdS/L-cys NPs was deposited onto the substrate as a strongly adherent film.

Varying the precursors Cd^{2+} and S^{2-} ions concentration during the synthesis process it was obtained that equal deviation from stoichiometry resulted in various change of the NPs' size and optical properties. The smallest absorbance edge λ_{edge} value (λ_{edge} = 406 nm that corresponds to the NPs diameter D = 3,7 nm) are reached at $[S^{2-}]/[Cd^{2+}]/[\text{L-cys}]$ = 1 : 2,9 : 6,1 ratio, the largest (λ_{edge} = 456 nm; D = 5,3 nm) at the precursors ratio $[S^{2-}]/[Cd^{2+}]/[\text{L-cys}]$ = 3,5 : 1,0 : 5,5. Maximal quantum yield QY = 26% of the stable solutions can be reached at $[S^{2-}]/[Cd^{2+}]/[\text{L-cys}]$ = 1,0 : 1,6 : 7,4. Deposited from this solutions thin films preserve such correlations and demonstrate remarkable (up to 80 nm) Stokes shift in all cases.

1. E. V. Krupko, G. Ya. Grodzyuk, Yu. B. Khalavka, G. M. Okrepka, and L. P. Shcherbak. Effect of the composition of the reaction mixture on the preparation of L-cysteine-stabilized CdS nanoparticles and their optical properties. / *Theoretical and Experimental Chemistry*. - Vol. 47, No. 2. – 2011. - P. 101-107.
2. Ю.Б. Халавка, О.В. Копач, В. М. Струтинський, Л.П. Щербак. Виготовлення плівок наночастинок кадмій телуриду, впроваджених у полімерну матрицю, за допомогою установки автоматизованого пошарового осадження. / Наук. вісник ЧНУ Хімія, Вип. 422. – 2008. - С. 34-39.

Thermally Stimulated Depolarization of Corona Poled Films of Polyvinylidene Fluoride

Sorokina O.G., Fedosov S.N.

Department of Physics, Odessa National Academy of Food Technologies

To study relaxation processes in ferroelectric polymers like polyvinylidene fluoride (PVDF), the thermally stimulated depolarization (TSD) method is the most appropriate, although a theory was developed only for thermally frozen Debye processes. It has been shown recently that trapped charges play an important role in the buildup of polarization in PVDF. Here the TSD currents are studied in corona poled PVDF in order to distinguish between relaxation of the polarization and that of the space charge. The study was performed on uniaxially stretched PVDF films of 20 μm thickness produced by Plastpolymer, Russia. A specially designed corona triode was used to pole samples at constant current conditions, while the value of the electret potential was continuously measured during poling. TSD currents in the poled samples were measured at the heating rate of 4 K min^{-1} in the open circuit (OC) mode with a 25 μm-thick FEP-Teflon spacer used as a dielectric gap. It is known that in the OC mode both the relaxation of dipoles and that of the space charge produce TSD currents flowing in the opposite directions. A set of the corona poled samples was studied 1 h after poling, while another set was stored after poling for 14 months before performing the TSD measurements. There were two oppositely directed TSD peaks in the samples studied immediately after poling. Comparing TSD currents at the freshly poled samples with those stored for 14 month, we have found that two additional peaks appear in the range from 60 °C to 80 °C at the sample stored for a long time. The obtained results indicate that almost certainly four relaxation processes are involved, two of them associated with the dipole relaxation and another two related to the space charge.

To explain existence of the four relaxations, one should consider that ferroelectric polymers differ distinctly from polar electrets. The former has not only ferroelectric crystallites, but also a polar amorphous phase typical for electrets. Polarization in electrets is thermally frozen and thermodynamically unstable, while the ferroelectric polarization is stable, if the depolarizing field is neutralized by real charges. Our calculations have shown that the surface or space charge can stabilize not only the ferroelectric polarization in crystallites, but also the dipole polarization in amorphous phase. It follows from our results that a very slow redistribution of charges and polarization takes place in PVDF after completion of poling, until the electret and ferroelectric components of polarization are finally separated, both accompanied by the trapped charges.

Synthesis of Boron Nitride Nanotubes by Ammonia Nitriding of Boron Fibers and Powder

Sylenko P.M., Shlapak A.M.,Solonin Yu.M.

Frantsevich Institute for Problems of Materials Science of National Academy of Sciences of Ukraine, Kyiv, Ukraine

Due to the unique properties of boron nitride nanotubes (BNNT) and the prospects of their use is now conducted numerous investigations of the processes of their synthesis and properties.

In this paper a study of the process of synthesis of boron nitride nanotubes by nitriding continuous fibers and boron powder and research of their morphology and structure is carried out. Nitidation was carried out in a flow alumina reactor, placed in a tubular electric furnace. Through reactor in which were powder or crushed continuous fiber boron, ammonia was passed at a specified speed. Research of product synthesis has been studied by scanning and transmission electron microscopy. In Fig. 1 is shows the results of the product synthesis research.

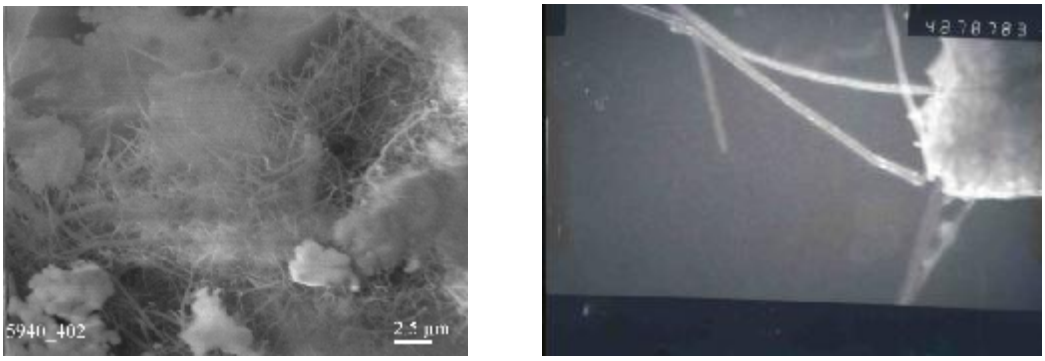

а б

Fig. 1. SEM and TEM images of nanotubes BN, synthesized at 1300 °C (a) and 1550 °C (b) for 1 hour.

It was found that the used method of synthesis of boron nitride nanotubes allow us BNNT in the amount of several grams per experiment to obtain. In collaboration with scientists from the Minsk State University (Belarus) research on the use of BNNT to create a composite material based on phosphates for protection from heat and ionizing radiation are conducted at present [1].

1. Kuzhir P. et al. Broron enriched unfired phosphate ceramics as neutron protector // Nanoscience and Nanotechnology Letters. – 2012. – Vol. 4, No. 11. – P. 1104-1109.

Simulations of the SiO_2/Si(100) Interface with Implanted Selenium Atoms

Tkachenko A.V., Mikaelyan G.R.

Zaporozhye National University, Department of Semiconductors Physics, Zaporozhye, Ukraine

The implantation of dopant atoms and ions is a traditional and effective way of modifying semiconductor electro-physical properties [1]. Ions implantation can lead to an increase the concentration of surface point defects; ions can penetrate into vacancies as well as behave as substitutional impurities. The aim of the current work was to investigate the physical and chemical properties and find the equilibrium states of the Si(100) interface covered with a thin layer of oxide with implanted Se atom. From theoretical estimates and experimental data [2], isolated selenium atoms mainly occupy sites in the silicon lattice. In this work selenium atoms were placed in oxygen and silicon vacancies of the oxide layer.

Quantum chemical calculations were performed for a $Si_{78}O_{60}H_{86}$ cluster that served as a model of a SiO_2/Si(100) interface, using a software package Mopac2009. The MNDO method (Modified Neglect of Diatomic Overlap), based on the solution of the Schrodinger equation in the Hartree–Fock approximation for a cluster, was used in our theoretical investigations.

The modeling of vacancies in the SiO_2/Si(100) oxide layer was done by eliminating oxygen or silicon atoms from the cluster. States with oxygen vacancies were obtained as a result of cluster geometry optimization with eliminated oxygen atoms in the oxide layer. All of the obtained states were characterized by the formation of new bonds between the unbounded silicon atoms when a vacancy appeared.

The Si–vacancy modeling was performed by eliminating the silicon atoms in the first layer of the carrying base. As a result of cluster geometry optimization, atoms with broken bonds do not form any new bonds in the area of silicon vacancy. The making of a strong chemical bond between oxygen and silicon atoms in the Si–vacancy area requires a noticeable change in their positions and can lead to the formation of mechanical stresses and an increase in the full system energy.

The search for the equilibrium states of a SiO_2/Si(100) interface with implanted selenium atoms was performed by placing Se atom into oxygen and silicon vacancies. Geometric parameters of the obtained systems, the charge distribution on atoms, the bond orders, valences, orbital hybridizations, atomic orbital populations, molecular and localized orbitals and total cluster energies were calculated.

1. Pleshivtsev N.B. and Bazhin A.I. Fizika vozdeistviya ionnykh puchkov na materialy, Moscow: Vuzovskaya kniga, 1998 – 391 p.
2. Overhof H., Scheffler M., and Weinert C. M., Phys.Rev.B, 1991, vol. 43, p. 12494-12506.

The growth kinetics of compound nanoshells under finite reaction rate at the interphase boundaries

Zaporozhets T.V., Podolyan O.M., Gusak A.M.

Cherkasy National University, Cherkasy, Ukraine

Prediction of time and efficiency of pore formation in the radial symmetric "core / shell" nanosystems [1,2] requires estimates of the time of the intermediate phase growth by reaction diffusion. For nano-systems, the features at the initial diffusion stage (delay at the interface, the existence of nucleation barriers) can significantly affect the total time of the phase formation. Phenomenological model of the growth of the intermediate phase layer during reactive diffusion in "core a –shell b " nanosystem is proposed. The effective rate coefficient of the reaction at the interface was introduced to take into account both curvature and the finite reaction rate at the boundaries of the growing phase layer: $K^{eff} = \dfrac{K_{ab} r_{ab} K_{bg} r_{bg}}{K_{ab} r_{ab}^2 + K_{bg} r_{bg}^2}$ (K_{ij} – reaction rate coefficient for the case of planar boundary between i and j phases). Both constant D and parabolic concentration-dependent diffusion coefficients $D(c) = D_{\min} + p(c - c_s)^2$ have been considered.

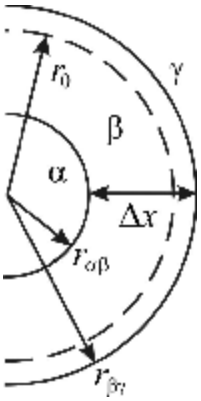

Some results:

- the concentration dependence of the diffusivity $D(c)$ may significantly alter the average diffusion coefficient $\bar{D}$ due to the deviation of the concentration range of the phase equilibrium values (leading to its nonmonotonic change during the phase growth and the increase in the last stage of the core exhaustion, regardless of the ratio of other model parameters);
- with increasing K^{eff} rate m of growth phase ($\Delta x \sim t^m$) is asymptotically approaching 0.5 (diffusion controlled parabolic growth), and with decreasing K^{eff} – tends to 1 (linear growth, which is controlled by the boundary kinetics); with increasing particle size r_0 the trend to parabolic law increases;
- the practical value of the proposed model is the ability to predict the full reaction time t to exhaustion of one components: there is a characteristic length $l = D/K^{eff}$, which determines the linear $r_0 << l$ or parabolic $r_0 >> l$ growth mode, depending on the eventual width of the phase (in our case, particle radius r_0).

3. Yin Y., Rioux R.M., Erdonmez C.K., Hughes S., Somorjai G.A., and Alivisatos A.P. Formation of hollow nanocrystals through the nanoscale Kirkendall effect // Science. – 2004. – V. 304. – P. 711–714.

4. Запорожец Т.В., Гусак А.М., Подолян О.Н. Эволюция пор в нанооболочках. Обзор // Успехи физики металлов. – 2011. – Т. 12. – С. 1-72.

Process of Structure Formation in Thin Polymer Films Obtained in a Vacuum

Zadorozhniy V.G., Polishchuk S.G., Keybal E. A., Kobrin V.L.

Odessa National Academy of Food Technologies, Odessa, Ukraine.

The features of structure formation in thin polymer films obtained without additional stimulation were studied. During the film growth, it was found that $300<M_n<7200$ and $1,1<M_\omega/M_n<1,82$. For films with $1,5< M_\omega/M_n <2$, MMP was represented by a linear combination of the Schulz distribution of zero and first order that allowed to calculate their MMP.

Experimental results and theoretical data were in accord. Analysis of MMP in the films suggests that for a number of polymers (PE) the free radicals formed in the evaporator disappear before evaporation.

Under reducing the rate of evaporation, a decrease in M_n and expansion of MMP of the condensed fragments were observed. Under the thermal evaporation, M_n is larger and MMP is narrower than those values at the electron beam evaporation.

Effect of T_k and E of electrons on MM of macromolecules in the films of the FT-3 is presented in Table 1

Table 1

$T_к$, °C; j, mA/cm^2; E, eV	molecular weight	
	M_ω	M_n
-195	5000	1500
-50	10000	2900
+100	40000	5600
+100	80000	20000
+150	120000	36400
+200	140000	50600
j=0,1; E= 50-100	55000	62000
j=0,1..0,2; E=100-150	145000	55600
j=0,3..0,5; E=200-500	80000	22700
original polymer	200000	-

Films of some polymer produced by electron-beam and HF irradiation are cross-linked. Additional increase of T_k from 280 to 430K results in a slight increase in the content of cross-links from 75 to 80%.

Irradiation in the condensation process in a vacuum at above T_k and below T_f leads to the formation of intermolecular effective links.

Metrological Support of Surface Diagnostic at Submicron and Nanometer Scales by Scanning Probe Microscopy

Lytvyn O.S. , Lytvyn P.M., Prokopenko I.V.

V. Lashkaryov Institute of Semiconductor Physics NAS Ukraine, Kyiv, Ukraine

To ensure quality standards in production at submicron and nanometer scales the unity of measurements needed at these ranges [1]. Scanning probe microscopes (SPM) is a unique tool for measurements of geometric, mechanical, electrical and other parameters in the ranges of submicron and nanometer sizes. Accordingly, it was necessary to extend SPM from academic, scientific and research applications to the industrial utilization as measuring equipment. Solution of this problem involved scientists and engineers since the start of SPM mass production. Solving this task can be divided into the three stages. The microscope as a measuring device consists of three parts: 1) a system that implements and controls the relative movement of the tip and sample as well as measures tip-sample interaction, 2) tip that directly carries microscope interaction with the surface, and 3) software algorithms that manage the process of scanning and processing the resulting image. Each of these tasks contribute to accuracy and resolution of measurements and require calibration, verification, and, hence, appropriate methodologies and standards. The lack of methodologies and standards is the main problem of metrological support for some SPM techniques. Measurements of geometrical parameters of surface are more or less regulated by national and international standards [1], the possibility of quantification for nanomechanical properties measurements is extensively studied too [1]. Nevertheless, the electrostatic, magnetic, conductive and capacitive SPM currently used mainly as visualizations tools without the possibility of standardized rigorous quantitative analysis of corresponding characteristics of surface.

This report discusses the problem of creating adequate metrological support of SPM measurements for diagnostic and control assistance both scientific development and some practical industrial implementation aspects.

The National Scientific and Technical Program «Nanotechnologies and Nanomaterials» supported this work.

1. Nanoscale Calibration Standards and Methods. Dimensional and Related Measurements in the Micro-and Nanometer Range / Edited by G. Wilkening, L. Koenders. - Verlag GmbH & Co. KGaA, Weinheim, 2005. - 528 p.

The Infrared Spectra of Thin Films of PbTe:Sb

Achimova E.A.[3], Freik D.M.[2], Kryskov Ts.A.[1], Lyuba T.S.[1], Meshalkin A.Yu.[3], Rachkovsky O.M.[1], Tsykanyuk B.I.[1]

[1] *Ivan Ohienko Kamyanets-Podilsky National University, Kamyanets-Podilsky, Ukraine*
[2] *Vasyl Stefanyk Precarpathian National University, Ivano-Frankivsk, Ukraine*
[3] *Institute of Applied Physics AS of Moldova, Chisinau, Moldova*

All experimental IR spectra of PbTe:Sb thin films were recorded on a Spectrum 100 FTIR spectrophotometer by PerkinElmer. The resolution was set at 1 cm^{-1} and a scan number of 32 was chosen to ensure good signal to noise ratio. The samples were deposited by thermal evaporation on BaF_2 substrate which is transparent in IR region. During all recordings the temperature of 298 K was maintained.

The absorption coefficient and optical band gap are the most significant parameters in chalcogenide thin films. Visible, NIR and IR spectroscopy is a powerful technique to explore the optical properties of semiconducting thin films. The optical transmittance spectrum of PbTe:Sb thin film was measured at room temperature. From the transmittance spectrum we can evaluate the absorption coefficient and optical band gap with the aid of the program PARAV.

The variation of the absorption coefficient as a function of wavelength for PbTe:Sb film is shown in Fig. It is observed that the absorption coefficient decreases with wavelength.

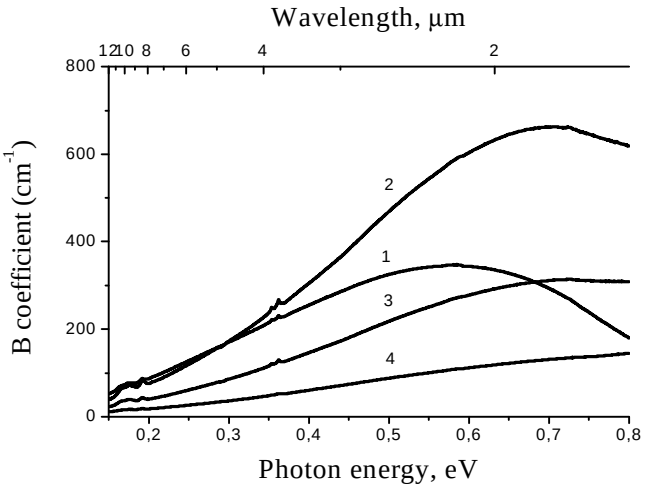

Fig.1. The infrared spectra of thin films of PbTe:Sb: 1 – 0% Sb, 2 – 0,1% Sb, 3 – 0,3% Sb, 4 – 1% Sb

The electronic transition between valence band and conduction band is given by $\alpha h\nu = A(h\nu - E_g)^p$, where A is a constant, α the absorption coefficient, E_g the energy gap, ν the frequency of the incident radiation, and "h" the Planck's constant. The exponent p is 0.5 for direct allowed transitions, 1.5 for direct forbidden transitions, 2 for indirect allowed transitions, and 3 for indirect forbidden transitions [1].

1. Chao I.N. Growth and characterization of IV-VI semiconductor heterostructures on (100) BaF_2 / I. N. Chao, P. J. McCann, W. L. Yuan et.all // Thin Solid Films. – 1998. - vol. 323, no. 1-2. - pp. 126–135.

Termal Stability Phase Composition and Structure of Films Diborides of Hafniuм

Agulov A.V.[1], Goncharov A.A.[1], Vasileva L.V. [1], Stupak V.A.[2], Kudelin Y.V.[3], Pokintelica A.S. [2], Goncharova S.A.[1]

[1]Donbass State Academy of Mechanical Engineering, Kramatorsk, Donetsk reg. Ukraine;
[2]Donetsk National University, Donetsk, Ukraine;
[3]SME «Gormashinstrument», Donetsk, Ukraine

In given article attempt to make the analysis, thermal stability thin wearproof nanostructure on a basis diborides transitive metals is spent. Influence of high temperatures on phase structure, structure and physics-mechanical characteristics of investigated coverings is shown.

Films of borides or nitrides of borides transitive metals are investigated in very limited quantity, basically on a basis diboride of titan [1-3]. Research of thermal stability of films $TiB_{2,4}$ [2] with fine columned (columnar) structure show that the synthesized films keep the structure and superhardness 48,5 GPa at temperature up to 900^{o}C.

Comparison of the structural data to results of research of hardness and the module of elasticity of condensates a method nanoindentation has shown that in system $(W,Ti)B_2$ – a covering - «the silicon substrate» at increase of structural streamlining of a covering which is observed in the range of temperatures
300-700^{o}C, occurs continuous growth of hardness and the module of elasticity from H=28,6 GPa and E=290 GPa at TS=300^{o}C to H=34,6 GPa and E=323 GPa at TS=700^{o}C [2].

That is, for films put in "inadequate" conditions [4] the increase in hardness connected with process of streamlining, i.e. film crystallization is characteristic.

Thus, from the point of view of practical application has interest of research kinetics of process of high-temperature annealing on air depending on temperature and annealing time. The given process represents a great interest from the point of view: to use the given coverings in processing of metals cutting since cutting process occurs in the air. environment and knowing kinetics covering destructions, it will be possible to predict without special work period firmness and time before full breakage of the cutting tool.

1. C. Mitterer, P. H. Mayrhofer and J. Musil. Thermal stability of PVD hard coatings // Vacuum. 2003. V. 71, Is. 1-2, P. 279-284.
2. P. H. Mayrhofer, C. Mitterer, J. G. Wen, I. Petrov,. Thermally induced self-hardening of nanocrystalline Ti–B–N thin films // Journal of Applied Physics. 2006. V. *100 (4).*
3. P.H. Mayrhofer and M. Stoiber. Thermal stability of superhard Ti–B–N coatings // Surf. and Coat. Technol. 2007. V. 201, Issue 13, P. 6148-6153.
4. A. D. Pogrebnyak, A. P. Shpak, N. A. Azarenkov, and V. M. Beresnev. Structures and Properties of Hard and Superhard Nanocomposite Coatings // Usp. Fiz. Nauk. 2009. V. 179. Issue. 52 (1), P. 29–54.

Dispersion of Refractive Index in Thin Y_2O_3 Films at Different Method of Obtained

Antonyuk V.G., Bordun I.O., Opryshko O.Yu.

Ivan Franko National University of L'viv,Lviv, Ukraine

Thin films Y_2O_3 with thickness 0.3–1.5 μm obtained by the method of discrete evaporation and RF-sputtering in this work have been investigated. X-ray diffraction data shoved the polycrystalline structure with predominant orientation in plain (222) and (440).

The dispersion of the refractive index of thin Y_2O_3 films, obtained by the method of the discrete evaporation and RF-sputtering in different atmospheres was investigated. The dispersion dependents $n(E)$ for films Y_2O_3 obtained by the method of the discrete evaporation (I) and RF-sputtering in atmosphere 50%Ar:50%O_2 (II) and RF-sputtering in atmosphere Ar (III) in visible region good approximated one-oscillator threeparametric models:

$$n^2 - A = \frac{E_0 E_d}{E_0^2 - E^2},$$

here A – coefficient of approximation; E_0 – energy of maximum absorbtion band, which determined spectral course of refractive index; E_d – parameter, named dispersion energy.

The parameters of one-oscillator approximation are determined, the dispersion energy E_d, coefficient A and value E_0, ionicity degree f_i and coordination number N_c are calculated.

Crystalchemical and energetic parameters of dispersion curve in thin Y_2O_3 films

Films	A	E_0, eV	E_d, eV	f_i	N_c
I	0.15	6.53	18.29	0.63	2.54
II	0.56	6.52	15.91	0.64	2.21
III	1.32	6.36	13.26	0.69	2.13

The dispersion curve in the visible region, inrespective of a production method, is mainly determined by the transition from the top of the valence band formed by the 2p-states of oxygen to the bottom of the conduction band formed by the 4d5s- states of yttrium.

Magnetoresistance Size Effect in Polycrystalline Bismuth Films

Aseyev A.S., Ravlik A.G.

National Technical University "Kharkiv polytechnical institute", Kharkiv, Ukraine

Bismuth is a convenient matter for observation of various effects in solid state related to carrying of the charge. In particular, the unique combination of charge carrier properties – a long mean free path, low concentration and high mobility of carriers (in comparison to traditional metals) – causes the large-scale magnetoresistive effect even at room temperature.

While investigating the magnetoresistance in vacuum condensed bismuth films, we have found the mutual presence of two axial textures with planes (003) and (012) oriented parallel to the film surface [1]. The formation of the texture types and their perfection were shown to be affected by substrate temperature T_S. Such structural rearrangements have lead to extremum appeared on the T_S dependence of the magnetoresistance $\Delta\rho/\rho_0$ and resistivity ρ_0. In this paper we study the magnetoresistance MR in the field of 2 Tesla and resistivity without magnetic field of bismuth films of various thicknesses h, prepared by electron beam evaporation at definite substrate temperature.

As was revealed, the variation of thickness has no conspicuous effect on the value of ρ_0 of the specimens with T_S at room temperature. This effect is probably caused by insufficiently high level of crystal structure perfection of the films. As film thickness increases the MR is substantially rises and tends to saturate (ref. to fig.).

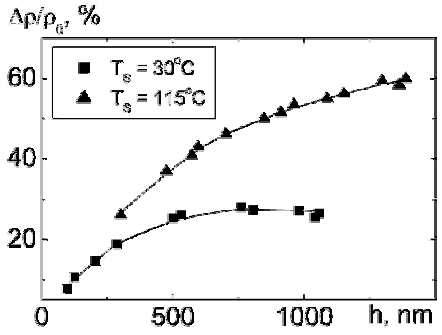

The resistivity of specimens with T_S exceeded 100ºC was noticeably lower than that with T_S at room temperature and ρ_0 was decreasing while thickness rising. Such $\rho_0(h)$ dependence is mostly related to more perfect crystal structure of specimens and the presence of two texture types. The magnetoresistance of the specimens was increasing with thickness increased and also the tendency to saturation has occurred. The observed dependence of ρ_0 on h is the manifestation of classic resistivity size effect, that in turn affects on the MR(h) dependence.

The results obtained allow producing bismuth films with designated values of magnetoresistance and are the data for analyzing the influence of crystal structure on the MR value.

1. Асеев А.С., Авраменко Б.А., Равлик А.Г. , Колупаева З.И. Влияние структурных факторов на магнетосопротивление конденсированных пленок висмута // Вестник ХНУ им. В.Н. Каразина. Серия «Физика». – Харьков, 2012. – №1020. – Вып. 17. – С. 36 – 41.

Raman Spectroscopic Study of Zn-Doped As_2Se_3 Thin Films

Azhniuk Yu.M.[1], Loya V.Yu.[1], Gomonnai A.V.[1],Zahn T.[2]

[1] *Institute of Electron Physics, Ukr. Nat. Acad. Sci., Uzhhorod, Ukraine*
[2] *Chemnitz University of Technology, Chemnitz, Germany*

Raman spectroscopy has proven to be an effective tool for the characterization of thin films providing important information on their structure. With regard to amorphous arsenic chalcogenide films, the application of Raman spectroscopy is considerably encumbered by photostructural changes which are observed in these materials [1–3]. In this case special attention should be paid to the proper choice of the wavelength and intensity of the laser beam being used for excitation.

Here we report on a Raman scattering study of Zn-doped As_2Se_3 thin films grown by a thermal evaporation technique. Micro-Raman measurements were performed using a Dilor XY 800 spectrometer equipped with a CCD camera and a broad set of excitation lines provided by Ar^+ and Kr^+ lasers. Measurements were carried out at room temperature.

For As_2Se_3 films with a low Zn concentration (0.7 %) the observed Raman spectrum basically reproduces the one of undoped As_2Se_3 films with a dominating broad feature centered near 225 cm^{-1}. For more heavily Zn-doped (8.6 %) samples, however, a different behaviour is revealed. In particular, at excitation with the 676.4 nm laser line and at low power density (0.35 MW/cm^2) the observed Raman spectrum strongly resembles that of undoped amorphous As_2Se_3 films. However, at higher power density (0.7 MW/cm^2) two distinct peaks at 196 and 244 cm^{-1} appear on the background of the broad maximum at 225 cm^{-1}. These new peaks are evidence for local irreversible photoinduced changes in the film structure since they do not disappear after the excitation power density is reduced back to 0.35 MW/cm^2. The frequencies of the new peaks are slightly below the values for ZnSe TO and LO phonons, therefore it can be concluded that ZnSe crystallites are formed in the laser spot. The observed new features appear in the Raman spectra of Zn-doped As_2Se_3 film within the acquisition time of 1 min, hence the crystallite formation is quite fast. The behaviour of ZnSe-related Raman features as a function of excitation wavelength and power density is discussed.

1. K. Tanaka, Current Opinions in Solid State & Mater. Sci. 1 (1996) 567–571.
2. A.V. Kolobov (ed.), Photoinduced Metastability in Amorphous Semiconductors, Wiley-VCH, Berlin, 2003.
3. O.I. Shpotyuk, Opto-Electron. Rev. 11, (2003) 19–25.

Mechanisms of Illumination Influence on the Adsorption Processes on the Phthalocyanines Thin Films Surface

Burlachenko J., Snopok B.

V.Lashkaryov Institute of Semiconductor Physics NAS of Ukraine

It was shown that illumination has strong influence on the adsorption processes on the surface of phthalocyanines (Pc) [1].The response to ethanol and water vapors decrease on 18-78 % dependently on Pc type and illumination wavelength. The adsorption kinetics becomes faster and the repeatability of measurements increases. Previously we proposed a new method for the classification of mixtures with dominate components based on suppressing of sensors sensitivities to dominate components in conditions of illumination.

Here we consider possible mechanisms of the light influence on the adsorption processes on the surface of Pc films.

On the figure the responses of QCM sensor with CuPc film as sensitive coating to water vapor are shown. There are three measurement conditions: (1) without illumination, temperature 20 °C, (2) without illumination, temperature 28 °C and (3) under illumination by red light, temperature 20 °C.

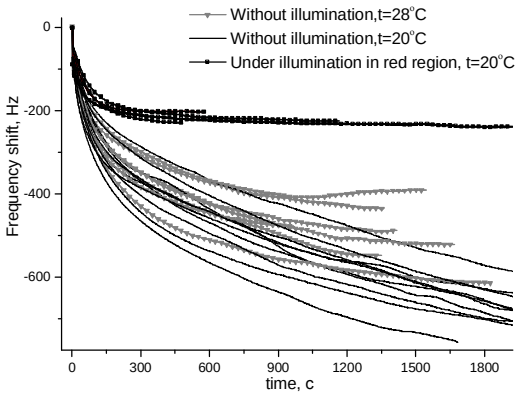

It is clear that illumination has much higher influence on the adsorption processes than temperature. So, the possible heating of the surface due to light absorption is not the mechanism of the illumination influence.

The influence of illumination on the adsorption-desorption processes on the c surface can be explained taking into account the mechanism of light absorption by these materials. It is known that the Q-band of Pc (around 650-700 nm) is concerned with $\pi - \pi^*$ transitions of Pc macrocycle. This causes the significant redistribution of electronic density within the molecule, especially near the nitrogen atoms. In our opinion, this effect together with “switching off” a low-energy adsorption centers (defects of different nature etc.) are the main reason for decreasing of surface adsorption capacity towards some analytes, adsorption kinetics changes and increase of measurement repeatability.

1. J. Burlachenko, B. Snopok Controlling of the adsorption-desorption processes on the surface of chemical sensors coated by photosensitive ptthalocyanine films // Optoelectronics and Semiconductor Techniques.- V. 40 - 2005, p. 136-142.

Structural and Optical Studies of Copper Enriched Thin Films Based on Cu_6PS_5I Superionic Conductors

Chomolyak A.A.[1], Studenyak I. P.[1], Buchuk R. Yu.[1], Izai V. Yu.[1], Kúš P.[2], Plecenik A.[2], Zahoran M.[2], Greguš J.[2], Roch T.[2]

[1]*Uzhhorod National University, Uzhhorod, Ukraine*
[2]*Comenius University, Mlynska dolina, Bratislava, Slovakia*

Cu_6PS_5I crystal belongs to argyrodite family and is well known as a superionic conductor. At room temperature it possesses high ionic conductivity and low activation energy what makes it, similarly to the most efficient solid electrolytes, promising for applications as an electrochemical energy source. It should be noted that the investigations of physical properties of Cu_6PS_5I thin films are only being started.

The thin films were deposited onto silicate glass substrates by radio frequency magnetron sputtering. Co-deposition was performed from two tilted magnetrons – one equipped with Cu_6PS_5I target (pressed powder) and second with pure Cu target. The deposition was carried out at room temperature in Ar atmosphere, the films thickness were 0.5-1.5 μm. Structural studies of copper enriched $Cu_{6.1+x}P_{0.93}S_{4.46}I$ thin films were performed using atomic force microscopy, scanning electron microscopy and energy-dispersive X-ray spectroscopy.

Optical transmission spectra of thin films based on Cu_6PS_5I superionic conductor were studied by an MDR-3 grating monochromator. From the spectrometric studies of interference transmission spectra, the spectral dependences of the absorption coefficient (or the extinction coefficient) as well as dispersion dependences of the refractive index were derived. Besides, the optical pseudogap values E_g^* (E_g^* is the absorption edge energy position at the fixed value of the absorption coefficient α=10^3 cm^{-1}) and Urbach energy values E_U (E_U is the energy width of the exponential absorption edge) were determined.

It is shown that with copper content increase the red shift of both the short-wavelength part of the absorption spectrum (related to the temperature behaviour of the absorption edge), and the interferential maxima were observed. Besides, the broadening of short-wavelength part of the absorption spectrum as well as the decrease of transmission in the interferential maxima with copper content increase were revealed. The optical pseudogap decrease and refractive index increase with copper content increase in thin films based on Cu_6PS_5I superionic conductor were observed.

Post-Deposition Thermally Driven Formation and Morphology of Thin Metal Nanoparticle Films

Dmitruk N. L., Dvoynenko M. M., Taborska M. I., Romanyuk V. R.

Institute for Physics of Semiconductors NAS of Ukraine, Kyiv, Ukraine

Thin metal films are important element of various photonic devices based on surface plasmons excitation. With resonance matching of the exciting light frequency and the frequency of surface plasmons, it is possible to reach a maximal increase of near-surface electromagnetic field together with corresponding enhancement of intensity of various photophysical phenomena. Therefore the ability of surface plasmon resonance (SPR) frequency control is very desirable [1], especially in sensorics, SERS and SEIRA applications, where vibrational spectra suffer from low absorption cross-section. Besides, as was shown recently, the morphology of discontinuous metal film (island size and inter-island gaps) may have influence on surface-enhanced spectra obtained.

Typically, nanoparticle sizes and interparticle distances on a substrate are controlled during nanoparticle growth in wet chemical or electrochemical processes. In this work ultrathin gold nanoparticle films with mass thickness from 3 to 20 nm, thermally evaporated in vacuum on the glass substrates, were investigated. The morphology of these films was intentionally modified by post-growth annealing which caused optical properties change, especially in the region of SPR excitation.

Structure and morphology of films were examined with SEM and AFM techniques. Statistical analysis of nanoparticle sizes and interparticle distances shown that nanoparticle array characteristics, formed after thermal treatment, depend on initial film mass thickness, temperature and annealing duration. The conditions allowing fabrication of relatively narrow size distributed island films with average particle size from 15 to 60 nm have been determined.

Optical parameters of thin Au nanoparticle films were determined from transmittance/reflectance spectroscopy (350-1100 nm) of polarized light. An implementation of various effective medium approximations for observed morphologies of island films is discussed. These results are very important for many applications exploiting plasmonic field enhancement, notably in polaritonic optoelectronics, plasmonic photovoltaics and sensorics.

1. V.R.Romanyuk, O.S.Kondratenko, S.V.Kondratenko, A.V.Kotko, N.L.Dmitruk Transformation of thin gold films morphology and tuning of surface plasmon resonance by post-growth thermal processing. *Eur. Phys. J. Appl. Phys*. – 2011.-V.56. -P.10302-10307.

High Temperature Oxidation of NiSi and $NiSi_2$ Film

Dranenko A.S., Koshelev M.V.

Frantsevich Institute for Problems of Materials Science of NASU, Kyiv, Ukraine

Nickel silicides are one of the most widely studied silicide systems due to their high temperature performance and microelectronics application. They are widely used in microelectronics as interconnectors, ohmic contact, and gate materials for integrated circuits. Characteristics which make them promising high temperature electronic materials include chemical and thermal stability.

In this work the phase formation and thermal oxidation stability of NiSi and NiSi2 thin films on n-type Si (111) substrates have been investigated. The objects to study were thin-film layers of Ni (200nm) on crystalline Si substrate of orientation (111) doped with phosphorus. Thin-film system Ni/Si obtained by electron-beam deposition in vacuum $2 \cdot 10^{-4}$ Pa. After deposition the samples were annealed in a furnace with oil-free vacuum pumping $1.33 \cdot 10^{-3}$ Pa in the temperature range 470 – 1270 K.

For phase identification was performed in ″Electronograph EMR-100″ using reflection diffraction method. The thermogravimetric analysis (TGA) was carried out in ″Derivatograph Q-1500D″ thermoanalytical instrument. The sample mass of 20mg was heated in a platinum crucible in static air atmosphere at a rate 5 K/min and a maximum temperature of 1270 K.

The values of interplanar distances were compared with tabulated values. In the initial state in thin-film system Ni (200 nm)/Si with a layer of ″natural″ oxide SiO_2 (~ 6–10 nm) was present nickel phase. At annealing temperature 770 K a number of nickel phase remains after annealing the system. Further increase in annealing temperature to 970 K leads to formation of Ni_2Si and NiSi. Remaining phase of nickel is not observed. Nickel disilicide $NISi_2$ formed at temperature of 1270 K.

According to data TGA, oxidation of silicon substrate and silicide films can be concluded that the oxidation of the films and the associated increase in weight begins at about 250 degree higher than the oxidation of a silicon substrate. As temperature rises (up to 1270 K), the rate of oxidation increases and weight gain for the films is much smaller (~2.5 times) than the silicon at the same temperature. For both NiSi and $NISi_2$ oxidation types the SiO_2 thin protective layers have been formed. The oxidation of NiSi film is beginning at 930 K that is by 100 K lower than in case of $NISi_2$. With the increase of NiSi film mass gain proved to significantly higher than that for $NISi_2$ film, and at 1270 K this difference is by 3 times more that is explained by the difference of their structure and stoichiometry.

Magnetization Reversal of Synthetic Antiferromagnets Using Magnetic Field Pulse Perpendicular to Reference Plane

Dzhezherya Yu.[1], Iurchuk V. [2], Demishev K.[2], Korenivski V. [3]

[1]*Institute of Magnetism, National Academy of Sciences of Ukraine, Kiev, Ukraine*
[2]*National Technical University of Ukraine "Kiev polytechnic institute", Kiev, Ukraine*
[3]*Royal Institute of Technology, Stockholm, Sweden*

The properties of novel systems – so-called synthetic antiferromagnets (SAF) which are the basic elements for magnetoresistive random-access memory (MRAM) cells – are widely studied now. SAF consists of two dipole-coupled elliptical magnetic layers with a small aspect ratio separated by thin non-magnetic spacer. Previous works devoted to the investigation of spin dynamics revealed collective acoustical and optical spin resonant modes in such systems. High-frequency investigations of the two coupled macrospins in SAF cell showed that system's behavior is similar to Kapitsa pendulum. In-plane AC magnetic field was proposed to use for the cell's state operation.

Here we study the magnetization dynamics of SAF for the case when the external magnetic field is perpendicular to cell's basic plane. Switching conditions between SAF's equilibrium states have been considered. It has been shown that at definite conditions a high-speed switching without any relaxation processes can take place.

A major problem in controlling the magnetization process in SAF is to organize a switching between two ground states with opposite values of antiferromagnetism vector to avoid long-lasting relaxation processes. Analysis of SAF dynamics equations in different external perpendicular magnetic field configurations allows deriving an optimal profile for the excitation field as

$$H_z(t) = -H_0 / ch(nt), \qquad (*)$$

where H_0 is the field amplitude and n is the pulse duration parameter. No relaxation oscillations near the new equilibrium state should be observed for such field profile. The amplitude of the external field can be reduced by adjusting of the duration parameter, which is extremely important for MRAM operation. It should be noted that remagnetization can be done using the field pulses with the shape close to (*) (e. g. Gaussian or Lorentzian) but in this case we cannot totally avoid the damping oscillations during transition to the new SAF state.

The possibility to operate SAF cell using by means of perpendicular magnetic field pulses has been demonstrated. It has been shown that remagnetization of the system can be realized in non-inertial mode using field signals of a specific shape.

Structural and Optical Properties of Si and Ge Nanocrystal Arrays in Oxide Matrices Prepared by Annealing of Multilayer Structures

Ershov A.V., Grachev D.A. , Malekhonova N.V., Pavlov D.A.

Lobachevsky State University of Nizhni Novgorod, Nizhni Novgorod, Russia

A direction of solid state electronics evolution is integration with optical semiconductor devices on one chip. A modern common technology bases on silicon. There is a fundamental prohibition to make light emitting diodes of bulk silicon, but ordered arrays of silicon quantum dots in the dielectric matrices is a way to fabricate new devices such as durable flash memory and LEDs integrated in a standard planar CMOS process. Germanium quantum dot approach is close to silicon technology enough to form similar structures using the same method.

The test samples were multilayered nanoperiodical structures Ge/SiO_2 and $SiO_{x\approx1}$/Oxide, 5-10 nm 10-30 periods, containing silicon or germanium nanocrystals. They were obtained by vacuum evaporation from separate sources. The systems were annealed at 500-1100 °C during 0.5-2 hours with using dry nitrogen, where oxide was one of SiO_2, Al_2O_3 or ZrO_2. Atomic scale structural studies were carried out by high resolution transmission electron microscopy by JEM-2100F apparatus. Photoluminescence spectra were investigated in the range of 350-900 nm with excitation at 337 nm or 448 nm at room temperature.

The hottest temperature influence leads to synthesis of crystalline silicon nanoparticles. Their location follows the initial structure. Diameters of nanocrystals were approximately equal to original thickness of SiO_x layers; its density was about $1 \cdot 10^{12}$ cm^{-2}. When varying the the SiO_x thickness, the size of quantum dots was controlled, which was confirmed by photoluminescence. They produce diameter-depended radiation in wavelength range 750-850 nm.

According to high resolution electron microscopic images the Ge/SiO_2 structures consist of continuous layers with sharp boundaries. In the annealed structures it was observed nanocrystals in the amorphous phase. On the photoluminescence spectra there are two peaks, 380 nm and 430-480 nm wavelength ranges. This light emission is likely to be caused of irradiation transitions from defect levels at the Ge/SiO_2 interface.

It is argued distinctive features of the directed temperature modification in the cases of using different dielectric materials. Ge quantum dot application is due to its high compatibility with high-k dielectric host thin films. Also it is discussed the abilities to observe the quantum size effects in the optical properties of the structures.

Electric Relaxation Processes in Electret Films

Fedosov S. N.

Odessa National Academy of Food Technologies, Odessa, Ukraine

The electret state of dielectrics is usually studied by the surface potential decay method, but obtained information is rather limited. A new method of a constant corona charging was successfully introduced for studying space charge and polarization processes in electrets. We suggest here to combine advantages of the electret potential decay method and the constant current corona method.

The principle consists in analyzing the electret potential during the application of rectangular current pulses of infra-low frequency. The current is supplied by a corona triode in such a way that the whole process of the charging is divided into several cycles, each consisting of a stage of the potential growth and a stage of the potential decay when the charging current is zero.

The method was applied for studying corona poling and electric relaxation in polyvinylidenefluoride (PVDF). The current pulses were produced by a corona triode and applied to a PVDF samples of d=25 μm thickness. The control grid was made vibrating for continuous surface potential measurement by Kelvin's method during both charging and discharging stages. The current density was set at I=80 μA/m^2 and the charging time of each cycle was T=300 s. The potential of 3 kV was reached after application of 10-12 cycles.

By solving differential equations we obtained the following formulae for the surface potential during charging and the potential decay

$$V(t) = \frac{Id}{g} + \left(U - \frac{Id}{g} \right) \exp\left(-\frac{t}{t_o} \right) \text{ at } t<T, \tag{1}$$

$$V(t) = \left[\frac{Id}{g} + \left(U - \frac{Id}{g} \right) \exp\left(-\frac{T}{t_o} \right) \right] \exp\left(-\frac{t-T}{t_o} \right) \text{ at } t>T \tag{2}$$

where g is the apparent conductivity, U the residual potential after a preceding cycle, t the time from the beginning of each charging-discharging cycle, t_o the Maxwell relaxation time.

By fitting experimentally observed electret potential curves to Eqs. (1-2) we were able to separate contributions of ε and g to the relaxation time t_o and to follow their dynamics during poling. During corona poling, the dielectric constant and conductivity can be considered as not material constants, but rather apparent parameters dependent on the electric state of the dielectric. Therefore, their analysis can give valuable information on space charge and polarization processes in such dielectrics.

The proposed method might have some limitations in the case of very stable homoelectrets. However, it is reliable and convenient, if applied to dielectrics with noticeable conductivity, such as polar or ferroelectric polymers.

Pyroelectric Activity and Switching of Polarization in Polyvinylidene Fluoride Films

Fedosov S.N.[1], Seggern von H.[2], Sorokina A.G.[1]

Odessa National Academy of Food Technologies, Odessa, Ukraine
Darmstadt Technological University, Darmstadt, Germany

Pyroelectric study of polyvinylidene fluoride (PVDF) films is of great interest, because PVDF is widely used for the manufacturing of pyroelectric sensors. The aim of our study was to compare curves of the pyrocoefficient with the corresponding curves of the residual polarization in PVDF films.

Experiments were carried out on the stretched samples of Kureha Co. (Japan) PVDF having thickness of 12.5 microns with gold electrodes of 0.2 cm^2 area deposited by the cathode sputtering. For initial electrification voltage of 2.0 kV was applied to the sample through an electronic switch during 200 sec in order to insure the uniform ferroelectric polarization of the order of 9.2 $\mu C/cm^2$.

Polarization switching has been performed by applying a high voltage (from 0.5 to 2.0 kV) of the opposite polarity during a definite time in a wide time range from 10^{-6} to 100 sec. The value of the switched polarization was determined by processing the voltage pulses on the measuring 0.2 μF serial capacitor after the switching, short circuiting, and forward poling with the application of high voltage without changing its polarity.

After each switching of polarization we measured the pyrocoefficient by a Collins dynamic method of a heat wave. Light pulses of 50 ms duration were generated by flash Metz 45 CT-3, and illuminated the surface of the metal electrode used as a source of the heat waves. Pyroelectric current and voltage on the measuring capacitor were recorded using a broadband oscilloscope Tektronix TDS 510A. By measuring the pyroelectric coefficient we have found that the total polarization switching occurred when the duration of the switching pulse voltage of 2.0 kV was more than 100 sec.

It was found that the polarization switched by several consecutive short voltage pulses was much smaller than the polarization switched by a single voltage pulse, the duration of which was equal to the total time of the multiple pulses application. This indicated that the distribution of the switching times exists.

The joint study of the pyroelectricity and the polarization switching in PVDF films have showed that the corresponding curves of the pyrocoefficients and polarization dependences from duration of the voltage pulses and from the voltage values are almost identical. This allowed us to conclude that the value of the ferroelectric polarization, which usually obtained after complex measurements and calculations can be easily estimated using a rather simple method of the pyroelectric measurements.

Electrochromic Properties of Niobium (V) Oxide Films

Fomanyuk S. S., Krasnov Yu. S., Kolbasov G. Ya.

Vernadskii Institute of General and Inorganic Chemistry of the Ukrainian National Academy of Sciences, Kyiv, Ukraine

It is known that most of the metal oxide films possess electrochromic effect. Niobium oxide (V) of nanocrystalline structure is the least studied electrochromic material. Of particular interest are films electrochemically deposited from aqueous electrolyte solutions. This procedure allows one to obtain optically homogeneous thin film, and is distinguished from others by simplicity and relatively lowcost. The optimal composition of the electrolyte and the parameters of deposition of niobium (V) oxide films from aqueous electrolyte based on hydrogen peroxide and sulfuric acid. Analysis of optical absorption spectra of the electrolyte solution showed that it consists of complex compounds of niobium acid with hydrogen peroxide. It has been found that the electrochromic properties of niobium (V) oxide films depend on the mode of electrodeposition and solution pH. Films obtained at more negative potentials and the lowest value of pH, had larger nanocrystals (20-100 nm), and a content of crystal water (of to 20 mol.%). The optical spectra in Fig. 1 show that the films deposited at potentials of +300 to 0 mV absorb light in the visible spectrum it the case of electrochromic coloring, while the films deposited at potential values from 0 to -500 mV had a broader absorption band in the visible and near-IR regions, it the case of electrochromic coloring.

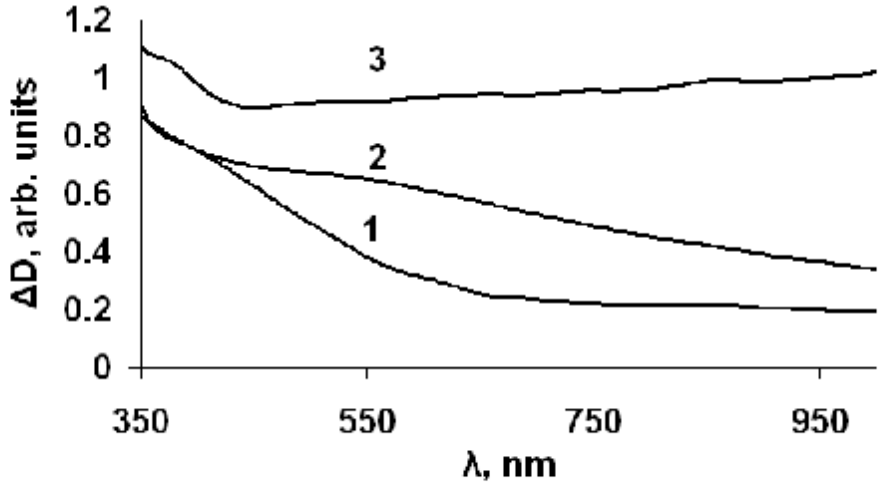

Fig. 1 Coloring spectra of Nb_2O_5 films at potential - 1B in 1 mol / L $LiClO_4$ in propylene carbonate, obtained by electrodeposition at potentials: +200 mV (1), 0 mV (2) and -200 mV (3) from a solution of niobium peroxocomplexes on electrodes with conductive SnO_2 layer.

Photoinduced Changes of Transmission Spectra of Sb_xSe_{1-x} Thin Films

Gera E.V.[1], Pop M.M.[2], Maryan V.M.[1], Yasinko T.I.[1], Durkot M.O.[1], Mykulanynets-Meshko O.S.[1], Tarnaj A.A.[1], Shpyrko G.N.[1]

[1]*Uzhgorod Scientific-T echnological Center of the Institute for Information Recording, NASU, Uzhgorod Ukraine*
[2]*Uzhgorod National University, Uzhgorod, Ukraine*

This paper presents the results of investigation of laser radiation influence on transmissions spectra and optical parameters of Sb_xSe_{100-x} ($3 \le x \le 30$) amorphous films.

Thin films were obtained on unheated glass substrates by way of vacuum evaporation of glasses and alloys of corresponding compositions from quasiclosed effusion cells. The thickness of films was 1 μm. Investigation of transmissions spectra of films was carried out by means of "МДР-23" spectrometer in the wavelength region of 550-1100 nm at 300 K. Disfocused radiation of semiconductor laser (λ=530 nm, P=100 mW) was used for exposure of films.

Table. Values of the pseudogap width E_g, (eV), and refractive index (n) for Sb_xSe_{100-x} films versus the exposure time.

		Exposure time, min			
		0	1	5	10
Sb_3Se_{97}	E_g	1,949	1,941	1,928	1,926
	n	2,527	2,532	2,550	2,687
Sb_5Se_{95}	E_g	1,947	1,942	1,940	1,939
	n	2,510	2,536	2,574	2,598
$Sb_{10}Se_{90}$	E_g	1,932	1,927	1,926	1,925
	n	2,423	2,437	2,461	2,482
$Sb_{30}Se_{70}$	E_g	1,702	1,686	1,684	1,682
	n	2,827	2,861	2,878	2,971

The investigations have shown that with growing of antimony content in the composition of Sb_xSe_{100-x} films, transmission spectra are shifted into longwave range testifying to decrease of pseudoforbidden gap width (E_g) and increase of refractive index (n) of films (Table). The values of E_g were determined from Taus relationship ($\alpha(h\nu)=B(h\nu-E_g)^2/h\nu$). The slope of the edge changes significantly with increasing concentration of antimony. This indicates a change in the type of structural matrix during the transition from Se to Sb_2Se_3 – from a chain-ring structure of selenium to a random two-dimensional structure based on trigonal pyramids $SbSe_{3/2}$.

Laser exposure of Sb_xSe_{100-x} films results in a shift of absorption edge to the longwave range. It means one observes photodarkening of the films.

The value of E_g is decreasing and n – increasing (Table). The maximum shift (ΔE) of the absorption edge takes place in the film with Sb content 30 at. % under the same exposure conditions.

Photoluminescence and Structural Properties of High Quality CdSe Films Deposited by Closed Space Vacuum Sublimation

Gnatenko Yu. P.[1], Bukivskij P. M.[1], Faryna I. O.[1], Opanasyuk A.S.[2], Dobrozhan O. A.[2]

[1]*Institute of Physics of NAS of Ukraine, Kyiv, Ukraine*
[2]*Sumy State University, Sumy, Ukraine*

CdSe films with direct bandgap energy about 1.75 eV at room temperature have *n*-type conduction and high photosensitivity in the visible spectral region. At present, such films are intensively studied. It is caused by the fact that they are suitable material for elaboration of a number of optoelectronic devices such as photoelectrochemical solar cells, photo- and gas detectors, high-performance thin film transistors, gamma ray detectors, light-emitting diodes, etc. Furthermore, CdSe thin films can also be used as the absorber layers in the top of tandem solar cells and they are considered to be an important material for photovoltaic applications.

In this work, we study the photoluminescence (PL) and structural properties of CdSe films deposited on the glass substrates by means of closed space vacuum sublimation technique. Comparison of the CdSe films PL properties deposited at different substrate temperatures with the results of the structural investigations allowed us to determine the optimal conditions of their deposition. The energy position of the exciton PL lines and the bands, caused by the donor-acceptor recombination, have been analysed as a function of the substrate temperature. This allowed to determine the nature and the energy structure of intrinsic and impurity defects as well as to evaluate the optical quality of the investigated thin films.

CdSe polycrystalline films were deposited on the glass substrates at the evaporator temperature T_e = 700 ^{0}C. The substrate temperature T_s varied from 200 ^{0}C to 600 ^{0}C, a growth time was 10 minutes. The films obtained at T_s < 400 ^{0}C have a highly dispersed structure with the grain size (d) from 0.1 μm to 3.0 μm. In this case the layer-by-layer mechanism determines the layers growth process. At $T_s \geq$ 400 ^{0}C the films have a columnar-like structure with the clear growth texture. For T_s = 600 ^{0}C the films with grain size D =(3-4) μm and layers thickness l = (5-6) μm were obtained. In this case the crystallites are preferentially oriented with the (102) planes parallel to the substrate.

The presence of a narrow intensive D^oX-line caused by the excitons bound to neutral donor in PL spectrum of CdSe films obtained at T_s = 600 ^{0}C indicates about the high optical quality of the investigated films which are n-type. Besides, another PL bands observed which are due to DAP recombination. It was shown that the donor and acceptor centers in CdSe films are mainly caused with Li(Na) resudial impurities.

This research was supported by the Ministry of Education and Science of Ukraine (Grant № 52.21.04-01.13/15 ЗФ).

Optical and Photoelectric Properties of $Cd_{1-X}Mn_XTe$ Thin Films

Gnatenko Yu.P.[1], Bukivskij P.M.[1], Faryna I.O.[1], Gamernyk R.V.[2], Kosyak V.V.[3], Koval P.V.[3]

[1]*Institute of Physics of NAS of Ukraine, Kyiv, Ukraine*
[2]*Lviv National University, Lviv, Ukraine*
[3]*Sumy State University, Sumy, Ukraine*

Semimagnetic or diluted magnetic semiconductors are promising materials for various applications in modern optoelectonics. Recently this material is also considered as alternative to $Cd_{1-x}Zn_xTe$ solid solutions in room temperature radiation detectors. It should be noted that the segregation coefficient of Mn atoms in CdTe is less than of Zn, about укажите значение and 1.35 respectively. The special interest is devoted to polycrystalline $Cd_{1-x}Mn_xTe$ films since it can be used as a base layer in compact and cheap radiation detectors.

The photoluminescence and Raman spectroscopes are powerful methods for the study of electronic and vibrational properties of semiconductor materials including the determination of their crystal phases and the nature and energy structure of intrinsic and impurity defects. Also the photoelectric measurements could be used to obtain additional information relative to various defects and photosensitivity of the investigated materials.

In this work the studies of the photoluminescence and Raman scattering as well as photo-diffusion current spectra of $Cd_{1-x}Mn_xTe$ films were carried out. The main goal of present study is to determine the effect of growth conditions on chemical composition and optical quality of the films deposited by close-spaced vacuum sublimation technique.

The Raman scattering spectrum for $Cd_{1-x}Mn_xTe$ films obtained at the substrate temperature T_S=400 ^{0}C shows the peaks at 179 and 204 cm^{-1} which can be associated with Mn-like LO-phonons of hexagonal and cubic symmetry, respectively. Other peaks at 353 and 408 cm^{-1} are correspond to 2LO-phonons, while the presence of peak at 644 cm^{-1} may be due to 3LO-phonon. The increasing of substrate temperature to T_S=500 ^{0} C lead to substantial increase in intensity of the peak at 204 cm^{-1} as well as its 2LO-phonon line. It indicates the transition of MnTe crystal phase from hexagonal to cubic. This, in turn, provides formation of $Cd_{1-x}Mn_xTe$ solid solution. Low-temperature photoluminescence investigations of $Cd_{1-x}Mn_xTe$ films indicate improvement of their optical quality due to solid solutions formation. The joint photoluminescence and photodiffusion current analysis allowed us to determine a manganese concentration in different films which changes from 2% to 4%.

This research was supported by the Ministry of Education and Science of Ukraine (Grant № 52.21.04-01.13/15 3Ф).

Computer Simulation of Plasmochemical and Electronic Processes on the Semiconductors' Surface with Quantum-Size Structures

Grankin D.V.

Priazovskyi State Technical University, Mariupol, Ukraine

When the atomic particles from plasma interact with the surface of solids, the nonequilibrium phenomena are possible, which are associated with the electronic excitation of solid. The nonequilibrium processes of the atomic particles interaction with the surface and the energy exchange in the acts of "gas – solid" interactions determine the behavior of the catalytic structures, semiconductor opto- and microelectronics, protective coatings reentry spacecrafts. Creation of the nanoscaled structures on the surface changes the optical, electrophysical, magnetic, catalytic and other surface properties. This paper considers the impact of nanostructures on the catalytic and optical properties of semiconductors.

We investigate the chemiluminescence (CL) of Zn_2SiO_4-Mn, which was excited by the recombination of H-atoms on the surface. A bright CL was observed in the visible spectrum with λ_{max} = 525 nm. The samples of the willemite with the deposited Pd-nanodots were also applied. The nanodots were deposited using "reverse-micelles" method. The Pd clusters sizes lay in the range of (3–12) nm. The samples also had a system of the electron traps, which act as the centers of energy accommodation via the electronic channel.

It was obtained that irradiation of Zn_2SiO_4-Mn by the UV light from the intrinsic adsorption band leads to increase in accommodation rate of reaction heat of H-atoms recombination via electronic channel by more than two orders of magnitude. This effect is associated with a high efficiency of accommodation of the reaction energy via electronic channel with participation of the electron traps. On the other hand we found that the deposition of Pd-nanodots on the surface leads to the total luminescence quenching. It is concluded that the effects were associated with the accommodation of energy of the vibrationally-excited precursor molecules H_2^v via the electronic channel.

The model of plasmochemical and electronic processes on the spatially inhomogeneous surface was created, according to which it was carried out the computer simulations.

We obtained the dependencies which illustrate the effect of the characteristics of nanodots on the luminescence intensity and the rate of the plasmochemical processes, depending on the concentration of the spatial centers of accommodation and its configuration.

In simulations we demonstrate that the deposition of nanodots leads to luminescence quenching up to its complete disappearance.

Thermoelectric Properties of *p*-PbSnTe Thin Films

Ivanov V.A.[1], Gremenok V.F.[1], Seidi H.[1], Bente K.[2], Lazenka V.V.[2]

[1] *State Scientific and Production Association "Scientific-Practical Materials Research Centre of the National Academy of Sciences of Belarus", Minsk, Belarus*
[2] *Institut für Mineralogie, Kristallographie und Materialwissenschaft, Leipzig, Germany*

Lead-tin telluride ($Pb_{1-x}Sn_xTe$) alloys are materials with good thermoelectric properties [1,2] and also are semiconductors of current interest for possible applications as long wavelength infrared detectors. Ternary $Pb_{1-x}Sn_xTe$ alloys are narrow gap semiconductors characterized by an energy gap that is linearly proportional to the tin concentration *x*. At 4 K, the energy gap of PbTe is 190 meV and pure SnTe (corresponding to x=1) is a *p*-type semiconductor with energy gap of ~200 meV [3]. The $Pb_{1-x}Sn_xTe$ compound is a *p*-type semiconductor whose carrier concentration increases with increasing *x* [2]. The physical properties of $Pb_{1-x}Sn_xTe$ thin films are influenced by the elemental composition and substrate temperature. The purpose of this study is to prepare by hot wall vacuum deposition of bulk material onto glass substrates and investigate a thermoelectrical properties of the $Pb_{1-x}Sn_xTe$ thin films (x = 0.05 – 0.95). The $Pb_{1-x}Sn_xTe$ films were deposited at different substrate temperatures.

Thermoelectric properties (Seebeck coefficient) of the films were investigated at the room temperature. The temperature difference between the „hot" ends and „cold" ends of the probes was $\Delta T = 25$ K.

The as-deposited films were high densely packed, pinhole free, microcracks free and strongly adherent to the surface of the substrate. The films obtained were polycrystalline monophase in nature and had a cubic crystal structure. The thickness of the films varied from 0.9 to 2.3 μm. The as-prepared films showed *p*-type electrical conductivity, which is confirmed by the thermoelectric probe measurement. The Seebeck coefficient and the conductivity of the films was in the range of α = 20 - 400 μV/K and $\sigma = 3 \cdot 10^1 - 1 \cdot 10^4$ $\Omega^{-1} \cdot cm^{-1}$ respectively, at room temperature depending on concentration of the lead in the films. The increase of concentration of lead atoms leads to increase of Seebeck coefficient and decrease of conductivity.

The reported results give an indication that the technologies using hot wall deposition of the PbSnTe thin films may find applications in the fabrication of thin film thermoelement.

1. Goldsmith J.H. Thermoelectric Refrigeration, Plenum, New York. - 1964.
2. Jovovic V., Thiagarajan S.J. Low temperature thermal, thermoelectric, and thermomagnetic transport in indium rich $Pb_{1-x}Sn_xTe$ alloys // Journal of applied physics. – 2008. - V.6. - P.053710.
3. Nicolic P.M. Optical energy gaps of PbSe-SnTe, PbTe-SnTe and PbTe-SnSe // Brit. J. Appl. Phys. – 1967. - V.18. - P.897-903.

Electric and Photovoltaic Properties of ZnO/*p*-CdTe Surface-Barrier Structures

Khomyak V.V, Ilashchuk M.I, Parfenyuk O.A, Gavaleshko N.M

Chernivtsi National university named after Yuri Fedkovych, Chernivtsi, Ukraine

Zinc oxide belongs to the semiconductor materials that are quite intensively studied in the present. Transparency of ZnO in a wide spectral region (E_g=3.3 eV at T=300K) combines with its high resistance to radiation. That is why the practical usage of ZnO in heterojunctions as wide-gap semiconductor for the transparent part of structure is of special interest. Taking into account the prospects of cadmium telluride for photovoltaic transformation of solar radiation, creation of ZnO/*p*-CdTe structures and investigation of their properties are rather actual .

In this paper the results of electric and photovoltaic properties of ZnO/*p*-CdTe heterojunctions are presented. These structures were fabricated by zinc oxide thin films deposition onto freshly cleaved CdTe substrates by means of magnetronic sputtering.

CdTe single crystals were grown by Bridgman method at low pressure of Cd vapour ($P_{Cd} \approx 2.0 \cdot 10^3$ Pa). Concentration of holes and their mobility found from the electric properties of crystals were $3{,}0 \cdot 10^{15}$ cm^{-3} and 70 $cm^2 \cdot V^{-1} \cdot s^{-1}$ respectively.

Investigated surface-barrier structures ZnO/*p*-CdTe had good rectifying properties. The height of the potential barrier estimated from direct branches of *I-V* characteristics equaled to 0,7eV at *T*=295K. The analysis of *I=f(V)* dependences showed that the tunnel-recombination processes involving energy levels with a depth of 0,13 eV play the dominant role in formation of currents through the barrier at direct and reverse voltages. It is known that these levels in CdTe are due to the complex defects of $\left(V_{Cd}^{-2} D^{+}\right)^{-1}$.

It is determined that linear dependence of barrier capacitance on voltage is observed in $1/C^3 = f(V)$ coordinates. This indicates at the smooth distribution of uncompensated acceptor impurity in barrier locking layer of heterojunctions under the research. Since the properties of the initial CdTe are determined by acceptor defects (V_{Cd} or associates with their participation), their gradual decrease in the direction to barrier border can be explained by diffusion of Zn atoms and their placement in cadmium sublattice during manufacture of structures.

Obtained heterojunctions were characterized by rather high photosensitivity. When illuminated by the radiation close by power and spectral distribution to sunlight open circuit voltage, short-circuit current and filling factor equaled to: V_{xx} = 0,62 V; $I_{кз}$ = 0,28 mA; *F*=0,63 respectively.

The Influence of Density of Porous Silicon on the Electrical Parameters of Transistors

Khrypko S.L.[1], Kidalov V.V.[2]

[1] *Classical Private University, Zaporozhye, Ukraine*
[2] *Berdyansk State Pedagogical University, Berdyansk, Ukraine*

Annotation. In work the received concrete results about influence of conditions of electrochemical anodizing on the main parameters of the porous silicon: thickness, porosity, density, the sizes. Processes of anodizing show the opportunity of management. Were brought up epitaxial a film on porous silicon, which had a high level of perfection.

The use of porous silicon (PS) in electronic technologies sufficiently wide. Currently, the technology of manufacturing of electronic devices comprising the steps towards the formation of effective sinks for defects and rapidly diffusing impurities [1]. Practical implementation of the controlled process epitaxial on PS would create a new design of semiconductor devices, to improve their electrical parameters, increase reliability.

For research were used wafers of silicon grown by the Czochralski method, the p-type conductivity, boron-doped with a resistivity of 10 ohm·cm, diameter 76 mm, thickness of 380 microns, disoriented by 40 relative to the plane (111). Transistor structures fabricated by planar-epitaxial technology with individual n + and p + hidden layers doped with antimony and boron, respectively. Formation of PS layers was carried by the method of electrochemical treatment in the electrolyte based on hydrofluoric acid [2] in the galvanostatic mode at a current density in the range of 5 - 50 mA/cm^2.

When PS 1,1-0,8 g/cm^3 density decreases the breakdown voltage of collectors in-base and emitter-base junctions. The results may be useful for manufacturers of semiconductor devices and integrated circuits.

1. Zholudev G.K., Khrypko S.L. Study gettering in silicon transistor structures // Russian Microelectronics. 1996. – T.**25**. – №6. – P. 436 – 441.
2. Zholudev G.K., Khrypko S.L. Influence of a hydrochloric acid on mechanisms of creation of porous silicon// Physics and chemistry of solid state. – 2009. – т.**10**, №1. – p. 149-156.

Diffusion Parameters of Transition Metals in Zinc Selenide

Kinzerska O.V. [1], Tkachenko I.V. [1], Pohrebennyk V.D. [2], Pashuk A.V.[2]

[1] *Yuri Fedkovych Chernivtsi National University, Chernivtsi, Ukraine*

[2] *V. Chornovil Institute of ecology, environmental protection and tourism University National "Lviv Polytechnic", Lviv, Ukraine*

Most recently intensively investigated wide-II-VI compounds doped with transition metals, which possessing a number of specific properties. Among of them a special place is occupied by zinc selenide as one of the most promising optoelectronic materials. Since active regions most devices are thin semiconductor layers, the primary task is to choose the optimal technology for their reception. Analysis of the literature shows that doping of II-VI compounds 3d-elements are diffusion from the vapor phase in a closed volume, which allows to obtain sufficiently uniform distribution of impurities in each section of the diffusion layer. To ensure reproducible technology production of doped layers need information about the basic parameters of diffusion of impurity elements. In particular these include the diffusion coefficient D and surface concentration N_s diffusant, which actually determines the solubility of impurities in the surface layer of the semiconductor. Tasked in this paper is solved for the diffusion layers of zinc selenide doped with several transition metal atoms Me (Ti, V, Cr, Mn, Fe, Co, Ni). The process was carried out in evacuated to 10^{-4} Torr and sealed quartz ampulla at 1200°C within a few hours. The diffusion coefficient was determined by the formula $D \approx d^2/t$. Thickness d of the diffusion layer is determined visually using an optical microscope. Surface concentration of transition metals in layers ZnSe: Me measured by X-ray analysis, and the parameters D and N_s shown in the table.

Me	Ti	V	Cr	Mn	Fe	Co	Ni
D, cm^2/s	$7\cdot10^{-7}$	10^{-6}	$5\cdot10^{-7}$	$5\cdot10^{-9}$	$7\cdot10^{-7}$	$6\cdot10^{-8}$	$5\cdot10^{-7}$
N_s, cm^{-3}	$5\cdot10^{18}$	$2\cdot10^{19}$	$2\cdot10^{18}$	$3\cdot10^{18}$	$4\cdot10^{18}$	$9\cdot10^{18}$	$4\cdot10^{18}$

Largest diffusion coefficient and solubility at these conditions with annealing obtained atoms V and the smallest value of D is inherent Mn, although its solubility is at the level most of the 3d-elements. However solve this problem as well as finding the activation energy of diffusion, determines the need some special studies that are the subject of another work.

Dynamic Conductivity of Ultrathin Silver Films

Koltun N.S.

Ivan Franko Lviv national university, Lviv, Ukraine

Optical properties of thin metal films have important information about kinetic parameters of electron transport. Optical properties of thin silver films have been studied already before, but fundamental analysis of thickness dependencies of effective optical parameters is lacking. We have developed methodology for assessing transport kinetic parameters on the basis of the thickness dependent optical constants of the films. Ultrathin silver films in the vicinity of percolation threshold (thicknesses about d = 8-25 nm) have been studied. The critical thickness of the films, mean linear grain size and grain boundary scattering parameters of charge curriers have been determined from the size dependencies of the effective optical constants. The experimental data are in good agreement with those obtained by structural and electro physical investigations of the samples.

Ultrathin silver films have been obtained by the thermal evaporation on the glass substrate under high vacuum condition ($P \sim 10^{-7}$torr) at the room temperature. Mass thicknesses of the films have been assessed by the shift of the resonance frequency of the piezoquartz vibrator. Measuring the resistance of the films was carried out electronically by the Ohmmeter ИЦ301-1. Transmittance and reflectance spectra were measured by broadband spectrophotometer Shimadzu uv 3600.

Dynamic conductivity size dependencies of silver films with thicknesses from 8 to 25 nm in the wavelength range 200-2500 nm were investigated. Optical coefficients n and k have been calculated from the spectral data using Murmann's equations [1]. Optical conductivity, effective charge carrier mass, effective relaxation time, skin depth values were calculated. The critical thickness at which metallic phase is formed was found to be 15 nm. It was determined within the framework of the percolation theory [2] (in the vicinity of the percolation threshold transmittance and reflection spectra do not depend on the frequency). This is confirmed by the dynamic conductivity data which are frequency independent for this thickness value of the film. Another proof is the dramatic change of the sign of the first derivative of the dielectric permittivity on frequency ($d\varepsilon_1/d\nu$) around the thicknesses of silver layer 15-16 nm. The effective mass of the charge carrier was around $1,2 \pm 0,2\ m_0$, which allowed us to use the free electron model [3] in finding of dielectric constants. Mean grain sizes were estimated. They proved to be commensurable with film thicknesses. For example, for film thickness d = 15 nm linear grain size is D =22 nm and for thickness d = 20 nm, D = 25 nm. The skin depth thickness was evaluated [4]. It was shown, that its thickness dependence has descending character up to the percolation region. For thin films with thicknesses above 15 nm this parameter

remains constant and approximately 25 nm. Structural investigations of the films showed that grain sizes of the samples similar to those obtained by the optical studies. The intergrain tunneling coefficient for thin silver films with metallic type conduction were calculated. Its value is about t ~ 0,6-0,7. The data is in good agreement with those obtained by the electro physical investigations of the films in the framework of grain boundary scattering theories.

On the basis of the curried out optical and structural studies was found kinetic charge transport parameters for the silver films with the thicknesses 8-25 nm. It is shown, that the average linear grain sizes obtained in different ways are the same and are commensurable with the thickness of the films. Grain-boundary scattering parameters obtained from spectral characteristics are in full agreement with those previously obtained values from electrical resistivity studies of the films. Effective critical thickness of silver film with metal phase conductivity was estimated and, it was found to be 15 nm.

1. Murmann H. 1933 Z. *Phys.* 80, p. 161-77
2. Pavel Smilauer, *Contemporary Physics,* 1991, Vol. 32, no. 2, p. 89-102
3. M. Dressel, G. Grüner, *Electrodynamics of Solids,* Cambridge University Pres,Cambridge, 2002.
4. P. W. Gilberdt, J. Phys. F: Met. Phys., 12(1982)1845-60.

Structural Changes of $As_{40}Se_{60}$ Nanolayers Studied by X-Ray Photoelectron Spectroscopy

Kondrat O.[1], Popovich N.[1], Holomb R.[1], Mitsa V.[1], Tsud N.[2]

[1]*Institute of Solid State Physics and Chemistry, Uzhhorod National University, Uzhhorod, Ukraine;*
[2]*Charles University, Faculty of Mathematics and Physics, Department of Surface and Plasma Science, Prague, Czech Republic*

The sensitivity to near band-gap light and photo-structural transformations in chalcogenide glasses are key features of phase-change memories [1]. In addition, ChGs exhibit large third-order optical nonlinearities and can be excellent candidates as future materials in modern photonic devices for all optical non-linear switching, data signal processing, optical regeneration, Raman and parametric amplification etc. Many researchers consider that due to the nano-phase separation in as deposited films the manufacturing of holographic gratings and rewritable optical disks, using the optomechanical effect discovered in g-$As_{50}Se_{50}$ will be possible. Therefore, the study of structural changes at the atomic scale in nanostructured amorphous semiconductors induces by laser irradiation is an important scientific and applied task.

The bulk $As_{40}Se_{60}$ samples were prepared by conventional melt-quenching route in evacuated quartz ampoules from a mixture of high purity 99.999% As and Se precursors. Amorphous $As_{40}Se_{60}$ thin films with thickness of about 0.5 μm were prepared by thermal evaporation from bulk glass on the (100) silicon crystal wafer substrates. The irradiation of amorphous $As_{40}Se_{60}$ thin film was carried out by using a He-Ne (632.8 nm) laser of 50 mW/cm^2 intensity. The high-resolution photoemission spectra were taken using the Mg K-α (hν=1253.6 eV) X-rays source. The Ar-ion sputtering were applied to remove adsorbed carbon and oxygen from the surface. The photoelectron As 3d and Se 3d core-level spectra of as-prepared and laser irradiated $As_{40}Se_{60}$ films were measured and analyzed.

The structural modifications of near surface nanolayers under the laser irradiation were detected. The significant increase of the Se-**Se**-As structural units (s.u.) amount with simultaneous disappearing of the 2As-**As**-Se s.u. are taking place. The mechanisms of photostructural changes are discussed in detail [2].

1. K. Shimakawa, A. Kolobov and S. R. Elliott, Adv. Phys. 44 (1995) 475.
2. O. Kondrat, N. Popovich, R. Holomb, V. Mitsa, V. Lyamayev, N. Tsud, V. Cháb, V. Matolín, K.C. Prince, Thin Solid Films 520 (2012) pp. 7224.

Photoluminescence of Tb^{3+} Ions in Nanocrystalline $Gd_3Ga_5O_{12}$

Kostyk L. , Luchechko A., Tsvetkova O.

Ivan Franko National University of Lviv, Lviv, Ukraine

It is well known that rare earths doped oxide materials with garnet structure are widely used as efficient luminescent material in many applications due to their high light output, high chemical stability and well-mastered technology. Recently a great interest attracted oxide nanopowders for possible using in the production of nanostructured garnet ceramics with the same or similar physical characteristics with respect to single crystal analogues [1, 2].

This paper presents the results of photoluminescent investigations of $Gd_3Ga_5O_{12}$ nanoceramics doped with 0,1 - 1 at % Tb^{3+} ions. The nanopowder (grain at about 30 nm) was prepared using a co-precipitation method and characterized by X-ray diffraction on diffractometer STOE STADI P [2]. Nanocrystalline powder was used for ceramic preparation via cold pressed into pallets (8 mm in diameter) and heated at 900 ^oC. AFM was used to the obtain information about the morphology and size distribution of grain. An average size of agglomerates in the nanoceramics is about 80 nm.

The luminescence excitation spectra in $Gd_3Ga_5O_{12}$: Tb^{3+} nanoceramics exhibit intense broad band with λ_m =266 nm related to the allowed f-d transition and narrow several lines in the spectral region 400-650 nm attributed to f-f transitions in Tb^{3+} ions. Sharp lines peaked at 273, 308, 312 nm were assigned to the Gd^{3+} ions. Photoluminescence spectra of garnet nanoceramics are characterized by groups of lines in blue and green spectral regions, which are caused by $^5D_3 \rightarrow {}^7F_j$ and $^5D_4 \rightarrow {}^7F_j$ transitions in activator ions. The similar Tb^{3+} luminescence lines were also observed in the X-ray luminescence spectra [2], indicating that the same luminescence centers are involved in emission under photo- and X-ray excitation. The changing of excitation wavelength affect to the ratio of the $^5D_3/^5D_4$ emission intensity. The relative intensity of blue and green emission is similar upon excitations into the f-d band of Tb^{3+} and 312 nm (Gd^{3+} lines). The blue emission intensity ($^5D_3 \rightarrow {}^7F_j$ transitions) decreases at 378 nm excitation (Tb^{3+} lines). Efficient energy transfer from Gd^{3+} to Tb^{3+} ions has been evidenced by excitation spectra in UV region.

Revealed peculiarities are discussed in terms of correlation between preparing conditions and luminescence properties of Tb^{3+} nanoceramics.

1. Lupei V. Comparative spectroscopic investigation of rare earth-doped oxide transparent ceramics and single crystals. J.Alloys and Compounds. – 2008. – Vol. 45 – P. 52–55.
2. Kostyk L., Luchechko A., Varvarenko S., Pavlyk B., Tsvetkova O. Preparation and luminescence properties of $Gd_3Ga_5O_{12}$ nanocrystalline garnet. Chemistry of Metals and Alloys. – 2011. – Vol. 4 – P. 77–80.

Impact of the Silver Surface Morphology on the Eu^{3+} Ions luminescence in Some Inorganic Coordination Compounds

Kozak D., Nedilko S., Rozuvan S., Sherbatskii V., Amirkhanov V., Litsis O.

Taras Shevchenko National University of Kyiv, Kyiv, Ukraine

Surface enhancement of the light provided by thin metallic films and actively discovered for the recent two decades, gives the ability to observe the spectroscopic properties of even several molecules. This feature makes them preferable for modern bio-medical applications. We investigated the dependence between luminescence intensity of coordination complexes with carbacilamidophosphate (CAPh) ligands and morphology of silver films, modified by ND: YAG laser pulses (532 nm). Europium doped coordination compounds with general formulas $Eu(L)_3(i\text{-}prOH)_2$, $Eu(L)_3Phen$ and $Eu_2L_6(i\text{-}prOH)_2 \cdot \mu\text{-}\gamma,\gamma'Dipy$ (L = $CCl_3C(O)N(H)P(O)[N(CH_2)_5]_2$–2,2,2– trichloro-N-(dipiperidin-1-yl-phosphoryl) acetamide, CAPh type ligand) were synthesized.

Compounds based on carbacilamidophosphate, CAPh ligand, are geteroanalogues of β - diketones and they are very promising from the various practical approaches particularly resulting from their good biocompatibility. Luminescence intensity of these materials is generally higher in comparison with similar red phosphors intensity of emission. Luminescence of these compound micropowders is characterized by good monochromaticity of their linear spectra and relatively high efficiency of luminescence, chemical stability and the luminescent spectra under light, X - Ray and VUV excitation and the spectra of the luminescence excitation were obtained as well.

Experiments using VUV synchrotron radiation were made on SUPERLUMI station (HASYLAB laboratory, DESY synchrotron), Project II - 20080221.

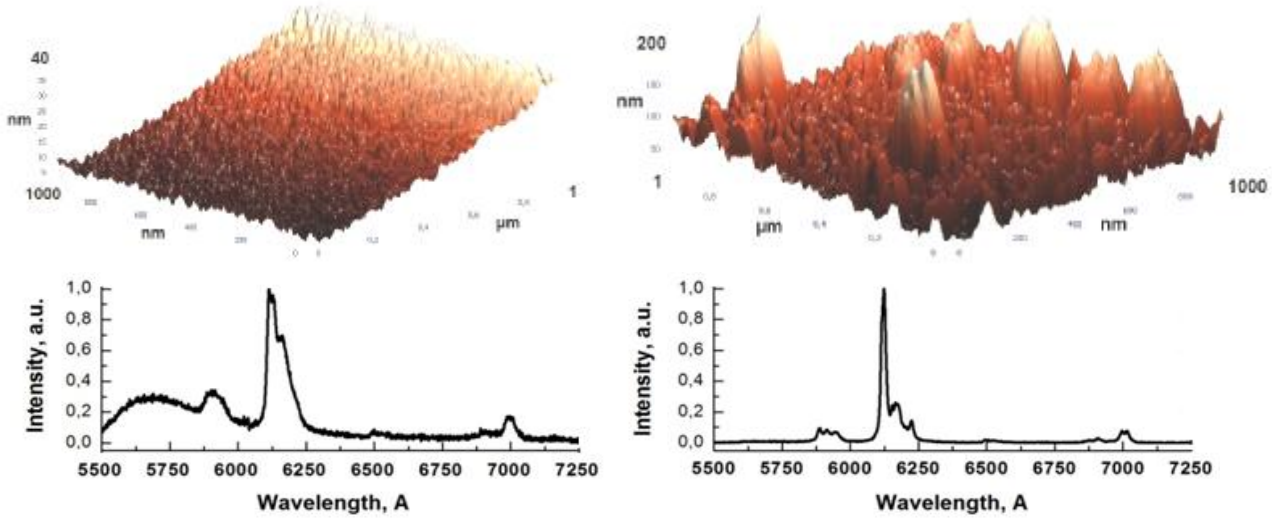

Quantum Chemical Simulation of Silica Protolytic Equilibrium in Acidic Medium

Kravchenko A.A., Grebenyuk A.G., Lobanov V.V., Demianenko E.M.

Chuiko Institute of Surface Chemistry of National Academy of Sciences of Ukraine
Kyiv, Ukraine

Adsorption properties of silica surface in contact with aqueous solutions depend on many factors such as the energy of interaction between surface functional groups and segments of adsorbate molecules, surface charge, ionic strength, and the pH value of the solution. X-ray photoelectron spectra of silica surface at pH <2 contain Cl 2p and Cl 2s bands, so indicating protonation of surface silanol groups, positively charged surface absorbing counter-ions Cl^-. This work is devoted to theoretical modeling of the protonation of surface hydroxyl groups: $\equiv Si-OH + H^+ \leftrightarrow \equiv Si-OH_2^+$.

The calculations have been carried out by density functional theory method using correlation-exchange functional B3LYP and valence-split basis set 6-31++G(d, p). The effect of water environment was taken into account within the frameworks of the continuum model for the solvent (PCM).

The localization has been examined of positively charged hydroxyl group among the ion pairs of hydronium cations and chloride anions formed due to hydration and ionic dissociation of three hydrochloric acid molecules. In this paper we investigated thermodynamic parameters of the equilibrium between molecular associate (Fig. *a*) and an ion-pair complex (Fig. *b*). The value of deprotonation constant (pK_{a1}) of silanol group has been found to be -0.10 what is quite close to the experimental values given in the literature (-0.95). This testifies the actuality of the proposed model for adsorption systems involving ion pairs at the interface silica surface - aqueous solution of hydrochloric acid.

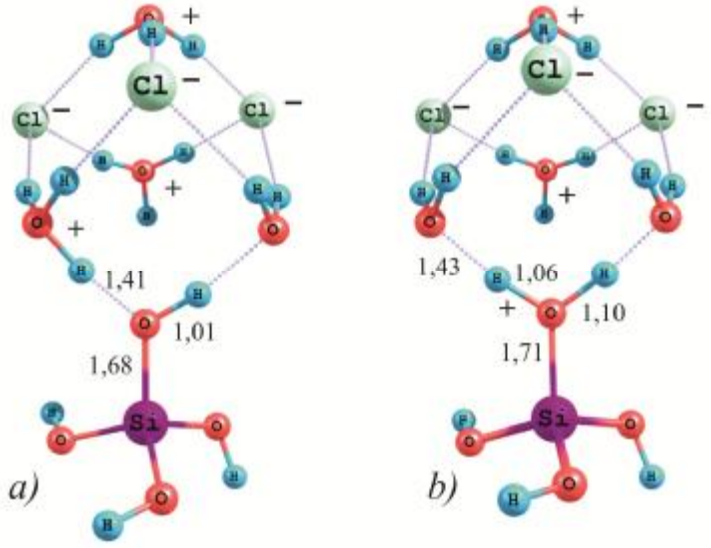

The equilibrium structures of the complex $3Cl^-\cdots 3H_3O^+\cdots HOSi(OH)_3$: molecular state (*a*) and an ion-pair state (*b*)

Electrostriction Effects at Laser Ablation of Quartz Surface Layer

Krylov O., Nedilko S., Rozouvan S.

Taras Shevchenko National University of Kyiv, Kyiv, Ukraine

Quartz plates were engraved using focused laser light in both nano and femtosecond time range and studied afterward by applying atomic force microscopy technique.

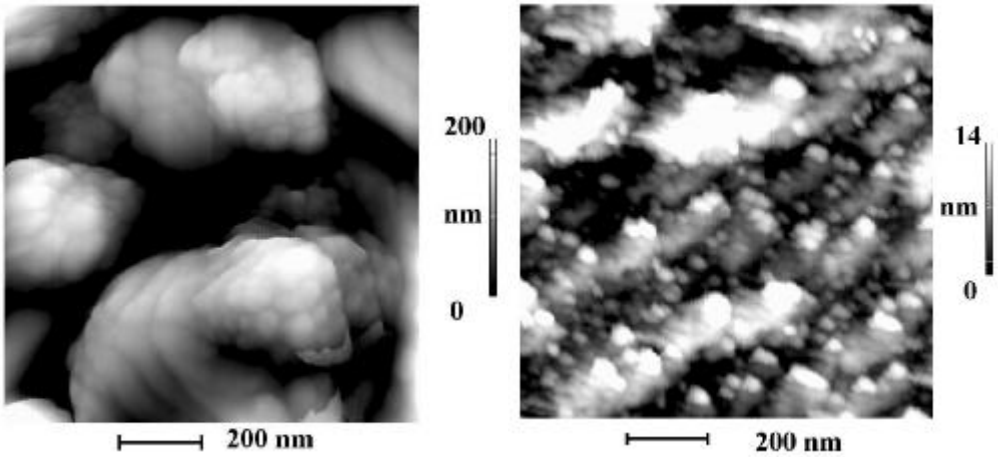

The size and numbers of nanoparticles on the samples surfaces were found to be strongly depended on a distance from a focal point and the laser pulses duration. The ablation was explained taking into account an advanced formula for electrostriction force which was found to be a degenerate tensor with tangential components along the irradiated surface. The ablation was found possessing two key features:

1. Melted glass parts are removed from the focal point either by thermal force (nanosecond pulse duration) or electrostriction force (femtosecond). Thermal forces form relatively slow flows of melted glass. The glass droplets initially having spherical form are flatterned by gravitational forces. At the contrary, the electrostriction force very fast removes glass droplets from the focal point so they have spherical form. Femtosecond pulses form almost ideal spherical nanoparticles on the treated surface (left figure). Flatterned objects can be seen on the surface for nanosecond laser pulses (right figure).

2. Focused femtosecond pulses should work as optical tweezers keeping the nanoparticles in the focal point instead of removing its from there. For steady flows, extra elecrostiction pressure in the focal point is compensated by lower air pressure there which prevents glass droplets from leaving focal point area. In the case of femtosecond laser pulses, AFM scans reveal an opposite process - the less size of a glass nanodroplet - the larger distance separates it from the focal point area. The result can be explained by using the extended ratio for electrostriction pressure which introduces electrostiction force tangential components.

Formation of Nanosized Structure by Thermolythographic Laser Recording

Kryuchyn A.A., Gorbov I.V., Lapchuk A.S., Lytvyn P.M.

Institute for information recording of NAS of Ukraine, Kyiv, Ukraine

Formation of nanosized structures by laser radiation focused by diffraction-limited optical systems requires special photo (or thermo) sensitive materials with nonlinear or threshold exposure characteristics. These materials were widely used for creation of WORM-type optical media. Recording modes of these media were chosen in order to geometrical dimensions of obtained marks were about half of exposure emission wavelength. Materials with ablative recording (thin films of organic dyes or composite polymer-organic dye materials), phase and photo transformations, and local oxidation of metal films can be used for thermolythographic laser recording. The choice of recording medium depends on thin films deposition possibility on specified substrates, laser radiation recording power, etc. It is necessary to provide an adiabatic heating operation of thermosensitive film and minimum fluctuation of exposure level in recording area for carrying out of thermolythographic recording by Gaussian distribution laser beam.

The possibility of 120-220 nm raised structure formation on the thermosensitive dye-polymer materials by 405 nm wavelength laser emission focused by 0.9 numerical aperture lens is shown experimentally.

Structure of Splat-Quenched Multiprincipal Component $CoCrCuFeNiSn_{0.5}$ High-Entropy Alloy

Kushnerev A.I., Bashev V.F.

Oles Honchar Dnipropetrovsk National University, Dnipropetrovsk, Ukraine

In recent years, one kind of new alloys, high-entropy alloy with multiple principal elements in equiatomic or near-equiatomic ratios, has received more and more attentions due to its unique structure and excellent properties [1]. Promising properties in hardness, wear resistance, oxidation resistance and corrosion resistance can be obtained by proper composition design. Because of the high mixing entropy of alloys with multi-principal elements, the microstructure of high-entropy alloys usually displays some simple solid solutions during solidification, instead of complex phases or inter-metallic compounds A series of multiprincipal component alloy systems have been explored in the past few years. The most commonly used elements are Al, Ti, Cr, Fe, Co, Ni and Cu. Structure of multiprincipal component as-cast and splat-quenched (cooling rate ~ 10^6 K s^{-1}) $CoCrCuFeNiSn_{0.5}$ alloys are investigated for the first time in this paper.

From the XRD analyses, the crystal structures of the as-cast $CoCrCuFeNiSn_{0.5}$ alloy are found to consist of a simple face-centered cubic (FCC) and body-centered cubic (BCC) solid-solution structures. The lattice parameters were calculated from the positions of their peaks as 0,3586 nm and 0.2944 nm, respectively for FCC and BCC phases. The sizes of coherent scattering areas have been determined by the Selyakov–Sherer formula as 110 nm for BCC and 85 nm for FCC phase. Similar structures, with slightly different lattice constants, are found for the splat-quenched alloy (the XRD pattern of this alloy also included two major phases, one BCC and one FCC, with lattice constants of 0.2941 and 0.3587 nm, respectively). The sizes of coherent scattering areas were about 145 nm for BCC phase and 120 nm for FCC phase. The process of splat quenching of the alloy is also accompanied by a simultaneous increase of about twice the values of microstrains to 0.006. As compared with FCC phase the estimated degree of texturing for the BCC phase significantly increased and the density of dislocations decreased by three times from $1.1 \cdot 10^{13}$ cm^{-2} to $3.8 \cdot 10^{12}$ cm^{-2}. Such a change in the density of dislocations is not typical for the alloys obtained by quenching. Probably observed changes can be explained by the appearance of primary BCC orientation of nonequilibrium solidification during the splat-quenching process.

1. C. Lia, J.C. Lia, M. Zhaoa, Q. Jiang. Effect of alloying elements on microstructure and properties of multiprincipal elements high-entropy alloys//Journ. of Alloys and Compounds.– 2009. –V. 475. – P. 752–757.

Size Dependent Effects of Contact Melting in Alternating Layered System with Various Thickness

Lazarev V.I., Sukhov V.N.

V.N. Karazin Kharkiv National University

Some of us earlier observed the effect of contact melting in two-layer films of various metals which in our experiments formed eutectic alloys: In/Bi, Au/Pb, Au/Sn, In/Pb, etc. Such two-layer systems start melting under heating at eutectic temperature. The question of manifestation of contact melting in multilayered system is interesting both from fundamental and applied points of view.

Functional materials of the Sn/Pb system are widely used in various applications, you just have to mention that such an eutectic alloy is broadly applied in soldering, there is a need for it in modern nanotechnology. However, the physical processes that occur in this system, in ultrathin layers and multilayer materials at temperatures close to melting are not well understood.

The present paper examines the processes occurring during heating of a layered system consisting of three pairs of thin alternating layers of Sn/Pb of various thickness, but with a complete eutectic composition at each point on a film plane. Layered system was obtained by condensation of metals on the substrate in vacuum ($P = 10^{-8}$ Torr), followed by the creation of a temperature gradient along it. The method developed previously and described in detail in [1], allows one to observe a front of contact melting on the layered film visually and to determine its temperature as compared with the thick film of the same composition.

If the layers do not interact then in such a system each layer is melted at its own temperature, taking into account the size dependence effect. The total thickness of the layered system was chosen in the range in which we can detect the size dependence effect of its melting temperature. For our system, where the diffusion of layers interacts during heating, it is interesting to examine the manifestation of their individual and collective properties of melting.

Experiments performed in situ showed that the Sn/Pb multilayer system melts when heated through the diffusion mechanism of contact melting at the same temperature as the film of eutectic alloy of the same thickness. Decreasing the temperature of contact melting exceeding 1K is observed for a layered system, with a total thickness of layers of 36 nm being due to the size effect, as compared with a thick (1000 nm) film of the same eutectic composition.

1. A method of phase diagrams of binary systems. N.T. Gladkikh, A.V. Kunchenko, V.I. Larin, V.I. Lazarev, A.L. Samsonik and V.N. Sukhov. Functional Materials 6, No.5 (1999).

Electrophysical Parameters of the Film Resistors Based on Glass-RuO_2 Nanodispersed Composites Grinded by Ultrasound

Lepikh Ya.I., Lavrenova T.I., Bugayova T.M., Kurmashev Sh.D.

Interdepartmental scientific-educational physics-technical centre of Odessa I.I.Mechnikov National University, Odessa, Ukraine

Abstract. Current-carrying phase agglomerates (RuO_2) size influence on electrophysics characteristics of the heterophase system "glass-RuO_2" was investigated. RuO_2 agglomerates mid-size reduction (at glass particles fixed sizes) results in "glass-RuO_2" heterophase system specific superficial resistance increase.

Dioxide ruthenium nanodisperst powder morphology, dispersion and phase structure after their processing in water by ultrasound is investigated and electrophysical parameters of film resistors based on these powders are determined.

Initial RuO_2 powder consists of volumetric agglomerates with diameter ~ 6 micrometers which contain RuO_2 monocrystals in the size ~ 50 nanometers.

It is established, that at after RuO_2 agglomerates ultrasonic grinding during 20 minutes there is a sharp reduction of their sizes from 6 micrometers up to 2,8 micrometers, then there is a process of coagulation with a small increase of agglomerates sizes and then further reduction of their sizes up to 3 micrometers.Thick-film resistors specific surface resistance (ρ_s) and temperature resistance factor (TRF) dependence on time of ultrasonic processing are received (fig. 1,2).

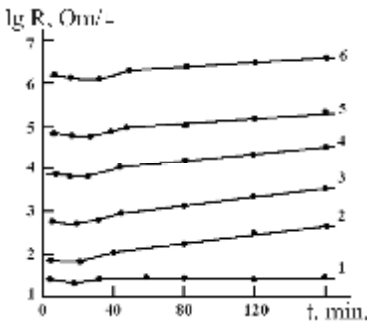

Fig. 1 Dependence ρ_s (lgR) on ultrasonic grinding time and Ru_2O concentration (1-50 %, 2 - 40 %, 3 - 30 %, 4 - 20 %, 5 - 15 %, 6 - 10 %)

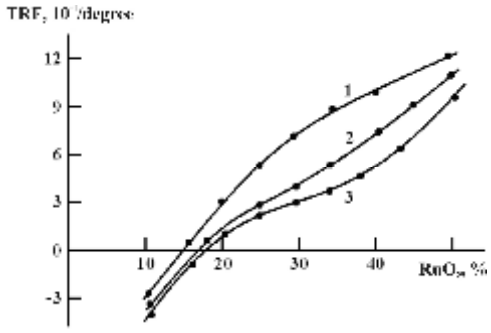

Fig. 2 Dependences TRF on RuO_2 concentration and ultrasonic grinding time, minutes**:** **1**-0; **2**-90; **3** - 160

It is established, that RuO_2 agglomerates ultrasonic grinding time increase (till 160 minutes) results in increase film specific surface resistance for all ratios RuO_2:glass (RuO_2 from 10 up to 50 %), and TRF passes from area of negative in area of positive values. The resistors resistance increase at ultrasonic processing can be connected with RuO_2 agglomerates sizes reduction (at the fixed glass particles sizes), that results in contacts amount and conducting phase chains lengths increase and accordingly in ρ_s increase.

AFM – Exploration of Film Relief of Surface Fe and Cu/Fe

Loboda V.B., Kolomiets V.M., Shkurdoda Yu.O., Kulyk S.G.

Sumy State A.S. Makarenko Pedagogical University, Sumy, Ukraine,

Atomic force microscope (AFM) is widely used for the exploration of microstructure and topographical peculiarities of surface of various materials. In case of thin films it helps to define size and form of microparticles of its surface as well as its roughness; it is important for understanding of electroconductive properties of multilayers films.

The exploration of the relief of surface of as-deposited and annealed films Fe(30 nm)/S та Cu(15 nm)/Fe(30 nm)/S (S – substratum of polish glass) below the temperatures 550 K and 700 K is performed with the help of Scanning Probe Microscope Nano Scope 3a Dimension 300^{TM} in the rate of periodic contact. These films are the constituent parts of three-layers Co/Cu/Fe/S, for which the phenomenon of giant magnetoresistance (GMR) is typical.

As one can conclude from the figure 1 (a, b), copper changes the topography of the surface of film Fe (a) greatly. The maximum fluctuation of the profile of as–deposited films (b) Cu(15 nm)/Fe(30 nm)/S makes 7 – 20 nm. After the process of annealing in the extreme oil-free vacuum below the temperature 550 K, crystal grains, ranging from 35 nm to 200 nm in size and 17 nm to 50 nm in height correspondingly, can be observed. Annealing below the temperature 700 K (d) results in significant smoothing of the surface, but at the same time it causes the emersion of microholes in the cooper surface.

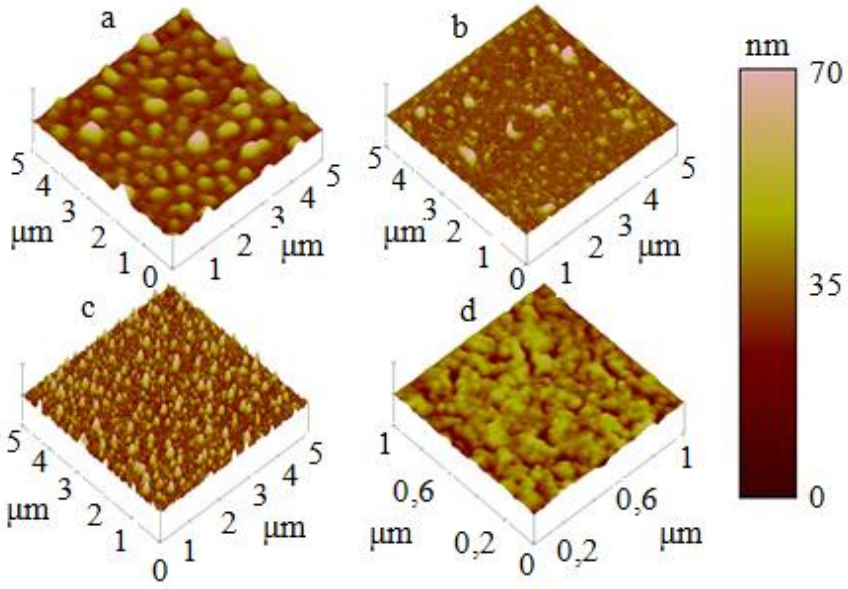

Fig. 1. AMF – image of relief of surface: a – as-deposited film Fe/S, b – as-deposited film Cu/Fe/S, c – annealed film (550 K) Cu/Fe/S, d – annealed film (700 K) Cu/Fe/S.

Photoelectric Properties of Oxidized Macroporous Silicon Structures

Lytvynenko O., Karachevtseva L., Goltviansky Yu., Karas' M., Stronska O.

V. Lashkaryov Institute of Semiconductor Physics, NASU, Kyiv, Ukraine

Macroporous silicon is a promising material of micro- and optoelectronics. The main drawback to the use of macroporous silicon in optoelectronics is the instability of its photoelectric properties. Passivation of silicon by the thermal oxidation was used to improve the stability of the macroporous structure surface. In this work the influence of the oxide coating on the photoconductivity of macroporous silicon structures was investigated for use as photodetectors.

Macropores with depth of 100 micron and a diameter of 4 micron were formed by electrochemical etching in a solution of hydrofluoric acid. Silicon oxide coatings of thickness 7-30 nm were formed by dry oxidation. The ohmic contacts were deposited by vacuum evaporation of indium on the surface of the structures.

The volt-watt sensitivity of macroporous silicon structures with SiO_2 coating was measured. The sensitivity of the structure with SiO_2 coating of 15 nm thickness more than 5 times higher of macroporous silicon without oxide coating and monocrystalline silicon due to the increase of the surface barrier on the border of Si-SiO_2 and decreasing concentration of surface states.

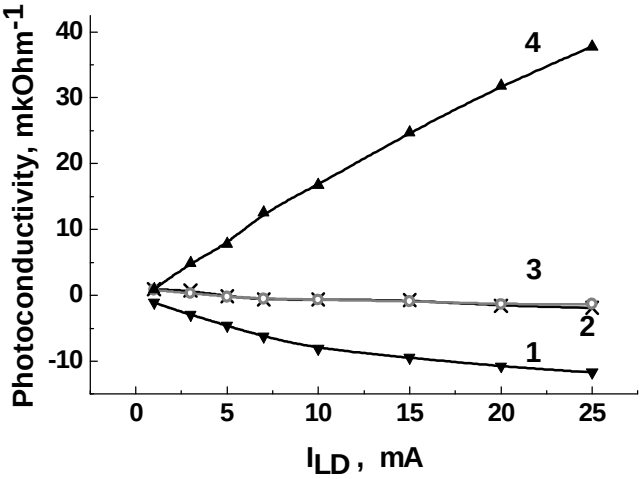

Dependence of the photoconductivity of macroporous silicon at a wavelength of 0.4 microns on the intensity of light at different thicknesses of the oxide coating:
1 – "own oxide" (~ 3 nm),
2 – 7 nm,
3 – 15 nm,
4 – 30 nm.

Photoconductivity of investigated macroporous silicon structures depends on the thickness of the oxide coating (Figure), which affects the absolute values of photoconductivity, its sign and the dependence of photoconductivity on light intensity. The mechanism of the photoconductivity sign change was explained by the accumulation of negative charge in the silicon and the accumulation of positive charge in the layer of silicon oxide or on the Si-SiO_2 boundary.

Electronic Properties of Heterogeneous Materials with Volume-Filling Defects

Marenkov V. I. , Zubkov O. Yu.

Odessa I.I. Mechnikov National University, Odessa, Ukraine

One of the current hot topics in nanotechnology is the creation of new materials (electrically conductive threads, metal foams, etc.) [1].

In this regard, an important and still unresolved aspect of electronics-oriented applications consists in the simulation of the electronic characteristics of micro-porous materials (silicon, etc.). Especially, this concerns the controlled design of their electronic properties by creating tailored sets of volume-filling nano-scale defects. Applications of these materials can be imagined in electronics industries, space technology as well as in environmental protection.

Usually, the electrical properties of nano-defective materials are modeled with the help of rather complicated quantum-mechanical calculations of the density of electron states in nano-defects (such as quantum dots, nano-wires, cracks and nano-pores). The major draw-back of these calculations is in the large number of freely adjustable parameters entering them - what makes it very difficult to apply the corresponding results directly to concrete practical problems.

Here we circumvent these difficulties with the help of techniques from the statistical theory of quasi-neutral micro-cells in heterogeneous plasmas [2, 3]. We assume that the electrons are in statistical equilibrium in the volume-filling defects (VFD) of the micro-inhomogeneous material as well as in the matrix of the underlying basis material (the metal or the semiconductor). The proposed method allows for an efficient derivation of the main electronic characteristics of heterogeneous materials.

Lower dimensional material defects like nano-cracks etc lead to a redistribution of the free electrons in the metal matrix and the defects what, on its turn, induces local deviations from the Maxwell distribution of the free-electron density. Here we consider materials with a rather high volume concentration of defects. We analyze the influence of the geometrical characteristics and concentration of defects on the effective level of the local chemical potential for electrons in the bulk. It is shown that slight changes of the Fermi level may lead to strong changes (by several orders of magnitude) of the self-consistent electrostatic potential. This opens up new possibilities for the design of highly sensitive micro-sensors for temperature, ionization, concentration of gas components, etc.

The basic ingredient of our model building concept [4] is the simultaneous solution of two electrostatic problems, which reduce to solving the Poisson-Boltzmann equation together with the Poisson-Fermi equation for the self-consistent electrostatic potential and the effective charge in the volume of the

defect and elements of the basis material. Technically, an essential role plays the isolated simply-connected section S_C of the surface Π corresponding to the extremum of the self-consistent effective potential which describes the effective electro-neutrality cell C_{ξ}^{z} .

The conjugacy condition for the solutions on the boundary surface of a VFD results in a system of transcendental equations for the electrochemical potential F in the sample. We reduced this system to a single transcendental equation which analytically describes the functional relationship of the defining thermodynamic parameters of a micro-heterogeneous porous sample with given VFD characteristics and effective Fermi level F. Finally, we present a detailed discussion of a possible application of our results to modern high-tech temperature sensors and to measuring tools for ionization products in combustion processes.

1. Nanoporous Materials IV, Proceedings of the 4th International Symposium on Nanoporous Materials Niagara Falls, Ontario, Canada 07-10 July 2005. – 243 p.
2. V.I. Marenkov and M.N. Chesnokov, Physical models of plasma with a condensed sispesre phase.- Kyiv: UMK VO, 1989. –188 p.
3. O. Zubkov, A. Kucherskiy Vibrations in the ensemble of charged macroparticles in plasma // 24th Symposium on Plasma Physics and Technology, Prague , June 14–17, 2010. – P. 151.
4. A.Zagorodny, V. Mal'nev, S. Rumyantsev. The influence of elelctron emission on the charge and effective potential of a dust particle in plasma// UJP. – 2005. – 50, N5. – P. 448–454.
5. Marenkov V.I., Kuchersky A.Y. Statistical concept review and the Thomas Fermi approximation in the theory of plasma properties of heterogeneous systems // Physics of Aerodisperse Systems. – 2007. – № 44. – P. 107– 120.

Effect of Microwave Radiation Treatment on the Photoluminescence and Absorption Properties of Epitaxial GaAs

Milenin V.V., Red'ko S.M., Red'ko R.A.

V. Lashkaryov Institute of Semiconductor Physics of the National Academy of Sciences of Ukraine, Kyiv, Ukraine,

Epitaxial structures of n-n^+-GaAs with a thickness of 3 and 300 μ for top epitaxial layer and substrate, respectively, and n-type doped with Te (~$5\cdot10^{16}$ cm^{-3} and ~$1\cdot10^{18}$ cm^{-3} for epitaxial layer and substrate, respectively) were objects of the investigation. Some of the structures were covered by a thin film of gold (~10 nm). The photoluminescence (PL) (77 K) and reflectance (300 K) spectra of studied structures were measured during a month in the 500-2000 nm and 800-1100 nm wavelength range, respectively.

Microwave irradiation of the samples was conducted at the frequency 2.45 GHz and power was 7.5 W cm^{-2}. To prevent the samples from overheating, the microwave irradiation was conducted in special conditions: the samples were treated with three radiation pulses with the interval between them 5 s. The duration of treatment was 60 and 120 s.

The initial spectrum of PL exhibits an impurity bands at 1.02 and 1.21 eV and edge emission at 1.52 eV. The first and second related with donor-acceptor pairs, which consists V_{Ga} and impurities. PL intensity of the bands after the treatment changes over time. These changes are non monotonous, and in some cases oscillatory. The magnitudes of relative intensities for impurity peaks were ranged from 0.3 to 4.5 times. An uncorrelated change in the intensity of impurity bands testifies about changes both channels radiative and non-radiative recombination. The most efficiency changes after microwave treatment was detected for near-edge emission. Repeated microwave treatment leads to qualitatively the same changes. The initial spectrum of reflectance consisted oscillations in 980-1100 wavelength region. These oscillations are attributed to the interference formed by the air–GaAs and top-GaAs–substrate interfaces. The changes of reflectance spectra after microwave treatment were not detected: the interference has persisted. Later the increase of the reflectance was observed with interference, related to two-layers structures with different n.

Thus, the microwave radiation influences on the structural quality of the near-surface layers of the epitaxial GaAs. A non-equilibrium state arises as a result of the microwave treatment. The high level of structural and impurity defects inherent in this state. Its relaxation results in long-term oscillatory features of observed spectra. More detailed experimental and theoretical studies are needed for better understanding the phenomena, stimulated by microwave processing, and its practical use.

Changing the Structure and Optical Properties of the Films Under Swift Heavy Ions

Myroniuk D.V.[1], Lashkarev G.V.[1], Lazorenko V.Y.[1], Shtepliuk I.I.[1], Skuratov V.A.[2], Strelchuk V.V. [3], Kolomys O.F.[3], Timofeeva I.I. [1], Khomyak V.V. [4]

[1]Frantsevich institute for problems of materials science NAS Ukraine, Kyiv
[2]Flerov Laboratory of Nuclear Reactions, Dubna, Russia
[3]Lashkaryov Institute of semiconductor physics NAS Ukraine, Kyiv, Ukraine
[4]Fedkovich Cherinvtsi national university, Chernivtsi, Ukraine

Zinc oxide films were grown by DC magnetron sputtering on n-and p-type Si substrates. The samples were irradiated at room temperature by 167 MeV Xe^{26+} ions at fluences up to 10^{13} cm^{-2}. As-grown and irradiated samples were investigated by X-ray diffraction (XRD), photoluminescence (PL) and resonance Raman scattering. It was found that irradiation in ZnO films causes (i) the appearance a lot of point defects, (ii) reduce in the size of coherent scattering regions (CSR), (iii) reorientation of crystallites and (iv) the intensity increase of the deep-level emission band.

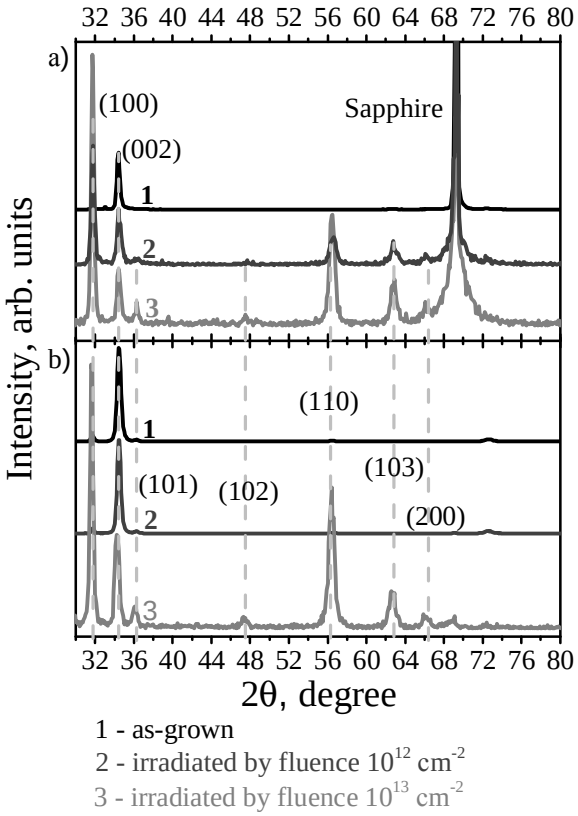

Fig.1. XRD pattern of as-grown and irradiated with ions Xe^{26+} ZnO films, deposited on the n-and p-type Si substrates

In order to compare the peak intensity values in an accurate way, the values obtained after each irradiation were normalized relative to the peak intensity of the reflex plane (002) of initial samples. As-grown samples are textured along the c axis (fig.1). In irradiated films, the dominant reflex (002) is decreased in the intensity with appearance and increasing in the intensity of reflexes for additional planes (100), (101), (102), (103), (110), (200).

When comparing of CSR as-grown and irradiated samples show that after irradiation CSR size for main peak (002) decreases. The grain sizes for the planes (100), (110), (101), (102), (103) are proportionate to or even greater than the size of CSR for reflections (002).

The effect of swift heavy ions on ZnO films properties is discussed.

Synthesis of Nanobelts Tin (IV) Oxide by CVD Method

Nagirnyak S.V., Dontsova T.A., Ivanenko I.M.

Department of Chemistry, National Technical University of Ukraine «KPI», Kyiv, Ukraine

The tin (IV) oxide is a semiconductor with a band gap of 3.6 eV at 300 K. Through to this it has unique electrical and optical characteristics. Thin films of doped tin (IV) oxide are widely used in transparent conductor electrodes and solar batteries. The gas sensors based on SnO_2 widely used as detectors that react to the presence in the atmosphere of harmful to human health or hazardous gases, including CO, NO, NO_2, H_2, etc. In both cases, tin (IV) oxide should have a large surface area.

It is known that increasing the ratio of surface area to volume for SnO_2 nanostructures leads to improved electrical and optical characteristics. This can be achieved by using one-dimensional nano- and microrods or whiskers based tin (IV) oxide.

The aim of this work was the synthesis of SnO_2 nanobelts by CVD method. For this SnO powder was placed in quartz reactor, through which passed a stream of nitrogen (50 ml/min) at temperatures 1050°C for 4 hours. The obtained nanobelts are shown in Fig. 1, and their elemental analysis is presented in Table 1.

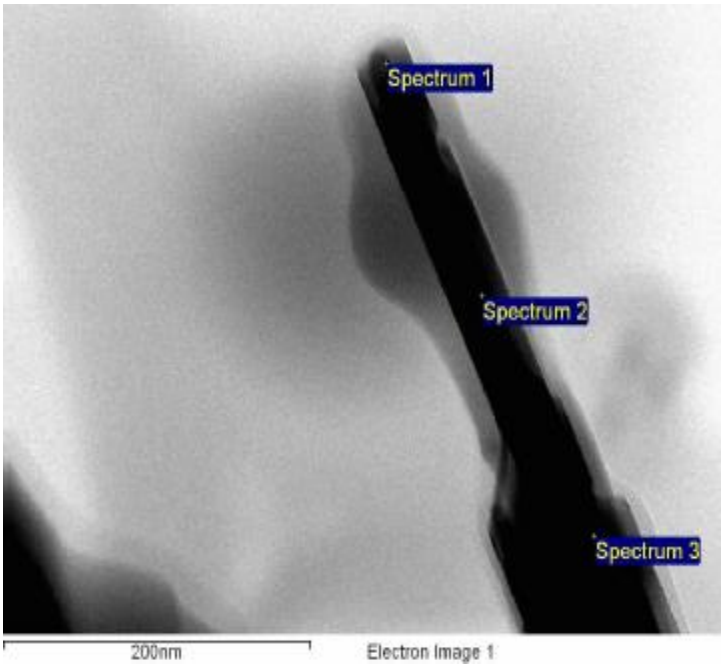

Fig. 1. TEM images of SnO_2 nanobelts.

Table 1. The elemental composition of the products of synthesis (from Fig. 1)

Spectrum	In stats.	O	Sn
Spectrum 1	Yes	81.23	18.77
Spectrum 2	Yes	81.83	18.17
Spectrum 3	Yes	83.98	16.02

Thus, it was synthesized SnO_2 nanobelts by simple CVD method. It can be used for receiving of pure functional materials based on SnO_2. Such pure materials are used to obtain sensitive layers in the manufacture of sensors, electrodes, solar cells.

Annealing Influence on Cinetics of Structure Changes of Gold Nanofilms Deposited Onto Oxide Materials

Naidich Y.V., Gab I.I., Stetsyuk T.V., Kostyuk B.D.

Frantsevich Institute for Materials Science Problems of NASU, Kyiv, Ukraine

Cinetics of structure changes of gold nanofilms by thickness of 100 nm deposited onto oxide (alumina ceramics, sapphire, quartz glass) substrates and annealed at temperatures 800 – 1000 °C during different time intervals from 2 min up to 20 min was investigated. Surfaces of all substrates have been well polished up to roughness R_z = 0,03 – 0,05 μm. After polishing all samples have been degreased and annealed in vacuum at temperature 1100 °C during 1 h. Gold nanofilms 100 nm thickness have been deposited onto annealed substrates surfaces by method of electron beam dispersion and then the films onto oxides were annealed on air. The samples have been annealed and were investigated by methods of optical, scanning electronic and atomic-power microscopy. With use of the obtained microphotos the areas of gold islets which were remained onto the nonmetallic samples surfaces were determined by planemetric method and were presented on graphs.

It is established that character of dispergation during annealing on air gold nanofilms on all investigated oxide materials has approximately identical and it develops from enough slow films fragmentation in result annealing up to 800 °C. The fragmentation was considerably accelerated during temperature rise especially in a range 900 – 950 °C when nanofilms dispergation on separate fragments of the different sizes and forms at enough long exposure which achieves up to 20 min, practically is finished. As a result of the further annealing at temperatures 950 – 1000 °C there is only a process of nanofilms fragments acquisition of more or less round forms. In this case the area of the surface oxide substrates which is covered by these fragments remained almost constant and amounted to approximately 15 – 25 % of all surface substrate.

The data on gold nanofilms behavior during annealing are not only scientific interest but and can be applied in process of optimum characteristics of gold coverings on oxide surfaces development according to the certain conditions of their operation, and also at development of new technological processes of the soldering or welding by pressure of the details from oxide materials were covered by gold as in this case it is important to know behavior of a metallic covering depending on temperature and time of details connection process carrying out.

Temperature Investigation of Optical Absorption Edge in $(Ag_3AsS_3)_{0.45}(As_2S_3)_{0.55}$ Thin Film

Neimet Yu.Yu.[1], Studenyak I. P.[1], Buchuk R. Yu.[1], Izai V. Yu.[1], Trunov M. L.[1], Makauz I. I.[1], Kökényesi S.[2]

[1]Uzhhorod National University, Uzhhorod, Ukraine;
[2]*University of Debrecen, Debrecen, Hungary*

Chalcogenide glasses are of a great interest at a development of new solid electrolytes because of high values of their electrical conductivity in comparison with oxide glasses. The As-S-Ag glasses were extensively studied in the first place due to the potential possibility of their application as a solid electrolyte. Therefore, in such a case, the present ternary As-S-Ag thin films introduce a considerable interest.

Synthesis of $(Ag_3AsS_3)_{0.45}(As_2S_3)_{0.55}$ glass was carried out at a temperature of 700°C during 24 h with following melt homogenization during 72 h. Homogeneous films with thickness d~1 μm were prepared by thermal evaporation in vacuum by VUP-5 equipment from the bulk glass with a deposition rate of 3-6 nm/s onto glass substrates held at 300 K. Film thickness was measured during the deposition using the interferometric method. X-ray diffraction studies show that fresh evaporated films were obtained in amorphous state. The transmission spectra were studied in the interval of temperatures 77–300 K by a MDR-3 grating monochromator; an UTREX cryostat was used for low-temperature studies.

With temperature increase the long-wave shift of high-energy parts of transmission spectra and decrease of transmittance at interference maxima are observed. Based on the interferential transmission spectra, the spectral dependences of absorption coefficient were obtained. It is shown that the optical absorption edge in the region of its exponential behavior is described by the Urbach rule. The main parameters of the Urbach absorption edge as well as the temperature dependences of optical pseudogap and Urbach energy are determined. It should be noted that the temperature dependences of optical pseudogap and Urbach energy for $(Ag_3AsS_3)_{0.45}(As_2S_3)_{0.55}$ thin film are well described within a framework of the Einstein model.

From the interferential transmission spectra, the dispersion dependences of the refractive index for $(Ag_3AsS_3)_{0.45}(As_2S_3)_{0.55}$ thin film in the 450-800 nm spectral range are obtained. In the transparency region a slight dispersion dependence of refractive index is observed, the dispersion increases while approaching the optical absorption edge. It is shown that the refractive index increases with temperature.

The small-Angle X-ray Scattering Study of Nanosize Inhomogeneities in Ni^{2+}-Doped Gallium-Containing Magnesium-Aluminum-Silicate Glasses

Nishchev K.N., Panov A.A., Zaikin A.I.

Ogarev Mordovia State University,, Saransk, Republic of Mordovia, Russia

The transparent Ni^{2+}-doped glass-ceramics are promising materials for active optical fibers, because they possess broadband fluorescence covering the whole 1200-1600 nm telecommunication window.

Glasses of $28MgO\text{-}10Al_2O_3\text{-}8TiO_2\text{-}xGa_2O_3\text{-}(54\text{-}x)SiO_2$ (mol%) systems (MATS) were used as the host of Ni^{2+} (where x=0, 3, 5, 8). The glass samples were prepared by a conventional melting method. Raw materials were melted in a corundum crucible in atmosphere at 1500-1550 °C for 2h in an electric furnace.

The influence of secondary on the structure of the glass (at different temperature-time conditions) was investigated by small-angle X-ray scattering (SAXS) (fig. 1), using system Hecus S3-MICRO.

Addiction of Ga_2O_3 into host glass systems leads to change kinetics of nucleation the crystalline phase. Growths of inhomogeneity in bulk glass were obtained with increasing of temperature of treatment. The average radius of gyration of the inhomogeneities varies from 2 nm to 6 nm.

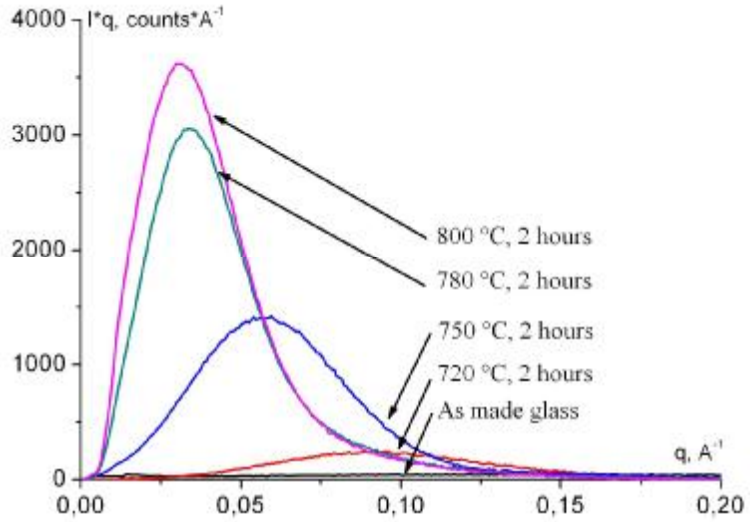

Fig. 1. SAXS pattern of MATS glasses, treated with different temperature.

This work supported by The Ministry of Education and Science of the Russian Federation (project №2.6247.2011).

1. B.N. Samson, L.R. Pinkley, J. Wang, G.H. Beall. Nickel-doped nanocrystalline glass-ceramic fiber//Opt. Lett., 27 (15), pp. 1309-1311 (2002)

Fabrication and Properties of Photosensitive Structures of $Cu_{1-x}Zn_xInSe_2$ Single Crystals

Novosad O.V., Bozhko V.V., Parasyuk O.V., Kozer V.R., Gerasymyk O.R.

Lesya Ukrainka Eastern European National University, Lutsk, Ukraine

Of late years, the interest in ternary chalcogenide compounds and their alloys has grown up. The ternary compound $CuInSe_2$ and solid solutions on its basis are used as materials for thin-film heterojunctions in solar cells.

In this work photosensitive structure of $Cu_{1-x}Zn_xInSe_2$ (x=0−20) solid solution single crystals with n-type conductivity has been produced and studied. For the growing of solid-solution crystals on the basis of $CuInSe_2$, the horizontal variant of the Bridgman–Stockbarger method, as described in detail in [1], was chosen. The measurements were carried out using the specimens fabricated in the form of plates ~3×3×1 mm^3 in size.

Photosensitive structures were produced by heat-treatment of monocrystalline n-$Cu_{1-x}Zn_xInSe_2$ (x=0−20) plates in air at temperatures near 550 °C for t≈25 min. It is known [2, 3] that the interaction of $CuInSe_2$ with oxygen of ambient air at T≈400−700 ^{0}C can form contact of the $CuInSe_2$ with layer of wide band n-type In_2O_3 oxide. Then the crystals cooled down to room temperature at a rate of 300 K/min, so as in the article [2]. As a result, on the $CuInSe_2$–$ZnIn_2Se_4$ plates homogeneously colored layers of purple were formed. After heat treatment the formed layers were removed from all sides except one. Thus, taking into account [2, 3] it can be argued that the resulting structure is a contact of n-In_2O_3 and compounds n-$CuInSe_2$−$ZnIn_2Se_4$ of various composition.

Studies of the stationary current-voltage characteristics have shown that In_2O_3/$CuInSe_2$–$ZnIn_2Se_4$ structures have rectifying properties. Rectification coefficient (K) at voltages U≈2−5V was in the range of ~2 to 7. Best rectifying properties are typical for the structures based on $CuInSe_2$–$ZnIn_2Se_4$ with 10 mol. % $ZnIn_2Se_4$ (K≈6). When illuminated using integral light of halogen lamp, photovoltaic effect was observed. The photosensitivity of the best structures reached S_u≈4 V/W at T≈300 K.

1. V.V. Bozhko, G.Ye. Davydyuk, O.V. Parasyuk, O.V. Novosad, V.R. Kozer. Electrical and optical properties of solid solutions $Cu_{1-x}Zn_xInSe_2$ (x=0,05-0,2) // Ukr. J. Phys. – 2010. – Vol.**55**, №3. – p. 312–316.
2. M.A. Magomedov, G.A. Medvedkin, Yu.V. Rud', and V.Yu. Rud'. Preparation and properties of isotype heterostructures of n-$CuInSe_2$ // Fiz. Tekh. Poluprovodn. – 1992. – Vol.**26**, №3. – p. 556–558.
3. M.A. Abdullaev, I.K. Kamilov, D.Kh. Magomedova, P.P. Khokhlachev. Effect of thermal oxidation on the electrical conductivity and photoresponse of In_2O_3/$CuInSe_2$ structures // Inorganic Materials. – 2007. – Vol.**43**, №12. – p. 1424–1428.

Defect Nanostructure Changing and Ultrasound Measuring of SiO_2 Films

Onanko A.P., Kulish N.P., Onanko Y.A.

Kyiv national university, Kyiv, Ukraine

Introduction. The influencing of ultrasonic deformation ε was researched on elastic and inelastic characteristics of SiO_2 + Si. Strain σ can collect up in non-ideal crystals, changing their inelastic and elastic characteristics.

Experiment. For measuring of elastic module E and internal friction (IF) the impulse method on frequency f ≈ 1,67; 5 MHz and the method of complete piezoelectric oscillator on frequency f ≈ 118 kHz were used at deformation e ≈ 10^{-6} in vacuum P ≈ 10^{-3} Pa [1].

Experimental results. There was a small value of IF background in SiO_2 $Q^{-1}_0 \approx 2 \cdot 10^{-6}$ to T ≈ 385 K. Puasson's coefficient μ:

$$m = \frac{(\frac{1}{2}V_{\mathbf{b}}^{\ 2} - V_{\leftrightarrow}^{\ 2})}{(V_{\mathbf{b}}^{\ 2} - V_{\leftrightarrow}^{\ 2})}. \qquad (1)$$

It's showed, that inelastic Q^{-1} and elastic E characteristics are essentially depended from morphology of surface layer. Atomic force microscopy (AFM) are testified the presence of wafer-plate relief on fig.1.

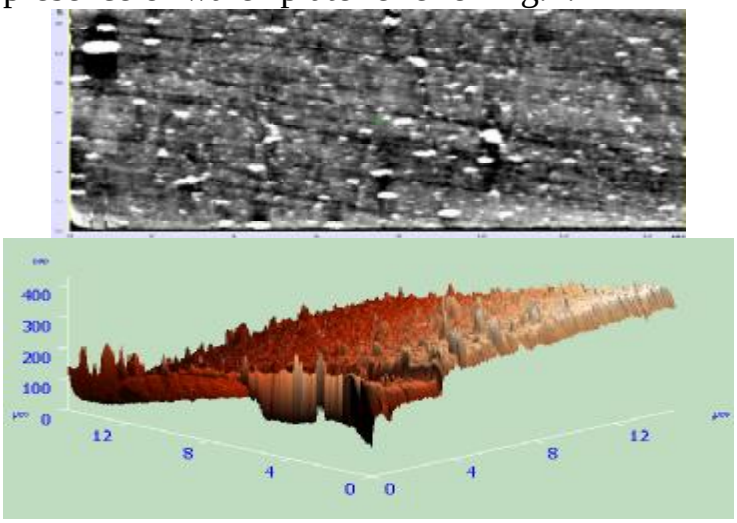

Fig. 1. 3D atomic force microscopy of microstructure image of SiO_2 + Si type KDB-6,0 with orientation (100) (15x15 mkm).

Conclusions. Thus, the study of influence of structure defects on attenuation of elastic vibrations in SiO_2 + Si wafer-plates allows to estimate the degree of nanostructure. Outcomes of an evaluation of dynamic characteristics interstitial atoms Si_i, vacancy V and O-complexes can be applied for account of a condition of an annealing with the purpose of deriving specific structural defects in SiO_2 + Si.

The Ampere-Volt Characteristic of the Macroporous Silicon Structure That Self-Heating.

Onyshchenko V.F.

Lashkaryov Institute of Semiconductor Physics of NAS of Ukraine, Kyiv, Ukraine

Two-dimensional macroporous silicon structures with microporous layer are used as gas sensors and photoelectric [1]. In this paper, the volt-ampere samples when self-heating is measured also they are theoretically calculated and explained. We investigated the samples characterized by the [100] orientation, the thickness H=500 μm, the n-type of conductivity, the specific resistance of 4.5 Ω×cm. The macropores had the diameter D_p=1-6 μm, the depth h_p=40-100 μm, the distance between the pores of *a*-D_p=1-4 μm. The ampere-volt characteristics were measured in the constant current mode.

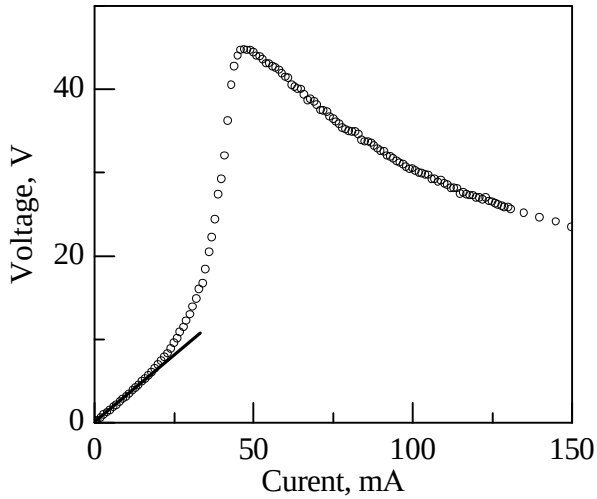

Fig. Experimental data of the ampere-volt characteristic for the macroporous silicon structures on the silicon substrate.

The voltage increased when I>11 mA due to reduction of carrier mobility (see Figure.). The decrease voltage after its maximum (T=550 K, I=50 A) due to the thermal generation of charge carriers. The dependence between the temperature and the current becomes linear after maximum. When the sample temperature is higher than the melting temperature of the gold-silicon eutectic (T=650 C, I=105 A) then the contacts were molten but that does not influence on the measurement. We found that the ampere-volt characteristic of the macroporous silicon structures described Ohm's law, the temperature dependence of the conductivity of the macroporous silicon structure and the temperature dependence of the electric power on the sample.

1. Onyshchenko V.F., Sachenko A.V., Karachevtseva L.A. Anomalous-sign photo-emf in macroporous silicon at photon energies comparable to that of indirect band-to-band transition // Ukr. J. Phys. – 2009. – Vol.54, No12. – P. 1212-1218.

The Mobility Relaxation in Two-Dimensional Macroporous Silicon Structures

Onyshchenko V.F.

Lashkaryov Institute of Semiconductor Physics of NAS of Ukraine, Kyiv, Ukraine

Two-dimensional macroporous silicon structures with microporous layer are used as gas sensors and photoelectric [1, 2]. The large internal surface microporous layer promotes adsorption of gases that cause marked changes in electrical, photoelectric and optical properties of macroporous silicon with a layer of micropores. In this paper, the relaxation voltage at the terminals of the sample are measured and the relaxation times of mobility in two-dimensional macroporous silicon structures after turn out infrared lighting that warmed the sample are calculated.

We investigated macroporous silicon structure on silicon substrate characterized by the [100] orientation, the thick H=400 μm, the n-type conductivity, specific resistance of 4.5 Ω×cm. The macropores had the diameter D_p=1-6 μm, the depth h_p=40-100 μm, the distance between the macropores a-D_p=1-4 μm. The samples were gold ohmic contacts. The macroporous silicon structure lit IR LED with a wavelength of 0.95 microns. We ascertained that the voltage at the terminals of the sample decrease after turn out infrared lighting, it means that the conductivity of the structure increases. This situation can be explained by the fact that the infrared emission LEDs not only generate electron-hole pairs, but also decreased their mobility due to heating of the sample. The relaxation processes are described by the differential equation of heat conduction. From experimental data the relaxation times of mobility (temperature) τ_1=53 s, τ_2=73 s. The heat transfer coefficient determined from two sizes and relaxation times the voltage at the terminals of the sample. This allows you to calculate the relaxation times due to the influence of other sample sizes τ_3=121 s, τ_4=0,027 s (the relaxation time of mobility due to the thickness of silicon between the macropores).

We found that the relaxation voltage at the terminals of the sample due to the relaxation of mobility which depends on temperature. Calculated relaxation time mobility for the distance between the pores of 1 mm, the heat transfer coefficient α = 122 W/(m^2K) and surface recombination velocity of 90 m/s is almost three orders of magnitude larger than the relaxation time of the charge carrier concentration.

1. Karachevtseva L., Onyshchenko V. and Sachenko A. Photocarrier transport in 2D macroporous silicon structures // Opto-Electronics Review. – 2010. – Vol.18, No4. – P. 394-399.
2. Karachevtseva L.A., Onyshchenko V.F., Sachenko A.V. Photoeffect Peculiarities in Macroporous Silicon Structures // Chemistry, Physics and Technology of Surface. – 2010. – Vol.1, No1. – P. 87-93.

CZTSe Films Investigations by XRD and μ-PIXI Methods

Opanasyuk A.S.[1], Koval P.V.[1], Ponomarev A.G.[2], Magilin D.V.[2], Cheong H.[3]

[1]*Sumy State University,Sumy, Ukraine*
[2]*Institute of Applied Physics of NAS of Ukraine, Sumy, Ukraine*
[3]*Department of Physics, Sogang University, Seoul, Republic of Korea*

Recently the films of $Cu_2ZnSnSe_4$ (CZTSe) four-component compound have attracted a special attention of researches as alternative to CdTe, $CuInSe_2$, and $CuIn_{1-x}Ga_xSe_2$ absorbing layers at fabrication of cost-effective thin film solar cells. This material has band gap (E_g=1.0-1.5 eV) which is close to optimal for the conversion of solar energy, p-type conductivity and high coefficient of radiation absorption ($a>10^4$-10^5 sm^{-1}) because it is a direct-gap semiconductor. It consists of elements that are widely distributed in the crust and have low production costs [1].

CZTSe films obtained by Cu, Zn, Sn, and Se co-evaporation onto glass substrates with Mo sublayer was studied in the work. Structural investigations were carried out with using X-ray diffractometer DRON 4-07 (Ni-filtered K_α – radiation of Cu-anode). The spectra was registered in the angle range 2θ from 20^0 to 80^0, where 2θ is the Bragg angle. The phase analysis was carried out by using X-ray characteristic emission induced by proton beam (PIXE, μ-PIXE methods). Corresponding studies were performed in microanalytical accelerator complex "Sokol" (IAP, Sumy, Ukraine). Energy of protons beam was equal 1.5 MeV. Further analysis of PIXE spectra was carried out with using of GUPIXWIN program.

X-ray investigation was found CZTSe films have almost monophase tetragonal crystal structure. The samples have growth texture along [211]. Lattice constants of the material varried in range a = (0.56640-0.56867) nm, c = (1.13466-1.13776) nm ($c/2a$ = 0.9983-1.0017, V = (0,364044-0,367469) nm^3). Coherent scattenig domain size was equal $L_{(211)}$ = 20.4-36.4 nm.

Using the results obtained by μ-PIXE method, there were constructed the distribution maps of the elements which are components of compound of the surface area. The elemental composition of the films depending on the obtaining samples modes was determined.

1. Properties of the Window Layers for the CZTSe and CZTS Based Solar Cells / Opanasyuk A.S., Kurbatov D.I., Ivashchenko M.M., Protsenko I.Yu., Cheong H. // Journal of Nano- and Electronic Physics. –2012.–V. 4**,** №1.–P. 01024-1–3.

Research Defective Condition at the Surface Layers of p-Si with Deposited Film of Metal Bi and Al

Pavlyk B.V., Kushlyk M.O., Didyk R.I., Slobodzyan D.P.

Department of Electronics, Ivan Franko National University of Lviv, Lviv, Ukraine

Using microscopic researches and calculated data for heterostructures on silicon with metal films, appearance of the surface layer was found. This layer with its structure and physical characteristics is different from characteristics of monocrystalline silicon.

Various physical parameters of films of Bi and Al cause specific effects on the structure of the surface layer of silicon. Found that the surface layer of silicon is deformed through gratings of a crystal and film mismatch as well as various coefficients of thermal expansion. This leads to the formation of subsurface deformation potential, which facilitates the seizure of defects from the volume of crystal to surface layer for example through dislocations that reach to the surface.

We have shown a possible mechanism of low-temperature diffusion of silicon atoms from the surface layer into aluminum film based on defects in its structure and mechanical stresses in the junction silicon layers.

Microscopic researches of surface structure allow stating that detected surface defects are clusters of point defects.

Theoretical calculations of the energy distribution of near-surface, deformed layer under the films for Al and Bi were performed. From the analysis of these calculations the highest possible depth of capture defects under bismuth film to 10 nm obtained, the deposition conditions described, it is several orders of magnitude lower than under the aluminum film (1 - 2 microns). Estimated parameters penetration depth of deformation potential in the surface layer of silicon correlate well with experimental results.

1. M.Yu. Gutkin, I.A. Ovid'ko Defect structure on the internal boundaries in nanocrystalline and polycrystalline films / / Materials Physics and Mechanics. –2009. – № 8. – p.p.108-148
2. N.T. Gladkih, A.P. Kryshtal, R.V. Suhov islet Formation of nanoistel by self-organizing during melting condensed films of Bi and Sn at the Si // Nanosystems nanomaterial, nanotehnologiy. – 2010. – V. 8. – № 1. – p.p. 79-90
3. B. Pavlyk, R. Didyk, M. Kushlyk [et al.] Electro-physical characteristics of surface layers of crystals p-Si films deposited Al, subjected to elastic deformation // Electronics and information technologies. – 2012. – Issue 2. – p.p.57-64.

Structural Transfomations and Magnetic Properties of Amorphous Films of Gd-Fe System

Prysyazhnyuk V.I., Mykolaychuk O.G.

Ivan Franko National University of Lviv, Ukraina

Magnetic properties of films and volume samples of binary compounds of Gd-Fe system ($GdFe_2$, $GdFe_5$ i Gd_2Fe_{17}) and also agency of formation of structure on magnetic properties were explored. Amorphous films deposited a method of thermal evaporation on teflon substrates. The temperature of substrates had two values 300 and 500 K. At increase of temperature of a substrate or at annealing of films, the percentage ratio of a polycrystalline phase was incremented. A thickness of films measured by means of optical interferometer MIO-1 (it was equal 200 nanometers). For structural studies of films electronic microscope UEMV-100K and high-temperature attachment PRON-2 was used. For magnetic studies the modernised vibrating magnetometer was used.

The hysteresis curves for volume and thin-film samples specify in that fact that these materials belong to the class of magneto-soft compounds. It is necessary to score also the significant differences in character of hysteresis loops for volume and thin-film samples of all compounds of this system. Absolute values of a coercive force for amorphous and polycrystalline films, and volume compounds was determinate. Value of a coercive force decreases at formation of amorphous films in comparison with volume samples in 2 times. Formation of a polycrystalline phase in films give rise to increasing coercive force in 1.5 times in comparison with volume samples (polycrystalline films become more magneto-hard). For absolute value of a coercive force does not matter how there is a crystallisation, or in the process of film formation on the warmed-up substrate, or in the process of annealing of amorphous films after their deposition. Though as have shown the previous structural researches in these cases different structures was formatted [1].

1. V.Prysyazhnyuk, O.Mykolaychuk. Structure formation in Gd-Fe thin films// J. of Non-Cristalline Solids. -2006. -Vol.352. -P.4299-4302.

Charging Mechanism of Si Real Surface Due to Wet Ammonia Adsorption

Ptashchenko F.O.

Odessa National Maritime Academy, Odessa, Ukraine

A quantum-chemical modeling of different types of surface centers, due to NH_3 and H_2O molecules adsorption on the natural oxide layer over Si crystal is carried out. The modeling subject was the hydroxyled cristobalite (111) face. All calculations were performed with the PCGAMESS code by DFT method. The B3LYP hybrid exchange-correlation functional has been adopted for all calculations in cluster approximation. To minimize the computing time, different clusters were used for different problems. The broken bonds of Si and O atoms on the cluster faces were saturated with OH-groups and H atoms, respectively. There was a capability of the full system geometry optimization, or freeze the cluster edge- (not surface-) atoms for variations of the SiO_2 cell parameters.

The calculations showed that the adsorbed single NH_3 molecules constitute some states in cristobalite with bounding energies over the range of 0,25–0,8 eV. These states have occupied electron levels, corresponding to energies deep in the v-band, and empty electron levels, corresponding to energies high in the c-band of Si. These centers in the cristobalite layer cannot charge the Si surface.

The creation of an ion pair $NH_4^+ \ldots OH^-$ on SiO_2 surface as a result of NH_3 protonation in a pyramidal cluster, consisting of three H_2O molecules and one NH_3 molecule, as described in [1] for SiO_2 in the NH_3 water solution, is a highly improbable event in gas atmosphere.

The calculations showed that more realistic charging mechanism of the SiO_2 surface, due to wet ammonia adsorption, is NH_3 molecule protonation under the assistance of a number of adsorbed H_2O molecules, resulting in NH_4^+ ion formation. The systems with 2 to 6 H_2O molecules on the cristobalite surface were calculated. In this model, a surface silanol group $\equiv$Si–OH, which is located in a neighboring to the NH_3 surface cell, transfers a proton to an H_2O molecule, which simultaneously transfers another proton to the NH_3 molecule. In this process another H_2O molecule can take part, and there is a possibility of a chain protons migration. As a result, a $\equiv Si–O^-$ and NH_4^+ ion pair is formed, and the ions are located far from each other. The $\equiv Si–O^-$ ion has a strong electric field and interacts with an H_2O molecule, resulting in a silanol group $\equiv$Si–OH and OH^- ion. This ion can transfer its electron to the Si crystal as $OH^- \rightarrow OH + e^-$. The bounding energy of resulting NH_4^+ ion is of 1,5 eV.

1. Kravchenko A.A. et al. // Chemistry, Physics and Technology of Surface. 2010.– V.1, No 2.– P. 177–181.

Transformation of Energy Gap of Amorphous GeS Films after Modification by Bi

Romanyuk R. R.[1, 2], Mykolaychuk O. G.[2]

[1]*Western Scientific Centre, Lviv, Ukraine;*
[2]*Ivan Franko National University of L'viv, Lviv, Ukraine*

Bi-additions to the amorphous materials based on Ge-S are an effective tool for changing their physical properties. Bi and Pb additives lead to inversion of the type of conductivity of these compounds. Other elements of the bismuth group, even at high concentrations in chalcogenide matrices, do not change the type of conductivity. But among scientists, there is uncertainty about the mechanism of entry of Bi into amorphous matrices and the coordination of Bi.

The thesis is dedicated to experimental research of the influence of bismuth modification on the structure, electrical and optical properties of amorphous GeS films. We studied film compositions $(GeS)_{1-x}Bi_x$ (x = 0; 0.03; 0.07; 0.11; 0.15) of thickness 0.5-1.2 microns. Bulk samples were obtained in ampoules by melting stoichiometric GeS with the addition of Bi of certain concentrations. The ampoules were subjected to vibration and hardening in cold water. The thin films under investigation were obtained by using the method of discrete evaporation of fine-dispersive mixture on the surface in a vacuum (10^{-4} Pa) from fresh cleaves NaCl at 293 K followed by annealing in a vacuum at T = 350 K. The thickness of the films was measured with an optical interferometer. Electron diffraction patterns were filmed on the electron-diffraction apparatus EG-100M at accelerating voltage U = 80 kV by using a rotating sector.

It was found on the base of short-range order studies that by condensation of $(GeS)_{1-x}Bi_x$ ($x \leq 0.15$) films on substrates at T = 293 K the amorphous structure with tetrahedral coordination of Ge atoms and double coordination of chalcogen atoms is formed. The atoms of Bi attempt to form the structural units of pyramidal type $BiS_{3/2}$. The concentration dependences of the width of optical gaps (E_o) and refractive index of amorphous $(GeS)_{1-x}Bi_x$ films are shown. Mechanism and electroconductivity type for $(GeS)_{1-x}Bi_x$ condensates and energetic position of recombination centers have been established. It is shown that in $0.11 < x < 0.15$ concentration region the change of conductivity type from *p*- on *n*-type occurs.

The model for energy gap for amorphous films of germanium monochalcogenides and feature of its transformation after modification by Bi is proposed.

Signal Decrement Investigation in CdS-Cu_2S Heterostucture

Smyntyna V.A., Borschak V.A., Brytavskyi Ie.V.

Department of Experimental Physics, Odessa I.I. Mechnikov National University, Odessa, Ukraine

The mechanisms of signal decrement, associated with the removal processes of nonequilibrium charge from the space charge region of the image sensor on the basis of non-ideal heterojunction were investigated. The mechanism of the observed two-stage process was determined: phase of slow relaxation - implementation of the thermal emission of localized charge, that depends on temperature; phase of rapid relaxation - the result of tunneling mechanism of ejection.

The research of current transfer processes in nonideal geterojunction CdS-Cu_2S allowed developing image sensor in the X-rays and optical range with high sensitivity and possibility of signal accumulation [1, 2].

Data-storage time and sensitivity of the sensor are determined by relaxation time of nonequilibrium positive charge. Possible ways of captured by traps holes removing from the barrier of non-ideal heterojunction were considered: the thermal holes emission to the CdS valence band; direct holes tunneling from trapping centers to the Cu_2S valence band; two-stage free-electron tunneling from CdS quasi-neutral region to the space charge region and subsequent recombination with nonequilibrium hole; tunnel-hopping recombination.

Experimentally observed phenomenon of investigated sensor signals relaxation were analyzed theoretically within the model of relaxation processes in the heterojunction CdS-Cu_2S.

Relaxation curves of short-circuit current at different points of the sensor were obtained experimentally (Fig. 1). It is seen, that relaxation curve has two well-marked area: rapid initial photocurrent drop (region I) and then its relatively slow decay (region II). At different points signal showed decrease with the same characteristic relaxation time, but very different in magnitude. This suggests, that sensor heterogeneity on the photosensitivity is caused by a substantial change of trapping centers concentration along the surface, that determines the thermal emission probability.

To clarify mechanisms implemented by charge release, sensor signal relaxation characteristics at different temperatures were studied (curves 1 – 4, Fig. 1). It's clear, that the time constants of later relaxation stage decrease with temperature increasing (region II, Fig. 1). This shows the implementation of thermal mechanism, which determines relaxation kinetics at this region. Relaxation time constants derived from experimental data and theoretical calculations are in good agreement and demonstrate the same temperature dependence. Thus, the current relaxation in considered part of current dependence is determined exceptionally by thermal charge emission from the deep hole traps.

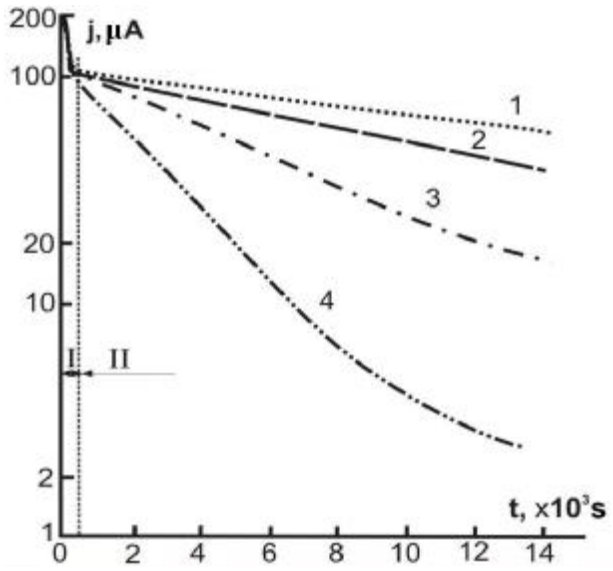

Figure 1: Sensor signal relaxation (of short-circuit current) at different temperatures: 1–T=15°C, 2–T=25°C, 3–T=40°C, 4–T=60°C.

Such parameters as magnitude and the slope of initial part of the photocurrent decay (region I, Fig. 1) don't depend on temperature. This demonstrates the implementation of photocurrent relaxation mechanism in this region, which isn't due to the thermal release and has apparently, tunneling character. Assessing the contribution of tunneling mechanisms in trapped charge relaxation was carried out by calculating the barriers tunneling transparency coefficients for the corresponding transitions. Calculations were made taking into account the changes of potential barrier shape under illumination [3]. The lack of temperature dependence of relaxation curve is due to the fact, that the values of barriers tunneling transparency coefficients don't depend on temperature. Account of tunneling processes leads to characteristics harmonization of the short-circuit current relaxation curves obtained experimentally and theoretically.

Research results, that are discussed in this work, enabled to supplement the modeling of developing sensor optoelectrical characteristics and to compare fabrication parameters with processed CdS-Cu_2S films properties.

1. Vassilevski D.L., Vinogradov M.S., Borschak V.A. Photon induced modulation of surface barrier: investigation and application for a new image sensor // Applied Surface Science. – 1996. – 103. – pp. 383-389.
2. Smyntyna V.A., Borschak V.A., Kutalova M.I., Zatovskaya N.P., Balaban A.P. Sensor on the basis of nonideal heterojunction for registration of the X-ray images // in Proc. of EUROSENSORS XVIII Conference, Rome, September 12-15. – 2004.
3. Borschak V.A., Smyntyna V.A., Brytavskyi E.V., Balaban A.P., Zatovskaya N.P. Dependence of Conductivity of an Illuminated Nonideal Heterojunction on External Bias // Semiconductors. – 2011. – vol. 45. – pp. 894-899.

Electron Microscopic Study of Thin Composite Films Based on Fullerite C_{60}

Solonin Yu.M., Grayvoronskaya E.A.

Institute for Problems of Materials Science NAS Ukraine, Kiev, Ukraine

For the electron microscopic studies of thin composite films based on fullerite the systems C_{60}-WO_3 and C_{60}-Cu were chosen. The films were synthesized by thermal evaporation and simultaneous deposition in vacuum on KCl salt crystals. The temperature of substrates was 293 K. After researching the structure of the samples, they were annealed in vacuum at 573 K, and then further studies of the structure of the films were conducted. For the synthesis of thin composite films of C_{60}-WO_3 two methods were used – simultaneous deposition from two sources and layered deposition.

a b

Figure 1. Film C_{60} + WO_3 and microdiffraction from it (simultaneous deposition): a – initial sample, b – after annealing at 573K.

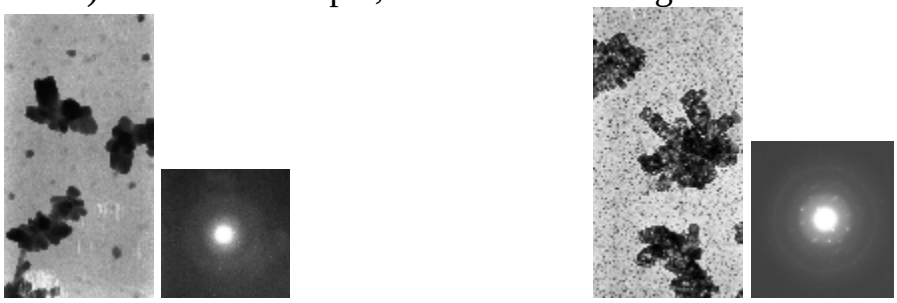

a b

Figure 2. Film C_{60} + Cu and microdiffraction from it (simultaneous deposition): a – initial sample, b – after annealing at 573K.

For composite films of C_{60}-WO_3 and C_{60}-Cu obtained at 293 K heterogeneous amorphous structure was observed. After annealing at 573 K crystalline structure appears, manifesting diffraction rings and point microdiffraction patterns.

The Effect of Doping on the Photocatalytic Properties of TiO_2 Films

Sylenko P.M., Dan'ko D.B., Shlapak A.M., Andrushchenko D.I., Okun' I.Y., Solonin Yu.M.

Frantsevich Institute for Problems of Materials Science of National Academy of Sciences of Ukraine, Kiev, Ukraine

Titanium dioxide remains the most investigated photocatalytic material for hydrogen production by water decomposition under sunlight. Its significant drawback is a large band gap (about 3eV), which leads to the absorption of UV light only that is the small fraction of sunlight spectrum (~ 4 %). One of the most promising way to reduce the band gap is doping of TiO_2 by carbon or nitrogen [1–2]. In our work the TiO_2 films were doped in two ways: 1 - by isothermal calcinations in doping element atmosphere at elevated temperatures, 2 – by adding the vapor or the gas of doping element to the gas-vapor mixture for TiO_2 synthesis.

The results of photocurrent studies of nitrogen doped TiO_2 films are shown in Fig 1. Ammonia was used at the films synthesis as the source of nitrogen.

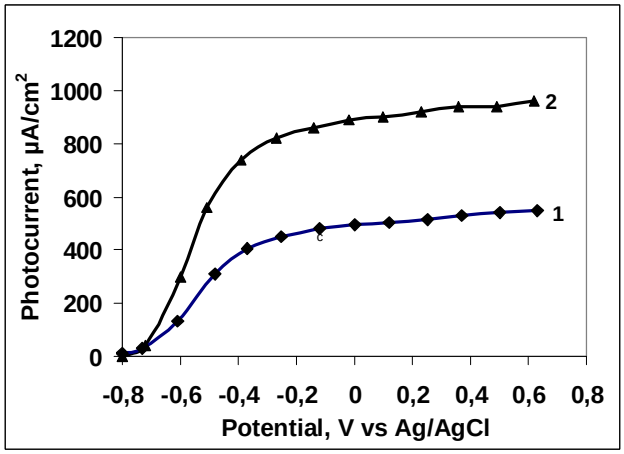

Fig.1. Photocurrent of TiO_2 photoanode as a function of electrode potential in 1M KOH solution under 100 mW/cm^2 xenon lamp illumination (1 sun). 1 – undoped, 2 – nitrogen doped.

It was found that doping with carbon (carbon source - toluene) did not significantly affect on the magnitude of the photocurrent, while doping with nitrogen increased photocurrent by 1.5-2.0 times.

1. Franco L. M. et al. Photocatalytic activity of nitrogen-doped and undoped titanium dioxide sputtered thin films // Superficies y Vacío. – 2012. - 25(3). – P. 161-165.
2. Chen F.Y., Lin Y.T. Effect of C Content and Calcination Temperatures on the Characteristics of C-doped TiO_2 Photocatalyst// Nanotech. – 2010. - Vol. 1. –P. 491 – 493.

Determination of Crystallite Size and Strain in PzT Thin Films Using X-Ray Diffraction

Tsaly V.Z.[1], Martynyuk Ya.V.[2], Kleto G.I.[1]

[1]*Chernivtsi National University by Yuriy Fedkovich, Chernivsi, Ukraine*
[2]*National Technical University of Ukraine «KPI», Kyiv, Ukraine*

In connection with the synthesis and study of nanocrystalline materials becomes relevant question of the size of the particles. The size of small particles can be determined by different methods. One of the most accessible and common ways of finding the crystallite size and microstrain in polycrystalline films is the analysis of the broadening of X-ray diffraction peaks. Crystallite size D can be determined using the simple of Debye - Scherrer formula: $D = \frac{Kl}{b\cos q}$, where K=0,9 – is Scherrer constant; λ – X-ray wavelength; θ – diffraction angle, β – the full width at half maximum (FWHM) of all the peaks of the diffraction reflection after adjusting for instrumental component β_0. The method of measuring the size of the crystallites on the Debye - Scherrer formula can be used only when the diameter of the individual free from stress crystallites in a polycrystalline film as low as 1.0 nm. Use of the Gaussian function and Lorentzian function to fit the FWHM of all the peaks yields correct results. However, the method of the Williamson–Hall equation [1] allows to calculate strain and particle size of the each sample: $b\cos q = \frac{Kl}{D} + 2e\sin q$, where ε – the lattice strain. According to this method, $b\cos q$ is plotted against $2e\sin q$. Using a linear extrapolation to this plot, the intercept gives the particle size Kl/D and slope gives the strain (ε).

In this work we report about the results of investigation of thin ferroelectric films of lead zirconate-titanate using X-ray diffraction method.

X-ray diffraction was performed in θ - 2θ configuration using a DRON-3 diffractometer with CuKα radiation (Ni – filter). For instrumental corrections, a standard quarts and Si samples were used.

The obtained results well correlated with electronic microscopic investigations [2].

1. Williamson G.K, Hall W.H. // Acta Metallurgica. 1953. V.1. Iss.1. P.22-31.
2. Kleto G.I., Martynyuk Ya.V., at al. // Nanosystems, nanomaterials, nanotechnologies. 2009. V.7. Iss.1. P. 65-71.

Tensoresistive Properties of Thin Film Systems Based on Fe and Pt

Tyschenko K.V., Pazukha I.M., Shumakova N.I.

Sumy State University, Sumy, Ukraine

The results of experimental investigation of strain properties for thin film systems based on Fe and Pt on deformation intervals $\Delta\varepsilon_{l1} = (0 – 1)$ % and $\Delta\varepsilon_{l2} = (0 – 2)$ % subject to thickness and concentration of Fe atoms was presented in work.

Dependences $\Delta R/R$, R and γ_{li} versus ε_l for double-layer system Fe(55)/Pt(20)/S (S – substrate, the value of thickness is in nm), which are shown at fig. 1, characterize by differ first deformation cycle from another; a narrow interval of elastic deformation (till 0,2%) and relatively high value of strain coefficient (near 10 units). Starting from second cycle strain properties stabilized. Besides, the dependences of instantaneous longitudinal strain coefficient γ_{li} versus deformation ε_l characterize by local maximum [1]. This effect appears at deformation interval $\Delta\varepsilon_{l2}$ at $\varepsilon_l = 0{,}7\%$. The value of deformation, which corresponds to local maximum, increases at the increases of atom Fe concentration.

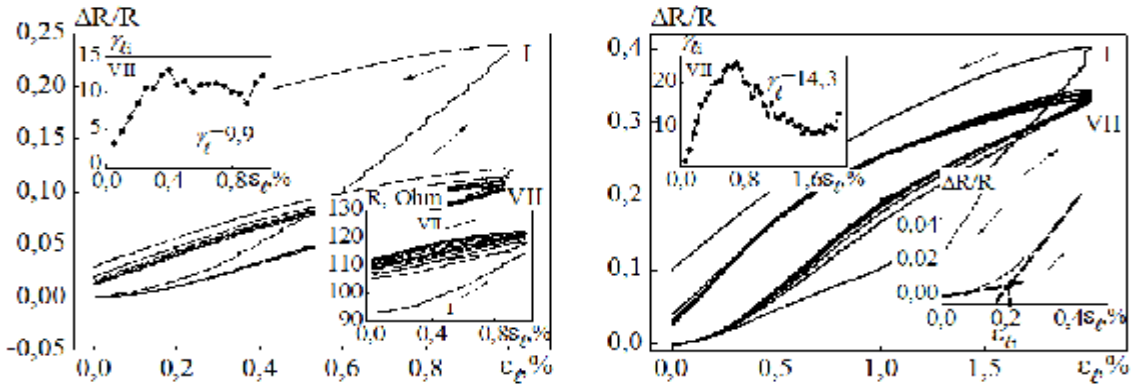

a b

Fig. 1 – Dependences $\Delta R/R$, R and γ_{li} vs. ε_l for thin film system Fe(55)/Pt(20)/S at two interval: $\Delta e_{l1} = (0\text{-}1)\%$ (a) and $\Delta e_{l2} = (0\text{-}2)\%$ (b). I, VII – number of deformation cycles “load – unload”. γ_l – mean value of strain coefficient

Notices, that deformation value at maximum ($\varepsilon_l = 0{,}7\%$) differ from deformation value which corresponds to transition from elastic to plastic deformation ($\varepsilon_{lt} = 0{,}2$ %, insert in fig. 1b). According to work [2], this maximum explained by nonlinear changes of resistance at deformation (insert at fig.1a).

Work was in the framework of state project № 0112U001381

1. К.В. Тищенко, І.Ю. Проценко // *Металлофизика и новейшие технологии*, **34**, № **7**, pp. 907-917 (2012).
2. K.V. Tyschenko, L.V. Odnodvorets, C.J. Panchal, I.Yu. Protsenko // *JNEP*, **4**, № 4, pp. 04014-04018.

Study of Magnetoresistive Properties of Thin Film Systems Based on Co and Gd or Dy

Vorobiov S.I., Shutileva O.V., Shpetnyi I.O., Chornous A.M.

Sumy State University, Sumy, Ukraine

The work is devoted to studying the influence of heat treatment and thickness of the layer of rare earth metals on the structural and phase state and magnetoresistive properties of three-layer films of Co / Gd / Co / S and Co / Dy / Co / S (S – substrate).

Film samples were obtained by electron-beam method by layer condensation in vacuum (residual gas pressure $P \sim 10^{-4}$ Pa) at substrate temperature ($T_s \cong 450$ K). As the substrates for studying the phase composition and crystal structure used film-substrate of amorphous carbon. For research magnetoresistive properties used ceramics substrate. Heat treatment of samples was carried out in the working volume of the vacuum setup on a «heat → preconditioned during 15 min → cooling to room temperature».

Investigation of structural and phase state using transmission electron microscopy (device TEM-125K) showed that freshly condensed films have phase composition HCP-Co+FCC-Co+quasi amorphous Gd or Dy. After heat treatment the structural-phase composition does not undergoes changes, and there is only a consolidation of Co crystallites, as evidenced by information as electron microscopy and electron-diffraction studies.

Research of magnetoresistive properties was conducted for 4 Precision measurement scheme at 3 geometry orientation of the sample in an external magnetic field intensity of to B = 500 mT. Has been found that the system Co(10) / Gd(x) / Co(10) / S (x – effective thickness of the intermediate layer, n = 1, 2, ... 10 nm) is not dependent on the thickness of layer Gd manifests anisotropic magnetoresistance (MR), whose value, for example, a three-layer film Co(10) / Gd(6) / Co(10) / S in the perpendicular geometry measurement is 0,18% in the transversal – 0,14%, in the longitudinal – 0,04%.

For film systems Co(5) / Dy(x) / Co(20) / S (n = 5-20 nm) by analogy with the previous system manifests anisotropy field dependences of MR, the average value of which, for example, for the system Co(5) / Dy(15) / Co(20) / S is in the perpendicular geometry – 0,39%, in the transversal – 0,15%, in longitudinal – 0,21%.

For a system of Co / Gd / Co is a characteristic oscillatory dependence of the thickness of the MR layer of Gd, while for films of Co / Dy / Co with increasing thickness of the Dy value of MR increases.

After treatment in the studied samples stored anisotropic magnetoresistance, and its value is not dependent on the geometry of measurement increased by an average of 10 to 20%.

Optically Transparent Photocured Adhesives with a High Refractive Index

Yarova N.V.

Institute of Macromolecular Chemistry,
National Academy of Sciences of UkraineKiev, Ukraine

Polymeric optics allows deciding the new technological tasks in optoelectronics. In the present report the formation and properties of optically transparent photocured adhesive are considered. In this regard, the study of kinetic features of photocuring of ED-20 epoxy resin and compositions based on it allows determining the optimal conditions for the formation of three-dimensional polymers. The study of the concentration dependence of the kinetics of photoinitiated polymerization allowed determining the optimal ratio of the components in terms of a more complete and rapid cure of polymer composition under consideration. To determine the optical, physical and chemical characteristics comprehensive research of developed compositions was carried out.

Physicochemical characteristics of optically transparent epoxide compositions

Parameters	Results of tests
The spectral bandwidth, %	98
The refractive indices at 20°C for uncured compositions for cured compositions	1,558-1,600 1,654-1,657
The working temperature range of the adhesive joint, °C	-170 - +140
Moisture resistance at 40°C and relative humidity of 98%, days, no less than	70
Rupture strength of the joint, MPa, no less than	14-15
Time of fixation for items upon gluing, min	1-2
Polymerization time, min, no more than	10
Yield of conforming products, %	98
Viability at 10–20°C, months, no less than	12

As seen from the data, composition is of the significant interest as an ecologically pure adhesive or coating for industrial goods of photoelectronics due to its technological effectiveness.

Absorption Spectrum of Thin $CsPbI_3$ and Cs_4PbI_6 Films

Yunakova O. N., Miloslavsky V. K., Kovalenko E. N.

Kharkov National University, Kharkov,Ukraine
Kharkov National University of Radioelectronics, Kharkov,Ukraine

It is known that two ternary compounds $CsPbI_3$ and Cs_4PbI_6 are produced in the system CsI – PbI_2. The first compound is formed at 20°C in the orthorhombic lattice with four molecules per unit cell, and at T> 563K it transformed into the monoclinic phase, according to the other sources – into the cubic. Cs_4PbI_6 has a hexagonal lattice. The structural elements of the two compounds lattice are $(PbI_6)^{4-}$ octahedra.

The absorption spectra of $CsPbI_3$ and Cs_4PbI_6 thin films were investigated in the spectral range of 2 – 6 eV and a temperature range of 90–530 K. It is found that in the sequence of compounds PbI_2, $CsPbI_3$ and Cs_4PbI_6 the long-wavelength exciton bands are linearly shifted to the higher energies and converge at $x \rightarrow 0$ into the position of Pb^{2+} impurity bands in CsI, indicating the excitation and excitons localization in the cation sublattice of the ternary compounds, that is in octahedra $(PbI_6)^{4-}$. The structure of the $CsPbI_3$ and Cs_4PbI_6 absorption spectra is similar to that of the CsI:Pb^{2+} impurity spectra and are treated like its, based on the electronic transitions in the $(PbI_6)^{4-}$ octahedra.

With increasing of the temperature, the long-wavelength exciton band A_1^I in $CsPbI_3$ is linearly shifts to the longer wavelengths with $dE_m/dT=-2.45\cdot10^{-4}$ eV/K down to T = 367 K, and at T = 402 K is abruptly shifted to the shorter wavelengths by 0.4 eV. The structure and position of the main bands of spectrum are similar to Cs_4PbI_6 (Fig. 1, c. 2). Upon the subsequent cooling of the film the $CsPbI_3$ absorption spectrum is not recovered. Consequently, when the $CsPbI_3$ film is heated to T> 400 K, apparently a compound Cs_4PbI_6 is formed, and the excess lead is arise in the spectrum in the form of impurity absorption. The near spectral position of the bands in the CsI:Pb^{2+} and Cs_4PbI_6 spectra, as well as the much higher oscillator strength of the A_1^I band in this film in comparison with Cs_4PbI_6 stoichiometric film is evidence in support of this assumption.

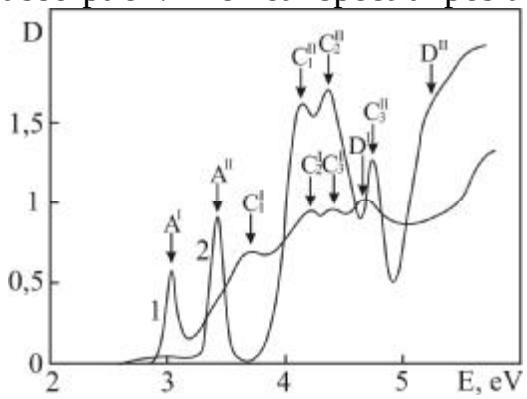

Fig.1. The absorption spectrum of the $CsPbI_3$ film (T=90K) (1) before and (2) after heating above 400 K.

The temperature dependence of the spectral position and half-width Γ(T) of A_1 bands in $CsPbI_3$ and Cs_4PbI_6 is determined by the exciton-phonon interaction. From the analysis of the function Γ(T) is set three-dimensional character of exciton excitations in both compounds.

After-Condensation Processes and Electrical Properties of Nanostructures PbTe:Bi of the Electric-Technical Model

Dzundza B.S., J.S. Jaworski J.S., Mateik G.D., Hatala I.B., Kushnir T.P.

Precarpathian National University named after Vasyl Stefanik, Ivano-Frankivsk, Ukraine

The change of resistivity ρ polycrystalline PbTe:Bi on time t of exposure at 300 K have been studied. Based on the electrical model of the resistance calculation films have been shown that the change in ρ (t) is related to the restructuring process of the crystal structure of the films. The dependence of the linear size of crystallites films of PbTe: Bi since their exposure have been find.

Films of lead chalcogenides are promising materials for making based on these active elements of micro-and optoelectronics: detectors and infrared radiation source, thermoelectric energy converters. Note that the performance characteristics of the device structures and their stability over time are determined by the structural condition and degradation processes that occur in the thin-film material. Doping impurity basic matrix leads to the formation of a stable time of the material n-type conductivity.

Films PbTe: Bi obtained from the vapor phase by vapor deposition in vacuum on fresh chips (0001), muscovite mica. Measurement of electrical parameters was carried out at constant electric and magnetic fields. For each sample a series of measurements over time during the week was carried out and then subjected to annealing in air and measured the thermoelectric parameters depending on temperature.

Experimental results of resistivity values of films PbTe:Bi at different times of exposure is characterized by a significant change only in the initial stages. With further aging of the resistivity changes slightly all the curves ρ(t) tends to saturation. The resistivity ρ of fine nanostructures on mica (0.08 - 0.67) microns is smaller of two orders of magnitude than 1.08 microns thick.

The analysis of calculated based on the electrical model dependencies crystallite size of polycrystalline PbTe:Bi since their exposure indicates the decay processes of large crystals into smaller blocks which leads to an increase in resistivity due to the formation of new boundaries section. These processes are active only during the first few hours after growth in the future practically suspended and the electrical parameters of the structures are stabilized over time. Estimated grain size after recrystallization process termination in good agreement with the average grain size obtained from AFM profilograph.

The work supported by an integrated project of MES of Ukraine (N 0113U000185) and by projects of FRSF State Agency for Innovation and Informatization of Ukraine. (Contracts: R54, F53, 3), NAS of Ukraine (N 0110U006281)

Scattering of Charge Carriers in Pure and Doped Lead Telluride Films

Dzundza B.S., Javorsky J.S., Tkachuk A., Kostyuk O., Letsyn R.B.

Precarpathian National University named after Vasyl Stefanik, Ivano-Frankivsk, Ukraine

The effect of the phase boundaries on the scattering of charge carriers in lead telluride nanostructures deposited on substrates of polyamide webbing on their thickness have been studied. The dominant role are played by scattering on the surface and grain boundaries.

Nanostructures obtained from the vapor phase by evaporation in vacuum open on the polyamide substrate strip type PM-1. Measuring of electrical parameters of the films was carried out in air at room temperature at constant magnetic fields. These samples were also investigated by atomic force microscopy films consist of nanoscale crystallites of pyramidal shape. The dependences of the size of the crystallites and in the lateral direction normal to the substrate thickness from the condensate have been defined. With increasing thickness of the crystallite size is also increased in both directions from the output saturates at a thickness larger than 1 micron.

Fig. 1 is shown the experimental dependence of conductivity on the reciprocal thickness of the nanostructure.

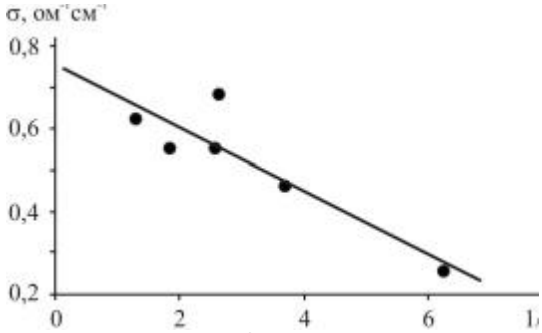

Fig. 1. Dependence of specific conduction from inverse thickness of PbTe nanostructures for (σ_0=0,75 ohm^{-1} cm^{-1}, λ = 0,27 mm) at 300 K.

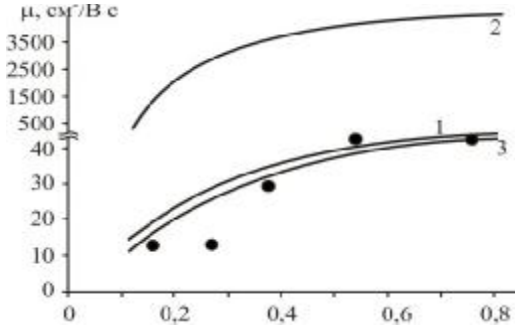

Fig. 2. The dependence of the carrier mobility (μ) of the thickness (d) for new growth condensates of PbTe at 300 K. μ_v = 65 cm^2/Vc.

The observed decline in conductivity with decreasing thickness due to a significant diffuse scattering of carriers at the surface, which becomes dominant at d <200 nm. This is also confirmed by the experimental and calculated depending on the thickness of the carrier mobility (Fig. 2). Insignificant contribution of the grain boundaries (Fig. 2 - curve 2) in scattering carriers is due to a sufficiently large size of crystallites.

The work supported by an integrated project of MES of Ukraine (N 0113U000185) and by projects of FRSF State Agency for Innovation and Informatization of Ukraine. (Contracts: R54, F53, 3), NAS of Ukraine (N 0110U006281)

Diagnosis of Thermoelectric Parameters in Semiconductor Materials

Galuschak M.O. [1], Zapukhlyak R.I. [2], Ralchenko V.G. [3], Tkachuk A.I. [1,2]

[1]*Ivano-Frankivsk National University of Oil and Gas, Ivano-Fvankivsk, Ukraine*
[2]*Vasyl Stefanyk Precarpatian National University, Ivano-Frankivsk, Ukraine*
[3]*A.M. Prokhorov General Physics Institute, Moscow, Russia*

Diagnose of solid state – to evaluate it's condition. To evaluate condition of the solid state, we need measure its thermoelectric parameters: thermal conductivity, electrical conductivity, Seebeck coefficient. Therefore advisable to describe the main methods of measuring thermoelectric parameters of solid state. Measure the conductivity and Seebeck coefficient is not difficult. Difficulties arise when measuring thermal conductivity.

Methods for measuring the thermal conductivity divided into fixed and dynamic. In the first case, measurements are made after the establishment of equilibrium. It is essential to achieve a high degree of accuracy, but establishment of equilibrium, especially for poor heat conductors, may be a long process. At the same time required for measurements on a given sample at several different temperatures will be very high. Dynamic methods based on measure of heat flows, according to the temperature can be much faster and do us measure in wide range of temperatures. However, dynamic measurements have their shortcomings, as very difficult have high degree of accuracy.

It is necessary to distinguish between absolute and comparative measurement. In absolute method directly measured heat that passes through the sample. Of course heat to the sample through one end in the electricity form. In the comparative method is the same amount of heat passing through the sample and through a sample with known thermal conductivity which consistent with study sample. Heat flux calculated by reference to the temperature gradient on the sample. Absolute methods are usually applied at temperatures below room temperature, but due to the small size of conventional semiconductors at higher temperatures better use the comparative method. This heat dissipation by radiation in the surrounding area is not so essential.

The work supported by projects of FRSF State Agency for Innovation and Informatization of Ukraine. (Contracts: R54, F53, 3)

Electrophysical Properties of Modified Films Based on Glassy Arsenic Chalcogenides

Yurkovych N.V., Mar'yan M.I., Loya V.Yu[1]

Uzhgorod National University, Uzhgorod, Ukraine
[1]Institute of Electron Physics, National Academy of Sciences of Ukraine, Uzhgorod, Ukraine

Introducing of elements chemically different from matrix atoms modifies the physical properties of chalcogenide glassy semiconductors. This change is observed both when element are introduced into the molten glass during synthesis and when deposition is compatible with chalcogenide glassy semiconductors and chemical element. This lead to active develop of a new approach to control the properties of semiconductors based on the formation of the nanoscale atomic formations in the semiconductor matrix, the composition of which can include atoms of introduced impurity, atoms of its own components, and also own point defects in the glass matrix. These new formations cause changes of energy state in the forbidden zone while maintaining the same phase of the base material.

The gradient of $As_2S(Se)_3$ + Zn (Te) thin films with various concentrations of zinc and tellurium by thermal evaporation in vacuum is obtained [1]. A set of studies of the temperature dependence of resistance were performed and the activation energy of the investigated structures is determined. Experimental results showed that the conductivity of film is greatly increase with increasing the temperature and concentration of the chemical element - a modifier that is associated with changes in their atomic - faulty subsystems. The temperature dependence of the resistance is described by the expression:

$$R = R_0 \cdot \exp\left(-\frac{Ea}{kO}\right), \qquad (1)$$

where R-studied resistance; R_0 - coefficient of proportionality; Ea - activation energy; k - Boltzmann constant; T - temperature.

Unlike the tellurium based structures, where with increasing concentration the exponential curve becomes less sharp and the range of variation in the resistance decreases. This is related with the presence of a large concentration of impurity defects in the film in the structures. In zinc contained structures the significant change in resistance can be explained by the metallic nature of Zn. The study of current-voltage characteristics of these materials is revealed their sensitivity to the light. The analysis of determined activation energies shows that with increasing of modifier concentration the conductivity activation energy decreases. The self-organization processes of mentioned glassy materials were also studied and the possibility of formation of dissipative structures with different levels of functional ordering was established.

1. N.V. Yurkovych, M.I. Mar'yan. The processes formation of thin-film heterogeneous structures based on Ge_2S_3 glass in dependence of the technologies conditions of their preparation. Uzhhorod university scientific herald. Series Physics. Issue 28. – 2010. p. 64-69.

СЕКЦІЯ 4 (усні доповіді)
ТОНКОПЛІВКОВІ ЕЛЕМЕНТИ ЕЛЕКТРОННИХ ПРИСТРОЇВ, НАНОЕЛЕКТРОНІКА

21-24 травня 2013 р.

SESSION 4 (oral)
THIN FILM ELEMENTAL COMPOUNDS FOR ELECTRONIC DEVICES

May, 21-24, 2013

The Structural and Electrical Characteristics of Non-Rectifying Contacts to High-Resistance *n*-AlN Films

Belyaev A.E.[1], Boltovets N.S.[2], Zhilyaev Yu.V.[3], Panteleev V.N.[3], Konakova R.V.[1], Sachenko A.V.[1], Sheremet V.N.[1], Kapitanchuk L.M.[4]

[1]*V. Lashkaryov Institute of Semiconductor Physics, NAS of Ukraine, Kyiv, Ukraine*
[2] *State Enterprise Research Institute "Orion", Kyiv, Ukraine*
[3]*Ioffe Physico-Technical Institute, RAS, Sankt-Peterburg, Russia*
[4]*Paton Electrical Welding Institute, NAS of Ukraine, Kyiv, Ukraine*

Formation of non-rectifying contacts to high-resistance wide-gap semiconductors makes a complicated physico-technological problem, especially for high-resistance *n*-AlN films. In this case, the electron affinity is appreciably lower than bandgap, and Fermi level practically is not pinned at the surface.

Using successive vacuum deposition, we formed, in a single technological cycle, contact metallization Au(100 nm)-Pd(70 nm)-Ti(50 nm)-Pd(30 nm)-*n*-AlN-n^+-SiC on substrates heated to 350 °C. Then test structures with linear and radial geometry of templates were prepared to measure contact resistivity ρ_c in the 100-380 K temperature range. Ohmic contacts were formed using rapid thermal treatment at $T = 900$ °C for 30 s. The concentration depth profiles in metallization layers were taken using Auger electron spectroscopy. The cleavages of ohmic contacts and morphological features of AlN films (both initial and after removal of metallization layers were studied with an Auger microprobe JAMP-9500F in the scanning electron microscopy mode.

The contact *I-V* curves were linear in the 100-380 K temperature range; the descending dependences $\rho_c(T)$ were observed in the 100-250 K temperature range. At further increase of temperature, ρ_c varied but slightly and was $(6\text{-}7)\times10^{-2}$ Ω·cm^2 for different specimens. The portion of weak temperature dependence of ρ_c was owing to current flow through metal shunts associated with dislocations, with allowance made for diffusion limitation of electron supply to the contact. This is in agreement with our model for ohmic contact [1] and measured density of structural defects in *n*-AlN films ($>10^{10}$ cm^{-2}).

The descending dependences $\rho_c(T)$ in the 100-250 K temperature range were exponential. We suppose that such a behavior of $\rho_c(T)$ curves at low temperatures may be related to the effects of disordering in conduction of metal shunts of atomic sizes. These effects lead to conduction transition from metallic- to activation-type [2].

1. A.V. Sachenko et. al. J. Appl. Phys., **111**(8), 083701 (2012)
2. B.I. Shklovskii, A.L. Efros. Electronic Properties of Doped Semiconductors (Moscow, Nauka, 1979).

Tb-doped Carbon-Enriched Silicon Oxide Films for White-Green Electroluminescence Devices

Gordienko S.O.[1], Nazarov A.N.[1], Tiagulskyi S.I.[1], Vasin A.V.[1], Rusavsky A.V.[1], Gomeniuk Yu.V.[1], Lysenko V.S.[1], Nazarova T.M.[2], Rebohle L.[3], Voelskow M.[3], Skorupa W.[3]

[1]*Lashkaryov Institute of Semiconductor Physics, NAS of Ukraine, Kyiv, Ukraine*
[2]*Department of Common and Inorganic Chemistry, National Technical University of Ukraine "KPI", Kyiv, Ukraine*
[3]*Institut für Ionenstrahlphysik und Materialforschung, Helmholtz Zentrum Dresden-Rossendorf e.V., Dresden, Germany*

An electroluminescence device utilizing a heterostructure of amorphous terbium doped carbon-rich SiO_x (a-SiO_x:C:Tb) on silicon has been developed. The a-SiO_x:C:Tb active layer was formed by RF magnetron sputtering of a-$Si_{1-x}C_x$:H(:Tb) film followed by high-temperature oxidation. Chemical and physical properties of the film before and after oxidation were studied by Fourier-transform infrared (FTIR) transmittance spectroscopy, electron energy-loss spectroscopy (EELS), Rutherford backscattering spectroscopy (RBS), Raman scattering (RS) spectroscopy and photoluminescence spectroscopy (PLS). Electrical properties of the films were investigated by capacitance-voltage (CV) and current-voltage (IV) characteristics at different temperatures. Electroluminescence (EL) properties were studied by EL spectroscopy at constant current regime, dependence of EL intensity vs. applied voltage and EL intensity vs. electron injection time at constant current.

It was shown that after oxidation at temperature near 700°C amorphous Tb-doped SiC film transformed in carbon-rich SiO_2 film with terbium oxide nanoinclusions. The CV characteristic of the Me/a-SiO_2:C:TbO_X/p-Si heterostructure represents one of typical metal-oxide-semiconductor (MOS) capacitor. Depending on polarity of the applied voltage the electroluminescence of this structure is either green or white, which can be attributed to different mechanisms of current transport through the oxide film – space charge limited current for green electroluminescence and trap assisted tunneling or Fowler-Nordheim tunneling for white electroluminescence. Thus, at different polarity of the applied voltage the different mechanisms of the EL excitation are exhibited. At forward bias the EL is excited by mechanisms of irradiative electron-hole recombination, and at reverse bias – by impact ionization mechanisms.

Non-Equilibrium Green's Function Method in Matrix Form and Transport Problems Modeling in Nanoelectronics

Kruglyak Yuriy A.

Odesa State Environmental University, Odesa, Ukraine

Any nanoelectronics device has active conduction channel described by the Hamiltonian [H]. The channel interacts with the source and drain, and with both contacts which stay in local equilibrium defined by the appropriate electrochemical potentials. The interaction between the channel and the contacts are described by the self-energy contact matrices [Σ_1] and [Σ_2]. Interaction of an electron in the channel with its environment is described by the self-energy matrix [Σ_0]. The dimension of these matrices is determined by the number N of the basis functions used for quantum-mechanical description of the conduction channel and contacts. Concrete form of the matrices is specified by the method used to solve the Schrodinger equation and the choice of the basis functions. Once these matrices are composed the further procedure for calculating the conductivity, current and other electrophysical properties are straightforward which is the main purpose of this report illustrated with the 1D and 2D transport problems modeling in nanoelectronics.

There are usually considered two limiting cases of electron transport – diffusional and ballistic. In the ballistic limit electron transport is controlled by the self-energy matrices [Σ_1] and [Σ_2], whereas the interactions inside the channel are negligible. In contrast, in the diffusional limit the transport of electrons is controlled by interactions within the channel described by the matrix [Σ_0], and the role of the contact matrices [Σ_1] and [Σ_2] is negligible.

Classical description of transport processes is based on the Boltzmann transport equation. Non-Equilibrium Green's Function method (NEGF) is a quantum analogue of the Boltzmann equation; its foundations were laid by Martin and Schwinger, Kadanoff and Baym and Keldysh. Both approaches are common in a sense that they both take into account the dynamic and entropic forces. In the ballistic limit, however, dynamic and entropic processes are spatially separated. Electrons skip from one contact to another one under the influence of only dynamic forces. Electrons inside the contacts are happend not be in equilibrium, but quickly come to equilibrium under the influence of entropic forces (Landauer model for elastic resistor). Today it was indeed well established that ballistic resistors withstand fairly strong currents because Joule heating is negligible. Heat is released at the terminals, which due to their relatively massive quickly dissipate the heat. This separation of the dynamics from the thermodynamics to be one of the primary reasons that makes a bottom – up approach [1] starting with ballistic devices scientifically and pedagogically attractive.

Our objective is to present the compact NEGF formalism with an account of the Landauer model for nanodevices.

In our bottom – up approach we will start with elastic resistors for which energy exchange is confined to the contacts, and the problem of resistance can be treated within a one-electron picture by connecting contacts to the Schrodinger equation $[H]\{\psi\} = E\{\psi\}$ and add two more terms to it representing the outflow $[\Sigma] = [\Sigma_1] + [\Sigma_2]$ and inflow from the contact $\{s\} = \{s_1\} + \{s_2\}$, namely: $E\{\psi\} = [H]\{\psi\} + [\Sigma]\{\psi\} + \{s\}$, where the Schrodinger equation is written directly in the matrix form, bearing in mind that the basis functions have been already chosen, so that the square matrices are shown in square brackets, and the column matrices – in curly brackets. Using this modified Schrodinger equation, the wave function can now be written in terms of the inverse matrix $\{\psi\} = [EI - H - \Sigma]^{-1}\{s\}$, where I is unit matrix.

Matrix $G^R = [EI - H - \Sigma]^{-1}$ **(1)** is called Retarded Green's function and its Hermitian conjugate matrix $G^A = [G^R]^+$ is called Advanced Green's function. We note that the NEGF formalism applied to problems in nanoelectronics is reduced to four equations, the first of which is the expression (1) for the Retarded Green's function.

Then the Schrodinger equation can be rewritten as $\{\psi\} = [G^R]\{s\}$. The product of the column $\{\psi\}$ by Hermitian conjugated row $\{\psi\}^+$ gives $\{\psi\}\{\psi\}^+ = [G^R]\{s\}\{s\}^+[G^A]$. Non-equilibrium Green's function is defined as $G^n = 2\ \{\psi\}\{\psi\}^+$, so that the number of electrons is given by $N = Tr\,[G^n] / 2$.

Similarly inflow of electrons is described by $\Sigma^{in} = 2\ \{s\}\{s\}^+$, and now the non-equilibrium Green's function is $G^n = G^R\,\Sigma^{in}\,G^A$ **(2)** and serves as the second equation in the NEGF formalism.

The third equation is a matrix form of the density of states $D(E)$, multiplied by 2 , and is called the spectral function $A = 2\ \cdot D(E) = G^R \Gamma G^A = G^A \Gamma G^R = i[G^R - G^A]$, **(3)** where matrix $[\Gamma]$ is the anti-Hermitian part of the corresponding contact matrix $\Gamma = i[\Sigma - \Sigma^+]$ and describes the interaction of electrons in the channel with contacts.

The fourth equation of the NEGF formalism is the equation for the current through the terminal with number m $I_m = \frac{q}{h} Tr\left[\Sigma_m^{in} A - \Gamma_m G^n\right]$, **(4a)**. Lets take into account (2) and (3), as well as $\Gamma = \sum_n \Gamma_n$, $\Sigma^{in} = \sum_n \Sigma_n^{in}$, $\Sigma_n^{in} = \Gamma_n f_n(E)$, where $f_n(E)$ – the Fermi function of contact n. Then $I_m = \frac{q}{h} \sum_n \bar{T}_{mn}\left(f_m(E) - f_n(E)\right)$, **(4b)** where the transmission coefficient between contacts m and n $\bar{T}_{mn} \equiv Tr\left[\Gamma_m G^R \Gamma_n G^A\right]$.

Examples of modeling 1D and 2D resistors including graphene are given.

1. Kruglyak Yu.O., Kruglyak N.Yu., Strikha M.V. Lessons of nanoelectronics: current generation, Ohm's law formulation and conduction modes in «bottom–up» approach // Sensor Electronics Microsys. Tech. – 2012. – V. **3**(**9**), N 4. – P. 5 – 29.

Temperature, Magnetic Field and Multifunctional Sensors for Cryogenic Application

Mitin V.F., Kholevchuk V.V., Venger E.F.

V. Lashkaryov Institute of Semiconductor Physics, National Academy of Sciences of Ukraine, Kyiv, Ukraine

In this report we review and discuss the properties of a range of Ge-on-GaAs film resistance thermometers that cover the temperature range 0.02 K to 500 K and dual function sensor (DFS) for concurrent and coincident measurements of temperature (1.5 K to 400 K and 0.1 K to 400 K) and magnetic field. The constructions and characteristics of the sensors are presented together with a discussion of their sensitivities to temperature, magnetic fields and ionising radiation.

The temperature sensors are based on Ge film resistors deposited onto semiinsulating GaAs substrates using vacuum technology. This technology makes it possible to vary temperature and magnetic field sensitivity of Ge film resistance over wide limits in different temperature ranges as well as make different versions of resistance thermometers with preset properties, i.e., the necessary resistance and heat sensitivity in the required temperature range. The prepared Ge-on-GaAs film sensing elements are then employed in different packages. Nowadays three types of sensor packages are offered:- cylindrical canister package, made from gold plated copper (3 mm in diameter and 5.0 mm long), micropackage (1.2 mm in diameter and 1.0 mm long) and micro-package with plate (2 mm square by 0.15 mm thick).

The DFS consists of a Ge-on-GaAs film resistance thermometer and an InSb-on-GaAs film Hall-effect magnetic field sensor. These sensors are incorporated in a parallelepiped package, made from gold plated copper, sealed with epoxy. The dimensions of this package are 3.5 mm wide, 2.2 mm high and 10.1 mm long. The DFS has eight copper contact leads:- four leads for the resistance thermometer and four leads for the Hall-effect magnetic field sensor. The DFS approach can be applied to the problem in cryogenic thermometry of temperature measurements in high magnetic fields, since, by simultaneous, direct measurements of temperature and local magnetic field, it enables computational correction of the field effects on the thermometer.

This work was partially funded under Ukrainian State Program “Development of knowledge-intensive sensor’s products” Project No. 2.2.3/18.

Some Methodological Aspects of Studying Ohmic Contacts to *n*-InP

Novytskyi S.V.

V. Lashkaryov Institute of Semiconductor Physics, NAS of Ukraine, Kyiv, Ukraine;

Currently InP Gunn diodes are widely used in radar systems, radio spectroscopy, telecommunications, for road accident prevention etc. [1, 2]. Stable operation of Gunn diodes under extreme conditions puts special requirements on ohmic contacts connecting the devices into a circuit. Therefore, these contacts must be resistant to different actions and maintain low contact resistivity at Gunn diode operating temperatures.

The problem of contact thermal stability can be solved by applying contact metallization with a diffusion barrier that prevents mass transfer in the contact metallization. We studied the contact structure Au/TiB_2/Au/Ge/n-n^+-n^{++}-InP with a TiB_2 layer serving as diffusion barrier. An Auger analysis showed diffusion stability of TiB_2 at annealing (formation) temperature of 400–490°C. In this case, the contact resistance value did not change.

We studied also how the contact resistivity ρ_c of ohmic contacts Au/TiB_2/Au/Ge/n-n^+-n^{++}-InP depended on the ambient temperature T. An uncharacteristic (growing) dependence $\rho_c(T)$ at diode operating temperatures was obtained. This dependence is well described with the model for current flow via metal shunts that were formed at the metal-semiconductor interface due to In atoms deposition on structural nonuniformities [3]. After microwave irradiation of the contact structures (frequency of 2.45 GHz, irradiation of 7.5 W/cm^2), the contact resistivity decreased and was uniformly distributed over the contact area. This may be caused by local heating at the defects that leads to redistribution of In atoms in the semiconductor near-surface region.

1. H. Eisele, R. Kamoua. Submillimeter-Wave InP Gunn Devices. IEEE Trans. Microw. Theory Techn. - 2004. - 52, no 10. - P. 2371-2378.
2. H. Okazaki, T. Sato, N. Yoshizawa, T. Hashizume. Optical and electrical properties of InP porous structures formed on *p*-*n*-substrates. Proc. 22nd 2010 Intern. Conf. "IPRM-2010". - Japan, Kagawa. - 2010. - P. 77-80.
3. A.V. Sachenko, A.E. Belyaev, N.S. Boltovets, R.V. Konakova, Ya.Ya. Kudryk, S.V. Novitskii, V.N. Sheremet, J. Li, S.A. Vitusevich. Mechanism of contact resistance formation in ohmic contacts with high dislocation density. J. Appl. Phys. - 2012. - 111. - 083701.

Radiation Resistance of SiO_x<Ti> Thermosensitive Films

Shepeliavyi P.E.[1], Indutnyi I. Z.[1], Dan'ko V.A.[1],
Neimash V.B.[2], Povarchuk V.Yu.[2]

[1]*V.Ye.Lashkaryov Institute of Semiconductor Physics, NAS of Ukraine, Kiev, Ukraine*
[2] *Institute of Physics, NAS of Ukraine, Kiev, Ukraine*

It was shown by us earlier [1] that metal-dielectric films, deposited in vacuum, can be used as active elements for microbolometers. An important problem of practical exploitation of these bolometers for high-energy physics and space applications is the stability of their parameters under extreme conditions of external factors (ionizing radiation, strong magnetic fields, etc.). In this work we investigate thermosensitive properties of metal-dielectric SiO_x<Ti> coating under the influence of ionizing radiation (gamma-ray photons).

The composite $SiO_x\langle Ti\rangle$ films were prepared by the thermal evaporation of a mixture of silicon oxide (SiO_2) and Ti powders. The optical transmission of the films in the IR spectral range and their temperature-sensitive properties were studied. By varying the contents of the metal in vaporizer and time of evaporation it was possible to obtain $SiO_x\langle Ti\rangle$ layers with resistance (for monopixel of 0,8x1 mm) from tens kOhm to MOhms and a value of the temperature coefficient of resistance (TCR) equal to -2.22 $\%K^{-1}$. IR spectrum of $SiO_x\langle Ti\rangle$ film is characterized by a broad absorption band in the range of 8-12 microns which is associated with the Si–O–Si stretching mode.

Gamma irradiation of the $SiO_x\langle Ti\rangle$ bolometers was carried out at room temperature using a ^{60}Co (E = 1.33 MeV) gamma rays source (MPX-γ-25M) with the dose rate of 0.18 Gy/s from small doses up to integral doses of 10^6 Gy. After each gamma-ray exposition measurements of the sample resistance were done at the temperature range of 273÷333 K, and then values of TCR were calculated. Gamma irradiation has very little effect on sample resistance up to a dose of γ-radiation of 10^5 Gy, while TCR does not change up to 10^6 Gy.

These results suggest that $SiO_x\langle Ti\rangle$ films can be used as materials for production of radiation-resistant thermosensitive layers operated in γ-radiation fields and combined functions both IR-absorption and formation of an electric signal. Offered thermosensitive layers have the following advantages: high stability of physical and chemical properties, absence of toxic components, compatibility with IC fabrication technology, low commercial cost.

1. E. V. Michailovskaya, I. Z. Indutnyy, and P.E. Shepeliavyi. Inhomogeneous SiO_x•Fe Metal-Dielectric Films as a Material for Infrared Thermal Radiation Detectors // Technical Physics, Vol. 48, No. 2, 2003, pp. 261–264.

Current flow Mechanism in Ohmic Contacts to GaN Through Metallic Shunts

Sheremet V.N.

V. Lashkaryov Institute of Semiconductor Physics of NAS of Ukraine, Kyiv, Ukraine

Information about anomalous current flow mechanisms in ohmic contacts to semiconductors with high dislocation density has appeared in [1-3]. Such mechanisms are characterized by contact resistivity increasing with temperature *T*. One cannot ascribe such a behavior to thermionic or field emission. An assumption was made that current flow in such contact structures occurs via metal shunts formed by metal atoms deposition on dislocations [1]. Later a model for such current flow in semiconductors with high dislocation density and current limitation by diffusion supply of electrons was proposed [2]. It gives the possibility of conductive and scattering dislocations calculation.

The ohmic contacts studied by us were formed using successive magnetron sputtering of metallization layers Ti (50 nm)-Al (20 nm)-TiB_x (100 nm)-Au (200 nm) onto the GaN surface grown on an Al_2O_3 substrate, followed with rapid thermal annealing at $T = 900$°C for 30 s in an N_2 atmosphere. X-ray spectroscopy study showed that dislocation density in GaN was ~10^8 cm^{-2}. We observed increasing of ohmic contact resistivity ρ_c with temperature at $T > 250$ K. This is uncharacteristic of the conventional current flow mechanisms in ohmic contacts and can be explained by assuming current flow via metal shunts [1-3]. According to the model proposed in [2, 3], we obtained the density values $N_{D1} = 5\times10^6$ cm^{-2} and $N_{D2} = 1\times10^7$ cm^{-2} for conductive and scattering dislocations, respectively. After microwave treatment of the specimens for 800 s (frequency of 2.45 GHz, irradiation of 7.5 W/cm^2), the dislocation density values increased to $N_{D1} = 3.3\times10^7$ cm^{-2} and $N_{D2} = 2\times10^7$ cm^{-2}, and after treatment for 1000 s - to $N_{D1} = 1.3\times10^8$ cm^{-2} and $N_{D2} = 2\times10^9$ cm^{-2}. The increase of conductive dislocation density resulting from microwave irradiation is followed by contact resistivity drop from 1.8×10^{-4} Ω·cm^2 (initial value at $T = 300$ K) to 4.1×10^{-5} Ω·cm^2 (after irradiation for 1000 s). Such an increase can be explained by redistribution of metal atoms (associated with dislocations) as a result of microwave treatment. This feature is accounted for in the model of current flow in semiconductors with high dislocation density and current limitation by diffusion supply of electrons [3]. No significant changes of dislocation densities and contact resistivity were observed after aging at room temperature for 270 days.

1. T.V. Blank et. al. Tech. Phys. Lett. **30**(10), 806 (2004).
2. A.E. Belyaev et. al. Semiconductors **46(**3), 330 (2012).
3. A.V. Sachenko et. al. J. Appl. Phys. **111**(8), 083701 (2012).

Space-Charge-Limited Current and Photoelectrical Spectra in Iso-Type PbTe-CdTe Heterojunctions

Tetyorkin V., Sukach A., Tkachuk A.[1], Krolevec N.

V. Lashkaryov Institute of Semiconductor Physics NAS of Ukraine
[1]V.Vinnichenko Kirovohrad State Pedagogical University

Carrier transport mechanisms and photoelectrical properties of iso-type *p*-PbTe/*p*-CdTe heterojunctions are investigated. The heterojunctions were grown on (111)BaF_2 substrates under near equilibrium condition using a hot-wall epitaxy technique. Because evaporation of both semiconductors is congruent, epitaxial layers of high quality were grown. Experimental set-up was equipped by two evaporators, each charged with a source material for successive growth of epitaxial layers. The source materials were single crystals of CdTe and PbTe of *p*-type conductivity grown by Bridgman technique. The hole concentration $p=(4\text{-}10)\times10^{15}$ cm^{-3} and mobility of the order of 20-80 cm^2 $V^{-1}s^{-1}$ were measured in *p*-CdTe at room temperature. The hole concentration and mobility in *p*-PbTe was $(2\text{-}6)\times10^{17}$ cm^{-3} and 10^3 cm^2/V s, respectively

The photovoltaic response in the long-wavelength infrared region with the half-peak cut-off wavelength ranged from 9.0 to 9.5 μm was observed in the investigated heterojunctions at T=77 K. The possible mechanism of the photoresponse is the internal photoemission of holes from *p*-PbTe across the heterojunction barrier.

The carrier transport mechanism was investigated by means of the current-voltage measurements. At temperature 77 K the dominant conduction mechanism was found to be the space-charge-limited current. At low bias voltages an ohmic region was observed, followed by a square-law region at higher biases. The crossover voltage, at which transition from the first to the second region occurs, shifts towards higher voltages with increase of CdTe layer thickness. The above features of the current-voltage characteristics are in accordance with Lampert's theory of the space-charge-limited current. In these heterojunctions holes may be injected from the narrow-gap PbTe to the wide-gap CdTe across a potential barrier at the interface.

The valence band offset in the investigated iso-type heterojunctions was estimated to be of the order of 0.13-0.14 eV. Thus, the conduction band offset in PbTe-CdTe heterojunctions is supposed to be of the order of 1.0 eV.

Comparative Characteristics of Ohmic Contacts to Heavily Doped *n*-Silicon Layers

Vinogradov A.O.

V. Lashkaryov Institute of Semiconductor Physics, NAS of Ukraine, Kyiv, Ukraine

It is known that all semiconductor devices require reliable ohmic contacts with low contact resistivity. This is of particular importance for devices applied in extreme electronics that operate under severe conditions (high temperatures, high current densities and voltages). Such devices are strongly heated because of high power dissipated in their active region.

At present there are practically no data on temperature dependence of contact resistivity ρ_c in the operating temperature region for such devices. So the aim of this work was investigation of dependence $\rho_c(T)$ for ohmic contacts to high-power silicon IMPATT diodes whose operating temperature was 200–250 °C.

We studied the samples of two types: (i) initial ones whose contact metallization was formed at a n^+-n-Si substrate heated to 350 °C and (ii) those subjected to heat treatment in a vacuum at $T = 450$ °C for 10 min. An Au(50 nm)–Ti(50 nm)–Pd(30 nm)–n^+-n-Si structure served as contact metallization. The n^+-layer was prepared using phosphorus diffusion into silicon substrate with resistivity of ~0.002 Ω·cm. The phosphorus concentration in the n^+-layer (thickness of ~0.8 μm) was about 10^{20} cm^{-3}.

When studying the dependences $\rho_c(T)$, it was found that contact resistivity ρ_c grew with temperature in the temperature range of 150–380 K (for the initial samples) and 220–380 K (for the samples subjected to heat treatment). Such a behavior differs from that in the conventional models for current flow in ohmic contacts. And ρ_c value for the initial sample was an order of magnitude higher than that for the heat-treated one. The effects observed can be explained using the model advanced in [1] according to which the anomalous dependence $\rho_c(T)$ is due to conductivity in metal shunts associated with dislocations in the Si near-contact region.

1. A.V. Sachenko, A.E. Belyaev, N.S. Boltovets, A.O. Vinogradov, V.P. Kladko, R.V. Konakova, Ya.Ya. Kudryk, A.V. Kuchuk, V.N. Sheremet, and S.A. Vitusevich. *Features of temperature dependence of contact resistivity in ohmic contacts on lapped n-Si* (J. Appl. Phys. 112, 063703 (2012)).

Control of Laser-Induced Barodiffusion of In in the Film In/CdTe System by an Acoustic Response

Vlasenko O.I., Veleschuk V.P., Gnatyuk V.A., Levytskyi S.N., Lyashenko O.V.[1]

V.E. Lashkaryov Institute of Semiconductor Physics of the NAS of Ukraine, Kyiv, Ukraine;
[1]Taras Shevchenko National University of Kyiv, Kyiv, Ukraine

Nanosecond laser irradiation of a metal film-semiconductor structure is one of perspective methods of formation of a shallow and abrupt *p*-*n*- junction, in particular for creation of diodes for ionizing radiation detectors, an In/CdTe is used. In this method, the nonthermal barodiffusion mechanism of introduction of In dopant into a surface layer of CdTe will be implemented due to sharp pressure gradients [1]. This requires in-situ control of pressure in processes of melting, ablation and defect formation. For this purpose, it is effective to use the photo-thermo-acoustic (PTA) phenomenon and accordingly the PTA-method.

PTA-control of the generation of pressure was carried out at irradiation of the system In film (d = 300-400 nm)/p-CdTe in water and air by pulses of a neodymium YAG:Nd laser (λ = 532 nm, τ = 7 ns). The frequency range of induced longitudinal acoustic pulses was 200-2000 kHz. It was established that the amplitude of a longitudinal acoustic pulse and hence pressure in the laser spot area under irradiation of the In/CdTe in water was much higher (up to 100 times) than that at excitation in air.

It was found that starting from the laser energy density E_{max} = 260 mJ/cm^2, the acoustic response amplitude sharply increased and it was accompanied by appearance of ablation tracks (craters) on the In film surface. The depth of craters reached the CdTe surface. Thus, laser irradiation with E higher than E_{max} is unreasonable for the effective doping.

The applied control of pressure, by using an induced acoustic response, allowed to determine the optimal range of laser pulse energies at which efficient diffusion of the dopant is implemented under condition of absence of significant defect formation. The In/CdTe diode structures, formed by laser-induced doping in water, were showed high rectification properties.

The work has been performed in frames of the Target Complex Program of Fundamental Researches of the NAS of Ukraine “Fundamental problems of nanostructured systems, nanomaterials, nanotechnologies” (Project No II-53/17/8/13-N).

1. V.P. Veleshchuk, A. Baĭdullaeva, A.I. Vlasenko, V.A. Gnatyuk, B.K. Dauletmuratov, S.N. Levitskii, O.V. Lyashenko, and T. Aoki. Mass transfer of indium in the In-CdTe structure under nanosecond laser irradiation // Physics of the Solid State. – 2010. – Vol. 52, No. 3. – P. 469–476.

СЕКЦІЯ 4 (стендові доповіді)
ТОНКОПЛІВКОВІ ЕЛЕМЕНТИ ЕЛЕКТРОННИХ ПРИСТРОЇВ, НАНОЕЛЕКТРОНІКА

23 травня 2013 р.

SESSION 4 (poster)
THIN FILM ELEMENTAL COMPOUNDS FOR ELECTRONIC DEVICES

May, 23, 2013

Modeling of the Basic Solar cells Characteristics on the Basis of *n*-ZnS/*p*-CdTe and *n*-CdS/*p*-CdTe Heterojunctions

Berestok T.O., Dobrozhan O.A., Kurbatov D.I., Opanasyuk A.S.

Sumy State University, Sumy, Ukraine

Nowadays the maximal efficiency of the best film solar cells (SC) on the basis of *n*-CdS/*p*-CdTe heterojunctions (HJ) is 17.3 %, but the rates of its increase had been essentially slowed down. The increase of SC efficiency with absorbing CdTe layer is possible, for example, by means of the replacement of optical window material. Meanwhile, CdS (E_g=2.42 eV) window layers may be replaced for more wide-gap material – ZnS (E_g=3.68 eV) [1]. According to the theory it can lead to the increase of SC photosensivity in the ultraviolet spectrum area and to their efficiency increase. From the ecological point of view, it's important that ZnS is nontoxic («Cd-free») material due to the absence in the composition of heavy metals. However, the efficiency of existing SC on the basis of *n*-ZnS/*p*-CdTe heterojunction doesn't exceed 4%. To increase the effectiveness of such SC one need the optimization of the characteristics of the separate layers and of the constructions of photovoltaic devices in general, that is possible with the help of modeling of physical processes in the device.

In this work we used SCAPS-3200 software environment for the realistic modeling of the basic electrical characteristics (current density of short circuit (J_{sc}), open circuit voltage (U_{oc}), fill factor (*FF*) and efficiency (h)) of thin solar cells films with *n*-ZnS/*p*-CdTe heterojunction. In order to compare the modeling of characteristics of photovoltaic devices with the traditional *n*-CdS/*p*-CdTe construction was held with the same parameters. Modeling of dark and light current-voltage characteristics of photovoltaic devices was held at different operational temperatures, thickness of window and absorber layers. Meanwhile, it was considered that the recombination of carriers on the interphase region is absent. As a result of modeling the optimal constructive SC parameters, that provide their maximal efficiency at the temperature 300 K, namely the thickness of absorber layer CdTe – 3.00 μm, of window layer ZnS – 0.05 μm were established. The analysis of the basic characteristics of two constructions showed that SC on the basis of *n*-ZnS/*p*-CdTe heterojunction have greater short circuit current (J_{sc}=28.91 mA/cm^2), fill factor (*FF*=87.61 %) and efficiency (h=26.46 %) in comparison with *n*-CdS/*p*-CdTe heterojunction (J_{sc}=28.06 mA/cm^2, *FF*=86.30 %, h=25.05 %).

1. Structural and electrical properties of ZnS/CdTe and ZnTe/CdTe heterostructures / Kosyak V.V., Kurbatov D.I., Kolesnyk M.M., Opanasyuk A.S., Danilchenko S.N., Gnatenko Yu.P. // Journal of Materials Chemistry and Physics. – 2013. - doi.org/10.1016/j.matchemphys.2012.12.049

Combined Effect of the Microwave Radiation and Chemical Treatment on Optical Characteristics of Thin Gold Films

Boltovets P.M.

V. Lashkaryov Institute of Semiconductor Physics, NAS of Ukraine, Kyiv, Ukraine

One of the most actual problems in modern materials science is development of new complex surface architectures with controllable properties for further applications in sensor systems. With this aim, different chemical, biological, physical phenomena and processes can be used to form complex structures at the sensor surface. In particular, microwave radiation is extensively used for modification of surfaces of different materials in microelectronic technologies [1]. However, its influence on properties of thin gold films widely used in sensor devices (especially those based on the surface plasmon resonance effect) has not been studied sufficiently yet. One of the aims of this work was to study the effect of microwave radiation on the optical properties of thin gold films and their possible restructurization. Besides, chemically active small molecules, e.g. thiocyanate (NCS), can cause some modification of a near-surface layer in the gold film during interaction with it [2]. In particular, whereas sulfur atoms bind the surface due to their capacity to bind three atoms of Au at once, CN group can form a complex compound with the gold atom by tearing it off the surface. Therefore, it seemed reasonable to investigate the possible mutual effect of the both factors on such characteristics of the gold film as the width of the SPR curve, its amplitude and position of the SPR minimum for the purpose to develop sensor surfaces with tunable properties.

To irradiate the samples, a magnetron with ν = 2.45 GHz, P = 7.5 W/cm^2 was used. Short series of sample irradiations for 2-3 s were carried out for 10 and 20 s with samples in air, water and different concentrations of GNCS. The width of the SPR curve, its amplitude and minimum position formed well-defined clusters for treated and untreated sensor surface except cases of irradiation in air and in high concentration of GNCS. Besides, the clear regularity concerning the broadening of the SPR curve, decrease in its amplitude and increase of the SPR angle is observed. It can serve as an evidence of the decrease in the thickness of the films under consideration as a consequence of chemical treatment as well as possible formation of nanostructured architectures under microwave radiation. Thereby, the combination of these two factors can allow obtaining surface structures with controllable parameters.

1. A.B. Kamalov, Modification of Au-Ti (W, Cr, TiBx)-GaAs contacts properties caused by external influences // Radioelectron. Communs. Systems, 52 (3), P. 160-164 (2009).
2. P.M. Boltovets, N.S. Dyachenko, B.A. Snopok, Yu.M. Shirshov, Ya.D. Lampeka Protein-orientating structures: thiocyanate layers as support for immobilization of bioreceptors // Proc. SPIE, 4425, P. 189-193 (2001).

Logical Model of Thin Film Display Elements

Bushma A.V.

Borys Grinchenko Kyiv University, Ukraine

Use of general analytical representations that are based on principles of information transform for research and the analysis will allow to provide the uniform methodological approach to the description of information display systems (IDS) hardware decisions. As a result, creation of technical realizations and their criterial optimization becomes simpler. However, these analytical approaches are developed insufficiently.

The analysis and analytical interpretation of information processing in the ergatic optoelectronic system and its units has been represented in this work.

The formalized approach to signal processing in IDS allows to simplify generalized description of symbol formation at display information area (IA). Let's consider formation of an optical image of a symbol S_n from the set $\tilde{\mathbf{A}}_n$ of separate thin film IA elements, that is $S_n \Leftrightarrow \tilde{\mathbf{A}}_n$. Then, for each element a_{i_n} it is possible to write down

$$a_{i_n} = y_{\mathrm{SO1}}\left\{ y_{\mathrm{SL1}}\left(Z_i^{\mathrm{E}} \right) \right\},$$

where a_{i_n} is the i-th element of an optical symbol S_n; y_{SO1} – operator corresponding to electrooptical transformation in an element of display; y_{SL1} – logic function of this element; Z_i^{E} – signal of excitation of an element $a_{i_n} \in \tilde{\mathbf{A}}_n$.

The functional analysis has shown that practically for all the types of IA elements used in output units of means for display and information registration, the logic component y_{SL1} of realized conversion y_{S} can be presented as a function of a logic gate.

Practical interest is related with definition of the logical function corresponding to the operator y_{SL1}. For this purpose, it is necessary to sequentially submit all possible combinations of logical signals to inputs of the investigated structure and to fix the received output response. Thus, we generate the truth table of a logic gate and, as a result, we can define its type.

It is shown that excitation of arbitrary thin film IAE $\tilde{a}_{p i_n}$ can be presented in the following aspect

$$\tilde{a}_{p i_n} = y_{\mathrm{SO1}}\left\{ \overline{\overline{z_1 + z_2}} \right\}$$

The obtained results allow formalizing the description and modeling of IDS used in electronic equipment both in whole and in their separate units by logical representation of appropriate functions. It forms an analytical basis for complex optimization and hardware minimization of technical decisions in thin film IDS, as well as essential increase in their reliability.

Optochemical Sensors on the Base of Surface Plasmon-Polariton Photodetectors with Thin Thiacalixarene Films

Dmitruk N.L.[1], Mamykin S.V.[1], Mynko V.I.[1], **Kalchenko V.I.[2],**
Drapailo A.B.[2], Kharchenko S.G.[2]

[1]*Institute of Semiconductor Physics of NAS, Kyiv, Ukraine*
[2]*Institute of Organic Chemistry of NAS, Kyiv, Ukraine*

Surface plasmon-polariton photodetectors based on Schottky barriers (Au/GaAs, Au/Si, etc.) are promising devices for different optoelectronic applications such as detectors for light polarization state, angle of light incidence and light wavelength, and as a base for optochemical sensors [1]. The last mentioned application needs to add to the construction of the device some sensitive and selective film.

Optochemical sensors on the base of Au/GaAs Schottky barrier with new periodically corrugated interface of anticorrelated type [2] and selective film of thiacalixarenes have been made. To make a periodically corrugated plasmon carrying interface we used simplified method which could be the final stage of manufacturing of this type photodetector. It consists in deposition of thin Au thin film (20 nm) with following evaporation of chalcogenide semiconductor (As_4S_6) photoresist film (120 nm) with subsequent exposition by laser holographic image of diffraction grating and chemical etching which forms mask of grating type. Then part of Au film was etched out and additional gold plasmon-carrying film with 60 nm thickness has been deposited.

Single layer of thiacalixarenes on the top of the structure have been used to enhance sensitivity and selectivity of the sensors. Sulfur atoms they are composed, chemically bind to gold surface. To deposit thin films it was choosen method of immersion plasmon-polariton fabricated elements in solution thiacalixarenes in chloroform followed by washing samples in pure chloroform. After deposition we obtained a slight shift in the spectral and angular position of the plasmon-polariton resonance of the photocurrent, which is proof of a thin dielectric film on the surface. Checked sensitivity of the shift of angular dependence of the resonance to presence of acetone and ethanol vapors in the air were $4.7*10^{-7}$ and $6.0*10^{-7}$ degrees/ppm respectively, which is about 5 times higher than for the corresponding structures without thiacalixarenes films.

1. Dmitruk N.L., Mayeva O.I., Mamykin S.V., Yastrubchak O.B., Klopfleisch M. Characterization and application of multilayer diffraction gratings as optochemical sensors // Sensors and Actuators, A: Physical. - 2001. - V. 88. - N. 1. - P. 52-57.
2. Dmitruk N.L., Mamykin S.V., Sosnova M.V., Korovin A.V., Myn'ko V.I. Diffraction gratings with anticorrelated relief for new surface plasmon polariton photodetectors & sensors // 27th International Conference on Microelectronics, MIEL. - 2010. - P. 175-176.

Impedance of Si Microwhiskers at Metal-Insulator Transition

Druzhinin A.A.[1,2], Ostrovskii I.P.[1], Khoverko Yu.N.[1,2],
Koretskyy R.N.[1], Nichkalo S.I.[1]

[1]National Lviv Polytechnic University, Lviv, Ukraine;
[2]International Laboratory of High Magnetic Fields and Low Temperatures, Wroclaw, Poland

The paper deals with investigation of doped to concentration near the metal-insulator transition (MIT) Si whiskers by impedance spectroscopy method at low temperatures (4.2-70 K) and frequencies region 0.01-250 kHz. The whiskers were grown by chemical transport reaction method in closed bromine system with use of gold as initiator of growth. Boron is used as doping impurity. The whisker diameters ranges from 30 to 40 μm. It was investigated whisker samples with concentration of boron impurity which corresponds to metallic (resistivity value ρ_{300K}=0.0094 Ohm·cm) and dielectric (ρ_{300K}= 0.0168 Ohm·cm) side of MIT. For each type of samples the Nyquist and Bode plots were obtained. For samples with impurity concentration which corresponds to metallic side of MIT the Nyquist plot has inductive, or so called negative capacity [1], nature of resistance at temperature range 4.2-70 K. It should be noted that the maximum of inductive nature of resistance on Nyquist plot for such samples is observed at 4.2 K and decreases with increasing temperature. At the same time, for samples with impurity concentration which corresponds to dielectric side of MIT the Nyquist plot the capacitive nature of resistance at 4.2 K was observed, though with decreasing of impurity concentration the impact of capacitive component into resistance rises. It was found that the nature of impedance imaginary component substantially depends on the degree of MIT occurrence in Si whiskers. In particular, at temperatures 4.2-20 K for samples from dielectric side of MIT the capacitive nature of resistance and in metallic samples – inductive nature of reactive component of impedance on the Nyquist plot were observed. Capacitive nature of impedance in dielectric Si whiskers at low temperatures could be explained by peculiarities of charge carriers hopping conduction on impurity band, what accompanied by recharging processes of impurity centers during the charge motion caused by radio-frequency alternating current. The observed maximum on frequency dependencies of dielectric dissipation in dielectric samples is caused by interaction with phonons, which is strongly manifested at the region of mechanical resonance occurrence that in Si whiskers takes place at ~ 70-100 kHz and low temperatures.

1. Poklonskyi N.A., Otritsatelnaia emkost (impedans induktyvnogo typa) kremnievykh p^+– n^- perekhodov, obluchennykh bystrymi elektronamy/ Shpakovskyi S.V., Gorbachuk N.I. // FTP, – 2006. – T. 40, № 7. – S. 824-828.

Extraordinary Optical Transmission Though Metallic Subwavelength Structure Under TE and TM Polarizations

Fitio V.M.[1], Yaremchuk I.Ya.[1], Bobitski Ya.V.[1,2]

[1]*Department of Photonics, Lviv Polytechnic National University, Lviv, Ukraine*
[2]*Institute of Technology, University of Rzeszow, Rzeszow, Poland*

Extraordinary optical transmission of metal submicron structures have been actively studied over the last decade, the first researches in this field were made by Ebbesen and colleagues [1], and further interest in this phenomenon is caused by its potential application in the fields of optics and photonics. Binary metal grating is mainly used to investigate this phenomenon, because they have a simple structure and the mechanism of transmission for TE and TM polarizations is different [3].

In this work is shown that a necessary condition for resonance absorption is waveguide effect in the dielectric film and resonance electromagnetic field if the thin dielectric film covers of the metal grating. In lack of the film the high absorption is achieved when the waveguide phenomenon occurs in the slits which form microresonators and standing wave is formed in microresonators. Resonant absorption is achieved for TM polarization by the occurrence of waveguide effect and excitation plasmon-polaritons on metallic surfaces by the dielectric or metallic gratings which are making a low perturbation in the metallic plane. Plasmon resonance increases of the absorption in the grating and thus reduces the transmittance. Waveguide effect can be for any width slit, and thus it is possible achieved the extraordinary optical transmission. Resonant absorption for TE waves occurs only in result of waveguide effect. There is a minimal slit width where possible waveguide effect and consequently high absorption. The high intensities of the fields in the slit or on the surfaces of the metal grating at plasmon resonance indicate on resonance phenomena that occur at high transmission. They are significantly larger than the amplitude of the incident wave on the grating.

This work was supported by grant GP/F36/117 from the State Fund for Fundamental Research of Ukraine and Research scientific work DB/Microlaser from State Agency for Science Innovation and Informatization of Ukraine.

1. T.W. Ebbesen, et al. Extraordinary optical transmission through sub-wavelength holes arrays// Nature. – 1998. – V. 391. – P. 667-669
2. J.A. Porto et al. Transmission resonances on metallic gratings with very narrow slits// Phys. Rev. Lett. – 1999. – V. 83. – P. 2845-2848.

Microstructure of Selecting Elements for Plasma Flow Sensors

Gasenkova I.V., Andrukhovich I.M.

Institute of Physics B.I. Stepanova NAS of Belarus, Minsk, Belarus

Sensors based on the Faraday cylinders were used for measurements of plasma parameters in near Earth space and in the interplanetary medium. High-precision metal microstructures are used as the selecting elements. One of the possible ways to obtain such structures is electrochemical deposition of the material of the electrodes in anodic alumina matrix, the topology of which corresponds to the given microstructure pattern, followed by removal of the matrix by means of etching. The matrix should ensure reproducible size of the electrodes structure. Due to the porous structure of anodic alumina, a wedge etching is very small (0.03-0.05) the thickness of the anodic oxide and holes are formed with high accuracy. So slight lateral etching can be explained by the specific structural features of the aluminum oxide structure.

Formation of the matrix for microstructures was performed as follows. Before anodizing aluminum samples grade A99 went through chemical cleaning and chemical polishing. Next were anodized in galvanostatic mode of 3% oxalic acid solution at 32 ÷ 34 °C during 60 s. The current density was 10 mA/cm^2. Obtained layer anodic oxide was removed and carried over the anodizing process. The process parameters are as follows: 3% solution of oxalic acid, current density of – 10 mA/cm^2, electrolyte temperature – 12 ÷ 15 °C, time anodizing determines the required thickness of the oxide film. Using photolithography method on the surface of the anodic aluminum oxide formed the desired pattern microstructure and obtain the matrix by selective etching of oxide in accordance with the required precision microstructures topology of selecting elements. Whereas nickel is used as the metal for plasma flow sensors microstructures, electrochemical deposition of nickel was held in the resulting matrix. $NiSO_4 \cdot 7H_2O$ (200 g/l), H_3BO_3 (25 g/l), NaF (2 g/l), $K_2S_2O_8$ (2 g/l), NaCl (2 g/l), Li_2SO_4 (20 g/l), H_2O were used as electrolyte. Process temperature of 35 ± 1 ºC was maintained by a thermostat MLW16. To decrease pitting mixing of electrolyte with compressed air was used.

It was established that to produce microstructures of the high-energy plasma flow sensor elements with dimensions 10 mm, it is necessary to carry out the electrochemical deposition in two stages. In the first phase-current density 2 mA/cm^2, deposition time 10 min. In the second phase the current density increases to – 20 mA/cm^2, the process depends on the desired thickness of the microstructure.

Impedance Spectroscopy of Lithium Batteries with Cathode-Based Spinel System Li-Mn-Fe-O

Gasyuk I.M., Boychuk A.M, Ugorchuk V.V., Boychuk T.Ya.

Vasyl Stefanyk PreCarpathian National University, Ivano-Frankivsk, Ukraine

The using of spinel $LiMn_2O_4$ as cathode of lithium power sources is accompanied by a number of problems, the most of whichis the degradation of the structure during lithium intercalation. It leads to a rapid decrease in both specific performance and the number of cycles of the LDS. Therefore, the attention of researchers is attracted on cation-substituted spinel, which have more stable structure and in which is maximum eliminated the possibility of manifestation Jan Teller effect. At work the impedance modeling study of lithium batteries with cathodes based on spinel $LiMn_{1.9}Fe_{0.1}O_4$ have been spent.

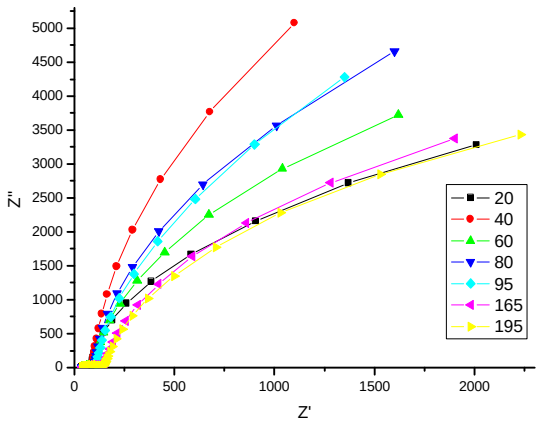

Figure. 1. Neykvist Charts electrochemical cell during the discharge

The study of polycrystalline spinel $LiMn_{1.9}Fe_{0.1}O_4$ synthesized by standard double sintering ceramic technology using oxides Fe_2O_3, MnO_2, and hydroxide LiOH. According to the results of X-ray diffraction studies (DRON3, Cu_{Ka} radiation) only spinel phase in the samples have been presented. Electrochemical cells were collected in a sealed box drained. Cathode mixture is consisted of spinel conductive additives (soot) and binding agent. Metallic lithium anode served as electrolyte - $LiBF_4$, dissolved in γ-butyrolactone. Impedance hodograph electrochemical cells have been treated with Autolab PGSTAT/FRA-2 spectrometer in the frequency range 10^{-2}-10^5 Hz the first cycle discharge.

Figure 1 shows the experimental Nyquist diagrams of cells at different stages of "guest" load lithium. All spectra are modeled another scheme, which consists of ohmic resistance and the two successive links with parallel combinations of resistance and phase shift element (CPE). The resistance R1 is the resistance of connecting contacts to the electrochemical cell and all other ohmic resistance, non-electrical double layers and diffusion regions. The second link is responsible for the charge transfer through the boundary solution / passive layer through passive layer and through the boundary layer passive / spinel. Last, low link associated with the transfer charge inside the cathode material, ie proper intercalation of lithium. The presence of this branch indicates electro-stumylated diffusion of lithium ions in the spinel matrix studied, which provides relatively high specific electrochemical parameters of lithium power sources

Organic-Inorganic Nanostructured Silicooligoetherurethaneurea Thin Film Resistive Humidity Sensors

Gomza Yu.P., Klepko V.V., Stryutsky A.V., Minenko M.M.

Institute of Macromolecular Chemistry NAS of Ukraine, Kyiv, Ukraine

The sol-gel organic-inorganic functionalized proton conductive materials based on silicooligoetherurethaneurea doped with polyhedral oligomeric silsequioxanes (POSS) with ionogenic groups in organic frame were synthesized. WAXS investigations shows the amorphous structure of such materials, SAXS data indicates the “macrolattice” type structures forming. The nanosized POSS-based functionalized dopant is uniformely distributed in such a lattice at minimal content and is aggregated at higher concentration. (See fig. 1).

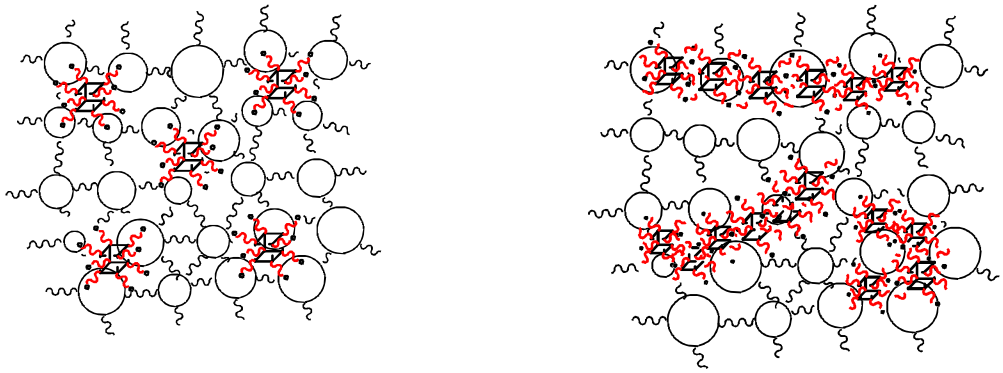

Figure 1. The scheme of structure of silicooligoetherurethaneurea based materials doped with POSS.

The materials were formed thin transparent films with high adhesion to metal electrodes and polymer substrates, high mechanical properties and thermoresistance up to 250^{o}C. The levels of proton conductivity of such materials are from 10^{-7} to - 10^{-3} Sm/cm at temperatures from 20 to 120^{o}C. The sensoric characteristics investigation of thin films of such materials applicated on the interdigital electrodes shows that R.H. variation from 20 to 90% leads to wide scale (up to 3-4 of decimal order), close to linear and reciprocal variations of protonic conductivity level. The recovering time of such devices was about 1-2 minutes. For practical sensoric applications we propose the using of the fixed frequency a.c. bridge sircuit which enables fast R.H. levels monitoring by measuring the capacity values.

So the sol-gel functionalized silicooligoetherurethaneurea materials are prospective for thin film resistive and capacity humidity sensor applications. Their high mechanical and thermoresistance properties enables using of them as ion conducting membranes for various electrochemical devices which operate at elevated temperatures (up to 200-250^{o}C).

Quantum-Sized Effects in Oxidized Macroporous Silicon Structures with Surface II-VI Nanocrystals

Karachevtseva L., Kolesnyk O., Kolyadina O., Matveeva L., Smirnov O.

V. Lashkaryov Institute of Semiconductor Physics, NASU, Kyiv, Ukraine

Nanotechnologies of II-VI nanocrystals in oxidized macroporous silicon structures are perspective for the manufacture of light emitting elements. In this work the interface Si-SiO_2 in oxidized macroporous silicon structures with surface CdS and ZnO nanocrystals was investigated by methods of electro-reflectance and photoconductivity.

Direct interband transition energy, the broadening parameter and the relaxation time of charge carriers were identified from electro-reflectance spectra of macroporous silicon structures with silicon oxide layer of a thickness of 7, 15 and 30 nm (Figure). There were revealed a built-in electric field and surface quantization of charge carriers in the surface Si-SiO_2 region. It was determined the occurrence of quantized energy levels and the corresponding quantum wells. The broadening parameter, built-in electric field and the number of quantized levels increased with increasing of the oxide thickness, and relaxation time of charge carriers decreased.

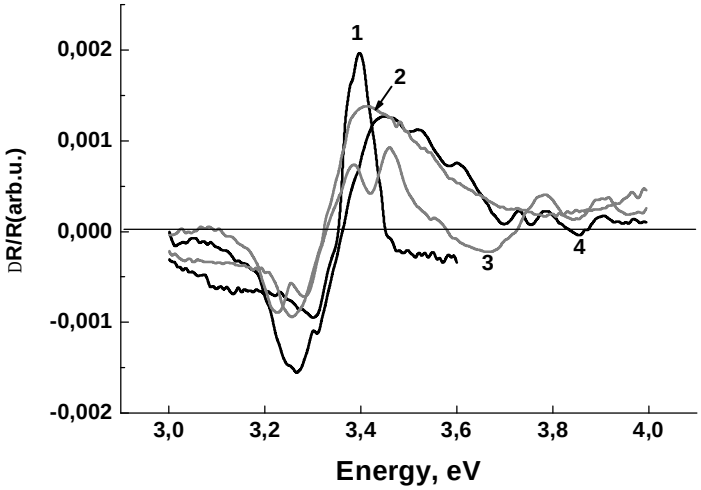

Electroreflection spectra of silicon substrate (1) and macroporous silicon structures with ZnO nanocrystals on SiO_2 nanocoatings of thickness:
7 nm (2),
15 nm (3),
30 nm (4).

Photoconductivity maxima of investigated structures were shifted to the short side at 0.17-0.20 eV, which can be attributed to the quantum-sized effect in the transition from silicon to SiO_x. This conclusion is confirmed by measuring the photoconductivity in spectral range 1/4-2/0 eV. It was detected splitting peaks in the area of main peak of photoconductivity of indirect interband transition for silicon oxide thickness 15 and 30 nm due to surface quantization of charge carriers in the surface region of silicon. Obtained data correlate with the results of electroreflectance spectra measurement in the area of direct interband transition of oxidized macroporous silicon structures with surface CdS and ZnO nanocrystals.

Surface Photoconductivity in Macroporous Silicon with Oxide

Karas' N.I.

V. Lashkryov Institute of Semiconductor Physics NAS of Ukraine, Kyiv, Ukraine

Porous silicon is a promising material micro-and optoelectronics also be of interest and use of the macroporous silicon as photodetectors. The main drawback for use in optoelectronics is the instability of its photoelectric properties. To stabilize the photoelectric properties of the surface passivation using macroporous structures by thermal oxidation. It is known that the oxide layer has built a positive charge localized in a narrow layer about 2 nm, adjacent to the interface Si-SiO_2. In [1] found a negative steady-state photoconductivity in the structures macroporous silicon at wavelenghs between 0.4 and 0.57 μm . The aim of this work is to study photoconductivity in macroporous silicon oxide-coated for different wavelength of lighting.

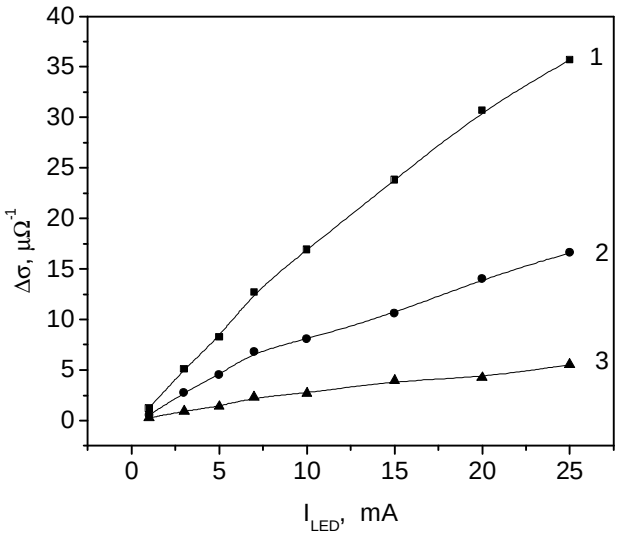

Fig. Dependencies of photoconductivity on I_{LED} for different LED wavelength (λ): 1 – 0.4 μm, 2 - 0.57 μm, 3 – 0.93 μm

The studies found that for thickness of the oxide coating of 30 nm is observed only positive photoconductivity, the spectral dependence of it has an anomalous character - with an increase of the absorption coefficient (from 200 to 105 cm^{-1}) decreasing the wavelength of light (from 0.93 to 0.4 μm respectively) the photoconductivity is not decreasing but increasing. It occurs in all cases where bipolar photoconductivity of space-charge region more of bipolar photoconductivity of quasineutral region space-charge region (called the localization effect of photoconductivity).

1. Karas' N.I. Negative photoconductivity in macroporous silicon structures // New technologic. – 2010. – V. 27, № 1. – P. 118-123.

Negative Photoconductivity in Macroporous silicon oxide-coated

Karas' N. I.

V. Lashkryov Institute of Semiconductor Physics NAS of Ukraine, Kiev, Ukraine

In [1] found a negative steady-state photoconductivity in the structures macroporous silicon at wavelengths between 0.4 and 0.57 μm. Negative photoconductivity is interpreted as a monopolar photoconductivity, which is concentrated in the space charge region and is associated with the surface trapping of majority carries in the so-called ‘‘slow’’ surface levels. In our work the influence of the oxide coating and the wavelength of light to the negative photoconductivity in macroporous silicon has been studied. The starting material consisted of n-type silicon with [100] orientation and 4.5 Ω·cm resistivity. Macropores with diameter D_p = 4 μm and depths h_p = 100 μm are formed by electrochemical etching.

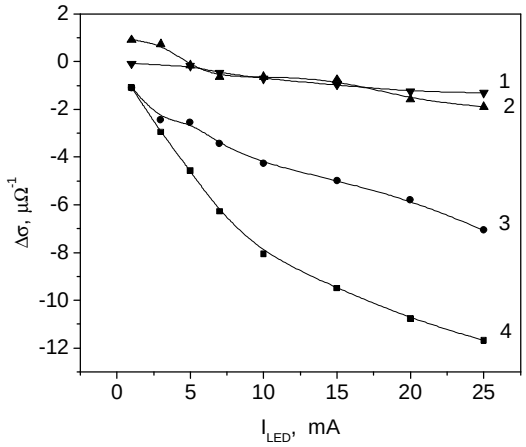

Fig. Dependencies of negative photoconductivity on I_{LED} for different oxide thickness and LED wavelength (λ): 1 – 15 nm, 2 – 7 nm, 3, 4 – 3 nm, 1, 3 – λ = 0.57 μm, 2, 4 - λ =0.4 μm.

The measurements were performed at room temperature with LEDs. As a result of these studies, we found that the value of negative photoconductivity in macroporous silicon with its own oxide (3 nm) is several times higher than in the macroporous silicon with an oxide coating thickness of 7 nm and 15 nm. We believe the reason of this is compensation negative charge of the surface by positive oxide charge.

1. Karas' N.I. Negative photoconductivity in macroporous silicon structures // New technologic. – 2010. – V.27, №1. – P. 118-123.

Fabrication and Photovoltaic Properties of the Thin-Film $CuIn_{0.5}Ga_{0.5}Se_2$/ZnSe/ZnO Solar Cells Without Using Cadmium-Related Compounds

Khomyak V.V.[1]., Shtepliuk I.I.[2]

[1] *Chernivtsi National University, Chernivtsi, Ukraine*
[2] *I. Frantsevich Institute for Problems of Material Sciense, NASU, Kyiv, Ukraine*

Development of the growth technology and studies of the diamond-like semiconductors - $CuInSe_2$ (CIS), $CuGaSe_2$ (CGS), $CuIn_xGa_{1-x}Se_2$ (CIGS) – with chalcogenide and chalcopyrite structure lead to the fabrication of the highly stable and radiation resistant devices with huge photoconversion efficiency of 20%. This value is a record high compared to the well-known solar cells. Typically, the active area of these structures contains CIGS / CdS heterocontacts. However, the removal of highly toxic cadmium from the thin-film solar cells based on CIGS is very desirable from the viewpoint of environmental safety. For this reason it is very important to replace the buffer layer by the material without cadmium. Therefore, use of ZnSe is an attractive alternative for the replacement of CdS buffer layer in widely used solar cells CIGS/CdS/ZnO.

The growth of $CuIn_xGa_{1-x}Se_2$ thin polycrystalline films ($x = 0.5$) with thickness of 1.5 - 2 μm and ZnSe ones with thickness of 200 nm was carried out by vacuum thermal evaporation in quasi-closed chamber with using diffusion cells. During deposition procedure the both substrate temperature and evaporator temperature were controlled. The most satisfactory growth of thin films with very high density of layers and large grains occurred at evaporator temperature of $T_e \approx 1200$°C and substrate temperature of $T_S \approx 300$ - 400°C. Our studies have shown that the XRD patterns of $CuIn_xGa_{1-x}Se_2$ contain the set of lines corresponding to the chalcopyrite structure.

It should be mentioned that ZnO films (used in $CuIn_{0.5}Ga_{0.5}Se_2$/ZnSe/ZnO heterostructures) were deposited by means of the reactive magnetron sputtering of the metallic target in the atmosphere of the gas mixture ($Ar+O_2$). Substrate temperature, during deposition of ZnO, did not exceed 300 - 350°C. The change of the ratio of argon and oxygen gives a possibility to change the concentration of free electrons. It provided an opportunity to obtain both high-resistance and low-resistance ZnO film in the frames of one technological process.

The height of the potential barrier (which was defined from direct branches of Volt-ampere Characteristic) was about 0.55 V. Additionally, the measurement of the light volt-ampere characteristics gives us a possibility to determine key parameters such as open circuit voltage (U_{OC}), short-circuit current (I_{SC}) and fill factor (FF). In the case of the best samples this parameters were $U_{OCV} = 530$ mV; $I_{SC} = 8.5$ mA; $FF = 0.72$ respectively.

Preparation and Characterization of n-TiO_2/p-$Co_{0.7}Ni_{0.3}O$ uv-Sensitive Heterostructure

Kleto G.I., Tsaly V.Z., Tkachuk P.N., Martynyuk Ya.V.[1], Makoviy V.V.

Chernivtsi National University, Chernivtsi, Ukraine
[1]National Technical University of Ukraine «KPI», Kyiv, Ukraine

Thin films of TiO_2 are highly interesting for UV sensor fabrication. The most common detectors currently in use are Schottky-type structures. However, UV photodetectors based on metal-semiconductor structures show a slow photoresponse in visible and IR regions due to effect of photoemission from metallic barrier layer. Recently, TiO_2 based p-n type photodiodes have also been extensively studied [1,2]. TiO_2/p-type wide band gap semiconductor heterostructures did not show any response in the visible light region attributing to Schottky junction [2]. In order to improve the sensitivity of UV sensors we have prepared and investigated the main characteristics of UV sensitive n-TiO_2/p- $Co_{0.7}Ni_{0.3}O$ heterostructure. Ultrathin film of the mixed Co-Ni oxide can be one of the best materials for p-part due to its high conductivity and high transparency in UV region [3].

In this work metallic targets of Ti and $Co_{0,7}Ni_{0,3}$ alloy were used to prepare TiO_2 and $Co_{0,7}Ni_{0,3}O$ films on quarts, sitall and silicon substrates by RF-sputtering process. X-ray diffraction patterns have been used to study the structural properties of TiO_2 and $Co_{0.7}Ni_{0.3}O$ films. In order to obtain high quality polycrystallinity form of the film material, postdeposition annealing was carried out. Multilayered structures were fabricated on sitall wafers. They consist of n^+- SnO_2 electrode layer, n- TiO_2 and ultrathin $Co_{0.7}Ni_{0.3}O$ layers. The typical current-voltage characteristic of heterogunction is rectifying. The maximum forward to reverse current ratio was 10^5 at voltage of 1V. For the most effective detection it is necessary to provide absorption of the light in photosensitive n- TiO_2 layer close to p-n interface region. For this purpose one has to irradiate the structure from side of ultrathin p-layer. Spectral range of sensitivity is well agreed with band gap of TiO_2. Maximum spectral sensitivity 16 ma/W is close to maximum possible one for Shottky-type TiO_2-based photodiodes. The results of this work suggests that TiO_2/$Co_{0.7}Ni_{0.3}O$ heterostructure is effective for fabrication of UV sensor devices.

1. Tsai T.Y., Chang S.I. et al // Nanoscale Res. Lett. – 2011. – V. 6, (1). – P. 575.
2. Masayuki Okuya, Katsauyuki Shiozaki, Nobuyuki Horkawa et al // Solid State Ionics. – 2004. – V. 172. – P. 527-531.
3. A. Banerjee, K. Chattopadhay // Progress in Crystal Grows and Characterization of Materials. – 2005. – V. 50 – P. 52-105.

Optical Investigation of Properties of $Zn_{1-x}Mn_xS$ Films

Klymov O.V.[1], Kurbatov D.I.[1], Kshnyakina S.I.[1], Starikov V.V.[2]

[1]*Sumy State University, Sumy, Ukraine*
[1]*National Technical University «KhPI», Kharkiv, Ukraine*

Recently interest of researches in the field of science materials in obtaining and investigation of new film material for micro- and optoelectronics, solar power and spintronics has increased. Such materials include compounds of A_2B_6 group – ZnS, ZnTe, CdTe, etc, and semimagnetic solid solutions based on them – $Zn_xMn_{1-x}S$, $Zn_xMn_{1-x}Te$ and $Cd_xMn_{1-x}Te$. It can be explained by their unique photoluminescence, optical and magnetic properties that are currently studied not enough.

In this work we carried out investigation of optical properties of $Zn_{1-x}Mn_xS$ films. Measurement of condensates optical properties (transmission and reflection spectra) was performed by using a spectrophotometer CF-46 in the range of wavelengths that are close to the red threshold of photoconductivity of materials at room temperature.

$Zn_{1-x}Mn_xS$ films were obtained onto cleaned glass substrates by close-spaced vacuum sublimation in vacuum setup VUP-5M. The evaporation of powder with semiconductor-quality purity was carried out. Manganese content was equal 7%. Temperature of evaporator was equal T_e = 1473 K. Substrate temperature varried in the range of T_s = (373-723) K.

Research has shown that transmittance was equal (34-58.5)% in $Zn_{1-x}Mn_xS$ condesates near red threshold of photoactivity of semiconductor. Coefficient of light reflection reached (0.8-9.2)% in $Zn_{1-x}Mn_xS$ films. As shown by scanning microscopy and X-ray diffraction, the difference between the coefficients of transmission and reflection of thin layers obtained at different condensation temperature was caused by the different crystal structure and phase of these samples, the presence of grain boundaries and different roughness of the surface.

Absorption coefficients by films were calculated and in the range of energy radiation higher than material band gap were equal $a = (2.07\text{-}3.31\cdot10^4)\cdot10^4$ см$^{-1}$. There were observed two linear plots on the dependences of $(ahn)^2 - hn$. And extrapolation of these linear plots allowed to determine material band gap. Obtained values of band gap E_g = (3.10-3.23) eV and E_g=(3.68-3.72) eV correspond to solid solutions based on MnS and ZnS (MnS – E_g = 3.1 eV, ZnS – E_g=3.72 eV). These data are in good correlation with those obtained by X-Ray method.

The Computer Simulation of 3D SOI-Structures for Sensitive Elements

Kogut I.T., Holota V.I., Dovhij V.V., Terletsky A.I., Fryk O.B.

Precarpathian National University, Ivano-Frankivsk, Ukraine

This paper presents the device-technological simulation results of the developed methods for local nonstandard with one- and two layers 3D "Silicon-on-Insulator" (SOI) - structures formation. These structures are combined with one- or two levels of microcavities under surface of silicon wafer. Is shown that proposed 3D SOI structures could be use as a constructive material for the sensitive elements design as well as with standard planar constructions on the bulk silicon and 3D architectures and their combinations. Such structures allow creation and monolithic integration the sensitive elements for IC, system-on-chip (SoC) and laboratories-on-chip (LoC).

The creation and use of SoC and LoC has significantly intensified for last years. Traditionally the planar CMOS and Bi-CMOS technologies are used for SoC and LoC sensitive elements fabrication. These technologies allow creating elements of digital and analog blocks, as well as sensor and actuator elements. The SOI-structures assumed to have better perspectives for development the new device structures based on higher speed, rigidity to external factors, growing degree of integration. The research and investigation of new low cost technological methods fabrication of local original non-standard SOI-structures are desirable for development of new MEMS, SoC and LoC elements with planar and three-dimensional (3D SOI) architectures.

The base method of compatible local 3D soi structures and microcavities fabrication. The proposed method of compatible local 3D SOI-structures and multilevel microcavities fabrication is based on the results of one level cavities creation under surface of substrate. Cross section of a hermetical microcavity fabricated by this method is showed on Fig.1**.** This technology is compatible with the base technology formation of the local non-standard 3D SOI structures. Hermetic sealing microcavities are provided by the selection of topological sizes and technology for the local oxidation of the surface of cavities, with the following joining of hanging in the cavity nitride films (4) and deposition of sealing material (5) [1].

Multilevel cavities are formed using processes of industrial CMOS-technology: lithography, local thermal oxidation with masking by a silicon nitride film, isotropic and anisotropic plasma etching, formation of tunnels and cavities in a substrate, etc [1, 2]. Such local structures can be created at designed places on a silicon substrate according to the device layouts. The computer simulation results of base steps are shown in Fig.2.

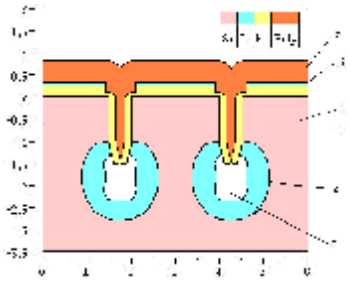

Fig. 1. Cross-section of a hermetical microcavity: 1 – substrate (100); 2 – thick local thermal oxide; 3 – thin oxide; 4 – silicon nitride; 5 – polysilicon; 6 – hermetical microcavity.

It is possible to fabricate 1, 2 and more microcavities levels in substrate by proposed method. The microcavities could be located one under other as showed on Fig.2. or on different levels and places. The hermetical cavities are obtained by thermal oxidation. At the same time could be fabricate two levels of local 3D SOI structures. These cavities and channels could be used as elements for fluidic transport in LoC, as resonators, as elements of cooling system-on-chip, as microbattery and energy storage embedded into chip and other applications [5, 6].

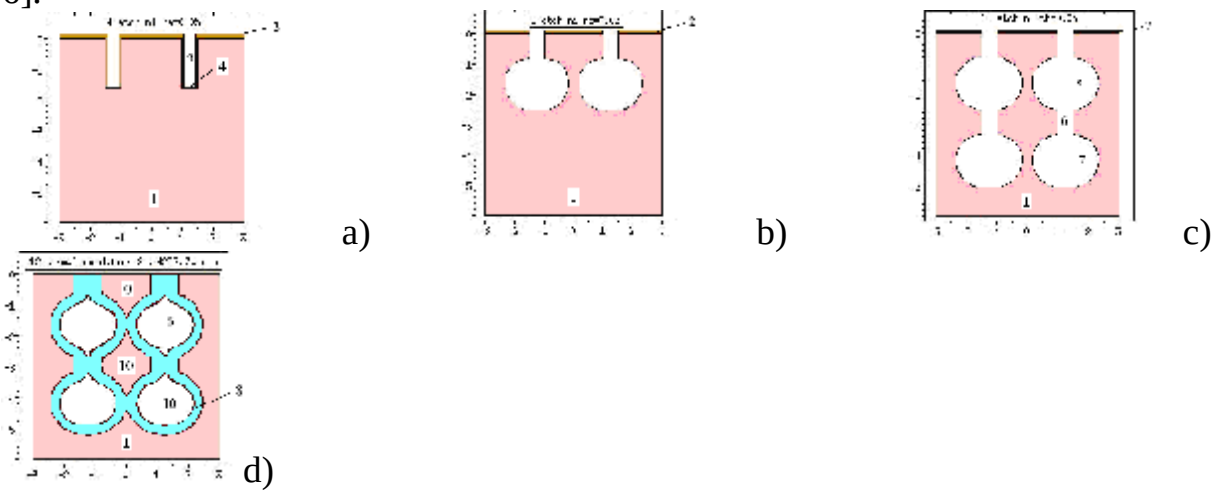

Fig. 2. The simulation results of base fabrication steps: a) initial substrate after anisotropic trenches etching; b) 1st level of cavities formed by isotropic etching; c) 2nd level of cavities formed by isotropic etching; d) hermetical microcavities: 1 – substrate, 2 – Si_3N_4, 3 – trench for 1st level, 4 – trench bottom, 5 – cavities of 1st level, 6 - trench for 2nd level, 7– cavities of 2nd level, 8 – local oxide, 9 – silicon-on-insulator, 10 – silicon-into-insulator.

Sensetive 3D soi transistor. 3D SOI sensitive transistor (Fig.3.) is formed by non-standard local one-level 3D SOI-structures and microcavities [2-5]**.** The results of technology simulation shows that non-standard multilayer 3D SOI-structures are compatible with the base method of multilevel microcavities fabrication. In the proposed sensitive 3D SOI transistor the channel region

connect with substrate via silicon with width *c*. Width *c* could be controlled by the technology process and layouts parameters.

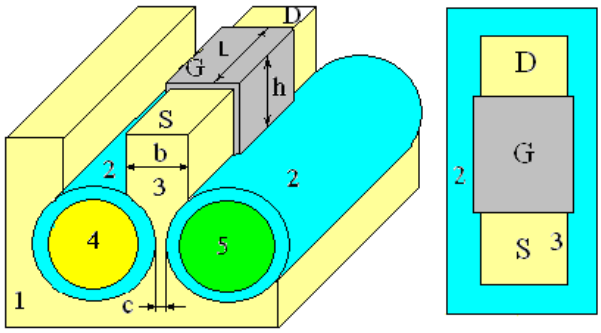

a) b)

Fig.3. The schematic base construction (a) and layouts of the sensitive 3D SOI MOS-transistor, combined with microcavities: 1- initial substrate, 2 – local thermal oxide of hermetical microcavities, 3-local SOI-island, 4, 5 – fluidics into microcavities with different potentials(charges). S, G and D – source, gate and drain of transistor, L - lengh and W=2h+b- width of channel, c - width of silicon between underchannel region and substrate.

On the base of sensitive 3D SOI transistor its possible to build the single sensitive *p*- or *n*-channel transistors, matrix transistors and SOI CMOS digital and analog elements and in the same time with their monolithic integration into processing blocks in one chip. Such 3D structures of “silicon-on-insulator” and “silicon-into-insulator” will extend possibilities of elements design for SoC and LoC.

Matrix transistors can transform difference of potentials or charges of fluidics with different properties, wich are moved in microcavities, into electrical form. Some simulation results of electrical potential distributions and influence of potentials in cavities for sensitive matrix transistors with common and single isolated gates are showed in **Fig. 4.**

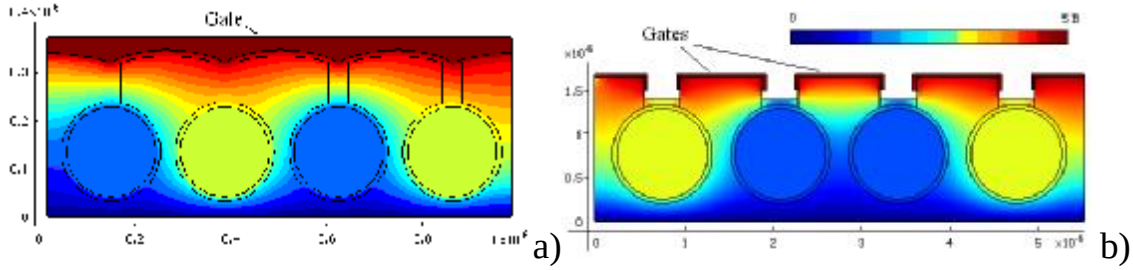

a) b)

Fig. 4. The simulation examples of electrical potentials distribution for 3D SOI matrix sensitive transistors: a) with common gate and cylindrical surface of channel, b) with isolated each other gates and standard 3D surface of channel (potentials: blue- 1V, yellow -3V, gates – 5V)

Conclusions. This paper presents the simulation results of developed technological methods for non-standard multilayer’s local 3D SOI-structures

and microcavities/microchanels fabrication. These methods are compatible each other and allows creation and monolithic integration the sensetive elements for MEMS, SoC and LoC

1. Патент №43198 UA. Спосіб формування герметизованих порожнин в кремнієвих пластинах./ Когут І.Т., Голота В.І.; опубл.15.08.2008. – Бюл. №15 (in Ukrainian).
2. Патент №36463 UA. Спосіб виготовлення локальних тривимірних структур «кремній-на-ізоляторі». Когут І.Т., Голота В.І., Дружинін А.О., Сапон С.В. – опубл. 27.10.2008. – Бюл. № 20 (in Ukrainian).
3. І.Т. Когут. Локальні КНІ-структури – перспективний матеріал для інтегрованих мікросистем-на-кристалі. // *Прикарпатський вісник НТШ* (*Фізика і хімія твердого тіла*). – 2008. – №1. – С. 164-172 (in Ukrainian).
4. A. Druzhynin, V. Holota, I. Kogut, S. Sapon and Y. Khoverko. The Device-Technological Simulation of the Field-Emission Micro-Cathodes Based on Three-Dimensional SOI-Structures // *Electrochemical Society Trans*. – 2008. – Vol. 14(1). – P. 569.
5. Druzhynin A.O., Holota V.I., Kogut I.T., The device-technological simulation of the local three-dimensional SOI-structures for microsystem applications. // Fifth Workshop of the Thematic Network on Silicon-On-Insulator, Technology, Devices and Circuits (EUROSOI-2009) / Conf. Proc., 19-21 January 2009, Goteborg, Sweden, pp. 103-104.
6. Druzhynin A.O., Holota V.I., Kogut I.T., The device elements for monolithic integrated SoC based on the local 3D SOI-structures //ULIS-2009, Yaachen, Germany. Mar.18-20, 2009.

Passivation Properties of Nanostructured ITO Films

Kostylyov V.P.[1], Sachenko A.V.[1], Slusar T.V.[2], Serba O.A.[1],
Tytarenko P.O.[1], Chernenko V.V.[1], Korkishko R.M.[1], Legkova G.V.[2]

[1]*V.E. Lashkarev Institute of Semiconductor Physics,*
National Academy of Science of Ukraine, Kyiv Ukraine
[2]*National Aviation University, Kyiv, Ukraine*

Until now indium-tin oxide (ITO) films are widely used for making transparent conductive contacts to the photosensitive structures and solar cells based on it. At the same time, it is known that depending on the conductivity type of the ITO-silicon heterojunction components it can be rectifying or antibarrier and thereby effects on the recombination processes at the ITO-silicon interface.

So it is interesting to research the effectiveness of applying ITO layers in order to reduce recombination (effective surface recombination velocity S_{ef}) and optical losses (light reflection coefficient) in silicon solar cells. In this work the passivation properties of ITO films deposited on the front surface of back-contact back-junction silicon solar cells also called interdigitated back contact (IBC) solar cells were experimentally investigated. Samples of IBC solar cells were made on *n*-type float-zone silicon wafers with resistivity of 2 Ω·cm. On the front side the n^+-*n* junction (front surface field) and thermal SiO_2 passivation layer with thickness of 100 nm were formed.

The researches were performed in several stages. The illuminated current-voltage characteristics at standard testing conditions AM1,5 and photocurrent spectral dependencies at constant monochromatic power mode in the wavelength range 400...1200 nm were measured on the initial samples and after each stage of the treatments. From *I-V* curves the photovoltaic parameters were determined, as well as from photocurrent spectral characteristics external and internal quantum efficiencies were obtained. In order to remove SiO_2 layer from the front surface of the initial samples it was treated in concentrated hydrofluoric acid. Then the ITO film with thickness of 75 nm was deposited on this treated surface by reactive sputtering of indium-tin target. The thickness and refractive index of deposited ITO films were determined by ellipsometry.

It was experimentally shown that the effective surface recombination velocity S_{ef} in both cases of passivated by thermal SiO_2 film and after its removal remains approximately constant. At the same time the formation of ITO-silicon heterojunction leads to a significant reduction of S_{ef} and increasing of the internal quantum efficiency in the short-wave region of the spectrum. Possible mechanisms of observed passivation phenomena are discussed.

The Inkjet Printing of Resistive Layers with Colloidal Solutions of Carbon Nanotubes

Kravchuk O.[1], Bobitski Y.[1,2]

[1]*Department of Photonics Lviv Polytechnic National University, Lviv, Ukraine,*
[2]*Institute of Technology, University of Rzesów, Rzesów, Poland,*

In this work the functional inkjet printing with *colloidal solutions of carbon* nanotubes to create resistive layers was investigated. We have tested different printing systems, substrates and solutions of carbon nanotubes. Printed samples were tested for resistance to environmental factors such as temperature, humidity and solar radiation.

The results showed that the technology of inkjet printing with solutions of carbon nanotubes can be used for the production of printed resistors. CNT demonstrate high resistance to high temperatures, but at the same time, the printed structures must be protected from moisture and mechanical damage.

For inkjet printing Epson Stylus D88, Epson Stylus R 200, Epson Stylus R800, Canon Pixma Pro 9500 Mark II, and the "PrintoLUX" system, which integrated printhead Epson Stylus Photo R1800, were used. It is important to choose a system that is suitable for printing with newest inks − solutions of carbon nanotubes. It should be able to apply CNT with high accuracy on different substrates. Integration of one or more printed resistances of CNT's is an important step in our research. Using of colloidal solutions of CNT's in conjunction with other nanoinks and insulating inks opens up possibilities for printing more complex electronics in the future.[1]

Electrical resistance of printed rectangular structures was measured using 4-point method with a Keithley 2701 Ethernet multimeter. The sheet resistance depending on the number of layers for different printers is shown in Figure 1. It is obvious, that sheet resistance decreases with increasing number of deposited layers. We can clearly see that values of the measured resistances for thermal inkjet systems (such as HP and Canon) in one to two orders lower than those for piezo inkjet systems (Epson). Printer ESPON Stylus Photo R800 in this experiment showed the worst results.

To simulate the effect of temperature fluctuations climate chamber "VMI 04/180" from Heraeus vötsch were used. The cycle lasted one hour; the temperature varies from −30 °C to + 120 °C, then again to −30 °C. The experiment took place continuously, 24 hours a day.

Epson printers use piezo-, and HP and Canon thermal inkjet technology. It was found that thermal inkjet printing systems are better suited for the use of solutions of carbon nanotubes. In piezo inkjet systems, mechanical deformation in the head, leading to clogged nozzles and adhesion of CNT's.[2]

Printing on various substrates showed that smooth surfaces are less suitable for printing with CNT solutions. This is due to the fact that coated CNT initially not very well stuck on the substrate and can be damaged under mechanical stress. Using of special coating allows improving the print quality on these smooth surfaces.

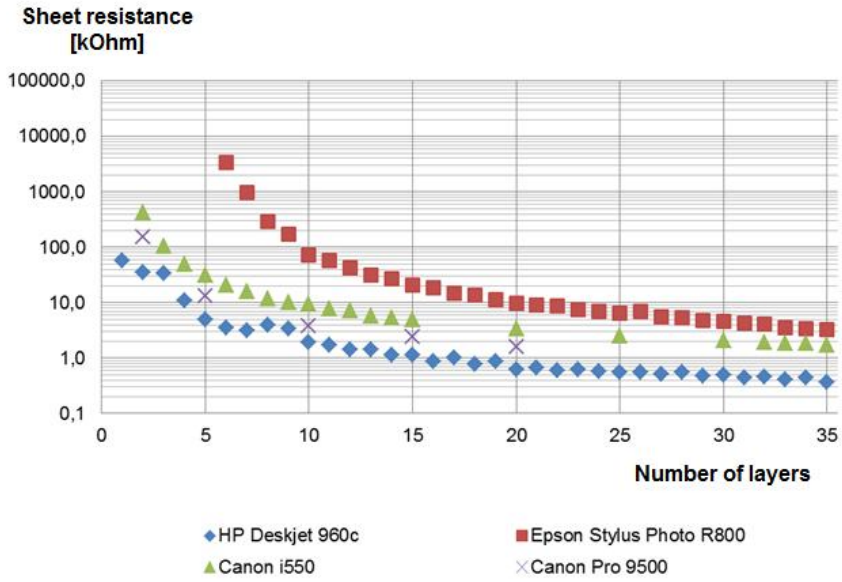

Figure 1. Sheet resistance depending on the number of layers for different printers (substrate: p_e: smart type 2 paper)

It was found that the effect of temperature on the structures causes only small changes in resistance. The greatest influence on carbon nanotubes does humidity. Surface resistance increases with the increase or decreases with decreasing water content in the air. This effect is due to the fact that the basis of the solution of carbon nanotubes is water.

Investigation of the relationship between mass ratio of CNT solution and distilled water and surface resistivity of structures showed that the mass fraction of CNT's is inversely proportional to the resistance, i.e. a tenfold increase in the mass fraction of CNT solution provides a tenfold decrease in surface resistance.

This study showed that it is possible to use the electrical properties of carbon nanotubes for functional inkjet printing. To check obtained results in practice conductive tracks and resistors has been manufactured.

By using solutions of carbon nanotubes in combination with other functional inks in the future it will be possible to print items such as resistors, batteries, capacitors and transistors.

An interesting area for functional inkjet printing is the production of prototypes. For example, a manufacturer of PCB can quickly and inexpensively produce prototypes using fairly simple inkjet printer before they go into production. The use of flexible substrates in the future will cause changes in the production of electronics.

1. Magdassi, Shlomo. The chemistry of ink jet inks. // World Scientific. – 2010.
2. Hofmann J. Erforschung der Integrationsmöglichkeiten von Carbon Nanotubes in die Inkjet-Leiterplatten-Drucktechnik. Georg-Simon-Ohm Hochschule Nürnberg : s.n., 2011.

Development of Thin Film Composite Coatings for Multi-Element Interference Colorimetric Sensor Array

Kukla O.L., Vahula O.O., Fedchenko O.M., Matvyenko L.M.

V.E. Lashkaryov Institute of Semiconductor Physics of NAS of Ukraine, Kyiv, Ukraine

The developed technology for manufacturing of composite calixarene-polymer films enabled to simplify the formation of multi-element sensor array on a single substrate for optoelectronic colorimetric analyzer. This is achieved by the using of photosensitive polymer as a binding component in composition of the films. Separate sensitive cells were produced by consistent layering of different types of composite films on a substrate and photolithographic forming of corresponding pattern in each subsequent layer.

Thin films were deposited by centrifugation from solution containing a calixarene and organic solvent (acetone), and the binding polymer (photoresist). The ratio of the calixarene solution to polymer was 8:1, the centrifuge rate of 3000 rpm, the thickness of the formed layer was in the range of 200-300 nm. Deposition of the film on a substrate followed by its annealing in air (to give the better sensitivity to inorganic gases) or in inert atmosphere or vacuum (for the forming dominant sensitivity to organics). As sensitive components were investigated calixarene materials of 14 species, including regular and tretbutilnye calixarenes of 4, 5, 6, 8 types, and modified by thia-, phosphorus-, carbonyl, aminocarbonyl, and other functional groups. From testing of the gas sensitivity the 4 defined composite film types were selected for multi-element array, they exhibit a more enhanced selectivity to the following four classes of organic compounds: aromatics (xylene, with a threshold sensitivity of about 10 ppm), alcohols (ethanol, 50 ppm), ketones (acetone, 200 ppm), chlorine organics (dichlorethane, 70 ppm), and inorganic one (ammonia, with a threshold detection level of 0.001 ppm).

Fig.1 shows examples of multi-element sensor arrays fabricated. Each of them is a structure of four isolated cells of different composite calixarene-polymer films of 6x6 mm sized on the surface of polished silicon wafer of 16x16 mm.

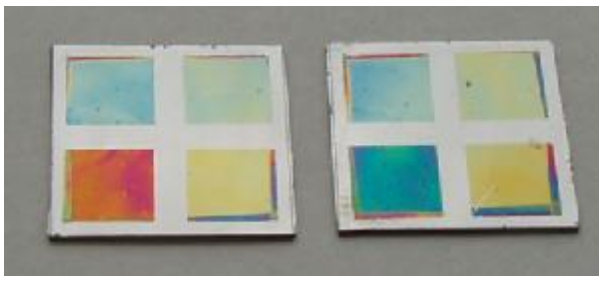

Fig.1 Samples with 4-element sensor arrays for the detection of organic

The sequence of layer's deposition was selected in accordance with the established annealing temperature of the film (with the falling of such temperature from the first element to the last one), it was due to the necessity to avoid a loss of sensitivity of consistently formed sensor elements.

ZnO Thin Film Deposited by ALD for CdS/CdTe/Cu_xS Solar Cells

Semikina T.[1], Yaroshenko N.[1], Mamykin S.[1], Godlewski M.[2], Luka G.[2], Pietruszka R.[2], Kopalko K.[2], Krajewski T.A.[2], Shmyryeva L.N.[3]

[1] *V. Lashkarev Institute of semiconductor physics NAS of Ukraine, Kyiv, Ukraine*
[2] *Institute of Physics Polish Academy of Sciences, Warsaw, Poland*
[3] *National Technical University of Ukraine "KPI", Kyiv, Ukraine*

In this work we use the atomic layer deposition (ALD) technology to get ZnO films for application as conductive electrodes in solar cells of the second generation based on heterojunctions of II-VI materials. It replaces molybdenum often considered as the best electrode for structures based on II-VI materials. We compare the photoelectrical characteristics of solar cells structures CdS/CdTe/Cu_2S deposited on pyroceram glass/Mo or quartz glass covered by ZnO.

Transparent conductive thin films of ZnO are grown in the Savannah-100 ALD reactor (Cambridge NanoTech) from diethylzinc and water vapor as zinc and oxygen precursors, respectively. ZnO films have thikness 200 nm and very low resistivity, i.e. 4×10^{-3} Ωcm. This is due to native defects, mainly zinc interstitial which can act as very efficient donors in ZnO.

Solar cells of CdS/CdTe/Cu_xS studied by us are prepared by quasi-closed sublimation method from CdS and CdTe powders. The thickness of the CdS is equal to 0.2 μm, for CdTe correspondingly is 1.0 μm. Since both CdS and CdTe layers have the n-type conductivity we deposited the layer of p-Cu_xS for barrier formation. Degenerated semiconductor Cu_xS is also as an electrode to CdTe. We concentrated on the search for the best material choice (Mo, ZnO,) for the bottom electrode and technological parameters deposition studying for preparing of high conductive ZnO films. Mo films are deposited on pyroceram substrates by magnetron sputtering using PVD 75 (Kurt J. Lesker) system.

The dark and illuminated current-voltage (I-V) characteristics of solar cells are measured under two illumination powers of 0.013 and 0.136 W/cm^2 (incandescent lamp and halogen bulb respectively) and analyzed. The calculated efficiency of the best prepared solar cells is 1.89 % for samples on ZnO (short circuit current I_{sc}= 0.249 mA, open circuit voltage U_{oc} = 0.3695 V, fill factor FF = 0.267). We observed that structure of solar cells deposited on ZnO show the better I-V characteristics in comparison with solar cells with Mo contact. The exchange of Mo contact by ZnO leads to current increasing by a factor of three. The observed difference in photo current can be explained by distinctive properties of Mo and ZnO structures and quality of interfaces between CdS and conductive materials. Most likely, the interface of CdS/ZnO has lower density of surface traps in comparison with CdS/Mo resulting in the observed increase of the current.

Quantity Determination of Gas Forming Admixtures, and Methods of Finding Them in Titanium Dispersion Systems

Sinyaeva N.P.

Zaporizzhya National University, City of Zaporizzhya, Ukraine

Titanium coarse-dispersion systems are the powders, which are used in modern technology for highly economical utilization of metal-ceramic products, getters, and solid propellants. Manufacturing processes of powders are various: electrolysis, the grinding of hydrogenated titanium with the following dehydrogenation. [1, 2, 3]

Powders produced by such manufacturing processes have a great number of parts having structural defects with the considerable proportion of free energy, which can be the adsorption centers of water, hydrogen, oxygen, and the chemical adsorption can create the thin films on the surface of particles.

Influence of various forms of the oxygen admixtures, hydrogen, oxygen films on the quality of powders is different depending on their content on the surface, volume and forms of their presence. The modern methods are allowed to determine only the total content of hydrogen and oxygen. Therefore, the development of a quantitative differentiated estimation method of hydrogen and oxygen is an actual goal.

The proposed differentiated estimation method represents as follows: a total content of hydrogen and oxygen is determined in powder samples which have different surface-to-volume ratios and then the coefficient of a mini regression line of the Y=A+BX quotation of the above gases is calculated on a specific surface of samples. The absolute term (a) of quotation corresponds to volume content of gases and the angular term (bx) to the surface content of them. This method can be used only in the case when the content of gases in volume is supposed to be independent on coarseness of powders [6, 7].

As for the powders used in our researches the volume content constancy is proved by special experiments. To choose technology of dispersion we have carried out evaluation of each component of the hydrogen and oxygen content and determined the form of their presence on the surface of powders.

It was proved by UK and KP spectrometry and electronic microscopy methods that hydrogen and oxygen can be found on surface in the H_2O form, OH groups, and TO thin films.

Correctness of differentiated method regarding titanium powders and titanium hydrides is proved by standard samples [8].

1. The electrolytic refining of titanium in melted environments. Edited by V.G. Gopienko. – M.: “Metallurgy”, - 90 pages.
2. Liskovich V.F., Rubtsov A.N. Author’s certificate No. 206087 dd 30.08.67; Bulletin of inventions, 1967, 24.
3. Shapovalova O.M. The absorption of gas admixtures while producing titanium powders.
4. Guardipee K.W. The differential method of determination of oxygen / K.W. Guardipee “Analytical chemistry”. – 1970. – Vol. 42, No.469. – P. 469-474.
5. Manita A.D. The probability theory and the mathematical statistic./A.D.Manita. M: UNDO department, MGU. – 2001. – 1200.
6. Smagunova A.I. Methods of mathematical statistic in the analytical chemistry/ A.I. Smagunova, O.M. Karpukova – Rostov-on Don, “Phoenix”. – 2012. – 346 p.

Saxs Investigation of the PbS Porous Films

Skatkov L.[1], Cheremskoy P., Gomozov V.[2]

[1]*PCB "Argo", Beer Sheva, Israel*
[2]*NTU "KhPI", Kharkov, Ukraine*

The way of changing of the character of porous structure of the same substance by means of sedimentation on the substrate of different types can be observed based on the sample of PbS films. High-porosity fractal structures, containing non-equiaxed chaotically-oriented SMP, are received at low-vacuum condensation of PbS on polycrystalline sub-layer of $BaCl_2$ at sufficient sub-cooling conditions ($1.3T_s$, T_s – melting temperature, K). As to the data of small-angle X-ray analysis of straight and inclined pictures of the samples in relation to molecular flow drop at condensation, almost no anisotropy of small-angle X-ray scattering (SAXS). At the same time, like in Al black films, being created at another conditions [1], specific surface as to the data of low-temperature Argon desorption reaches (40 – 60)x10^3 m^2/kg. at total porosity of ~ 32%, SAXS indicatrixes asymptotics is described by ~ $s^{-3,1}$ law, while invariant curves feature several maxima, caused due to poly-modality of SMP distribution as to the size (Fig.1).

However, by changing of polycrystalline sub-layer of BaCl2 with NaCl mono-crystalline matter (100) at the similar conditions (vacuum, substrate temperature, condensations velocity), it can be obtained more regulated porous structure of PbS, having nothing in common with fractals and containing pores in the form of "negative crystals" - elongated parallelepipeds, faceted with equilibrium plane sheets {100} having the same orientation as the substrate. It can be observed from small-angle X-ray pictures on the Pic.13b, where diagonal directions of the square coincide with crystallographic directions [001] и [010].

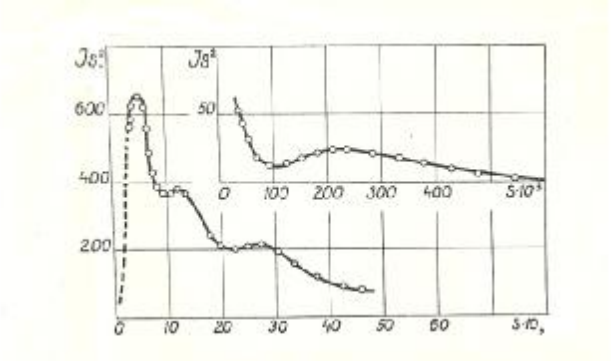

Fig.1. SAXS indicatrix invariant for the PbS condensates deposited on the polycrystalline sublayer $BaCl_2$.

1. Skatkov L., Cheremskoy P., Gomozov V., Bayrachniy B., Tulskiy G., Deribo S. The Influence of Space Environment on Substructure of Light-Absorbing Thermoregulating Al Coatings, Coatings – 2011. – V. 1, N. 2. – P. 108-116.

Ionizing Radiation Detectors with Schottky Contact

Sklyarchuk V.M.

Yu. Fedkovych Chernivtsi National University, Chernivtsi, Ukraine

One of possible ways of solving the problem of leakage current reduction is to create a rectifying contact, for instance, Schottky contact type, instead of one of the ohmic contacts. In this case the resistance of the depleted region is about 10^2-10^3 times larger than the resistance of homogeneous semiconductor part, which contributes to a considerable reduction of detector leakage current, and the electric field intensity is increased by a factor of 100. All this has a positive effect on the key parameters of detector, such as efficiency and resolution.

In this paper, current-voltage characteristics of structures based on p-type CdTe and n-type CdZnTe with the ohmic and rectifying contacts are studied. The resistivity of crystals under study for p-type CdTe was ~10^9 Ohm cm, and for n-type CdZnTe ~10^{10} Ohm cm at a temperature of 20^0C. Ohmic contacts to CdTe were created by thermal evaporation of Ni, and to CdZnTe – by thermal evaporation of In. Prior to metal deposition, the surface of crystals was subject to thorough mechanical polishing and etching in the bromine solution in methanol. Immediately prior to metal deposition the surface was treated in argon plasma. The rectifying contacts to CdTe and to CdZnTe were created by Ni evaporation, but with the difference that immediately prior to metal deposition the mode of surface treatment in argon plasma was different: current was reduced, and voltage was increased. Current-voltage characteristics of the ohmic contacts both for CdTe and for CdZnTe had two characteristic parts: linear ($I \sim U$) and quadratic ($I \sim U^2$). The voltage of transition U_o from a linear law to a quadratic one was a function of sample thickness d ($U_o \sim d^2$), and with the same crystal thickness – a function of product mt, and the larger is mt, the lower is voltage U_o. Thus, this procedure can be used for the determination of mt, which for semi-isolating crystals is not an easy task. Current-voltage characteristics of rectifying contacts had three characteristic parts: sublinear ($I \sim V^{1/2}$), linear ($I \sim V$) and superlinear ($I \sim V^2$). The voltage of transition from a linear part of current-voltage characteristic to a superlinear part also depended on crystal thickness d, and at d~1-2 mm this voltage was equal to 1000-1200 V, and dark currents did not exceed 3-5nA at a temperature of 20^0C and the rectifying contact area 10 mm^2. For the homogeneous detectors with the ohmic contacts on the same material at d~1-2 mm U_o was equal to ~ 5-10 V. From our standpoint, it must be taken into account in the manufacture of detectors for various application areas.

Electrophysical Properties of Ni-$Hg_3In_2Te_6$ Schottky Diodes

Sklyarchuk V.M., Rarenko A.I., Sklyarchuk O.F., Zakharuk Z.I.,
Dremlyuzhenko S.G., Kosyachenko L.A.

Yu. Fedkovych Chernivtsi National University, Chernivtsi, Ukraine

Direct-gap semiconductor $Hg_3In_2Te_6$ is a promising material for photodetectors of fiber-optical communication lines. The energy gap nearly 0.72 eV allows creating photosensitive structures efficient in maximum transparency region of quartz fiber (internal quantum efficiency of photoelectric conversion is almost 100% for the wavelength of 1.55 μm). High concentration of electrically neutral stoichiometric vacancies typical of this material accounts for its high radiation stability, which expands considerably the application area of such photodetector as compared to devices based on germanium and InGaAs, GaInAsP and AlGaAsSb solid solutions, but simultaneously complicates creation of p-n-junction by doping. Therefore, to obtain photosensitive structures, it is necessary to create heterojunctions or surface-barrier diode structures. Published results of research on Schottky barrier diodes prove good prospects of this material for creation of photodetectors sensitive in the region of 0.6-1.7 μm with a maximum at 1.55 nm. Such photodiodes can be employed in detectors of visible and near infrared radiation that can operate under increased radiation.

This paper presents the results of research on the photosensitivity spectra of Ni-$Hg_3In_2Te_6$-Ni diodes. The use of photodiodes included good quality mechanical treatment, chemical etching in the bromine solution in methanol and surface treatment in argon plasma. By the way, different modes of surface processing in argon plasma allowed using nickel both as an ohmic and a rectifying contact. Such technology facilitates fabrication of photodiodes as compared, for instance, to ITO/$Hg_3In_2Te_6$ heterojunctions. $Hg_3In_2Te_6$ crystals have a wide homogeneity range in the component distribution. Therefore their beginning is enriched by In_2Te_3 and their end - by HgTe at the zone melting. Accordingly, the band gap and the spectral dependence of the photoconductivity are changed (see fig., curves 1, 2).

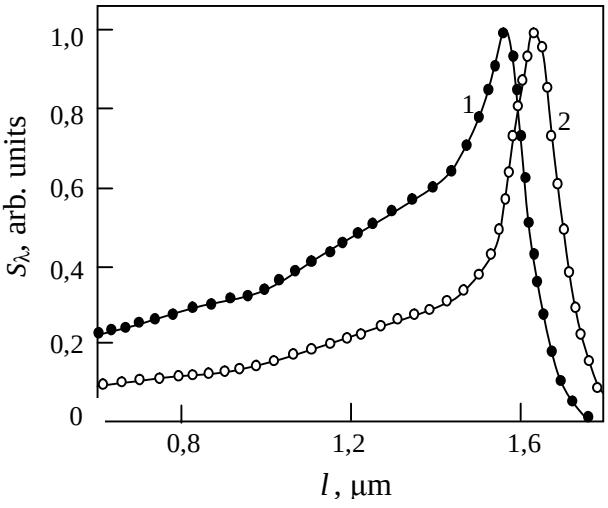

Diode Structures Based on $Cd_{1-x}Mn_xTe$

Sklyarchuk V.M., Sklyarchuk O.F., Rarenko I.M., Zakharuk Z.I., Shafrayuk V.P.

Yu. Fedkovych Chernivtsi National University, Chernivtsi, Ukraine

$Cd_{1-x}Mn_xTe$ has been recently considered as an alternative to traditional $Cd_{1-x}Zn_xTe$ solid solution for the manufacture of X-, γ-ionizing radiation detectors. The use of $Cd_{1-x}Mn_xTe$ as a detector material is motivated by a low segregation factor of Mn ($k \approx 1$) in $Cd_{1-x}Mn_xTe$, which allows producing semiconductor materials with a uniform distribution of components in the bulk of a crystal. Due to introduction of Mn impurity it is possible to control over a wide range the energy gap E_g of solid solution and to obtain a resistivity which is rather high. For instance, introduction of 5-6% Mn (that is, half that of Zn) yields material with E_g ~1.60 eV that has a resistivity 10^{10}-10^{11} Ohm cm. The ionicity degree of chemical bond in $Cd_{1-x}Mn_xTe$ crystals is higher than in $Cd_{1-x}Zn_xTe$ (since the electric negativity of Mn is smaller than the electric negativity of Zn by Pauling scale), which results in a higher material stability. Moreover, due to its magnetic properties, it is a promising spintronic material.

This paper presents the results of research on the electric and photoelectric characteristics of surface-barrier diodes based on p-type $Cd_{1-x}Mn_xTe$ single crystals.

The diode structures were prepared on $Cd_{1-x}Mn_xTe$ single crystals grown by Bridgman method. The resistivity of single crystals was ~10^5-10^6 Ohm cm. The energy gap, found from optical transmission curves, was equal to 1.78 eV, which corresponds to x=0.20. After chemical treatment in the bromine solution in methanol, the surface of single crystals was processed in argon plasma. As an ohmic contact use was made of nickel, as a rectifying contact – aluminum. Metals were deposited by thermal evaporation in vacuum. The shape and dimensions of contacts were assigned by molybdenum masks. The rectifying contact diameter was 0.5-1.0 mm. The resulting structures demonstrated pronounced diode characteristics. The current-voltage characteristics of obtained structures shown that the rectification factor at a voltage of 1 V was approximately equal to 10^5-10^6, with the area of rectifying contact 1-2 mm^2. The dark currents at a voltage of 1 V were equal to 10-20 pA. Measured the current-voltage characteristics are well described by the Sah-Noyce-Shockley model for currents generated by space charge. The results obtained hold out a hope of creating good quality photodiodes and ionizing radiation detectors based on $Cd_{1-x}Mn_xTe$.

Strained Mercury Cadmium Telluride Thin Films as Room Temperature IR Detector

Smirnov A.B.[1], Savkina R.K.[1], Sizov F.F.[1], Kladkevich M.D.[2], Samoylov V.B.[2]

[1] *V. Lashkaryov Institute of Semiconductor Physics at NAS of Ukraine, Kyiv, Ukraine*
[2] *Institute of Physics at NAS of Ukraine, Kyiv, Ukraine*

It is well known that thermal processes dominate at near room temperature in HgCdTe-based devices used for middle and long wavelength regions and in the conventional photon detector it is not possible to accurately detect any infrared radiation other than that of high output power as in a CO_2 gas laser. These detectors need significant cooling. Such requirement has long been thought to be fundamental and inevitable. At the same time, photodiode HgCdTe/Si structures based on the concept of the carriers' exclusion and extraction were manufactured for near-room temperature operation [1]. In addition, three types of IR photovoltaic detectors can operate at near-room temperature: photoelectromagnetic detectors, magnetoconcentration detectors, and Dember effect detectors [2]. The possibility to detect infrared radiation by HgCdTe-based structure investigated in this study without cryogenic cooling to achieve useful performance is based on the possibility the spatial separation of the nonequilibrium carriers in the stressed semiconductor heterostructure with piezoelectric properties [3].

Narrow-gap mercury cadmium telluride thin films grown by MBE methods onto various substrates (HgCdTe/Si, HgCdTe/GaAs) were investigated as a piezoelectric heterostructure for IR detection. Mechanical stresses at the layer-substrate interface were analyzed. It was determined that for [310] oriented MCT-based structures under the anisotropic restriction of the deformation the nonzero shear components of the strain tensor arise and stress induced piezoelectric polarization is generated. The photovoltage depends on the light power density and on the modulation frequency of the incident light were investigated. An element of the prototype achieves photovoltaic spectral sensitivity on a level $D^* = 2.6 \cdot 10^9$ ($W^{-1}cm\ Hz^{1/2}$) at 300 K.

1. Velicu S., Badano G., Selamet Y., Grein C.H., Faurie J.P., Sivananthan S., Boieriu P., Don Rafol, and Ashokan R. HgCdTe/CdTe/Si Infrared Photodetectors Grown by MBE for Near-Room Temperature Operation // Journal of Electronic Materials. – 2001. – V. 30. – P. 711-720.
2. Piotrowski J. and Rogalski A. Uncooled long wavelength infrared photondetectors // Infrared Physics Technology. – 2004. – V.46. – P. 115-131.
3. Kryshtab T., Savkina R., Sizov F., Smirnov A., Kladkevich M., and Samoylov V. Infrared radiation detection by a piezoelectric heterostructure at room temperature // Phys. Status Solidi C. – 2012. – V. 9. – P. 1793-1796.

Photoelectric Properties of Nanostructured Tin Oxide

Smirnov A.B.[1], Savkina R.K.[1], Sadovnikova M.L.[1], Gaskov A.M.[2]

[1]*Institute of Semiconductors Physics by V.E.Lashkaryov, Kyiv, Ukraine*
[2]*Moscow State University, Moscow, Russia*

Ones of the perspective materials to create the gas sensors, solar battery & photodetectors are composite structures based on porous semiconductor films of the tin oxide. The different degrees of oxide nonstoichiometric by oxigen stipulate functional properties of the SnO_2. The transport of charge carriers in the porous layers of SnO_2 support transformation of chemical signal (change of charge carrier's concentration in surface layer) into change of integral conductivity of the sensitive material. Conversion efficiency of the sensitive layer is defined by microstructure of material. The most change of this parameter expected for materials with nano sized functional particles. There were investigated photoelectric properties of the sensitive films (SF) based on the SnO_2 characterized by oxygen deficit. The studied samples were porous films with thickness ~10 μm and crystallite grains near 20 nm [1]. The kinetics of stationary photoconductivity (PC) of *n*- SnO_2 (E_g = 3,57 eV T = 300 K) (Fig.) with illumination of the samples by diode (λ_D = 535 nm) with electrical power of diode 1 W also spectral dependence of PC of the samples were studied. The kinetics of stationary PC consists of two parts: *I* – exposure and *II* – relaxation. The saturation PC to the maximal value σ_{max} = 0.0529 μS with permanent illumination occur during 35 min. There are long-time relaxations of PC observable on completion the illumination. The general time of PC relaxation is about 20 h. The analysis of times of instant relaxation $t = \frac{s_{max}}{ds/dt}$ (inset on Fig.) shows that *II* part there are two processes with different characteristic times [2]. The photosensitivity of the samples with maximum near λ = 0.47 μm (2.64 eV) in the range $hn < E_g$ are observed. The spectra of the photoconductivity of the samples were obtained by special procedure: illumination of the sample by green diode (15 ÷ 20) sec with time interval between measurements 60 min.

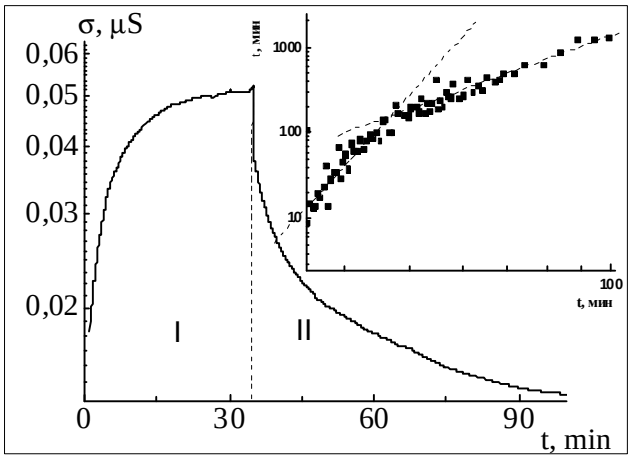

1. R.B. Vasiliev, M.N. Rumyantseva, L.I. Ryabova, A.M. Gaskov. Conductivity of SnO_2 ultradisperse ceramics in strong electric field // Semiconductors. – 2013. – V. 47, № 3. – C. 360-363.
2. M.K. Shenkmann, A.Ya. Shyk. Dolgovremennye relaxatsyi i ostatochnaya provodimost' v poluprovodnikah // FTP. – 1976. – V. 10, № 2. – P. 209-233.

Structural Investigations of Polycrystalline Yttrium Iron Garnet by Sol-Gel Method with the Subsequent Annealing

Fedoriv V.D.[1], Stashko N.V.[1], Fadeev M.S.[2], Kulyk Yu.O.[3]

[1]*Vasyl Stefanyk PreCarpathian National University, Ivano-Frankivsk, Ukraine*
[2]*National Technical University of Ukraine "Kyiv Polytechnic Institute", Kyiv, Ukraine*
[3]*Ivan Franko National University of Lviv, Lviv, Ukraine*

Yttrium Iron Garnet ($Y_3Fe_5O_{12}$), is a material used widely in electronic devices for the microwave region as well as in magnetic bubble domain-type digital memories. Some magnetic properties, such as saturation magnetization, remanence and coercitivity, depend critically on the structure and microstructure of the materials. Therefore, it is important to develop techniques to produce garnets with a strict control of the composition, homogeneity, size and particle shape [1]. In this regard, alternative methods of synthesis of garnet structures that ensure weak-agglomerated homogeneous in size nanoparticles actively began to be developed and implemented.

Studied material was synthesized by the sol-gel method of auto-combustion. Synthesized by us material for production of polycrystalline $Y_3Fe_5O_{12}$ was annealed at different temperatures.

The scanning electron microscopy indicates the formation of nanosized crystallites of ~200 nm in width and ~800 nm in length. However, the particles of $Y_3Fe_5O_{12}$ formed with very well pronounced agglomeration, indicating a good connectivity between the grains. The crystallites are necked to each other forming highly symmetric ornaments. The porous feature of agglomerates can be attributed to the release of large amount of gas during combustion.

Measuring of the spectra of small-angle X-ray scattering allowed to establish that in the initial sample homogeneous microscopic pores have been formed. Their contribution to the total number of pores is about 20%. The main part of the pores are mesopores (~ 80%). After annealing at 1000 ºC pore distribution changes significantly. Disappearance of micropores is observed in the sample, which is probably caused by the processes of structural relaxation of amorphous phase of initial sample during annealing.

Thus, sol-gel method of auto-combustion provides the chemical homogeneity and activity of obtained powders, which enables to get finely dispersed polycrystalline porous material with a homogeneous size particles.

1. Vaqueiro Paz, Arturo Lopez-Quintela M., Rivas Jose Synthesis of yttrium iron garnet nanoparticles via coprecipitation in microemulsion // J. Mater. Chem. – 1997. – V.7, № 3. – P.501–504.

Aliphatic Polyurethane as a Polymer Matrix for Thin Film Electronic Devices Based on Organic Dyes

Stratilat M.S.[1], Bezrodnyi V.I.[2], Negryiko A.M.[2], Kosyanchuk L.F.[1], Todosiichuk T.T.[1]

[1] *Institute of Macromolecular Chemistry NAS of Ukraine, Kyiv, Ukraine*
[2] *Institute of Physics NAS of Ukraine, Kyiv, Ukraine*

Dye-doped polymer materials are applied for the thin-film elements, such as waveguides, fibers and microscopic laser cavities of different configurations, in order to develop completely optical devices in the field of photonics. The main requirements to polymer materials are good solubility of laser dyes, high optical transparency, high beam strength and photochemical stability. The important factor is also a possibility to miniaturize a dye-doped polymer laser, which then can be integrated on micro-chip elements based on thin films. Nowadays, dye-alloyed PMMA films, obtained by radical polymerization method are used for this purpose. Since the method of polymer synthesis contains a usage of free radicals, this method for the production of miniature laser active media based on PMMA induces the reasons for the dye instability and absorption in a region of generation by the products of dye decomposition.

This work presents a creation of the polymer matrix based on aliphatic polyurethane (APU), synthesized by the two-stage method, for the thin-film dye-doped laser elements. The prepolymer, based on hexamethylene diisocyanate and oligodiethyleneglycol adipate is obtained at the first stage, and the second stage includes a synthesis of the polymer by solidification of the prepolymer with trimethylpropane.

Electrical and optical properties of APU have been investigated. In particular, dielectric permittivity is found to be $\boldsymbol{\varepsilon} = 8.8$, which is very important for the solubility of dyes. A high value of $\boldsymbol{\varepsilon}$ allows to eliminate the formation of different associations of organic dyes. The transmittance spectra showed that APU possesses high transparency in a wide spectral range, 260-2200 nm, involving nearly a whole region of dye laser operation.

The improvement in the photochemical properties of widely used laser dyes (Rhodamine 6G, Pyrromethene 567 and Pyrromethene 597), doped to APU has been demonstrated in the comparison with the polymer matrices, produced by radical polymerization. Photostability is increased by two orders under the irradiation in $\boldsymbol{S_0 \rightarrow S_2}$ transition, and it grows several times under the irradiation in $\boldsymbol{S_0 \rightarrow S_1}$. Generation characteristics is improved by order of magnitude.

This work contains discussions about the reasons for the observed improvements in the operation parameters of dye-doped thin-film elements based on APU, and the conclusion has been made about the perspective applications of the new polymer matrix in the dye-based miniature devices.

Influence of Crystal Thickness on the Temperature Hysteresis of Incommensurate-Commensurate Phase Transition

Sveleba S.A., Karpa I.V., Katerynchuk I.M., Phitsych E.I., Kunyo I.M.

Ivan Franko National University, Lviv, Ukraine

Currently, influence of the surface on physical properties of crystals attracts much attention of experimentalists. This is due both to the importance of understanding the properties of the surface and the need to experimental study the effect on the physical properties of the surface and near-surface layers of the crystal of the "defect" such as the surface. Processes at the surface accompanying the phase transitions are of considerable interest.

In crystals with an incommensurate (IC) superstructure the size effects may be associated with the modulation period of the IC ~ 1500-800 Å and can be seen in the values of the crystal thickness d> 100 nm.

In the work we study the effect of varying the crystal thickness d ($1 \leq d \leq 3500$ micron) on the phase transition temperature incommensurate-commensurate ferroelectric (T_c) phase and ferroelectric-ferroelastic (T_3) for the $[N(CH_3)_4]_2Zn_{0.75}Mn_{0.25}Cl_4$ crystals.

Magnitude of the temperature hysteresis of phase transitions ΔT_c, ΔT_3 and magnitude of global temperature hysteresis Δ decreases with decreasing thickness of the crystal. This is probably due to increased influence of mechanical stress, which is accompanied by an increase in the temperature range of the existence of metastable states, as well as a decrease of the relaxation time of the superstructure to its equilibrium state.

At a sample thickness of the crystal $[N(CH_3)_4]_2Zn_{0.75}Mn_{0.25}Cl_4$ less d_a ~ 80 micron the thermal hysteresis of the phase transition temperature T_c and T_3 increases sharply. Authors tend to assume that the internal mechanical stresses that accompany the formation of the new phase is affected by 180° domain structure and, consequently, the phase transition in $[N(CH_3)_4]_2Zn_{0.75}Mn_{0.25}Cl_4$ crystals. This is demonstrated by the suppression of the spontaneous polarization at imposing small uniaxial compressive stress to the $[N(CH_3)_4]_2ZnCl_4$ crystal.

Proton Irradiation Influence on In_2O_3 Thin Films and In_2O_3/InSe Structures

Sydor O.M.[1], Sydor O.A.[1], Kovalyuk Z.D. [1], Dubinko V.I.[2]

[1] *Chernivtsi Department of IPMS of NASU, Chernivtsy, Ukraine*
[2] *"Accelerator" R&D Complex at the NSC KIPT of NASU, Kharkiv, Ukraine*

Intrinsic oxide films of InSe layered semiconductor possess conductive properties, high mechanical strength and transparency to visible radiation. The method of thermal oxidation, being enough technologically simple, makes it possible to grow the oxide films and thus to create high-quality intrinsic oxide/InSe heterostructures (HS).

In this paper the influence of 30 keV proton by fluences 10^{11}-10^{13} cm^{-2} on intrinsic oxide films In_2O_3 and In_2O_3/p-InSe:Cd HS are investigated. The thermal oxidation of the layered semiconductor was carried out at a temperature of 400°C and duration of the process was 30 min and 96 h. Because of these conditions, we have created the intrinsic oxide films about of 90 and 400 nm thick, respectively.

Measurement of the surface resistance of the films depending on proton fluence showed that the resistance decreases slightly (within 1%). It can be supposed that the intrinsic oxide films In_2O_3 grown by the thermal oxidation method are low-insensitive to radiation of this type.

A comparison of the photoresponse spectra of the initial and proton irradiated intrinsic oxide/InSe HS did not find any changes after irradiation. Only a decreased value of photocurrent and, therefore monochromatic ampere-watt sensitivity S_I, was registered. In this sample any broadening of the spectral sensitivity range or a change in the position of the maximum were not observed.

The most significant changes in the photoresponse spectra of an In_2O_3/InSe HS can be observed when it was prepared by a short-term oxidation. After proton irradiation there is a shift of the high-energy edge of the spectral characteristics to the long-wavelength side. Additionally, its slope becomes different. After irradiation the spectra's width $\delta_{1/2}$ at their half-height decreases form 1.44 to 1.22 eV and the range of spectral sensitivity $\Delta\lambda$ gets narrower (from 0.34÷1.01 to 0.40÷1.01). The photosensitivity maximum of the In_2O_3/InSe HS (at 0.5 μm) shifts after irradiation to the long-wavelength side (to 0.56 μm). It is worth to note a good increase (by 23 %) in photosensitivity both at the long-wavelength edge and at λ_{max}. The monochromatic volt-watt and ampere-watt sensitivities of the In_2O_3/InSe HS become only improved after irradiation what is in agreement with the behavior of the parameters U_{OC} and J_{SC}.

It is made interpretation of processes occurring by proton irradiation of objects studied in this paper.

Microplasmas in InGaN/GaN Thin-Film Structures of High-Power light-Emitting Diodes at Reverse Bias

Veleschuk V.P., Vlasenko O.I., Kisselyuk M.P.,
Lyashenko O.V.[1], Vlasenko Z.K.

V. Lashkaryov Institute of Semiconductor Physics, NASU, Kyiv, Ukraine;
[1]Taras Shevchenko Kyiv National University, Kyiv,Ukraine

The increase of the area of light-emitting epitaxial thin-film heterostructures based on the GaN results in growth of heterogeneity of distributing of internal mechanical strains, dislocations of different type, dopants and components of indium or aluminium in the nano-layers of InGaN and AlGaN. It accordingly predetermines in the heterogeneous generation of defects and decrease of quantum yield due to increase of heterogeneity of flowing of the current. This, in turn, leads to forming of shunts and areas of local overheat, in particular in a thin-film heterostructure, or even to the breakdown.

Therefore appears considerable problem of operative revealing and control electrically active extended defects in such heterostructures.

At the certain threshold value of reverse voltage in the most imperfect areas of InGaN/GaN structure appears luminescence [1], or so-called microplasmas (MP), because the electric field of ionization in the areas of such defects less than in the homogeneous areas of *p-n-* junction.

Microplasmas in the InGaN/GaN heterostructures of high-power light-emitting diodes are studied and revealed that microplasmas parameters are related with the functional parameters of heterostructures. The voltage of origin (switching) of MP is established, three characteristic sites of low-voltage microplasmas found out: in the space-charge region of heterostructure, on the side, near a contact. Location of critical technological defects is very important for, in particular, improvement of the technological stages at making and development of light-emitting thin-film structures. Also it is necessary for reliability prognostication because a site of such defect (microplasmas) often determines the scenario (direction) of the degradation process at testing or exploitation.

1. V.P. Veleschuk, O.I. Vlasenko, M.P. Kisselyuk, and O.V. Lyashenko. Microplasma breakdown of InGaN/GaN heterostructures in high-power light-emitting diodes // *Journal of Applied Spectroscopy*. – 2013. – Vol. 80, N 1. – P. 121-127.

Response of Heterostructures of CeO_2-p-Si Nanostructured Film to Gaseous Nitrogen Oxide (IV)

Yushchenko A.V.

Vinnytsia National Technical University, Vinnytsia, Ukraine

The intensive investigations of heterostructures of metal oxide – semiconductor are performed for their application as gas sensors for qualitative and quantitative analysis of gas medium composition. In these structures the parameters of metal oxide films determine the sensitivity to the gas medium. It is known that a chemical element Ce may exhibit valence III, IV, mixed or intermediate valence. This allows to assume that the parameters of nanostructured films of Cerium oxide and the parameters of the entire heterostructure in tote will give a significant response to the changes of gas medium composition.

We investigated a heterostructure of nanostructured film of CeO_2 – p –Si. For the synthesis of CeO_2 films on the surface of p-Si we used a method of explosive evaporation. The volt-ampere (VA) characteristics of the test samples were investigated in the laboratory atmosphere and in the atmosphere of Nitrogen (IV) oxide. A relative response of VA characteristics of the heterostructures upon change of the laboratory medium to the gaseous medium was considered as following: $d = \frac{I_v - I_g}{I_v}$, where I_v, I_g are the correspondent currents in the laboratory and gaseous medium measured at the same values of voltage applied to heterojunction.

Our results lead to the following conclusions: VA characteristics of the heterostructures of the nanostructured film CeO_2-p-Si are different in the air atmosphere and in the atmosphere of Nitrogen (IV) oxide. This property potentially may be used for the development of the gas sensors based on the described nanostructured films. The response of VA characteristics to the changes of gaseous medium is determined by the height of potential barrier of a heterojunction and by changing of voltage drop on the nanofilm. The changing of voltage drop on the nanostructured adsorption active film significantly affects the response of heterostructure CeO_2 - p – S in respect to the changing of the air atmosphere for the atmosphere of of Nitrogen (IV) oxide. The dependence function of changing of voltage drop on nanofilm upon applied voltage to the heterojunction is non-linear. It depends on the charge change at the boundary of heterojunction and on the charge on the free surface of CeO_2. A sign of response at different voltages applied to heterojunction is different. The change of response sign to the presence of NO_2 in the direct and reverse heterojunction switching is determined by the changing of voltage drop on the adsorption active nanofilm CeO_2. The change of response sign at the direct switching of hetrojunction can be explained by redistribution of voltage drop at the potential barrier and on the nanofilm.

Cathode Properties of Mechanically Activated Nanocomposite SiO_2 - Al_2O_3

Zaulychnyj Ya.V.[1], Ilkiv V.Ya.[1], Zarko V.I.[2], Gasjuk M.I.[3]

[1] *National Technical University of Ukraine "Kyiv Polytechnic Institute"*
[2] *Chuiko Institute of Surface Chemistry of NASU, Kyiv, Ukraine*
[3] *Vasyl Stefanyk Precarpathian National University, Ivano-Frankivsk, Ukraine*

Given the growth of the lithium current sources (LDS), the attention of researchers focused on studying the properties of materials that can be used as a cathode material. Promising from this point of view is the solid solutions based on silica, due to their low cost and high structural stability to the intercalation-deintercalation processes. To set the properties of cathode mechanically activated composite SiO_2-Al_2O_3 (80% and 20% by weight. respectively) conducted electrochemical studies of cathode LDS models based on them.

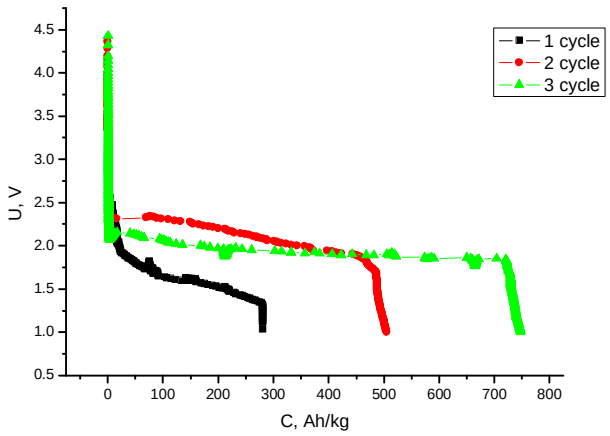

Mock LDS gathered in an airtight glass box with an atmosphere of argon. A mixture of the studied composite (88% wt.), Conductive additives (soot) and binding agent (2%) coated on nickel mesh, welded to molybdenum rod. Metallic lithium anode served in the role of the electrolyte used LiBF4 in γ-butyrolactone. Bit galvanostatic curves obtained by charge-discharge device at a current of 20 mA when the mass of the active substance cathode 7 mg. In Fig. 1 shows the characteristics of the first three cycles of discharge. The discharge curve of the first cycle is characterized as the lowest value of specific capacity (300 Ah / kg) and least stable operating voltage. This may be due to the formation of passivating films on the surface of the cathode in the first class. The second phase is characterized by higher capacity (500 Ah / kg) and a horizontal section of tension in the region in more than 2, indicating a clean surface when you first charge the cell and increase the number of intercalated lithium in the structure. Electrochemical parameters of the third cycle of the highest. The horizontal section shows the voltage lithium intercalation into homogeneous nanocomposite position, and high values of specific operating parameters can successfully use such composites as cathode materials of lithium batteries.

СЕКЦІЯ 5 (усні)
ФУНКЦІОНАЛЬНІ КРИСТАЛІЧНІ МАТЕРІАЛИ: РІСТ, ФІЗИЧНІ ВЛАСТИВОСТІ, ВИКОРИСТАННЯ
21-24 травня 2013 р.

SESSION 5 (oral)
CRYSTAL'S GROWTH AND THEIR PHYSICAL PROPERTIES
May, 21-24, 2013

Double Feeding of the Melt Method. Conditions for Growing of Uniform Si-Ge Single Crystals.

Azhdarov G.Kh., Aghamaliyev Z.A., Islamzade E.M.

Institute of Physics, National Academy of Sciences of Azerbaijan, Baku, Azerbaijan

The problem of component distribution in solid solution crystals grown from a melt fed by rods made of the components of the system, with allowance for the dependence of their segregation coefficients on the melt composition, has been solved in the Pfann approximation. Examples determining the conditions for growing homogeneous single crystals of solid solutions with a specified composition and obtaining (in a unified cycle) crystals composed of several uniform parts of different compositions are presented for the Si–Ge system. The good prospects of using the method of double feeding the melt for growing single crystals of semiconductor solid solutions with specified graded and/or uniform compositions are shown.

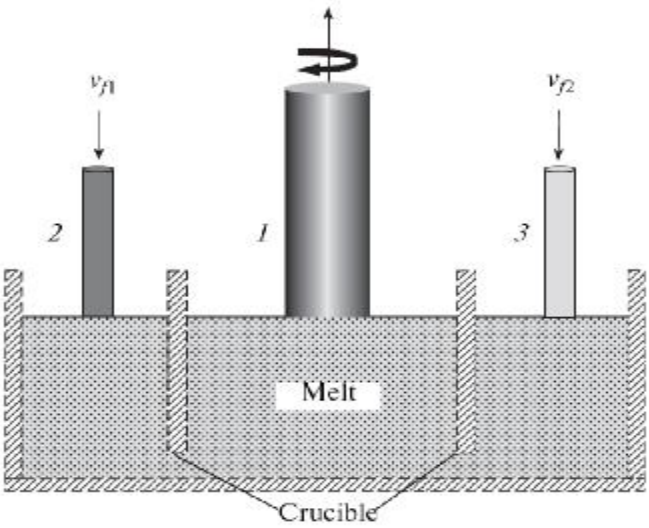

Schematic diagram of the growth of single crystals of binary solid solutions by double feeding of the melt. 1,2,3 - the growing single crystal and feeding rods consisting of the first and second components, respectively; v_c is the single crystal pulling rate; and v_{f1} and v_{f2} are the immersion rates for the first and second rods.

The essence of our approach is shown schematically in figure. When a solid solution begins to grow from a melt of a specified composition, rods of the first and second components are simultaneously introduced into the melt. Obviously, under these conditions the composition of the growing single crystal will be determined by the crystallization and melt feeding rates and the initial melt composition and volume.

On the Huygens Principle and Crystallization OF Thin Amorphous Films

Bagmut A.G.

National Technical University "KhPI", Kharkiv, Ukraine

Four types of crystallization reactions of amorphous films was distinguished. There are layered polymorphic crystallization, islands polymorphic crystallization, dendrite polymorphic crystallization and liquid-phase crystallization. It is noted, that the layered polymorphic crystallization can be regarded as a "coherent" crystallization, occurring in the accordance to the optical Huygens principle.

On the basis of systematic electron diffraction and electron microscopy studies of species of crystallization of thin amorphous films on structural and morphological features, shared between the layered polymorphic crystallization [LPC], island polymorphic crystallization [IPC], dendrite polymorphic crystallization [DPC] and fluid-phase crystallization [FPC] [1]. This enabled to classify adequately a variety of crystallization processes in the films.

One of the reasons for the implementation of a certain type of crystallization is the nature of the binding forces between the atoms of the elements. If dominated the covalent bonds, often the mechanism of LPC is implemented. Metallic bond initiates the mechanism of IPC.

When LPC takes place, the promoting of the crystallization line can be considered similar to the advancement of the light wave front in accordance with the Huygens principle (Fig. 1). In this case, to the crystallization of thin films can be applied the term "coherent" crystallization, as the single-crystal layer is provided by the same orientation (i.e. the "coherence") secondary nucleation centers. At the same time the LPC is an analog to layer growth of the film on the substrate from the vapor phase (growth accordance to Frank and van der Merwe mechanism). As a result of the phase transformation on the mechanism of LPC a crystalline film forms, where the dimensions of flat grains in the tangential direction by orders of magnitude greater than its thickness.

Island polymorphic crystallization is not a "coherent" crystallization. It is an analog of island film growth on the substrate from the vapor phase (growth accordance to Volmer and Weber mechanism). As a result of the phase transformation finely dispersed polycrystalline film is formed.

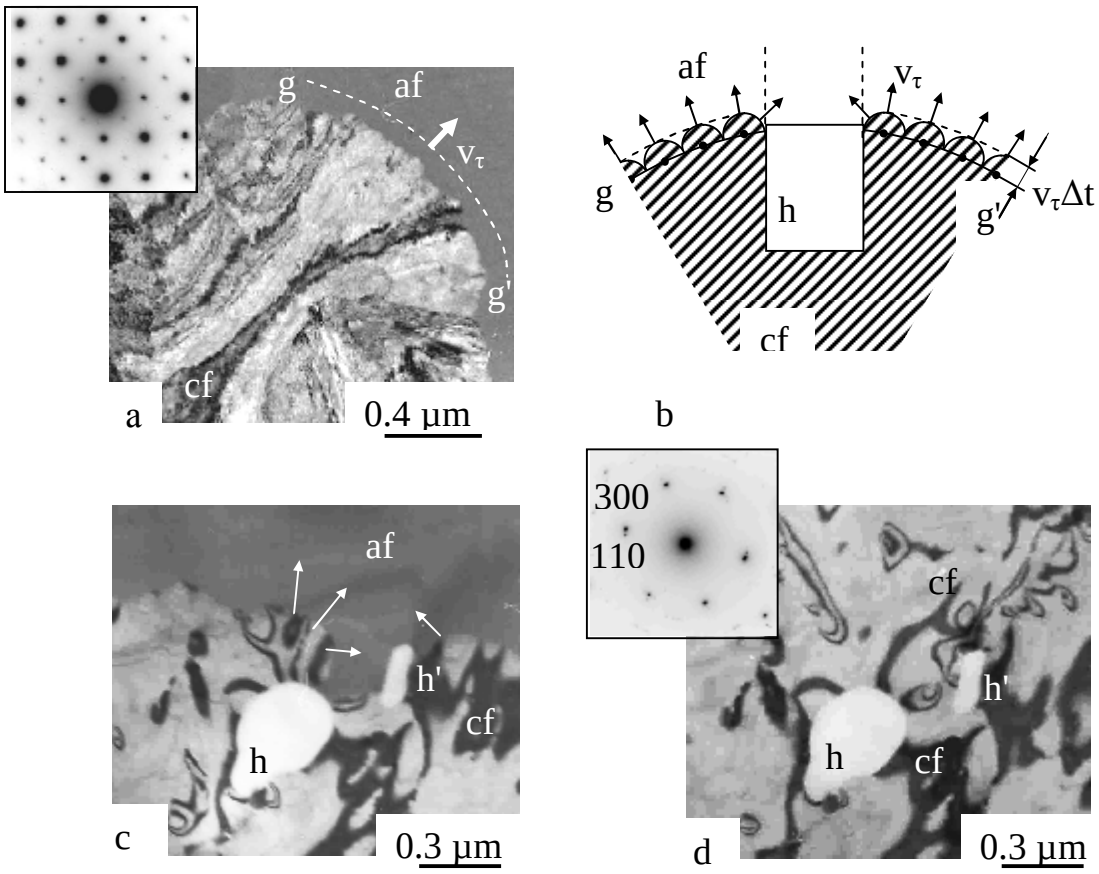

Fig. 1. Layered polymorphic crystallization of amorphous films: (a) - crystallization HfO_2 film by annealing in a muffle furnace on air, (b) - the scheme of a coherent crystallization, made by analogy with the optical principle of Huygens. (c), (d) - crystallization of amorphous film of Cr_2O_3 under the influence of the electron beam in a vacuum: bypass of obstacles (holes h and h') by moving line of crystallization g-g'. af - amorphous phase. cf - crystalline phase. The arrows indicate the direction of movement of the sections of line of crystallization. In the upper left corner of the micrograph (a) and (d) the patterns of micro diffraction are shown (contrast is inverted).

1. Bagmut A.G. Classification of the Amorphous Film Crystallization Types with Respect to Structure and Morphology Features // Technical Physics Letters.- 2012.- V.**38**, № 5.- P. 488–491.
2. Bagmut A.G. Structural and morphological features of crystallization reactions of amorphous films according to the electron microscopy data // Functional Materials.- 2012.- V.**19**, № 3.- P. 370– 377.

Crystal-Chemical Analysis of the Behaviour of the Transition Metals (Co, Ni) in Lead Telluride Crystals

Boychuk V.M.

Vasyl Stefanyk PreCarpathian National University, Ivano-Frankivsk, Ukraine

Lead Telluride attracts attention primarily because of its wide use in infrared technology and thermoelectric devices [1]. Important factors that determine performance characteristics of the device structures are point defects of the base material, which can be substantially controlled through doping.

The nature of the doping of transition metals (Co, Ni) is determined by unfilled *d*-shell ($3d^7 4s^2$ – Co; $3d^8 4s^2$ – Ni). Given the fact that for the impurity atoms of the transition metals (Co, Ni) characteristic oxidation levels are 2 and 3, so disproportionation of dopant charge state can be written according to the scheme: $M^{2+} \rightarrow M^{3+}_{1-z} + M^{2+}_{z} + (1-z)e^{-}$ (M = Co, Ni), where z – the value of disproportionation of dopant charge state. X-ray researches [2] have shown that in the boundaries of measurement precision lattice parameter is constant and equal to the lattice parameter of lead telluride; this indicates interstitial placement of trivalent dopants M^{3+}_{i}.

In this paper the crystal-quasichemical formulae of doped n- and p-PbTe:M crystals have been first proposed. Based on the found analytical expressions for the concentration of point defects and current carriers their dependences on the dopant content have been calculated. In the case of p-PbTe:M there are decrease of the hole concentration, conversion of the conductivity from p- to n-type and further increase of the electron concentration; in the case of n-PbTe:M there is increase of the major carrier concentration. It has been shown that cation vacancies V^{2-}_{Pb} are responsible for p-type conductivity of the material, and ionized impurity atoms M^{3+}_{i} – for n-type conductivity; concentration of these dominant defects increases with increasing content of the alloying component.

Coefficients of disproportionation of dopant charge state have been determined: $z \approx 0{,}15$ for cobalt; $z \approx 0{,}45$ for nickel. The character of the concentration of point defects and the Hall concentration of current carriers of PbTe:Co crystals is similar to PbTe:Ni due to close values of disproportionation of dopant charge state z.

Introduced crystalquasichemical approaches extend possibilities of scientific analysis of the defect subsystem in semiconductor crystals, and determine the technological aspects of managing their properties.

1. Shperun V.M., Freik D.M., Zapukhliak R.I. Thermoelectricity of lead telluride and its analogues. – Ivano-Frankivsk: Plai, 2000. – 250 p.
2. Kuznetsova T.A., Zlomanov V.P., Tananaieva O.I. Features of doping lead telluride by cobalt and nickel // Inorganic Materials. – 1998. – V. 34, No 9 - P. 1055-1061.

The work supported by project of MES of Ukraine (N 0107U006768)

Optical Probing of Dynamical Magnetic Spin Clusters in CdMnTe Spin Glass Compound

Bukivskij P.M., Gnatenko Yu.P.

Institute of Physics of NAS of Ukraine, Kyiv, Ukraine

Spin glass (SG) formation is one of the most complex and exciting problems in the condensed matter physics and material science. SG behavior has been found in many materials : crystalline and amorphous alloys , metalic and semiinsulating. Usually, a spin freezing process can be analyzed in terms of clustering. Far above the freezing temperature (T_f) SG properties are explained by a collection of independent finite superparamagnetic clusters with local order and fluctuations.

In spite of the intensive theoretical and experimental investigations of SG systems, a number of issues still remain open. In particular, the relative concentrations (RCs) of “loose” spins, i.e. the fraction of the spins which do not belong to any clusters (single spins), and various magnetic spin clusters in SGs is one of the important unanswered questions. Another problem is lack of detailed quantitative information on how these microscopic magnetic spin states (MMSSs) evolve with temperature, as well as how temperature affects the redistribution between the spin states.

In this paper we report the first estimation of the relative concentrations (RCs) of various MMSSs: in $Cd_{0.70}Mn_{0.30}Te$ (T_f=6.45 K) SG in the vicinity of its freezing temperature ($0.7T_f \leq T \leq 2T_f$). These results are based on the analysis of low-temperature PL spectra structure caused by the appearance of various localized exciton magnetic polarons. In this case these excitonic states are used as a probe of various MMSSs. This enables us to estimate the RCs of "loose" spins, finite superparamagnetic, and infinite or “locked” clusters. At T_f the proportions of these parts are equal to 5 : 20 : 75. This is the first such quantitative evaluation for any SG compounds. It should be noted that the RC value for the “loose” spins (5%) correlates with the effective concentration X^* of Mn atoms in the $Cd_{1-X}Mn_XTe$ SGs. Our studies are crucial for better understanding of the MMSSs temperature evolution in the dynamical freezing range $0.7T_f < T < 2T_f$, since the available concepts of SG treat the temperature evolution of various spin clusters only qualitatively In addition, we have also studied the temperature evolution of various MMSSs both above and below T_f. .

The results obtained may be used both for better understanding of the nature of aging, memory and chaos effects in SGs and for more effective using of these effects in various practical applications. Thus, this work provides a better insight into challenging issues of the freezing process of spins and also opens doors for a broad range of research opportunities to future investigations of the MMSSs in semi-insulating SGs.

Optical Properties of Tl1-xIn1-xSnxSe2 (x=0-0.25) Single Crystals

Danylchuk S.P., Bozhko V.V., Myronchuk G.L., , Parasyuk O.V., Kityk I.V.

Volyn National University, Lutsk, Ukraine

Thallium indium selenide is a typical representative of layered semiconductors and is attractivedue to an interesting couple of properties and their anisotropy resulting from the specifics of the crystal structure [1].

Compounds of the $A^{III}B^{III}C^{VI}_2$ type and their solid solutions with the clearly defined layered structure are characterized by the presence of structure defects of which vacancies and dislocations are the dominant ones. According to X-ray diffraction analysis data [2], main part of the defects in the $Tl_{1-x}In_{1-x}Sn_xSe_2$ single crystals is comprised of thallium vacancies (V_{Tl}), the concentration of which increases with *x*. All crystals are *p*-type semiconductors according to the sign of thermo-EMF coefficient which may be caused by the acceptor character of the thallium vacancies.

One of the principal methods of the investigation of the defect state of a semiconductor is the study of the energy dependence of the absorption coefficient.

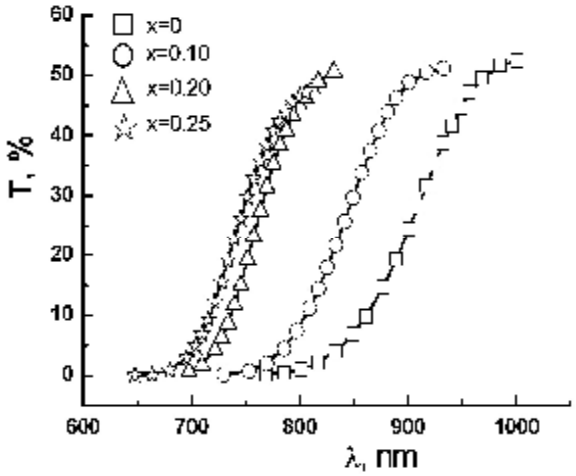

Spectral dependence of the transmission coefficient in the $Tl_{1-x}In_{1-x}Sn_xSe_2$ crystals (x=0–0.25) at 300 K.

Using light quantum energy near the fundamental absorption edge at $\alpha = 300\ cm^{-1}$, the bandgap energy was estimated depending on temperature and composition (*x)* of the crystals.

Band gap energy increases with the $SnSe_2$ content in the solid solution reaching its maximum for the largest content (*x*=0.25). Such E_g increase may be related to the mechanism of the formation of solid solutions, where the statistical substitution of Sn atoms for In atoms is accompanied by the increase of the concentration of thallium vacancies V_{Tl}.

Using the values of E_g determined from the absorption coefficient at the fundamental absorption edge, we have established that the value of temperature coefficient of the band gap energy equals to $\beta = (3.5–5)\cdot10^{-4}$ eV/K. Minor decrease of β in more defective alloys with higher *x* is, in our opinion, related to the disordering of the crystal lattice by the structure defects.

1. A.U. Sheleg, V.G. Gurtovoj, S.N. Mustafaeva, E.M. Kerimova, Fizika Tverdogo Tela 53 (2011) 443.
2. M.Yu. Mozolyuk, L.V. Piskach, A.O. Fedorchuk, I.V. Kityk, I.D. Olekseyuk, O.V. Parasyuk, J. Alloys Compds. 509 (2011) 2693.

Thermoelectric Parameters of IV-VI Crystals Compounds: Experiment, Calculation, Optimization

Dzumedzey R.O.

Vasyl Stefanyk Precarpatian National University, Ivano-Frankivsk, Ukraine

Lead telluride is the basic material for making thermionic energy converters. PbTe has bilateral homogeneity of the deviation from the stoichiometric composition as the metal side (n-type) and on the side of the chalcogen (p-type). The properties of lead chalcogenides can be modified due to doping.

Investigating crystals obtained by metalceramic-technology. Lead telluride crystals obtained by direct melting of initial components in graphitized quartz ampoules evacuated to a pressure of ~ 10^{-2} Pa. In one case, the doping was performed during the synthesis of compounds. To this vial for the synthesis of accurately calculated sample made right amount of impurities. In another dopant added in the binary compound.

Theoretical calculation of conductivity was carried out by the determination of carrier mobility by variation method. As we know the conductivity depends of the mobility and concentration - σ (μ, n), mobility depends of the concentration and effective mass - μ (n, m*). By entering the analytical dependence of the effective mass from the concentration as a power function ($m^*=\alpha n^{\beta}$, where α and β coefficients), we obtain the conductivity as a function of carrier concentration. Choosing the calculated values by their match with the experimental data on the electrical conductivity. Theoretical calculation of the Seebeck coefficient conducted on components for a particular scattering mechanism according to the expression Pisarenko for nondegenerate crystals and expression:

$$\alpha = \frac{k}{e} \cdot \frac{\pi^2}{3} \frac{kT}{\mu} \left(r + \frac{3}{2} \right),$$

for degenerate crystals. The total value of the Seebeck coefficient calculated by summing each of its component $a = \sum_i a_i$.

Optimization was performed separately for each material as n-type so p-type of conductivity. Optimum materials for each leg of the thermoelectric module chosen from the given technological conditions of synthesis, dopant content and maximum of thermoelectric figure of merit for a particular temperature range.

The work supported by projects of NAS of Ukraine (N 0110U006281) and by project of MES of Ukraine (N 0107U006768)

Crystal-Chemistry and Thermodynamics of Point Defects in Semiconductor Crystals of Samarium Mono-Sulfide and its Analysis

Freik D.M., Gorichok I.V., Shevchuk M.O., Godlevska M.A.

Precarpathion National University named after V. Stefanyk, Shevchenko Str.,57, Ivano-Frankivsk, 76000, Ukraine, e-mail: goritchok@rambler.ru.

This work investigates defective subsystem of samarium monosulfid crystals and undoped and doped by rare-earth elements (Sm, Gd, Tm) crystals of lead telluride.

Equilibrium values of concentration of chalcogen vacancies and antistructural samarium atoms in semiconductor and metallic phase of SmS at a given temperature and chemical composition were calculated for SmS crystals by minimizing the thermodynamic potential of the crystal. The dependence of electrons effective mass on their concentration in the samarium monosulfid conductive d-band was determined based on the experimental dependences of Hall concentration on temperature.

The calculation of the concentration of point defects and free charge carriers in metallic and semiconductor phase of single-crystal samarium monosulfid, which is in equilibrium condition with a pair of metal, was conducted. The temperature dependence of the solidus line of the excess metal was defined.

Based on the crystal model of the lead telluride defect subsystem, which takes into account vacancies in anionic and cationic sublattices, dependencies of the concentration of point defects and free charge carriers and the deviation degree from stoichiometry in PbTe crystals depending on the technological parameters of two-temperature annealing – annealing temperature T and vapor pressure of tellurium P_{Te} were calculated.

For doped crystals PbTe: Sm, PbTe: Gd and PbTe: Tm models of defect subsystems are proposed and thermodynamic parameters of impurity atoms introduction in the lattice are calculated.

The work supported by project of MES of Ukraine (N 0107U006768)

Chemical Properties and Defects Subsystem of Germanium Telluride and Solid Solutions Based on it

Freik D.M., Gorichok I.V., Yurchyshyn L.D.

Precarpathion National University named after V. Stefanyk, Shevchenko Str.,57, Ivano-Frankivsk, 76000, Ukraine, e-mail: goritchok@rambler.ru.

In this work the defective subsystem germanium telluride crystals and solid solutions GeTe-Bi_2Te_3: specifies type of dominant point defects, charge states and their concentration dependence of the deviation from the stoichiometric composition within the homogeneity. Methods crystal-quasichemical and thermodynamic potentials found that nonstoichiometric germanium telluride dominant defects are vacancies germanium, which determine the dependence of hole concentration on temperature and chemical composition of the crystal. Vacancies tellurium V_{Te}^{1+} and anti-structural germanium atoms Ge_{Te}^{1-} under any investigated process conditions do not affect the concentration of free holes, and the impact of anti-structural defects Te_{Ge}^{1+} on the concentration of charge carriers is noticeable only at temperatures above 750 K and excess tellurium concentrations above 0.04 at. % Te.

Found that annealing GeTe in tellurium pair go to a significant reduction in comparison to the as crystals, concentration anti-structural tellurium atoms $\left[Te_{Ge}^{1+}\right]$. Growth chalcogen vapor pressure go to a linear growth of hole concentration, and the increase of annealing temperature, at a fixed value of the vapor pressure of the chalcogen causes non-monotonic dependence of $p(T_в)$ with a maximum near 700 K.

Research of defect subsystem of solid solutions GeTe-Bi_2Te_3. Found that the main mechanism of their formation is the substitution of Bi atoms – vacancies germanium at low doses impurity compounds and complex formation $\left(Bi_i^{3+} - V_{Ge}^{2-}\right)^{1+}$ with subsequent release phase Bi_2Te_3 with Bi content higher than 1.0 at.%.

The work supported by project of MES of Ukraine (N 0107U006768)

Structure and Properties of ZrO_2-Ni/NiO Composites from Nanopowders

Glazunov F.I.[1], Danilenko I.A.[1], Konstantinova T.E.[1], Glazunova V.A.[1], Volkova G.K.[1], Burhovetsky V.V.[1]

[1] *Donetsk Institute for Physics and Engineering named after O.O. Galkin National Academy of Sciences of Ukraine*

Among various types structural ceramics, zirconia ceramics have been widely researched in the recent time, because it have high mechanical properties, chemical and thermal stability, biocompatibility, which allows its use for cutting tools, thermal coatings, biomedical implants etc. However ability to brittle fracture is a significant disadvantage for any ceramics. Composites have been found to be most successful in overcoming this drawback. Metals or metal oxides have been successfully used as reinforcing materials either as particles and whiskers [1]. Despite their success, the use of such systems is still poorly understood, especially for composites prepared from nanopowders. The aims of the present paper are development of composite materials based on nanopowders of yttria stabilized zirconia with the fillers of nickel and nickel oxide particles.

The zirconia and NiC_2O_4 nanopowders have been used as initial components. Synthesis of nanopowders of doped zirconia (ZrO_2-3 mol% Y_2O_3) was carried out by co-precipitation of hydroxides from solutions of salts of zirconium and yttrium nitrates with aqueous ammonia [2]. Nickel oxalate was obtained from commercial grade nickel chloride in reaction with oxalic acid. To produce the composites, powders of zirconia and nickel oxalate mixed by cavitation in an ultrasonic chamber and calcined at 700-1200^{o}C or co-precipitation of hydroxides zirconium and nickel. Compaction of samples was carried out at a pressure of 300 MPa. The samples were sintered at 1200-1500^{o}C, 2 hours in air or argon.

Structure and properties of nanopowders and dense composites has been studied. Kinetics of zirconia and nickel oxide nanopowder grain size growth was investigated. Effect of nickel oxide addition on the phase composition of zirconia during sintering in different atmospheres was found. Both Ni and NiO inclusions significantly enhances the strength and crack resistance of composites on 30% and 70%, respectively. The crack resistance increase was explained by phenomena of crack deflection and bridging.

1. Ajayan, P.M., Schadler, L.S. and Braun, P.V. Nanocomposites Science and Technology, Wiley-VCH Verlag, Weinheim 2003.
2. Konstantinova T, Danilenko I, Glazunova V, Volkova G, Gorban O. Mesoscopic phenomena in oxide nanoparticles systems: processes of growth//J. Nanopart. Res. – 2011. - №13. - p. 4015 - 4023.

The Formation Energy of Point Defects in Binary Compounds of Semiconductor Crystals

Gorichok I.V.

Precarpathion National University named after V. Stefanyk, Shevchenko Str.,57, Ivano-Frankivsk, 76000, Ukraine, e-mail: goritchok@rambler.ru.

In this work, given the results of the calculation of the formation energies E anionic and cationic monovakansie in semiconductor compounds $A^{III}B^{V}$, $A^{II}B^{VI}$, $A^{IV}B^{VI}$, which are the basis of active and passive elements of modern microelectronics. On the way to optimize the properties of these materials is a problem of effective management subsystem defective crystals. The level of development of modern experimental methods doesn't allow yet the direct determination of the concentration of point defects, especially in the cases when in the crystal there are several different types of defects - vacancies, interstitial atoms or their complexes, and measured parameters of the crystal are the result of their combined effect. Therefore it is necessary to use theoretical methods for determining concentrations of point defects. Thus, the fore a problem of determining the thermodynamic parameters of point defects: energy of their formation, the position of impurity levels in the energy band structure of the crystal, the free energy of vibration of the defect caused by a change in the oscillation frequency of the atoms in the vicinity of the point defect. Moreover, in most cases the assessment of concentration of point defects can be made only on the basis of known point defect formation energy, since the numerical value of the other two options, mainly, is smaller.

Along with ab initio methods of determining the energies of point defects is urgent search of relatively simple analytical methods of determining the value of E. In this work we used for this advanced method Hyukelya, and methods whith based are on the use of thermochemical, thermodynamic and electrical data. So, using thes parameters of crystal as energy of atomization, fusion, and others., we can estimate the energy changes in the system that occur when you remove an atom from its lattice site and lattice relaxation. In other cases - the energy formation of vacancies are calculated on the basis of experimentally determined parameters of the system to which the point defects have the greatest impact, particularly compress, the concentration of free carriers.

The calculated value of energies formation of vacancies of different methods are consistent with one another and with published data that shows their objectivity and ability to use for estimate the concentrations of defects in semiconductors.

The work supported by projects of NAS of Ukraine (N 0110U006281) and by project of MES of Ukraine (N 0107U006768)

Crystal-Chemical Model of Defect Subsystem in Nonstoichiometric Zink Calcogenides Crystals

Gurhula H.Ya.

Vasyl Stefanyk Precarpathian National University

Zink chalcogenides are perspective materials in electronic engineering for making detectors for γ - and x-rays, photo receiving and radiating structures of visible and infrared light spectrum. These materials are characterized by high quantum yield of photo-luminescence and cathode excitement. However, the largest quantum yield can be obtained only in homo-n-p-transition, which requires the ability to grow material of hole and electron conductivity type.

It is known that the basic electrical and photovoltaic properties of semiconductors are determined by their own defects and impurities, which are almost always present in the crystal. According to the results of the experimental studies, in particular PL, CL, EPR, defective crystals' structure of ZnX (X – S, Se, Te) compounds is extremely difficult, and only in rare case it becomes possible to interpret the experimental data using the approximation of one dominant effect. The concentrations of different types of defects depend on each other, and therefore, the development of the model of point defects that would enable, on one hand, to identify the relationships that exist between the concentrations of defects and on the other - to establish qualitative and quantitative dependency of the physical crystals' properties of compounds ZnX on the concentration of defects.

In this work, the crystalquasichemical formulas of the non-stoichiometric n- and p-ZnX have been proposed provided the realization of the complex spectrum of point defects after the scheme of Schottky-Frenkel. On their basis, the concentration dependencies of the prevailing defects have been calculated, as well as major current carriers and Hall concentration which would depend on the degree of deviation from the stoichiometric (α, β), disproportion of the charge state of point defects and content of alloying elements (Zn, X) respectively. Based on quasi-chemical equations of the formation of point defects, the annealing processes of double temperature treatment of ZnX crystals have been described and the dominant defects have been determined. Besides, the analysis of the principal models of point defects in ZnX crystals with the concomitant process of self alloying by p-ZnX and chacolgenide – n-Zn has been performed when interacting with oxygen, and also the mechanisms of defect formation in solid solution on the basis of metal chalcogenides.

The obtained two-dimensional diagrams of concentration of defects (charge carriers) – the chemical composition is determined by the technological factors (conditions of annealing), that provide obtaining of the crystals with already preset properties.

The work supported by project of MES of Ukraine (N 0107U006768)

Color Centers in Chemical Vapor Deposited Diamond Films

Khomich A.A.[1,3], Ralchenko V.G. [1], Bolshakov A.P.[1], Vlasov I.I.[1], Karkin A.E.[2], Khomich A.V.[3], Kmelnitskii R.A.[4], Konov V.I.[1]

[1] *A.M. Prokhorov General Physics Institute RAS, Moscow, Russia*
[2] *Institute of Metal Physics UB RAS, Yekaterinburg, Russia,*
[3] *V.A. Kotelnikov Institute of Radio Eng. & Electronics RAS, Fryazino, Russia*
[4] *P.N. Lebedev Physical Institute RAS, Moscow, Russia*

For the applications in quantum information and experiments on the foundations of quantum mechanics a robust narrow-band single photon source is desirable. One of the most promising candidates is a single photon source based on optically active defects in diamond, the so-called color centers, which are well localized, photostable at room temperature and demonstrates high brightness [1]. The unique physical and chemical properties of the host diamond crystal and progress in chemical vapor deposition (CVD) diamond films make these films suitable for practical quantum applications.

The ion implantation is one of the best ways to controllably introduce the impurities into diamond lattice in order to produce color centers [2]. The effect of isochronal vacuum annealing at temperatures up to 1680 ° C on the process of defect transformations in ion-implanted (energy 350 keV, H^+ or D^+ with fluencies $2 \div 12 \times 10^{16}$ cm^{-2}, ion energy 350 keV) and in fast neutron irradiated (fluence up to 2×10^{20} cm^{-2}) CVD diamond films was studied by photoluminescence and Raman spectroscopy. It was found that the grain boundaries in polycrystalline CVD diamond films did not significantly influence on the processes of radiation defect annealing and diffusion. In the photoluminescence spectra the new bands which are not observed before in diamonds was detected and investigated [3]. It is shown that the nonuniformity of the distribution of color centers along the surface of the [H^+] - and [D^+] - implanted layers appears to be of a nature similar to the island graphitization that is typical exclusively for hydrogen isotope implantation in diamond. The perspectives of defect engineering in CVD diamond films are discussed.

1. I. Aharonovich, A.D. Greentree, S. Prawer. Diamond photonics // *Nature Photonics* **5** (2011) 397—405
2. B.J.M. Hausmann, T.M. Babinec, J.T. Choy, J.S. Hodges, S. Hong, I. Bulu, A. Yacoby, M.D. Lukin, M. Lončar. Single color centers implanted in diamond nanostructures // *New Journal of Physics* **13** (2011) 045004 (11pp.)
3. A.V. Khomich, R.A. Khmelnitskii, N.A. Poklonski, N.M. Lapchuk, A.A. Khomich, V.A. Dravin, O.N. Poklonskaya, E.E. Ashkinazi, I.I. Vlasov, E.V. Zavedeev, V.G. Ralchenko. Optical and paramagnetic properties of polycrystalline CVD-diamond films implanted with deuterium ions // *J. Appl. Spectroscopy* **79** (2012) 600-609.

Crystalquasichemical Mechanism OF Catalysis IN THE Surface Layer OF Nanostructures $CuCl_n/Al_2O_3$

Kurta S.A.,Tatarchuk T.R., Mykytyn I.M.

Vasyl Stefanyk' Precarpathian National University, Ivano-Frankivsk, Ukraine

1,2-dichloroethane (1,2-DCE) is obtained in the oxidative chlorination of ethene (OCE) using nanostructured catalysts based on copper chlorides, immobilized (deposited or impregnated) on the surface of the carrier– γ-Al_2O_3. This process may change the mechanism of catalysis and therefore qualitative and quantitative composition of the OCE-reaction products.

On the base of comparison theoretical X-ray density and pycnometric density for $CuCl_2$ the presence of cation stoichiometry was detected and crystalquasichemical model of structure of the industrial catalyst (impregnated type MEDS-B) (firm «Sud-Chemie Catalysts», Germany) for oxidative chlorination ethene has been proposed:

$$(1-\alpha)\mathrm{Al}_{\mathrm{A}}^{\bullet}\left[\mathrm{Al}_{\frac{5}{3}}^{\times}\mathrm{V}_{\frac{1}{3}}^{\prime\prime\prime}\right]_{\mathrm{B}}\left(\mathrm{O}_4^{\times}\right)_{\mathrm{O}}+\alpha\mathrm{Cu}_{\mathrm{A}}^{\times}\left[\mathrm{Cu}_2^{\prime}\right]_{\mathrm{B}}\left(\mathrm{Cl}_4^{\bullet}\right)_{\mathrm{O}}\left(\mathrm{Cl}_2^{\prime}\right)_{\mathrm{i}}\rightarrow$$

$$\rightarrow\left(\mathrm{Al}_{1-\alpha}^{\bullet}\mathrm{Cu}_{\alpha}^{\times}\right)_{\mathrm{A}}\left[\mathrm{Al}_{\frac{5}{3}-\frac{5\alpha}{3}}^{\times}\mathrm{Cu}_{2\alpha}^{\prime}\mathrm{V}_{\frac{1}{3}-\frac{\alpha}{3}}^{\prime\prime\prime}\right]_{\mathrm{B}}\left(\mathrm{O}_{4-4\alpha}^{\times}\mathrm{Cl}_{4\alpha}^{\bullet}\right)_{\mathrm{O}}\left(\mathrm{Cl}_2^{\prime}\right)_{\mathrm{i}}$$

Ability to crystalquasichemical mechanism of catalysis for the OCE reaction in the nanostructures surface layer of the catalyst (impregnated type) was confirmed by massspectrometry and X-ray analysis of the active phase of $CuCl_2 \cdot 2HCl(H_2[CuCl_4])$ of OCE-catalyst and partially hydrolysed active phase of $CuCl_2 \cdot 2H_2O$ OCE-catalyst.

Formation of molecular chlorine on the surface of the catalyst has been shown by the Deacon reaction:

$$2\mathrm{HCl}_{(\mathrm{gas})}+\mathrm{O}_{\mathrm{O}}^{\times}\rightarrow\mathrm{H}_2\mathrm{O}+2\mathrm{Cl}^{\times}+\mathrm{V}_{\mathrm{O}}^{\bullet\bullet}+2\mathrm{e}^{\prime}$$

which reacts with ethene and leads to the formation of 1,2-dichloroethane:

$$2\mathrm{Cl}^{\times}+\mathrm{C}_2\mathrm{H}_4\rightarrow\mathrm{C}_2\mathrm{H}_4\mathrm{Cl}_2$$

A new crystalquasychemical mechanism of the OCE in the 1,2-DCE considers the formation and annihilation of electron-hole pairs and catalyst's antistructure during the reaction and can be applied to explain catalysis in the surface layer of nanostructures of industrial catalyst (impregnated type –MEDS-B) (firm «Sud-ChemieCatalysts», Germany). Adsorption-chemical processes in the catalytic OCE will proceed in a way of formation of cation and anion vacancies in the spinel structure of the catalyst. At the same time, the mechanism of catalysis of OCE in 1,2-DCE on the industrial catalysts (deposited type –X1) (company«Harshow», United States) explains well the metal complex model, proposed and described earlier.

Mo-Zr-V System with 3-Phase Transformation

Lutsyk V., Vorobjeva V.

Institute of Physical Materials Science SB RAS, Ulan-Ude, Russian Federation

Effect of 3-phase transformation in Mo-Zr-V system was discovered experimentally [1]. 3D computer model of T-x-y diagram, which consists of 23 surfaces and 14 phase regions (Fig.), are used to confirm and visualize it on the vertical or horizontal sections [2]. R is a solid solution of binary compounds R1=$ZrMo_2$ and R2=ZrV_2. Really, three-phase reaction L+R1→B of peritectic type has a place in the binary system Mo-Zr, and the binary eutectic is crystallizing according the reaction L→B+R2 in the system Zr-V. Obviously, that transfer from one type of phase reaction to another type must occur within the 3-phase region L+B+R.

Surface ***abc*** (Fig., left) of two-phase reaction L→B in the presence of the third phase R corresponds to this kind of transfer, when a mass increment becomes equal to zero: m_R=0. E. g., solidification of arbitrarily chosen melt G begins at the temperature 803.3°C. Vertical line in the point G(0.25, 0.61, 0.24) intersects the upper and lower borders of the three-phase region L+B+R at temperatures 749.5°C and 717.1°C, correspondingly. Peritectic reaction L+R→B with decreasing of liquid and R masses is carried out in the interval 749.5-733.8°C. After the section of the surface m_R=0 at 733.8°C the binary eutectic B+R is crystallizing within the interval 733.8-717.1°C. Corresponding section ***ab*** of the surface m_R=0 (originating segment of ruled surface) is shown on isothermal section 733.8°C within the L+B+R phase region (Fig., right).

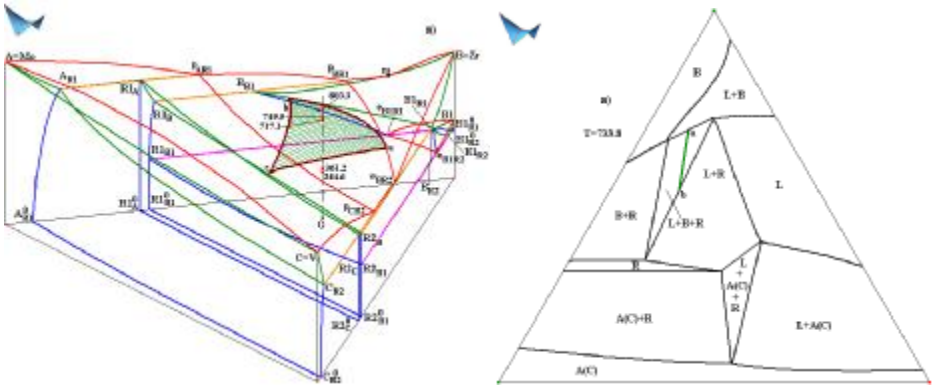

1. V.N. Yeremenko. *Chosen Works. Recollections. Devoted to 100th Anniversary*. Naukova Dumka, Kiev. 664 pp. (2011) (In Russian).
2. V.I. Lutsyk, V.P. Vorob'eva. Investigation of Three-Phase Transformation Type Changing Conditions in the System Ti-Ir-Ru // Perspectivnye Materialy, # 13 (Special Issue), pp. 191-197 (2011) (In Russian).

Quantitative Determination of Oxide Admixtures in Film-Forming Material ZnS

Magunov I.R., Mazur O.S., Zinchenko V.F.

A.V. Bogatsky Physico-Chemical Institute of the NAS of Ukraine, Odessa, Ukraine

Film-forming material based on zinc sulphide ZnS is widely used for obtaining thin films in optics and optoelectronics. Presence of oxide compounds of zinc in material worsens its mechanical properties of thin films (mechanical durability, adhesion to a substrate, homogeneity etc.), reduces long-wave IR domain of transparency to 14.5 micrometers, results in spoilage of equipment at evaporation of material.

Model exchange reactions of zinc oxide (basic oxide admixture) with dysprosium sulphide are studied thermo-gravimetrically. The exchange reactions pass at temperatures about 900°C quantitatively. Reactions in the system Dy_2O_3 – Dy_2S_3 for clear identification of the phases in the system ZnO – Dy_2S_3 were studied as well.

Synthesis of the composite materials with alloying additive is carried out in high-temperature quartz tube furnace RHTC 80-450, Nabertherm (Germany); inert (Ar) high purity medium was used.

Table – Phase composition of the systems ZnS – Dy_2S_3, ZnO – Dy_2S_3 and Dy_2O_3 – Dy_2S_3 after heat treatment at 900°C (XRDPA data)

System	Color	Phase composition of the system
ZnS – Dy_2S_3 (5 % mass.)	greyish-yellow	β-ZnS (hexagonal), α-ZnS (cubic), α-Dy_2O_2S (hexagonal) (small)
ZnS – Dy_2S_3 (20 % mass.)	light brown (reddish)	α-ZnS, α-Dy_2O_2S, ZnO (admixture)
ZnO/Dy_2S_3=2:1	dirtily green	α-Dy_2O_2S, ZnO, β-ZnS (very small)
Dy_2O_3/Dy_2S_3=2:1	dirtily green	α-Dy_2O_2S, Dy_2O_3 (very small)

Determining the amount of oxide admixtures is based on discoloration of standards as a result of exchange reactions, with formation of dysprosium oxy-sulphide, that has a characteristic spectrum of diffuse reflection in visible and near IR intervals of a spectrum.

Synthesis of High-Brightness $SrTiO_3:Pr^{3+}$ Phosphors without co-Activators by Sol-Gel Method

Marchylo O.M. [1], Nakanishi Y. [2], Kominami H. [2], Hara K. [2], Zavyalova L.V. [1], Svechnikov G.S. [1]

[1] *V.E. Lashkaryov Institute of Semiconductor Physics, National Academy of Sciences of Ukraine, Kyiv, Ukraine*

[2] *Research Institute of Electronics, Shizuoka University, Hamamatsu, Japan*

The $SrTiO_3:Pr^{3+}$,Al phosphors were synthesized by sol-gel method at the optimal conditions [1]. The starting materials were $SrCl_2$, $PrCl_3$, $Al(NO_3)_3 \cdot 9H_2O$ and $Ti(O\text{-}i\text{-}C_3H_7)_4$. Synthesis was carried out in a nitrogen atmosphere. A ratio of starting materials Sr/Ti = 1 was fixed. The concentration of Pr at 0.2 mol% was fixed, and concentrations of Al were varied of 0 to 15 mol%. The starting materials were dissolved in an ethanol (vol. 96%) and dried under stirring. The annealing was carried at temperature 1300 ºC in during 5 hours. PL spectra were measured with PMA-12 in the wavelength range of 450–750 nm under a He-Cd laser excitation (λ=325 nm) at room temperature. CL measurements were carried out at the anode voltage of 2 to 10 kV and current density 60 μA/cm^2.

The influence of Al addition on PL spectra and CL luminance of $SrTiO_3:Pr^{3+}$,Al with effective concentration of Pr^{3+} of 0.2 mol% were investigated (Fig.1 and Fig.2). Abnormally high level of brightness for the sample with no contain aluminum is observed. In this case, the brightness achieves 1840 cd/m^2 at the anode voltage of 10 kV. Al-addition even at 1 mol% leads to a sharp seven-fold reduction in the luminance level. Further increase in Al-concentration from 1 up to 15 mol% does not result to significant changes in luminance. In contrast to data [2], where the results of enhancement emission intensity of $SrTiO_3:Pr^{3+}$ due to Al addition in 200 times were reported.

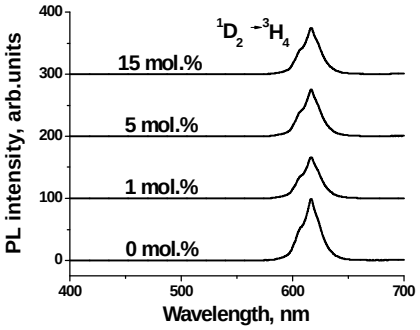

Fig.1

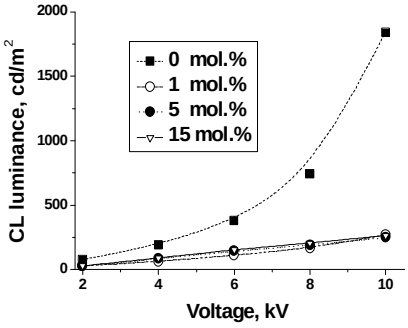

Fig.2

1. Marchylo, L.Zavyalova, Y.Nakanishi, H.Kominami, K.Hara, A.Belyaev, G.Svechnikov, L.Fenenko, V.Poludin, J. SPQE&O., **12** [4] 321-323 (2009).
2. S.Okamoto, H.Kobayashi and H.Yamamoto, J. Appl. Phys., 86[10] (1999) 5594-5597.

The Aging of Single-Crystal Yttrium-Iron-Garnet Epitaxial Films

Moklyak V.V.

G. V. Kurdyumov Institute for Metal Physics, Kyiv, Ukraine

Surface layer aging of yttrium-iron-garnet monocrystal epitaxial films were investigated by electron conversion Mössbauer spectroscopy. The specific changes for the all characteristic parameter of Mössbauer spectra were founded. For spectra obtained with one year time interval the next regularities were fixed: narrowing the width of the line for both *d*-positions on the ≈ 0,05 mm/s; increasing of isomer shift on ≈ 0,1 mm/s for all positions; decreasing of the effective magnetic fields for resonant nuclei for the all positions; changing of axial component of electric field gradient tensor value; the integrated intensity of the paramagnetic component is unchanged and stay on ≈ 2,5 % of the total intensity.

These changes were explained by the recovering of defect anionic sublattice in the epitaxial heterostructure surface layer. Partially reconstruction of oxygen polyhedras coursed the increasing of the chemical bonds ionicity degree in tetrahedral and octahedral complexes of iron and redistribution of electron density for $Fe_a^{3+} - O^{2-} - Fe_d^{3+}$ bonds with the localization of the 4s-electrons of iron wave function on the oxygen nuclei. These processes leads to increasing of isomer shift too. The 4s-electrons iron have took part in the formation of the Fermi contact field, which makes the main contribution to the resulting value of the effective magnetic field at the resonant nuclei. So the reducing of the effective magnetic field has caused by a decreasing in spin density 4s - electrons of iron. Narrowing of the line width for both *d*-positions is the result of a greater sensitivity this positions to changes in the anionic sublattice in comparison to *a*-positions. Simultaneous description of electric field gradient valence and crystal parts competitive impact is to complex so the changes of tensor axial components couldn't be correctly explained in our mode.

The effective magnetic fields vectors reorientation processes by Mossbauer spectroscopy in external magnetic field (up to 2,8 kOe) was experimentally observed. At the same time the values of magnetic field remained constant for all samples. This effect is caused by the "freezing" of spin moments and the disregarding of spin bipolar contribution in the external magnetic field during anionic sublattice reconstruction.

Influence of Synthesis Parameters on the Properties of Nanocrystalline Vanadium Oxide Films

Nikirin V., Goltvyanskyi Yu., Kychyk A., Melnik V., Khatsevych I.

V. E. Lashkaryov Institute of Semiconductor Physics of the National Academy of Sciences of Ukraine, Kyiv , Ukraine

Materials with high temperature coefficient of resistance (TCR) are basis for uncooled microbolometers production, therefore creation of such materials and investigation of their properties have a big practical interest. One such material is vanadium dioxide films. They have a high sensitivity to infrared radiation and ambient temperature changes. Our studies have shown that by changing of the VO_2 films synthesis conditions is possible to create materials (compositions close to $VO_2 – VO_x$, x = 2.12) with a high TCR (~ 7,0% / K) and low resistivity values at room temperature. It was found that for creation thermo-sensors based on vanadium oxide is need to provide conditions for the formation of a film containing a mixture of various vanadium oxides. The presence of V_2O_5 and VO_2 provide high TCR, presence V or V_2O_3 provides a high conductivity of the film. Unfortunately, each vanadium oxide phase have own optimal formation condition (temperature, stoichiometry, etc.), and the synthesis of suitable films is a complex technological problem. Our experiments have shown that vanadium oxide films with high TCR ~ 7.0% / K can be formed by magnetron deposition with next thermal annealing at temperatures of 250-350 ^0C for 30-300 min. A feature of this method is formation inclusions of crystalline phase V_2O_3 already at the process of deposition film VO_X ($1.4 \leq x \leq 1.6$). The presence crystalline inclusions in the film before annealing (Fig. 1, b, lower curve), provides formation and crystallization phases of various vanadium oxides during low temperature annealing (250-300 ^0C).

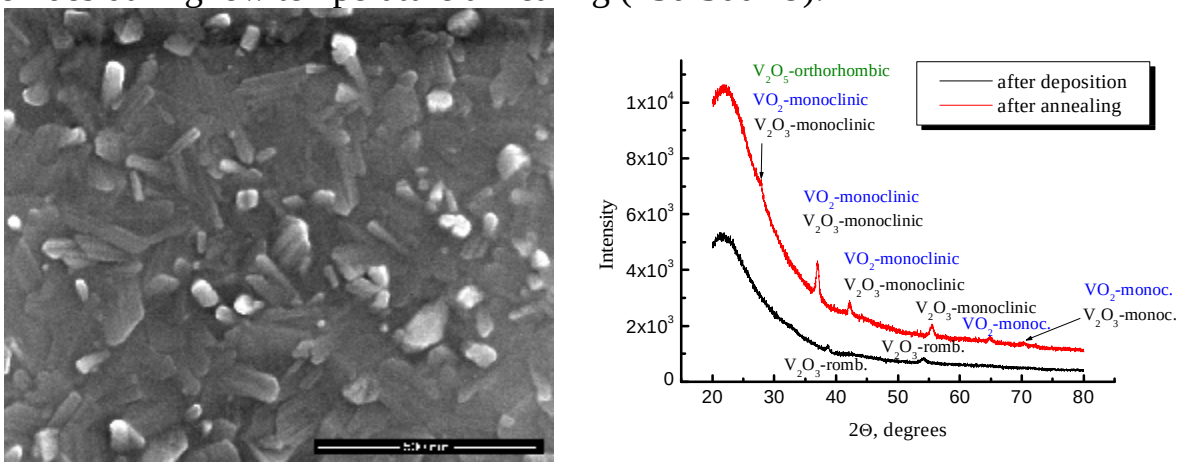

a) b)

Fig.1. SEM-image of vanadium oxide film (a), X-ray diffraction of the film before (lower curve) and after thermal annealing (upper curve).

Crystallites which formed in the film during deposition are the centers for further film crystallization, therefore crystallization occurs already at 250^0C. Since crystallization of vanadium oxide film occurs during annealing in oxygen-atmosphere simultaneously observed additional film oxidation. After annealing the film composition is close to VO_2 and consists nanosize crystallites with different phases of vanadium oxide (VO_2, V_2O_3 and V_2O_5), that is evident from the diffraction of x- rays (Fig. 1, b, upper curve). The size of crystallites in synthesised film is in the range from tens to several hundred nanometers (Fig. 1, a). This film with nanocrystalline inclusions of VO_2 and V_2O_3 provides high TCR (Fig. 2, a) and low resistivity values ~ 2 - 4×10^{-2} Ohm*cm (Fig. 2, b) at room temperature.

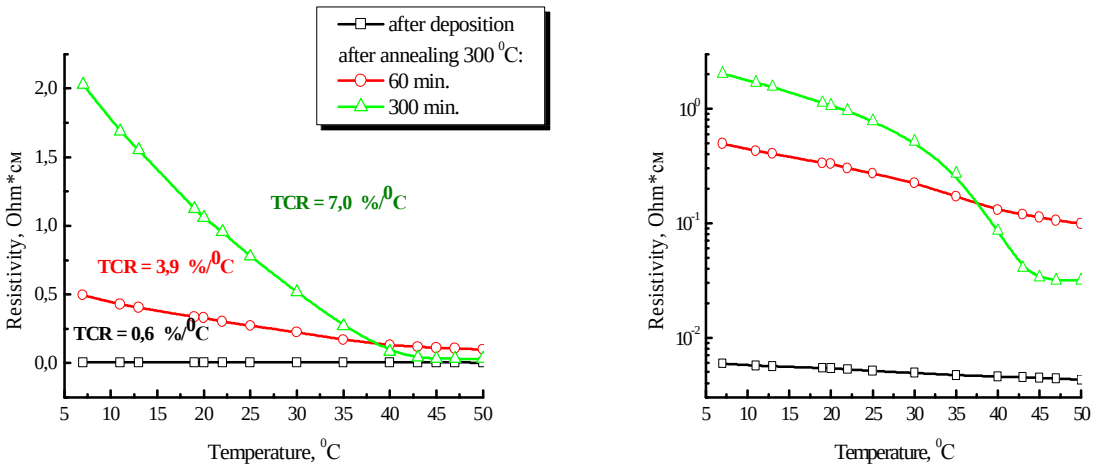

a) *b)*

Fig.2. Thermal dependence of the film resistivity immediately after deposition and subsequent thermal annealing: in linear coordinates (a) and semilogarithmic (b).

The proposed method for the synthesis of vanadium oxide films allows creating temperature-sensitive materials that could be used as a sensing element for uncooled microbolometers.

New System of Alternative Energy 'Solar Collector – Thermoelectric Generator'

Nykyruy L.I.

Vasyl Stefanyk Precarpathian National University, Ivano-Frankivsk, Ukraine

The purpose of this paper is developing a system of direct conversion of solar energy into thermal energy using the upgraded structure of heliostats and solar heat into electricity using of thermoelectric generators.

The idea is to develop of the new technology of thermoelectric materials based on IV-VI compounds, which will be the basis for the construction on their the thermoelectric modules, and further testing of these modules as thermoelectric generator engineered on solar energy collectors. The temperature difference between the coolant and the tabulation of the coolant will be in the range of 150 degrees, indicating on prospect of obtaining the thermoelectric power.

There are developed and patented technology for multicomponent compounds based on the lead telluride as base material, and its doping with different impurities (In, Ga, Tl, K, Na, Bi, Sb). The following are the examples of PbTe: Bi. Doped Bismuth alloys have electronic conductivity. Were calculated thermoelectric parameters with account of carrier scattering by phonons (acoustic and optical), vacancies, and impurity atoms in the approximation of the variational principle.

Electrical conductivity of pressed samples with different dopant concentration is about the same and consist 7.9 $(Ohm \cdot cm)^{-1}$ for $Pb_{49.95}Te_{50.00}Bi_{0.05}$ and 10.5 $(Ohm \cdot cm)^{-1}$ for $Pb_{49.00}Te_{50.00}Bi_{1.00}$ (for fraction of 0.05-0.5 mm). These values are significantly lower from electrical conductivity of samples obtained by hot pressing, and, at the same time, an order higher than the corresponding values for the undoped PbTe samples, obtained by cold pressing. Seebeck coefficient is lower by an average for samples with impurity concentration 1.00 at. % on 20 mV/K than for samples with 0.05 at.%.

The thermoelectric module is built on the basis of materials of n-and p-type, and consists of 48 columns (5 mm diameter and 3 mm high), connected by a switching plate with 24 thermocouple.

It was develop a business plan for the production of industrial lead telluride thermoelectric material and modules on their base.

The work supported by projects of FRSF State Agency for Innovation and Informatization of Ukraine. (Contracts: R54, F53, 3)

The work supported by project of MES of Ukraine (N 0107U006768)

Study of Oxide Crystals Growth on Refractory Metals Surface

Orlovskaya S.G., Karimova F.F., Shkoropado M.S., Kalinchak V.V.

Odessa National I.I. Mechnikov's University, Odessa, Ukraine

Transition metal oxides are widely used as catalysts, besides they are considered to be applicable in solar industry, microelectronics and other modern technologies. So development of effective methods of metal oxides production is subject of extensive investigations.

So this study is aimed at main characteristics (growth rate and mechanism) of oxide microcrystals formation on molybdenum and tungsten filaments during high temperature oxidation. Tungsten and molybdenum oxides exhibit unique physico-chemical properties: gasochromism, electrochromism and photocromism. So they are promising materials for electrochromic displays, gas sensors, smart windows and other applications.

To study oxides structures on the surface of refractory metals we developed an experimental setup based on "hot filament" method. This method consists in a controllable heating of metal filament in oxidizing atmosphere at a gas temperature T_g [1, 2]. The oxides growth is registered by videomicroscopy. Changes of crystal's dimensions are defined by image processing routine, then their growth rate is calculated.

In so way the mechanisms of oxide layers development are defined on the surface of tungsten and molybdenum filaments heated electrically. It is found that from the beginning a primary oxide film is formed on a tungsten surface. Then numerous whiskers appear above the oxide layer mainly along cracks. Gradually they transform into branched bush-like structures due to prismatic facets overgrowth (Fig.1).

Figure 1. Bush-like oxide structures on the surface of tungsten filament.

Oxide structures on molybdenum filament appear in the form of microplates, which are oriented in different directions. With time they interconnect and grow together [3]. It is found that the first tungsten oxide whiskers appear at 900 K, whereas molybdenum oxide plates are observed starting with temperature 800 K, because molybdenum oxides are more volatile.

By computer processing successive images of oxides structures we defined their growth rates, depending on growth direction. So for tungsten oxide rate of growth in height (outwards the filament) is distinctly less than growth rate in width –parallel to the filament surface (Fig.2).

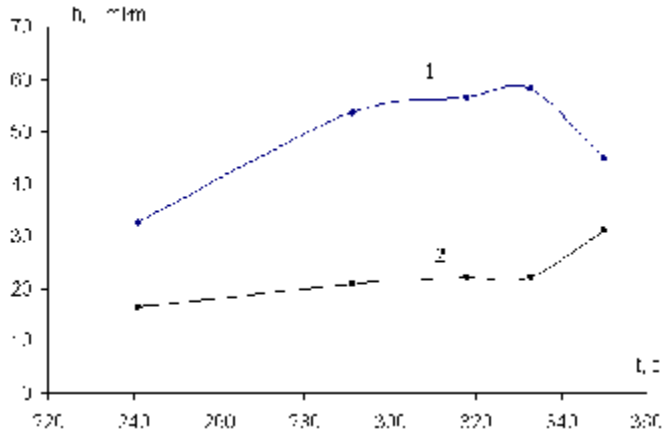

Figure 2. Crystal's dimensions histories: 1 – crystal height (h); 2 –crystal width (l).

Growth rates for tungsten oxides crystals varies in ranges: in height – 0.1÷0.5 mcm/c and in width – 0.1÷0.8 mcm/c. As to molybdenum oxide crystals – they increased with equals rates in height and in width: from 0.2 mcm/c up to 0.55 mcm/c for different crystals.

To clarify oxide crystals formation mechanism we fulfilled x-ray analysis of filaments. It was found substantial quantity of carbon on the tungsten surface, possibly as a result of graphite lubricant use during wire-drawing. After thorough surface peeling the whiskers are not formed under heating. So we conclude that the carbonaceous particles are perhaps the centers of oxide vapors condensation.

1. Sadiki H. et al. Properties and electrochromic performances of reactively sputtered tungsten oxide films with water as reactive gas // Surface & Coatings Technology 200 (2005) 232 – 235.
2. Orlovskaya S.G., Karimova F. F. and Shkoropado M. S. Formation of oxides on tungsten conductors heated by electric current // Powder Metallurgy and Metal Ceramics. – 2010. –Vol. **49**, N.6. – P.352-354.
3. Orlovskaya S.G., Shkoropado M.S., Karimova F.F. Growth Kinetics of Oxides Structures on Refractory Metal Surface During Heating in Air // Physics and Chemistry of Solid State. – 2012. – V. **13**, N.3. – P. 733-737.

Quantum-Chemical Calculation of the Thermodynamic Parameters of ZnS, ZnSe, ZnTe Crystals

Parashchuk T.O.

Vasyl Stefanyk Precarpathian National University, Ivano-Frankivsk, Ukraine, taras-parashchuk@i.ua

Zinc chalcogenides are promising materials for both techniques and scientific models. However, for the practical application of ZnS, ZnSe, ZnTe it is needed the reliable information about crystal structure of these materials.

For the calculation of the thermodynamic parameters we used the cluster approach. The calculations were performed using the software package Firefly within the limited Hartree-Fock approximation, using the valence basis set SBKJC, which includes the skeleton of the effective potential. Visualization of spatial structures was carried out using Chemcraft.

As a result of the calculation were obtained energies of formation, enthalpy of formation, entropy, Gibbs energy and the specific heats at constant pressure and at constant volume of ZnS, ZnSe, ZnTe crystals.

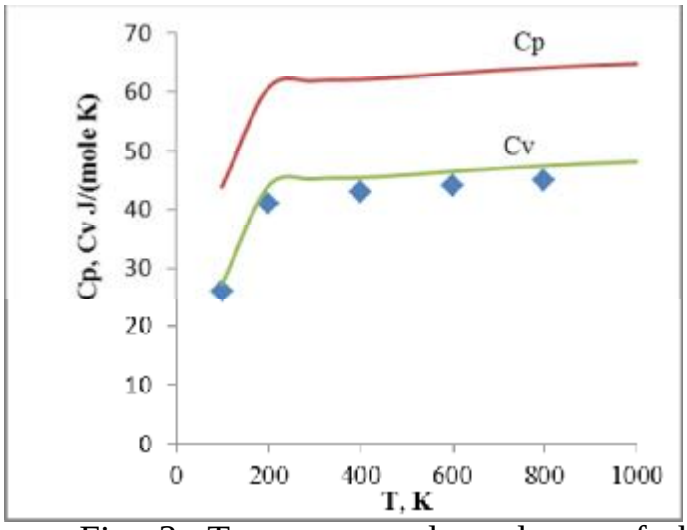

Fig. 3. Temperature dependence of the specific heats of ZnSe crystals at constant pressure C_P and constant volume C_V respectively; lines – is the calculations, points is the experiment.

The obtained values of the specific heats at constant pressure C_p and at constant volume C_v at different temperatures are shown in Fig. 3. We can see that our results of quantum-chemical calculations satisfactorily describe the experiment and theoretical calculations of other authors. In particular, the values of C_p and C_v are increases throughout the temperature range presented. At low temperatures there is a rapid increase in the value of the specific heats according to the theory of Debye and at higher - growth trend becomes weaker and close to the Dulong-Petit limit. Temperature dependence of the specific heats of crystalline structures has been defined the following functions:

$$C_p = a + b \cdot 10^{-3} T - c \cdot 10^{5} T^{-2}$$

Our calculated dependence is corresponding to known experimental data.

The work supported by project of MES of Ukraine (N 0107U006768)

Quasi-Chemical Description of Own Point Defects of Zinc Telluride

Prokopiv V.V.

Vasyl Stefanyk Prekarpathian University, Ivano-Frankivsk, Ukraine, e-mail:, prkvv@i.ua

Zinc Telluride is a promising material of light-emitting diodes with high brightness. It is needed reliable information about their defective condition for developing the science-based technology ZnTe material.

$0 = V_{Te}^{0} + V_{Zn}^{0}$	$K_S = \left[V_{Te}^{0}\right] \cdot \left[V_{Zn}^{0}\right]$
$Zn^{V} = V_{Te}^{0} + Zn_{Zn}^{0}$	$K_{Zn,V} = \left[V_{Te}^{0}\right] p_{Zn}^{-1}$
$\frac{1}{2}Te_2^{V} = V_{Zn}^{0} + Te_{Te}^{0}$	$K_{Te,V} = \left[V_{Zn}^{0}\right] p_{Te_2}^{-1/2}$
$V_{Zn}^{0} = V_{Zn}^{2-} + 2h^{+}$	$K_a' = \left[V_{Zn}^{2-}\right] \cdot p^2 / \left[V_{Zn}^{0}\right]$
$V_{Te}^{0} = V_{Te}^{2+} + 2e^{-}$	$K_b' = \left[V_{Te}^{2+}\right] \cdot n^2 / \left[V_{Te}^{0}\right]$
$0 = h^{+} + e^{-}$	$K_S = np$
$2\left[V_{Zn}^{2-}\right] + n = 2\left[V_{Te}^{2+}\right] + p$	

Stoichiometric Zinc Telluride can be changed by setting the partial pressure of the components (Zinc, Tellurium) on the solid phase or the temperature in the method of two-temperature annealing. Equilibrium of "crystal-vapor" can be described by quasichemical reactions equations which are listed in the table.

If you are calculated the equations system you can determine the concentration of holes p through the constant quasichemical reactions K and the partial vapor pressure of Zinc P_{Zn} (1) or Tellurium P_{Te_2} (2):

$$2\frac{K_b' K_{Zn,V} P_{Zn}}{K_i^2} p^4 + p^3 - K_i p - 2\frac{K_a' K_S}{K_{Zn,V} P_{Zn}} = 0 \qquad (1)$$

$$2\frac{K_a' K_S}{K_i^2 K_{Te,V} p_{Te_2}^{1/2}} p^4 + p^3 - K_i p - 2K_b' K_{Te,V} p_{Te_2}^{1/2} = 0 \qquad (2)$$

The calculation of defects concentration are showed that in crystals ZnTe vacancies of Tellurium $[V_{Te}^{2+}]$ are formed in small quantities and concentration of charge carriers which is determined by the mainly vacancies of Zinc $[V_{Zn}^{2-}]$.

The increased of the Zinc vapor partial pressure P_{Zn} as the decrease vapor pressure Tellurium P_{Te_2} thus a constant annealing temperature T it reduces the hole concentration p, which is caused by a decrease in the concentration of Zinc vacancies $[V_{Zn}^{2-}]$.

With the decrease of annealing temperature T by the constant partial pressure of Zinc vapor P_{Zn} (Tellurium P_{Te_2}) the concentration of Zinc vacancies have been decreased $[V_{Zn}^{2-}]$, which reduces the hole concentration p.

The work supported by project of MES of Ukraine (N 0107U006768)

Crystal Chemistry of Point Defects and Their Complexes in Cadmium, Stanum and Lead Telluride Thin Films

Prokopiv V.V., Prokopiv V.V (jr.), Strutynsky O.R.

Vasyl Stefanyk Precarpathian National University, Ivano-Frankivsk, Ukraine,
E-mail: prkvv@i.ua

Performance device structures are largely determined by the defect subsystem of the using material. The purpose of this study was to analyze the defective condition in Cadmium, Tin, Lead Telluride films grown from the vapor phase to choose the optimal conditions of the process.

The quasichemical reactions models of intrinsic point defects in the Cadmium, Tin, Lead Telluride films which were growing from the vapor phase by hot wall have been given. The analytical expressions for determining the concentration of free charge carriers and the prevailing point defects due to the equilibrium constant K quasichemistry reactions defect and partial vapor pressure of Tellurium P_{Te_2} have been received.

It is shown that Cadmium Telluride films at high temperatures, evaporation T_E receive only the n-type conductivity for the whole area of change of substrate temperature T_S. However, with increasing substrate temperature T_S, at a constant temperature evaporation T_E, the electron concentrations is decreased and if T_E <900 K conductivity inversion from n-to p-type have been occurred.

In tin telluride films grown at low substrate temperature T_S and high values of the partial vapor pressure of an additional source of tellurium P_{Te_2} predominant defects are doubly ionized vacancies Tin $\left[V_{Sn}^{2-}\right]$, and in the films grown at other values of these technological factors will prevail fourfold ionised vacancies Tin $\left[V_{Sn}^{4-}\right]$.

It was founded that PbTe films have complex disordering of Frenkel defect subsystem in cationic sublattice with the predominance of doubly charged vacancies and interstitial Lead, and increasing the temperature of deposition $420\,K \le T_D \le 620\,K$ and the partial vapor pressure of $1\,Pa < P_{Te_2} < 10^3\,Pa$ leads to decrease in the concentration of electrons, inversion of conductivity from n-to p-type and the continued growth of concentration of holes.

During the growing of SnTe, PbTe films the changing of tellurium vapor partial pressure at constant temperature and substrate temperature TS TV evaporation at low pressure values tellurium ($P_{Te_2} < 10^{-3}$ Pa) does not affect the concentration of free charge carriers and defects due to the fact that at low additional source of tellurium pressures, the pressure of tellurium in the system is determined by the temperature of evaporation T_E.

The work supported by project of MES of Ukraine (N 0107U006768)

Composite Films of Electrolytic Fe,Ni,Co,Mo-Sulfides and MnO_2 Dioxide with Carbon Nanotubes in Redox Reaction with Lithium

Apostolova R.D., Peskov R.P., Kolomoyets O.V., Kirsanova I.V., Shembel E.M.

SHEI "Ukrainian State Chemical Technology University", Dnepropetrovsk, Ukraine

Electrolytic synthesis technology of the composition electrode material range for thin-layer lithium accumulators and lithium-ion systems have been proposed and optimized. Electrolytic mono sulfides of the transitional metals (Fe, Ni, Co, Mo) and bimetallic sulfides (Fe-Ni; Fe-Co; Ni-Co) codeposited with carbon nanotubes (UNT) belong to their quantity. MnO_2-UNT-composites continue the range.

The composites obtained from the UNT suspension in aqueous electrolytes at the stainless steel (18H12X10T) cathode with active component mass of 0.7-2.0 mg/cm^2. Sulfides deposed from the electrolytes comprising metal sulfates in the presence of sodium tiosulfate, dioxide MnO_2 – from electrolyte comprising $KMnO_4$, H_2SO_4. It was added UNT (0.5 g/l) in the electrolytes.

Electrolytic synthesis products have been shown the raised ability to discharge-charge electrochemical transformation in redox reaction with lithium.

Electrolytic bimetallic sulfide composites with UNT provide the discharge capacity of 550-600 mAh/g in the model lithium accumulator that raises the theoretical capacity of the graphite using in the negative electrodes of the lithium-ion batteries (372 mAh/g). UNT enhance adhesion strength of the active electrode material to metal support increasing the life of the lithium accumulator on its base similarity to graphite in the composites with electrolytic sulfides of the transitional metals [1,2].

Because of UNT in MnO_2 composite the electron conduction of the electrode material, its the average discharge voltage, the discharge capacity and the lithium accumulator life enhance. The analysis of the kinetic regularity of the electrode process realizes with the utilization thin MnO_2 electrode (0.7 μm) made by the mechanical rubbing in aluminium support.

1. R.D. Apostolova, Yu. A. Tkachenko, O.V. Kolomoyets, E.M. Shembel // Surface Engin. and Appl. Electrochem. 48 (2012) 170-174.
2. R.D. Apostolova, O.V. Kolomoyets, E.M. Shembel // J. of Appl. Chem. (In Russian) 84 (2011) 571-577.

Photoelectric Properties of Pure and Cu,Au-Doped Cadmium Iodide Crystals

Rudka M.M[1]., Antonyuk V.G[2]., Stetsyk N.V[2]

[1]Lviv Polytechnic National University, Ukraine, Lviv, Department of Physics
[2]Ivan Franko National University of Lviv, Ukraine, Lviv, Department of Physical and Biomedical Electronics

The layered nanocrystals of cadmium iodide belong to the class $A^{II}B^{VII}_2$ and have a strong anisotropy of the internal crystal interactions. Within the limits of the structural sandwich package J-Cd-J there are strong covalently-ion interactions between the components, with dominate of covalent component, and there are weak van der Waals forces between layers. The fundamental absorption edge of the CdJ_2 crystals at room temperature is 3.2 eV and from decrease in temperature to 77 K shifts to 3.48 eV [1], [2].

It is known [3] that the dominant luminescence centers in pure crystals CdJ_2 are strongly oriented donor-acceptor (DA) complexes of point structure defects in the cation vacancy and interstitial cadmium. The spectral position and duration of donor-acceptor luminescence are determined using of energetical parameters of such luminosity centers and the rate of localization upon them the nonequilibrium genetic electron-hole pairs.

Investigated samples were the undoped as well as the Cu-doped and Au-doped CdJ_2 crystals of thickness varied within 0.8–10 nm. These nanocrystals were grown using the standard Bridgman–Stockbarger technique in sealed quartz ampoules (CdJ_2:Cu – 0,5 % by mass, CdJ_2:Cu,Au – 0,4 % by mass, CdJ_2 – 0,15 % by mass). Their crystalline structures were monitored using an x-ray diffractometer.

Activation CdJ_2 with using by impurities allows considerably to increase the intensity, and to change the spectrum of their fluorescent glow. The presence of impurities causes the increasing concentration both their own complexes, and the generate own-impurity or pure- impurity defects. It is shown in the absorption spectra, especially in photoluminescence excitation spectra of crystals [4], [5]. Impurities of copper and gold in cadmium iodide crystals are photochromic (Fig. 1). On the one hand, they are increasing the intensity of luminescence of cadmium iodide, on the other hand they make material CdJ_2:Me more sensitive to the high-energy electromagnetic radiation. It depending on the dose of radiation causing varying degrees of reduction of the afterglow.

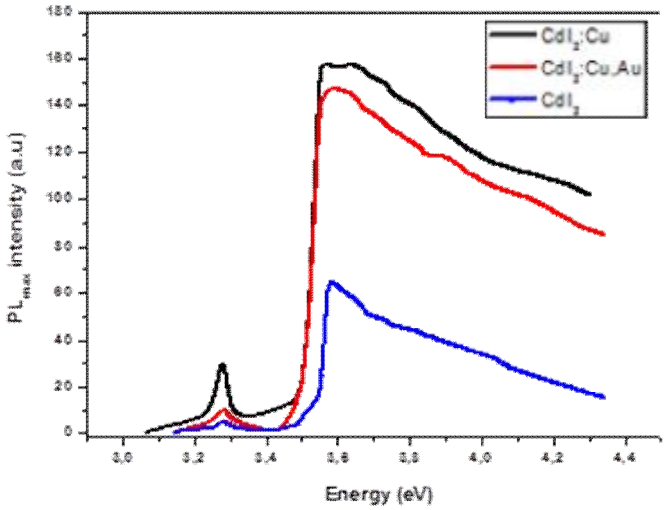

Fig 1. Excitation and luminescence spectra of cadmium iodide crystals doped by Cu and Au impurities.

It was shown that CdJ_2:Cu and CdJ_2:Au,Cu crystals are optically stable to the action of high electromagnetic radiation. Besides, this crystal has significant fluorescent yield and wide spectral range in luminosity as green-yellow and yellow region of the spectrum. The excitation of such crystals in selective absorption band at 3.23 eV at temperatures lower than 200 K causes also the donor-acceptor luminescence in the green and red spectral regions. Thus according to the time of afterglow the green luminescence can be attributed to the category of fluorescence, and the red luminescence can be attributed to the phosphorescence.

Abstract. The crystals CdJ_2 activated by gold and copper were investigated. It was shown that activation by gold and copper samples CdJ_2:Au,Cu are optically resistant to high-energy electromagnetic radiation. The behavior of the crystals with two activators confirms the hypothesis about recombination of nonequilibrium charge carriers which are created due to high-energetical irradiation, through donor-acceptor pair (DAP) defects.

1. Wide-layered crystals and their physical properties. Ed. A.B.Lyskovich. (Lviv, High School, 1982) 148 p. (In Russian)
2. M.S. Brodin, I.V. Blonsky. Exciton processes in layered crystals. (Kiev Sciences, Dumka, 1986) 256 p. (In Russian)
3. M. Rudka. Visnyk of Lviv Polytechnic National University. "Physics and mathematics science". - № 566, Vol. 97 (2006). (In Ukrainian)
4. M. Rudka, Lahotskyy T.V., Harambura S.B., Kravchuk I.M. ELEKTROinform. - № 3, Vol.12 (2009). (In Ukrainian)
5. M. Rudka Visnyk of Lviv Polytechnic National University. "Physics and mathematics science." – № 687, № 687, Vol. 181 (2010). (In Ukrainian)

Metal Induced Crystallization Mechanism of the Metal Catalyzed Growth OF Silicon Wire-Like Crystals

Sarikov A. V.

V. Lashkarev Institute of Semiconductor Physics NAS Ukraine, Kiev, Ukraine

The principle of the vapor-liquid-solid (VLS) growth of Si wire-like crystals is the formation of elongated Si crystals using catalytically active metals (such as Au, Al, Ti, Pt) upon the supply of Si containing species from the vapor phase. Variations of this process include the growth with solid metal catalysts (vapor-solid-solid process) and the growth on partly metal covered Si substrates without silicon rich vapor used (solid-liquid-solid process).

Up to now, no conclusive thermodynamic mechanism was proposed to explain the role of metal catalyst in the formation of crystalline Si wires. Traditional mechanisms relying on particular aggregate state of metal, increased sticking coefficient of Si to the metal as compared to that to the substrate, and preferential decomposition of Si containing species on the metal surface do not present a comprehensive picture each and thus cannot be considered general.

This work proposes a thermodynamic mechanism of the metal catalyzed growth of Si wire-like crystals featuring the mechanism of the metal induced crystallization of amorphous silicon. Si atoms incoming on the catalyst surface in any way are considered to form a disordered structure with higher chemical potential of Si atoms than in crystalline Si. Chemical potentials difference between the disordered and the crystalline Si states is the driving force for Si wire growth. Metal catalyst plays an important role to lower the energy barrier for the disordered state-to-crystal transformation, which is much higher for direct crystallization process (e. g. ~ 0.1 eV vs ~ 2.7 eV for amorphous Si).

Chemical potential difference between the disordered and the crystalline Si states, $\Delta\mu_{dc}=\mu_d-\mu_c>0$, is expressed in terms of equilibrium relative Si concentrations in metal in contact with disordered and crystalline Si (X_d and X_c):

$$X_d = X_c \times \exp\left(\Delta m_{dc} / RT\right) > X_c$$

This expression gives a clue how the driving force of the metal enhanced transformation of the disordered Si into the crystalline state is realized. Without crystallization Si would dissolve into the metal catalyst up to the relative concentration X_d corresponding to the equilibrium between the metal and the disordered Si. On the other hand, at Si concentrations above X_c metal catalyst becomes supersaturated with respect to crystalline Si. Supersaturation is released by the Si crystallization at the interface of metal catalyst with the Si wire-like crystal giving rise to its length. This process is qualitatively independent on the metal used, its aggregate state, and the way of Si deposition. It therefore accounts generally for the preferential growth of elongated Si wire-like crystals in the VLS and relative processes and may be also extended to the metal catalyzed wire-like crystal formation in other metal/semiconductor systems.

Effect of Microwave Action on Composite Materials

Shynkarenko V.V.

Lashkaryov Institute of Semiconductor Physics of NAS of Ukraine, Kiev, Ukraine

It is well known that after microwave action on material it starts heating and, as result, it changes it's physical properties. But what will be if microwave power will be not enough for heating such material? Every modern device contains microelectronic parts, which work at frequencies about 1-3 GHz. Cell phones emit such energy while working; computers, microcontrollers work at such frequencies and, as result, also emit electromagnetic waves in microwave range. In fact, any microelectronic device can be irradiated by itself during its work, so effect of such treatment must be investigated.

Previously we obtained results of characteristic improvement of metal-metal oxide-silicon (MOS) structures with thin (15-30 nm) oxide film [1] after low-power microwave action. But mechanism of such influence is still unknown. We tried to check its properties – do the changes continue after irradiation or stop after the influence. The microwave action changes defect structure or it may change chemical bonds.

Composite material TiB_2-C was choosen for such check. Usually it manufactured by sintering TiC and B_4C phases at temperature 800-1200^oC 8-12 hours by following endothermic reaction $2TiC+B_4C \rightarrow 2TiB_2+3C$. We created two samples with different phase ratio, one – with excess of TiC, another – with excess of B_4C. Technologically we sinter it under pressure to create composite structure at 1200^oC for the first 10 min. Next continuous sintering was changed into microwave treatment at frequency 2,45 GHz, power 1,5 W/cm^2 and time of exposition 3 s. Heating of samples has not exceeded 5 degrees, and we repeated treatment 5 times with delays about 20-30 s.

We created device for continuous measure of samples electrical resistance, and launched it after last microwave treatment. As will be shown on charts, time of relaxation, may continue up to 10-15 min. At least this period we continued registering changes of electric resistance.

Microhardness and phase ratio changes of material also were checked. In fact endothermic chemical reaction (which need in temperature 800^oC) had flown at room temperature and at liquid nitrogen temperature due to short low-power microwave treatment.

The obtained result can be interpreted as modern way to sinter crystal or composite material. But in fact, if we create any modern device with complex structure or even thin film structure we must check the influence of microwave action on it. Low power microwave irradiation may influence not only the intrinsic mechanical stress, but also the microstructure and chemical bonds in material. The changes in structure are strong enough to cause the relaxation of such material at least for few days.

1. E.D. Atanassova, A.E. Belyaev, R.V. Konakova, P.M. Lytvyn, V.V. Milenin, V.F. Mitin, V.V. Shynkarenko. Effect of active actions on the properties of semiconductor materials and structures. Kharkiv – 2007. – 216 p.

Point defects and Physicochemical Properties of Crystals of Pb-Sb (Bi)-Te systems

Turovska L.V.
Vasyl Stefanyk PreCarpathian National University, Ivano-Frankivsk, Ukraine

Lead Telluride crystals and solid solutions on basis of them are basic materials for making thermoelectric energy converters in medium-temperature region (500-750) K [1]. An important problem of thermoelectric material science is improvement of ZT, the value of which is crucial for estimation of expediency of practical use. Impurity introduction leads to increase of phonon dispersion and significant decrease of the lattice component of thermal conductivity, so it is one of the possible ways to improve the value of ZT.

In this paper within the crystal-quasichemical formalism defect subsystems of crystals of Pb-Bi (Sb)-Te systems have been analyzed. In doped crystals PbTe:Sb fraction of electrically active impurity atoms is significantly less than 1, and it evidences that dopants are distributed between the cationic and anionic sublattices [2]. Thus, in doped crystals PbTe:Sb dopant, replacing lead in its sublattice, ionizes from state $Sb^0(s^2p^3)$ into the state $Sb^{3+}(s^2p^0)+3e^-$ and relatively Pb^{2+} sublattice it is in the state Sb_{Pb}^{1+} (where it is a donor). In tellurium sublattice dopant ionizes $Sb^0(s^2p^3)\rightarrow Sb^{3-}(s^2p^6)+3h^+$ (where it is an acceptor) and relatively Te^{2-} sublattice dopant is in Sb_{Te}^{1-} state. This leads to the experimentally observed amphoteric effect of dopants of V group. Dependences of Hall concentration of point defects in PbTe:Sb crystals on the dopant content have been calculated. It has been shown that the dominant defects are antimony ions in lattice sites of lead telluride Sb_{Pb}^{1+}, Sb_{Te}^{1-}, doubly charged tellurium V_{Te}^{2+} and lead V_{Pb}^{2-} vacancies. Similar situation holds in PbTe:Bi crystals.

Based on the proposed crystal-quasichemical formulae it has been found that in PbTe-BiTe solid solutions replacement mechanism is realized with the predominance of concentration of dopant ions in the cation sublattices $[Bi_{Pb}^{1+}]$ and anionic vacancies $[V_{Te}^{2+}]$ in the case of n-PbTe-BiTe or cation vacancies $[V_{Pb}^{2-}]$ – in p-PbTe-BiTe. For PbTe-Sb_2Te_3 (Bi_2Te_3) solid solutions on basis of lead telluride along with impurity defects interstitial tellurium Te_i^0 (up to 3 mol. % Bi_2Te_3 and 2 mol. % Sb_2Te_3) or cation vacancies V_{Pb}^{2-} (at higher content of alloying compounds – to the limit of solubility) predominate.

1. Abrikosov N. Kh., Shelimova L. Ye. Semiconductor materials based on $A^{IV}B^{VI}$ compounds. – M.: Nauka, 1975. – 220 p.
2. Bytenskii L.N., Kaidanov V.I., Maksenko V.P., Melnik R.B., Nemov S.A. Self-compensation of the donor action of bismuth in lead telluride // Physics and Engineering of Semiconductors. – 1984. – V. 18, No. 3. – P. 489-492.

The work supported by project of MES of Ukraine (N 0107U006768)

Crystal-Chemical Mechanisms of Interections of Oxygen with Zinc Sulfide Crystals

Vadyuk M.P.

Vasyl Stephanyk Precarpathian National University, Ivano-Frankivsk, Ukraine

Zinc sulphide always contains oxygen. Polluting effects of the atmosphere, the ability of zinc sulfide oxidation and the need compensation distortions introduced its own defects and impurities have been promoted uncontrolled entry of oxygen in ZnS lattice. The main forms of oxygen in the presence of zinc sulfide (not isovalence doped impurities) are: solid solution of ZnS•O and allocation of ZnO:S. Talking about the interaction of oxygen with zinc chalcogenides, there are two crystal devices: Oxygen replacement of anion parts and rooting it in the interstices of the crystal lattice of the basic compounds.

Given that the dominant defects in n-ZnS (excess Zinc) are doubly charged zinc vacancies ($V_{Zn}^{//}$) and interstitial Zinc atoms ($Zn_i^{\S}, Zn_i^{\text{ФФ}}$), while Oxygen doping n-ZnS on the mechanism of substitution, the corresponding cluster will have the form: $V_{Zn}^{//}V_S^{\bullet\bullet} + \frac{1}{2}O_2 = V_{Zn}^{\times}O_S^{\times}$ and crystaloquasichemical formula is as follows: $\left(Zn_{Zn}^{\times}O_S^{\times}\right)_x \left(Zn_{(1-x)[(1-\alpha)+\alpha\gamma]-x}^{\times} V_{\alpha(1-\gamma)(1-x)+x}^{//}\right)_{Zn}$

$\left(S_{(1-\alpha)(1-x)}^{\times} V_{\alpha(1-x)}^{\bullet\bullet}\right)_S \left(Zn_{\alpha(1-\gamma)(1-\delta)(1-x)}^{\bullet} Zn_{\alpha(1-\gamma)(1-x)\delta}^{\bullet\bullet}\right)_i + \alpha(1+\gamma+\delta-\gamma\delta)(1-x)e' + 2xh^{\bullet}$.

The concentration of defects in this case would be: $\left[V_{Zn}^{"}\right]=A\alpha(1-\gamma)(1-x)+x$; $\left[V_S^{\bullet\bullet}\right]=A\alpha(1-x)$; $\left[Zn_i^{\bullet}\right]=A\alpha(1-\gamma)(1-\delta)(1-x)$; $\left[Zn_i^{\bullet\bullet}\right]=A\alpha(1-\gamma)(1-x)\delta$; $p=2Ax$; $n=A\alpha(1+\gamma+\delta-\gamma\delta)(1-x)$. Here α - deviation from the stoichiometric composition; γ - the proportion of Zinc atoms in the crystal lattice sites; δ - rate of disproportionation interstitial Zinc atoms; x - concentration of Oxygen; $Zn_{Zn}^{\times}$ - Zinc lattice sites; $V_S^{\bullet\bullet}$ - vacations doubly charged Sulfur; $e^{/}$ - electrons; "•", "/", "x", "0" - positive, negative, neutral and zero charges. $A=\frac{2Z}{a^3}$, Z = 4 - number of structural units in the unit cell, a^3 - the volume of the unit cell.

For p-ZnS (excess Sulfur) with predominant defects $V_{Zn}^{//}$, $V_{Zn}^{/}$ and $Zn_i^{\bullet\bullet}$ configuration of the cluster will aim as follows: $V_{Zn}^{//}V_S^{\cdot\cdot} + \frac{1}{2}S_2 \rightarrow V_{Zn}^{//}S_S^{\cdot\cdot}$, and the concentration of defects is equal to: $\left[V_{Zn}^{//}\right]=A(1-\mu)\left(\varepsilon(1-\beta)+\beta\right)$; $\left[V_{Zn}^{/}\right]=A\mu\left(\varepsilon(1-\beta)+\beta\right)$; $\left[Zn_i^{\bullet\bullet}\right]=A\varepsilon(1-\beta)$; $n=A\left(\varepsilon(2-2\beta+\mu-\mu\beta)+\mu\beta\right)$; $p=2A\left(\beta+\varepsilon-\beta\varepsilon\right)$, where β - deviation from stoichiometry; μ - coefficient of disproportionation Zinc vacancies; ε - partial Zinc sites in the crystal lattice.

The work supported by project of MES of Ukraine (N 0107U006768)

Influence of Coordinate Dependent Effective Mass to the States of Inhomogeneous Semiconductors

Voznyak O.M., Voznyak O.O.

Vasyl Stefanyk Prekarpatian National University, Ivano-Frankivsk, Ukraine

Quantum-mechanical systems with position-dependent mass play a key role in many physical problems. The most important cases are arising in physics of inhomogeneously doped semiconductors, semiconductor's heterostructures, quantum wells, super-lattices, and other. The practical availability of such systems encourages consideration of problems, where mass depends on the coordinates.

An important task of the theory of position-dependent mass is to find correct generalizations of the standard Hamiltonian, because coordinate-dependent mass no longer commutes with the momentum operator in the kinetic energy. For simplicity, in this paper we consider the one-dimensional case, where the wave function and mass depends on the coordinate x only.

Starting from the first principles, based on the requirement of Galilean invariance (see for example [1]), it was shown that the correct Hamiltonian can be obtained by writing it as a product of function $f(x) = 1/\sqrt{m(x)}$ and operator of momentum. Then, the Hamiltonian reads

$$\hat{H} = \frac{1}{2} f(x)\hat{p}\, f(x)\, f(x)\hat{p}\, f(x) + U(x), \qquad (1)$$

and such ordering of factors provides hermitian kinetic energy operator.

In [2] using the methods of elementary quantum mechanics and Hamiltonian (1), the behavior of particle with position-dependent mass in the case of a) finite potential barriers b) infinite potential barriers and c) Croning-Penny model has been studied. It was found that the behavior of transmission coefficient differs from the same coefficient in the case of constant mass.

In our work we use the factorization method based on the representation of Hamiltonian as a product of two operators, expressed through the momentum operator and so-called superpotential function. Varying the last one we can generate exact results for the ground state. Particularly, the regular periodic potentials have been studied when particle mass periodically depends on the coordinate x. In the case of regular and singular superpotential the exact solutions have been found and detailed analyses have been performed.

1. Levy-Leblond J. M., Elementary quantum models with positiondependent mass// Eur.J. Phys. – 1992. – v.13. – p.215.
2. Levy-Leblond J. M., Position-dependent effective mass and Galilean invariance //Phys. Rev.A. – 1995. – v.52. – p.1845.

The work supported by project of MES of Ukraine (N 0107U006768)

Synthesis and Magnetic Microstructure of Ultrafine Lithium Iron Phosphate

Al-Saedi Abdul Halek Zamil, Tadeush O. H.[2], Kotsyubynsky V.O.[1]

[1]Vasyl Stefanyk Precarpathian national university, Ivano-Frankivsk, Ukraine
[2]South-Ukrainian national pedagogical university named after K.D.Ushynsky, Odessa, Ukraine

Lithium iron phosphate $LiFePO_4$ is the most perspective cathode material for lithium-ion power sources nowadays. Its advantages in comparison with compounds of $LiMeO_2$type are the followings: - high discharge potential with presenceof horizontal region on discharge curve near 3.4 V vs Li / Li), high reversible specific capacity at about 200 mA·h / g), lower technology costs, safety for the environment in the production and utilization, thermal stability in the charged form. However, the successful commercial application of the material is constrained by relatively lower values of conductivity that causes a decline in discharge characteristics with the increasing of charge and discharge current. Perspective way for this problem solving is elaboration cathodes based on nanodispersed$LiFePO_4$, which will reduce the length of the electron and ion transport with the selection of the material morphology. In our research ultrafine $LiFePO_4$ was synthesized by the original multistep liquid phase method with using of low-cost precursors ($FePO_4 \cdot 7H_2O$, H_3PO_4, LiOH). Origin xerogel is amorphous (X-ray diffraction data); accordingly to the Mössbauer spectroscopy (Fig. 1) it contains Fe^{3+} ions (70%) and Fe^{2+} ions (30%). Thermal analysis of xerogels has demonstrated that processes of $LiFePO_4$crystallization were completed at 400°C. To prevent fromoxidation of Fe^{2+} material was obtained by the annealing in argon atmosphere. For increasing of ionic conductivity percolation component the presence of ions Fe^{3+} was formed by the synthesis conditions. The dominant doublet component of the Mössbauer specta with isomeric shift δ=1,20mm / s and quad-rupoles plitting Δ = 2,93 mm / sare evidence of the presence in the material after annealing at 390 and 500°C, the phase $LiFePO_4$. The second doublet component of the δ = 0,37 mm / s and Δ = 0,87 mm / s corresponds to Fe^{3+} in octahedral coordination in high spin state. Specific conductivity of the material obtained by annealing at 500°C is about 2300 Ohm·cm what is less than typical values about 10^4-10^5Ohm·cm.

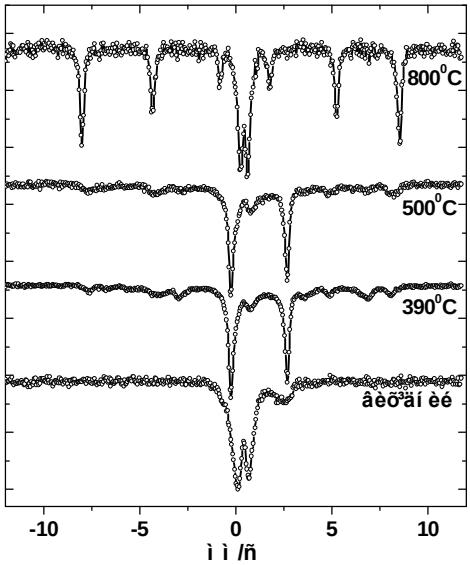

Fig.1

Structural Dependence of the Energy Distribution of Valence Fe (sd) – and O (p)-Electrons in Iron Oxide

Zaulychnyy Y.V.[1], Moklyak V.V.[2], Kotsyubynsky V.V.[3], Javorsky J.V.[1], Hrubyak A.B.[3]

[1]*National Technical University of Ukraine "Kyiv Polytechnic Institute", Kyiv, Ukraine*
[2]*G.V. Kurdyumov Institute for Metal Physics, N.A.S. Ukraine, Kyiv, Ukraine*
[3]*Vasyl Stefanyk Precarpathian national university, Ivano-Frankivsk, Ukraine*

The energy distribution of Fesd and Op electrons in mesoporous γ-Fe_2O_3 obtained by sol-gel method was investigated by X-ray emission spectroscopy. On the first stage of the synthesis iron citrate gel was obtained by mixing solutions of $Fe(NO_3)_3 \cdot 9H_2O$ and $H_2OC_6H_8O_7$ with next drying and annealing at the temperature 150°C. The aim of research was determination of precursors molar concentrations on the synthesized iron oxides electronic and magnetic properties. Three series were differ by molar concentration of precursors (0.1 M, 0.25 M and 0.5 M of the appropriate symbol series) in the case equal molar ratio between them was obtained. The method of low-temperature Mössbauer spectroscopy has showed that samples of all series are superparamagnetic (Fig. 1); for the 0.1 M sample at room temperature the presence of Fe^{2+} (20%) was fixed, in 0.25 M sample its content did not exceed 3%; for the sample 0.5 M spectrum consisted of doublet components formed by γ-rays scattering on Fe^{57} nuclei which are in an octahedral coordination in the particles whose size determine their superparamagnetic condition and relaxation component coursed by the presence of fractions with the particles size which are intermediate between superparamagnetic and magnetoordering states (particle size about 10-15 nm). According to a study by scanning electron microscopy material is dense xerogel. As it was revealed comparison OKα bands (Fig. 2) for the system 0.5 M narrowing was observed energy distribution Op-electrons in high-energy region due to their redistribution in the region of low energies. At the same time, for the system of 0.25 M, which is characterized by minimal particle size distribution narrowing occurs in the lower energy region of the spectrum and the energy position of these electrons increases as a result of the shift of OKα line to the high-energy region. The presence of Fe^{2+} in the surface layers of the material for the sample of 0.1 M is confirmed and Fesd-electron distribution in the short area narrowing was fixed.

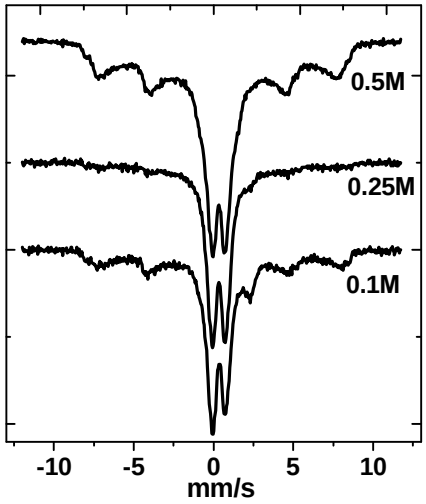

Fig.1

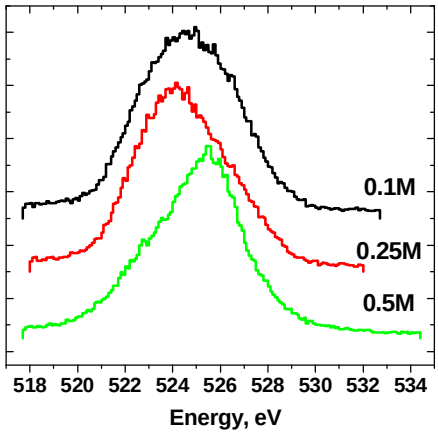

Fig.2

СЕКЦІЯ 5 (стендові доповіді)
ФУНКЦІОНАЛЬНІ КРИСТАЛІЧНІ МАТЕРІАЛИ: РІСТ, ФІЗИЧНІ ВЛАСТИВОСТІ, ВИКОРИСТАННЯ

21 травня 2013 р.

SESSION 5 (poster)
CRYSTAL'S GROWTH AND THEIR PHYSICAL PROPERTIES

May, 21, 2013

Peculiarity of the Growth Isotopically Enriched Single Crystals $Li_2B_4O_7$

Adamiv V.T.

Institute of Physical Optics, Lviv, Ukraine

The dosimetry and detection of neutrons is an important factor in the nuclear safety facilities. The solid-state neutron detector prepared from materials with high values of the interaction cross-section towards neutrons would be an optimal variant of neutron detector. The advantage of $Li_2B_4O_7$ borate is such that they can be obtained in the form of single crystals. The natural isotope distribution of the compounds $Li_2B_4O_7$ are ^6Li – 7.42 %; ^7Li - 92.58%; ^{10}B – 19%; ^{11}B – 81% and it is can directly to apply in the neutron detectors. This is ensured by their large thermal neutron absorption cross-section in nuclear reactions: $^6Li(n,\alpha)^3H$ (σ = 945 barn), $^{10}B(n,\alpha)^7Li$ (σ = 3840 barn).

The significant increasing of sensitivity to thermal neutrons has been fixed in isotopically enriched ^6Li and ^{10}B single crystals $Li_2B_4O_7$. Therefore, it is important to investigate the growth of the lithium borate crystals $Li_2B_4O_7$ enriched with isotopes ^{10}B or/and ^6Li.

The lithium carbonate (Li_2CO_3) and boric acid (H_3BO_3) of high purity enriched by corresponding isotopes (^6Li and ^{10}B to the level of 95% and 97.3 %, respectively) at heating decompose into oxides for synthesis of $Li_2B_4O_7$ borate. It is applieded the technique of multi-staged and multi-graded synthesis of Li_2B4O_7. The $Li_2B_4O_7$ compound isotopically enriched ^6Li and ^{10}B melts congruently (T_{melt} = 925^{o}C) that permits to grow its single crystals by Czochralsky technique. The growth has been performed from Pt-crucibles ∅40x40x2mm) on the single crystal [001] seed. Optimal growth parameters, obtained experimentally, were following: pulling rate 0.2 mm/h, and rotation rate of seed 10 rpm. Sustaining of necessary temperature gradient over the melt in process of single crystal growth (approximately 50^{o}C/cm) is very important, because, on the one hand, overheating of $Li_2B_4O_7$ melt quickly reduces viscosity at practically constant density, but it is not available for the next process of single crystal growth, because in overheated borate melt becomes apparent instability of [BO_4] – structural fragments that leads to formation of boron-oxygen complexes with larger number of [BO_3] – triangular fragments in the melt. And violation of structural balance between [BO_4] and [BO_3] fragments in the melt has an influence on stability of the growth conditions on the $Li_2B_4O_7$ crystallization front, because the inverse process of formation of tetraborate structural fragments (2[BO_4]+2[BO_3]), normal for the $Li_2B_4O_7$ crystal phase, in the melt is enough slow. Therefore, under precise control of all listed factors, there were obtained enriched ^6Li and ^{10}B $Li_2B_4O_7$ single crystals with sizes ∅20x30 of good quality.

TEGPAS a New Test System for Thermoelectric Generators

Ahiska R.[1], Freik D.[2], Nykyruy L.[2]

[1]*Gazi University, Faculty of Technology, Ankara, Turkey*
[2]*Vasyl Stefanyk Precarpathian National University, Ivano-Frankivsk, Ukraine*

Today, the studies of energy production from renewable energy sources such as wind, solar, biomass, hydro, geothermal and hydrogen continues rapidly. Thermoelectric generators (TEGs) are used to convert geothermal energy, which is one of the renewable energy sources available, into electrical energy. In this study, a new test measurement system and supervisory control and data acquisition application with programmable logic controller has been carried out to be enable the collection of the data of thermoelectric generator for the usage of thermoelectric modules as thermoelectric generator.

The electrical equivalent circuit of the TEG consists of an ideal voltage source V and an internal resistance R_{in}. It is similar to the equivalent circuit of a battery. When a temperature difference between surfaces of TEG occurs, a direct voltage (DC) across the TEG is achieved. If a load resistor R_L is connected across the TEG, the electric current passes through the load resistor and an electric power is obtained from the TEG. If the temperature difference between the surfaces of the TEG is increased, the electric power obtained from the TEG increases. The maximum power output obtained from the TEG is obtained when the internal resistor R_{in} value of the TEG equals that of the load resistor R_L. From the standpoint of TEG applications, it is highly desirable to maximize power output [1]. A hot-cold water circulator system has been established to carry out of thermoelectric generator experiments in the laboratory. During the production of the electric energy from the thermoelectric generator, the temperatures of the surfaces of the thermoelectric generator, current-voltage values obtained from output of the thermoelectric generator, hot and cold flows have been measured by the system instantly. All these data have been monitored continuously from the computer (MicroWin program) and recorded by a supervisory control and data acquisition program (PC SCADA program). At the same time, in environments where there was no computer, an operator panel with the ability to communicate with the programmable logic controller has been used for the monitoring of the instant thermoelectric generator data. The setup test measurement system has been implemented on the thermoelectric generator system with about 10W.

This study is supported by the Ankara Chamber Of Industry 1. Industrial District Office as Thermoelectric technology development project in Turkey.

1. R. Ahiska, S. Dislitas, Computer controlled test system for measuring the parameters of the real thermoelectric module, Energy Conversion and Management 52 (2011) 27-36.

Synthesis and Crystal Growth Compounds of Systems Pb-Sb(Bi)-Te and Sn-Sb(Bi)-Te

Arsenyuk I.O., Lyuba T.S., Kryskov Ts.A.

Ivan Ohienko Kamyanets-Podilsky National University, Kamyanets-Podilsky, Ukraine

The semiconductor compounds of systems Pb-Sb (Bi)-Te and Sn-Sb (Bi)-Te is the basic materials for thermoelectric converters of thermal energy into electric power that operate in the temperature range (500-800)K, photodetectors and emitting structures in infrared range of the optical spectrum.

Optimization of the thermoelectric parameters of PbTe and SnTe is needed for reducing the concentration of charge carriers by changing the lattice defects. This can be realized with doping impurities or appropriate cationic substitution in solid solutions. Thus we achieve the growth of thermoelectric coefficient, electrical conductivity with little change in thermal conductivity [1-2].

Synthesis of compounds of systems Pb-Sb(Bi)-Te and Sn-Sb(Bi)-Te conducted in vacuumed to a residual pressure of 10^{-4} Pa quartz ampoules, which were placed in a two-zone furnaces. We used the technologically pure components that were previously optional cleaning methods for improving the uniformity. Weighing of substances was performed on an analytical balance up to 0,0005 mg. Ampoules were heated for removing substances from the internal walls without changing the temperature of the filling substance, during vacuumation. Vacuumed ampoules were placed in two-zone electric furnace that can make forced oscillations. This device is designed to improve homogeneity of semiconductor compounds during their synthesis.

The growing of crystals was carried out in a vertical electric furnace by the method of Bridgman-Stockbarger. A narrow region of high temperature is situated in the middle part, which allows moving the ampoule as up and down. The synthesized compound was placed in quartz ampoules, which were at the bottom of the capillary transition to increase the likelihood of the emergence of a crystal.

The research of thermoelectric samples from all parts of the ingot showed results that show sufficient homogeneity of samples, increasing the percentage of the output material and the perspectives of the technological process of getting material to create devices of thermoelectricity, optoelectronics and infrared technology.

The work supported by an integrated project of MES of Ukraine (N 0113U000185) and by projects of NAS of Ukraine (N 0110U006281)

Study of Kinetic Dependencies of Conversion Process of Natural Surfaces Langbein with Sodium Sulfate and Potassium Chloride in Shenity

Artus M.I., Kostiv I. Yu.

Vasyl Stefanyk PreCarpathion National University, Ivano-Frankivsk, Ukraine

Reaction of Langbein with sodium sulfate or it's minerals occurs have been spend with the presence of moisture on the surface Langbein crystals with formed shenity by the equation:

$$K_2SO_4 \cdot 2MgSO_4 + Na_2SO_4 \cdot 10H_2O + 2KCl + 2H_2O \rightarrow 2[K_2SO_4 \cdot MgSO_4 \cdot 6H_2O] + 2NaCl \quad (1)$$

Surface moisture is reactionary environment. Ions from the surface of crystal salts and potassium chloride have been diffused into thought-crystal liquid phase, reacted with ions from the surface of the crystals Langbein with formation and crystallization of the solid phase shenity. Shenity have been stand on solid surface grains of Langbein. Crystals shenity that created in the reaction conversion Langbein on the surface and in the bulk solution, differ among themselves, which is typical for top chemical reactions. The degree of conversion of sodium sulfate Langbein and potassium chloride in shenity increases throughout the period of study, with the most intense in the first 5 days. The highest degree of conversion is achieved at a temperature of 30-50 ^{0}C.According to experimental results rate constant, reaction order, activation energy and defined area of the flow process have been calculated.

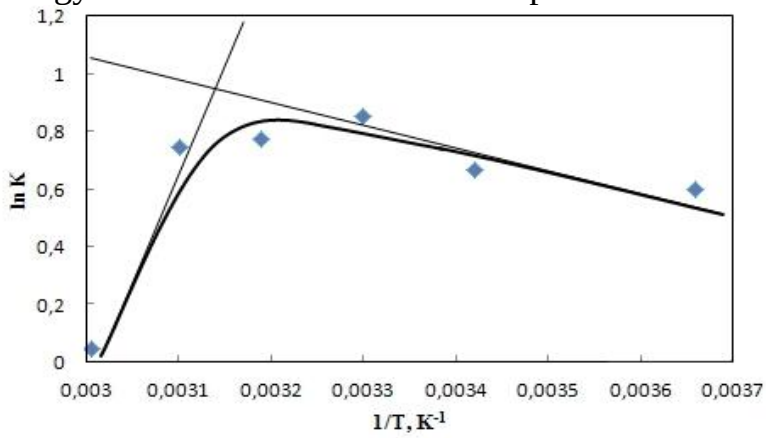

Pic. 1. The dependence of the logarithm of the reaction rate constant conversion of langbein from inverse tempe-rature 1 / T.

This dependence is not linear, but has the bend, which is divided into two temperature ranges. In Figure 1 identified the optimum temperature at which the reaction occurs with the highest conversion rate equal to 319 K (46 °C). The line equation can determine the activation energy for two temperature intervals. The value of the activation energy for the temperature range 273 ... 303 K is 28.5 kJ / mole for the temperature range 313 ... 333K is 22.52 kJ / mole.

Thus, the conversion process takes place in the diffusion close to the transition region. In the water Langbein is dissolved in the kinetic region where limiting is a chemical reaction with water molecules Langbein. Disqualification of the reaction products from the surface does not limit the process. In this case, the reaction rate is accelerated reaction product - sodium chloride. In the wet mixture slowest process is the moving ions to the surface Langbein. It becomes noticeable effect which have been limited the diffusion of ions in semi-dry mass.

Chemical Bond and Technology Peculiarities of Fe, Se, Te Based Materials

Ashcheulov A.A.[1], Manyk O.M.[1], Manyk T.O.[2], Bilynskyj-Slotylo V.R.[1]

[1]*Yuriy Fedkovych Chernivtsi National University, Chernivtsi, Ukraine*
[2]*Bukovyna State University of Finance and Economics, Chernivtsi, Ukraine*

The choice Fe, Se, Te, compounds FeSe, FeTe and based on them solid solutions as the object of the study conditioned by the fact that it is prospective semiconductor materials for new generation of optical, photoelectric, magnetic, and other electronics devices [1]. Therefore was tasked to detailed study and complex mathematical models constructing that describe dynamics of the chemical bonds formation Fe, Se, Te based crystals using methods of the theory of oscillations, the microscopic theory of crystal lattice and solving of inverse problems of elasticity theory [2].

Force and energy characteristics of chemical bond of Fe, Se, Te, FeSe, FeTe crystal and based on them solid solutions are investigated. Their numeric values for the separate constituting of chemical bonds FeSe and FeTe crystals given in table.

Force and energy characteristics of FeSe and FeTe

Parameter \ ℓ		1	2	3	4	5
FeSe	$f^{(\ell)}$, N/m	-51.3	-548.8	-168	-57.1	43.3
	$\omega_\ell \cdot 10^{13}$, Hz	16.14	15.79	8.34	8.86	8.16
	T_ℓ, K	1348	1292.4	360.6	406.9	345.2
FeTe	$f^{(\ell)}$, N/m	-44.7	-372.4	-92.6	-201.9	38.2
	$\omega_\ell \cdot 10^{13}$, Hz	12.84	12.15	10.52	6.18	5.31
	T_ℓ, K	1187	1061.6	796.1	275.1	202.6

The fine structure of the chemical bond and the cause of its formation are found. Shown that the presence of fine structure causes the formation of successive polymorphic transitions in the components themselves and their compounds. In this case, each of the polymorphic states characterized by its own set of physical and chemical properties. Discovery of this regularity can significantly extend the existing technological possibilities and suggest new approaches to the preparation of micro-and nanotechnology [3].

1. Ashcheulov A.A., Manyk O.M., Manyk T.O., Savchuk A.I., Bilynskyj-Slotylo V.R. Peculiarities of the chemical bond of FeSe and FeTe // Physics and Chemistry of Solid State. – 2012. – Vol. **13**, №1. – P. 136-141.
2. Manyk O.M. Bagatofaktornyj pidhid v teoretychnomu materialoznavstvi. – Chernivtsi: Prut, 1999. – 432 s.
3. Patent 67792, Ukraine. Process for producing of monocrystalline ingots of FeSe, FeTe and solid solutions of FeSexTe1-x / Ashcheulov A.A., Manyk O.M., Manyk T.O., Bilynskyj-Slotylo V.R., Savchuk A.I. – 2012. Bul.№5.3.

New Non-Stoichiometric Phases in Systems Tlbr-Tli-$Tl_2Se(Tl_2Te)$

Babanly D.M.

Institute of Chemical Problems of NAS of Azerbaijan, Baku

Chalcogen-halides of heavy *p* elements possess high-performance semiconductor properties making them perspective matrices for the creation of various types of new functional materials

Systems TlHal-Tl_2X (X-Se, Te; Hal-Br, I) are characterized by formation of ternary compounds of type Tl_5X_2Hal, crystallized in tetragonal structure such as Tl_5Te_3 (space group I4/mcm). Selenid-halides melt congruently at 745 and 720K, and telurid-halides - with decomposition on synthectic reaction at 750 and 775 K.

In this work the systems TlBr-TlI-Tl_2Se (A) and TlBr-TlI-Tl_2Te (B) are investigated using methods DTA and XRD as well as measurement EMF of concentration chains concerning a thallium electrode at 300-430 K temperature interval.

Alloys of systems (A) and (B) are received by melting preliminary synthesized and identified initial compounds in quartz ampoules under vacuum ($\sim 10^{-2}$Pa) with the subsequent homogenized annealing at 600K for 800h.

Some polythermal and isothermal sections and also projections of liquidus surfaces of systems (A) and (B) are constructed. It is established, that both systems are quasi-ternary planes of corresponding quaternary systems.

The system (A) consists of two subsystems Tl_2Se-Tl_5Se_2Br-Tl_5Se_2I and TlBr-TlI-Tl_5Se_2I-Tl_5Se_2Br, differentiated by quasi-binary section Tl_5Se_2I-Tl_5Se_2Br. The first subsystem is characterized by unlimited mutual solubility of components in solid state. Solid solutions on the base a selenohalides (δ-phase) have Tl_5Te_3 type tetragonal structure which are morfotropically transfer to the structure with less-symmetry such as Tl_2Se (space group P4/ncc). The second subsystem has more difficult character of phase equilibriums. In subsolidus it consists of heterogeneous areas β+δ, Tl_6SeI_4+δ, Tl_6SeI_4+β and Tl_6SeI_4+β+δ (β-solid solutions of boundary system TlBr-TlI).

There are not quasi-binary sections in the system (B). The section Tl_5Te_2Br-Tl_5Te_2I is stable in subsolidus and characterized by formation of continuous solid solutions (δ-phase) in Tl_5Te_3 structure. The homogeneity field of the δ-phase penetrates deep into the Tl_2Te–Tl_5Te_2Br–Tl_5Te_2I subsystem, occupying its large part.

On the base on phase diagrams and their isothermal sections methods to grow monocrystals with given composition are selected.

Structure and Secondary Phases Diagnostics of $Cu_2ZnSnSe_4$ by Means of Vibrational Raman Spectroscopy

Babichuk I.S.[1], Valakh M.Ya.[1], Dzhagan V.M.[1], Yukhymchuk V.O.[1], Maximo L.[2], Caballero R.[2], Liamas E.G.[3], Gurieva G.[3], Schorr S.[3,4]

[1]*V.E. Lashkaryov Institute of Semiconductor Physics of National Academy of Sciences of Ukraine, Kyiv, Ukraine*
[2]*Universidad Autónoma de Madrid, Madrid, Spain*
[3]*Helmholtz-Zentrum Berlin für Materialien und Energie, Berlin, Germany*
[4]*Freie Universität Berlin, Institute of Geological Sciences, Berlin, Germany*

$Cu_2ZnSnS(e)_4$ is a promising material for thin film solar cells due to suitable direct optical gap of about 1.5 eV and large band-to-band optical absorption coefficient (~10^5 cm^{-1}) [1]. In contrast to better studied CdTe and $Cu_2In(Ga)S(Se)_2$ materials, all constituents of CZTS are non-toxic and abundant in the earth crust. During the last decade the conversion efficiency of CZTS-based solar cells has been improved significantly and values over 11% have been reported recently [1]. However, compared to binary II-VI to ternary I-III-VI, for quaternary chalcogenide materials much more serious problems arise such as competing types of crystalline structure, non-stoichiometry, presence of secondary phases of binary and ternary compounds, point defects and their complexes, etc [1,2]. Raman scattering appears to be one of informative methods, complementary to X-ray diffraction methods, in establishing the structure of $Cu_2ZnSnS(e)_4$ [3].

The aim of this work was to determine the type of crystalline structure, composition homogeneity and identification of possible secondary phases in $Cu_2ZnSnSe_4$ (CZTSe) films formed on glass substrate covered with a thin layer of molibdenium.

The structural properties of films were investigated by X-ray diffraction and Raman spectroscopy . For excitation of Raman spectra the 514.5 nm wavelength of Ar^+-laser was used. The laser power was adjusted for the power density on the sample surface to be low enough to avoid affecting the structure of the film in the process of measuring Raman spectra. The structural characterization of the films by X-ray diffraction was carried out in grazing incidence geometry (GIXRD) using a PANalytical X'pert Pro MPD diffractometer with Cu-Kα -radiation (λ=1.54056 Å). The incident angle was chosen as 2^o, a collection time of 17s/step and a step size of 0.02^o was applied. All measurements were performed at room temperature.

CZTSe thin films were deposited by flash evaporation onto Mo coated glass substrates using ZnSe, CuSe and SnSe binary compounds in powder form at a nominal substrate temperature (T_{sub}) of 100°C or 350°C.

Analysis of experimental XRD data and modeling of corresponding diffraction patterns was performed using PowderCell software. Based on the experimental data and appropriate structural model calculation of the relative

intensity of the reflections was calculated and the parameters of the elemental cell refined (Table 1), using the Rietveld method and FullProf software [5]. The pseudo Voight profile was used for approximation of experimental reflexes. The obtained lattice parameters allow to conclude that the CZTSe thin films formed have structure of kesterite ($I\bar{4}$-symmetry) [1].

Table 1. Lattice parameters of $Cu_2ZnSnSe_4$ thin films.

sample	film thickness, nm	a (Å)	c (Å)	c/2a	Reference
F1D	190	5,6894	11,3358	0,9962	1
F2D	350	5,6771	11,2682	0,9924	1, 4
F3D	440	5,6728	11,2503	0,9916	4

The results of Raman study of $Cu_2ZnSnSe_4$ thin films is in a good agreement with X-ray data. But the samples with dominant content of kesterite phase have been distinguished from those being a mixture of kesterite with a minor content of stannite structure. The Raman results give evidence that the most important influence on quality of CZTSe structure has the conditions of their post-growing annealing. The possible presence of secondary phases of ternary compounds such as Cu_2SnSe_3 was inferred from the Raman spectra.

1. Siebentritt S. Kesterites - a challenging material for solar cells / S. Siebentritt, S. Schorr // Prog. Photovoltaics Res. Appl. – 2012. – v.20. – p. 512.
2. Amiri N.B.M. Secondary phase Cu_2SnSe_3 vs. kesterite $Cu_2ZnSnSe_4$: Similarities and differences in lattice vibration modes / N.B.M. Amiri and A. Postnikov // J. Appl. Phys. – 2012. – v.112. – p. 033719.
3. Fontane X. Vibrational properties of stannite and kesterite type compounds: Raman scattering analysis of $Cu_2(Fe,Zn)SnS_4$ / X. Fontane, V. Izquierdo-Rosa, E. Saucedo, S. Sohorr, V.O. Yukhymchuk, M.Ya. Valakh, A. Perez-Rodriguez, J.R. Morante // Journal Alloys and Compounds. – 2012. – v.539. – p. 190.
4. Olekseyuk I.D. Single crystal preparation and crystal structure of the Cu2Zn/Cd,Hg/SnSe4 compounds / I.D. Olekseyuk, L.D. Gulay, I.V. Dydchak, L.V. Piskach, O.V. Parasyuk, O.V. Marchuk // Journal of Alloys and Compounds. – 2012. –v.340. – p. 141.
5. Juan Rodriguez-Carvajal and Thierry Roisnel, www.ill.eu/sites/fullprof/.

Effect of Heating Rate on the Oxidation Process of Nanocrystalline ZnS: Mn Obtained by SHS

Bacherikov Yu.Yu.[1], Zhuk A.G.[1], Kravchenko S.A.[1], Okhrimenko O. B.[1], Kardashov K.D.[2]

[1]V. Lashkaryov Institute of Semiconductor Physics, NAS of Ukraine, Kyiv, Ukraine;
[2]Odessa National Maritime Academy, Odessa, Ukraine

High emittance and wide band gap of zinc sulfide determine trends of its wide using in new generation optoelectronic devices. In addition, the main properties of ZnS concerning a series of parameters are well studied to date and that allows obtaining more reliable data for investigations of effects of the technological production and post-technological processing features on ZnS properties.

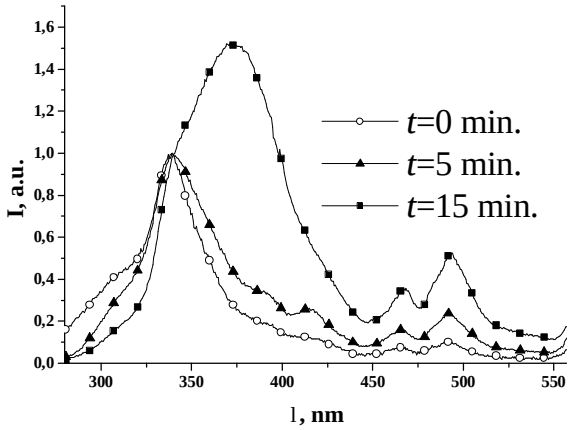

In this work the luminescence properties of ZnS: Mn obtained by self-propagating high temperature synthesis method (SHS) and annealed at T = 350°C for 7 hours with heating interval of 5 and 15 minutes were studied.

PL spectra were recorded on a SDL-2 equipment at T = 300°K with photoluminescence excitation by a Xe-lamp radiation.

6. Strong band caused by presence of oxygen and ZnO-phase in ZnS was shown by results obtained from PLE spectra (see fig.) to be present when the sample was heated during 15 min as distinct from the case of the heating during 5 min. This fact can be explained as follows. In slow heating physical adsorption of oxygen occurs on ZnS surface and oxygen molecule had sufficient time and energy for transition to chemical absorption state to form ZnO-phase. Increase the rate of heating allowed oxygen to adsorb on surface by physical adsorption like as in slow heating. However, fast heating of ZnS results in that oxygen gains sufficient energy to leave the surface for a time less than it is necessary for chemical absorption. Therefore oxidation processes on ZnS-surface occur in different ways at different intervals of heating.

Electronic Structure of Non-Centrosymmetric $AgCd_2GaS_4$ and $AgCd_2GaSe_4$ Single Crystals

Bekenev V.L.[1], Bozhko V.V.[2], Parasyuk O.V.[2], Davydyuk G.E.[2], Tretyak A.P.[2] Bulatetska L.V.[2], Fedorchuk A.O.[3], Kityk I.V.[2,4], Khyzhun O.Y.[1]

[1]*Institute for Problems of Materials Science, National Academy of Sciences of Ukraine, Kyiv, Ukraine*
[2]*Eastern European National University, Lutsk , Ukraine*
[3]*Lviv National University of Veterinary Medicine and Biotechnologies, Lviv, Ukraine*
[4]*Czestochowa University Technology, Czestochowa, Poland*

A quaternary compounds with the $AgCd_2GaS_4$ and $AgCd_2GaSe_4$ were synthesized at study of the quasibinary $AgGaS_2$-CdS and $AgGaSe_2$-CdSe systems [1,2]. The both compounds are n-type semiconductors with the width of energy gap, E_g, of 2.15 eV and 1.7 eV at about 300 K in the case of $AgCd_2GaS_4$ and $AgCd_2GaSe_4$, respectively [2,3].

X-ray photoelectron core-level and valence-band spectra for pristine and Ar^+-ion irradiated (001) surfaces of $AgCd_2GaS_4$ and $AgCd_2GaSe_4$ single crystals grown, respectively, by the Bridgman method and the method of direct crystallization have been measured in the present work. The X-ray photoelectron spectroscopy (XPS) results reveal high chemical stability of (001) surfaces of $AgCd_2GaS_4$ and $AgCd_2GaSe_4$ single crystals. Electronic structure of $AgCd_2GaS_4$ has been calculated employing the full potential linearized augmented plane wave method. For the $AgCd_2GaS_4$ compound, the X-ray emission bands representing the energy distribution of the valence Ag d-, Cd d-, Ga p- and S p-like states were recorded and compared on a common energy scale with the XPS valence-band spectrum. The theoretical and experimental data regarding the occupation of the valence band of $AgCd_2GaS_4$ were found to be in excellent agreement to each other. Second harmonic generation (SHG) efficiency of $AgCd_2GaS_4$ by using the 320 ns CO laser at 5.5 μm has been recorded within the temperature range 80–300 K.

1. Chykhriy S. Y., Parasyuk O. V., Halka V. O. Crystal structure of the new quaternary phase $AgCd_2GaS_4$ and phase diagram of the quasi-binary system $AgGaS_2$-CdS // J. Alloys Compd. 2000, V. 321, № 1–2, P. 189–195.
2. Growth and properties of the single $AgCd_2GaSe_4$ crystals / V.V. Bozhko, G.Ye.Davydyuk, L. V. Bulatetska, O. V. Parasyuk, A. P. Tretyak, N. Vainorius, V. Kažukauskas // Journal of Crystal Growth. – 2011. – Vol. 330, № 1. – P. 5–8.
3. Optical and Photoelectrical Properties Of $AgCd_2GaS_4$ Single-Crystal Compounds / L. V. Bulatetskaya, V. V. Bozhko, G. E. Davidyuk, O. V. Parasyuk // Fizika i Tekhnika Poluprovodnikov. – 2008. – Vol. 42, № 5. – C. 522–527.

Electrochemical methods for producing of highdispersive systems of semiconductor materials

Boruk S.D., Dremlyuzhenko S.G., Dremlyuzhenko X.S., Kapusch O.A., Yuriychuk I.M.

Yuriy Fedkovych Chernivtsi National University, Chernivtsi, Ukraine

Wide range of obtaining low-dimensional semiconductor systems is developed in present time [1]. All methods of synthesis of highdispersive and nanocrystalline semiconductor materials must meet certain criteria set, namely:

1. Nonequilibrium, which allows to gain a spontaneous nucleation and prevent the growth and aggregation of nanoparticles, which are formed.
2. High chemical homogeneity of obtained nanomaterial.
3. Monodispersity of the particles, which are formed.

Formation of nanocrystalline semiconductor has its own peculiarities. The conditions under which the process of synthesis or dispersing of compact coarse particles takes place play a significant role and determine the mechanism of their formation. However, mechanical dispersion for obtaining of nanoparticles is not enough widespread due to very high energy cost. The most effective methods are mechanochemical processes based on mechanical activation of solid-phase reactions during grinding. The average particle size of semiconductor material, which are obtained by mechanical grinding varies from 5 to 200 nm, depending on the melting point of the material and grinding time. Varying conditions of the process, one can get the desired particle size. However, the size distribution of particles obtained by mechanical grinding, is often quite wide [1, 2].

This causes the search of efficient way for dispersion of raw materials. Promising area is destruction of the crystals under the influence of a voltaic arc. We have obtained cadmium, tellurium and cadmium telluride highdispersive systems by an action of a voltaic arc in a solution of thioglycolic acid. Metallic cadmium and tellurium in various combinations are used as electrodes. Spectral studies of obtained systems have confirmed the formation of colloidal systems in tellurium (K) - cadmium (A), cadmium (K) - Te (A), tellurium (K) - Te (A) systems. Stability of the systems is 12-14 days.

1. Triboulet R. Fundamentals of the CdTe Sysnthesis / R Triboulet // J. Alloys Compd. – 2004. – Vol. 371, № 1-2. – P. 67-71.
2. Gusev A.I. Nanomaterials, nanostructures, and nanotechnology. 2-nd edition, revised and expanded /A.I.Gusev. – Moscow:Nauka-Fizmatlit, 2007. – 416 p.

Electrical, optical and photoelectrical properties of $Cd_{1-x}Zn_xTe$ (x=0,04) single crystals

Bozhko V.V., Novosad O.V., Gerasymyk O.R., Kozer V.R.

Lesya Ukrainka Eastern European National University, Lutsk, Ukraine

Electrical, optical and photoelectrical properties of p-type single crystals $Cd_{1-x}Zn_xTe$ grown by Bridgman method under Cd and Zn vapour pressure have been investigated. The resistivity of single crystals at T≈300 K is $\rho \approx 10^6$-10^7 Ohm·cm, the thermoelectric power factor - $\alpha \approx 700$ μV/K. According to studies of the magnetoresistance concentration ($p \approx 10^9$-10^{10} cm^{-3}) and mobility of holes ($\mu \approx 100$ cm^2/V) have been estimated. In a broad field interval (B≈0–0,7 Tl), the relative variation of the magnetoresistance is described well by the square-law dependence [1]

$$\frac{\Delta\rho}{\rho_0} = \mu^2 B^2 (C - A^2). \qquad (1)$$

In order to put the experimental results in agreement with formula (1), we took $C\text{-}A^2 \approx 6$, which is close to the characteristic value obtained at the holes scattering by ionized impurities [1].

On the position of the edge of intrinsic optical transitions, which is well described by the Urbach rule [2], the optical width of the forbidden zone of the compound was evaluated ($E_{g0} \approx 1{,}53$ eV at T≈300 K).

Single crystals $Cd_{1-x}Zn_xTe$ studied by us turned out to be photosensitive. The characteristic feature of photoconductivity of specimens is a well degenerate maximum which is probably associated with the intrinsic photoconductivity. The energy gap width in the single crystals at T≈300 K evaluated from the photoconductivity maximum located at $\lambda_m \approx 800$ nm agrees well with the optical, $E_{g0} \approx 1{,}53$ eV, widths obtained at the same temperature.

The temperature dependence of the electric conductivity for single crystals $Cd_{1-x}Zn_xTe$ has activation character and is described by the exponential dependence

$$\sigma = \sigma_0 e^{-\frac{E_A}{kT}} \qquad (2)$$

at high temperatures from room one to T≤700 K. The activation energy E_{A1} for the electric conductivity in region T>550 K determined from Eq. (2) is equal to $E_{A1} \approx 0{,}62$ eV. In low-temperature section T~300-400 K, the activation energy of electric conductivity equals $E_{A2} \approx 0{,}41$ eV.

1. P.S. Kireev, Semiconductor Physics (Mir Publishers, Moscow, 1978).
2. V.L. Bonch-Bruevich, R. Enderlein, B. Esser, R. Keiper, A.G. Mironov, and I.P. Zvyagin, Elektronentheorie Ungeordneter Halbleiter (Deutscher Verlag der Wissenschaften, Berlin, 1984).

Study the Dynamic of Excitons in the Layered PbI_2 Nanoclusters

Bukivskii A.P., Gnatenko Yu.P., Skubenko P.A.

Institute of Physics of NAS of Ukraine, Kyiv, Ukraine

At present there are a number of works devoted to the synthesis of the lead iodide nanocrystals (NCs) and study of their optical properties. This semiconductor crystal is a very promising high-sensitive noncooled radiation detector material for X- and γ-rays suitable for biomedical and industrial imaging applications. PbI_2 is a layered direct semiconductor with a repeating unit of a hexagonally closed-packed layer of lead ions sandwiched between two layers of iodide ions. Recently [1] we observed the formation of PbI_2 nanoclusters (NCLs) which are naturally formed in $Pb_{1-X}Cd_XI_2$ alloys as a result of non-isoelectronic substitution at cation sites. The layered structure of these alloys facilitates formation of quantum-confined nanostructure. Thus, these alloys present a three-dimensional semiconductor material with randomly distributed NCLs.

The aim of this work is thus to study the dynamics of excitons in the layered PbI_2 NCLs that may help determine the nature of the intense photo- and radioluminescence spectra of these crystals at room temperature. For this purpose we have performed time-resolved photoluminescence (PL) spectra measurements as well as measurement of the radioluminescence spectra for these crystals. It should be noted that earlier the time-resolved PL measurements for layered semiconductor NCLs have not been carried out.

The obtained results have been explained using the model of self-trapped excitons (STE) on Pb – I bonds at the nanocrystal surface which are formed as a result of the thermal activation or the quantum tunneling of the delocalized excitons through the barrier at room and liquid helium temperatures, respectively. The processes are rapid and occur on subnanosecond and nanosecond time scale and their rate depends on the NCLs sizes. It was shown that the investigated materials have very intense room-temperature PL and radioluminescence due to the existence of disclike PbI_2 NCLs with average lateral size about 2.5 nm and the height of two layers. Therefore, for these NCLs there exist many surface Pb – I bonds where the STEs are formed. The further increase of the emission intensity of such scintillator materials is possible by optimizing the size distribution of NCLs in the $Pb_{1-X}Cd_XI_2$ alloys and by means of thermoelectric cooling. The cooling of the NCLs allows us to decrease the nonradiative recombination from STE states into the ground state by tunneling through the barrier. Thus, the $Pb_{1-X}Cd_XI_2$ alloys can be considered as new scintillator materials, where the radioluminescence is determined by the emission of STEs in the layered semiconductor NCLs, and can be named bulk-nanostructured scintillators (or nanoscintillators).

Switching effect in solid electrochemical cells on the basis of Ag_8SnSe_6 argyrodites

Chekaylo M.V., Ilchuk G.A., Ukrainets N.A., Danylov A.B., Ukrainets V.O.

Lviv Polytechnic National University. Lviv, Ukraine

The subject of our research was volt-ampere characteristics (VAC) of solid electrochemical cells (SEC) $Ag/Ag_8SnSe_6/Ag$ with symmetrical non-turn-off Ag electrodes under the condition of circuit limitation of current (fig. 1). We manufactured SEC on the samples of Ag_8SnSe_6 argyrodite monocrystals. It was determined that the basic property of stationary VAC for $Ag/Ag_8SnSe_6/Ag$ SEC (fig.1) is the presence of two essentially different resistance states caused by ionic type of Ag_8SnSe_6 conductivity. The high resistance state $r = 4 \cdot 10^5 \Omega$ with current $I \approx 10^{-5}$ A is observed for $Ag/Ag_8SnSe_6/Ag$ SEC in the range of negative voltage $U = -4 \div 0$ V. When voltage increases from 0 V to 3 V current increases steadily but with sharp current oscillations and for $U = 4{,}5$ V current increases with "jump" from 10^{-5} A to 10^{-4} A.

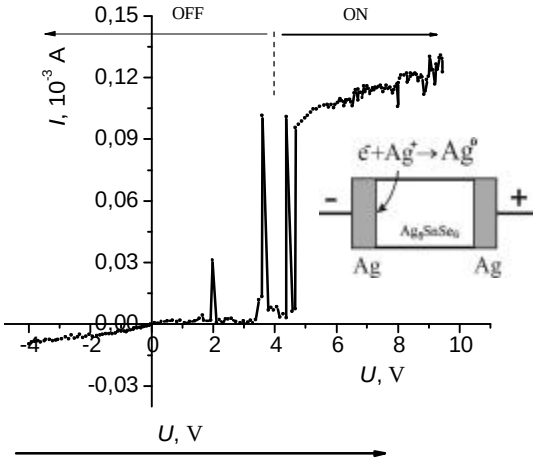

Fig. 1 Stationary VAC for $Ag/Ag_8SnSe_6/Ag$ SEC on the basis of monocrystal Ag_8SnSe_6 with circuit limitation of current ($I_{max} \leq 130$ mA). The direction of voltage change $U = (-4 \rightarrow +10)$ V is shown by arrow. The design philosophy of SEC and electrochemical reaction at the cathode are shown in the right insert.

When voltage is applied, Ag+ ions are generated in the region of positive bias (anode) and drift in electrical field through the solid electrolyte of argyrodite. In cathode region the reducing reaction of Ag, origination and further formation of Ag dendrite fiber take place, similar to electrocoating formation in liquid electrolytes. When dendrite fiber reaches to opposite electrode, as a result of SEC interelectrode bridging the high resistance cell (state OFF) switches in low resistance state ($r < 1 \cdot 10^5 \Omega$, state ON). Metal dendrite fiber growth ($U \approx 2 \div 4{,}5$ V) is accompanied by current instabilities (jumps). The instabilities are related to quantization of conductivity and manifest switching by separate atoms. When $U \geq 5$ V the cell switches to ON state.

Polymorphic "Sphalerite-Wurtzite" Transition in Zinc Chalcogenide Crystals

Chobanyuk V.M., Parashchuk T.O.

Physical-Chemical Institute,
Vasyl Stephanyk Precarpathion National University

In this paper the cluster approaches to calculate thermodynamic parameters of zinc chalcogenides was proposed. The enthalpy of formation of crystal data and the phase transition temperature for polymorphic sphalerite-wurtzite modifications have been determined. The calculation was carried out within the cluster approximation using the restricted Hartree-Fock method, using the valence basic set SBKJC [1], which includes an effective core potential, using FireFly.

For the calculation used five molecular models of zinc chalcogenides. The first cluster includes the zinc atom is surrounded by two ligands and has the general formula $ZnC_2H_2X_4$ (X = S, Se, Te). The second cluster, which $Zn_4C_6H_6X_{13}$ general formula contains sulfur atom surrounded by four atoms of zinc, which corresponds to the real placement of atoms in the crystal, all these atoms is four-coordinated. For the saturation limit relations used six ligands of HCX_2.

Wurtzite structure was investigated using three models. The first (general formula $Zn_{15}H_{15}$) is the base for calculating the spatial and electronic structure and thermochemical quantities, it consists of 30 atoms and contains of two four-coordinated pairs, six three-coordinated pairs and seven two-coordinated pairs of atoms. Another models were the similar with different quantities of atoms.

As a result of calculation obtained values of enthalpy of formation models, combining them in view of the coordination models allowed to remove the boundary conditions and thus to estimate the corresponding values for the real crystals of sphalerite and wurtzite. It was also obtained thermodynamic characteristics at different temperatures based on the calculated vibrational spectra of the nanoparticles. These data are built graph of Gibbs energy on temperature for two polymorphic modifications, where the intersection point corresponds to the phase transition temperature. For example, the calculated value of this quantity for ZnS is 1191^0C, slightly above the experimental data (1175^oC [2]) for volume.

As a result of quantum-chemical calculations verified the suitability of molecular models to compare the properties of wurtzite and sphalerite and determine the phase transition temperature. This approach proved to be quite suitable for calculating the heats of formation and phase transition temperature. Well played the main differences of polymorphs:

– bond length is shorter in wurtzite;

– sphalerite is thermodynamically more stable.

Satisfactory accuracy of the calculation is due to the choice of the appropriate model, and the mutual elimination of systematic errors.

1. M.Krauss, W.J.Stevens .Rev. Phys. Chem. 35 (1985), 357-385.
2. E. Spano, S. Hamad, C.R. Catlow. J. Phys. Chem. 107 (2003), 10337-10340.

Thermoelectric Figure of Merit of Composite Structures of Different Classes of Compounds

Freik D.M.[1], Galuschak M.O.[2], Krunutcky O.S[2], Matkivsky O.M.[1], Mateik G.D[2].

[1]*Vasyl Stefanyk Precarpatian National University, Ivano-Frankivsk,Ukraine*
[2]*Ivano-Frankivsk National Technical University Oil and Gas, Ivano-Frankivsk, Ukraine*

Thermoelectric phenomena obtained in recent years increasingly practical application for the direct conversion of thermal energy into electrical energy [1]. The effectiveness of this transformation depends on the properties of materials used in thermoelectric modules. They should have high values of conductivity (σ) and Seebeck coefficient (S) and low thermal conductivity (χ) provided that certain of the thermoelectric figure of merit (Z) ($ZT = S^2\sigma / \chi$, T-absolute temperature). A review of works devoted to the peculiarities of promising thermoelectric properties of semiconductor composite materials: bismuth telluride and antimony Bi_2Te_3, Sb_2Te_3; lead telluride PbTe; compounds (LAST-m) $AgSbTe_2$-$(PbTe)_m$; Mg_2Si, $CoSb_3$, Si-Ge; lanthanum chalcogenides; structure based half-Heusler compounds [3].

Composite materials Bi_2Te_3 and their alloys are among the most widely used for temperatures from 200 K to 400 K. composites based on lead telluride PbTe - effective for medium temperatures (450-800) K, and on the basis of Mg_2Si, Mg_2 (Si, Sn) attracted attention because of the high value of ZT ~ 1,1 at 800 K and and non-toxicity. Solid solutions Si_xGe_{1-x} occupy an important place for temperatures above 1000 K. The value of ZT for p-type and compound $Si_{80}Ge_{20}$ is 0.95 at 1273K. Composite structures based half-heusler compounds environmentally safe and ZrNiSn have matter ZT = 0,7 at 800 K.

Attention is focused on the possible areas of practical use of composite materials for power generators and cooling devices in space, vehicles, medicine and in solving specific problems.

1. Freik D.M., Galuschak M.O., Krunutcky O.S, Matkivskiy O.M. New Nanocomposite Thermoelectric Materials (Review) // Physics and chemistry of solid state 14, (2) p. 300-316 (2013).

The work supported by projects of FRSF State Agency for Innovation and Informatization of Ukraine. (Contracts: R54, F53, 3) and by projects of NAS of Ukraine (N 0110U006281)

Investigation of Temperature-Frequency Dependences of Electronic Conductivity of Solid Solutions of Li_2O-Fe_2O_3-Al_2O_3 by the Method of Electric Impedance

B.J. Deputat[1], L.S.Kaykan[2], V.V. Ugorchuk[2], T.O. Kritsak[1], T.M. Mazur[1].

[1]*The Ivano-Frankivsk National Technical University of Oil and Gas, Ivano-Frankivsk, Ukraine*

[2]*Vasyl Stefanyk Precarpathian National University, Ivano-Frankivsk, Ukraine*

Solid solutions of composition of $Li_2O-Fe_2O_3-Al_2O_3$, that characterized by mixed type conductivity and possibility of ion diffusion of lithium in the structure of the material, intensively investigated as active substance of electrodes or solid electrolytes autonomous power sources. However, the description of the electrical conductivity of polycrystalline multiphase ferrite materials is not simple and not completely solved task is related to the difficult crystal structure of ferrites and by heterogeneity of element composition in the volume of material [1, 2].

In this work, we have investigated the temperature-frequency dependence of electronic conductivity synthesized by traditional ceramic technology Al - substituted lithium iron spinels with the general formula $(1-y)LiFe_5O_8 + (y)LiAl_5O_8$ of the composition and mode of heat treatment on the final stage of the synthesis.

Undertaken temperature studies of the systems showed that in general with the increase of temperature conductivity increases, but dependences on the curves Arrhenius for the systems specimens Series № 1 (samples cooled from the synthesis temperature by tempering in water) and Series № 2 (samples slowly cooled with a stove) indicate on dominance of different mechanisms of conductivity in certain areas temperatures. Figure 1 shows the curves Arrenusa for both series of samples at y = 0.6

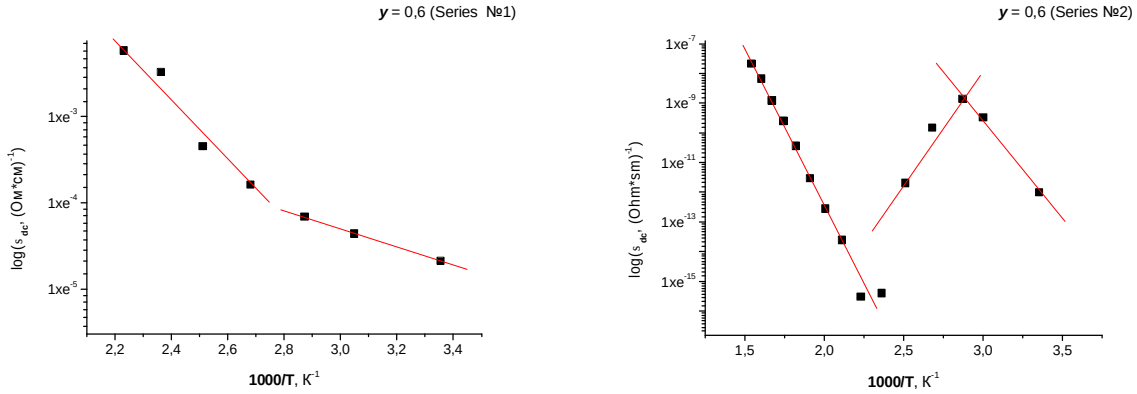

Fig. 1. Arrhenius curves for systems samples of composition $(1-y)LiFe_5O_8 + (y)LiAl_5O_8$

So for a system № 1 all curves Arrhenius are characterized by a change in the slope of the approximating line at temperatures ($T_k \approx 360$ K). At $T > T_k$ the dominant is activation mechanism of conductivity , and at $T < T_k$ - hopping. So

for the sample y = 0.6 the energies of activation calculated on the basis of the temperature dependences of the conductivity are ΔE_1 = 0,3 eB ΔE_2 = 0,1 eB. With increasing content of aluminum in the system value of energy activation, at which there is a change of the mechanism of conductivity, it is shifted toward higher temperatures.

For samples of Series number 2 on the curves Arrhenius observed area of approximating curve with a positive slope to the axis of temperatures, which is a display of the metallic type of conductivity (Fig. 1.a). Such course of curves of log (σ (1 / T)) indicates on the existence in the temperature range (350-400 K) of ferroelectric properties, that is confirmed temperature dependences of the real part of the dielectric constant (Fig. 2), which have the brightly expressed peak at the temperature transition.

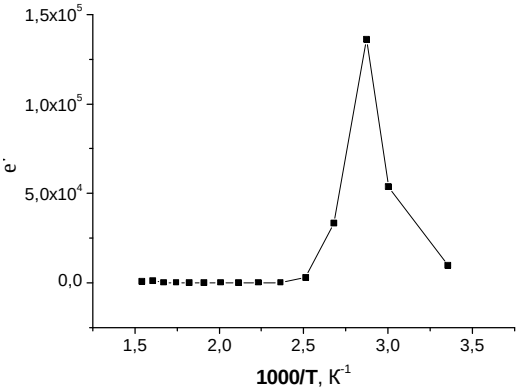

Fig. 2. Temperature dependence of real part of inductivity ε' for sample *y* = 0,6 Series №2.

Temperature region of existence of ferroelectric state is limited to two points of phase transition. The positive slope of the dependence curves of Arrhenius of samples of series № 2 (y = 0.6, 0.8, 1.0) in the temperature region, which corresponding to the ferroelectric state conditioned by remaining polarization microareas under external fields. Since the structurally samples with the content Al (y = 0.6, 0.8, 1.0) have areas stratification, in some local area are different and the phase transition temperature.

Arjunwadkar P.R., Patil R.R., Kulkarni D.K. Effect of sintering temperature on the structural, electrical and magnetic properties of $Li_{0.5}Al_{1.0}Fe_2O_4$ ferrite prepared by combustion method / P.R. Arjunwadkar, R.R. Patil, D.K. Kulkarni // J. Alloys and Compounds. – 2008. – Vol. 463. – P. 403-407

Malyshev A.V, Peshev V.V, Pritulov A.M. The temperature dependence of the dielectric properties of lithium-titanium ferrite ceramic / A.V. Malyshev, V.V Peshev, A.M Pritulov / / Solid State Physics. - 2004. - T. 26, no. 1. - S. 185-188.

Voltammetry investigation of the CdSb-electrolyte interface

Diychuk V. V.

Yu. Fedkovych National University, Chernivtsi, Ukraine

The method of voltammetry is widely used in the physico-chemical investigations of the electrode/electrolyte interface. The character of influence of electronic characteristics, crystallographic orientation of semiconducting electrodes and their surface treatment methods on interface redox processes can be revealed through the analysis of the voltage-current (v-c) curves.

In this short communication we report the results of the voltammetry investigation of the electronic characteristics of CdSb monocrystals in aqueous solutions HCl–NaCl and NaOH–NaCl at different pH.

Analysis of the v-c curves shows the potential ranges of the active and transpassive states of the electrode for all the solutions. The anodic current hysteresis has also been determined for the direct and opposite potential changes. Qualitative analysis of the v-c curves shows that pH of the solutions exerts a significant influence on electrochemical characteristics of CdSb electrode. Such characteristics as the maximum current value, passivation current value and angular coefficients of the v-c curves, which depend on the rate of electrochemical dissolution of CdSb, are decreasing with the increase of pH (within the increasing anodic current parts).

An active state of the electrode (anodic dissolution of CdSb) is registered in the strong-acid solutions within the range -0,211 to +0,456 V. Thermodynamic calculations show that the reactions of stoichiometric and selective (by Cd) dissolution of CdSb are thermodynamically allowed within the range of potentials mentioned above and the strong-acid pH.

The shift of pH towards the subacid and neutral solutions causes decrease of the maximum current value, which can be caused by passivation of the electrode with the deposit of new phase Sb_2O_3.

The active state interval of the electrode in the subalkali solution is quite wide (-0,065÷0,742 V) for pH=9. Further shifting of pH results in significant drop in the currents values, which is caused by formation of the poorly soluble compounds layer on CdSb at pH=11.

The atom-absorption and polarographic analysis of the electrolytes have been carried out after the electrode polarizations in order to determine the content of Cd and Sb compounds and support the abovementioned general conclusions. It was found that nearly-stoichiometric dissolution of CdSb in the solutions HCl–NaCl and NaOH–NaCl in fact takes place in a strong acid (pH=1), neutral and subalkali (pH=9) solutions.

Calculation of the Lattice Thermal Conductivity of Doped Lead Telluride Crystals

Dzumedzey R.O., Voznyak O.M., Gevak T.P., Bandura Yu.V.

Vasyl Stefanyk Precarpatian National University, Ivano-Frankivsk, Ukraine;

Exact calculation of the lattice component of thermal conductivity is generally possible but requires an examination of power structures and anharmonic processes in crystals and good agreement with the Boltzmann equation, which requires cumbersome mathematical calculations. The equation for the calculation lattice component of thermal conductivity can be written:

$$c_{lat} = \frac{1}{3} C_{гр} u^2 t \qquad (1)$$

were $C_{lat} = \frac{\mathbf{h}^2 w^2}{k_0 T^2} \frac{e^{\mathbf{h}w/k_0 T}}{(e^{\mathbf{h}w/k_0 T} - 1)^2}$. That is why there is a need to create models that simplify the theoretical calculations, which are primarily related to the phonon dispersion.

Among the existing models should note the following: Debye model, Dutch model, sinus model, Tiwari model and model boundary conditions Bryullyuen's area.

Comparing these models with experimental data, we can highlight the best matching Tiwari model and model boundary conditions Bryullyuen's area. These models agree well throughout most of the Bryullyuen's area.

Given the above it becomes clear presence of many empirical or semi-empirical expressions for calculating the lattice component of thermal conductivity. The best proven as follows:

$$c_{lat} = \frac{2k_0 c_{el}}{a e - 2k_0} \qquad (2)$$

The table shows the calculating results of the thermal conductivity doped crystals PbTe:Bi and PbTe:Sb for different impurity content in the temperature range (77-800) K.

Thermal conductivity (χ, $mWsm^{-1}K^{-1}$) of the doped crystals PbTe:Bi(Sb)						
at. %	77 K	200 K	300 K	450 K	600 K	800 K
	Bi					
0,25	20	9	8	–	–	–
0,5	17	8	8	–	–	–
1	12	11	8	–	–	–
2	–	–	12	10	9	6
Sb						
1	–	–	19	12	4	4
1,5	–	–	21	9	4	5
2	–	–	19	7	5	4

The work supported by projects of FRSF State Agency for Innovation and Informatization of Ukraine. (Contracts: R54, F53, 3) and by projects of NAS of Ukraine (N 0110U006281)

Raman Light Scattering of Solid State Phase Systems of Cadmium Diphosphide with Deviation from Stoichiometry

Fekeshgazi I.V., Sidenko T.S., Kolomys O.V., Trukhan V.M., Shovkova T.V.

V. Lashkarev Institute of semiconductors physics of NAN Ukraine, Kyiv, Ukraine

The surface and volume optical constants of solid state phase systems from some different materials are very important for them applications in the electronic devices. Therefore the problem of finding new active methods of properties influence and prediction in this systems and control of its structural changing in the surface and volume regions is actual. In the case of binary compounds especially actual are defects caused by deviation from stoichiometry as a result of one element substitute to another (A on B) or vice versa (B on A). This essentially changes both the internal elastic fields and electric fields in the system. The methods of the stoichiometry deviation's determination are based on the connection between physical properties and medium structure and its atoms concentration.

The most suitable method of determination for this deviation from stoichiometry on molecular level is micro-Raman spectroscopy. For example, in the case of binary compositions the excess of the one component means the lack of other one, that accompanied by appearance of the new characteristic lines in the Raman spectra.

The control of cadmium diphosphide samples was carried out by the analysis of Ramam light scattering spectra (LSS). The spectra of LSS were obtained at a room temperature in the reverse dispersion geometry on Horiba Joben Yvon T64000 and Renishaw spectrophotometers.

The frequency and spatially polarization of LSS spectra of the cadmium diphosphide systems without (and with) deviation from stoichiometry by excess of cadmium or phosphorus atoms were measured. Their analysis and comparison were made by the method of theoretical-group calculations of vibration spectra. The invariability of placing the LSS bands according beams direction and orientations of electric vectors of incident E_i and scattering E_s of light intensities was found. However, the intensities of bands at collinear orientation of $E_s||E_i$ were always higher, than at their perpendicularity.

The new characteristic bands appear at the annealing of crystals in the cadmium or phosphorus vapors as a result of excess the correspond atoms on stoichiometrical composition of CdP_2. The analysis of the obtained results were made with the using of model which is based on the presentation of structural chains from phosphorus atoms as weak interactive between molecular complexes itself.

Dielectric Relaxation Effect on Photoconductivity Decay in Indium Selenide Single Crystals

Fl'unt O. Ye.

Ivan Franko National University of Lviv, Lviv, Ukraine

The photoconductivity kinetic in frequency domain may be described by the frequency dependence of real $i_1(\omega)$ (in-phase) and imaginary $i_2(\omega)$ (shifted on $\pi/2$ by phase) components of modulated photocurrent caused by illumination of the semiconductor sample by intensity modulated light beam corresponding to sinusoidal law. Obeying the experimental intensity modulated photoconductivity spectra to fractional power law suggests the deviation model of behavior of excess charge carrier as from simple model of excess charge carriers trapping dynamics so from superposition model of releasing of charge carriers from trapping level distributed on energy in the forbidden gap. The reason of deviation from Debye model may be as the interaction of localized on traps charge carriers itself so the interaction of trapped charge carriers with surrounding media. Both processes may lead to formation of groups of localized charge carriers acting with some correlation. The macroscopically measured parameters as, for example, obtained from photoconductivity effect give characteristics of these groups, but not of elementary trapped carriers.

In this work the behavior of intensity modulated photoconductivity spectra and the low-frequency dielectric spectra of InSe and InSe:Ag (0.25 at. %) crystals at different temperatures have been compared. The light intensity beam modulation with sinusoidal shape on frequencies 10 Hz – 100 kHz were conducted using the infrared light emitting diode. The dielectric spectra are presented in the shape of frequency dependence of real $\varepsilon_1(\omega)$ and imaginary $\varepsilon_2(\omega)$ parts of complex dielectric constant, that have been measured by transducing the complex capacity into complex voltage under applying to samples 100 mV rms sinusoidal voltage. It is shown that as dielectric so intensity modulated photoconductivity spectra obey fractional power law on frequency and deviate from exponential time relaxation law (Debye law).

Intensity modulated photoconductivity spectra of InSe:Ag crystals show widering of the maximum on frequency dependencies of quadrature component of photocurrent with decreasing of temperature. Degree of deviation from Debye shape of photoconductivity kinetic at low temperatures correlates with the shape of low-frequency response, that begins to dominate below ~ 210 K. The revealed correlation has been explained by screening of trapped excess charge carriers by the medium of quasilocalized charge carriers displayed on the dielectric spectra by the frequency dependence $\sim\omega^{-(1-n)}$, where $n \approx 0.8$. The maximum observed on $i_1(\omega)$ may be connected with temporal dependence of trapping center parameters caused by dielectric relaxation of surrounding media.

Semiconductor Materials for p-Branches of Thermoelements which is Based on PbTe-SnTe Solid Solutions

Freik D.M.[1], Dzumedzey R.O.[1], Mazur M.P.[2], Lysyuk Yu.V.[1], Kalytchuk I.V.[3]

[1]*Vasyl Stefanyk Precarpatian National University, Ivano-Frankivsk, Ukraine;*
[2]*Ivano-Frankivsk National University of Oil and Gas, Ivano-Fvankivsk, Ukraine;*
[3]*Snyatyn' College of the Podillya State Agro-Technical University, Snyatyn, Ukraine*

Effective p-PbTe are using heavy doping sodium, which leads to deterioration of mechanical properties and a gradual decrease in thermoelectric power, thus reduce the operating time of thermoelectric module. As the p-type conductivity branches can use materials from GeTe, but they are expensive and have high evaporation, so really can not be used at temperatures above 750 K. For these purposes it is expedient to use a solid solution PbSnTe, which at high concentrations of tin has wide range of homogeneity, shifted towards chalcogen, which determines the hole conductivity of the material.

With metal-ceramic technology were prepared samples $Pb_{1-x}Sn_xTe$ with different composition x = 0.4, 0.5 and 0.6 which were used to study the kinetic parameters in the temperature range (300-800) K.

T, K	σ, $Ohm^{-1}sm^{-1}$			a , μV/K			c , $mWsm^{-1}K^{-1}$		
	x=0,4	x=0,5	x=0,6	x=0,4	x=0,5	x=0,6	x=0,4	x=0,5	x=0,6
350	1564	1814	2742	39	31	26	25	28	37
400	1208	1529	2357	63	44	33	24	25	33
450	871	1283	2031	88	61	48	22	23	30
500	706	1032	1684	119	81	62	21	22	28
550	492	809	1395	147	104	80	19	20	25
600	371	711	1182	175	128	102	18	18	22
650	298	552	994	197	153	126	18	17	21
700	271	498	802	209	169	142	19	16	20
750	254	443	756	215	180	155	20	17	19

After analyzing the tabulated values of electric conductivity, it is noticeable that it has a relatively high value (due to lower effective mass of holes and high electrical activity of metal vacancies) and smooth dependence on temperature (due to impurity scattering).

The value of the Seebeck coefficient also has a smooth dependence on temperature. At high temperatures (close to 800 K) the value is the optimal value for a single-band semiconductor (~ 200 μV/K).

Optimal values of thermoelectric parameters achieved for samples with x = 0.6 at temperatures close to 800 K. This fact is primarily associated with a decrease in the band gap, which reduces for the decrease of effective mass, and therefore to an increase electric conductivity.

The work supported by projects of FRSF State Agency for Innovation and Informatization of Ukraine. (Contracts: R54, F53, 3) and by projects of NAS of Ukraine (N 0110U006281)

Mechanisms of Formation of Solid Solutions PbTe-M_2Te_3 (M = Ga, In, Tl)

Freik D.M., Turovska L.V., Boichuk V.M., Boryk V.V., Andriishyn I.M.

Vasyl Stefanyk PreCarpathian National University, Ivano-Frankivsk, Ukraine

Lead telluride is promising semiconductor material for thermoelectric energy conversion devices that operate in medium-temperature range (500-850) K [1]. The important factors that determine the performance characteristics of device structures are point defects of the basic material, which can be controlled significantly by doping and solid solutions formation in the wide concentration range [2].

In this paper the analysis of possible mechanisms of formation of PbTe-Ga_2Te_3 solid solutions based on lead telluride has been presented. Based on the proposed crystal-chemical models of defect subsystem it has been shown that the basic physicochemical properties of solid solution crystals are determined by the concentrations of gallium ions in different charge states ($[Ga^{3+}] \rightarrow [Ga_{Pb}^{1+}]$, $[Ga^{1+}] \rightarrow [Ga_{Pb}^{1-}]$).

The possible mechanisms of formation of PbTe-Ga_2Te_3 solid solutions have been considered: substitution of gallium ions of lead position with the vacancy formation (mechanism I) and substitution Ga of Pb position with the interstitial tellurium formation (mechanism II). Obviously, the realization of mechanism II leads to increase of lattice parameter by rooting of tellurium atoms in tetrahedral blowholes of lead telluride, which is not typical for PbTe-Ga_2Te_3 solid solutions [3]. This speaks in favor of mechanism I. In this case, the majority carrier concentration decreases, the conductivity type changes and hole concentration increases with increase of Ga_2Te_3 fraction in n-PbTe-Ga_2Te_3. In this case, with increasing fraction of singly charged gallium ions Ga^{1+} the curve of n-p-thermodynamic conversion is shifted to the side of decrease of the doping compound. For p-PbTe-Ga_2Te_3 the majority carrier concentration increases.

The analytical expressions for the concentration of point defects and Hall concentration of current carriers in PbTe-Ga_2Te_3 solid solutions have been derived and their dependences on composition have been calculated.

It has been shown that the dominant defects are impurity defects Ga_{Pb}^{1+}, Ga_{Pb}^{1-}, doubly charged cation V_{Pb}^{2-} and anionic V_{Te}^{2+} vacancies, and the ratio between them determines the donor or acceptor doping effect of the compound.

1. Abrikosov N. Kh., Shelimova L. Ye. Semiconductor materials based on $A^{IV}B^{VI}$ compounds. – M.: Nauka, 1975. – 220 p.
2. Zaiachuk D.M., Shenderovskyi V.A. Intrinsic defect and electronic processes in A4B6 // Ukrainian Journal of Physics. – 1991. – V. 36, No 11. – P. 1692-1713.
3. Rustamov N.T., Alidzhanov M.A., Avilov Ch.I. Research of interaction PbTe-Ga2Te3 // Inorganic Materials. – 1979. – V. 15, No 7. – P. 1294-1295.

The work supported by project of MES of Ukraine (N 0107U006768)

Point Defects and Physics-Chemical Properties of Zinc Selenide Crystals Doped by Transition Metals

Freik D.M., Vadyuk M.P., Ptashnyk A.I.

Vasyl Stephanyk Precarpathian National University, Ivano-Frankivsk, Ukraine

Zinc selenide is used to create screens laser injection LEDs, lasers in the blue region of the spectrum, scintillation sensors, photoconductors and sources of spontaneous and coherent radiation. Of particular interest is the study of zinc selenide crystals doped with transition metals, because they are characterized by insidecentered transitions to unfilled 3d-shells - absorption and luminescence spectrum represented in the infrared light spectrum and high quantum output.

It is known that the inclusion of ions of transition metals (Ti, V, Cr, Mn, Fe, Ni and Co) leads to the features that make zinc selenide particularly attractive for use in solid-state laser devices at room temperature, working an average IR range.

In the n-ZnSe predominant point defects are doubly charged $Zn_i^{\bullet\bullet}$ and singly charged $Zn_i^{\bullet}$ interstitial zinc atoms, singly and doubly charged selenium vacancies $V_{Se}^{\bullet}$, $V_{Se}^{\bullet\bullet}$ and complexes $\left[V_{Zn}^{//}V_{Se}^{\bullet}\right]^{/}$, and in p-ZnSe range of point defects containing doubly charged $V_{Zn}^{//}$ and singly charged $V_{Zn}^{/}$ zinc vacancies, interstitial zinc atoms doubly charged $Zn_i^{\bullet\bullet}$ and doubly charged selenium vacancies $V_{Se}^{\bullet\bullet}$.

Fe impurity (metal with unfilled 3d-shell) can be in two different charge states 2+ and 3+ with different sizes of ionic radius with respect to Zn (Zn^{2+} - 0,74 Å, Fe^{2+} - 0,74 Å, Fe^{3+} - 0 64 Å), electronegativity values: - Zn^{2+} - 1,65, Fe^{2+} - 1,83. If Fe^{2+} is the place of Zn in the crystal lattice, it is due to the difference in electronegativity values in crystals of n-type conductivity Fe^{2+} can act as a nonradiative center, as a deep acceptor. If you charge state of impurity Fe^{3+}, and the value of the ionic radius of Fe^{3+} - 0,64 Å, is shorter than the Zn, may cause stress compensating voltage grid ZnSe - interstitial iron (Fe_i^{3+}) ions.

4. Alloying cobalt in zinc selenide crystals is in the doubly charged state (Co^{2+}), the most probable mechanism of formation of defects will be filling of zinc vacancies by cobalt ions Co_{Zn}. This contributes also a small difference between the ionic radius of cobalt and zinc (Zn^{2+} - 0,0715 nm, Co^{2+} - 0,0730 nm).

The influence of technological factors on the chemical synthesis of thermoelectric efficiency of PbTe-Bi_2Te_3 alloys

Freik D.M., Kryskov T.A., Gorichok I.V., Matkivskyi O.M., Luba T.

Precarpathion National University named after V. Stefanyk, Ivano-Frankivsk, Ukraine

The interest in studying of lead telluride properties that are modified by alloying elements of the fifth group in the periodic table and creating PbTe-Bi_2Te_3 solid solutions has increased during last few years. According to researches [1-2], dopping lead telluride should optimize thermoelectric parameters of the material: growth of models' electric conductivity and reducing their thermal conductivity. However, despite the already researched general influence of bismuth on properties of PbTe, the question of technological impact during samples' preparation for entry mechanism of impurity atoms into crystal lattice and its effect on the thermoelectric performance of the material is not still resolved.

Solid solutions were obtained by direct melting in evacuated quartz glass ampoules with purified Pb and Te components and previously synthesized Bi_2Te_3. Samples of metal for research were received by the faction powder synthesized material sized 0.05 - 0.5 mm under pressure (0.5-1) GPa. Pressed samples were again subjected to air annealing during 5 hours under temperature of 500 K. The magnitude of thermopower (α) and relative conductivity (σ) were calculated by a standard method: a sample was placed in an oven between two copper rods, one of which was heated to create a temperature gradient (≈ 10 K) for the sample. Temperature measurements were carried out by two chromel-alyumelevymy thermocouples, placed in drilled holes in the sample. Electrical conductivity was determined by measuring the voltage drop in the sample generated by a constant voltage source. Herewith, one of the branches in each thermocouple was used as electric conductor.

These samples had n-type conductivity. Their electrical conductivity decreases while temperature increases, the absolute value of the thermoelectric coefficient - is growing. Increase of Bi_2Te_3 content leads to a simultaneous decrease of both size ϭ and α.

1. Д.М. Фреїк, І.В. Горічок, Р.О. Дзумедзей, Ю.В. Лисюк, В.П. Кознюк, А.П. Кознюк. Синтез і термоелектричні властивості PbTe:Sb // ФХТТ. – 2012 – Т. 13, № 1. – С. 220-223.
2. L.D. Borisova. Thermoelectric Properties of Impurity Doped PbTe // Phys. stat. sol. (a).– 1979. – 53. – K19–K22.

The work supported by projects of NAS of Ukraine (N 0110U006281) and by project of MES of Ukraine (N 0107U006768)

Laser-Stimulated Increase in the Reflectivity of High-Resistivity CdTe Single Crystals and CdZnTe Solid Solutions

Gentsar P.O.[1], Vlasenko O.I.[1], Levytskyi S.M.[1], Gnatiuk V.A.[1], Yanchyk I.B.[1,2], Lavoryk S.R.[1,2]

[1] *V.Lashkaryov Institute of Semiconductors Physics of NAS of Ukraine, Kyiv, Ukraine*
[2] *LLC "NanoMed Tech", Kyiv, Ukraine*

By use laser irradiation of functional materials for electronic equipment can be change their optical and electrical properties. This paper presents the results of investigations of optical reflectance spectra before and after laser irradiation in the energy range 66 - 164 mJ/cm^2. Experimentally shown to increase the reflectivity of the studied crystals by a given laser irradiation.

As the samples are used monocrystalline plates p-CdTe (compensated chlorine) single crystals with orientation (111) and $Cd_{1-x}Zn_xTe$ (x = 0.1) solid solutions. The resistivities at room temperature of CdTe (linear dimensions of the samples were $5 \times 5 \times 0.5$ mm^3) and CdZnTe ($5 \times 5 \times 2$ mm^3) were (2-5) $\cdot 10^9$ Ohm·cm and $3 \cdot 10^{10}$ Ohm·cm respectively. The surface of the crystals were subjected to mechanical processing (cutting, grinding, polishing) with subsequent chemical processing (washing, etching, washing) and drying of samples.

Reflection spectra high-resistivity CdTe single crystals and CdZnTe solid solutions depending on the energy of the laser irradiation in the range 0.2 - 1.7 microns are obtained. Increasing the reflectivity of high-resistivity CdTe and CdZnTe solid solutions under laser irradiation in the energy range 66 - 164 mJ/cm^2 can be explained as follows: the processing of the investigated crystals led to laser-stimulated structural transformations of thin surface layer and, as a result, total reflectance is consisted both reflection from thin surface layer and the reflection from volume of material. Thus, this is the result of interference of reflected light (electromagnetic) waves from the interfaces of the air - a thin surface layer and a thin surface layer - the crystal volume. Reflective ability of the crystals determined refractive index n and extinction coefficient c. Differences between the optical characteristics of the surface layer and the volume and lead to the integral effect.

1. The work was supported by the Target Complex Program of Fundamental Researches of the NASU “Fundamental problems of the nanostructured systems, nanomaterials, nanotechnology” (Project No II-53/17/8/12-N).

Laser Processing of $Ge_{1-x}Si_x$ Thin Surface Layers

Gentsar P.O.[1], Vlasenko O.I.[1], Levytskyi S.M.[1], Yanchyk I.B.[1,2], Lavoryk S.R.[1,2]

[1] *V.Lashkaryov Institute of Semiconductors Physics of NAS of Ukraine, Kyiv, Ukraine*
[2] *LLC "NanoMed Tech", Kyiv, Ukraine*

As known, there are many ways of surface treatment of functional materials for electronic equipment. For example are the ion bombardment, laser irradiation and deposition of film on the surface. This leads to changes in particular, electrical and optical properties of the material that is essential for the production of electronic devices of the modern generation. The last time very successfully used for the surface treatment (surface layers) laser irradiation. In this paper, the effect of laser irradiation on the optical properties of solid solutions $Ge_{1-x}Si_x$ is shown. For this purpose, spectra reflectance and transmittance solid solutions in the field of fundamental optical transition are investigated.

Single crystals $Ge_{1-x}Si_x$ (x = 0.85) were grown by crystallization from a melt (Czochralski method). Samples were treated with laser irradiation, namely the crystal surface was uniformly irradiated at room temperature (T = 300 K) neodymium laser radiation pulses (λ = 532 nm) nanosecond duration (τ = 7-8 ns) with energy density E from 46.6 to 163.5 mJ/cm^2.

From the analysis of transmission spectra of solid solutions $Ge_{0.15}Si_{0.85}$ defined numerical value of the optical transition E_0 investigated samples that equal to 1.051 eV (1180 nm). It should be noted that the peak refractive index corresponds to the fundamental absorption edge. At the same time, the decline in refractive index corresponds to the peak absorption.

In the assumption of a linear dependence of the energy E_0 of the solid solution performed relation:

$$E_0(Ge_{1-x}Si_x) = E_0(Ge) + k \cdot x; \qquad E_0(Ge_{1-x}Si_x) = E_0(Si) - k(1-x),$$

where E_0(Ge) = 0,66 eV; E_0(Si) = 1,11 eV; k =0,45 eV.

The calculated value of the energy E_0 from the equations for solid solution composition x = 0.85 equal to 1.043 eV. The deviation of the calculated values of the energy E_0 and the experimental values of the energy E_0 equal to about 8 meV. In our experiments observed the effect of enlightenment. This is the result of interference of light reflected from the boundary air - enlightened surface layer and from the border enlightened surface layer - solid solution.

The work was supported by the Target Complex Program of Fundamental Researches of the NASU “Fundamental problems of the nanostructured systems, nanomaterials, nanotechnology” (Project No II-53/17/8/12-N).

Thermodynamics of Crystal Defects in Crystals of Zinc Telluride

Gorichok I.V., Bardashevska S.D., Lysak A.V., Korzchenevskyj O.Y.

Precarpathion National University named after V. Stefanyk, Shevchenko Str.,57, Ivano-Frankivsk, 76000, Ukraine, e-mail: goritchok@rambler.ru.

Zinc telluride belongs to a relatively little-studied direct-gap semiconductors and is interest in terms of expansion components of modern electronics. Besides the direct-gap semiconductors, ZnTe has a high photosensitivity and can be successfully used for efficient conversion of solar energy.

In this work, the method of thermodynamic potentials defined predominant type of point defects in a two-temperature annealing of crystals in a pair of components. The concentration of point defects were determined directly from the system of equations, wich describ the equilibrium in two-phase two-component system of crystal - pair:

$$\pm m_{D_i}^s = m_i^g$$

where $m_{D_i}^s$ – chemical potential of the defect and i - component (i = A, B), m_i^g – chemical potential of i-component in the pair. The chemical potential of the defects determined by the differentiation of Gibbs energy of the crystal of concentrations of defects.

As a result, the study found that the predominant type of defects in zinc vapor pressure range (10^3 - 10^5) Pa and annealing temperatures (1000 - 1200) K is doubly ionized zinc vacancies, whose concentration increases with both increasing T and decreasing P_{Zn}. By annealing the crystals in a pair of tellurium observed dominance of singly ionized cation vacancies. This is a very high concentration of neutral vacancies and tellurium, which at temperatures above $\approx$ 1100 K exceeds the concentration of singly ionized defects of this type. Significant influence donor tellurium vacancies in the investigated range of process parameters is observed. Most vacancies chalcogen is in charge state 2 +, and the number of neutral and singly ionized vacancies is much smaller.

Revealing in terms of the adequacy of evidence considered defective subsystem model is the fact that the energy formation of neutral zinc vacancy (E_0 = 4.59 eV) obtained by the way of variation for better coordination of the theoretical dependence of p (T, P_{Zn}, P_{Te}) with experimental virtually equal theoretically counted using thermochemical data value (E_0 = 4.39 eV).

The work supported by project of MES of Ukraine (N 0107U006768)

Synthesis and Properties of Thermoelectric Materials of the Compound Pb-Sb-Te

Gorichok I.V., Luba T.S., Krynytskyi O.S., Kryskov T.A., Makovyshyn V.I.

Precarpathion National University named after V. Stefanyk, Ivano-Frankivsk,

Lead Telluride is a promising thermoelectric material for medium-temperature (500-700) K thermal energy converters whose properties can be improved by doping antimony. Therefor, the actual problems to be solved are both the optimal amount of dopant and the influence of technological conditions of obtained material on its properties.

Undoped and doped Lead Telluride was received by direct fusion previously purified components and their stirring during synthesis. The resulting material was crushed in an agate mortar and, after dividing into fraction sized (0.05 - 0.5) mm, was compressed under pressure 0.75 GPa, resulting in receiving cylindrical samples with 5 mm diameter and $l \approx 10$ mm height. Then samples were calcined on air during 5 hours under 500 K again. These samples had stable n-type conductivity, there coefficient of Seebek and electrical conductivity increases while increasing temperature.

Conductivity activation energy analysis was based on dependence $\sigma(T)$ presented in coordinates $\ln(\sigma)$-1/T. This energy was ≈ (0.01-0.02) eV for samples antimony doped 0.1 and 0.3 at. %.

We assumed that electrons scattering on optical phonons is dominant under analyzed temperatures. The position of the Fermi level is calculated on $\alpha(T)$ obtained dependences. Thus, chemical potential of electrons at temperatures of 300 K and 500 K is 0.075 eV and 0.080 eV for the impurity concentration 0.3 at. % Sb, and the corresponding electron concentration equal to lg (n) = 18.54 cm^{-3} and lg(n) = 18.97 cm^{-3} (determined using numerical calculation of Fermi integral). Analysis of the calculated temperature n(T)-dependency (represented in coordinates ln(n) - 1/T) showed that activation energy is 0.01 eV for PbTe crystals containing antimony 0.3 at. % Sb. We can conclude that the main reason in growth σ is activation of electrons in defect levels, as determined activation energies and the temperature dependences of electrical conductivity and electron concentration are approximate.

We concluded that samples of lead telluride with impurity concentration 0.3 at.% Sb have the optimal parameters for usage as a material for n-branch in thermoelectric converters.

The work supported by projects of NAS of Ukraine (N 0110U006281) and by project of MES of Ukraine (N 0107U006768)

Formation Mechanisms of Point Defects and Their Complexes in ZnTe Crystals Doped by Indium and Oxygen

Gurhula H.Ya., Vintoniak T.P., Mezhylovska L.Y., Mudryk H.

Vasyl Stefanyk Precarpathian National University

Zinc Telluride – a promising material of light-emitting diodes with high brightness. As a direct-gap semiconductor, it has a high photosensitivity and can be successfully used to convert solar energy into the electric energy. Doping of ZnTe crystals by the isovalent impurity of oxygen leads to the appearance of localized states in the forbidden gap, that are most likely to be created during the replacement of oxygen tellurium (O_{Te}). In this work, first proposed crystalquasichemical formulas of nonstoichiometric n-and p-ZnTe:O with the realization of a complex range of point defects and it is done on its base the analysis of dominant point defects in ZnTe crystals doped with oxygen and analyzed in term of their thermodynamic n-p-transitions. Received two-dimensional and three-dimensional diagrams of "concentration of defects (carriers of charge) – composition" technological determine factors (chemical composition, annealing conditions) that provide of the crystals with predetermined properties.

Given that the interaction of oxygen with zinc telluride crystals can be in neutral or twice negatively charged state, there are several mechanisms for the formation of point defects in ZnTe:O, namely:

1 – substitution mechanism (A) – $O_{Te}^{\times}$; 2 – the mechanism of rooting (B) – O_i^{2-}; 3 – simultaneous formation of defects by mechanisms A and B – $O_{Te}^{\times}$, O_i^{2-} (mechanism C); 4 – the formation of defect's complex $(V_{Te}^{2+}O_i^{2-})^{\times}$ and $O_{Te}^{\times}$ (mechanism D).

The predominant defects in n-ZnTe:O at low concentrations of impurity ([O] < $1{,}2\cdot10^{-4}$ atomic particles) is doubly charged vacancy of tellurium V_{Te}^{2+}. Reducing the concentration of tellurium vacancies is due to their "healing" by ions O^{2-}. This provide for the increases concentration of zinc vacancies $[V_{Zn}^{2-}]$ and their effect on the conductivity of the material is dominant. If crystals ZnTe:O initially have n-type conductivity, then with increasing [O] electron concentration decreases, responsibly we have inversion of conductivity from n- to p-type and a further increase of the holes concentration, which confirms the donor action of oxygen in ZnTe crystals.

The material p-ZnTe:O with increasing of oxygen content in all cases of the impurity defects formation we have increasing concentration doubly charged zinc vacancies $[V_{Zn}^{2-}]$ and increasing concentration of impurity defects $[O_{Te}^{\times}]$, $[V_{Te}^{2+}O_i^{2-}]$. Doping [O] crystals of p-type conductivity increases the electron concentration.

1. Similar calculations are performed for ZnTe crystals doped indium.

The work supported by project of MES of Ukraine (N 0107U006768)

Investigation of Temperature Distribution for the Optically Opaque Anisotropic Thermoelement under the Laser Excitation

Gutsul I.V., Gutsul V.I.

Chernivtsi National University, Chernivtsi, Ukraine

In the paper we study the anisotropic optical thermoelement (AOT) consisting of the rectangular plate with the length a, height b and width c, produced from the material which is anisotropic over the coefficient of thermal conductivity χ. The rectangular impulse of ray current q_0 falls at the upper surface $y=0$ during the period of time τ. We assume that the crystal is optically opaque for the falling laser radiation. It means that the whole radiation energy is absorbed by the surface of the crystal and is transformed into the heat. Such situation can be realized when the metal layer is dusted at the upper surface of the sample. In this case, the unitary source of the heat is the impulse surface absorption. The internal sources of the heat are absent. The lower surface of the plate $y=b$ is hold at the constant temperature T_0, which is equal to the temperature of thermostat. The side surfaces of the sample are adiabatically isolated. The primary temperature of not radiated plate is assumed as equal to the temperature of thermostat T_0.

In order to estimate the temperature distribution of AOT we use the equation of thermo conductivity

$$c_0 r \frac{\partial T(y,t)}{\partial t} = c_{22} \frac{\partial^2 T(y,t)}{\partial y^2},$$

where $T(y, t)$ – the searched temperature, y – coordinate, t – time, χ_{22} – the component of thermo conductivity tensor, c_0 – specific thermal capacity, ρ – density.

5. The problem of investigation of temperature distribution inside of AOT is studied within two parts corresponding to the time intervals: when the laser ray current falls ($0 \le t \le \tau$) and when its action is stopped ($\tau > t$). The analysis of the results shows that the character of the temperature distributions depends on the relationship between the duration of impulse τ and parameter $t_0 = \frac{4b^2 r c_0}{p^2 c_{22}}$, which has the dimension of time and characterizes the temperature fluctuation in the whole volume of the plate. Taking into account that the parameters τ and τ_0 are independent, there are two cases: $\tau >> \tau_0$ – the long impulses of laser excitation and $\tau << \tau_0$ – the short impulses of laser excitation. In the first case ($\tau >> \tau_0$) AOT is rapidly heated (the exponential law) and during the time τ the duration of the impulse of ray current is almost in the stationary state with the temperature distribution linear over coordinate. When the short impulse ($\tau << \tau_0$) propagates through the AOT the temperature distribution over coordinate is non-linear and the stationary states are absent.

New Intermetallic Phase with Tl_5Te_3 Structure in System Tl-Er-Bi-Te

Imamaliyeva S.Z., Gasanova T.M., Babanly M.B.

Baku State University, Baku, Azerbaijan

Thallium subtelluride Tl_5Te_3 (I4/mcm) possess thermoelectric characteristics owing to features of the crystal structure has a lot of ternary analogs. One of them - Tl_9BiTe_6 have been widely used as material for thermoelectric energy conversion at around room temperature due to his high thermoelectric performance [1].

In our previous study [2] we reported the new ternary compound Tl_9LnTe_6 (Ln-Ce, Nd, Sm, Gd) also crystallizing in Tl_5Te_3-type crystal structure with following unit cell parameters: a=8.890, c=13.015Å, Z=2; a=8,888, c=13.014 Å, Z=2; a=8.888, c=13.013Å, Z=2 and a=8.887, c=13.012Å, Z=2 respectively.

In this paper we reveal the compound Tl_9ErTe_6 - the new ternary analog of Tl_5Te_3. Tl_9ErTe_6 melts incongruently at 1190K and crystallizes in the tetragonal system with the unit cell parameters a=8.892, c=13.062Å, Z=2 (space group I4/mcm). Phase equilibriums in Tl_5Te_3-Tl_9ErTe_6-Tl_9BiTe_6 (A) system are investigated by combination of differential thermal analysis (DTA) and X-ray diffraction (XRD) techniques as well as measurements of microhardness and electro-motive force (EMF) with thallium electrode at 300-430K temperature interval.

Based on experimental data, a series of polythermal sections and isothermal sections at 750, 770 and 800K of phase diagrams and also a projection of liquidus and solidus surfaces of the system (A) were constructed. Concentration dependences of crystal lattice parameters, microhardness and partial thermodynamic functions of thallium ($\Delta\bar{G},\Delta\bar{H},\Delta\bar{S}$) in alloys were determined.

It was established, that system Tl_5Te_3-Tl_9ErTe_6-Tl_9BiTe_6 is characterized by formation of continuous field solid solutions with Tl_5Te_3-type structure (δ-phase).

The conditions of single crystal growth from non-stoichiometric solution by Bridgman techniques are selected using the obtained experimental data on phase equilibriums

1. Sh.Yamanaka, A.Kosuka, K.Korosaki // J. All.Comp. 2003, v.352, p.275-278.
2. M.B.Babanly, S.Z.Imamaliyeva, D.M.Babanly, F.M.Sadygov. // Azerb. Khim. J., 2009, N2, p.122-125.

The Distribution of Activation Energy Adsorption Centers of Chemisorption and Phys-Chemical Processes on Semiconductor Surface

Ivankiv L.I., Gavreluh V.M.

"Ivan Franko" Lviv National University, Lviv, Ukraine

Formulas for the distribution of adsorption centers (a.c.) with chemisorption activation energy is:

$$Ea = kTln(Na)$$

The activation energy of chemisorption and catalysis on semiconductor surface were analyzed. Experimental dependence of the activation energy of dehydrogenation of ethanol bandgap semiconductor-catalyst (E_g) were determined.

The physical content of the semiconductors theory are known the empirical formula $\varepsilon^2 E_g = 1$, where ε - dielectric constant of semiconductor catalyst, and relation E_g with the activation energy of catalysis. We analyzed the change of the dielectric constant in the transition from adsorbate ($\varepsilon = 1$) to the adsorbent-catalyst ($\varepsilon > 1$) with the formation of the surface layer, which is responsible for the process of chemisorption and catalysis. Analysis and synthesis of knowledge on this issue showed that the activation energy of any catalytic reaction is determined by the energy E_g. From simple physical concepts constructed empirical Arrhenius equation, and the use of the distribution function a.c. of E_a for catalytic reactions to explain the phenomenon, not disclosed until now, the compensation effect.

Analyzed the binding energy of atoms chemisorbed molecule binding energy of the molecules of cellulose acetate phthalate and their relationship with E_a and Q (heat of adsorption) and change them to fill the absorption centers.

The model of chemisorption and catalysis of simple molecules on semiconductor catalysts were.

1. Волькенштейн Ф.Ф. Электронные процессы на поверхности полупрово-дников при хемосорбции. М. Наука, 1987, 48с.

Higher-Order Dielectric Susceptibilities for $M_2P_2X_6$ (M=Sn, Mn, X=S, Se) Compounds

Klevets V.Yu., Savchenko N.D., Shchurova T.N., Slivka A.G.

"Uzhgorod National University", Uzhgorod, Ukraine

Theoretical calculation of non-linear properties of functional materials is still nowadays urgent problem. In present work first-order, second-order and third-order dielectric susceptibilities for $M_2P_2X_6$ (M= Mn, Sn, X=S, Se) ternary compounds have been calculated.

We have used theoretical approach developed by W.A. Harrison [1] and applied by us earlier to the calculation of the electronic structure of $M_2P_2Se_6$ (M = Sn, Mn) compounds [2].

In calculations of the dielectric susceptibilities matrix elements used for the determination of the energies of covalent and polar bonds between Mn-X and P-X atoms have been determined from *p*-orbitals with atomic terms obtained within Hartree-Fock approximation. The dependence of dielectric susceptibilities on internuclear Mn-X and P-X distances and the effect of metallization have been analyzed. The calculation of susceptibilities for ternary compounds was performed by the direct summing up of the values for atomic pairs under consideration.

Comparison of theoretical and experimental values of non-linear optical coefficients for $Sn_2P_2S_6$ [3] shows the applicability of the proposed approach to the calculation of physical properties of ternary compounds of the investigated group.

1. Harrison W. A., Elementary Electronic Structure. New Jersey, London, Singapore, Shanghai, Hong Kong, Taipei, Chennai: World Scientific Publishing Co. (2004).
2. Клевець В.Ю., Савченко М.Д., Щурова Т.М., Сливка О.Г. Моделювання електронної структури складних халькогенідів типу $M_2P_2Se_6$ (M = Sn, Mn) // Uzhhorod University Scientific Herald. Series Physics. – 2012. – Issue 31. – P. 55-60.
3. Haertle D., Jazbinšek M., Montemezzani G., Günter P. Nonlinear optical coefficients and phase-matching conditions in $Sn_2P_2S_6$ // Optics Express. – 2005. – Vol. 13, No. 10. – P. 3765-3776.

FeF_3 as a Cathode Material for Lithium Power Sources

Kolkovskyy P.I.

Vasyl Stefanyk Precarpathian National University, Ivano-Frankivsk, Ukraine

The main task nowadays is to develop the methods of increasing the specific capacity of power sources which work on the intercalation principle. Iron fluoride is one of the most promising cathode material for lithium-ion power sources (LPS). Its advantages are such as relatively high voltage open circuit (up to 4 V) and reversible capacity at 200 mA h/g

The origin precursor was a mixture of β-$FeF_3 \cdot 3H_2O$ (ICSD #14134) and dehydrated FeF_3. The relative content of high-pressure phase FeF_3 (HP) was 20 wt.%. Taking into account the data of thermal analysis for ultra FeF_3, annealing includes several stages: annealing to 420 K (1h, remove physically adsorbed water) and 573 K (2h, removing crystal bound adsorbed water) in a stream of argon. As a result, according to data MS spectra we received FeF_3 without inclusions of hematite.

Measurement of kinetic parameters of lithium ion intercalation process was carried out in two-electrode models LPS. The synthesized material was used for preparation of the cathode in solution as a paste for non-woven polypropylene using acetone as a dispersion medium in the presence of surfactant. As electrolyte we used 1M solution $LiBF_4$ in PC+DMK (1:1) and as anode - metallic lithium. Discharge of LPS was carried out in galvanostatic regime at 100 μA current discharge.The figure shows a curve which traces two separate stages of the discharge, the transition between which apparently corresponds to the structural changes of the cathode material. Specific capacity at discharge at 1V voltage was 500 mAh/g and at deep discharge of LPS the specific capacity was 750 mAh/g. For cathode material after contact with the electrolyte relative content of Fe^{2+} is reduced to 9%. $LiBF_4$ dissolved in PC+DMK with forming two complexes $[Li (PC+DMK)2]^+$ or $[Li (PC:DMK)3]^+$.

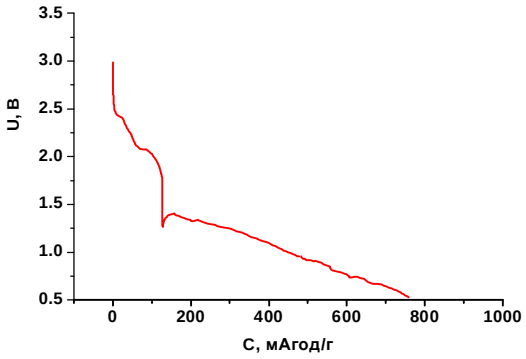

Structure Formation Mechanisms of Porous Systems Hard Crystalline Materials Condensed under Quasi-Equilibrium Steady-State Conditions

Kononenko I.N., Denisenko V.L.

Institute of Applied Physics NAS of Ukraine, Sumy, Ukraine

The method of formation of nanodimensional porous structures of hard crystalline materials is developed, structurization occurs under quasi-equilibrium statinary condensation in accumulative ion-plasma systems [1].

In the present study porous titanium condensates have been deposited by means of ion-plasma sputtering under the quasi-equilibrium conditions and their structure formation mechanisms have been investigated. At the beginning, we introduce to the low-dimensional porous system formation mechanisms,which are based on both the different rate growth of condensate surface local parts and partial coalescence of structural elements. Then we consider the quasi-equilibrium steady-state condensation peculiarities within the accumulative plasma-condensate system and discuss the formation mechanisms of titanium condensates produced on glass and cleaved KCl substrates. The condensate structure has been investigated by means of scanning and transmission electron microscopy. It has been shown that the self-assembly of the porous Ti layers is due to the following key processes: the self-organization of time-constant extremely low supersaturation and the continuous structural and morphological transformation of the growth surface as well.

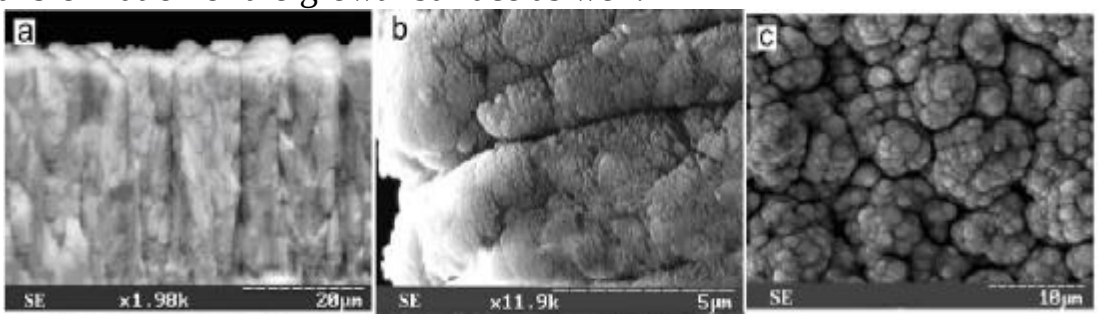

Fig. 1. SEM images of exsitu grown Ti condensates at P_{Ar}= 10 Pa and P_w =5.8 Won glass substrates. The images obtained at back-scattered electrons registration mode (BSE) and secondary electrons registration mode (SE): (a), (b) cross fracture at two magnifications, t =9 h, (c) t = 9 h.

The method of the Rutherford backscattering spectroscopy (RBS) was applied to definition of element structure. For RBS the beam of protons with energy of 1 MEV with a scattering angle of 135 degrees was used. The electrostatic «Sokol» accelerator with energy to 2 MEV of Institute of Applied Physics of NAS of Ukraine was a source of protons.

1. Perekrestov VI, Kornyushchenko AS, Kosminskaya YuA. Selective processes that proceed during formation of aluminium layers near the phase equilibrium in a plasma-condensate system. J Tech Phys 2008;53:1364e70.

Methods Employed for Minimization of Detrimental and Hazard Factors, Impact on a Human Body in the Process of Nanostructures Fabrication and Investigation

Koshel V. I., Poplavskyy O.P., Dzundza B.S., Poplavskyy I.O.
Vasyl Stefanyk PreCarpathian National University, Ivano-Frankivsk, Ukraine

Metal work, as well as labour conditions affect human body greatly. Scientists' labour conditions assessment is based on differential analysis of separate industrial environment factors impact. Under the simultaneous influence of several detrimental factors their integral power should be analysed. Under present-day conditions minimization of detrimental and dangerous factors impact on a human body is of vital importance.

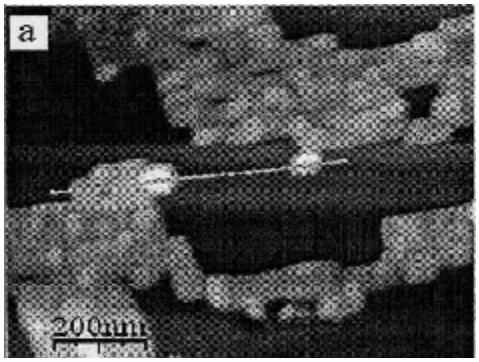

Fig. 1. Topogram of film

In the process of semiconductor devices fabrication the technologies of nanofilms application are used, and the study upon them is conducted. In most cases scientists work with polycrystalline materials, the crystals of which is the size of dozens manometers (see Figure 1), and contain such elements as mercury, lead, chlorine, fluorine etc. These substances refer to extra and highly dangerous hazard classes. Technical processes cause air, working surfaces, clothes contamination, and taking into account the size of nanomaterials, crystals may enter a human body through respiratory and digestive organs, as well as through skin and mucuous membrane. As a result, the conditions are created for the detrimental substances to reach the blood flow.

In most cases technical processes of nanomaterials fabrication, and their investigation is carried out on various plants, though, nanomaterials are transported through air by hand, or stored in laboratory for some time. Therefore, local contamination of air, as well as working surfaces and clothes is observed. This contamination may exceed the maximum permissible concentration. It facilitates additional entering of detrimental substances into a human body. In some laboratories two or more working places are situated and classes for students are conducted, which means that not only main executors of scientific studies work in a hazard environment.

For detrimental and hazard factors impact minimization it is necessary to use a complex of such measures as creation of a healthier air environment, technical equipment and technologies application, usage of individual security means. Special attention should be payed to remote technologies implementation, as well as to the work performed in closed plants, without transporting materials through air.

This work was partly carried out under scientific topics (state registration number 0113U000790).

Nanomaterials - the Risks and Perspective of the Application

Koshel V.I., Dzundza B.S., Poplavskyy O.P.

Vasyl Stefanyk PreCarpathian National University, Ivano-Frankivsk, Ukraine

At present there is extensive proliferation of nanotechnology worldwide. A technology that provides a nano-objects and nano with desired properties, which are used in microelectronics and energy, chemical and food industry, kosmetolohichniyi in agriculture [1,2]. Nanomaterials have opened new possibilities in pharmacology and medicine.

Questions about the toxicity of nanoparticles and nanomaterials remains open. Situation is aggravated by the lack of standardized protocols assess the impact of nanoparticles on the environment and objects relevant regulations [3]. Toxicity of nanoparticles of different elements are of paramount importance, especially in view of the steady increase in the number of employees who have professional contact with nanomaterials. Nanoparticles can penetrate unchanged across the cell barrier and the blood-brain barrier into the central nervous system, circulate and accumulate in tissues and organs, causing more pronounced pathomorphological changes in internal organs, and also have a long half-life.

The priority is issues such as nanobezpeky: study toxicity of nanoparticles and new materials, monitoring of professional effects, and analysis of potential risks to human health, environmental and occupational hazards, mitigation and dissemination of information regarding potential risks [5].

Assessment of risk using traditional methodology complicates that existing approaches do not consider physical and chemical properties of nanoparticles and their biological characteristics of action. For example fusiform nanoparticles are more permeable ability and cause more devastating effects in the body than similar spherical particles. The size, shape and density of the nanoparticles must be considered when calculating the maximum allowable concentrations. It should be noted that the risk assessment and its management requires a much larger base of experimental data than the currently accumulated on this issue.

1. Prodanchuk NG Nanotoksykolohyya: condition and prospects for research. / NG Prodanchuk, G. Balan / / Modern problems and prospects toksykolohyy research. -2009. - № 3. -C. 4-20.
2. B. Kurland A. Oh Nanotechnology and svyazannыh with her toksykolohycheskyh problems / BA Kurland / / Toksykolohycheskyy Journal. -2007. - № 6. -C. 2-3.
3. OV Demetska, k.biol.n., OB Leonenko the problem of regulating nanomaterials / / Modern problems of toxicology. - 2012. - № 1. - C. 52-56.

Influence of Heterogeneities in the Division of Alloying Admixtures on Elektrophysical Properties of Monocrystals of CdSb

Koval Yu.V.[1], Yashchynskyy L.V.[1], Fedosov S.A.[2], Zakharchuk D.A.[1], Korovytskyy A.M.[1]

[1]The State Technical University of Lutsk, Lutsk, Ukraine
[2]Lesya Ukrainka East European National University, Lutsk, Ukraine

It became clear lately, that now subsequent increase of reliability and economy of devices of semiconductor electronics cannot be carried out only by the improvements of technology, and is limited by heterogeneities of physical and chemical properties of semiconductor materials. That is why the problem of heterogeneities research both in general and in particular at different influences was and remains actual.

The purpose of our work was to explore influence of heterogeneities in the division of alloying admixtures Te on elektrophysical properties of cadmium antimonide monocrystals.

During the researches of division of specific resistance on length of the exemplars cut out parallel (I group) and perpendicular (II group) to growth to the crystal, the presence of the stratified periodic heterogeneities is discovered in direction of growth of monocrystals of CdSb, that results in appearance in this direction of gradients of specific resistance, and accordingly, predetermines formation of the internal electric fields. It is confirmed by researches of switching effect from high-resistance in the low-resistance state of monocrystals of CdSb(Te), which volt-ampere characteristic were taken off during at the different levels of illumination. From experimental data the value is expected $j=f(E)$. The substantial difference of thresholds values of tension of the electric field is marked for the exemplars of different groups subject to the condition identical, both for unlit and at the different levels of illumination, that contacts with existence of the compensating electric fields between the layers of growth.

Research of Hall effect is conducted for the exemplars of both groups at different intensities of illumination. Sharp growth of mobility of transmitters of charge is marked at the increase of intensity of illumination in the exemplars, cut out parallel to growth that is explained by the change of potential relief amplitude.

On the basis of the conducted researches it is possible to draw conclusion that the presence of heterogeneities in the crystals of CdSb results in anisotropy of properties. The study of these features creates pre-conditions for the account of the effects marked higher at constructing of different sort of semiconductors sensors, and also will provide the real ways of minimization of displays of these effects wherein they can appear undesirable enough.

Magnetic Properties of Crystals $(3HgSe)_{0.5}(In_2Se_3)_{0.5}$, Doped by Manganese or Iron

Koziarskyi I.P., Maistruk E.V., Marianchuk P.D., Koziarskyi D.P.

Yuriy Fed'kovytch Chernivtsi National University, Chernivtsi, Ukraine

The crystals of solid solutions $(3HgSe)_{0.5}(In_2Se_3)_{0.5}$ (doped by 3d-elements), were got by Bridgeman method.

Analysis of magnetic susceptibility (χ) was performed by Faraday method in the interval of T=77-300K and H=0,25-4 kOe. Samples $(3HgSe)_{0.5}(In_2Se_3)_{0.5}$ are diamagnetic, their magnetic susceptibility $\chi_0 = -0{,}3\cdot10^{-6}$ cm^3/g and does not depend on tension of the magnetic field (H) and temperature (T). Samples $(3HgSe)_{0.5}(In_2S_3)_{0.5}$ (doped by 3d-elements) are paramagnetic and their magnetic susceptibility has a paramagnetic character.

Dependences $\chi_{3d}^{-1} = f(T)$ for the explored samples $(3HgSe)_{0.5}(In_2Se_3)_{0.5}$, doped by manganese or iron, are described by Curie law or by Curie - Wase law with negative paramagnetic Curie temperature (θ). Value $\theta < 0$ points that in the explored crystals the exchange interaction of antiferromagnetic characte between the atoms of Mn or Fe.

$$c_{Mn} = \frac{C}{T-q}; \tag{1}$$

$$C = \frac{xN_0g^2S(S+1)m_B^2}{3k_BM_0} = \frac{N_{Mn}\cdot m_{ef}^2}{3k_Br}; \tag{2}$$

Established that the peculiar properties of magnetic characteristics of $(3HgSe)_{0.5}(In_2S_3)_{0.5}$, doped by manganese or iron, crystals are stipulated by nano formations – clusters of multiple size where exchange (Mn-Se-Mn, Fe-Se-Fe) interaction take place. This exchange interaction is similar MnS faze because there obtained as a result of substitution atoms of Hg by atoms of Mn or Fe. In the crystals $(3HgSe)_{0.5}(In_2Se_3)_{0.5}$:<Fe> Fe atoms can be found in the interstices, and may not be interacting with other atoms or Fe-Fe-Fe clusters can form with direct exchange interaction between atoms Fe within the cluster.

Extrapolation to zero averaged in the high-temperature dependencies $\chi_{3d}^{-1}=f(T)$, which described by Curie - Wase law, gives value of θ for each sample. This allows to get on the basis of the dependencies $\chi_{3d}^{-1}=f(T)$ and formula (1, 2), values of 3d-elements concentrations (N_{Mn} or N_{Fe}) for each sample. Increase effective magnetic moment of Mn or Fe atoms (μ_{ef}), with increasing temperature (set by the Curie-Weiss law (formula 1, 2) based on changes in slope of linear plots at $T=T_s$ the dependences $\chi_{3d}^{-1}=f(T)$), confirms that at $T=T_s$ clusters conversion from "antiferromagnetic" in the paramagnetic state.

The chemical Polishing of Undoped and Doped ZnSe Crystals by the H_2O_2 – HBr – Organic Solvent Etching Compositions

Kravtsova A.S., Tomashyk V.M., Tomashyk Z.F., Stratiychuk I.B., Kuryk A.O., Kalytchuk S.M., Galkin S.M.[1]

V. Lashkaryov Institute of Semiconductor Physics,
National Academy of Sciences of Ukraine, Kyiv, Ukraine;
[1]Institute for Scintillation Materials,
National Academy of Sciences of Ukraine, Kharkiv, Ukraine

The process of chemical treatment of the undoped and doped ZnSe crystals surface by bromine emerging solutions has been investigated. The depending of dissolution rate on the etchants composition, their mixing and temperature has been studied. The concentration regions of polishing solutions and the surface state after chemical etching have been established using electron microscopy and low temperature photoluminescence. The compositions of etchants for semiconductors chemical polishing have been optimized. The comparative characteristics of three etching compositions H_2O_2 – HBr – ethylene glycol (EG), H_2O_2–HBr–oxalic acid ($C_2H_2O_4$) and H_2O_2–HBr–H_2O to obtain high-quality polished surface of the semiconductors have been shown.

The mechanical grinding of samples was performed using aqueous suspensions of abrasive powder marks M10 and M5. To remove the damaged layer of ≈ 100-150 mkm thickness, which was remained after mechanical treatment, we performed a process of chemical-mechanical polishing (CMP) of zinc selenide plates by developed by us universal etchants H_2O_2–HBr–EG with the etching rate $\boldsymbol{v}_{CMP} \approx 13$ mkm/min. After etching the samples were washed with $Na_2S_2O_3$ aqueous solution and a lot of distilled water and isopropanol using ultrasound.

The process of chemical-dynamic polishing (CDP), using the method of the rotating disk at T = 283–308 K and rotation speed drive γ = 36–120 min^{-1}, is the final stage of treatment. A series of etchants for the controlled elimination of thin layers from the ZnSe crystal in order to achieve high-quality surfaces was developed based on compositions H_2O_2–HBr. We have found that the process of dissolution of these materials in the investigated polishing etchants is limited by the diffusion stages, as the calculated apparent activation energy does not exceed E_a = 35 kJ/mol.

It was found that the polishing mixture were formed in the ratio of components (in vol. %): (10-16) H_2O_2: (35-90) HBr: (0-55) EG, (10-16) H_2O_2: (38-90) HBr: (0-49) $C_2H_2O_4$ and (10-16) H_2O_2: (35-90) HBr: (0-55) H_2O. Using the electron microscopy the high quality of the semiconductors surface after the chemical polishing process was confirmed.

Nanocomposite on the Basis of Carbon Polymer – New Promising Material

Levchenko V.A. [1], Matveenko V.N. [1], Buyanovsky I.A.[2], Ignatieva Z.V.[2], Bol'shakov A.N.[2], Zakharov K.A[2].

[1] *Department of Colloid Chemistry, Lomonosov Moscow State University, Moscow*
[2] *Department of tribology, Blagonravov Mechanical Engineering Research Institute, Moscow*

In this work the results of a new type nanocomposite of diamond like carbon (DLC) namely nanostructural new coating-orientants and dynamic metallization process is developed to produce thick (DLC + aluminum, copper, zinc, nickel) coating on any metal or ceramic substrates. A new type nanocomposite of diamond like carbon (DLC) namely nanostructural coating-orientants and dynamic metallization process is developed to produce thick (DLC + aluminum, copper, zinc, nickel) coating on any metal or ceramic substrates. New type nanocomposite is considered having at present time no analogues in triboengineering [1-3].

Authors have made a number of theoretical and experimental studies directed to optimal synthesis parameters finding, coatings structure and tribological characteristics analyzing and establishing correlation between the mentioned factors (the triad "synthesis parameters- structure-performances").

Use as top layer DLC coatings-orientants in nanocomposite allows simplifying the composition of oil materials by reducing amount of antifriction, antiwear additives, etc. As the coatings under study have high corrosion resistance, it is possible to use them in friction units operating in aggressive media.

The research was done by financial support of the RFFR grants: № 11-08-00519-а; № 11-08-00958-а

1. Modern tribology: Results and perspectives. Ed. by K.V. Frolov. Moscow, publishing house LKI, 2008, 480p.
2. Levchenko V.A., Buyanovsky I.A., Ignatieva Z.V., Matveenko V.N. New generation of tribological DLC coatings. Proceedings of the Institution of Mechanical Engineers. Journal of Engineering Tribology, Part J, 2010, v.224, NJ6, pp.384-392.
3. Levchenko V.A. , Matveenko V.N. , Buyanovsky I.A., Ignatieva Z.V., Bol'shakov A.N. Synthesis of new generation nanocomposite coatings. In: The fifth international conference : «Chemistry of a surface and nanotechnology», 24 - 30 Sept., Hilovo - Petersburg, 2012, p.71-75.

X-ray Diffraction Studies of System $Fe_{25}Ni_{20}Mn_{15}Co_{10}Cr_{20}Al_{10}$ High-Entropy Alloy

Makarenko E.S[1]., Karpets M.V[2]., Tsebrii R.I[3]., Myslyvchenko O.M[1].

[1] *National Technical University of Ukraine "Kyiv Polytechnic Institute", Kiev, Ukraine*
[2]*Institute for Problems of Materials Science, NAS of Ukraine, Kiev, Ukraine*
[3]*Ternopil National Economic University, Ternopil, Ukraine*

X-ray studies of alloy $Fe_{25}Ni_{20}Mn_{15}Co_{10}Cr_{20}Al_{10}$ were made. X-ray research of high-entropy alloy samples were carried out by DRON UM1 diffractometer with using scanning in monochromatic CuKα radiation. The X-Ray diffraction pattern were scanned with the diffraction angle 2θ from 18-88°. Scanning step is 0.05° and exposure time is 2 sec. The processing of the experimental XRD data was performed using PowderCell 2.4. program for analysis of X-ray spectra from a mix of polycrystalline phase components.

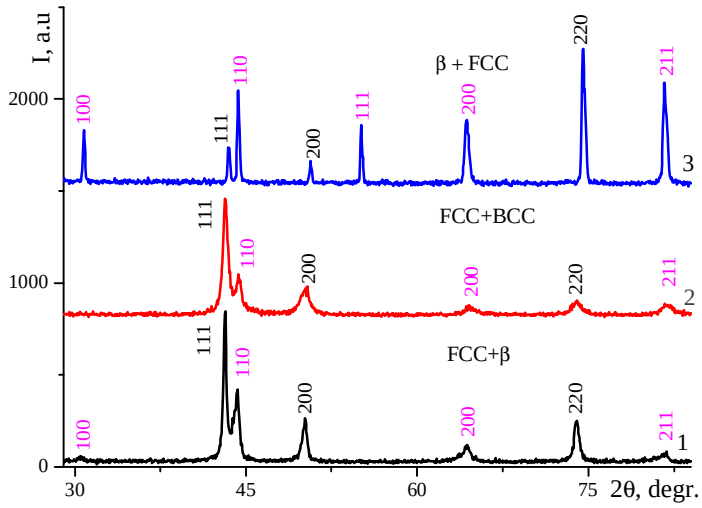

Fig. Fragments of the XRD patterns of high-entropy $Fe_{25}Ni_{20}Mn_{15}Co_{10}Cr_{20}Al_{10}$ alloy in the initial (1), deformed on 75% (2) and annealed at 1100 ° C / 3 hour (3) states. Cu Kα–radiation.

A high-entropy alloy $Fe_{25}Ni_{20}Mn_{15}Co_{10}Cr_{20}Al_{10}$ belong to FCC and BCC solid solutions (fig.). In the process of melting of alloy is formed an ordered β (35 wt.%) structure in the BCC lattice (sample 1) with the lattice period of a = 0.2594 nm. Deformation of alloy caused to the disappearance of superstructure maximums (sample 2). The period of the cubic FCC lattice after deformation (a=0.3633 nm) has increased compared to initial cast state (a=0.3620 nm). The quantity of FCC solid solution in the initial state of 65 wt.% and 79 wt.% after deformation. Clearly defined orderliness in β solid solution after annealing at 1100 ºC for 3 h (sample 3). Lattice parameters of a=0.2881 nm. X-Ray diffraction patterns has the anomalous intensity in β solid solution along the direction [100] and [111]. Therefore, fullprofile analysys of the diffraction patterns was performed the calculation of sample structure, using a textured model of March-Dollase [1]. Texture factor of τ=0.48 in direction [100] and τ=0.33 in direction [111]. Thus, the of FCC solid solution (54 wt.%), lattice parameter of a=0.3592 nm also has the texture in the direction of [220] in annealed condition with τ=0.27.

1. Dollase W.A. Correction of intensities for preferred orientation of the March model // J. Appl. Cryst. – 1986. – V. 19, – P. 267–272.

Features of the Crystal Structure of Bone Regeneration under Lead Poisoning

Maksimova E.M.[1], Nauhatsky I.A.[1], Strugatsky M.B.[1], Mostovoy S.O.[2]

[1] *V.Vernadsky Taurida National University, Simferopol, Ukraine*
[2] *S. Georgievsky Crimean State Medical University, Simferopol, Ukraine.*

Hydroxyapatite $Ca_{10}(PO_4)_6(OH)_2$ is the main mineral constituent of human bones.

Non-stoichiometric hydroxyapatite is of a hexagonal structure $P6_3/m$. Apatites of biological tissues, as well as products of laboratory synthesis, are objects of variable crystal structure parameters. Range of variability of bioapatite structure parameters can be considered as a = 9,48 ÷ 9,35Å; c = 6,88 ÷ 6,84Å [1-4].

The main aim of the work is estimation of lead poisoning effect on bone formation.

It was carried out x-ray analysis of mandible bone regenerate of 72 white rat males weighting 110-150g in the first – the fourth generation with lead intoxication.

Powder x-ray diffraction method on the base of diffractometer DRON-3 with copper tube (λ = 0,1542 nm) was used.

For the first generation of rats it was shown the active lead accumulation in bone crystal structure with substitution of calcium. Parameters of the crystal lattice increase. This way it broke the mineralization processes. As a result of the mineralization process was broken.

We found also for rats in fourth generation that crystal lattice is not changed. Observed strong broadening of diffraction peaks can be due to decreasing of crystallization rate and the presence in regenerate of various distortions, such as stresses and deformations.

1. S.N. Danilchenko, Journal of SumSU. A series of "Physics, Mathematics, Mechanics', 2 (2007).
2. S.O. Mostovoy, V. S. Pikalyuk, E.M. Maksimova, I. A. Nauhatsky, Morphology, 1 (2009).
3. V.S. Picaluk, S.O. Mostovoy, E.M. Maksimova., I.A. Nauhacky, K.A. Plehanova, Morphology, 4 (2011).
4. E.M. Maksimova, I. A. Nauhatsky, M. B. Strugatsky, S. O. Mostovoy, Scientific Notes of Taurida National V.I. Vernadsky University. A series of Physics and Mathematics Sciences, 1 (2012).

Chemical-Mechanical Polishing of PbTe and $Pb_{1-x}Sn_xTe$ by the H_2O_2–HBr–Ethylene glycol Etching Compositions

Malanych G.P., Tomashyk V.M., Kolomys O.F., Tomashyk Z.F., Strelchuk V.V., Lytvyn O.S., Lytvyn P.M., Stratiychuk I.B.

Інститут фізики напівпровідників ім. В.Є. Лашкарьова НАН України, Київ,Україна

Method of high quality polishing surfaces formation of PbTe and $Pb_{1-x}Sn_xTe$ single crystals including string cut ingots into plates, their mechanical grinding, chemical mechanical (CMP) and chemical dynamic polishing (CDP) using developed by us bromine evolving etchants has been developed. Single crystals of PbTe and $Pb_{0,83}Sn_{0,17}Te$, $Pb_{0,8}Sn_{0,2}Te$ (II) solid solutions grown by the Bridgman method as well as $Pb_{0,8}Sn_{0,2}Te$ (I) obtained through the vapor phase have been investigated.

Mechanical grinding of the plates was carried out by water suspensions of abrasive powders M10-M1. The disturbed during cutting and grinding layer with the thickness of 100-150 μm was removed by CMP using (in vol. %): 6 H_2O_2 – 74 HBr – 20 ethylene glycol (EG) etchant at a polishing rate of ≈ 80 μm/min. CMP was carried out on a glass polisher covered with lawn cloth with a continuous supply of etchant at a speed of 2-3 ml/min for 3 min and a pressure on the plates in 2-3 kPa. The etching rate was determined by reducing the thickness of the plates before and after etching by multy-rotatory watch indicator 1MIGP to within ± 0.5 mm. The etchants were prepared using 48 % HBr, 35 % H_2O_2 and EG (the composition is given in vol. %).

Microstructure of the plates surfaces after various stages of the mechanical and chemical treatments was studied using table scanning microscope JEOL JCM-5000 NeoScope. Morphological study of the polished surface of PbTe and $Pb_{1-x}Sn_xTe$ spent on scanning probe microscope NanoScope IIIa Dimension 3000TM (Digital Instruments, USA). Micro-Raman spectra were measured at T = 300 K using Horiba Jobin Yvon T64000 spectrometer equipped with confocal microscope and automated piezo-driven XYZ stage. Discrete lines of Ar-Kr ion laser (λ_{exc} = 488.0) with power on sample surface of 1-2 mW were used for excitation.

It was shown that at the dilution of the polishing etchants with the composition (in vol. %) 6 H_2O_2 – 94 HBr (based solution – BS) at the polishing and CMP rates of ≈ 10 μm/min and 100 μm/min correspondingly it is possible to ameliorate the quality of polished surfaces with the CMP polishing rates from 26 to 100 μm/min at the ratio (in vol. %) 100–40 BS : 0–60 EG. The proposed compositions of H_2O_2–HBr–EG polishing etchants and the treatment methods of PbTe and $Pb_{1-x}Sn_xTe$ single crystal surfaces contribute to a significant decrease in surface roughness (R_z < 40 нм) compared with its value obtained after cutting ingots into plates with the next grinding.

The Local Electron Scattering on the Crystal Lattice Defects in InSb

Malyk O.P.

Semiconductor Electronics Department, Lviv Polytechnic National University, Lviv, Ukraine

Usually the charge carrier scattering models in indium antimonide are considered in relaxation time approximation or using the variational principle. However, these models have essential shortcoming: a) they contradict the special relativity according to which the charge carrier would interact only with the neighbouring crystal region; b) they contradict the atomistic hypothesis according to which the charge carrier interacts (and transfers the energy respectively) only with one atom but not simultaneously with many atoms which are situated in different points of space. From the other side in [1-3] the short range models of carrier scattering were proposed for $A^{II}B^{VI}$ and $A^{III}B^{V}$ semiconductors in which the above mentioned shortcomings were absent. The purpose of the present work is to use this approach for description of the electron scattering in InSb.

For the charge carrier scattering on the nonpolar optical and acoustic phonons and static strain potential the interaction radius of the short-range potential is limited by one unit cell. For the charge carrier scattering on the ionized impurity, polar optical and piezoelectric (piezoacoustic and piezooptic) phonons the interaction radius of the short-range potential is founded in a form $R=g\ a$ (a - lattice constant, g – the respective adjusting parameters).

To calculate the conductivity tensor components the method of a precise solution of the stationary Boltzmann equation was used [4]. The temperature dependence of the electron mobility in the range 8 –700 K in InSb crystal (defect concentration ~8.3×10^{14} cm^{-3}) was calculated. The influence of the different scattering mechanisms on the charge carrier mobility is considered. The scattering parameters γ for different scattering modes are determined. The temperature dependences of the thermoelectric power in indium antimonide with different defect concentration in the same temperature range were calculated. A good agreement between theory and experiment in all investigated temperature range is established.

1. O.P. Malyk. Materials Science & Engineering. 2006. B 129. 161-171.
2. O.P. Malyk. Physica B:Condensed Matter. 2009. 404. 5022-5024.
3. O.P. Malyk. Diamond Relat. Mater. 2012. 23, 23-27.
4. O.P. Malyk. WSEAS Trans. Math. 2004. 3. 354-357.

Determination of the refractive index profile of GGG single crystals implanted by He^+ ions

Mokhnatskiy M.L.

Vasyl Stefanyk Precarpathian National University, Ivano-Frankivsk, Ukraine

One of the methods of the materials subsurface layers modification in order to give them certain properties is ion implantation. Its main advantages are the possibility to control the content and distribution of implanted adulterant and also to do the modification under the room temperature. Such technology is perfect for making of planar lasers waveguides, due to the high precision of radiation dose control [1].

Ion implantation causes the partial disordering of the subsurface layers of materials due to the defects, which arise along the trajectories of interstitial ions. Structural changes of modified by implantation layer are described by profile of relative deformation, which can be determined by X-ray diffractometry methods [2]. There is the correlation between the values of relative deformation and refractive index of material.

The object of research was gadolinium gallium garnet (GGG) single crystals implanted by He^+ ions with energy of 100 KeV and doses of $1\cdot10^{16}$ sm^{-2}, $6\cdot10^{15}$ sm^{-2}, $4\cdot10^{15}$ sm^{-2}, $2\cdot10^{15}$ sm^{-2}, $1\cdot10^{15}$ sm^{-2}. In order to determine the refractive index profile of implanted layer of single crystal it was carried out the measuring of refractive index of subsurface region of disturbed layer of material. The values of relative deformation on the surface were determined from the X-ray analysis results. These researches made it possible to determine the relation between deformation and refractive index of subsurface region of disturbed layer and approximating them on the whole modified by implantation layer to find the distribution of refractive index with depth.

1. Townsend P. D. Optical effects of ion implantation / P. D. Townsend, P. J. Chandler, L. Zhang. – Cambridge : Cambridge University Press, 1994. – 280 p.
2. Механізми дефектоутворення при імплантації монокристалів ГГГ іонами B^+ та He^+ / Б. К. Остафійчук, В. Д. Федорів, С. І. Яремій [та ін.] // Металлофизика и новейшие технологии. – 2008. – Т. 30, № 9. – С. 1215-1227.

The Method of Crystal Quartz Cleaning from Impurity Metal Cations

Myronyuk I.F.[1], Mandzyuk V.I.[1], Tsyba V.I.[2]

[1]*Vasyl Stefanyk Precarpathian National University, Ivano-Frankivsk, Ukraine*
[2]*Co.Ltd "KM LABS", Kyiv, Ukraine*

Crystalline silica is a unique material for producing of quartz glass used in electronic and optoelectronic products. Some kind of high purity quartz are also used to produce poly-and monocrystalline silicon. However, a natural material contains impurity Fe^{3+}, Al^{3+}, Na^{+}, K^{+}, Li^{+}, Cs^{+} cations, which limit its use. The known methods for purification of natural quartz based on the mechanical-chemical treatment of the powder material and not provide complete removal of impurity metal oxides. The analysis of the mechanism and kinetics of passing of quartz structural polymorphic transformations enabled to established that cyclic heating and cooling of the material in the range above and below the temperature of 573°C, at which the phase transition α-quartz ↔ β-quartz take place, must ensure a segregation of impurity metal cations and their concentration on the silica particle surface, since these phase transitions are accompanied by changes in specific material volume and are made instantly in the time dimension. Experimental verification of the effect of cyclic heating-cooling of quartz powder test samples close to temperature of α-quartz ↔ β-quartz phase transformation confirmed prediction made. Deintercalation of impurity metal cations, their segregation and concentration on the quartz surface is accompanied by a decreasing in the lattice parameters of the material. A complete removal of impurity metal cations from the bulk quartz particles with size of 160 – 200 microns and the mass content of the basic substance of 98,4% is achieved after 40-50 heating-cooling cycles of the material in the temperature range 520-870°C. The metastable compounds (KO_2, NaO_2, CrO_2, MnO_2, CsO_3) with boiling point of 540 ÷ 730°C are formed at segregation of impurity cations. This provides the removal of part of impurity metal oxides by their evaporation and condensation outside powder quartz. It is found out that quartz powder thermocyclic treatment should be carried out in several stages and a number of heating-cooling cycles must be greater than 8 at each stage. After each stage of thermocycling impurity metal cations, segregated on the quartz particles surface, washed by solution reactive hydrochloric acid and deionized water at 40 - 80°C and every 7-10 minutes quartz slurry is agitated for 2-3 minutes by ultrasound at frequency of 24 kHz and density of sound energy of 40-80 $W \cdot dm^{-3}$. Thus, the technology made, which combines thermocyclic and chemical treatment of powder quartz, can increase the mass content of the basic substance in the material from 98,4% to 99,995%.

Thermoelectric Properties of Crystals PbTeSe

Nykyruy L.I.[1], Ahiska R.[2], Klanichka V.M.[1],
Dzumedzey R.O.[1], Boryk V.V.[1]

[1]*Vasyl Stefanyk Precarpatian National University, Ivano-Frankivsk, Ukraine;*
[2]*Gazi University, Ankara, Turkey*

Solid solutions $PbTe_{1-x}Se_x$ have great interest, especially as the material for heterostructure devices for infrared optoelectronics, balanced by the lattice parameter. However, studies have shown that $PbTe_{1-x}Se_x$ have good thermoelectric properties, including improving figure of merit by (35-40)% compared to PbTe. This effect is on reducing of the thermal conductivity without degrading the electrical properties of alloys.

With metal-ceramic technology were prepared samples $PbTe_{1-x}Se_x$ with different composition x = 0,15; 0,25; 0,75; 0,85 та 0,95 which were used to study the kinetic parameters in the temperature range (300-800) K.

Electrical conductivity has relatively high values at room temperature. With increasing temperature its value sharply decreases as a result of intensification of scattering on the defects and optical phonons. The presence a minimum value of conductivity with composition x = 0.25 for all temperatures, this can be explained by the transition from soluble to concentrated solid solutions due to increase of atomic substitution.

The Seebeck coefficient sharply increases with increasing temperature. Its value is already at temperatures close to 600 K has optimal value for the single-band semiconductor (~ 200 μV/K). With composition x = 0.25 for all temperatures there is maximum.

From the values analysis of thermal conductivity, it is clear that there is a reduction of its temperature increase. It is obvious that the decrease rate is lower than the conductivity as the defining electronic component of thermal conductivity proportional to the multiplication $s\,T$. This increase in temperature covers decreases of conductivity values. Thermal conductivity is also characterized by a minimum in the composition x = 0.25.

Awarded the behavior of the kinetic parameters are legitimate, as they relate to each other the physical nature of the material: growth of the Seebeck coefficient a reduce for decreases of conductivity σ and growth of thermal conductivity χ through the recession carrier concentration.

The optimal thermoelectric parameters have samples of $PbTe_{0,75}Se_{0,25}$ at temperatures (600-800) K.

The work supported by projects of FRSF State Agency for Innovation and Informatization of Ukraine. (Contracts: R54, F53, 3) and of NAS of Ukraine (N 0110U006281)

Scattering Mechanisms in Crystals PbTe p-type Conductivity

Nyzhnykevych V.V., Galushchak M.O.

Ivano-Frankivsk National University of Oil and Gas, Ivano- Ivankivsk Ukraine

The theoretical analysis of scattering mechanisms of carriers by thermal vibrations of crystal lattice is done. The calculation provided of the mobility of carriers in a wide temperature (4,2 – 300 K) and concentration (10^{16} – 10^{20} sm^{-3}) bands in view of interacting conduction of holes of deformation potential acoustic and optical phonons and polarization potential of optical phonons.

Kinetic parameters of semiconductor materials are largely determined by the scattering mechanisms of carriers. Scattering mechanisms of carriers in lead chalcogenides have been studied repeatedly by different authors. But despite this, at present there is no consensus on the concentration and temperature limits the dominance of certain types of scattering. In this paper, based on comparison of theoretical calculations with the experimental Hall mobility data of specified concentration and temperature limits the use of approximate models of the band structure and the prevailing scattering mechanisms of charge carriers in lead selenide crystals p-type conductivity.

The dominant scattering mechanisms of carriers in hole lead selenide crystals are the scattering of short-range potential vacancies for the concentrations of $l0^{19}$ – 10^{20} sm^{-3} and the lattice thermal vibrations.

Scattering of phonons gives a correct picture of the quality necessary to characterize transport phenomena. The role of polar optical phonon significant at temperatures of 77 and 300 K for concentrations of 10^{16} – 10^{18} sm^{-3}. When increasing the concentration scattering on optical phonons is reduced due to screening.

At high concentrations (higher 10^{18}-10^{19} sm^{-3}) scattering on optical phonons is manifested through their deformation potential, whose influence on the total scattering at certain concentrations is very essential at room temperature. Scattering of carriers by acoustic phonons significant for all temperatures in the considering the whole studied concentration range. For temperature 77 K influence on the total scattering dominates deformation potential scattering on optical phonons.

1. Ravich Yu.L., Efimova B.A., Tamarchnko V.I. Scattering of current carriers and transport phenomena in lead chalkogenides. I. Theory // Phys. Stat. Sol. – 1971. – Vol.43, № 1. – P. 11-33.
2. Freik D.M., Nykyruy L.I., Ruvinsky M.A., Shperun V.M., Nyzhnykevych V.V. Scattering of charge carriers in lead chalcogenides crystals n-type // Physics and Chemistry of Solids. – 2001. – Vol.2, № 4. – P. 681-685.

Calculation of the Static Debye-Waller Factor Considering Anisotropic Effects

Ostafiychuk B. K., Yaremiy I. P., Tomyn U. O., Yaremiy S. I., Umantsiv M. M.

Vasyl Stefanyk Precarpathian National University, Ivano-Frankivsk, Ukraine

One of the promising methods of waveguide structures creating having a number of advantages over the other methods is ion implantation. Refractive index profile of implanted materials depends not only on the shape, size and concentration of radiation defects, but in the case of dislocation loops and cylindrical or disc-shaped clusters also on their spatial orientation. In order to take into account the anisotropy in the orientation of the radiation caused dislocation loops in the theory of X-ray scattering was calculated the coefficient h in the formula of the static Debye-Waller factor L for a set of diffraction vectors $\vec{H}$ and Burgers vectors of the loops $\vec{b}$. Here are the results of calculations for the reflection (111) and dislocation loops with Burgers vectors of $\langle 100 \rangle$, $\langle 110 \rangle$ and $\langle 111 \rangle$ types.

For $\vec{b}^0 = [100]$, $\vec{b}^0 = [\bar{1}00]$ h =0,516; $\vec{b}^0 = [010]$, $\vec{b}^0 = [0\bar{1}0]$ h =0,506; $\vec{b}^0 = [001]$, $\vec{b}^0 = [00\bar{1}]$ h =0,501. Average value for a set of the loops with Burgers vectors of $\langle 111 \rangle$ type $\bar{h}$ =0,508.

For $\vec{b}^0 = [110]$, $\vec{b}^0 = [\bar{1}\bar{1}0]$ h =0,775; $\vec{b}^0 = [\bar{1}10]$, $\vec{b}^0 = [1\bar{1}0]$ h =0,173; $\vec{b}^0 = [101]$, $\vec{b}^0 = [\bar{1}0\bar{1}]$ h =0,729; $\vec{b}^0 = [\bar{1}01]$, $\vec{b}^0 = [10\bar{1}]$ h =0,143; $\vec{b}^0 = [011]$, $\vec{b}^0 = [0\bar{1}\bar{1}]$ h =0,722; $\vec{b}^0 = [0\bar{1}1]$, $\vec{b}^0 = [01\bar{1}]$ h =0,722. Average value for a set of the loops with Burgers vectors of $\langle 110 \rangle$ type $\bar{h}$ =0,450.

For $\vec{b}^0 = [111]$, $\vec{b}^0 = [\bar{1}\bar{1}\bar{1}]$ h =1,028; $\vec{b}^0 = [\bar{1}11]$, $\vec{b}^0 = [1\bar{1}\bar{1}]$ h =0,237; $\vec{b}^0 = [1\bar{1}1]$, $\vec{b}^0 = [\bar{1}1\bar{1}]$ h =0,284; $\vec{b}^0 = [11\bar{1}]$, $\vec{b}^0 = [\bar{1}\bar{1}1]$ h =0,292. Average value for a set of the loops with Burgers vectors of $\langle 111 \rangle$ type $\bar{h}$ =0,460.

Thus for dislocation loops with the certain orientations coefficients h gravely differ from the corresponding average values.

Average values are in good agreement with those obtained in [1] and [2].

1. Dederics, P. H. Effect of defect clustering on anomalous x-ray transmission / P. H. Dederics // Physical review B. – 1970. – V. 1. – № 4. – P. 1306-1317.
2. Даценко Л. И. Динамическое рассеяние рентгеновских лучей реальными кристаллами / Л. И. Даценко, В. Б. Молодкин, М. Е. Осиновский. – К. : Наукова думка, 1988. – 200 с.

Specific energy characteristics of carbon activated by orthophosphoric acid

Ostafiychuk B.K., Budzulyak I.M., Mykyteychuk P.M., Rachiy B.I., Kuzyshyn M.M., Lisovski R.P.

Vasyl Stefanyk Precarpathian National University, 57 Shevchenko Street, Ivano-Frankivsk, 76025, Ukraine, e-mail:bogdan_rachiy@ukr.net

Obtaining of porous carbon materials (PCM) with a large (~ 1000 m^2/g) specific surface area and controlled pore size distribution, opened a wide industrial range for their practical use. The structure of the material can successfully apply them in medicine, nanotechnology, domestic sphere and particular for forming electrodes of electrochemical capacitors.

PCM obtained by carbonization of plant raw material, however at this stage is almost impossible to obtain carbon material with a large specific surface area and sufficient volume of micropores. Therefore, further carried out the chemical activation it's by orthophosphoric acid. The task of this work was to investigate the influence of orthophosphoric acid on the structural and energy characteristics of PCM.

It was found that the chemical activation of carbon by orthophosphoric acid leads to the formation of micropores, which constitute 95% of the total number of pores with an average radius 1,74 nm (Tab. 1). Using of galvanostatic method we calculated the specific capacitance PCM depending on the discharge current. Electrochemical studies were carried out in two-electrode cell size "2525". Specific capacitance of obtained PCM in 30% aqueous KOH solution is 150 F/g at discharge current 20 mA. With increasing current discharge rapidly increases the electrical resistance of PCM and decreases the specific capacity (Fig. 1).

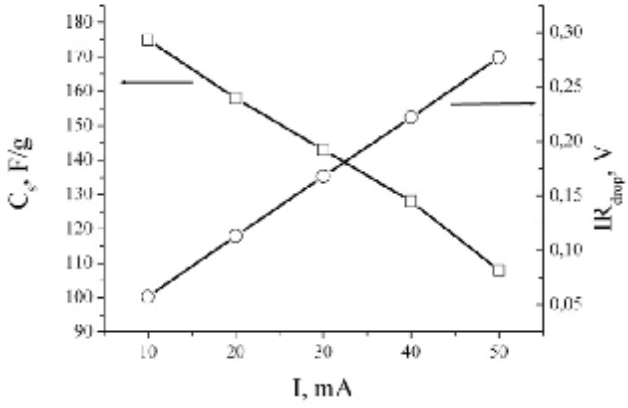

Fig.1. Dependence of specific capacitance and voltage drop of PCM from the discharge current.

Table 1.
Structural and adsorption characteristics of PCM

Specific surface, m^2/g	965
Micropore surface, cm^2/g	927
Total pore volume, cm^3/g	0,41
Micropore volume, cm^3/g	0,36
Average pore diameter, nm	1,74
Specific capacitance, F/g	150

Ab initio Calculation of Vacancies Formation Energy in Zinc and Cadmium Telluride Crystals

Parashchuk T.O., Voznyak O.M., Freik N.D., Grytsak R.I.

Vasyl Stefanyk Prekarpathian University, Ivano-Frankivsk, Ukraine

Structural and electronic parameters of Zinc and Tellurium vacancies have been calculated by Density Functional Theory. For the calculations were used the cluster approach: from the scope of the crystal was chosen restriction fragment, in which the initial positions of the atoms correspond to their position in the real nodes of the crystal lattice. All calculations were performed using the software package Firefly (pcgames) [1]. Atomic wave functions described by basis set B3LYP, the use of which allows one to accurately calculate the energy of chemical bonds in the crystal structures.

Building a computer model of the jobs carried out by the removal of a cluster node corresponding atom: Zn in the case of V_{Zn} or in the case of Te V_{Te} (for zinc telluride). The bond length Zn-Te in the cluster was chosen to be 2.64 A, and the lattice constant answered the bulk crystal lattice constant of ZnTe - 6,01 A.

The calculation were obtained energy necessary for the formation of a crystal of ZnTe to the constituent atoms of the sphalerite modification. To account for the calculation of the initial conditions, the resulting value of the total energy T must be clarified by the formula [2]:

$$E_{tot}=T-\sum E_{el}+\sum \Delta H_{at}, \quad (1)$$

where E_{tot} - the energy required for the formation of the cluster; T - the total energy of the system; E_{el} - the electronic energy of the atoms that make up the system; ΔH - the atomization energy of the atoms. The total energy of the system, T and E_{el} were taken from the results of the calculation, and all other values - from reference materials.

To calculate the structure of the defect was carried out full gradient optimization of geometrical characteristics of the cluster (bond lengths, bond and torsion angles) in the first coordination sphere. This approach allows to determine the relaxation of the crystal lattice in the region of the defect with the influence of the crystal field environment.

Edef defect formation energy was calculated as the difference between the full quantum-mechanical energy E_{tot} in the presence of a defect cluster and the cluster with a defect-free structure. Moreover, the number of additional carbon atoms and hydrogen atoms, which close dangling bonds must match in both cases. The calculation was obtained vacancy formation energy of metal and chalcogen.

The work supported by project of MES of Ukraine (N 0107U006768)

Quasi-Chemical Modeling of Point Defects in Iodine-Doped Cadmium Telluride

Pysklynets U. M.

Ivano-Frankivsk National Medical University, Ivano-Frankivsk, Ukraine

Cadmium telluride crystals have long been the subject of extensive studies owing to their special physicochemical properties, which make CdTe attractive material for high-efficiency optoelectronic devices and nuclear radiation detectors. An important issue is to study the physicochemical properties of halogen-doped CdTe crystals.

The influence of high-temperature processing conditions on the defect structure and physicochemical properties of iodine-doped cadmium telluride has been analyzed in terms of quasi-chemical defect reactions and equilibria in a heterogeneous system comprising an imperfect doped crystal and vapor.

To analyze the defect state of CdTe<I>, we examined two models: a model that included I_{Te}^{+} substitutional defects and their complexes with native point defects, $(V_{Cd}^{2-}I_{Te}^{+})^{-}$ and $(V_{Cd}^{2-}2I_{Te}^{+})^{0}$, and a model that, in addition, took into account the formation of DX^{-} centers. Without allowance for DX^{-} centers, there was unsatisfactory agreement between the calculated carrier concentration and the high-temperature Hall measurement results.

Both models took into account the formation of electrically inactive precipitates: some of the iodine atoms were thought to be aggregated.

The results suggest that the role of the iodine dopant in CdTe crystals is connected with the I_{Te}^{+}, substitutional defects; their complexes with native point defects, $(V_{Cd}^{2-}I_{Te}^{+})^{-}$ and $(V_{Cd}^{2-}2I_{Te}^{+})^{0}$ and the DX^{-} center.

The formation of the $(V_{Cd}^{2-}I_{Te}^{+})^{-}$ complex and DX^{-} center can be represented by the quasi-chemical reactions

$$I_{Te}^{+} + V_{Cd}^{2-} \Leftrightarrow (I_{Te}^{+}V_{Cd}^{2-})^{-} \equiv A^{-}, \quad K_{A^{-}} = \frac{[(I_{Te}^{+}V_{Cd}^{2-})^{-}]}{[I_{Te}^{+}][V_{Cd}^{2-}]};$$

$$I_{Te}^{+} + 2e^{-} \Leftrightarrow DX^{-}, \qquad K_{DX^{-}} = \frac{[DX^{-}]}{[I_{Te}^{+}]n^{2}}.$$

The mass-balance constraint has the form

$$I_{tot} = [I_{Te}^{+}] + [A^{-}] + [DX^{-}].$$

The electroneutrality condition is given by

$$n + [V_{Cd}^{-}] + 2[V_{Cd}^{2-}] + [Te_{i}^{-}] + [A^{-}] + [DX^{-}] = p + 2[Cd_{i}^{2+}] + 2[V_{Te}^{2+}] + [I_{Te}^{+}].$$

The concentrations of native point defects, impurities, their complexes, and charge carriers have been determined as functions of two-temperature annealing parameters (annealing temperature and cadmium vapor partial pressure).

The equilibrium constants of formation of the $(V_{Cd}^{2-}I_{Te}^{+})^{-}$ acceptor complex $K_{A^{-}} = 2 \cdot 10^{-29} \exp(-2.5 / kT)$ and DX^{-} center $K_{DX^{-}} = 2 \cdot 10^{-40} \exp(-1.0 / kT)$ have been evaluated.

Growth Peculiarities of Radiation Resistant $Hg_3In_2Te_6$ Semiconductors

Rarenko I.M., Zakharuk Z.I. , Galochkin A.V., Rarenko A.I., Tsaly V.Z.

Yuriy Fedkovych Chernivtsi National University, Chernivtsi, Ukraine

Semiconductor crystals of $A_2^{III}B_3^{VI}$ group such as In_2Te_3 and based on them solid solutions have extremely high radiation resistant electrical and photovoltaic parameters. The nature of high radiation resistance phenomenon in these materials is caused by the presence of stoichiometric vacancies in their crystal lattices. Therefore, regardless of the concentration and chemical identity of impurities, conductivity of $A_2^{III}B_3^{VI}$ group crystals is intrinsic. It remains intrinsic under irradiation of the crystals with a total radiation flux of fast neutrons, protons, electrons up to 10^{19} cm^{-2}. The most successful in this direction was the creation, research and application of $Hg_3In_2Te_6$ solid solutions.

We have found experimentally that in order to grow the crystals with improved electrophysical characteristics the synthesis of $Hg_3In_2Te_6$ crystals should be carried out from binary components. Their melting at 10.6 mm Hg vacuum must be implemented in a quartz ampoule graphitized with a minimum free volume. Growth of $Hg_3In_2Te_6$ have been carried out by modified zone melting method with zone temperature of 740°C, background temperature is of 380°C, zone heater speed ~ 2 mm/h. For X-ray diffraction studies $Hg_3In_2Te_6$ single crystals were grounded and compacted into quartz ditch. Reflection angles from polycrystalline samples are obtained at room temperature using a Seifert URD-6 diffractometer (Germany) under θ-2θ scheme according to Bragg-Brentano focusing. It is found that obtained material consists mainly of $Hg_3In_2Te_6$ phase with lattice parameters a=6,2900 Å. Some rather weak lines (3-6 rel. units) can be attributed to $Hg_5In_2Te_8$ phase.

$Hg_3In_2Te_6$ phase is a semiconductor with virtually intrinsic conductivity. Carrier concentration at 300 K is within $5\cdot10^{12}$–$2\cdot10^{13}$ cm^{-3}, and mobility –400-520 $cm^2/V\cdot s$, band gap is 0.74 eV at 300 K. Electrical conductivity and Hall coefficient vary exponentially with temperature. Mobility of carriers in $Hg_3In_2Te_6$ increases with increasing temperature up to 350 K, which is not typical for classical semiconductors such as Ge, Si, A^3B^5. In addition, unlike germanium, which band gap is close to the band gap of $Hg_3In_2Te_6$, the latter semiconductor has direct optical transitions with a maximum photosensitivity at λ=1,5 μm, that is very important for their application in high-speed photoelectronic systems, such as fiber optic transmission and detecting information signals devices.

Perspective Cathode Materials of Lithium Power Source Based on the Lithium Orthoferrite

Regush L. V., Kotsyubynsky V.O.
Precarpathian National University named after Vasyl Stefanyk, Ivano-Frankivsk, Ukraine

Lithium orthoferrite α-$LiFeO_2$ was synthesized by ion exchange reaction in the system $LiOH \cdot H_2O$ / β-FeOOH in ethanol environment with the next dehydration at 65° C.

The dependency of Li^+ and Fe^{3+} cations ordering degree in the octahedral positions of the crystal structure versus reaction duration was detected by the X-ray analysis (Fig. 1).

The presence for all samples only one iron-containing phase α-$LiFeO_2$ was proved by the Mossbauer spectroscopy method. The superstructure ordering of iron ions also was fixed for samples obtained at reaction time 24 and 48 hours. Cationic disordering growth for this samples on the Mesbauer spectra (Fig. 2) reflected by the quadrupole splitting values decreasing as a result of the ions Fe^{3+} symmetric surrounding probability increasing. The increasing of the spectrum doublet component lines width was coursed by the structure disordering.

Obtained systems were tested as a cathode material for lithium power sources (LPS). Model sources was discharged in galvanostatic mode at a current density 1,0 C in the voltage range of 1.5-3.0 V. The specific capacity of the material increases with the increasing of the material cation disordering degree and reached a value about 120 mA·h/g for LPS with the cathode based on α-$LiFeO_2$ obtained for ion exchange reaction time 72 h.

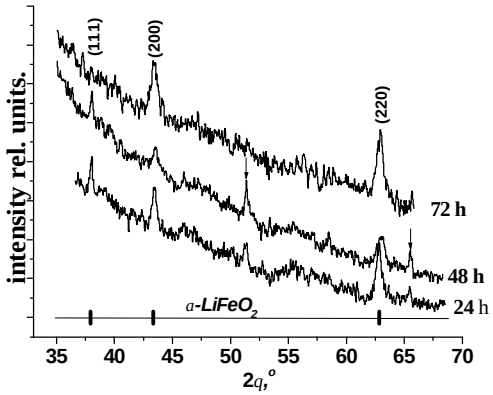

Fig. 1. X-ray diffraction patterns of α-$LiFeO_2$ samples obtained for different durations of ion exchange reactions

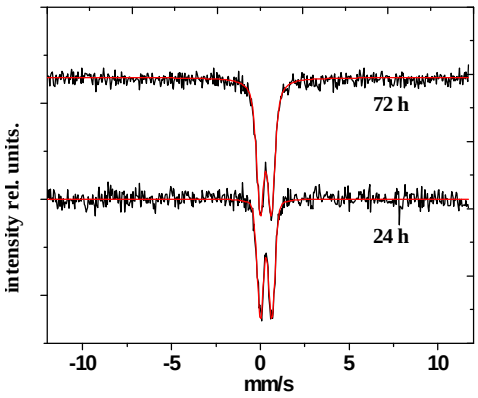

Fig. 2. Mesbauer spectra of of α-$LiFeO_2$ samples obtained for different durations of ion exchange reactions

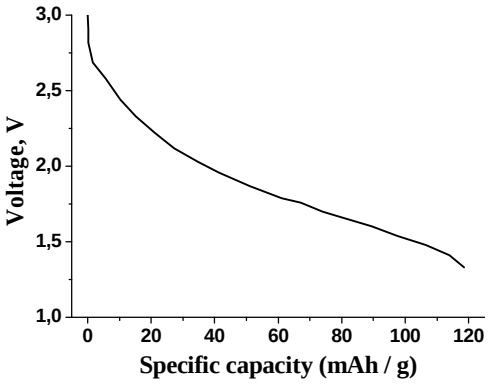

Fig. 3. The discharge curve of the LPS with the cathode based on α-$LiFeO_2$ obtained at reaction time 72 h

Electronic Structure of $HfNi_{1+x}Sn$ Solid Solution

Rogl P.[1], Romaka V.A.[2,3], Krayovskii V.Y.[3],
Romaka L.P.[4], Stadnyk Yu.V.[4], Goryn A.M.[4]

[1]*Vienna University, Vienna, Austria;*
[2]*Ya. Pidstryhach Institute of Applied Problems of Mechanics and Mathematics NationalAcademy of Sciences of Ukraine, Lviv, Ukraine;*
[3]*Lviv Polytechnic National University, Lviv, Ukraine;*
[4]*Ivan Franko Lviv National University, Lviv, Ukraine*

Electronic structure calculation of $HfNi_{1+x}Sn$ solid solution was performed by KKR-CPA and FLAPW methods and showed that the energy of mixing ΔH_{mix} decreases with the increasing of Ni content. The main factor that stabilizes the structure at low concentrations of Ni and decreases Gibbs energy is entropy (vibrational and configurational entropy). With further increasing of concentration of Ni atoms in vacant 4*d* crystallographic site of HfNiSn the secondary phase $HfNi_2Sn$ appears due to the clustering effect in solid solution.

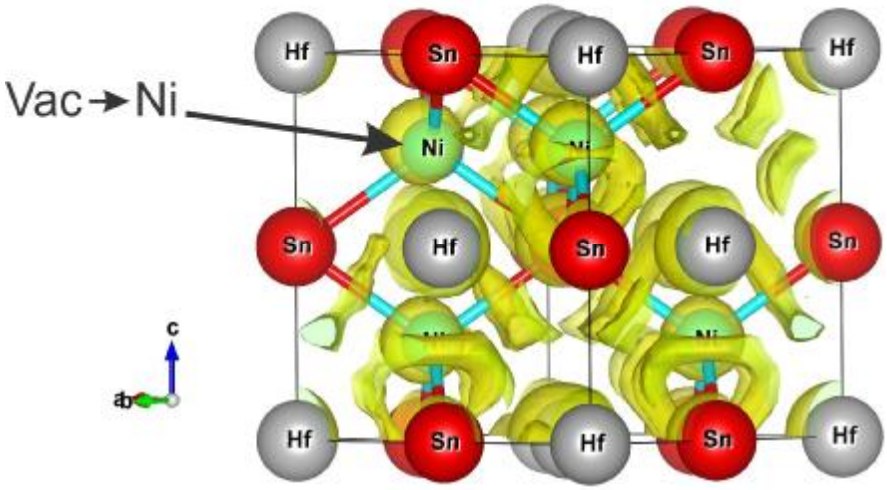

Fig. Electron localization function at 0.40 of $HfNi_{1.25}Sn$ (the arrow shows the position of admixture Ni in the structure)

Topological analyses of calculated electron density and electron localization function showed, that additional Ni atoms (4*d* site) practically do not take part in formation of chemical bonds (due to $3d^{10}$ electron configuration) with Sn atoms (4*b* site). However, Sn atoms form strong covalent bonds with Ni atoms in 4*c* crystallographic site that could be easily seen from electron localization between them (Fig). With further increasing of Ni content the system of tetrahedral bonds changes to octahedral which is typical for $HfNi_2Sn$ compound. Such change leads to complete transformation of band structure, and, as a result, to disappearing of the energy gap.

Mechanisms of Structural Defects Formation of Donor Nature in *n*-HfNiSn Intermetallic Semiconductor

Rogl P. [1], Romaka V.A. [2,3], Krayovskii V.Y.[3],
Romaka V.V.[1,3], Grytsiv A.[1], Lakh O.I.[4]

[1]*Vienna University, Vienna, Austria;*
[2]*Ya. Pidstryhach Institute of Applied Problems of Mechanics and Mathematics National Academy of Sciences of Ukraine, Lviv, Ukraine;*
[3]*Lviv Polytechnic National University, Lviv, Ukraine;*
[4]*SPA "V.I. Lakh NVO "Termoprylad", Lviv, Ukraine.*

In [1] it was showed that crystal structure of *n*-HfNiSn is disordered – crystallographic position of Hf is occupied up to ~1% ($y \leq 0.01$) by Ni atoms, that generate defects of donor nature in the crystal, and the formula of compound could be presented like $(Hf_{1-y}Ni_y)NiSn$.

Crystal structure investigation and electronic structure calculations of *n*-HfNiSn (half-Heusler phase), doped by Ni atoms, revealed accumulation of additional Ni_{1+x} atoms in vacant 4*d* site of $(Hf_{1-y}Ni_y)Ni_{1+x}Sn$ (Fig. 1), and predicted the donor nature of such defects that determine physical properties of semiconductor. Filling of such vacant site leads to change in crystal symmetry and starting from some concentration – formation of $HfNi_2Sn$ compound (Heusler phase).

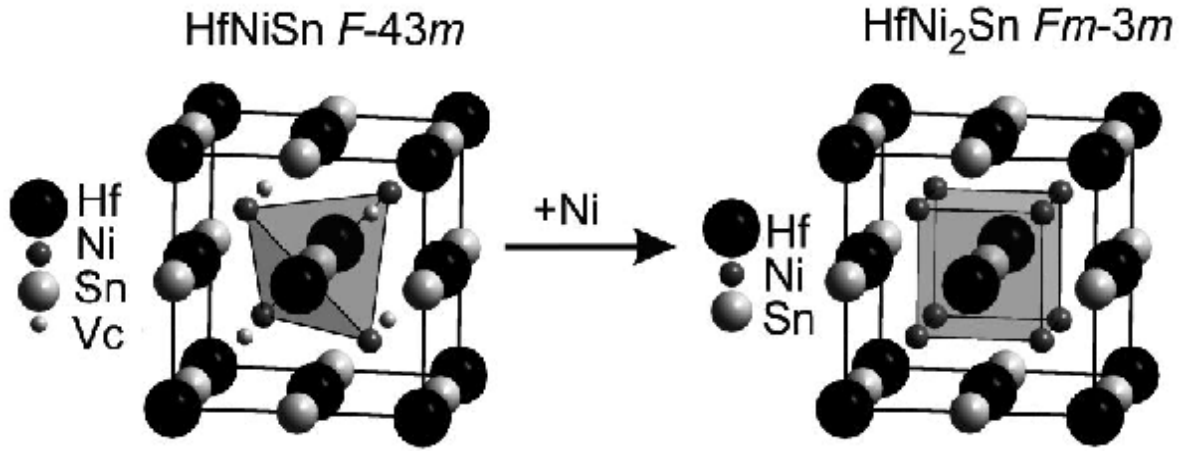

Fig. 1. Structural transformation of HfNiSn into $HfNi_2Sn$ by filling vacant 4d site with Ni_{1+x} atoms.

Structural investigation of $(Hf_{1-y}Ni_y)Ni_{1+x}Sn$ allowed to reveal several features of this solid solution. 1) Doping initial structure by additional Ni_{1+x} atoms leads to structural ordering – amount of Ni_y atoms in 4*a* crystallographic site decreases, and, as a result, number of donors also decreases. 2) Analysis of Fourier electron density maps showed the presence of additional peaks in 4*d* site, that correspond to Ni_{1+x} atoms ($R_{Br} < 3\%$). The existence of homogeneity region was also confirmed by EPMA.

For determination and prediction of Fermi level e_F position, energy gap, electrical and magnetic properties, and contribution of additional Ni_{1+x} atoms in 4*d* crystallographic site, the electronic structure was calculated using KKR-CPA method (Fig. 2).

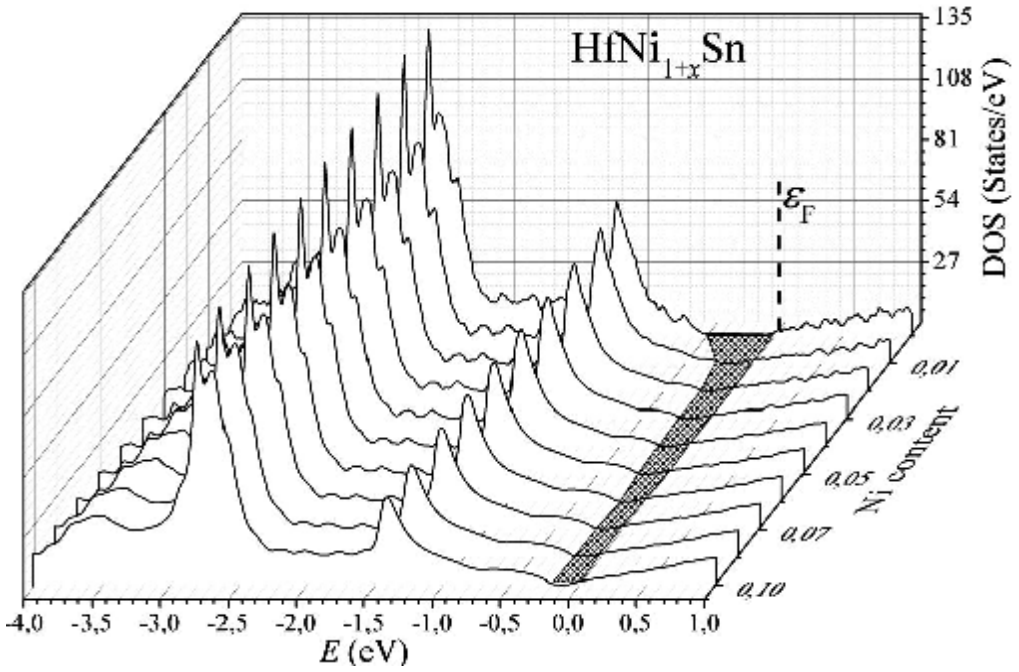

Fig. 2. Distribution of the total density of states $HfNi_{1+x}Sn$ solid solution.

Calculation showed that with increasing of concentration of Ni_{1+x} atoms the density of states at Fermi level in $HfNi_{1+x}Sn$ also increases, and the Fermi level shifts toward conduction band, that is typical for *n*-type of semiconductors doped by donor impurities. The energy gap e_g in $HfNi_{1+x}Sn$ decreases very fast from 287 meV for $x = 0$ ($Hf_{0.99}Ni_{0.01}$)NiSn) to 165 meV for $x = 0.1$ ($HfNi_{1.1}Sn$). The shift of Fermi level near the edge of conduction band has more complex nature, than just effects of donors, due to change in bands profile (growth of "bands tails").

1. Romaka V.V, Rogl P, Romaka L., Stadnyk Y., Grytsiv A., Krayovskii V., Lakh O. Peculiarites of Structural disorder in Zr- and Hf- Containing Heusler and Half-heusler Stanides // Intermetallics. – 2013. – Vol. 35. – P. 45-52.

Microwave Processing of Silicon Carbide Diode Schottky Barrier Stuctures TiBx-n-6H-SiC

Abdizhaliev S.K., Kamalov A.B., Tagaev M.B.

Karakalpak State University, Nukus, Uzbekistan

The use of microwave treatment, as shown in several studies [1-3], to manage physical and chemical properties and influence on the parameters of materials and semiconductor device structures, allowing the use of its technology in order to control the parameters of structural materials, activation of gettering of defects and reduce the thermodynamic equilibrium semiconductor structures. Data on the effect of microwave radiation on the parameters of the contact TiBx-n-6H-SiC, as well as at the metal-SiC in the literature. In this paper, the influence of microwave radiation on the parameters of the contact TiBx-n-6H-SiC.

Before and after the microwave treatment for diode structures were measured current-voltage characteristics and capacity-voltage characteristics of which determine the parameters of the Schottky barriers. The data show that the use of microwave processing as external influences at optimal doses, resulting in improved parameters silicon carbide diode structures with Schottky barrier TiBx-n-6H-SiC.

The results of the pilot studies, we can conclude that the change in the parameters of the Schottky barrier may be due to radiation-induced structural ordering of the impurity at the metal-n-6H-SiC.

1. Ageev O.A. Problems of technology contacts to silicon carbide. (Taganrog. from TSURE of 2005).
2. Ageev O., Belyaev AE, Boltovets NS, Konakova RV Milenin VV Pilipenko V.A. Implementation phase in semiconductor technology and VLSI (Kharkov: STC "Institute for Single Crystals . "2008).
3. Shalich I., Shapira Y. Stability of Schootky contacts with Ta-Si-N amorphous diffusion barriers and Au over layers on 6H-SiC. J. Vac. Sci. Technol. B. V. 8. Number 15. P. 2477 (2000).

Thin Film Interference Multichannel Light Filters on $In_4(Se_3)_{1-x}Te_{3x}$ and $Cd_{1-x}Zn_xSb$ Single Crystals

Strebezhev V.V., Strebezhev V.N., Nichyi S.V., Yuriychuk I.M.

Yuriy Fedkovych Chernivtsi National University, Chernivtsi, Ukraine

Creation of interference-absorption filters on A^3B^6 and A^2B^5 single crystals enables efficient selection of radiation in near and middle infrared region [1,2]. Technological processes of formation of cryo-resistant multilayer thin film interference multichannel light filters on $In_4(Se_3)_{1-x}Te_{3x}$ and $Cd_{1-x}Zn_xSb$ single crystals are investigated. Bandpass filters with different short wavelength cut-off edge within λ_{cut}=1.8–4 μm range have been simulated and practically obtained on the base of multilayer thin film interference systems, calculated by equivalent layers method. Filters with multiple optical channels are obtained by deposition of interference systems on metallized thin film Al or Cr diaphragm with separate light zones.

Morphology, composition and structure of SiO, SiO_2 thin films and ZnS, Ge, Al films deposited on $In_4(Se_3)_{1-x}Te_{3x}$ and $Cd_{1-x}Zn_xSb$ substrates by electron beam and thermal evaporation are studied by scanning electron microscopy and electron diffraction method. It is found that high adhesion and low porosity of films (filters components), that provide mechanical stability of the filter and stability of its characteristics with cooling, are achieved at a combination of optimal deposition rates, ion cleaning of substrates and their heating.

The dependence of optical characteristics and parameters of bandpass interference-absorption $In_4(Se_3)_{1-x}Te_{3x}$ and $Cd_{1-x}Zn_xSb$ based filters on technological conditions of their production and temperature operating conditions is investigated.

1. Gritsyuk B.M., Moschkova T.S., Ogorodnik A.D., Rarenko I.M., Volianska T.A. In4(Se3)1-xTe3x solid solution – material for absorption optical filters // Journal of Applied Spectroscopy. – 1999. – T.66, №4. – P. 577-579.
2. Dremluzhenko S.G., Konopaltseva L.I., Kulikovskaya S.M., Stetsko Yu.P., Strebezhev V.N., Rarenko A.I., Ostapov S.E. Interference IR-filters on the CdSb monocrystal substrates // Proc. of SPIE. – 1999. – Vol. 3890. – P. 104-110.

Peculiarity of the Synthesis $Li_6GdB_3O_9$ for the Single Crystals Growth

Teslyuk I.M.

Institute of Physical Optics, Lviv, Ukraine

Detection and dosimetry of neutrons continues to be an important factor in the nuclear power engineering, scientific investigations, mining industry and the nuclear safety facilities. The optimal neutron detector would be a solid-state device operating at or above the room temperature and prepared from materials with a large neutron capture cross-section. The advantage of $Li_6GdB_3O_9$ borate is such that they can be obtained in the form of single crystals. Even with natural isotope distribution (^{6}Li – 7.42 %; ^{7}Li - 92.58%; ^{10}B – 19%; ^{11}B – 81%; ^{155}Gd – 15% and ^{157}Gd – 15%) the compounds $Li_6GdB_3O_9$ are suited particularly for application in the neutron detectors. This is ensured by their large thermal neutron absorption cross-section σ in corresponding nuclear reactions: $^6Li(n,\alpha)^3H$ (945 barn), $^{10}B(n,\alpha)^7Li$ (3840 barn), $^{155}Gd(n,\gamma)^{156}Gd$ (61000 barn), $^{157}Gd(n,\gamma)^{158}Gd$(260000 barn).

For synthesis of $Li_6GdB_3O_9$ borate compounds with natural isotope distribution there was used multi-staged solid-phase synthesis in special installation consisting of furnace Ø90 mm with resistive heating that gives the possibility to perform synthesis of the growth mixture for one complete loading (95 g) of platinum crucible ∅40×40 mm simultaneously in crucible from aluminum oxide ∅85×100 mm. For synthesis of $Li_6GdB_3O_9$ compound there was used the gadolinium oxide (Gd_2O_3) of high purity with natural isotope distribution had been added to mixture from lithium carbonate (Li_2CO_3) and boric acid (H_3BO_3). Sampling of initial components has been performed by chemical formula for $Li_6GdB_3O_9$.

All this process of synthesis of $Li_6GdB_3O_9$ compound can be described by equation of chemical reaction:

$$6Li_2CO_3 + 6H_3BO_3 + Gd_2O_3 \rightarrow 2Li_6GdB_3O_9 + 6CO_2\uparrow + 9H_2O\uparrow$$

$Li_6GdB_3O_9$ compound formation starts at temperature 560^{o}C, and this process significantly goes faster when temperature reaches 670^{o}C. Synthesis itself has the multi-graded character owing to transient formations: on initial stage $2Li_2O{\cdot}B_2O_3$ and $3Li_2O{\cdot}2B_2O_3$ lithium borates are formed, then at higher temperatures (≥670^{o}C) interact with Gd_2O_3 with generation of $Li_6GdB_3O_9$ compound. Final synthesis (100%) of gadolinium-lithium borate $Li_6GdB_3O_9$ has been finished at melting in platinum growth crucible before single crystal growth.

Modification of the Properties of Chalcogenide As_2S_3 Glasses with Silver Iodide and Silver

Varvaruk V.[1], Lishchynskyy I.[1], Lytvyn P.[2], Kaban I.[3], Vasylyshyn I.[1]

[1]*Vasyl Stefanyk Precarpathian National University, Ivano-Frankivsk, Ukraine*
[2]*V.E. Lashkaryov Institute of Semiconductor Physics, Kyiv, Ukraine*
[3]*Institut für Physik, Technische Universität Chemnitz, Deutschland*

Amorphous chalcogenide compounds are interesting objects of study because they are intensively used in infrared optics, laser technology, systems, copying current optical storage devices, glass fiber optic data transmission systems and others.

This work investigates the thermodynamics and structure of chalcogenide glasses As_2S_3, $(As_2S_3)_{1-x}Ag_x$, $(As_2S_3)_{1-x}(AgI)_x$, with x = 5, 8, 10, 12, 15, 25, 30. Based taken by differential scanning calorimeter NETZSCH DSC thermogram 404C defined in the glass transition temperature. According to the model defined Kissinger activation energy for glass transition Eg investigated alloys.

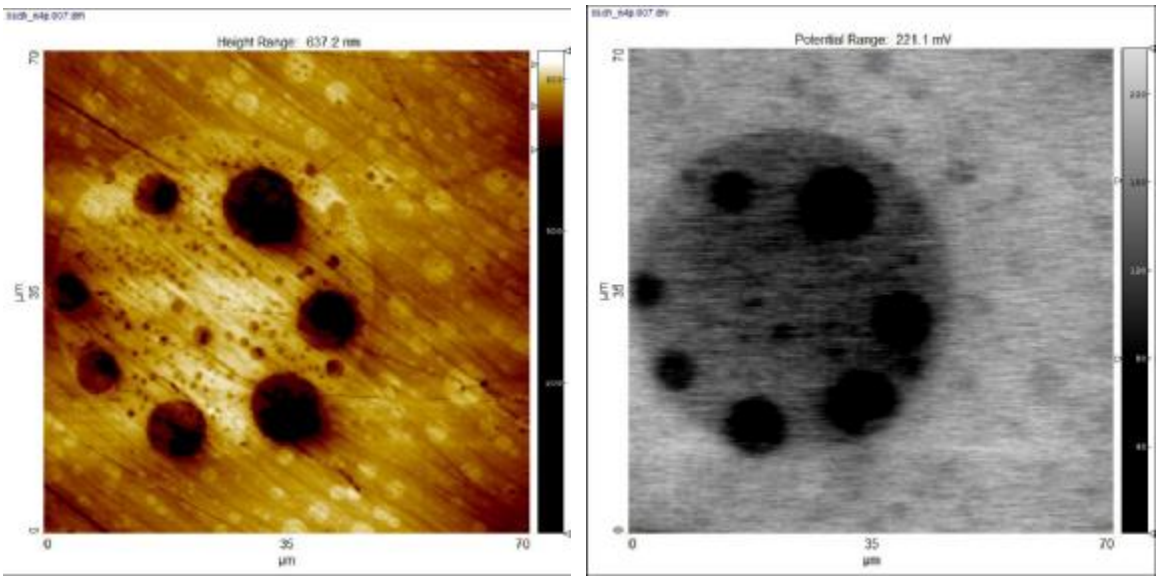

a b

AFM image (a) and surface potential map (b) for alloy $(As_2S_3)_{88}Ag_{12}$

Polishing the surface of glasses to drive mikrovorsystyh manifested in the relief phase with different durability. Atomic force microscopy visualized area harder for the matrix in which there are softer inclusion. Power-Kelvin probe microscopy showed a significant reduction in surface potential in softer inclusions, which is typical for saturated metal systems.

Changing the Surface Properties of Inorganic Materials under the Influence of Ionizing Radiation with Energy up to 24 MeV

Vasylyeva H.V.[1], OsypenkoA.P.[1], Yakovlev V.I.[2], Kylivnyk Y.M.[2]

[1]*Department of Theoretical Physics of Uzhgorod national university, Uzhgorod, Ukraine*;
[2]*Institute of Sorption and Endoecology Problems NAS of Ukraine, Kyiv, Ukraine*

A number of scientific and ecological problems are related to increased background radiation. Hence, the strength of materials involved with respect to ionizing radiation is of great importance.

It is also important to analyze changes on the materials surface under irradiation and effect of these changes on the general properties of the materials under study. On the other hand, ionizing radiation can be used for targeted variation of the surface parameters by variation of the dose, intensity, and type of the irradiating particles.

Here we report on the strength of titanium phosphate and zirconium silicate to ionizing radiation and variation of their surface parameters under irradiation. The samples were irradiated by gamma quanta with energy from 8 MeV to 24 MeV using a Betatron B–25 of the Department of Theoretical Physics of Uzhgorod National University.

The surface characteristics (specific surface area, pore volume and radius) were studied using a Quantachrome AS1 Win analyzer in the Institute of Sorption and Endoecology Problems.

All the above parameters of titanium phosphate and zirconium silicate are shown to vary with irradiation. The initial pore radius for titanium phosphate is within 50 nm. After irradiation it increases to 60–66 nm. Zirconium silicate has the radius of surface pores of 1.5 nm which decrease on the average by 0.35 nm after the irradiation (the device error is 1%).

Amorphous zirconium silicate with micro porous structure is a new sorption material and the composition of its surface groups is still under study. The sorption capacity of the materials under investigation with respect to divalent ions decreases after the irradiation.

Quasychemical Description of Own Point Defects in Zinc Telluride Enriched Zinc

Volochanska B.P., Pylyponyuk M.A., Boychuk M.T., Starko I.Yu.

Vasyl Stefanyk Prekarpathian University, Ukraine

Zinc Telluride is a promising material of light-emitting diodes with high brightness. It is widely used as a barrier material to create all sorts of low-dimensional structures. It is needed reliable information about their defective condition for developing the science-based technology ZnTe material.

Stoichiometric Zinc Telluride can be changed by setting the partial pressure of the components on the solid phase or the temperature in the method of two-temperature annealing. Equilibrium of "crystal-vapor" can be described by equations quasichemical reactions which is listed in the table.

There is $K = K_0 \exp(-\Delta H / kT)$ equilibrium constant, where ΔH is the enthalpy of reaction; P_{Zn} is the partial vapor pressure of Zinc; e^- is an electron; h^+ is hole; n and p are concentration of electrons and holes respectively, «v» is vapor.

$0 = V_{Te}^0 + V_{Zn}^0$	$K_S = \left[V_{Te}^0\right] \cdot \left[V_{Zn}^0\right]$
$Zn^V = V_{Te}^0 + Zn_{Zn}^0$	$K_{Zn,V} = \left[V_{Te}^0\right] p_{Zn}^{-1}$
$V_{Zn}^0 = V_{Zn}^{2-} + 2h^+$	$K_a' = \left[V_{Zn}^{2-}\right] \cdot p^2 / \left[V_{Zn}^0\right]$
$V_{Te}^0 = V_{Te}^{2+} + 2e^-$	$K_b' = \left[V_{Te}^{2+}\right] \cdot n^2 / \left[V_{Te}^0\right]$
$0 = h^+ + e^-$	$K_S = np$
$2\left[V_{Zn}^{2-}\right] + n = 2\left[V_{Te}^{2+}\right] + p$	

When you are calculated the system of equations you can determine the concentration of holes p through the constant quasichemistry reactions K and the partial vapor pressure of Zinc P_{Zn}:

$$2\frac{K_b' K_{Zn,V} P_{Zn}}{K_i^2} p^4 + p^3 - K_i p - 2\frac{K_a' K_S}{K_{Zn,V} P_{Zn}} = 0$$

The calculation of defects concentration are showed that in crystals ZnTe vacancies of Tellurium $[V_{Te}^{2+}]$ are formed in small quantities and concentration of charge carriers which is determined by the mainly vacancies of Zinc $[V_{Zn}^{2-}]$. The increased of the Zinc vapor partial pressure P_{Zn} thus a constant annealing temperature T it reduces the hole concentration p, which is caused by a decrease in the concentration of Zinc vacancies $[V_{Zn}^{2-}]$.

With the decrease of annealing temperature T by the constant partial pressure of Zinc vapor P_{Zn} the concentration of Zinc vacancies decreases $[V_{Zn}^{2-}]$, which reduces the hole concentration p.

Note that both isothermal and pressure dependence have good agreement with experiment.

The work supported by project of MES of Ukraine (N 0107U006768)

Effect of Finishing Chemical Treatment of Si-Wafers Surface on the Adsorption/Desorption of Ag^{+}, Fe^{3+}, Ca^{2+} ions

Vorobets M.M.

Yuriy Fedkovych Chernivtsi National University, Chernivtsi, Ukraine

The effectiveness of different methods of finishing chemical treatment, which are used to reduce uncontrolled technological impurity, of surface Si-wafers is investigated by the method of radioactive indicators. Criterion of qualitative and quantitative evaluation of the effectiveness of finishing chemical treatment chosen as value change of contact potential difference, work function of electron and surface resistance caused by adsorption/desorption of Ag^{+}, Fe^{3+} and Ca^{2+} ions. The thickness of the layer of adsorbed ions exceed the value of monolayer coverage ($N > 7 \cdot 10^{14}$ at/sm^2).

Experimentally, the adsorption of Fe^{3+} and Ca^{2+} ions decreases and Ag^{+} ions – to increase the value of the contact potential difference, which is caused by different mechanisms process. Specifically adsorbed ions Fe^{3+} are surface centers acceptor type and capable of capturing electrons on their free 4*p* and 4*d* energy sublevel, which leads to increased work function of electron. Increasing the contact potential difference as a result of adsorption of Ag^{+}-ions due to the reaction of their recovery, and reduces the surface concentration of free electrons and the value of the work function of electron. Above considerations are confirmed by measuring the surface resistance.

It is shown, that in the case of Si-wafer processing in ammoniac-peroxide solutions the degree of desorption of ions iron does not exceed 40 %, while the ions Ag^{+} the degree of desorption 100 %. Introduction to ammoniac-peroxide solutions potassium hydroxide, treatment of acid-peroxide solution or combination treatment in ammoniac-peroxide solutions and acid-peroxide solution increase the degree of desorption of ions Fe^{3+} to 100 %.

Desorption of Ca^{2+} ions to study options of finishing chemical treatment occurs with less efficiency than ions Fe^{3+} and Ag^{+}. This is due to the fact that Ca^{2+} ions do not form complex compounds with components desorption compounds. With lower electrochemical potential than Fe^{3+} (-2,67 eV for Ca^{2+} compared with -0,04 eV for Fe^{3+}), adsorbed Ca^{2+}-ions are capable of a stronger interaction with the surface of the semiconductor. One may assume that in the case of other alkaline earth and alkali metals such interaction will increase. It is logical to propose the addition of desorption compounds of components that can form complexes with ions of alkali or alkaline earth metals. Si-wafers surface treatment in ammoniac-peroxide solutions is not effective enough to desorption clean from Fe^{3+} ions and other ions are prone to hydrolysis in alkaline medium. Therefore, this treatment should be used in combination with acid-peroxide solution.

Monocrystals Based on Iron Borate for Researches in Solid State Physics and Magnetism

Yagupov S.V., Strugatsky M.B., Postivey N.S., Seleznyova K.A.,
Yagupov V.S., Milyukova E.T.

Taurida National University, Simferopol, Ukraine

Weakly-ferromagnetic monocrystals of iron borate, $FeBO_3$, thanks to a rare combination of its magnetic, magneto-optical, magneto-acoustic and resonance properties are the model object of numerous fundamental researches in condensed matter physics and magnetism. It is one of few materials combining room temperature magnetism and a high transparency up to a near ultraviolet. Additional opportunities to investigate new effects we open by growing and using crystals of iron borate containing various additives, isomorphically replacing the iron atoms, $Fe_{1-x}Me_xBO_3$ (Me = Mn, Ni, Co, Ga,…). Partial substitution of magnetic ions by diamagnetic ones in magnetically ordered crystals is a powerful method that allows a detailed study of many properties of magnetic materials. This is due to difference in dependences of mechanisms that contribute to the formation of such properties on the degree of diamagnetic dilution. In particular, diamagnetic dilution of iron borate is a possibility to investigate the nature of the surface magnetism and magneto-acoustic effects we had found in $FeBO_3$. For optical, magnetic, magneto-optical and magneto-acoustic effects research, $Fe_{1-x}Ga_xBO_3$ crystals are of great interest.

Traditional method of Iron borate growth is solution-in-melt crystallization. We develop and use also gas-transport synthesis.

$Fe_{1-x}Ga_xBO_3$ monocrystals with different x

It was determined the technological conditions and synthesized by solution-in-melt spontaneous method the series of $Fe_{1-x}Ga_xBO_3$ monocrystals of high structural perfection and optical quality in wide range of substitutions, $0 \leq x \leq 1$ (see fig.).

To determine the perfection degree of the samples we used rocking curve X-ray diffraction method. Concentrations of Fe and Ga in the grown crystals were defined by X-ray fluorescence analysis (XRF) and electron microscopy methods. It is important to note that the concentrations of magnetic and diamagnetic ions significantly differ from the ratio of these ions in the starting charge. Moreover, we found a spread of Fe and Ga concentrations, even among crystals grown in the same crucible.

Synthesis and Electrochemical Properties of $Vi_2Fe_4O_9$ Micro-Fine Ferrite Powder

Yuryev S.O., Yushchuk S.I., Grygorchak I.I., Tsiupko F.I.

National University "Lviv Polytechnic", Lviv, Ukraine

Today extensively studied electrochemical properties of cathode materials based on oxide systems with different chemical composition and structure that can absorb lithium ions. In its crystal structure bismuth ferrite $Bi_2Fe_4O_9$ be regarded as one of the most promising cathode materials for lithium-ion power sources.

Micro-fine powder of $Bi_2Fe_4O_9$ ferrite with particle size up to 100 μm obtained using the co-precipitation of hydroxides from solutions of salts of iron (III) and bismuth using ammonium hydroxide.

X-ray studies revealed that the crystal structure is orthorhombic (space group Pbnm), and unit cell parameters of the compound have the following meanings: $a = 7{,}94\ \text{Å}$, $b = 8{,}44\ \text{Å}$ і $c = 6{,}01\ \text{Å}$ and that is consistent with the literature data. The architectural framework of $Bi_2Fe_4O_9$ crystalline structure are columns of the oxygen octahedra each connected by edges. Columns are placed on the middle of the *a* and *b* parameters and are parallel to the *c* axis. Between octahedral columns are relationships, each of which consists of two oxygen tetrahedra. In the unit cell falls four octahedrons and four tetrahedrons. The iron ions are equally distributed between the tetrahedral and octahedral positions in the of $Bi_2Fe_4O_9$ crystalline structure.

Discharge characteristics of lithium intercalation were studied in three-electrode cell with one molarity solution of $LiBF_4$ in gamma-butyrolactone with chlorine-silver electrode. Kinetic processes of intercalation current formation studied using the method of impedance spectroscopy in the frequency range 3,10 ...106 Hz by measuring complex "AUTOLAB" of "ECOCHEMMIE" company (Netherlands) and FRA-2 and GPES programs .

The resulting discharge curves for micro - fine powder of $Bi_2Fe_4O_9$ ferrite characterized horizontal sections with constant voltage value in the neighborhood of 2,8 V. The energy and volume parameters of electrochemical cell commensurate with the corresponding values known lithium power sources. In our opinion the mechanism of electrochemical introduction of lithium ions in micro-fine powder of $Bi_2Fe_4O_9$ ferrite is determined by several factors. High values of energy and volume parameters obviously related to its layered structure. This fact contributes to the high degree of "guest" filling of Li^+ ions in the studied compound.

Determination of Displacement of the Deep Levels Radiation Origin at the Ge and Si n -Type

Zakharchuk D.A.[1], Fedosov S.A.[2], Koval Yu.V.[1], Yashchynskiy L.V.[1]

[1]*The State Technical University of Lutsk, Lutsk, Ukraine*
[2]*Lesya Ukrainka East European National University, Lutsk, Ukraine*

Influence of radiating defects with levels E_C *-0,2eV* in n-Ge and E_C *-0,17eV* in n-Si on piezoresistance crystals is investigated at temperatures of their ionization and on the basis of it the size of their displacement is appreciated at uniaxial elastic deformation for main crystal the schedule directions: [111], [110], [100]. Behind a rectilinear inclination of pieces of recession of dependences $lg\rho=f(X)$ in the field of the big mechanical pressure (when deformation redistribution is completed), or after corresponding processing experimental dependences $\rho=f(X)$ not irradiated and irradiated samples (when piezoresistance it is defined only by the second mechanism) the size of change of a power crack $\delta(\Delta E)$ between deep levels and a bottom of a c-zone for all mainstreams is determined. But change $\delta(\Delta E)$ can be caused due to displacement of levels E_C *-0,2eV* (in n-Ge) and E_C *-0,17eV* (in n-Si) so and offset of the valleys of the zone to conductivities.

That is why using the received experimental values $\delta(\Delta E)$ and known sizes of displacement of valleys of a c-zone which fall at one axis elastic deformation, it is determined sizes and directions of displacement of deep levels for main crystal the schedule directions. Anisotropy of sizes of their displacement allows to judge on the basis of measurement piezoresistance anisotropy of a structure of researched radiating defects: in a direction [110] in n-Ge V_2D (to which posesses level E_C *-0,2eV*) and [100] for the A-center (to which posesses level E_C *-0,17eV*) in n-Si. Such conclusion about anisotropy of the A-center is well coordinated with results of other authors with use of method EPR.

Electronic Properties of (111) Surface in ZnTe, ZnS, CdTe Crystals

Zubkova S.M.[1], Rusina L.N.[1], T.V.Gorkavenko[2]

[1]*I. N. Frantsevych Institute for Problems of Materials Science, National Academy Sciences of Ukraine, Kyiv, Ukraine*
[2]*Kyiv National Taras Shevchenko University, Kyiv, Ukraine*

Electronic band structure, local densities of states (LDS) (total and layer-resolved ones), and a charge density contour and 3D plots at the (111) polar surface in ZnTe, ZnS, CdTe crystals have been studied. The properties of anion- and cation-terminated surfaces have been analyzed separately. The self-consistent three - dimensional pseudopotentional method has been used for numerical calculations in the framework of a model of layered superlattice. In this model the surface was defined as a thin film, which is repeated periodically in the direction that is perpendicular to the surface. Films are separated by the vacuum gaps. Software package for calculation of electronic properties in the bulk and at the surface of sphalerite and wurtzite type crystals are proposed. The application of an original iterator in the self-consistent procedure allowed difficulties associated with the surface-induced presence of reciprocal-lattice vectors shorter than 1a.u. to be overcome.

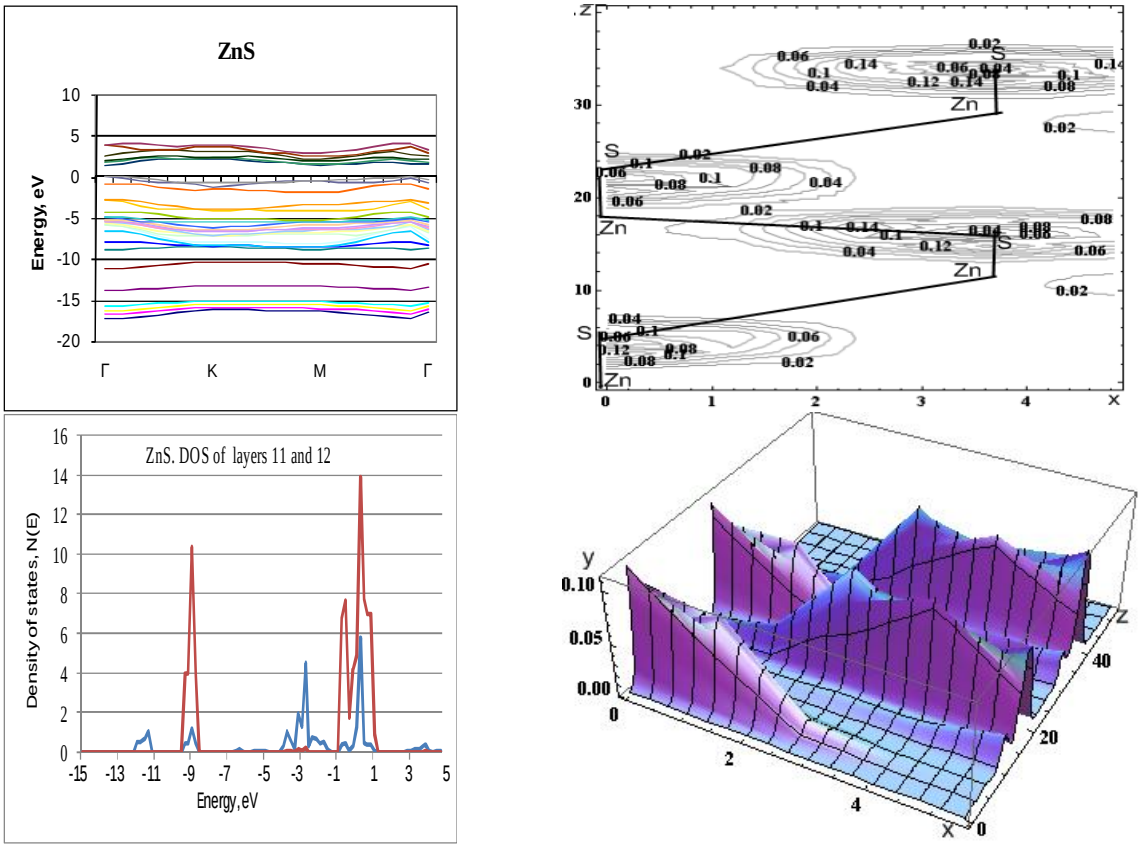

Figure displays the two-dimensional band structure of the 12-layer ZnS (111) film, LDS and charge density of contour and 3D plots for unrelaxed surface geometry.

ЗМІСТ

ПЛЕНАРНІ ДОПОВІДІ
PLENARY SESSIONS

Секція 1
Технологія тонких плівок (метали, напівпровідники, діелектрики, провідні полімери) і методи їх дослідження
(усні доповіді)

Session 1
Thin films technology (metals, semiconductors, dielectrics, conductive polymers) and their research methods
(oral)

Секція 1
Технологія тонких плівок (метали, напівпровідники, діелектрики, провідні полімери) і методи їх дослідження

(стендові доповіді)

Session 1
Thin films technology (metals, semiconductors, dielectrics, conductive polymers) and their research methods
(poster)

Секція 2
Нанотехнології, наноматеріали і квантово-розмірні структури
(усні доповіді)

Session 2
Nanotechnologies and nanomaterials, quantum-size structures
(oral)

Секція 2
Нанотехнології, наноматеріали і квантово-розмірні структури

(стендові доповіді)

Session 2
Nanotechnologies and nanomaterials, quantum-size structures

(poster)

Секція 3
Фізико-хімічні властивості тонких плівок
(усні доповіді)
Session 3
Physical-chemical properties of the thin films
(oral)

Секція 3

Фізико-хімічні властивості плівок та наноструктур.

(стендові доповіді)

Session 3

Physical-chemical properties of the films and nanostructure

Секція 4
Тонкоплівкові елементи електронних пристроїв, наноелектроніка
(усні доповіді)
Session 4
Thin film elements for electronic devices and nanoelectronics
(oral)

Секція 4
Тонкоплівкові елементи електронних пристроїв, наноелектроніка
(стендові доповіді)
Session 4
Thin film elements for electronic devices and nanoelectronics
(poster)

Секція 5
Функціональні кристалічні матеріали: ріст, фізичні властивості, використання
(усні доповіді)
Session 5
Crystal's growth and their physical properties
(oral)

Секція 5
Функціональні кристалічні матеріали: ріст, фізичні властивості, використання
(стендові доповіді)
Session 5
Crystal's growth and their physical properties
(poster)

ДЛЯ НОТАТОК

ДЛЯ НОТАТОК

ДЛЯ НОТАТОК

Наукове видання

ФІЗИКА І ТЕХНОЛОГІЯ ТОНКИХ ПЛІВОК ТА НАНОСИСТЕМ
Матеріали XIV міжнародної конференції
МКФТТПН-XIV

PHYSICS AND TECHNOLOGY OF THIN FILMS AND NANOSYSTEMS
Materials of XIV International Conference
ICPTTFN-XIV

ФИЗИКА И ТЕХНОЛОГИЯ ТОНКИХ ПЛЕНОК И НАНОСИСТЕМ
Материалы XIV международной конференции
МКФТТПН-XIV

Редактор *Володимир Прокопів*
Технічний редактор *Олександр Соколов*
Верстка *Роман Дзумедзей, Тарас Паращук, Іван Биліна, Остап Матківський*
Відповідальний за випуск *Любомир Никируй*

Усі матеріали подані у авторській редакції

Підписано до друку 15.04.2013.
Формат 60x84/$_{16}$. Гарнітура «Times New Roman».
Папір офсетний. Тираж 400.

Видавництво
ДВНЗ «Прикарпатський національний університет імені Василя Стефаника»,
вул. С. Бандери, 1, м. Івано-Франківськ, 76018,
Тел. +38(0342)715622,
E-mail: vdvcit@pu.if.ua

Фізика і технологія тонких плівок та наносистем. ***Матеріали XIV Міжнародної конференції*** / За заг. ред. заслуженого діяча науки і техніки України, д.х.н., проф. **Фреїка Д.М**. – Івано-Франківськ: Видавництво Прикарпатського національного університету імені Василя Стефаника, 2013. – 624 с.